

1997

The interpretation and characterisation of lineaments identified from Landsat TM imagery of SW England

Rogers, John David

<http://hdl.handle.net/10026.1/2022>

<http://dx.doi.org/10.24382/3888>

University of Plymouth

All content in PEARL is protected by copyright law. Author manuscripts are made available in accordance with publisher policies. Please cite only the published version using the details provided on the item record or document. In the absence of an open licence (e.g. Creative Commons), permissions for further reuse of content should be sought from the publisher or author.

**The interpretation and characterisation of lineaments identified from
Landsat TM imagery of SW England**

by

John David Rogers

A thesis submitted to the University of Plymouth in
partial fulfilment for the degree of

DOCTOR OF PHILOSOPHY

Department of Geological Sciences

August 1997

90 0342524 2



UNIVERSITY OF LYMOUTH	
Item No.	900 3425242
Date	25 NOV 1997 S
Class No.	T 554.23 R0 G
Contl. No.	X703594647
LIBRARY SERVICES	

REFERENCE ONLY

LIBRARY STORE

The interpretation and characterisation of lineaments identified from Landsat TM imagery of SW England

John David Rogers

Department of Geological Sciences, University of Plymouth

Abstract

Two Landsat TM scenes of SW England and a sub-scene of North Cornwall have been analysed visually in order to examine the effect of resolution on lineament interpretation. Images were viewed at several different scales as a result of varying image resolution whilst maintaining a fixed screen pixel size. Lineament analysis at each scale utilised GIS techniques and involved several stages: initial lineament identification and digitisation; removal of lineaments related to anthropogenic features to produce cleansed lineament maps; compilation of lineament attributes using ARC/INFO; cluster analysis for identification of lineament directional families; and line sampling of lineament maps in order to determine spacing.

SW England lies within the temperate zone of Europe and the extensive agricultural cover and infrastructure conceal the underlying geology. The consequences of this for lineament analysis were examined using sub-images of North Cornwall. Here anthropogenic features are visible at all resolutions between 30m and 120m pixel sizes but lie outside the observation threshold at 150m. Having confidence that lineaments at this resolution are of non-anthropogenic origin optimises lineament identification since the image may be viewed in greater detail. On this basis, lineament analysis of SW England was performed using image resolutions of 150m. Valuable geological information below the observation threshold in 150m resolution images is likely, however, to be contained in the lineament maps produced from higher resolution images. For images analysed at higher resolutions, therefore, knowledge-based rules were established in order to cleanse the lineament populations.

Compiled lineament maps were 'ground truthed' (primarily involving comparison with published geological maps but included phases of field mapping) in order to characterise their geological affinities. The major lineament trends were correlated to lithotectonic boundaries, and cross-cutting fractures sets. Major lineament trends produced distinct frequency/orientation maxima. Multiple minor geological structures, however, produced semi-overlapping groups. A clustering technique was devised to resolve overlapping groups into lineament directional families. The newly defined lineament directional families were further analysed in two ways:

(i) Analysis of the spatial density of the length and frequency of lineaments indicates that individual and multiple lineament directional families vary spatially and are compartmentalised into local tectonic domains, often bounded by major lineaments. Hence, such density maps provide useful additional information about the structural framework of SW England.

(ii) Lineament spacing and length of the lineament directional families were analysed for the effect of scale and geological causes on their frequency/size distributions. Spacing of fracture lineaments were found to be power-law, whereas lengths showed power-law and non-power-law distributions. Furthermore the type of frequency/size distribution for a lineament directional family can change with increasing resolution.

Contents

Abstract	i
Contents	ii
List of Figures	vii
List of Tables	xv
List of Abbreviations	xvii
CHAPTER 1 INTRODUCTION	1
1.1 Introduction and background.....	1
1.2 Aims.....	8
1.3 Objectives	9
1.4 Remote sensing and Geographic Information System hardware and software –	11
CHAPTER 2 CAUSES OF LINEAMENTS IN SW ENGLAND: REGIONAL GEOLOGY AND GEOMORPHOLOGY	12
2.1 Introduction.....	12
2.2 Geological history of SW England.....	12
2.3 Lithotectonic units of SW England.....	15
2.3.1 Gramscatho Basin of South Cornwall	15
2.3.2 Middle Palaeozoic 'northward' facing fold and thrust zone.....	17
2.3.3 Middle-Upper Palaeozoic 'southward' facing fold and thrust zone	19
2.3.4 The 'Culm Synclinorium'	20
2.3.5 The Upper Devonian rocks of North Devon.....	21
2.4 Post-Variscan cover.....	21
2.4.1 Late/Post Variscan intrusives.....	21
2.4.2 Post-Permian cover	22
2.5 Major post-Late Carboniferous/Early Permian brittle structures	22
2.6 The relationship between lineaments and bedrock geology in SW England -	24
2.6.1 Geological features which can form a surface expression	25
2.7 Morphological features of SW England	31
CHAPTER 3 LINEAMENT ANALYSIS - IMAGE PROCESSING AND LINEAMENT IDENTIFICATION	33

3.1 Introduction	33
3.2 Remote Sensing of the land surface in SW England	34
3.2.1 Ground reflection, transmission and absorption mechanisms of materials	34
3.2.2 Remote sensing platforms	38
3.2.3 Spectral responses of the major land-uses	41
3.2.4 Rationale for determining suitable satellite imagery	54
3.3 Image processing techniques	55
3.3.1 Geometric correction	55
3.3.2 Resolution and image degradation	60
3.3.3 Image enhancement	60
3.4 The effect of resolution on the visual impact of linear features on Landsat TM images	66
3.5 Criteria for the lineament interpretation of Landsat TM images	71
3.6 The determination of the optimum image processing techniques for the lineament analysis of SW England	72
3.7 Combining overlapping lineaments maps interpreted from images of Cornwall and Devon	85
3.8 Image processing techniques of higher resolution images	86
3.8.1 Removal of anthropogenic lineaments from lineament maps	87
3.9 Regional lineament patterns across SW England	92
3.10 Lineament populations of North Cornwall	99
3.11 The effect of pixelated images on lineament analysis	110
3.12 Discussion	125
3.13 Conclusions	130

CHAPTER 4 GEOLOGICAL INTERPRETATION OF THE LINEAMENT

PATTERNS OF SW ENGLAND	133
4.1 Introduction	133
4.2 Characteristic lineament patterns of the four main lineament groups	134
4.2.1 E/W trending lineaments	134
4.2.2 NW/SE lineaments	137
4.2.3 NE/SW trending lineaments	139
4.2.4 N/S trending lineaments	140

4.2.5 Analysis of common lineament patterns	140
4.3 Characteristics of localised lineament patterns	156
4.3.1 Characteristic lineament patterns	156
4.3.2 Geological analysis of the characteristics in localised and anomalous lineament patterns	158
4.4 Lineament mixtures in SW England	171
4.5 Lineament analysis of SW England	173
4.6 Conclusions	175
CHAPTER 5 EFFECT OF RESOLUTION ON THE INTERPRETED LINEAMENT POPULATIONS	177
5.1 Introduction	177
5.2 The effect of resolution on lineament analysis in the sub-area Cambeak	180
5.2.1 Lineament maps	180
5.2.2 Lineament patterns of the Rusey and the Strangles cliffs	185
5.2.3 Relationships between the lineament patterns and large scale lithotectonic features	189
5.2.4 Relationships between lineament patterns and small scale lithotectonic features	191
5.2.5 Discussion of the effect of resolution on lineament analysis of the sub-area Cambeak	202
5.3 The effect of resolution on lineament analysis in the sub-area Bridgerule	204
5.3.1 Lineament maps	204
5.3.2 Lineament patterns and lithotectonic trends in the sub-area Bridgerule	208
5.3.3 Discussion on the effect of resolution on lineament analysis in the sub-area Bridgerule	210
5.4 The effect of resolution on lineament analysis in the sub-area Laneast	212
5.4.1 Lineament maps	212
5.4.2 Lineament patterns and lithotectonic trends in the sub-area Laneast	215
5.4.3 Discussion on the effect of resolution on lineament analysis in the sub-area Bridgerule	217
5.5 Discussion on the effect of resolution on images of North Cornwall and the extrapolation of the regional lineament map	218
5.6 Conclusions	220

CHAPTER 6 DIFFERENTIATING LINEAMENT DIRECTIONAL FAMILIES	
USING CLUSTER ANALYSIS	222
6.1 Introduction	222
6.2 Description of the lineament frequency/azimuth distributions	225
6.2.1 Lineament directional families and normal distributions	227
6.3 Previous research in the identification of lineament directional families	229
6.4 Cluster analysis	230
6.4.1 Introduction	230
6.4.2 Cluster processing using hierarchical methods	232
6.4.3 Results of the hierarchical clustering methods	233
6.4.4 Discussion and interpretation	234
6.4.5 Cluster processing using an iterative partitioning method	240
6.4.6 Results of the k-means clustering method	241
6.4.7 Discussion and interpretation	243
6.4.8 Application of k-means clustering to other lineament populations	245
6.5 Image resolution, image size and lineament directional families	247
6.5.1 Mixtures of lineament families	247
6.5.2 Resolution	247
6.6 Number of clusters	251
6.7 Discussion	253
6.8 Conclusions	254
CHAPTER 7 GEOLOGICAL ANALYSIS OF LINEAMENT DIRECTIONAL	
FAMILIES IN SW ENGLAND	257
7.1 Introduction	257
7.2 Characteristics of lineament directional families identified from SW England	261
7.2.1 Analysis of characteristics of neighbouring lineament directional families	263
7.3 Density maps of lineament directional families identified from SW England	269
7.3.1 Construction of lineament density maps	269
7.3.2 Lineament density maps of SW England	270
7.3.2.a E/W lineaments (families M and N)	270

7.3.2.b NW/SE lineaments (families U, V and W)	273
7.3.3 Discussion	273
7.4 Scaling relationships of lineaments	276
7.5 Analyses of lineaments related to the SLFZ	279
7.5.1 Results	279
7.5.2 Discussion	283
7.6 Analyses of lineaments divided into lineament groups	285
7.6.1 Results	286
7.6.2 Discussion	286
7.7 Analyses of lineaments divided into lineament directional families	291
7.7.1 Scaling relationships of combined lineament directional families	295
7.7.2 Effect of image resolution on the scaling relationships of lineament length	301
7.7.3 Effect of image resolution on the scaling relationships of lineament spacing	305
7.7.4 Extrapolating the scaling relationships	308
7.8 Conclusions	309
CHAPTER 8 CONCLUSIONS AND FUTURE WORK	311
8.1 Conclusions	311
8.2 Future work	317
References	319
Appendix 1	336
Appendix 2	339
Publications	353

LIST OF FIGURES.

Chapter 1

Fig. 1.1. Geographical location map of SW England.

Chapter 2

Fig. 2.1. Geological map and lithostratigraphic history of SW England.

Fig. 2.2. Map showing the major lithotectonic trends in SW England.

Fig. 2.3. Location map illustrating the major NW/SE trending faults within SW England.

Fig. 2.4. Block diagram illustrating the geomorphological features associated with uniformly dipping strata.

Fig. 2.5. Block diagram illustrating the geomorphological features associated with upright folds.

Fig. 2.6. Block diagrams illustrating the geomorphological features associated with fault-line scarps.

Fig. 2.7. Block diagrams illustrating the geomorphological features associated with fold and thrust belts.

Fig. 2.8. Block diagrams illustrating the geomorphological features associated with the contact relationship between normal faulting and steeply plunging folds.

Chapter 3.

Fig. 3.1. The electromagnetic spectrum.

Fig. 3.2. The effect surfaces have on reflected electromagnetic radiation.

Fig. 3.3. Location of atmospheric windows within the electromagnetic spectrum.

Fig. 3.4. Image illustrating the patchwork field effect within SW England.

Fig. 3.5. Spectral signatures of wet/dry soils, vegetation and water.

Fig. 3.6. Spectral signature of a leaf and its controlling factors.

Fig. 3.7. Spectral signatures of different vegetation types and wet soils over the visible region of the electromagnetic spectrum.

Fig. 3.8. The effect of plant moisture on water absorption features.

Fig. 3.9. The relationship between slope angle and the degree of reflected electromagnetic radiation.

Fig. 3.10. Small map-scale image indicating large scale geomorphological features within SW England.

Fig. 3.11. Location map of the area covered by distorted Landsat TM scenes of SW England.

Fig. 3.12. Image showing the degree of geometric distortion within the Landsat TM images of SW England.

Fig. 3.13. Geometric correction of the Landsat TM images.

Fig. 3.14. A convolution matrix.

Fig. 3.15. Directional and non-directional filters.

Fig. 3.16. Examples of: (i) an image produced by a directional filter; (ii) and a full colour composite.

Fig. 3.17. Schematic diagram illustrating the effect pixel size has on reducing electromagnetic reflectance across field boundaries.

Fig. 3.18. Chart showing the frequency/length distribution of fields identified from images of North Cornwall.

Fig. 3.19. A series of images illustrating the decrease in the visual impact fields with increasing image resolution.

Fig. 3.20. A schematic diagram showing how large scale geomorphological features are preferentially interpreted from low resolution images.

Fig. 3.21. Location map of the areas covered by the different scenes used for interpreting lineaments.

Fig. 3.22. Flow diagram indicating the different stages in the construction of the lineament map of scene 1.

Fig. 3.23. Charts indicating the effect of band number and processing technique on the number of lineaments interpreted from scene 1.

Fig. 3.24. Frequency/length distribution of lineaments interpreted from scene 1.

Fig. 3.25. Frequency/length distribution of lineaments up to 5000m, interpreted from scene 1.

Fig. 3.26. Frequency/length distribution of lineaments from 5000m to 13500m, interpreted from scene 1.

Fig. 3.27. Flow diagram indicating the different stages in the construction of the lineament map of scene 2.

Fig. 3.28. Example of how lineaments relating to anthropogenic features were removed from the lineament maps.

Fig. 3.29. Diagram illustrating the rules used to remove lineaments relating to anthropogenic features from the lineament maps.

- Fig. 3.30. Chart showing the effect of resolution on the numbers of lineaments removed from the lineament maps.
- Fig. 3.31. Lineament map of SW England.
- Fig. 3.32. Frequency/length distribution of lineaments interpreted from SW England.
- Fig. 3.33. Rose diagrams of lineaments interpreted from SW England.
- Fig. 3.34. Map illustrating the lineament trends across SW England.
- Fig. 3.35. Lineament map of North Cornwall, interpreted from images with resolutions of 150m.
- Fig. 3.36. Lineament map of North Cornwall, interpreted from images with resolutions of 120m.
- Fig. 3.37. Lineament map of North Cornwall, interpreted from images with resolutions of 90m.
- Fig. 3.38. Lineament map of North Cornwall, interpreted from images with resolutions of 60m.
- Fig. 3.39. Lineament map of North Cornwall, interpreted from images with resolutions of 30m.
- Fig. 3.40. Frequency/length distributions of lineaments interpreted from images of North Cornwall with resolutions of 150m to 30m.
- Fig. 3.41. Rose diagrams illustrating lineament trends identified in North Cornwall.
- Fig. 3.42. Frequency/azimuth distribution of lineaments interpreted from SW England.
- Fig. 3.43. Frequency/azimuth distributions of lineaments interpreted from different resolution images of North Cornwall.
- Fig. 3.44. Frequency/azimuth distributions illustrating the anomalous peaks and troughs present within the lineament populations identified in this study.
- Fig. 3.45. Schematic diagram showing lineament dragging.
- Fig. 3.46. Schematic diagram showing how pixelated images can effect lineament trend.
- Fig. 3.47. Cartoon diagrams suggesting the pixel patterns which can define a lineament.
- Fig. 3.48. Graph indicating the curved length/trend distributions of lineaments around the anomalous peaks and troughs.

Fig. 3.49. Chart showing that data can fall between the curved length/trend distributions of lineaments identified around the anomalous peaks and troughs.

Fig. 3.50. Graph indicating the curved length/trend distributions of lineaments around anomalous peaks and troughs identified in a lineament population interpreted from linear stretched band 5 images.

Fig. 3.51. Diagrams suggesting how the curved lineament/length distributions maybe formed.

Fig. 3.52. Diagram suggesting how the pixel pattern can influence the spacing of the lineament/length curved distributions.

Fig. 3.53. Worked example of how lineament patterns can influence the spacing of the lineament/length curved distributions.

Fig. 3.54. Graph showing the degree of error imparted by pixelated images to lineament trend.

Chapter 4.

Fig. 4.1. Lineament map of SW England illustrating different lineament patterns.

Fig. 4.2. Lineament map of East Devon and West Somerset showing different lineament patterns.

Fig. 4.3. Lineament map of SW England indicating the major NW/SE lineament zones.

Fig. 4.4. Rose diagrams illustrating the trends within the major NW/SE lineament zones.

Fig. 4.5. Lineament map of the fold and thrust belt of South Devon.

Fig. 4.6. Lineament map of the fold and thrust belt of West Devon/East Cornwall.

Fig. 4.7. Geological map of the Plymouth area.

Fig. 4.8. Lineament map of Mothercombe Bay.

Fig. 4.9. Lineament and geological maps of the Falmouth area, South Cornwall.

Fig. 4.10. Schematic diagram illustrating the complex fracture history in South Cornwall.

Fig. 4.11. Lineament map of North Devon and the northern area of the Culm Basin illustrating different lineament patterns.

Fig. 4.12. Lineament and geological map of North Devon.

Fig. 4.13. Major curved lineament zones within North Devon.

Fig. 4.14. Lineament map of North Devon illustrating displaced and possibly

rotated primary lineaments.

Fig. 4.15. Diagram of a domino-type block rotation system.

Fig. 4.16. Diagram suggesting how a block rotation system could occur within North Devon.

Fig. 4.17. Lineaments trends with the granites of SW England.

Chapter 5.

Fig. 5.1. Geological map of North Cornwall.

Fig. 5.2. Geological and lineament maps interpreted from image resolutions of 150m to 30m, of the sub-area Cambeak.

Fig. 5.3. Chart illustrating the relative frequency of lineament groups within Cambeak.

Fig. 5.4. Topographic map of the sub-area Cambeak.

Fig. 5.5. Sample map of the area between Rusey and Strangles cliffs.

Fig. 5.6. Planar discontinuities at location 1.

Fig. 5.7. Planar discontinuities at locations 2, 3 and 4.

Fig. 5.8. Planar discontinuities at location 5.

Fig. 5.9. Planar discontinuities at location 6.

Fig. 5.10. Planar discontinuities at location 7.

Fig. 5.11. Planar discontinuities at location 8.

Fig. 5.12. Planar discontinuities at locations 9 and 10.

Fig. 5.13. Planar discontinuities at location 11.

Fig. 5.14. Planar discontinuities at location 12.

Fig. 5.15. Planar discontinuities at location 13.

Fig. 5.16. Planar discontinuities at location 14.

Fig. 5.17. Faults identified within the area between the Rusey and Strangles cliffs.

Fig. 5.18. Fault map of the Rusey cliffs.

Fig. 5.19. Geological and lineament maps interpreted from image resolutions of 150m to 30m, of the sub-area Bridgerule.

Fig. 5.20. Chart illustrating the relative frequency of lineament groups within Bridgerule.

Fig. 5.21. Topographic map of the sub-area Bridgerule.

Fig. 5.22. The effect of resolution on the interpretation of lithotectonic features

within Bridgerule.

Fig. 5.23. Geological and lineament maps interpreted from image resolutions of 150m to 30m, of the sub-area Laneast.

Fig. 5.24. Chart illustrating the relative frequency of lineament groups within Laneast.

Fig. 5.25. Topographic map of the sub-area Laneast.

Chapter 6.

Fig. 6.1. Frequency/azimuth distribution of lineaments interpreted from SW England.

Fig. 6.2. Frequency/azimuth distribution of lineaments interpreted from different resolution images of North Cornwall.

Fig. 6.3. Frequency/azimuth distribution of a lineament directional family.

Fig. 6.4. A series of graphs illustrating the distributions obtained from different mixtures of normal distributions.

Fig. 6.5. Dendograms produced by the hierarchical clustering methods.

Fig. 6.6. The cluster distributions produced by the centroid and median hierarchical clustering methods on the 150m resolution lineament population of North Cornwall.

Fig. 6.7. Diagram explaining the convergence criteria used in the *k*-means cluster analysis.

Fig. 6.8. The cluster distributions produced by the *k*-means cluster analysis from the 150m lineament population of North Cornwall.

Fig. 6.9. The cluster solutions obtained by *k*-means cluster analysis from the 120m to 30m lineament populations of North Cornwall and the lineament population of SW England.

Fig. 6.10 The effect resolution has on cluster distributions.

Fig. 6.11. Detailed analysis of the effect resolution has on cluster distributions.

Chapter 7.

Fig. 7.1. Distribution of the lineament directional families within the lineament population of SW England.

Fig. 7.2. Lineament maps of the lineament directional families T, U, V, W and X.

Fig. 7.3. Lineament maps of the lineament directional families B, C, D, E and F.

Fig. 7.4. Lineament density maps of the linked lineament directional families M, N.

Fig. 7.5. Lineament density maps of the linked lineament directional families U, V, W.

Fig. 7.6. The sampling biases truncation and censoring.

Fig. 7.7. Map illustrating the sample areas used for the analysis of the scaling relationships of lineaments.

Fig. 7.8. Scaling relationships of lineaments interpreted from the Sticklepath-Lustliegh fault zone.

Fig. 7.9. Scaling relationships of approximately NW/SE trending lineament groups identified from the Dartmoor and Bodmin granites.

Fig. 7.10. Scaling relationships of approximately NW/SE trending lineament groups identified from the Land's End granite.

Fig. 7.11. Trends of the lineament directional families identified from the lineament populations of North Cornwall.

Fig. 7.12. Diagram illustrating the method used for line-sampling lineament spacing.

Fig. 7.13. The effect of combined lineament directional families on the scaling relationships of lineament length.

Fig. 7.14. The effect of combined lineament directional families on the scaling relationships of lineament spacing.

Fig. 7.15. The effect of resolution on the scaling relationships of the length of lineaments in lineament directional families, interpreted from lineament populations of North Cornwall.

Fig. 7.16. The effect of resolution on the scaling relationships of the spacing of lineaments in lineament directional families, interpreted from lineament populations of North Cornwall.

Appendix 2.

Fig. A2.1. The trends of lineament directional families identified from the SW England lineament population.

Fig. A2.2. Lineament density maps of the linked lineament directional families Z, A.

Fig. A2.3. Lineament density maps of the lineament directional family B.

Fig. A2.4. Lineament density maps of the linked lineament directional families C, D, E.

Fig. A2.5. Lineament density maps of the linked lineament directional families F, G.

Fig. A2.6. Lineament density maps of the linked lineament directional families H, I.

Fig. A2.7. Lineament density maps of the linked lineament directional families J, K.

Fig. A2.8. Lineament density maps of the lineament directional family L.

Fig. A2.9. Lineament density maps of the linked lineament directional families O, P.

Fig. A2.10. Lineament density maps of the lineament directional family Q.

Fig. A2.11. Lineament density maps of the linked lineament directional families R, S.

Fig. A2.12. Lineament density maps of the lineament directional family T.

Fig. A2.13. Lineament density maps of the linked lineament directional families X, Y.

List of Tables.

Chapter 3.

Table 3.1. Landsat MSS sensor specifications.

Table 3.2. Landsat TM sensor specifications.

Table 3.3. Results and statistics of lineaments interpreted from scene 1 by different image processes and bands.

Table 3.4. Lineament trends within SW England.

Table 3.5. Statistics of lineament populations interpreted from images of North Cornwall.

Chapter 4.

Table 4.1. Lineament lengths of lineaments related to major NW/SE fault zones within SW England.

Table 4.2. Lineament trends within granites in SW England.

Table 4.3. Summary of the lineament characteristics identified from the lineament map of SW England.

Table 4.4. Summary of the lineament pattern characteristics from which different lithotectonic features in SW England were interpreted.

Chapter 5.

Table 5.1. The effect of resolution on lineament trends between the Rusey and Strangles cliffs.

Table 5.2. The strike of the major shallow to vertical dipping planar discontinuities in the Rusey and Strangles cliffs.

Chapter 6.

Table 6.1. Cluster difference coefficients for the hierarchical centroid cluster analysis.

Table 6.2. Cluster difference coefficients for the hierarchical median cluster analysis.

Chapter 7.

Table 7.1. Results from the analysis of the similarity in neighbouring lineament directional families.

Table 7.2. Results from the analysis of the scaling relationships of lineaments related to the Sticklepath-Lustliegh fault zone.

Table 7.3. Azimuth ranges of the lineament groups sampled from granites within SW England.

Table 7.4. Results from the analysis of the scaling relationships of lineament groups identified from granites within SW England.

Table 7.5. The azimuth ranges of the combined lineament directional families.

Table 7.6. Results from the analysis of the scaling relationships of the lineament lengths in lineament directional families identified from North Cornwall.

Table 7.7. Results from the analysis of the scaling relationships of the lineament spacing in lineament directional families identified from North Cornwall.

Table 7.8. Results from the analysis of the effect of image resolution has on the scaling relationships of the lineament length in lineament directional families identified from North Cornwall.

Table 7.9. Results from the analysis of the effect of image resolution has on the scaling relationships of the lineament spacing in lineament directional families identified from North Cornwall.

List of Abbreviations.

SW England: South-West England

GIS: Geographic Information Systems

EMR: Electromagnetic radiation

SLFZ: Sticklepath-Lustleigh fault zone

Landsat MSS: Landsat Multi-Spectral Scanner

Landsat TM: Landsat Thematic Mapper

SPOT: Système Probatoire de l'Observation de la Terre

FCC: False colour composite

I would like to thank Dr Mark Anderson and Dr Jim Griffiths for supervising and for help in the preparation of this thesis.

The time spent by Dr Kevin Morris and Sam Hudson in discussing remote sensing, GIS and computer programming, was invaluable. I also acknowledge the input Dr Dave Peacock gave on fault populations and modifying an early draft of the scaling relationships of lineaments. Many other people have contributed to my research either by discussion or friendship, Laura Smithurst, Stacey Murphy, Mike Carroll, Dr Darren Randall, Gary Aillud, Amanda Hopper, Simon West, Chris Vevers, Dr Tony Morris, Stella Pickard, Kirsty Lowe and Catie Brown, to all of these, and also people not mentioned I would like to say thanks.

Finally, I would like to extend my deepest gratitude to my parents who provided continuous help and support.

Author's Declaration

This is to certify that at no time during the registration for the degree of Doctor of Philosophy has the author been registered for any other University award.

This research was supported by a studentship from the University of Plymouth.

Publications (abstracts):

Rogers, J.D. 1994. Scaling relationships of lineament populations from Landsat TM imagery, South West England. (Extended abstract), *Tectonics Studies Group Special Meeting on Fault Populations*, 82-84.

Rogers, J.D. & Anderson, M.W. 1995. Interpretation of lineament populations from Landsat TM images. *Terra Nova*, **7**,(1),27.

Rogers, J.D. & Anderson, M.W. 1996. The interpretation of lineaments from Landsat TM imagery of S.W. England and their relationship to regional structural trends. *Proceedings of the Ussher Society*, **9**, 139.

Conferences attended:


(i) Usshers, 1993, 1995 and 1996;

(ii) Tectonic Studies Group, 1994, 1995;

(iii) Tectonic Studies Group special meeting on Fault Populations, 1994;

and (iv) European Union of Geosciences, 1995.

Signed



Date

18/11/97

Chapter 1 Introduction

1.1 Introduction and background

It has long been recognised that the bedrock geology of South-West (SW) England records a complicated and protracted history including the development and closure of basins, progressive Variscan ductile deformation, several phases of contractional and extensional faulting, granite intrusion and a post-Variscan cover (e.g. Dearman 1963, Dobson & Rex 1973, Sanderson & Dearman 1973, Shackleton *et al.* 1982, Seago & Chapman 1988, Selwood 1990). Evidence of this is largely restricted to coastal exposures, whereas the geology of the extensive inland area is comparatively less well known due to a covering of superficial deposits and vegetation typical of the temperate zone of northern Europe. Furthermore, such a complex history has resulted in multiple and often discontinuous lithotectonic trends making extrapolation inland difficult and imprecise. In such circumstances the information gained from the synoptic view offered by satellite images could quickly (relative to field mapping) and accurately identify the surface expression of the geology, particularly by lineament identification and analysis. O'Leary *et al.* (1976) defined lineaments as linear alignments of physiographic and tonal features whose parts are rectilinear or slightly curvilinear, which differ from adjacent features and presumably reflect a subsurface phenomenon. As such they represent linear lithotectonic features including primary lithostratigraphic and tectonostratigraphic boundaries, the analysis of which could further delineate the inland geology. Furthermore, SW England is largely unaffected by glaciation which northwards of the North Devon

coastline (Fig. 1.1) may form linear geomorphological features which are unrelated to bedrock geology (Charman *et al.* 1996).

Satellite images consist of pixels which represent an area of the land surface, resolution quantifies the amount of area covered by each pixel. Maximum resolutions for the suite of commonly available satellite images are 80m for Landsat Multi-Spectral Scanner (MSS), 30m for Landsat Thematic Mapper (TM) and 20m (in multi-spectral mode) for Système Probatoire de l'Observation de la Terre (SPOT). As the land surface of SW England is typical of the temperate zone of northern Europe the geomorphological features within the region which are identifiable as lineaments, and relate to geology from such satellite images, are topographic relief, fluvial systems and vegetation.

Identifying lineaments in images from geomorphological features in a temperate agricultural terrain is unfortunately complicated by the alteration of the landscape by man (particularly by modern agriculture) resulting in: a reduction in exposed rock; spurious linear noise produced by field boundaries and infrastructure (anthropogenic features); and the disturbance of the usually direct relationship between bedrock and cover (Drury 1986, Smithurst 1990). Such spurious features are visible in large map-scale high resolution Landsat MSS, TM and SPOT images. Drury (1986) and Smithurst (1990) have found that spurious noise caused by anthropogenic features may be reduced for regional mapping with small map-scale, high resolution (1:250,000) TM images, hence highlighting large scale geomorphological features. The priority for these authors was to reduce the effect of anthropogenic features within temperate regions, whilst enhancing structural content. Using such small map-scale images, however, results in a loss of important geological information since lithotectonic features occur over a range of scales (e.g. Heffer & Bevan 1990, Yielding *et al.* 1992,

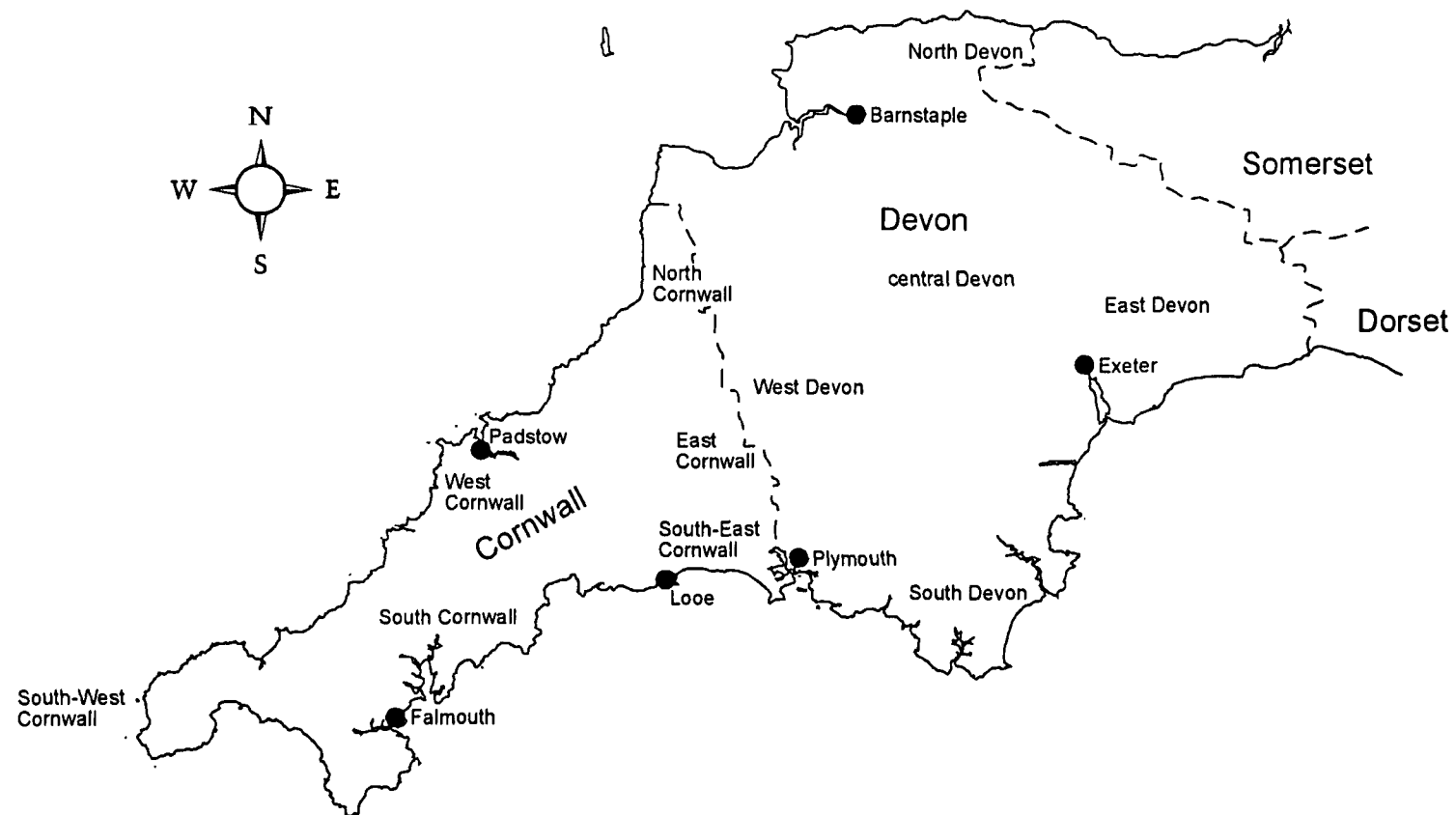


Fig. 1.1. Geographical map illustrating the areas and place names in SW England used to describe the data obtained in this study.

Gillespie 1993, Watterson *et al.* 1996a) or scale limited lithotectonic features may occur below the observation threshold of the image. Thus, previous lineament analyses in temperate agricultural terrains are limited in two ways: (i) they do not identify the optimum image scales where anthropogenic features are suppressed whilst at the same time maximising the geological information gained; and (ii) they do not indicate the amount of missing geological information. Woodcock & Strahler (1987), however, found that the visual disruption from anthropogenic features in an agricultural scene disappears when resolution is decreased to approximately double the size of the field boundaries within the particular image. This suggests that the optimum geological information may be obtained by decreasing image resolution while image map-scale can be increased, accordingly. Increasing the image map-scale, however, causes pixels to become visible (referred to in this study as pixelated images), a situation generally not documented in lineament analysis.

Lineament analysis of small map-scale, low resolution regional images of temperate agricultural terrains may increase the degree of geological information sampled (relative to other studies). However, this method would not be suitable for the lineament analysis in small areas of interest where the aim is to identify the detailed local geology (i.e. small scale lithotectonic features). Higher image resolutions also increase the degree of geological information sampled. Drury (1986) indicates that in a temperate agricultural terrain anthropogenic features are highly visible in high resolution large map-scale images, partly masking linear geomorphological features related to the underlying geology. As sampling anthropogenic features is therefore unavoidable in higher resolution images, previous lineament studies in SW England have typically concentrated on regional lineament analysis and not on techniques needed to separate

anthropogenic lineaments from the geological lineaments. Woodcock & Strahler (1987) suggests that the visual impact of the 'patchwork effect' of fields greatly increases for very high resolution images (e.g. 30m resolution Landsat TM images). Consequently, the ability of the technique used to identify geological lineaments from anthropogenic lineaments, could change with increasing resolution. Therefore, systematic interpretation of lineaments from images across a range of resolutions could indicate a cut-off resolution beyond which interpretation of geological lineaments by this technique might be avoided.

The common methods used to assess the geological information from lineament maps is the comparison of lineament trends to geological trends identified from published data (e.g. Wise *et al.* 1985, Conradsen *et al.* 1986, Smithurst 1990) and published maps (e.g. Drury 1986), and by comparing lineament trends to lithotectonic trends measured directly from the rock mass (ground truthing) (e.g. Whittle *et al.* 1983). Previous work by Smithurst (1990) on lineament analysis of large scale sub-scenes of SW England also suggests that distinct lineament patterns relate to major faults within the region. Hence, it is possible that lineaments interpreted from other lithotectonic features in SW England may also form characteristic lineament patterns (e.g. 'primary' lineaments relating to lithotectonic features which are cross-cut by 'secondary' lineaments related to faulting). The successful identification of the geological causes of lineaments within SW England will also suggest the amount of geological information sampled from the satellite image.

As identified by Smithurst (1990) certain lineaments can be related by their lineament pattern to particular lithotectonic features. Geological features, such as faults, have been identified to possess power-law scaling relationships, where the fault property (e.g. length, displacement, density) can be estimated across a

range of scales (e.g. Childs *et al.* 1990). These studies have typically been constrained by the analysis of seismic profiles which are compared to populations sampled at an outcrop-scale (e.g. Heffer & Bevan 1990, Yielding *et al.* 1992). The analysis of the effect of map-scale has not been previously investigated from remotely sensed images, where the image map-scale can easily be altered by changing the pixel resolution thus also allowing a wide range of map-scales to be sampled. The investigation of the scaling relationships of lineaments related to faults therefore may allow the correlation of power-law distributions of populations sampled at different map-scales without changing the sampling technique. The successful identification of scaling relationships in lineaments related to faults also means that an estimation of a lineament population at higher image resolutions can be achieved from lower resolution images. This circumvents the need to use high resolution images to sample small scale lithotectonic structures, consequently reducing the time taken for such an analysis. Furthermore, sampling from low resolution images negates the visual disruption caused by anthropogenic features.

Lineament density maps have been used to accurately map the extent of different geological features or identify areas containing high concentrations of fractures (e.g. Sawatsky & Raines 1981, Greenbaum 1985). To identify the extent of individual lithotectonic domains of the unexposed inner region of SW England lineaments may be related to geological features by their lineament patterns. Previous analysis of the lineament patterns relating to different lithotectonic features showed that the geological causes of some lineaments could not be distinguished (Chapter 4). Lineaments which are related to the same set of linear lithotectonic features will possess, at the least, near similar trends. Therefore, density maps of similar trending lineaments could accurately resolve the extent of

individual lithotectonic domains within SW England which may not be identifiable by just characterising lineament patterns.

In the regional, complex geological setting of SW England a high number of different geological features with dissimilar or similar trends could be interpreted. To obtain accurate scaling relationships from lineaments related to faults the analysed lineament sub-population needs to be 'pure'. Contamination by lineaments related to other geological features may lead to the mixing of different scaling relationships causing inaccurate results. Furthermore, density maps of lineament mixtures, the components of which may possess different spatial distributions, would also result in the identification of incorrect lithotectonic boundaries. Thus the method used in the division of the lineament populations into subsets is critical in selecting unmixed lineaments. Therefore, a technique was needed which could separate the lineament populations into unmixed subsets. For some lineaments, however, the absence of a characteristic lineament pattern meant that their geological causes could not be distinguished. Lineaments which relate to the same set of linear lithotectonic features typically possess similar trends. In lineament analysis the commonest technique used to differentiate lithotectonic-related lineament subsets by trend are rose diagrams (e.g. Smithurst 1990). However, more sensitive methods have been devised by other authors which identify the concentrations in the frequency/azimuth distributions of a lineament population relating to a particular lithotectonic feature (Wise *et al.* 1985, Conradsen *et al.* 1986, Hardcastle 1995).

1.2 Aims

The previous section described the problems associated with regional and local lineament analysis of SW England and determining geological information from such datasets. The aims of this study are to:

(i) Identify lineament analysis techniques in which the complex geological structure of the extensive inland region of SW England could be mapped at a larger map-scale than previously investigated (thus maximising the geological information) while minimising the effect of anthropogenic features.

(ii) Develop a technique which removes anthropogenic lineaments within lineament populations interpreted from still larger map-scale satellite images of North Cornwall.

(iii) Assess the effect the developed technique designed to remove anthropogenic lineaments on the geological information within the lineament maps interpreted from images from SW England and North Cornwall.

(iv) Quantify the lineament density (at the smallest image map-scale) and scaling relationships (over the range of image map-scales) to further delineate and estimate geological information in the lineament maps of SW England and North Cornwall.

(v) Use the analytical results to suggest refinements to our understanding of the underlying structural framework of SW England and scaling relationships of lineaments.

(v) Assess and develop new techniques which can identify subsets of lineaments with unmixed geological origins.

1.3 Objectives

In order to meet the stated aims, the following approaches were taken:

- (i) Identification of major lithotectonic trends and resultant geomorphological expressions in SW England from published data and geological maps for subsequent comparison with the compiled lineament maps.
- (ii) Reviewing the available satellite sensors to identify which provides the greatest advantages for lineament analysis of the previously identified geomorphological features from a temperate agricultural terrain and possessed the largest coverage of SW England.
- (iii) Visual assessment of Landsat TM images over a range of resolutions to identify the optimum image resolution at which geological information gained is maximised, whilst the visual effect of anthropogenic features is minimised.
- (iv) Evaluation of the effect of image processing techniques and band widths to further increase the geological information contained within the regional (SW England) and local (North Cornwall) images by analysing with statistical techniques the interpreted lineament populations.
- (v) The synthesis of post-lineament interpretation techniques in order to remove anthropogenic lineaments from lineament maps interpreted from higher resolution images of North Cornwall.
- (vi) Visual analysis of the regional lineament map to identify lineament patterns typical of particular geological properties (e.g. cross-cutting relationships indicating relative ages of formation). Evaluation of the identified lineament patterns relationship by comparison to previously identified lithotectonic trends, published maps and analysis of how these patterns vary spatially across SW England.

(vii) Evaluation of the completeness and accuracy of geological information contained within the regional lineament maps through comparison with geological interpretations of local higher resolution lineament maps of North Cornwall. Identification of the degree of geological information in these maps by investigation the differences in lineament characteristics with basic statistical techniques and identification of lineament patterns and their geological significance by analysing geological maps, lithotectonic trends identified by ground surveys and published data.

(viii) Analysing the frequency/trend distributions of the interpreted lineament populations to identify concentrations in the data. Assessment of the available techniques to determine unmixed subsets from lineaments interpreted from pixelated images. Investigation of different clustering methods to identify which method produced the most geological realistic division of lineaments (*lineament directional families*).

(ix) Evaluation of the clustering technique to identify unmixed lineament subsets by: (a) analysis of the lineament patterns in the lineament maps containing different lineament subsets of SW England; and (b) determination of the scaling relationships of different subsets of lineaments (related to faults) interpreted from North Cornwall.

(x) Construction and analyses of lineament density maps of SW England to obtain further information on the lithotectonic domains of SW England.

(xi) Analysis of the effect of resolution on the scaling relationships of fault-related lineament subsets by obtaining lineament lengths and spacings from the lineament maps and visually identifying the related cumulative frequency-size distributions.

1.4 Remote sensing and Geographic Information System hardware and software

Landsat TM images of SW England were processed on a NERC International Imaging System (I²S) Model 75 running System 600 software supported by a Vax 11/750 mini-computer. Lineament interpretation and analysis, however, was conducted on the images with the aid of the vector based geographic information system (GIS) ARC/INFO using a SUN workstation running on a UNIX platform. Unlike pure image processing programs, GIS allows data-handling and spatial analysis of a dataset in a geographical referenced framework. In a vector based GIS the dataset may consist of points, lines or polygons (areas), with lineaments generally represented as a series of lines. Therefore, in comparison to traditional lineament analysis where the hard copy may be geographically stretched (J. Griffiths, pers. com. 1997) the digitised lineaments are spatially more accurate. Furthermore, relative to the traditional lineament analysis techniques of interpreting hard copies of images, the GIS allowed a quick on-screen lineament interpretation from TM images of SW England and North Cornwall in under two years (although six months was lost due to hardware problems). GIS also facilitated the relatively rapid evaluation of lineament attributes interpreted from images of SW England and North Cornwall by allowing: (i) comparison of lineament maps with digitised geographical and geological maps; (ii) classification of lineaments by trend and length; (iii) estimation of the spacing between lineaments; and (iv) production of lineament density maps based on lineament frequency and lineament length per unit area.

Chapter 2 Causes of lineaments in SW England: regional geology and geomorphology

2.1 Introduction

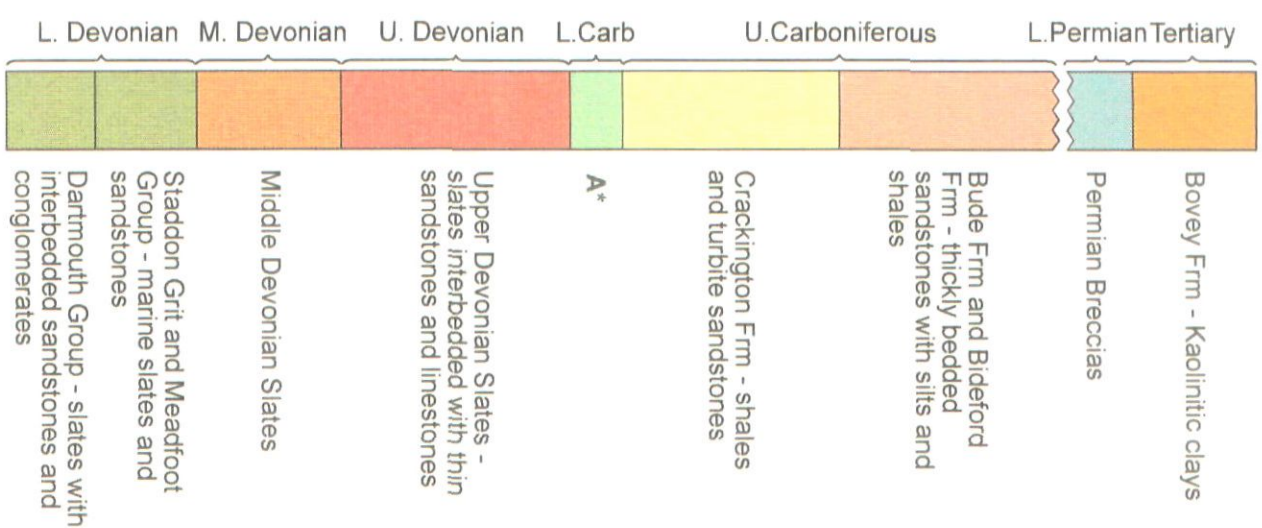
Lineaments are the representation of a linear surface feature in remotely sensed images. In SW England lineaments are formed by the interplay between the geology and geomorphological processes; geomorphological process can either emphasise or mask the geology. Linear geological structures which can form lineaments are: lithological differences formed by depositional change; lithological differences formed by later deformation; and deformation within lithologically similar rocks. In this Chapter, SW England is divided into lithotectonic domains which form similar trending linear features. An outline of the geological history of SW England provides a framework on which the main linear geological trends in the tectonic domains are highlighted. The morphological expressions that could be formed by geomorphological processes from these linear geological features are then described.

2.2 Geological history of SW England

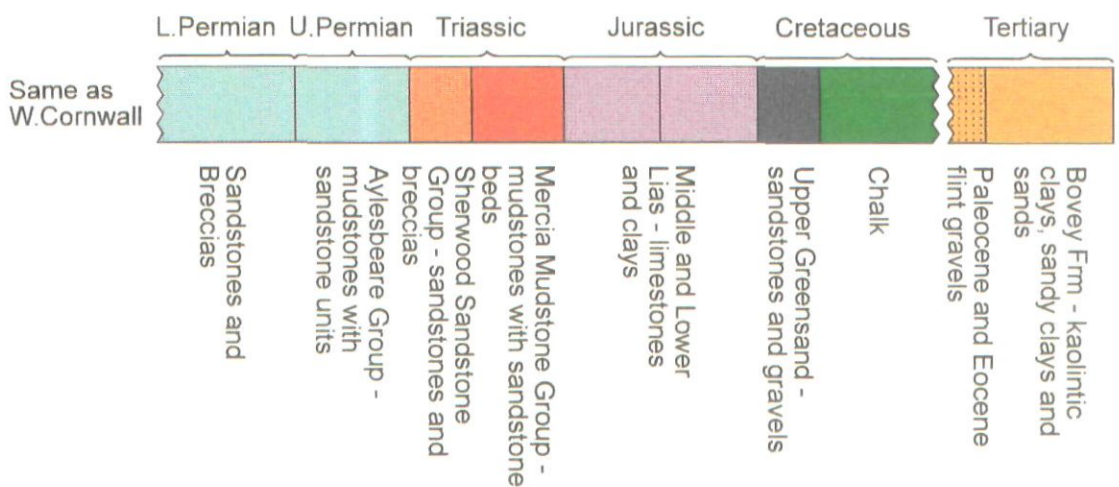
There is evidence in the geology of SW England to suggest a complicated sedimentary, igneous, metamorphic and deformation history. Rocks in the area studied range in age from the Lower-Middle Palaeozoic Variscan basement (Lizard and Start Complexes) to the Tertiary Bovey and Petrockstow Basins (Fig. 2.1). Early work in the region was conducted by Sedgwick & Murchison (1837), De la Beche (1839), Hendriks (1937, 1959) and Dearman (1963). Building on this, more recent research has included partial mapping of the poor rock exposure

Original Contains Pullouts

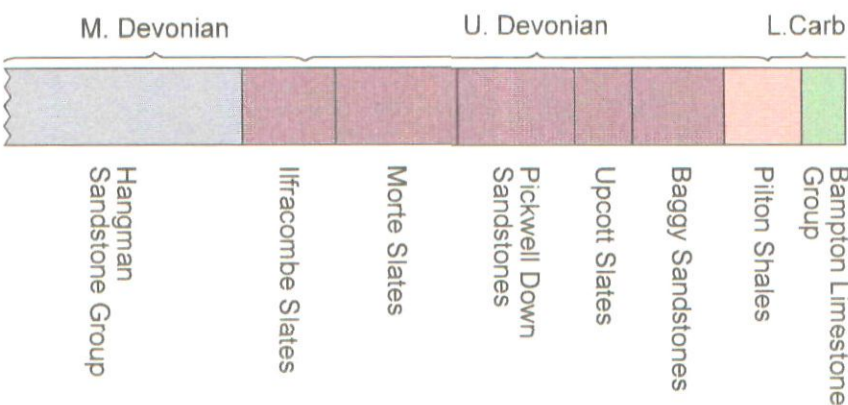
Devon and East Cornwall



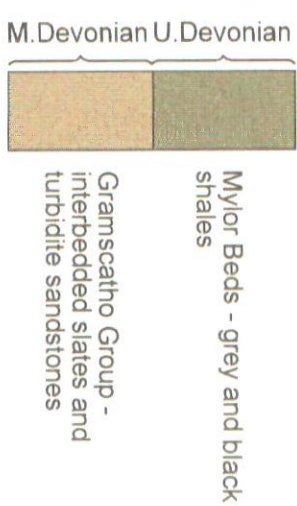
East Devon and West Somerset



North Devon

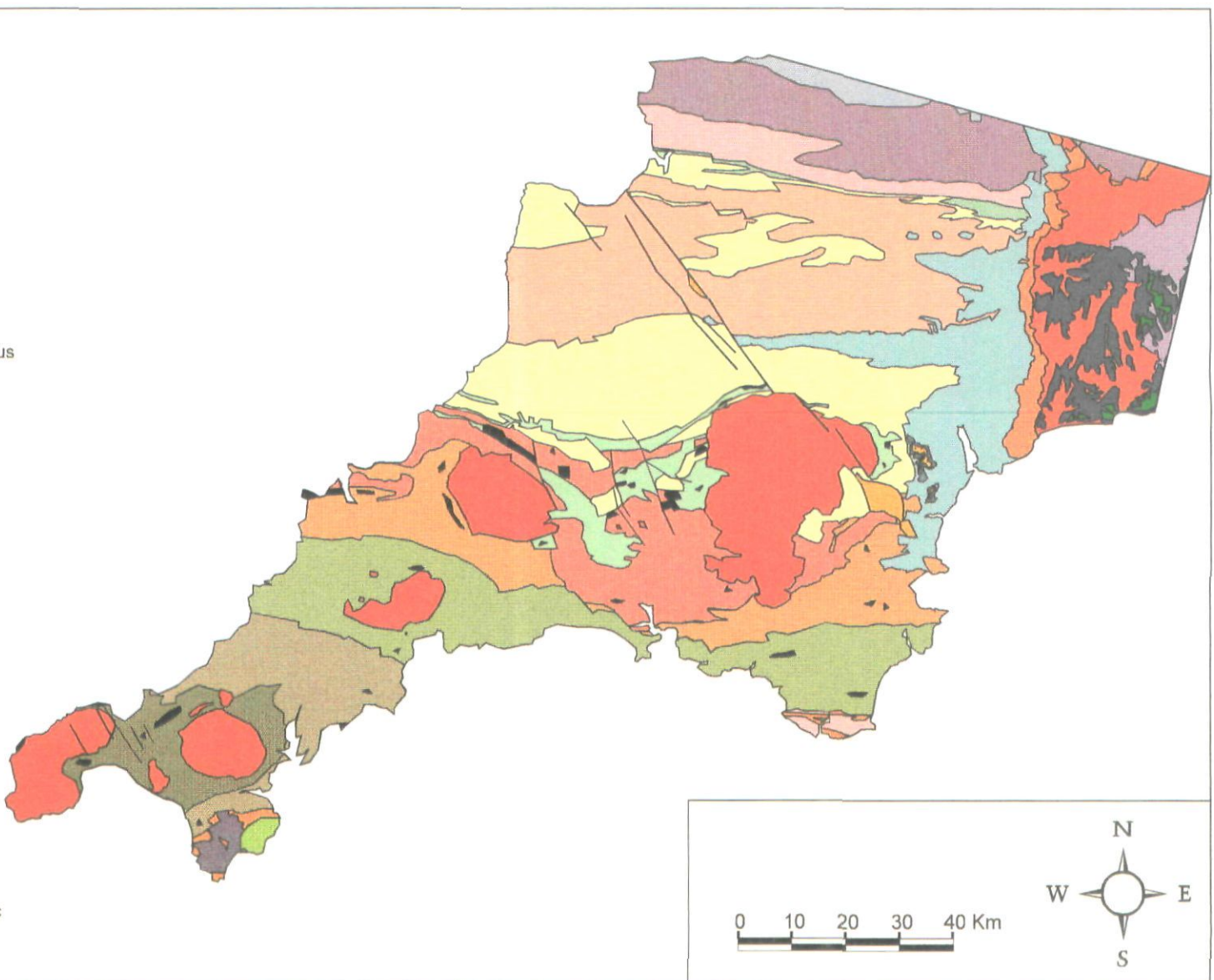


South and west Cornwall



A* North Cornwall - Fire Beacon Chert Fm, Buckator Fm, Trambley Cave Fm, Tintagel Volcanic Fm, Barras Nose Fm, Yeolmbridge Fm, West and central Devon - Meldon Chert Fm, Meldon Shale and Quartzite Fm, Meldon Volcanic Beds

Fig. 2.1. Geological map and lithostratigraphic history of the area of SW England covered by the interpreted satellite images (redrawn from Edmonds et al. 1975, BGS 1983, 1985, 1988, Holder & Leveridge 1986).



- Tertiary
 - Bovey Fm
- Cretaceous
 - Chalk
 - Upper Greensand
- Jurassic
 - Lias
- Triassic
 - Mercia Mudstone Grp
 - Sherwood Sandstone Grp
- Permian
 - Aylesbeare Grp and Breccias
 - Bude Fm
- Carboniferous
 - Crackington Fm
 - Bampton Limestone Grp
 - A*
- Devonian
 - Pilton Shales
 - Upper Devonian Slates
 - Baggy Sstns, Upcott Slates, Pickwell Down Sstns, Morte Slates, Ilfracombe Slates
 - Hangman Grits
 - Middle Devonian Slates
 - Staddon Grit, Meadfoot Grp, Dartmouth Grp
 - Mylor Beds
 - Gramscatho Group
- Intrusive Igneous Rocks
 - Granite
 - Basic Larva and Tuffs
 - Gabbro
 - Peridotite
- Metamorphic Rocks
 - Gneiss and Mica Schist
 - Hornblende Schist

0 10 20 30 40 Km



inland (e.g. Isaac 1985), which contrasts to the well exposed geology of the coastal sections (e.g. Shackleton *et al.* 1982).

Lineaments are not able to indicate the age of rocks, therefore separating SW England by chronostratigraphy and lithostratigraphy would be of little relevance to the interpretation of lineament maps. Different lithotectonic trends within SW England, however, would produce an expression in a lineament map. Hence, the geology of Rhenic SW England is divided by lithotectonic trends. SW England lies in the outer, or Rhenic zone of the European Variscan orogenic belt (Holder & Leveridge 1986b) and has been interpreted to be dominated by Upper Palaeozoic, NNW transported fold and thrust tectonics (Shackleton *et al.* 1982, Chapman *et al.* 1984). However, it is argued that dominantly southwards facing folds occur from North-East Cornwall and East Devon, forming a confrontation zone to the northward facing folds to the south (e.g. Andrews *et al.* 1988, Seago & Chapman 1988). Seago & Chapman (1988) have mapped this zone which occurs from the Padstow Confrontation Zone to Cargreen north of Plymouth and it is considered to be caused by under-thrusting of the northward propagating thrust sheets. Sanderson & Dearman (1973) suggested that SW England could be divided into 12 zones based on the assemblages of fold axis and facing directions, cleavage fabrics and the polyphase deformation history. These may be further simplified into ENE/WSW and NE/SW fold axial trends in South Cornwall and ENE/WSW and E/W fold axial trends from north of the Start-Perranporth line to the overlapping Permian strata.

The fold and thrust belt has produced a dominantly E/W trending lithological and structural grain to the region. However, areas of SW England have distinctly different trends. Dobson & Rex (1973) have dated the main phase of slate formation in SW England into zones, from which a south to north

movement in deformation can be interpreted. The order in which the lithotectonic units of SW England are discussed follows this spatial change in deformation. Late/Post Variscan intrusives and a post-Variscan cover then form contrasting trends. Post-dating the main phase of folding and thrusting, spatially extensive brittle structures either cross-cut or are concordant to the main E/W lithostratigraphic trend. These regional structures are described separately.

2.3 Lithotectonic units of SW England

2.3.1 Gramscatho Basin of South Cornwall

The northern boundary of this lithotectonic unit corresponds to the stratigraphic boundary of the older Meadfoot Group and approximately to an E/W dextral strike-slip zone, the Start-Perranporth Line (Holdsworth 1989) (Fig. 2.2). Internally it comprises a parautochthonous area and an allochthonous area which are to the north-west and south-east, respectively, of the Carrick Thrust (Holder & Leveridge 1986a) (Fig. 2.2).

Probable deep-water marine sediments of the Gramscatho Basin form the parautochthonous Upper Devonian, Mylor Slate Formation and Middle Devonian, Gramscatho Group (Leveridge *et al.* 1984, Shail 1989, Holder & Leveridge 1986a, Leveridge *et al.* 1990). The allochthonous region of South Cornwall is divided into four tectonic units: the Lizard Nappe, the Dodman Nappe, the Veryan Nappe and the Carrick Nappe (Leveridge *et al.* 1990). Closure of the Gramscatho Basin by the earliest Carboniferous was probably associated with the emplacement of the northwards moving allochthonous equivalent sedimentary units, contained in the Carrick, Veryan and Dodman Nappes and the Lizard Complex (Leveridge *et al.* 1984, Wilkinson & Knight 1989). The Lizard Complex is considered to exhibit ophiolitic affinities which suggests that the Gramscatho Basin was either partially

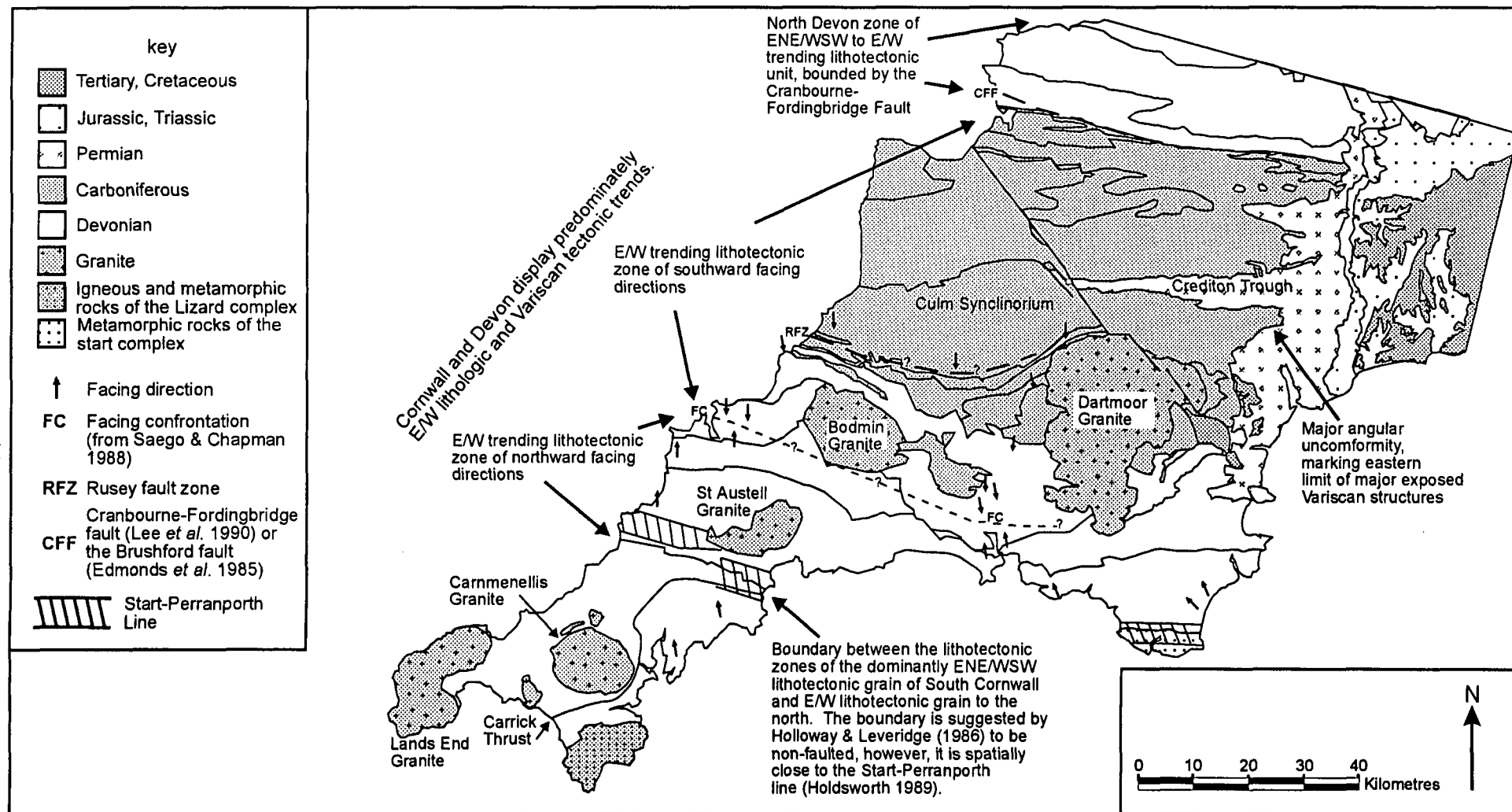


Fig. 2.2. Map illustrating the major lithotectonic divisions of SW England, highlighting the major lithologies and facing directions.

floored by oceanic crust (Holder & Leveridge 1986a) or was formed from a 'leaky' transform fault with the main ocean to the south (Barnes & Andrews 1986).

The primary structures are bedding (which generally dips to the SSE and youngs to the NW) and a bedding parallel early cleavage, which forms a dominant ENE/WSW grain to this region. However, large localised changes in these trends can occur (Leveridge *et al.* 1990) (Fig. 4.20a). Later folds and mineralised fractures predominantly follow the main ENE/WSW trend.

2.3.2 Middle Palaeozoic 'northward' facing fold and thrust zone

This zone of SW England is defined by the predominantly E/W lithotectonic trend and northward facing directions (Fig. 2.2). The southern part of this zone consists mainly of the Lower Devonian Dartmouth Group and Meadfoot Group and parts of the series of Middle Devonian Slates, which covers SW England from East Cornwall to South Devon (Fig. 2.1). The southern boundary of the ~E/W outcrop pattern of this lithotectonic unit in East Cornwall is marked in part by the Start-Perranporth Line (Fig. 2.2). This line is extrapolated across to South Devon where it marks the northern boundary (which is therefore faulted) of the Start Complex (Holdsworth 1989). Between the Dartmouth Group and Meadfoot Group the contact can be normal or faulted (Hobson 1976a, Chapman *et al.* 1984). These trends are dominantly controlled by E/W trending thrusts (Chapman *et al.* 1984, Seago & Chapman 1988). Northwards of this zone the lithotectonic trend of the Middle and Upper Devonian rocks to the south-east of the Dartmoor granite changes to the NE/SW, which is again mainly controlled by thrusting (Fig. 4.13). Klippen in this area, however, can form variable outcrop trends (Selwood *et al.* 1984).

The geochemistry of greenschists present within the Start Complex are interpreted by Floyd *et al.* (1993) to have oceanic affinities, although this does not link the sequence to the Lizard Complex. The remaining Palaeozoic rocks of SW England are considered to have formed within basins associated with rifted continental crust (Selwood 1990, Floyd *et al.* 1993). Thus the boundary of the Gramscatho Basin and the Start-Perranporth Line coincides with an ocean-continent boundary in the Devonian (Floyd *et al.* 1993). The Meadfoot Group and Dartmouth Group are considered to be pre-rift deposits, the Middle Devonian Slates to Lower Carboniferous rocks, syn-rift (Selwood 1990). These early Devonian rocks are considered to have formed in a series of small intracontinental basins related to the dextral strike-slip faults of the Start-Perranporth Line. Development of the Middle Devonian to Lower Carboniferous basins is proposed to be by the interaction of NNW/SSE and E/W trending basement connected faults, causing differential vertical movements (Turner 1986), which in this zone formed the South Devon basin (Selwood & Thomas 1986a). Inversion of the South Devon basin began in the Late Namurian by thrusting and folding resulting in flysch deposits and nappes (Isaac *et al.* 1982, Selwood & Thomas 1986a).

The internal tectonic grain of the Start Complex and Lower Devonian rocks is similar, with multi-phase deformation forming predominantly NE/SW to E/W trending folds and cleavages (Hobson 1976b, Hobson & Sanderson 1983, Tanner 1985, Burton & Tanner 1986, Seago & Chapman 1988). In the northward facing fold and thrust zone of South Devon, the internal structures of folds and cleavages are similar to the NE/SW thrusts. However, these are not apparent in areas of klippen (Selwood *et al.* 1984).

2.3.3 Middle-Upper Palaeozoic 'southward' facing fold and thrust zone

An arcuate zone of Upper Devonian to Lower Carboniferous rocks trends across North-East Cornwall to East Devon, this zone is argued to be a southwards facing back-thrusted fold and thrust belt (Fig. 2.2) (Seago & Chapman 1988). In North-East Devon the main trend is E/W to NW/SE. In East Devon the fold and thrust belt trends E/W, which changes to NE/SW to the east of the Dartmoor granite and swings to an E/W trend to the north of the Dartmoor granite. The southern boundary of this zone is the facing confrontation and the northern boundary is the Rusey fault zone. Northwards across the Rusey fault zone a major decrease in deformation and a small reduction of metamorphic grade occurs, hence, it is interpreted as a major tectonic break although the implications of the fault on the tectonic history of the region are contentious (Freshney *et al.* 1972, Rattey & Sanderson 1982, Selwood *et al.* 1985, Selwood & Thomas 1986b, Andrews *et al.* 1988).

The Upper Devonian to Lower Carboniferous rocks of this zone were deposited into the 'Trevone Basin' (Selwood 1990), forming varied sedimentary deposits (Isaac 1981, Isaac *et al.* 1983, Isaac 1985, Turner 1985, Selwood & Thomas 1986a). Basin inversion began in the Late Visean to Early Namurian forming a series of nappes (Fig. 4.19) (Selwood & Thomas 1986a).

The multiphase deformation history has imparted a complex set of internal structures to the northern zone, forming multiple minor trends common to the southern and northern sections of the northern zone. A difference in the steepness of the structures, however, can be identified; the southern section covered by the Kate Brook Tectonic Unit dominantly consists of flat lying structures (Isaac *et al.* 1983, Seago & Chapman 1988) (Fig. 4.14). Elsewhere the bedding and cleavages tend to be steeper (e.g. Isaac *et al.* 1983, Turner 1985).

2.3.4 The 'Culm Synclinorium'

The Culm deposits occupy an area ranging northwards from the Rusey fault zone of the North Cornwall coast, the Dartmoor granite, to North Devon, from near Barnstaple towards Wellington, Somerset (Fig. 2.1). These deposits form a thick sequence of repetitive sandstone and shale successions, of which the largest stratigraphic divisions are the Upper Carboniferous Crackington and Bude Formations. These sequences are folded and hence are repeated across North Cornwall, forming dominantly an E/W outcrop trend. The Culm deposits are considered to be formed mainly in a marine basin, the Culm Basin, caused by movement on listric faults (Selwood & Thomas 1986a).

The dominant fold structures evident within the area are upright chevron folds which have been overturned southwards from Hartland to Rusey, by southwards directed simple shear (Ratley & Sanderson 1982, Lloyd & Whalley 1986). Also, the intensity of associated E/W trending cleavage increases southwards (Hobson & Sanderson 1983). Ratley & Sanderson (1982) argue that a regional structure was formed, the 'Millook Nappe', which is also known as the Southern Culm Overfold (Freshney *et al.* 1972, Selwood *et al.* 1985). This structure is interpreted to be bounded by the Rusey fault zone (Fig. 2.2), which acted as a major thrust to the overriding Southern Culm Overfold. Lloyd & Whalley (1986), however, argue that the Southern Culm Overfold is not a regional structure as the chevron folds could have been overturned by multiple discrete simple shear zones which decrease in intensity northwards.

2.3.5 The Upper Devonian rocks of North Devon

Bounding the northern edge of the Culm Synclinatorium lie the Devonian sediments of North Devon. These areas are partially divided by the Brushford fault (Edmonds *et al.* 1985) or the Cranbourne-Fordingbridge fault, which are clearly visible in magnetic and aeromagnetic imagery of the region (Lee *et al.* 1990). Folded by the regional Lynton Anticline, the lithostratigraphic trend changes from ENE/WSW to E/W, from North-West Devon to North-East Devon. The fold style for North Devon changes from moderately upright facing to the north to steeply upwards facing southwards near Barnstaple (Hobson & Sanderson 1983).

2.4 Post-Variscan cover

2.4.1 Late/Post Variscan intrusives

Five large granite bosses are exposed across Devon and Cornwall extending along a WSW/ENE axis; Dartmoor, Bodmin Moor, St. Austell, Carnmenellis and Land's End (Fig. 2.2). Smaller bosses (e.g. Castle-an-Dinas and Beloda Beacon) are exposed around many of these major intrusives. The granites are aged between Upper Carboniferous and Lower Permian, and generally young eastwards towards the Dartmoor granite (Darbyshire & Shepherd 1985). Intrusion of the granites is therefore later than the main phases of folding and thrusting. These granites are considered to be linked at depth forming a much larger batholith (Bott *et al.* 1958, Bott & Scott 1964). The base of the granites is suggested by Shackleton *et al.* (1982) to be southwards dipping as the granites were injected northwards along a thrust. Cross-cutting relationships occur between the older Upper Devonian to Upper Carboniferous meta-

sedimentary rocks and also the structures caused by the main phase of northwards migrating deformation.

2.4.2 Post-Permian cover

The relatively un-deformed post-Permian strata rest over the deformed Palaeozoic rocks of the Variscan basement with a distinct angular unconformity. The area covered by these rocks (apart from the Crediton Trough) is to the east of a N/S line running through Exeter (Fig. 2.2). The Upper Cretaceous progressively oversteps westwards from the older Mesozoic succession of the Wessex Basin, across the Permian and Variscan basement of SW England. The general dip of this strata is to the east, forming N/S to NNE/SSW outcrop trends. Finally, small infilled Tertiary aged basins have been identified predominantly along the mainly dextral strike-slip Sticklepath-Lustleigh fault zone (SLFZ) (Fig. 2.1).

2.5 Major post-Late Carboniferous/Early Permian brittle structures

Late Variscan brittle structures are found throughout the peninsula. NW/SE dextral strike-slip faulting is shown by Dearman (1963) to have a regional distribution (Fig. 2.3). A sub-ordinate set of conjugate NE/SW sinistral strike-slip faults (Freshney *et al.* 1979b, Edmonds *et al.* 1985) is also considered to be regional in extent. E/W trending, moderately to steeply dipping normal faults have been identified within the Culm Basin (Freshney *et al.* 1972). Mineralised faults within the granites and meta-sediments trend mainly E/W in Devon and East Cornwall and ENE/WSW in South Cornwall (Dearman 1963). Darbyshire & Shepherd (1985) proposed the main age of mineralisation to be 269 ± 4 Ma. However, at least three subsequent phases of mineralisation are known to have

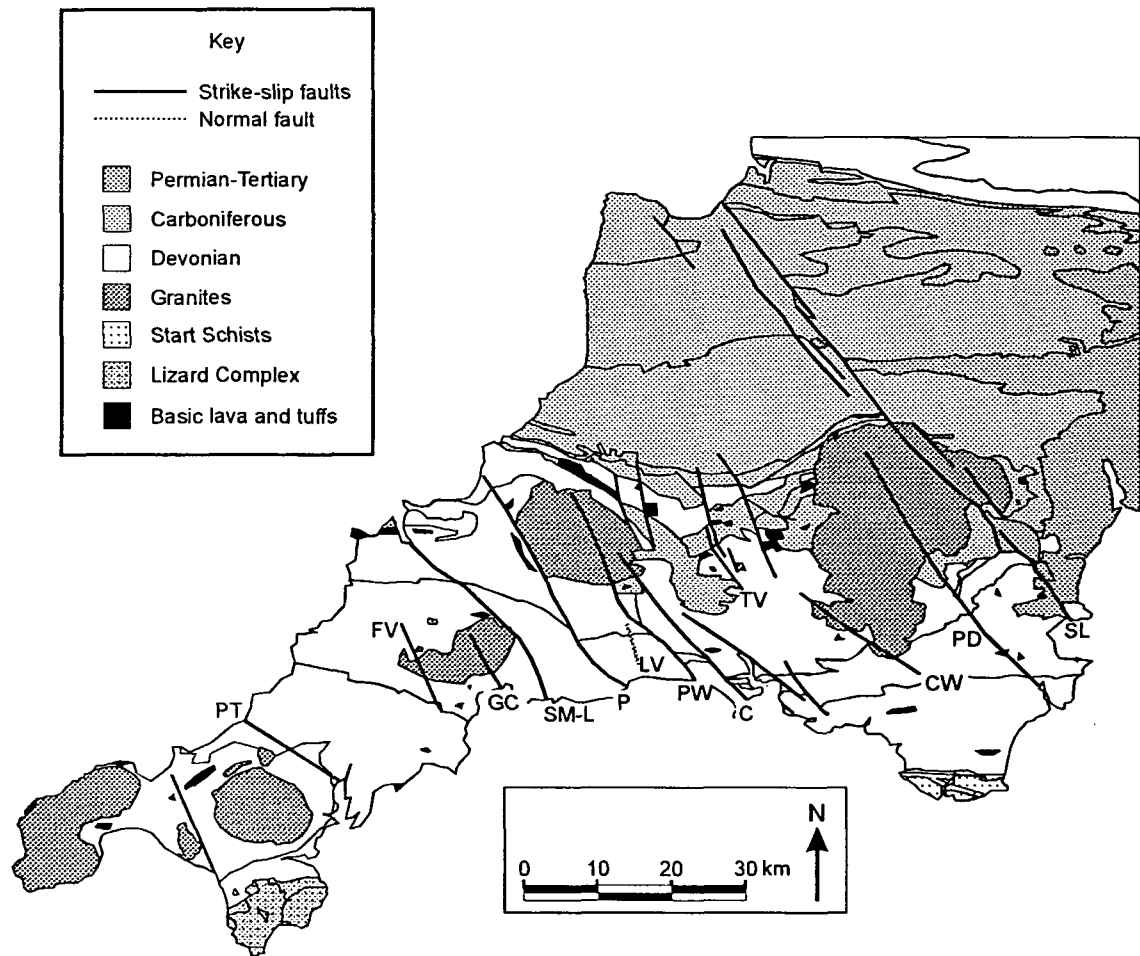


Fig. 2.3. Map of SW England illustrating the major faults which are discordant to the main lithotectonic trends of the region. PT, Porth Towan; FV, Fal Valley; GC, The Great Cross-Course; P, Portland; SM-L, St Minver-Lantivet; LV, Looe Valley; PW, Portwrinkle; C, Cawsand; TV, Tamar Valley; CW, Cornwood; PD, Prewley-Dartmouth; SL, Sticklepath-Lustleigh fault zone. Modified from Dearman (1963), Hobson & Sanderson (1983), Turner (1986) and Bristow & Robson (1994).

occurred (Jackson *et al.* 1982). A later set of N/S trending lodes known as cross-courses are present throughout the peninsula (Dines 1956). Some of these N/S fractures are mineralised and are considered to be the result of E/W extension associated with the formation of Permo-Triassic basins around the Cornubian massif (Scrivener *et al.* 1994). Reactivation of the basement Variscan structures can also occur, this is seen within South Cornwall (Shail & Alexander 1997) and the SLFZ (Holloway & Chadwick 1986). This can further complicate the already complex deformation history and lithotectonic trends of SW England.

2.6 The relationship between lineaments and bedrock geology in SW England

This section describes how lineaments may be formed in an area with a bedrock comprising of linear elements similar to those described previously in SW England. Lineament analysis has been successfully applied in areas of the world that have high erosion, minimal superficial cover and where the underlying geology has a strong control on surface relief at all scales (Sawatsky & Raines 1981, Bagheri & Kiefer 1986, Drury 1986, Mah *et al.* 1995). The direct interpretation of geological features from satellite images within SW England, however, is made difficult by superficial deposits which mask the bedrock, e.g. head deposits formed by periglacial activity (Freshney *et al.* 1979a). Interpretation of geological features within the region therefore depends on the recognition of the contrasting geomorphological features and how these relate to processes acting on heterogeneous bedrock (e.g. stream erosion of least-resistant rocks).

2.6.1 Geological features which can form a surface expression

Differential degradation of a surface is primarily controlled by rocks being resistant or non-resistant to geomorphological processes and the length of time over which these processes operate. As described in the previous sections, the geology of SW England is typified by sedimentary, meta-sedimentary and igneous rocks. Marked surface expressions will form when rocks with differences in their resistance to geomorphological processes are juxtaposed by a variety of geological structures, or when geological structures form zones of weakness in rocks which elsewhere are homogeneously resistant to geomorphological processes. Within this section only geological structures which can form a marked surface expression and have been identified to occur within SW England, are discussed.

(i) Homoclinal structures

Uniformly dipping or flat sequences of sedimentary rocks expose strata to the land surface, where differential erosion and weathering can form topographic features whose differences are caused by the angle of strata dip. Horizontal strata form exposure traces controlled by topography, dendritic drainage patterns, and mesa landforms. Differential weathering and erosion of tilted alternating resistant and non-resistant rock produce strike valleys and ridges, which may form subsequent streams and ideally a trellis stream pattern (Fig. 2.4). Streams, however, may cut across strike valleys by retaining their original direction and are known as consequent streams. These streams may be formed from previous topography of a peneplaned surface. Increasing strata dip produces changes to ridge morphology from mesas, cuestas, homoclinal ridges to hogbacks.

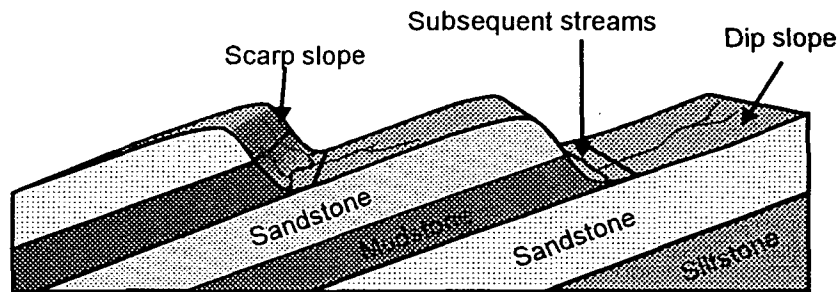


Fig. 2.4. Perspective block diagram showing differential erosion of relatively un-resistant mudstone and siltstone beds and resistant sandstone beds, forming dip slopes and homoclinal ridges. Erosion forms strike valleys and rivers and perpendicular streams on the dip slopes, ideally producing a trellis stream pattern.

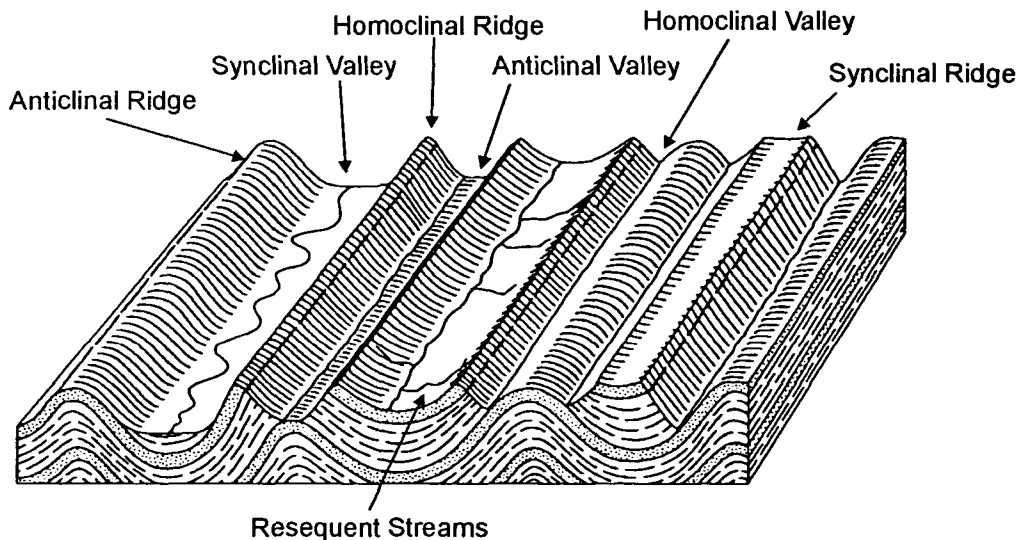


Fig. 2.5. Geomorphological features produced by the differential erosion of upright folds, after initial truncation, modified from Thornbury (1954).

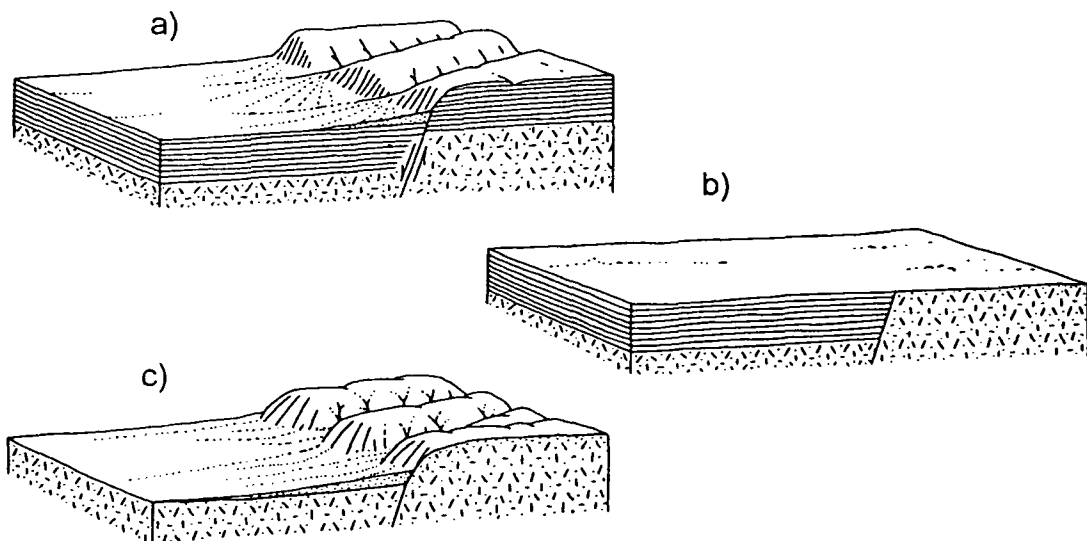


Fig. 2.6. Block diagrams showing a formation of a fault-line scarp; a) normal movement on a fault produces a fault scarp, b) destruction of the fault scarp by erosion, c) formation of a resequest fault-line scarp by continued erosion (from Thornbury 1954).

Uniformly dipping rock exposed at a small map-scale within SW England is restricted to the Permian to Cretaceous cover of East Devon and Somerset.

(ii) Folded strata

As identified, SW England has undergone a major phase of folding and differential degradation of the exposed folded strata can lead to topography outlining folds (Fig. 2.5). The style of fold leads to different outlines. Horizontal fold hinges produce parallel trending exposure patterns, with increasing plunge of the fold hinge the outcrop pattern becomes increasingly similar to the fold profile. A shallowly dipping fold axis can produce increasing distances between fold hinges of folds by the longer fold limbs, resulting therefore in larger distances between scarps.

(iii) Faulted strata

Faults exposed in SW England are predominantly Early Devonian to the Late Triassic in age (see Section 2.5). These ancient ages suggests that morphological features related to faulting are fault-line scarps and not fault produced (Thornbury 1954) (e.g. the faulted boundary between the Dartmouth Group and Start Complex). Formation of a fault-line scarp is shown in Fig. 2.6, where post-faulting erosion forms the scarp. Typical features which are also considered by Thornbury (1954) as common to fault-line scarps are: scarps situated to the downthrow side of the fault, good correlation between rock-resistance, structure and topography and super-imposed drainage across faults. These features are caused by faults juxtaposing strata with changes in strike, dip or rock types.

Thrust faults, high-angle reverse faults, normal faults and strike-slip faults have all been identified within SW England. Thrust faults are low angle reverse faults and hence produce an irregular fault trace which follows topography. These faults can be directly recognised by the following (Fig. 2.7) (Prost 1989):

(1) differences in structure and rock type generally occurs within the footwall and hanging wall, and a break in slope along the upper plate;

(2) bedding is often parallel to the thrust strike;

and (3) folds carried along on the thrust have analogous symmetry and typically verge towards the foreland.

Faults with steeper dips generally form surface traces which are near-independent of topography and hence become increasingly linear irrespective of the nature of displacement along the fault. These linear traces can be identified in SW England by:

(a) structural control of streams forming linear segments;

(b) higher permeability of fault zones and joints (Drury 1987) allows water saturation, forming depressions and an easier access to root systems, thus controlling vegetation;

and (c) displacement causes different rocks to be juxtaposed resulting in differential erosion.

Therefore, lineaments interpreted from images related to fault-line scarps formed by differential erosion correspond to the fault plane, and displaced lineaments correspond to displaced linear features (Fig. 2.8).

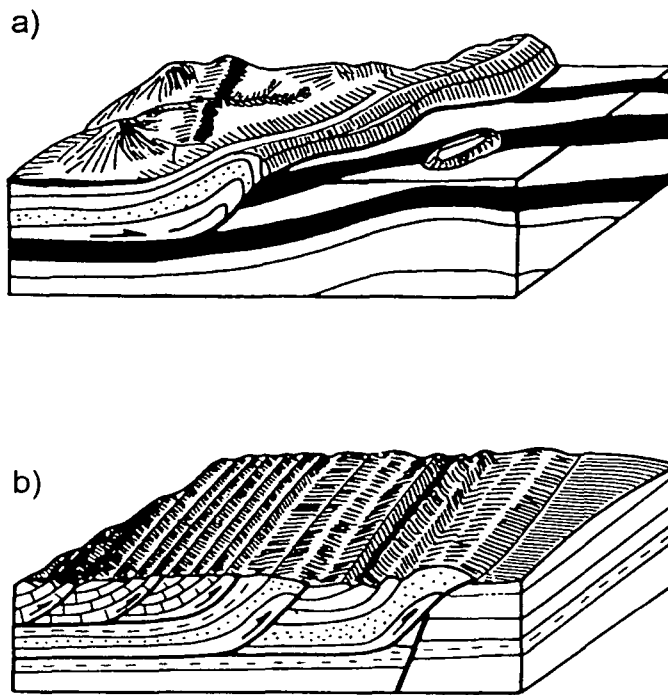


Fig. 2.7. Block diagrams showing the geological and morphological features produced by thrust faults, a) a leading-edge anticline forming an irregular fault trace, klippe and discordant strikes and dips across the thrust fault, b) changes in structural style from imbricate sheets to leading edge folds (from Prost 1989).

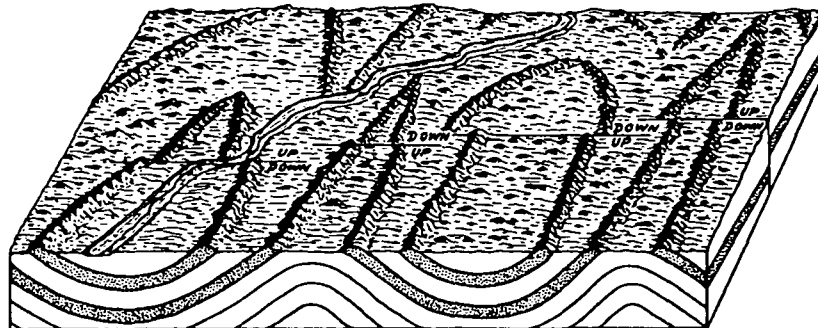


Fig. 2.8. Schematic block diagram indicating how normal faulting can effect topographic expression of fold noses formed by plunging synclines and anticlines (from Thornbury 1954).

(iv) Igneous intrusions and mineralised lodes.

The relative resistance to erosion of igneous intrusions generally produces positive topographic features. Granitic plutons have a general domal form, producing circular intrusions which cross-cut country rocks. Weathering and erosion of the granites of SW England is slow compared to less-resistant country rocks, producing topographic highs. Sills, dykes and mineralised lodes can produce identifiable, linear features (Drury 1987). Dykes and mineralised lodes can, however, have trends concordant or discordant to lithological and structural trends.

(v) Unconformities.

Angular unconformities are generally more visible in satellite images as they describe a change in dip between older and younger rocks. These unconformities are recognisable within images by differences in the degree of deformation and the truncation of lithological units or structural features (Gupta 1991). Hence, lineament trends and density can change across an angular unconformity. An angular unconformity often dips relatively shallowly and hence is topographically controlled (Gupta 1991). Therefore, most angular unconformity planes produce an irregular trace. Parallel unconformities form between analogously dipping beds, and these may only become visible within satellite images when an unconformity separates rocks which are non-resistant and resistant to geomorphological processes. These unconformities therefore produce similar topographic features to simple tilted strata.

(vi) Differential erosion of heterogeneous rock masses

Discontinuities within a rock which can cause linear features include tectonic foliations and fractures. Differential erosion of these features relies on fractures or a cleavage producing a relatively weaker rock, from which a topographic effect can form, or control stream direction and vegetation. Chemical weathering can, however, occur within the granites of SW England. Weathering of granite feldspars and biotite is concentrated along the exposed joints and faults, allowing later differential erosion of the now relatively unresistant regolith, forming valleys or lowlands (Embleton 1984). Changes in the trends of the surface expression caused by discontinuities in heterogeneous rocks within SW England therefore relate to changes in structural trends, time of rock deposition or emplacement and deformation properties of the rock.

2.7 Morphological features of SW England

The relative topographic highs of SW England are formed by the granite cupolas and their associated aureoles (200m - 600m), the Devonian sandstones of Exmoor (400m) and the Quantock Hills and the Upper Greensand and Chalk ridges of the Blackdown Hills. Lowland areas correlate to the Permo-Triassic sediments of East Devon. The remaining parts of the region generally show a large variance in relief, of up to 150m on the northern margins of Dartmoor.

The major stream patterns of SW England generally have two directions of flow and length. Rivers draining into the Atlantic generally exhibit E/W or N/S trending shorter streams, while the major rivers draining into the English Channel normally have an overall north-south trend and are longer. North coast rivers are typically perpendicular in trend to the direction of the coastline and in North Cornwall often discharge into the sea from hanging valleys. The N/S trending

rivers draining into the English Channel are discordant to the major Variscan geological trends. These discordant rivers are possibly related to a super-imposed drainage system influenced, in part, by a former Cretaceous cover (Embleton 1984). The trends of these rivers can be explained partly by the control exerted by the E/W lithotectonic grain and the regional NW/SE and N/S fracture sets, as basement Variscan bedrock has become exposed. Stream patterns over the granites, however, can show a good structural control. Land's End granite has a series of parallel NW/SE draining streams, formed along the NW/SE fault and joint trends, and South Dartmoor has a distinct N/S river trend controlled by jointing. The North Dartmoor granite, however, displays a radial drainage pattern typical of domal structures.

Morphological features produced by glaciation can cause the masking of surface linear features. The Pleistocene glacial advances are believed to have encroached as far as Barnstaple Bay (Croot *et al.* 1996), but further evidence of glaciation in SW England is highly questionable (Charman *et al.* 1996). Periglacial conditions are considered to have occurred within SW England to a greater extent producing extensive head deposits (Charman *et al.* 1996). The major effect of these processes were the infilling of valleys with solifluction deposits and the general smoothing of the landscape, particularly of the softer Devonian and Culm sequences (Embleton 1984). However, the effects of glaciation within SW England were minimal compared to northerly counties, allowing a reasonable correlation between bedrock and topography to be recognised (Durrance & Laming 1982).

Chapter 3 Lineament analysis - image processing and lineament identification

3.1 Introduction

SW England has a temperate climate which has enabled an intensive arable and pastoral farming to develop. It also contains an extensive road and rail infra-structure. These anthropogenic features cause linear features on large map-scale, high resolution images. Furthermore, agriculture has disturbed the soils and changed the vegetation making geobotany or soil type a poor aid to geological mapping of bedrock (James & Moore 1985). Hence, within such an area features interpreted from satellite images as lineaments are both the linear geomorphological surface expression of bedrock and structures, and the above anthropogenic features. Consequently, previous interpretations of lineaments from satellite images in temperate agricultural regions have relied on enhancement of topographic shadows combined with a reduction in non-geological visual linear disruption, at small map-scales, e.g. 1:250000 (Drury 1986, Smithurst 1990). This Chapter describes the procedures and images used to obtain a regional lineament map of SW England at relatively larger map-scales.

The smallest image map-scale (1:75000) is used for compilation of the regional map since anthropogenic objects are largely imperceptible. Further lineament maps of a small sub-area in North Cornwall are interpreted at successively higher image resolutions (and therefore larger map-scales), where the linear visual domination of the transport network and boundaries between different crop types, is increased. Procedures are described to help identify and

remove interpreted lineaments correlating with anthropogenic linear features, thereby 'cleaning' the interpreted lineament populations.

3.2 Remote Sensing of the land surface in SW England

Remote sensing comprises a range of techniques which allows information to be obtained by a sensor that is a physical distance from an information source. Electromagnetic radiation (EMR) serves as the 'information' link between the sensor and the source. The electromagnetic spectrum is the ordering of EMR into wavelength frequency. For remote sensing studies, the important spectral regions are in the optical and microwave ranges. However, the electromagnetic spectrum covers a much wider range from very short cosmic wavelengths, to the long wavelength occupied by radiowaves (Fig. 3.1). The major source of EMR for passive sensors (sensors which capture images representing the reflection or emission of EMR from the Earth which have a natural source) such as Landsat TM, Multispectral scanner (MSS) and Système Probatoire de l'Observation de la Terre (SPOT) is the Sun, with the Earth producing smaller amounts of longer wavelength EMR.

3.2.1 Ground reflection, transmission and absorption mechanisms of materials

The basic physical principles discussed in this section have been obtained from several general texts: Siegal & Gillespie (1980), Drury (1987) and Gupta (1991). The intensity of EMR reaching a sensor over a range of wavelengths from an object has a characteristic wavelength-variation imparted by the object. Furthermore, variations in the intensity of EMR moving from the source to the object and then sensor can be affected by the Earth's atmosphere.

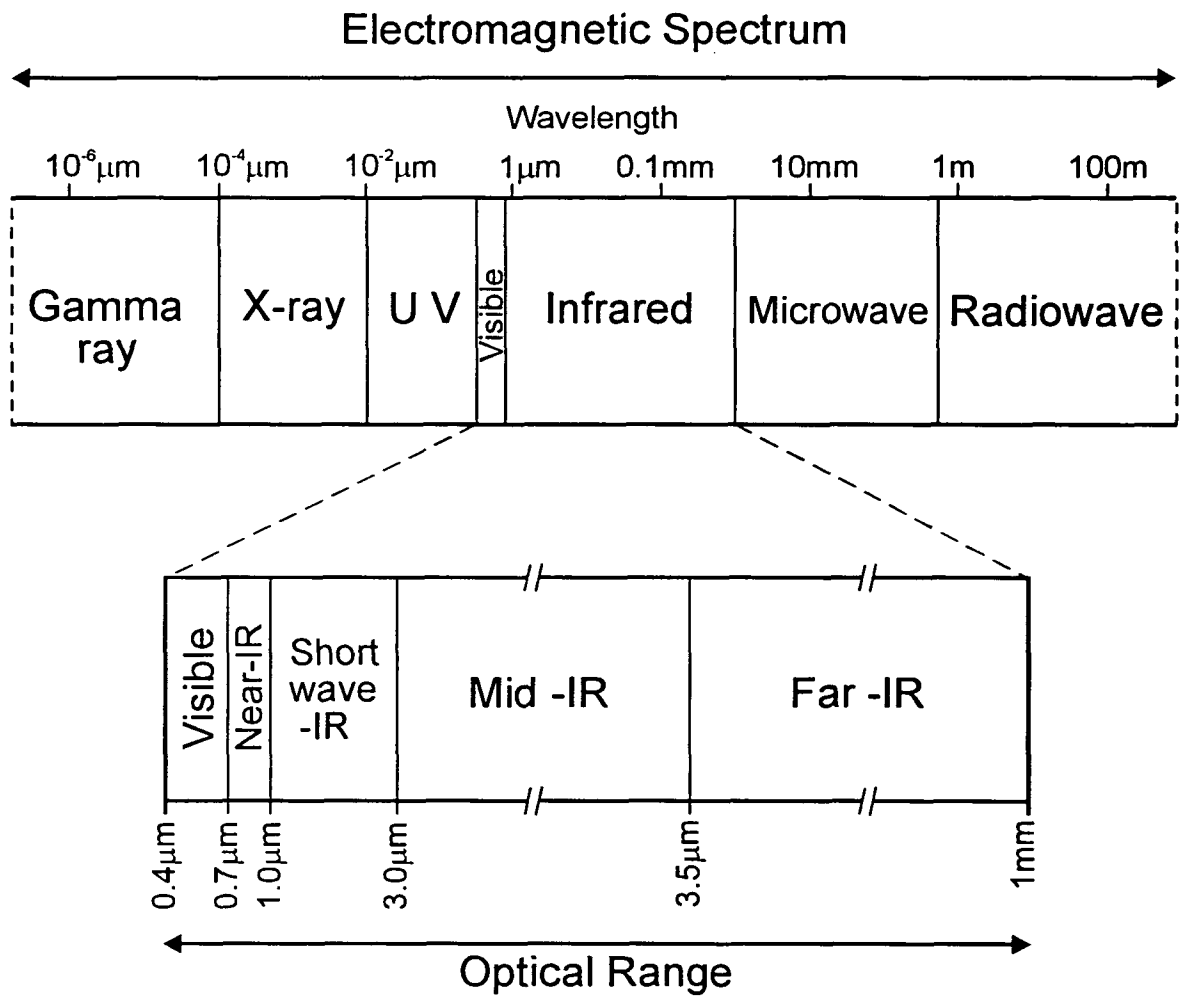


Fig. 3.1. The electromagnetic spectrum from gamma ray to radiowave, with the exploded diagram showing the optical range (modified from Gupta 1991).

There are three basic physical processes which allow an object and the Earth's atmosphere to change the amount of EMR reaching a sensor:

- (i) EMR being reflected from the object;
- (ii) transmission of radiation through the object;
- and (iii) absorption of EMR.

Following the law of conservation of energy the interaction between EMR and matter can be written as:

$$Ei_{(\lambda)} = Er_{(\lambda)} + Ea_{(\lambda)} + Et_{(\lambda)} \quad (\text{equ. 3.1})$$

the incident energy at one wavelength $Ei_{(\lambda)}$ is distributed between reflection $Er_{(\lambda)}$, absorption $Ea_{(\lambda)}$ and transmission $Et_{(\lambda)}$ (Gupta 1991). These processes interacting with linear geomorphological features and anthropogenic features of SW England, affect the degree of spectral response.

Incident EMR on a surface is in part reflected and in part transmitted through the object (equ. 3.1). Reflection of EMR is dependant upon several physical factors of the object's surface (Fig. 3.2). Specular reflection occurs when the object behaves as an ideal mirror (Fig. 3.2a) causing the incoming radiation to reflect according to Snell's law to reflect such that the angle of reflection (θ) is equal to the angle of incidence (i). Lambertian reflection (Fig. 3.2b) characterises an idealised rough object, and results in radiation being reflected equally in all directions. Natural surfaces, however, typically contain planar features and edges that reflect and diffract EMR in different directions (Fig. 3.2c). Consequently, most natural bodies have a reflection pattern between the idealised specular and Lambertian reflections (Fig. 3.2d) resulting in a semi-diffuse pattern that has a maximum peak which corresponds to Snell's law (Gupta 1991).

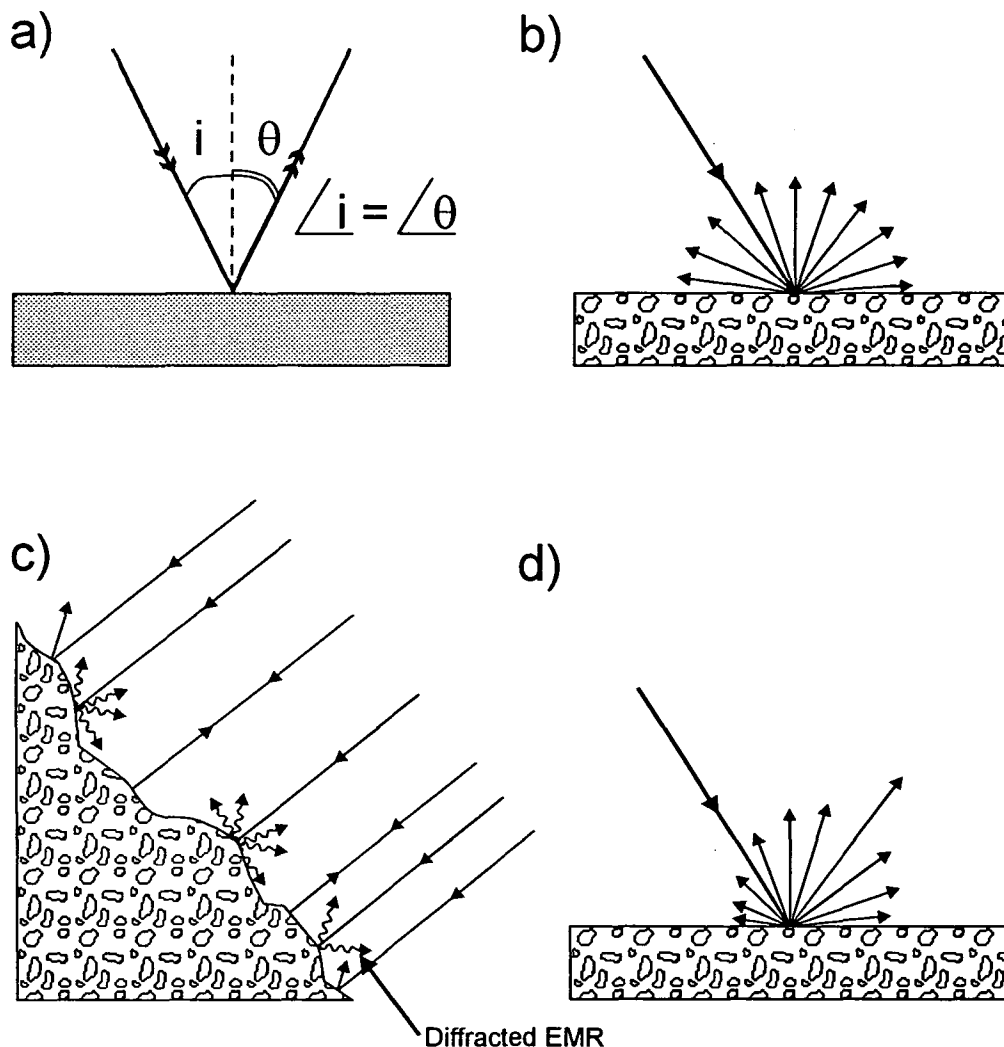


Fig. 3.2. Reflection patterns of electromagnetic radiation on objects with different degrees of roughness: a) specular reflection from a planar surface (idealised); b) lambertian reflection from an idealised rough surface (diffused reflection); c) natural uneven surfaces can produce numerous reflection directions and diffractions at fine edges and small irregularities; d) natural objects with a combination of planar and rough surfaces produce semi-diffuse reflections (from Gupta 1991).

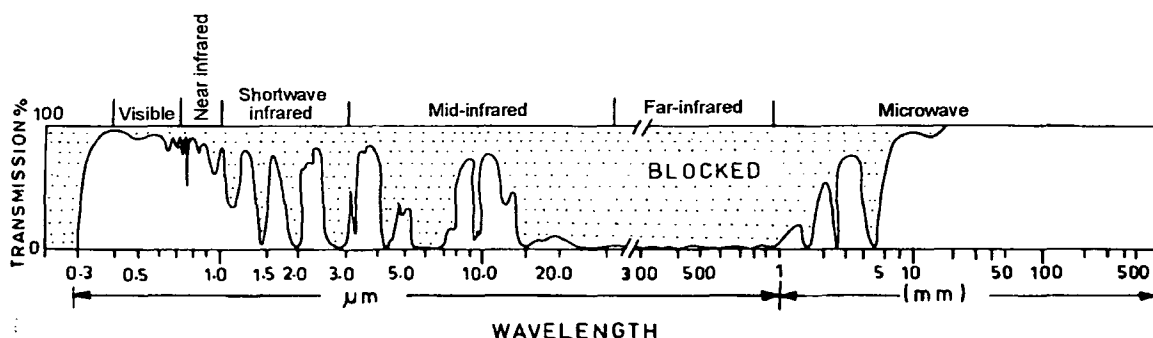


Fig. 3.3. Absorption spectrum of electromagnetic radiation passing through the atmosphere. Peaks in transmission of radiation forms atmospheric windows (from Gupta 1991).

Transmission of EMR in homogeneous objects is greater than in heterogeneous objects where 'contact boundaries' between materials further scatter or reflect EMR.

Selective absorption of EMR by materials can occur when the energy levels of the materials atomic-molecular system is changed. Atmospheric gases, primarily H₂O vapour, CO₂ and O₃, can selectively absorb particular wavelengths of EMR reducing the range of electromagnetic wavelengths available for passive remote sensing (Gupta 1991). These available ranges form 'atmospheric windows' (Fig. 3.3).

3.2.2 Remote sensing platforms

The main platforms used in remote sensing are aircraft, unmanned spacecraft and manned spacecraft. All provide potential data for the geologist. However, specific problems identified during lineament analysis from images of a temperate agricultural terrain (Section 3.2.3) mean that not all systems are suitable.

(i) Aircraft and manned spacecraft.

Aircraft may carry cameras, multi-spectral scanners and radar systems. High resolution images from these systems have been found to provide information for the geologist (Dury 1986a). However, due to high costs, aircraft surveys with multi-spectral scanners and radar systems have been limited in SW England to small survey areas (Hopper 1996).

Manned spacecraft have allowed collection of extremely high resolution photography (e.g. S-190B Earth Terrain Camera with a resolution of ~15m) and images from passive and active sensors (active sensors capture images by

radiation from an artificial source) (Drury 1987). Manned spacecraft orbits are confined between 60°N and 60°S and images therefore may have different sun illumination angles, improving the detection of linear topographic features (Drury 1987). The main problem of images obtained from manned spacecraft is a lack of coverage, and SW England is no exception.

(ii) Unmanned spacecraft

Recently sensors which are carried by satellites and designed for the remote sensing of land have been launched. Coverage of SW England by images provided by Landsat MSS, Landsat TM and SPOT in the NERC remote sensing archive are typically more extensive than from aircraft and manned spacecraft. The sensors capture EMR in a series of wavelength ranges, known as bands. These, however, vary in specification and therefore suitability for geological remote sensing.

(a) Landsat Multispectral Scanner (MSS)

Landsat -1, -2, -3, -4 and -5 were launched between 1972 and 1984 and provided a maximum ground resolution of 79m for Landsat -1, -2 and -3 and 82m for Landsat -4 and -5 . The MSS sensor has four spectral bands (Table 3.1).

Band number	Spectral range
4	0.5-0.6 μ m
5	0.6-0.7 μ m
6	0.7-0.8 μ m
7	0.8-1.1 μ m

Table 3.1. Landsat MSS sensor specifications.

(b) Landsat Thematic Mapper (TM)

Landsat-4 carrying the TM was placed in orbit in July 1982. Since then there have been relaunches and the TM has become the most widely used space sensor for geological investigation and exploration. The TM is a line-scan system incorporating several innovations over the MSS to the extent that it is considered a second generation sensor.

The Landsat 4 spacecraft was launched into a circular near-polar sun-synchronous orbit providing a good coverage of the globe with the scanning parameters optimised for scenes located near 40° north latitude (Engel & Weinstein 1983). The local capture time of scenes for SW England is 9.30 am. (Smithurst 1990) and has a revisit frequency of 16 days.

The TM sensor has seven bands and the spectral limits of the bands (Table 3.2) are based on knowledge of spectral characteristics of common natural objects and transmission characteristics of the atmosphere. The six bands (1 through 5, plus 7) possess an obtainable maximum ground resolution of 30m. Band 6, the thermal band, provides a ground resolution of 120m (Engel & Weinstein 1983).

Band number of Landsat TM 4 and 5.	Spectral range	Name	Maximum ground resolution
TM1	0.45-0.52 μ m	Blue-green	30m
TM2	0.52-0.6 μ m	Green	30m
TM3	0.63-0.69 μ m	Red	30m
TM4	0.76-0.9 μ m	Near-IR	30m
TM5	1.55-1.75 μ m	SWIR	30m
TM7	2.08-2.35 μ m	SWIR	30m
TM6	10.4-12.5 μ m	Thermal IR	120m

Table 3.2. Landsat TM sensor specifications, modified from Gupta (1991).

(c) Système Probatoire de l'Observation de la Terre (SPOT)

The identical French satellite systems SPOT-1 and SPOT-2 were placed in orbits on February 1986 and January 1990 respectively and carry two identical high resolution visible sensors. SPOT can scan in two modes providing different configurations. Nadir-looking panchromatic mode provides data with a 10 x 10 m ground resolution. Combined sensors in multi-spectral mode provide data in three bands with reflectance widths of green (0.49-0.59 μm), red (0.62-0.71 μm) and near-infrared (0.80-0.91 μm) and a 20 x 20 m ground resolution. The high resolution visible sensors can be commanded to look off-nadir giving the SPOT satellite the ability to form a parallax difference, and the production of stereo pairs of images.

3.2.3 Spectral responses of the major land-uses

This section discusses the spectral responses within the optical wavelength range covered by Landsat MSS, Landsat TM and SPOT satellites, of the major features visible on satellite images of SW England which are likely to cause lineaments.

(i) Soils and Vegetation.

Linear agricultural features that are visible in high resolution satellite images are the boundaries between arable, pastoral and fallow fields formed over large areas of SW England causing a patchwork field effect (Fig. 3.4).

Throughout the growing season, neighbouring fields regularly have different crops at different stages in their maturity, hence different spectral signatures.

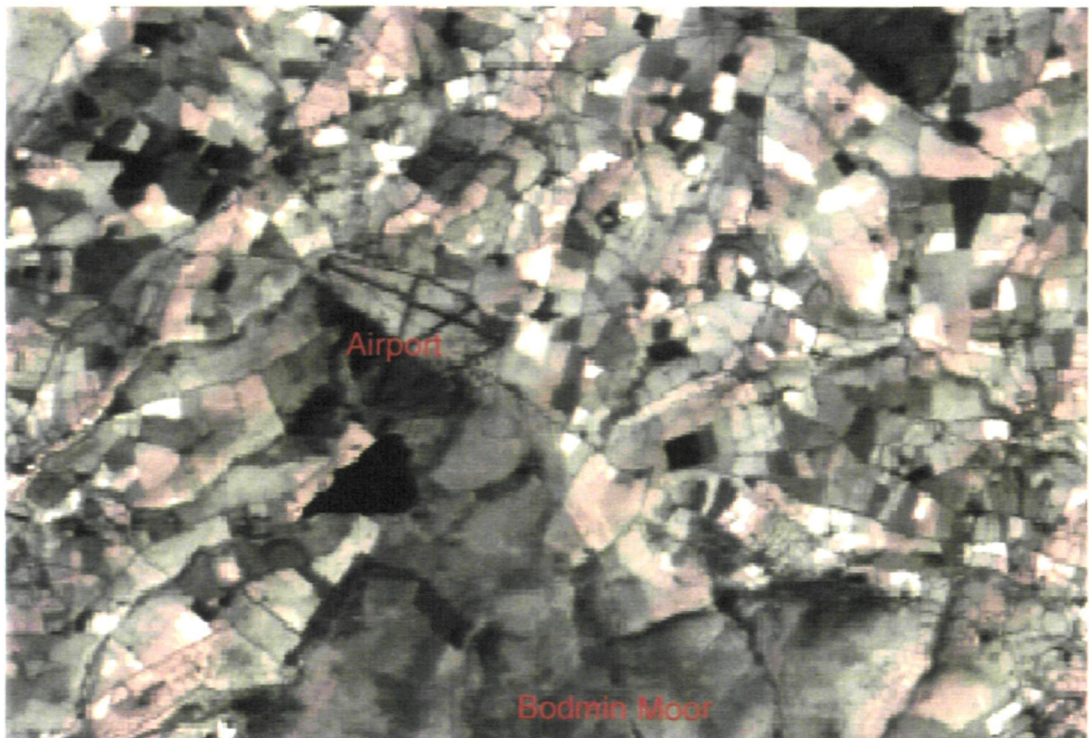


Fig. 3.4. An image showing the impact anthropogenic linear features have on the analysis of lineaments from Landsat TM images of SW England. This image is a linear stretched high resolution (30m) band 4 scene of an area northwards of Bodmin Moor. The effect agricultural practices have on lineament analysis is the highly visible 'patchwork' field pattern, highlighted by the reduction of this effect on the non-agriculturally developed Bodmin Moor. Also highly visible within the scene is the road network and runways of an airport, both of these form linear features which can be interpreted as lineaments.

The spectral responses from the road and rail network not only reflect the materials used in construction, but also different vegetation planted in the infrastructure verges.

Differences in the spectral responses and reflectances of EMR from linear anthropogenic features, creates edges (linear differences between the relative brightness in an image) which can result in the incorrect identification of an anthropogenic feature as a lineament. Spectral signatures of wet and dry soils, vegetation and water are shown in Fig. 3.5, indicating the large changes and differences in reflectance possible through the spectrum. The occurrence and wavelength ranges of the band widths of the sensors Landsat MSS, Landsat TM and SPOT are also illustrated. The degree of difference in the electromagnetic reflectance from fields with different vegetation or soil moisture levels in these bands, can clearly result in a field boundary being suppressed or enhanced.

Landsat TM bands 1-4, all SPOT and Landsat MSS bands have large spectral differences between wet and dry soil and vegetation type (Fig. 3.5). The degree of leaf reflectance of EMR is controlled by leaf pigments in the visible wavelengths and cell structure in the near-infrared (Fig. 3.6). The chlorophyll group in leaves absorb EMR in the visible region at $0.68\mu\text{m}$ and $0.45\mu\text{m}$, these absorption troughs are widened by other chlorophyll bands to leave a green peak at $0.54\mu\text{m}$. Similar reflectance curves are obtained for different vegetation types and wet soils in the TM bands 1 and 3 (Fig. 3.7). The patchwork field effect, however, is still highly visible in TM bands 1 and 3. Drury (1987) suggests that the visual disruption occurs because strong absorption by chlorophyll gives dark tones to vegetation relative to bare soil in TM band 3. Landsat TM band 4, has the greatest difference in reflectance between wet and dry soil and types of

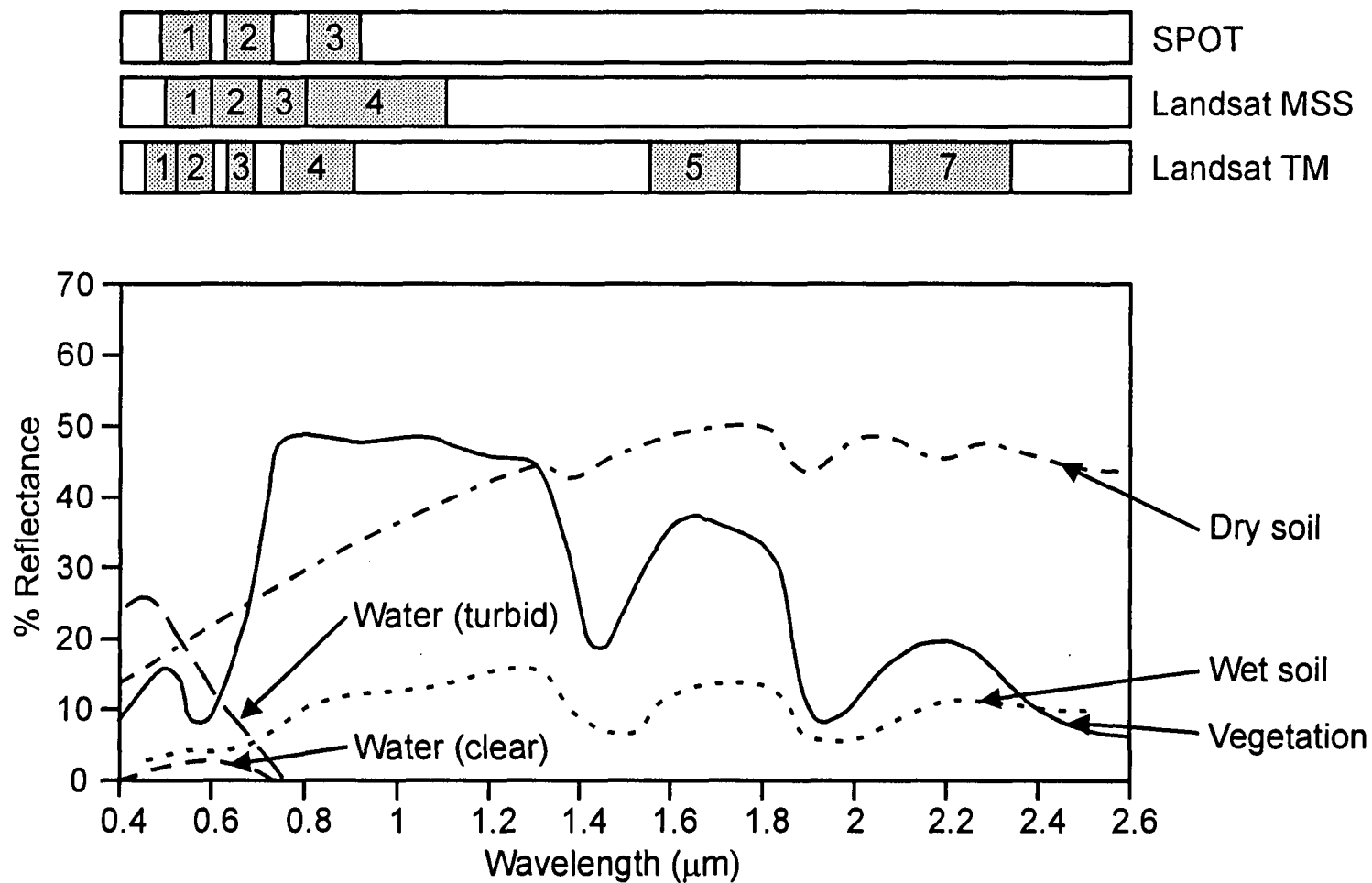


Fig. 3.5. Reflectance curves of 4 major natural features. Above are the spectral band widths (shaded in grey) of 3 satellite sensors (modified from Gupta 1991).

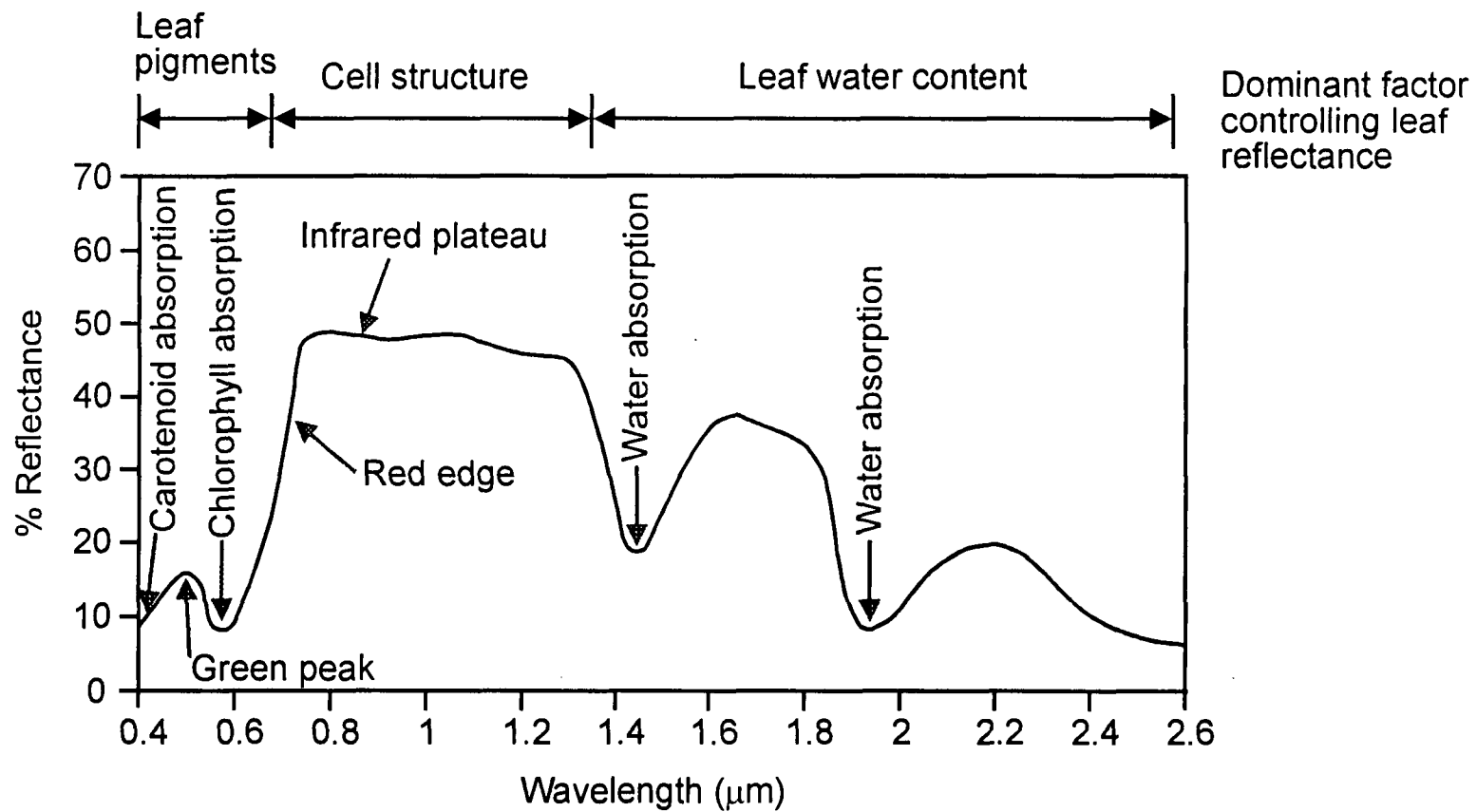


Fig. 3.6. Diagram of the reflectance spectra of leaves, illustrating the effect of leaf structures and contents on the degree of reflectance (redrawn from Goetz & Rock 1983, Gupta 1991).

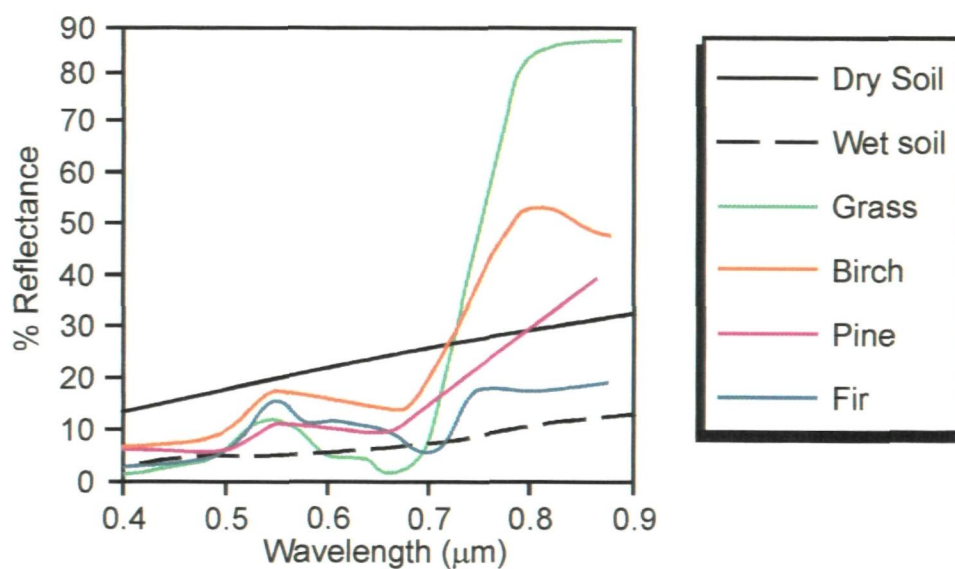


Fig. 3.7. Spectral reflectance curves for 4 different plant species of the visible to very near infrared parts of the electromagnetic spectrum (modified from Goetz & Rock 1983).

vegetation, hence the agricultural pattern dominates this band (Figs. 3.4, 3.7). This band is therefore particularly useful in the identification of linear features formed by field boundaries.

Leaf water content affects vegetation electromagnetic reflection in the shortwave-infrared, the spectral region covered by the TM bands 5 and 7 (Fig. 3.6). Molecular water stored in plant cells, filled soil pore spaces, and loosely bonded in minerals absorbs EMR by vibrational transitions (Drury 1986). Vibrational transitions involves the stretching or bending of H-O-H bonds in the water molecule from one equilibrium state to another. A fundamental transition is the change from the ground state to the first excited state and an overtone is the change from the ground state to the second excited state (Siegal & Gillespie 1980). Fundamental transitions occur at 2.09 μm , 3.11 μm and 6.08 μm (Gupta 1991) outside the visible and near infrared region atmospheric window. Overtones occur, however, within this atmospheric window at 0.94 μm , 1.14 μm , 1.4 μm and 1.9 μm (Drury 1986). The absorption of energy produces a reduction in the reflectance of EMR forming an absorption feature. Water absorption features become wider and deeper with higher plant moisture contents (Fig. 3.8) (Goetz *et al.* 1983).

Landsat TM bands 5 and 7 have different reflectance values, although exhibit similar reflectance response curves for vegetation, and wet or dry soils (Fig. 3.5). Landsat TM bands 5 and 7 were designed to measure plant moisture content, with TM bands 5 and 7 lying on the long-wavelength shoulders of the 1.4 μm and 1.9 μm water absorption features. Drury (1986) suggests that it is the 1.4 μm feature that affects the degree of vegetation reflectance for band 5.

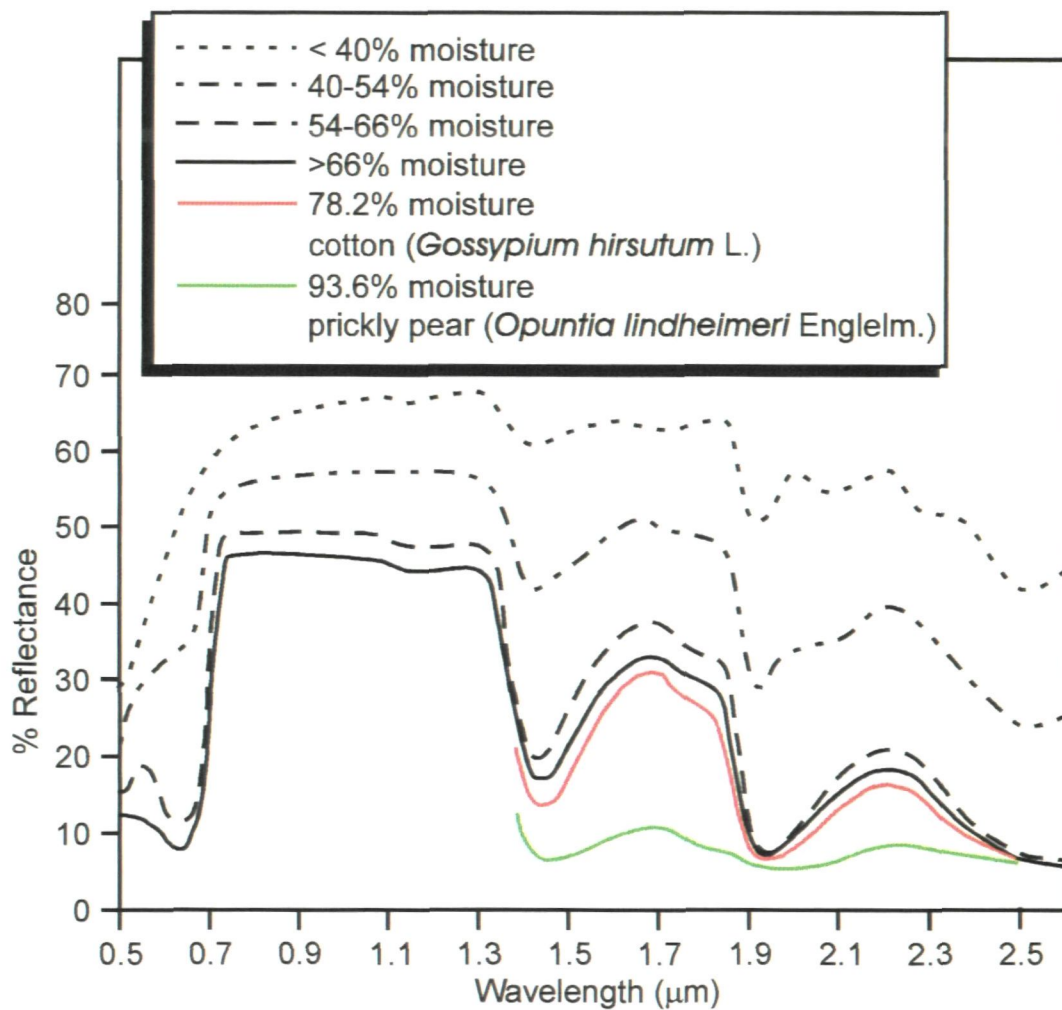


Fig. 3.8. Spectral reflectance curves of leaves with various degrees of moisture content. Black lines represent data for corn leaves, redrawn from Goetz and Rock (1983). Reflectance curves for cotton and prickly pear plant species are shown in colour, modified after Gausman *et al.* (1978).

The spectral reflectance curve of plants in the shortwave infrared is controlled by water (Fig 3.6). The effect of increasing water content is to suppress the degree of reflectance and increase the width of the water absorption feature, which lowers the vegetation reflectance further (Fig. 3.8). This is also observed to occur for Landsat TM band 7 (Fig. 3.8). Consequently, the degree of reflectance from vegetation becomes similar to wet soils.

Drury (1986) suggests that in a humid terrain, with uniform soil moisture, all green vegetation except trees should have roughly the same moisture content. Hence, for images of Landsat TM bands 5 and 7, EMR reflectance from different types of vegetation on a flat illuminated ground should be similar. Any variation in EMR reflection should therefore be caused by a change in the angle of solar incidence to the ground surface caused by a topographic feature, or a change in the trend of the topographic feature to the EMR source. Consequently, the structural interpretation of an image from Landsat TM bands 5 and 7 from a humid terrain, with grass and cereals dominating, should be simplified due to less agricultural disruption (Drury 1986). Lineaments would, therefore, mainly represent geomorphological features.

Soil moisture and plant moisture content can be varied by agricultural practices and crop maturity throughout the year. Agricultural dominance in band 5 TM images from late Spring may occur due to good soil drainage of cereal fields relative to pasture combined with a seasonal decrease of rainfall (Drury 1986). Lighter coloured fields continue to persist through summer as ripening cereals have reduced moisture content in their leaves and fruiting heads (Drury 1986). The relative water content for wheat can be reduced from a relatively high 100-90% to 60% in 40 days after post-flowering (Connor 1975, as referenced by Kirkham & Kanemasu 1983) and hence have a reduced reflectance compared to

pasture which retains a high moisture content (Drury 1986). Autumn ploughing creates fields of moist soil which appear dark against relatively brighter pasture. However, fields with the new shoots of cereals have a reflectance of a mixture of wet soil and leaves that is similar to pasture. The appearance of these new shoots occurs between the months between January and March and it is at this time field patterns become muted and conditions are optimised for geological interpretation (Drury 1986). The parent material can also control the degree of moisture in the overlying soil which is a large influence on the amount of moisture in plants. Only broad lithologies though, can be identified and little structural information is provided (Drury 1986).

Moore & Camm (1982) and James & Moore (1985) using Landsat MSS images, found that winter scenes provided the best data for structural interpretation. The low angle illumination (less than 15°) of relief by the winter Sun increased the degree of shadowing enhancing the topography. James & Moore (1985) used winter scenes with a coverage of snow to be able to mask the visual disruption caused by agriculture when using Landsat MSS images. However, the climate of SW England is too warm for snow coverage to frequently occur and imagery containing snow coverage is only available on the longer time series available from Landsat MSS data.

(ii) Transport system

Infra-structure such as roads, rail lines and buildings generally have a systematic and regular structure and appear light grey to grey in the visible wavelengths and darker in the near infrared. Road and rail networks can be highlighted by vegetation, either by different vegetation on embankments or by the linear alignment of fields. Hence, linear road and rail networks are visible at

smaller map-scales than expected from the relatively small area occupied.

However, because they can be highlighted by vegetation they are less visually intrusive for Landsat TM bands 5 and 7.

(iii) Relief

Natural objects have a semi-diffuse reflectance pattern (Gupta 1991) (see section 3.2.1). The relative degree of EMR reflected from relief is dependant on the incidence angle of the incoming ray, the object slope direction and the location of the sensor. Solar reflection sensors generally have a vertical viewpoint and hence the degree of reflectance varies due to the angle between the Suns' rays and the objects slope dip direction (Fig. 3.9). An example of linear features highlighted by relief is shown in Fig. 3.10.

(iv) Fluvial systems

Silted and shallow water bodies reflect EMR in the visible region of the electromagnetic spectrum while at longer wavelengths EMR reflection is negligible (Fig. 3.5). Hence, for a Landsat TM band 5 image of SW England with a linear stretch applied (see Section 3.3.2) the water body is black. The most visible feature of a fluvial system in the smallest map-scale scale Landsat TM images of SW England examined, however, is the effect of fluvial systems on relief (Fig. 3.10).

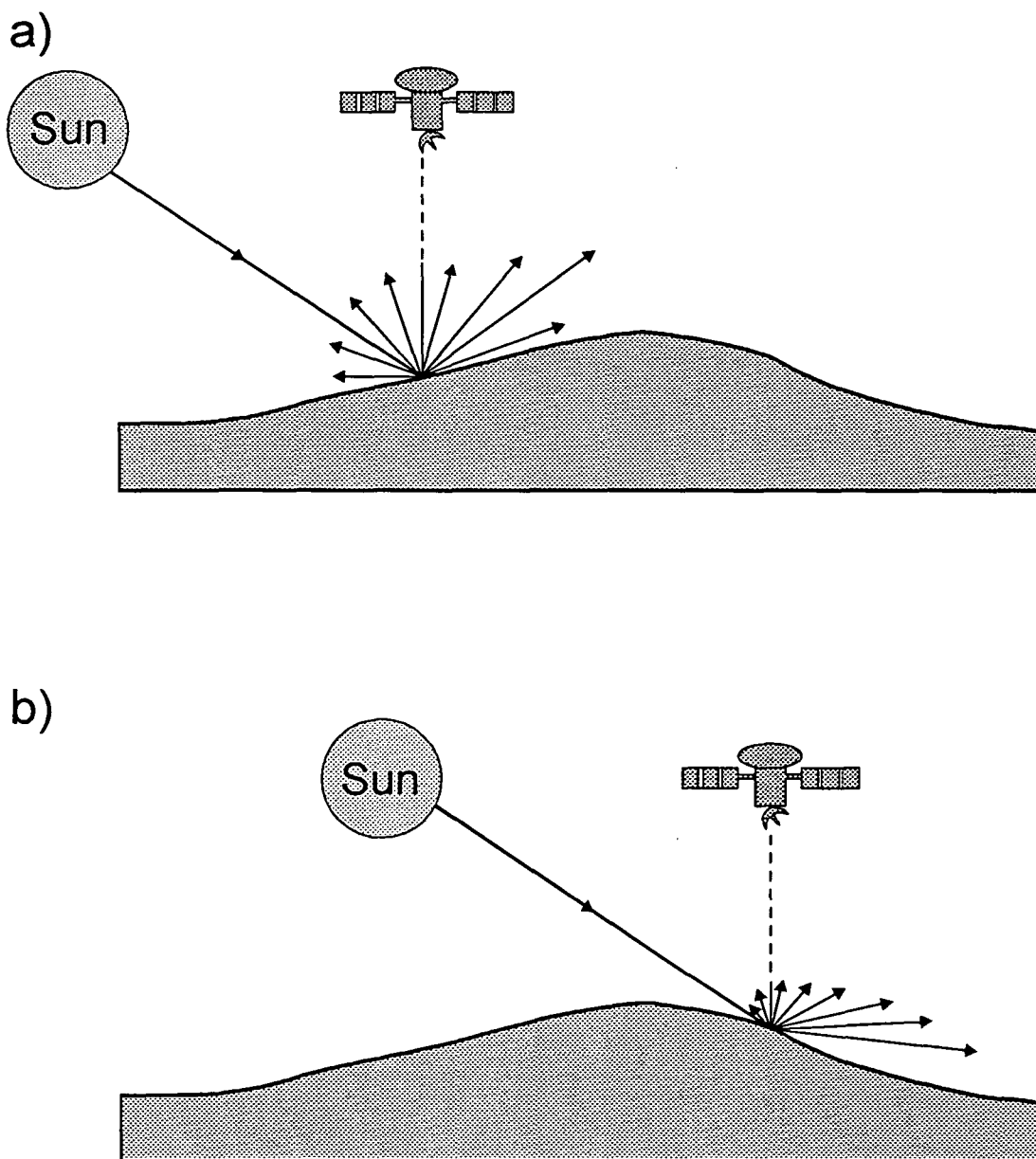


Fig. 3.9. The effect of the angle of slope on the geometric reflectance of solar radiation for a low sun azimuth. In a) a high reflectance value results from a high angle of incidence between the Sun and the slope, and b) low reflectance values result from a low angle of incidence between the sun and the slope.

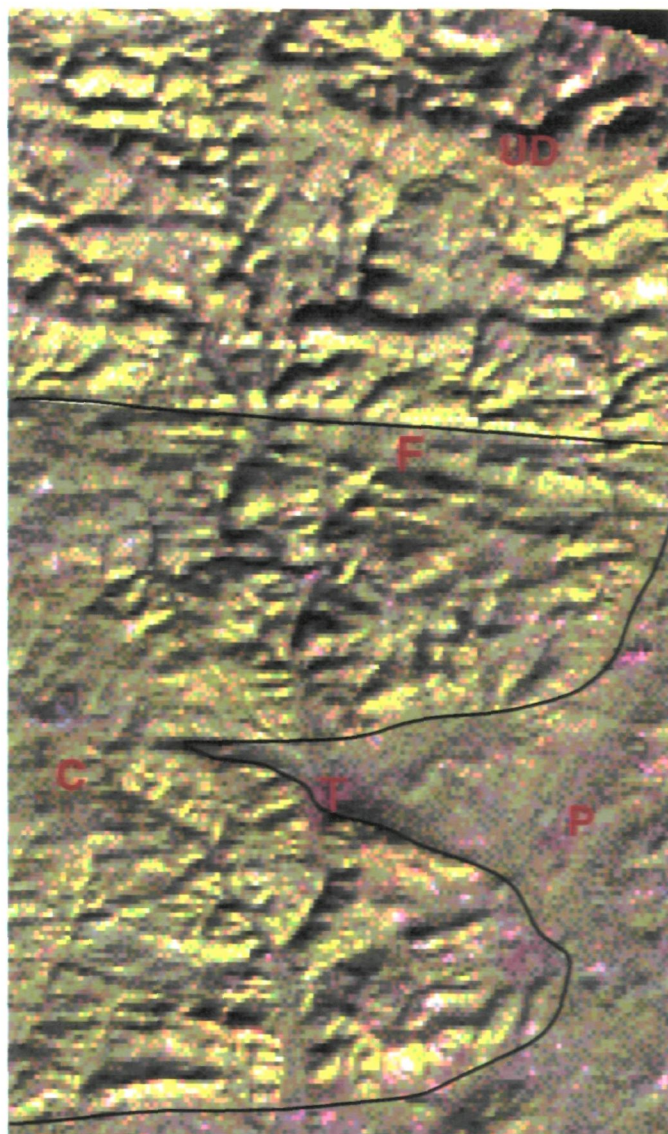


Fig. 3.10. Full colour composite image of TM bands (5,4,1) with a pixel resolution of 150m. The image covers North-East Devon and is centered on Tiverton (T). The image clearly shows the drainage basin of the N/S trending River Exe and shadowed topography. Visible within the image is a large E/W trending fold, marked by the letter F, and differences in image texture and tone relating to broad changes in tectonostratigraphy of the Upper Devonian sediments of North Devon (UD), Carboniferous Culm deposits (C), and the overlaying Permian sediments (P).

3.2.4 Rationale for determining suitable satellite imagery

All three sensors discussed, Landsat MSS, TM and SPOT, produce images which can be used for a lineament interpretation at a regional scale. Total coverage of SW England is available from the NERC remote sensing archive only in Landsat TM images, while only partial coverage by SPOT and Landsat MSS images are available.

Landsat TM covers a larger part of the electromagnetic spectrum and in more detail than Landsat MSS and SPOT and hence allows a wide range of data to be investigated. Landsat TM band 5 has been suggested by Drury (1986) to suppress the patchwork effect of fields, and hence is considered to be ideal in the interpretation of lineaments from a temperate agricultural terrain. Landsat MSS and SPOT bands are, however, placed in the visible and very near-infrared regions of the electromagnetic spectrum, generally enhancing field boundaries. In conclusion Landsat TM images are considered most likely to produce a successful regional analysis of lineaments in SW England.

Drury (1986) and Smithurst (1990) conclude that Landsat TM winter images have the greatest reduction on the patchwork effect of fields. Landsat TM winter scenes available for the region are restricted to the area of Devon and Somerset (path/row 203/025) and were recorded on 6th December 1984. Scenes available of the area of Cornwall and West Devon were limited to spring, summer and autumn. Consequently, in comparison to winter images, these images had relatively enhanced agricultural features and reduced shadowing from relief. The summer images compared to spring and autumn images, contained the largest spectral differences between soil and vegetation and the highest sun angle causing a muting of topography. Spring and autumn images had similar spectral differences and sun-angles. The autumn scene was chosen, however, because

of comparatively reduced cloud cover and was recorded on 11th September 1985 (path/row 205/024). The areas covered by these scenes are shown in Fig 3.11.

3.3 Image processing techniques

Images produced by remotely sensed data consist of pixels that represent an average radiation intensity of a specific area, recorded in an analogue form by a sensor and converted to digital numbers. Each image consists of rows and columns of pixels in an image plane which are all registered within an external co-ordinate system.

The 'raw' Landsat TM scenes of SW England were geometrically skewed, comprised of a 30m resolution and possessed a low contrast between image features. Consequently, the scenes needed to be:

(i) geometrically corrected resulting in spatially accurate lineament maps (Section 3.3.1);

(ii) degraded to resolutions of 60m, 90m, 120m and 150m, to investigate the effect of resolution on lineament populations (Section 3.3.2);

and (iii) enhanced, allowing the visual identification of lineaments from the images by increasing the contrast between image features (Section 3.3.3).

3.3.1 Geometric correction

Geometric distortion which occurs in Landsat TM images of SW England (Fig. 3.12) is related to the Earth's shape and spin and the orbital properties of the satellite. The process of geometrically correcting an image is termed a *warp*. Spatial correction of the scene was achieved using a polynomial warp with

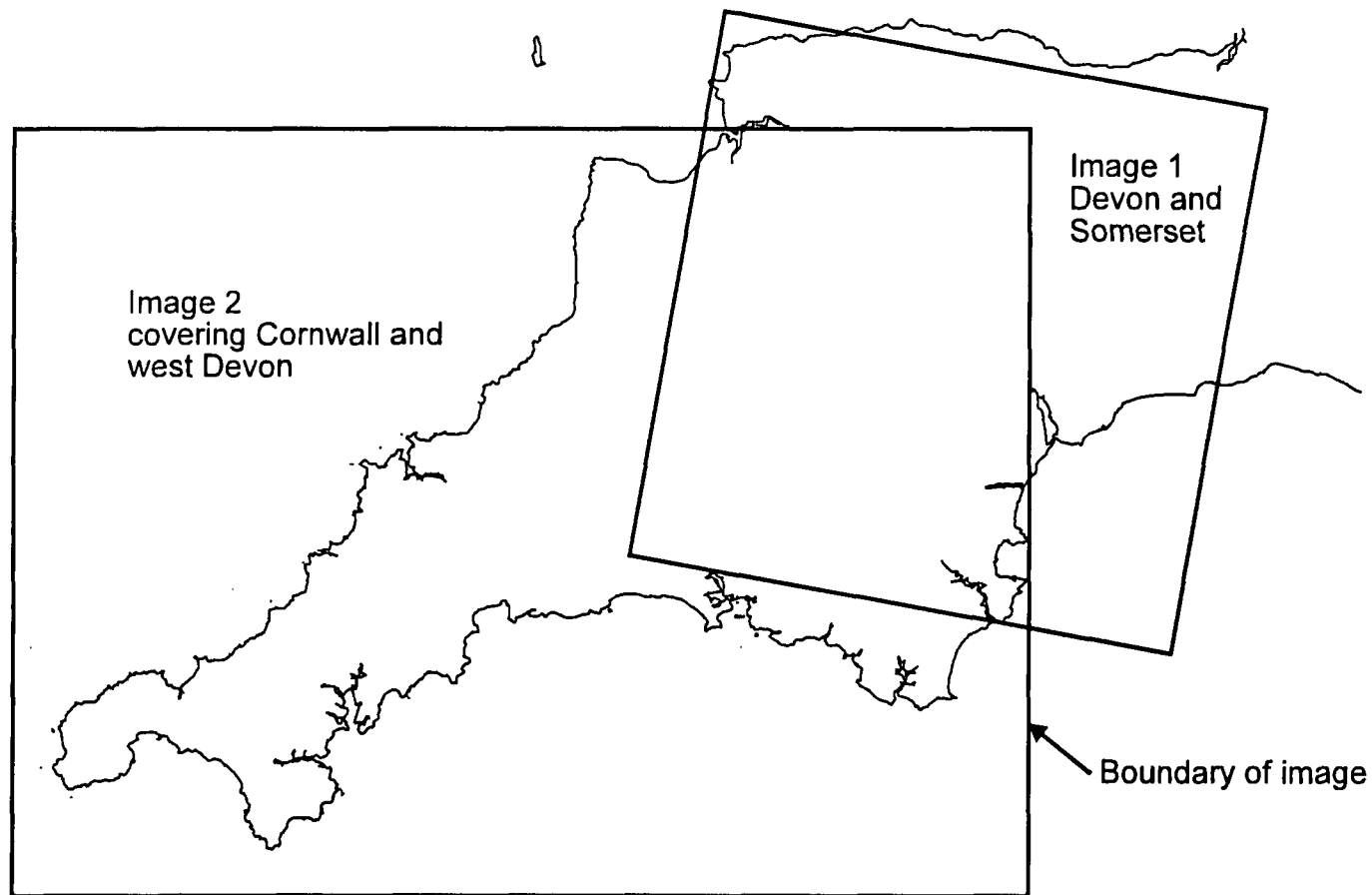


Fig. 3.11. Map of SW England, showing the approximate areas covered by the two Landsat TM images of Devon and Somerset (image 1) and Cornwall and west Devon (image 2).

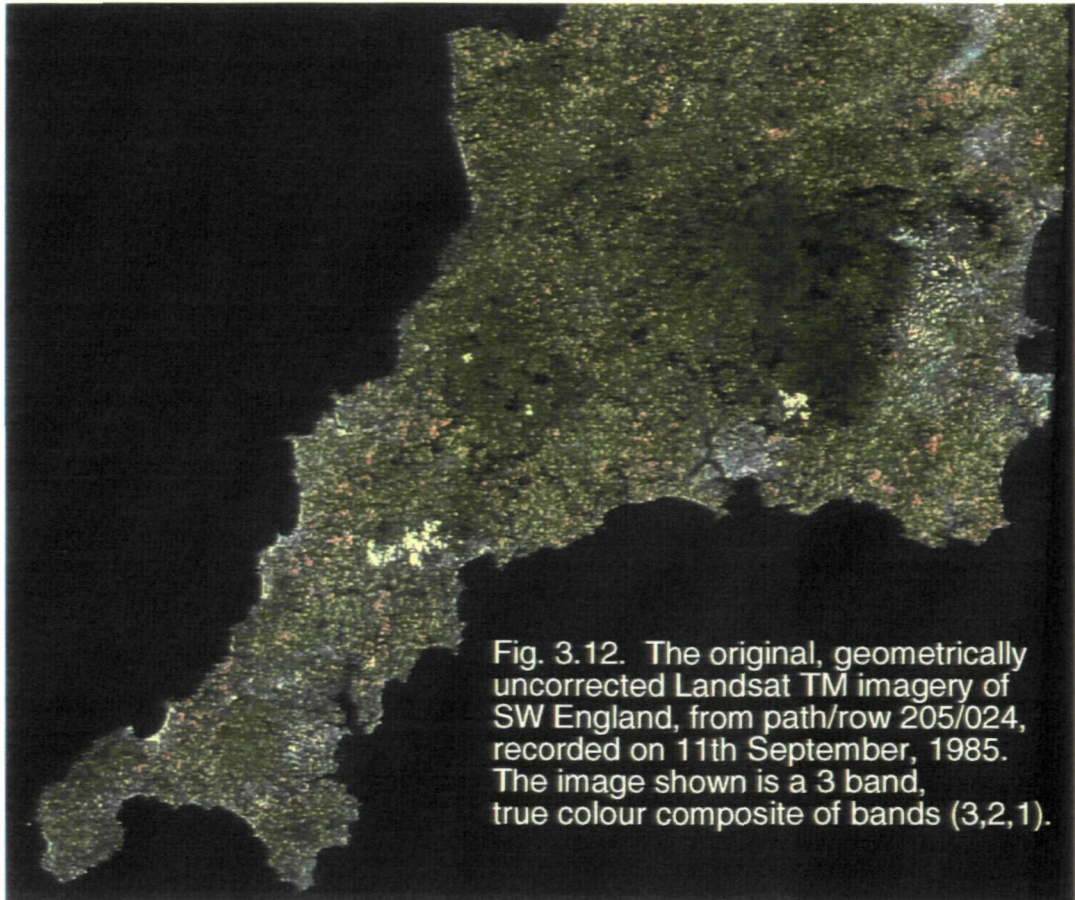


Fig. 3.12. The original, geometrically uncorrected Landsat TM imagery of SW England, from path/row 205/024, recorded on 11th September, 1985. The image shown is a 3 band, true colour composite of bands (3,2,1).

nearest neighbour interpolation (Schowengerdt 1983) of control points on the scene to control points located on the Bartholomew's digitised coastline map of SW England (Fig. 3.13).

The degree of error in distance of the corrected scenes were measured by the root means squared (RMS). RMS errors achieved for the warp of the Devon/Somerset and Cornwall/East Devon scenes were <1 , suggesting that the average spatial error of the images is <1 pixel in size (for scenes of SW England which were degraded to a resolution of 150m, the error is therefore $<150\text{m}$). Spatial errors up to approximately 3km, however, were produced by the warp. These large errors were restricted to the Devon/Somerset scene in the area of the Quantock Hills (Fig. 3.12) because of the relative large distance to the nearest coastline control point within the scene.

Sub-scenes of North Cornwall consistently had RMS errors <1 across the full range of resolutions examined. Therefore, all spatial errors were below the respective size values. However, the Bartholomew's coastline map of SW England contains inherent spatial errors related to the conversion of the original Casino projection to the British National Grid system. This was discovered after lineament interpretation of each of the scenes, and sometimes caused a small spatial displacement to occur between the geometrically corrected scenes and published British Geological Survey maps. As a result, the real spatial error was found to be up to 0.5km for scenes of Devon/Somerset and Cornwall/East Devon with resolution of 150m, and less for images with smaller resolutions.

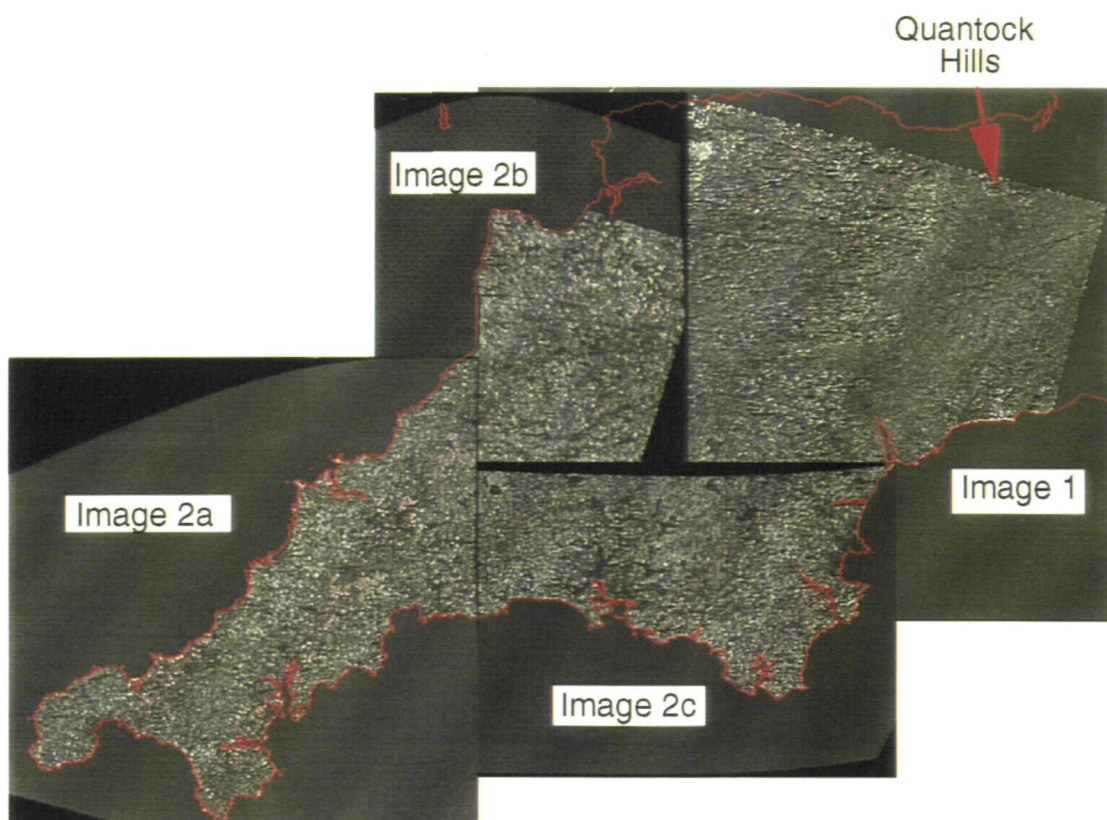


Fig. 3.13 Non-directional edge enhanced, band 5 TM images of SW England showing the regional accuracy of the applied geometric correction. The images were corrected to the digitised coastline of SW England obtained from the Bartholomews data set, shown as red lines. The degree of spatial error in the correction is relatively higher for the area of the Quantock Hills because of the absence of the coastline, to which the images were warped. Blank spaces between the images are caused by the overlapping of image 1 by 2b and image 2b by 2c. Lineaments of these areas are interpreted from the underlying image.

3.3.2 Resolution and image degradation

Landsat TM images have an initial resolution of 30m. To obtain images with resolutions of 60m, 90m, 120m and 150m, the geometrically corrected, un-enhanced, 30m resolution scenes was degraded by the nearest neighbour averaging technique. This involves the automatic combination of grey level values of 30m pixels with the surrounding pixels grey levels, to form each new resolution and a new grey level value for each new pixel.

Lineaments were interpreted from enlarged images with a screen pixel dimension of ~2mm. The image map-scale was therefore controlled by the area of ground represented by individual pixels. Hence, a decrease in resolution results in a relatively smaller map-scale image. The map-scale of images interpreted with 30m, 60m, 90m, 120m, and 150m resolutions were therefore ~1:15000, ~1:30000, ~1:45000, ~1:60000 and ~1:75000, respectively.

3.3.3 Image enhancement

(i) Contrast enhancement

Contrast enhancement is a pixel-by-pixel radiometric transformation, designed to enhance visual discrimination of low contrast image features (Schowengerdt 1983). The initial scenes contained a small grey level range resulting in low contrast of features, and therefore a linear contrast stretch was applied. This expands the original grey level range to fill the dynamic range (typically black and white for a single band image) of the display device. Although some image saturation was seen at the extremes of the output range, no important information was lost.

(ii) Spatial filtering

Spatial filtering is a 'context-dependant' operation that alters the grey level of a pixel, according to its relationship with the grey levels of other pixels in the immediate vicinity (Schowengerdt 1983). The main spatial filters employed are low-pass, high-pass and band-pass filters. Low-pass and high-pass filters have the effects of defocusing and increasing detail of an image respectively. Band-pass filters are used to isolate periodic noise from an image.

High-pass filters increase the high frequency spatial data of an image, by removing the low frequency components. These high frequency variations or edges, are defined by the sharp intensity differences between neighbouring pixels, the boundary being the edge (Drury 1987). These edges correspond to local changes that can be caused by relief, fluvial systems and vegetation (Gupta 1991). In SW England, as in other areas, the filtering process when applied to high resolution Landsat TM images, normally results in a sharpening of edges that relate to relief, fluvial systems, field boundaries and the road network.

The high-pass filters used employ the technique of spatial neighbourhood averaging using a box-filter algorithm, a process termed a *convolution*. In general, the box-filter or convolution matrix dimensions consists of an odd numbered matrix, such that the central pixel is evenly weighted. The centre of the convolution matrix overlies a pixel in the image, and the digital numbers covered are multiplied by the corresponding weighting factor. The results are summed and the value is then ascribed to the central pixel of the matrix (Fig. 3.14). This process is applied repeatedly to all pixels in the image.

High-pass filters were used to enhance edges in images which trended in any direction (i.e. a *non-directional filter*), and edges with specific trends (i.e. a *directional filter*). The non-directional high-pass filter consists of a matrix

a)

1	1	1
1	1	1
1	1	1

b)

	A	B	C
	D	E	F
	G	H	I

c)

$$\text{Central Pixel E} = \frac{1}{9} * \left[\begin{array}{l} (A*1) + (B*1) + (C*1) \\ + (D*1) + (E*1) + (F*1) \\ + (G*1) + (H*1) + (I*1) \end{array} \right]$$

Fig. 3.14. The convolution matrix a), is a 3x3 matrix low-pass filter consisting of equally weighted cells. The image consists of a matrix of pixels b), each representing a digital number. The pixels are overlain by the matrix and are multiplied by the corresponding weighting factor. The products are then averaged c), to compute the value of the shaded pixel, letter E.

containing a positive number for the centre pixel, surrounded by negative numbers corresponding to the encompassing pixels (Fig. 3.15a). Directional filters based on square convolution matrices have a symmetrical distribution of positive and negative weightings about a particular direction. The convolution results in an increase in detail at right angles to the axis of symmetry of the matrix. Edges are enhanced to about 45° either side to this direction, all others being suppressed. The directional filters used in this study consisted of convolution matrices in four gradient directions N/S, NE/SW, E/W and NW/SE; as this is sufficient to obtain an edge direction map covering all linear trends (Robinson 1976).

Since the images studied were taken with the sun illuminating from the SE, NE-SW orientated topographic features were naturally highlighted, causing a bias in the identification of NE/SW lineaments. Directional filters were used to remove such bias by increasing detail in other orientations (Figs. 3.15b, c). Smithurst (1990) using identical directional filters, concluded that they were the most useful for the structural interpretation of SW England (Fig. 3.16a).

High-pass filters enhance features that are approximately half the size of the matrix (Chavez 1982). Increasing the size of the matrix results in a reduction of lower frequency components subtracted from the original. Consequently 5x5 directional filters (Fig. 3.15c) were used in order to obtain a better interpretation of large scale features while still increasing the detail. The human visual acuity in vertical and horizontal directions is generally superior to the visual acuity in diagonal directions for a large range of spatial frequencies (Leibowitz 1953). To compensate for this, matrices were weighted higher in the diagonal directions. The high-pass filters produced images with a relatively narrow grey level range and therefore a linear contrast stretch was applied to all convolutions.

a)

-1	-1	-1
-1	9	-1
-1	-1	-1

b)

S

-1	-1	-1
0	0	0
1	1	1

SW

0	-1	-1
1	0	-1
1	1	0

W

1	0	-1
1	0	-1
1	0	-1

NW

1	1	0
1	0	-1
0	-1	-1

c)

S

-2	-2	-2	-2	-2
-1	-1	-1	-1	-1
0	0	0	0	0
1	1	1	1	1
2	2	2	2	2

SW

0	-1	-2	-3	-3
1	0	-1	-2	-3
2	1	0	-1	-2
3	2	1	0	-1
3	3	2	1	0

W

2	1	0	-1	-2
2	1	0	-1	-2
2	1	0	-1	-2
2	1	0	-1	-2
2	1	0	-1	-2

NW

3	3	2	1	0
3	2	1	0	-1
2	1	0	-1	-2
1	0	-1	-2	-3
0	-1	-2	-3	-3

Fig. 3.15. High-pass convolution matrices used for edge-enhancements of features present in the TM images; a) 3x3 non-directional filter, b) 3x3 directional filter and c) 5x5 directional filter. The directional filter name is above the matrices indicating the direction of maximum response, e.g. a south directional mask produces a maximum output for northwards directed luminance, hence highlighting E/W features.

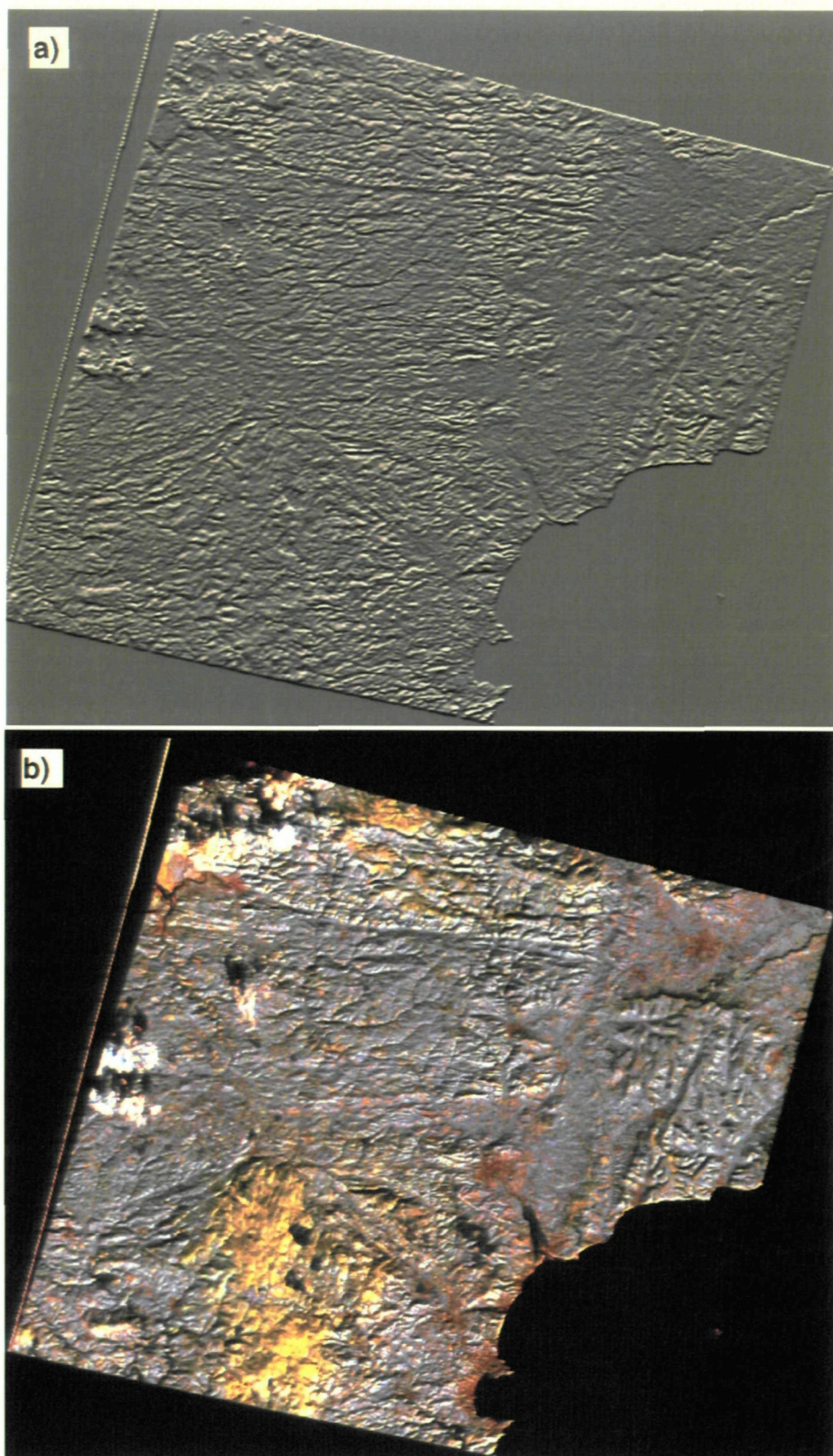


Fig. 3.16. Two images of the same scene 1 (Devon and Somerset) displaying the differences in the type of geological information obtained. Image a), is an E/W directionally enhanced image of TM band 5, showing less textural content and better defined lineaments in compared with image b). Image b), is a 3 band, false colour composite of Landsat TM bands (7,5,4) and highlights elevated areas relating to the Dartmoor granite and the sandstones of Exmoor, as pale yellow.

(iii) Colour processing

Digital Landsat TM images are typically displayed on colour visual display units, utilising an additive colour composite system with three primary colours; red, green and blue. A three band false colour composite (FCC) is typically stored in three refresh memories with each image band as one of the primary colours. An example of this type of processing is shown in Fig. 3.16b.

3.4 The effect of resolution on the visual impact of linear features on Landsat TM images

Landsat TM images of SW England contain a range of linear features formed by anthropogenic and natural objects. Natural objects such as relief and the river network are more likely to relate to underlying bedrock geology (Section 2.6.1) and it is therefore desirable that they are more prominent within the images. Band choice and processing techniques outlined in the previous sections were clearly made to optimise such features. Image map-scale, however, is a further variable that can be altered to enhance or suppress particular objects within an image (Drury 1986).

Generally, anthropogenic objects in SW England are smaller in scale than natural objects. With large map-scale high resolution Landsat TM images, the dimensions of a field are larger than the pixel size. Hence, a pixel typically contains the reflectance values of a single field. Multiple pixels within a field would therefore contrast heavily against multiple neighbouring pixels contained within a different field which possesses a dissimilar spectral response (Fig. 3.17). This results in a 'patchwork' effect which masks geomorphological objects (Fig. 3.4). In smaller map-scale Landsat TM images, the different spectral reflectance values of multiple fields are merged and as a result the patchwork effect

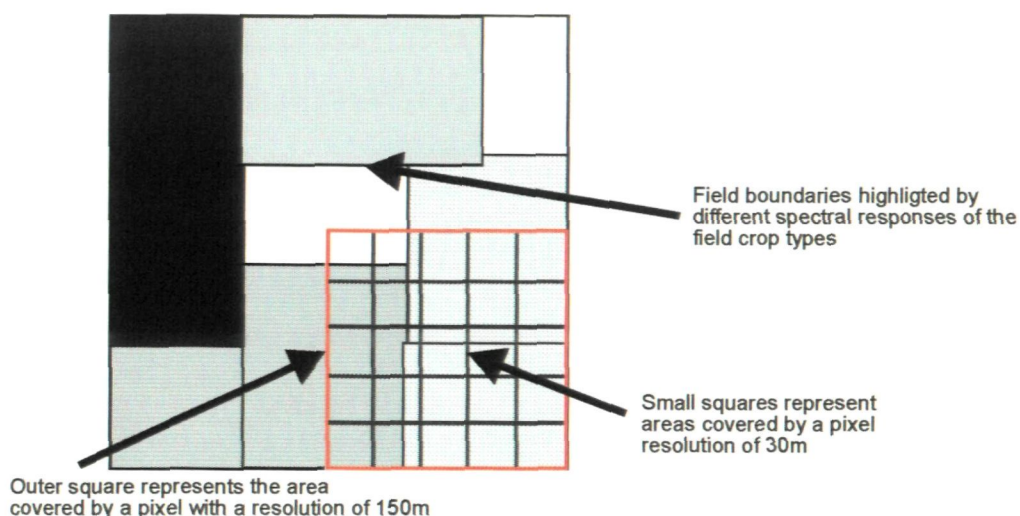


Fig. 3.17. Plan view cartoon of the EMR reflectance in a Landsat TM band 4 image, of an area dominated by fields. Multiple fields are covered by pixels with a resolution of 150m, hence reducing the reflectance differences across them. Pixels within high resolution images, however, generally contain the reflectance values of a single field. Therefore, these pixels are more sensitive to changes in EMR reflectance caused by the fields, consequently highlighting them.

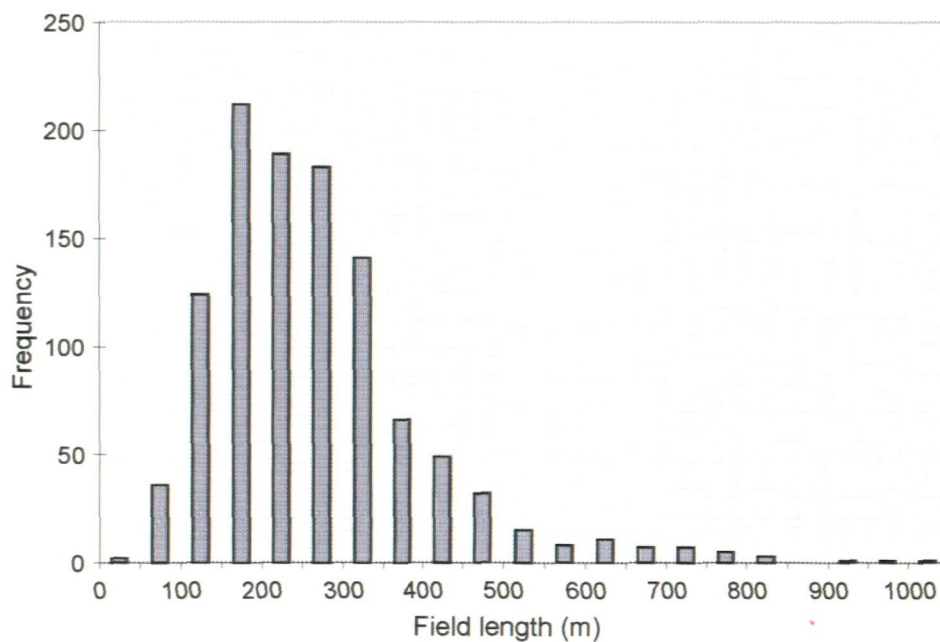


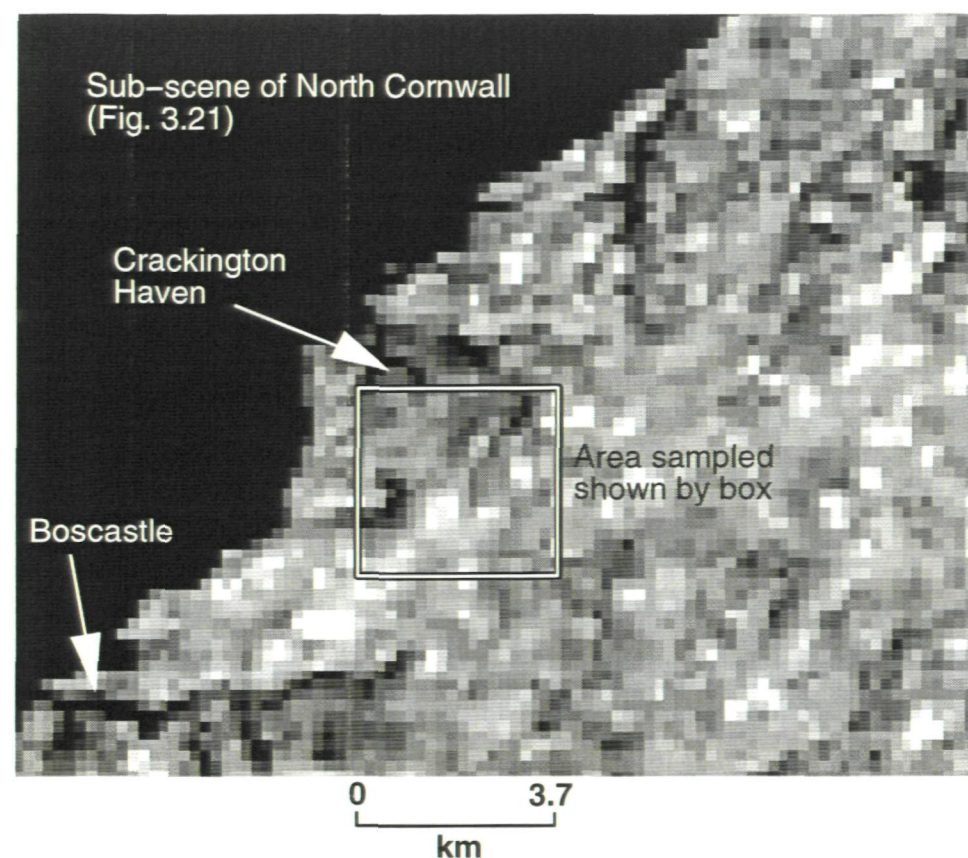
Fig. 3.18. Bar chart of the frequency distribution of field lengths identified from a band 4, Landsat TM image of North Cornwall.

is reduced. Drury (1986), however, found that the image map-scale needed to be reduced to 1:250000. As a consequence, small scale linear geomorphological features could be missed. This section describes the method devised to be able to conduct a lineament analysis on a Landsat TM images at 1:75000, while the patchwork field effect on the image is negligible.

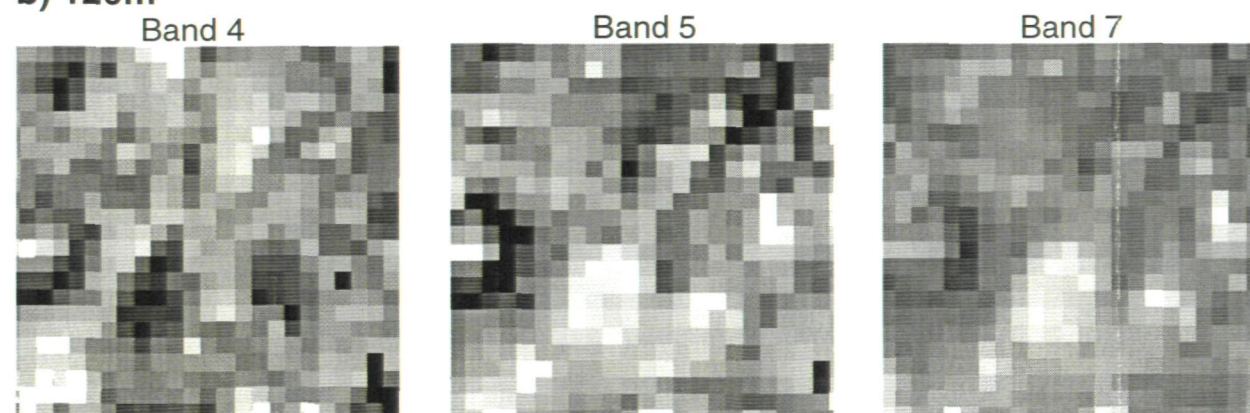
Woodcock & Strahler (1987) found that the patchwork effect for an agricultural scene which possesses an average field boundary of 420m, occurred within images up to a pixel resolution of 240m. This is approximately half the field boundary length. Field length boundaries have been measured from images of North Cornwall (Fig. 3.18). These are generally between 150m and 300m, suggesting that field boundaries cause a visual intrusion in Landsat TM images, up to a pixel resolution size of 150m. Field boundaries become increasingly blurred and less visible at lower resolutions as pixels overlapping contrasting fields produce merged reflectance values (Fig. 3.19). This suggests that the visual intrusion of smaller anthropogenic objects would become subdued at a resolution size of approximately 120m. At lower resolutions, therefore, large scale features such as valleys and ridges (i.e. non-anthropogenic) influence pixel reflectance values.

Decreasing the image resolution therefore would most likely increase the number of lineaments in a lineament population related to large scale features in the bed-rock geology (Fig. 3.20). Smaller scale features, however, may only be identified at higher image resolutions (<150m) where the local differences in electromagnetic reflectances can be detected, and hence form edges in images. For example, small scale faults in a large scale fault zone may only be expressed as changes to local relief and would, therefore, remain undetected in images with low resolutions (Fig. 3.20).

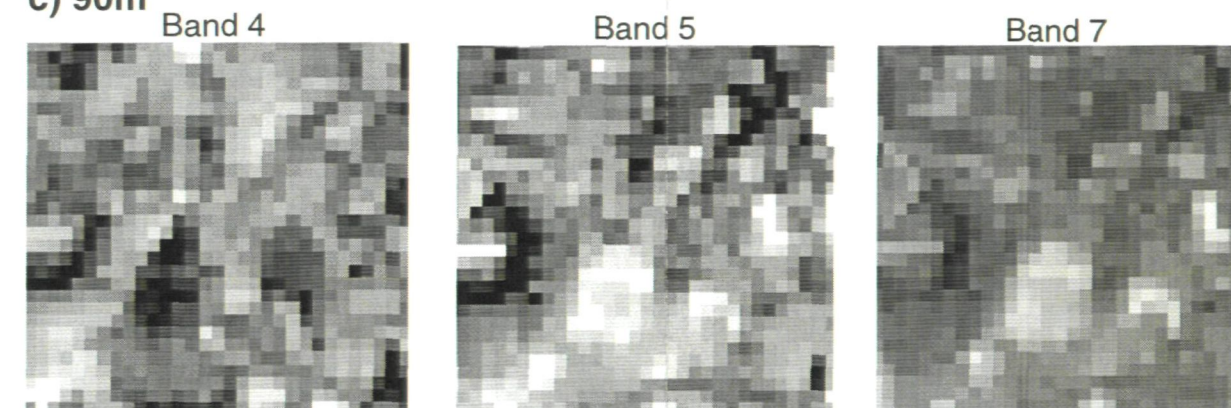
a) 150m



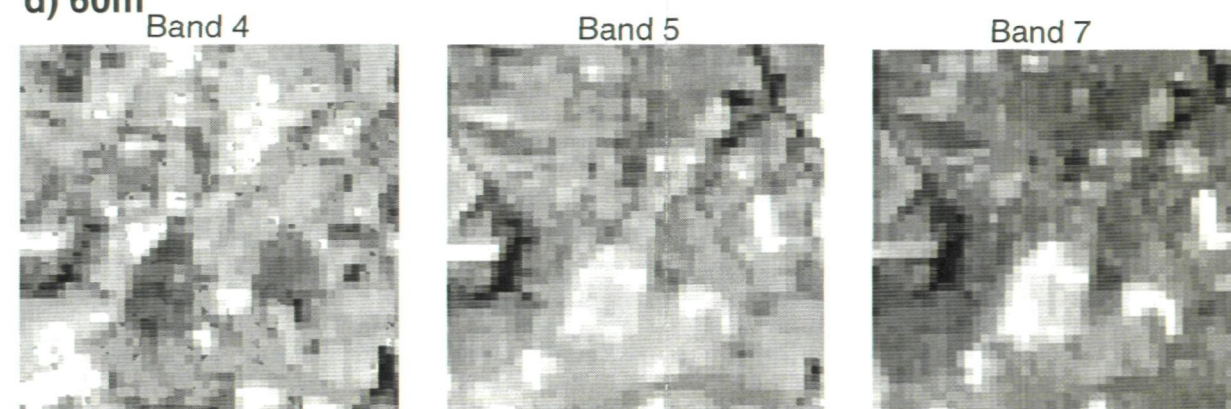
b) 120m



c) 90m



d) 60m



e) 30m

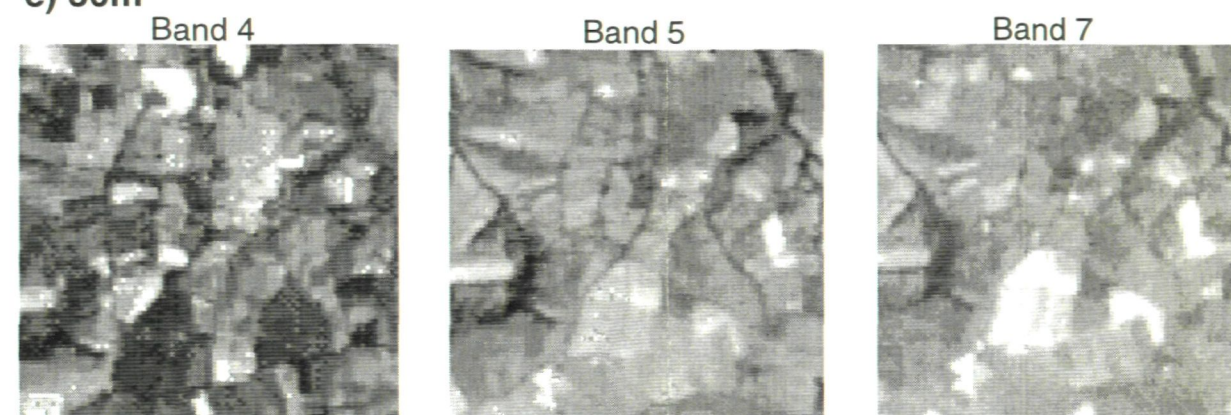


Fig. 3.19. Series of linearly stretched Landsat TM sub-images showing the effect of resolution on the visibility of fields, roads, rivers and relief within the imagery. The series of images in the left hand column is of band 4, middle column band 5, and the right hand column band 7. Image resolutions range from a) 150m, b) 120m, c) 90m, d) 60m and e) 30m. Image a) is a band 5 image, and shows the area covered by the sub-images b), c), d) and e), outlined as the black/white square.

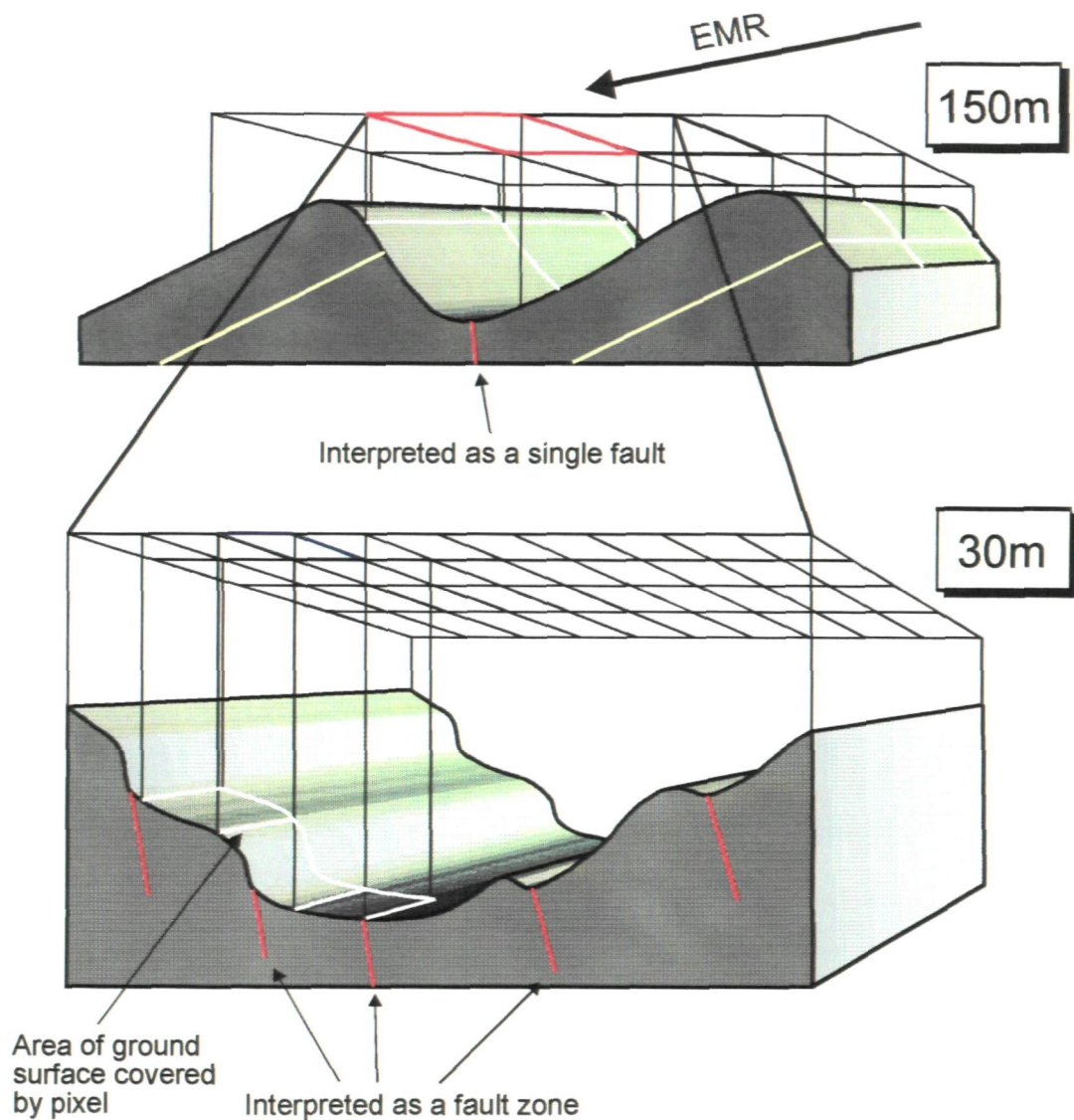


Fig. 3.20. Schematic block diagram of the relationship between pixel size and the interpreted geomorphological features. With a pixel resolution of 150m relatively large features can only influence the spectral reflectance to produce a difference in grey scales from a uniformly reflecting surface. At a pixel resolution of 30m, relatively smaller features can influence the level of EMR reflectance, hence producing greater frequencies of lineaments. High EMR reflection is illustrated as light grey. In this example, an apparent single fault in low resolution images may be interpreted as a fault zone with high resolution images.

From the previous discussion it seems fair to conclude that the optimum resolution for lineament interpretation in temperate agricultural regions may be regarded as the resolution at which the visual impact of anthropogenic linear features becomes subdued, whilst the geological information obtained is maximised. For Landsat TM images of SW England, this is best achieved at a resolution of 150m. However, for other temperate agricultural terrains the optimum resolution depends on the size of the anthropogenic features. As the anthropogenic features are subdued in these images, the image map-scale can be increased from 1:250000 to 1:75000 so that smaller scale linear features could be discerned.

3.5 Criteria for the lineament interpretation of Landsat TM images

The identification and interpretation of lineaments from a satellite image is considered by Wise (1982) to be largely subjective to the analyst. Consequently, the validity of lineament analysis can be questioned unless the methods used in the identification are both systematic and theoretically sound. In contrast, Wheeler (1983) suggests that the analyst should: devise and adhere to operational guidelines; test if the features interpreted from a single image are reproducible by independent analysts; and divide features into classes of confidence. Wise (1983), however, concludes that operational guidelines based on anything but the most simple system are difficult to formulate and apply consistently.

In the present study several pre-determined criteria were applied during lineament identification: linear segments of image with a width greater than half the length were not interpreted as lineaments; lineaments were interpreted from an image with a directional filter applied if they were within $\pm \sim 30^\circ$ to the enhanced

direction; linear features less than four pixels in length were removed from the analysis; and a greater qualitative confidence was placed in relatively longer lineaments as these are more likely to relate to the relatively longer natural features.

3.6 The determination of the optimum image processing techniques for the lineament analysis of SW England

Visual disruption from field boundaries found in images of the visible region of the electromagnetic spectrum are subdued in low resolution images (see Section 3.4). Therefore, Landsat TM bands in the visible region of the electromagnetic spectrum in such images could be interpreted for lineaments. Landsat TM images with a pixel resolution of 150m were chosen for an initial lineament interpretation of an area covering Devon and Somerset (scene 1) (Fig. 3.21). Images of Landsat TM bands 1, 3, 4, 5 and 7 with linear stretches and directional filters applied, and colour composites of bands (3,2,1), (5,4,1), (7,5,1) and (7,5,4) were interpreted and lineaments identified.

A final composite lineament map of scene 1 was interpreted from each lineament map identified from the above images. The process used in the compilation is described in the flow diagram in Fig. 3.22. It was found that some lineaments were found to occur in single images, alternatively, other lineaments occurred in multiple images forming *lineament zones*. A higher level of confidence was given to lineaments which were found to occur in multiple images as these lineaments are considered to be a function of larger linear geomorphological features. To remove low confidence lineaments from the final compilation lineament map, lineaments that were identified on more than three different images were retained (lineament zones).

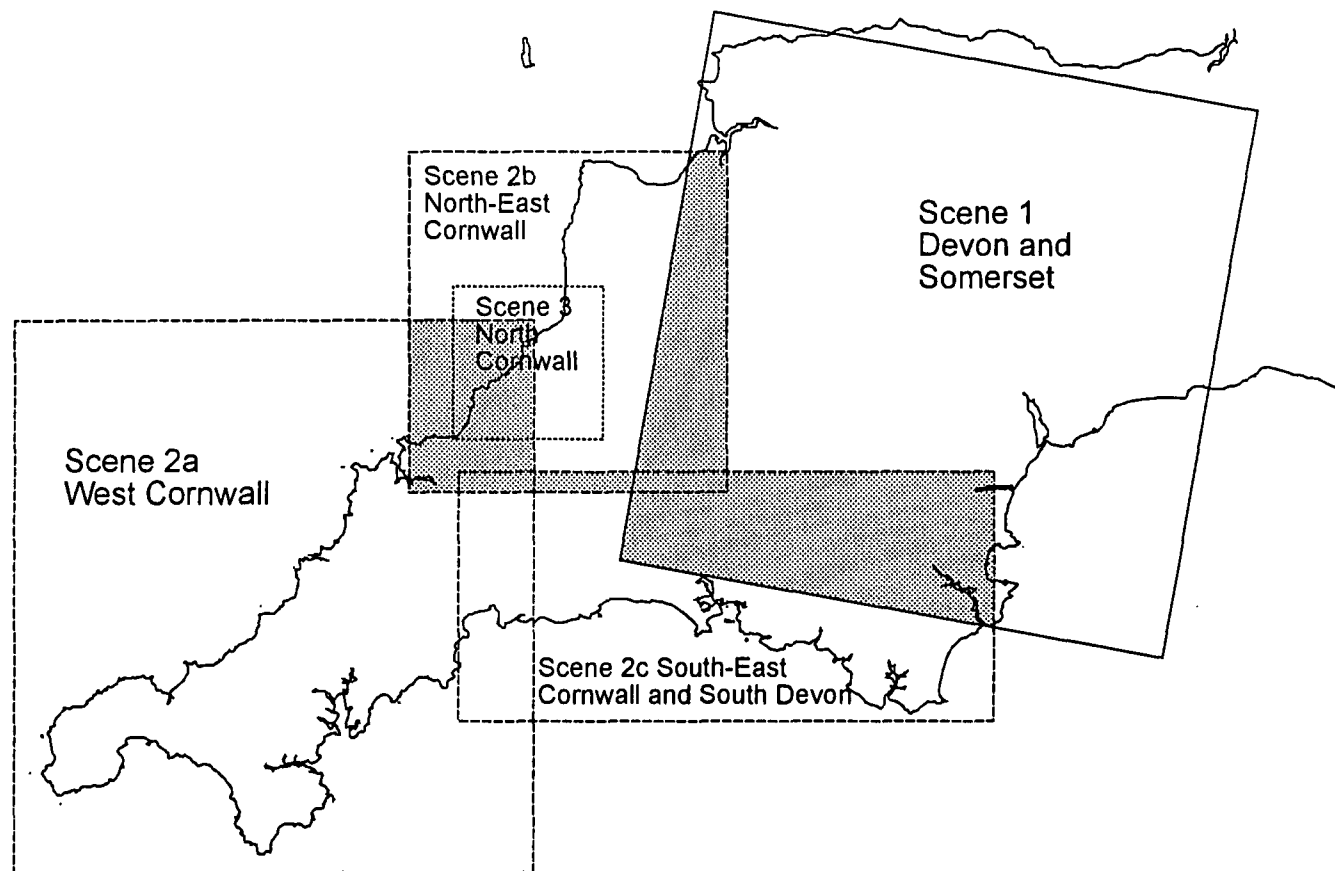


Fig. 3.21. Map illustrating sub-division of Landsat TM images interpreted in SW England. Shaded areas indicate overlapping images.

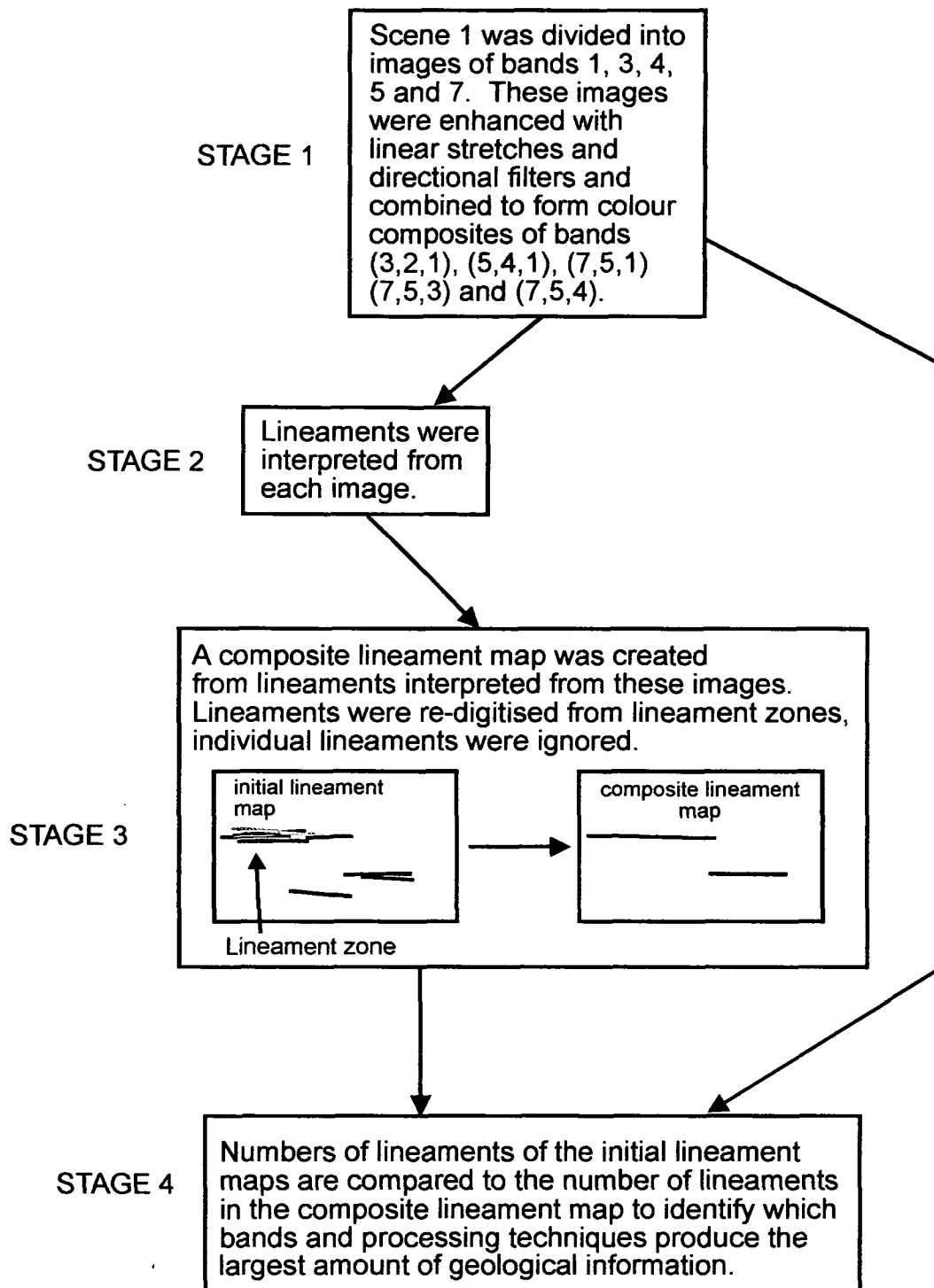


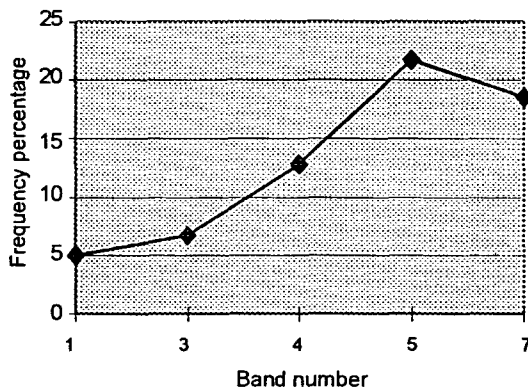
Fig. 3.22. Flow chart of the stages that were undertaken to produce the composite lineament map of scene 1.

Lineaments which did not form lineament zones were found to be interpreted predominantly from images of bands 1 and 3. One effect of combining lineament maps in this way was to increase the length of lineaments on the map by overlapping individual lineament segments identified on different images.

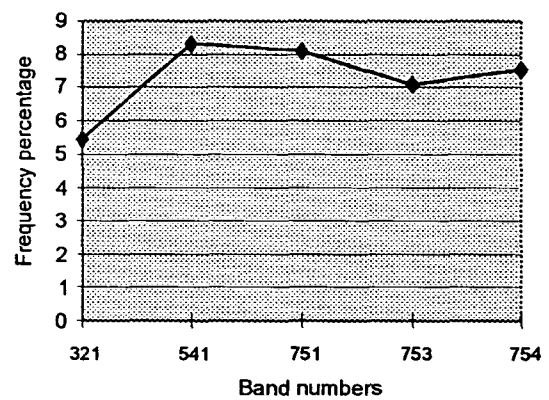
As linear anthropogenic features in images with a resolution of 150m of image 1 are muted, the interpreted lineaments are all considered to correlate to geological features. Comparatively high numbers of lineaments interpreted from the above images would therefore suggest an increase in the geological information obtained. High frequencies of lineaments and numerous short lineaments, however, may also suggest that the population consists of lineaments which only represent multiple short sections of zones of longer linear geological features. Consequently, the quality of the interpreted lineament populations from different bands and images may be assessed by the analysis of lineament frequency and length.

By comparing the number of lineaments interpreted from each image to the number of lineaments in the composite lineament map of scene 1, an indication can be gained of how successful each image band or processing technique is in highlighting geomorphological features in SW England. Lineament percentage (%) frequencies for each band and the processing techniques are illustrated in Fig. 3.23, and are expressed as a proportion (in %) of the number of lineaments within the composite lineament map of image 1. This shows that linear stretched images could form up to 21% (Fig. 3.23a), FCC's up to 8.5% (Fig. 3.23b) and images, with directional enhancements applied, up to 120% (Fig. 3.23c) of the lineaments in the composite lineament population of image 1. A value >100% was obtained for images with directional edge enhancements applied because four directionally enhanced images are needed to identify linear features

a) Linear stretch



b) FCC



c) (3x3) Directional filter

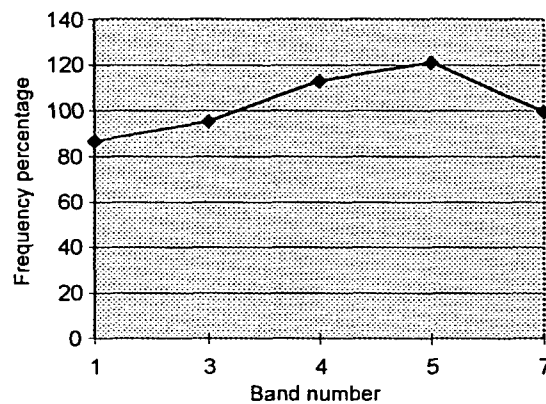
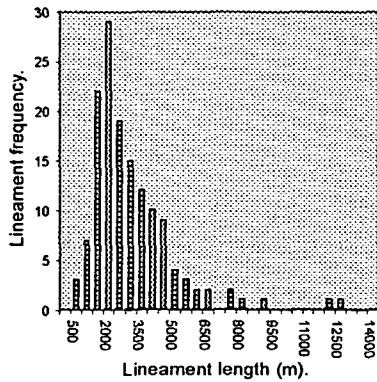


Fig. 3.23. Three line graphs illustrating the effect of band number and image processing technique on the number of lineaments interpreted from images of Devon. The number of lineaments are relative against the number of lineaments in the composite lineament map of scene 1. Plot a) shows the number of lineaments interpreted from images of single bands, plot b) the results from images of FCC's and plot c) the effect of the (3x3) directional filter, on single bands.

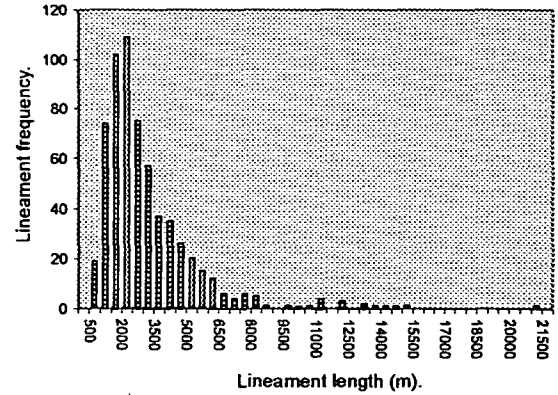
in all directions (see Section 3.3.3). As lineaments were interpreted from directionally enhanced images within $\sim\pm 30^\circ$ to the enhanced direction, lineaments therefore may be duplicated on more than one image resulting in higher frequencies of lineaments in the sample population. The occurrence of this was quite low, however, for short lineaments and negligible for longer lineaments. The overall effect was therefore small in respect to the large differences in frequencies interpreted from images enhanced by different processing techniques. Analysis of the percentage frequency of lineaments interpreted from individual bands also showed that the highest frequencies of lineaments were interpreted from Landsat TM bands 4, 5 and 7.

The characteristics of lineament lengths of a sample population were investigated by looking at histograms of lineament length. The overall distribution of the frequency of lineament lengths interpreted from sample populations all show a uni-modal distribution, with variable degrees of positive skewness (Table 3.3) (Fig. 3.24). Analysis of lineament lengths up to 5000m shows that lineaments from edge enhanced images were interpreted more frequently than lineaments from linear contrast stretched images and FCC's (Fig. 3.25). Lineaments interpreted from linear contrast stretched images, however, were more frequent than lineaments interpreted from FCC's. Lineaments lengths of the range between 5000m and 13500m show a large reduction in lineament numbers in comparison to the lineament range up to 5000m (Fig. 3.26). The effect of the image enhancement technique in this lineament length range, however, is negligible. These results suggest that the enhancement technique influences the frequency of relatively shorter lineaments and has no effect on longer lineaments. This may be due to the high visibility of large scale features and hence they are visible within most of the images investigated.

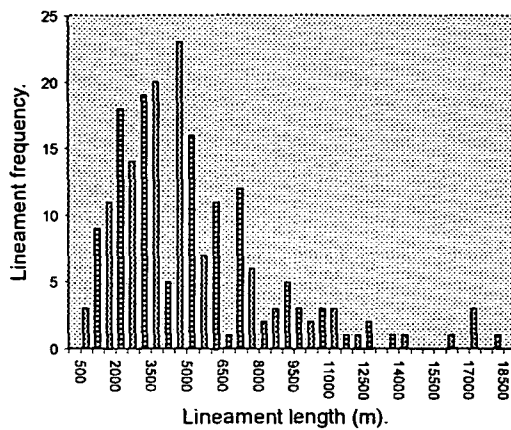
a) Linear stretch, band 1



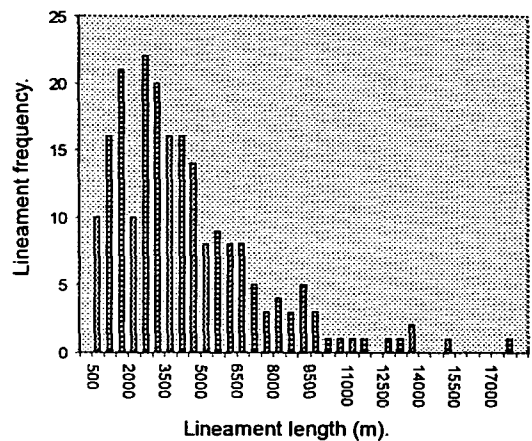
b) Linear stretch, band 5



c) FCC (bands 5,4,1)



d) FCC (bands 7,5,4)



e) Edge enhanced, band 5

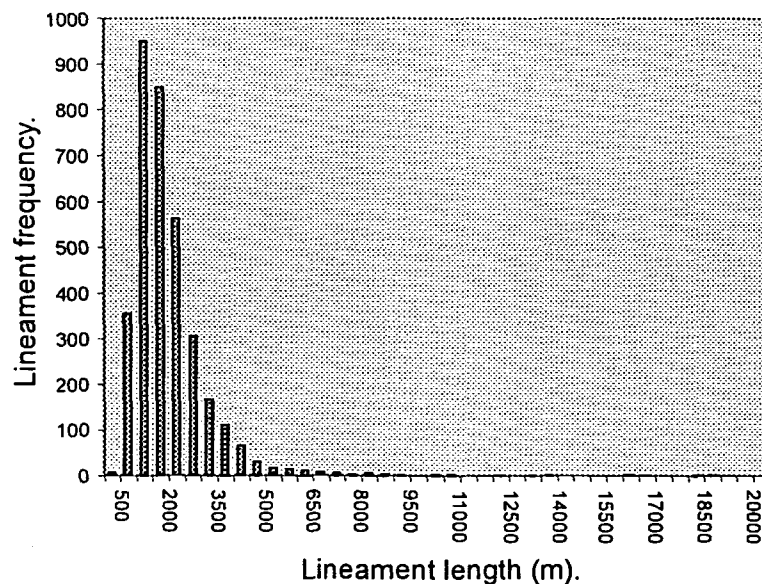


Fig. 3.24. Examples of frequency distribution plots of the length of lineaments interpreted from Landsat TM images of scene 1. Images which the lineaments are interpreted from are: a) a linear stretched, band 1 image; b) linear stretched, band 5 image; c) full colour composite of bands 5, 4 and 1; d) full colour composite of bands 7, 5 and 4; and e) directionally enhanced, band 5 image.

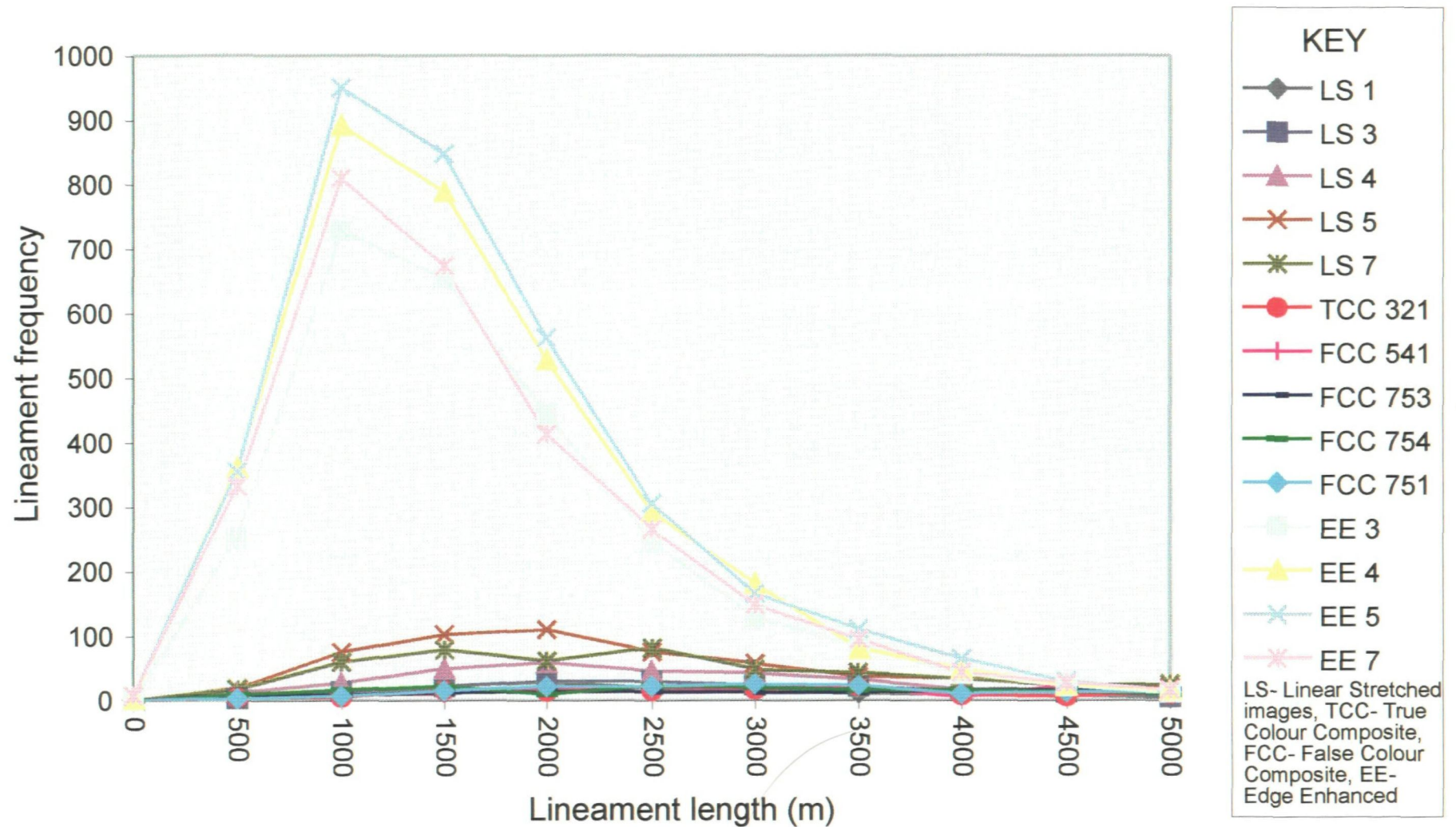


Fig. 3.25. Plot showing the effect of image enhancement technique and band number on the frequency of lineaments interpreted from scene 1, for lineament with lengths up to 5000m. The enhancement techniques and band numbers used for the interpretation of lineaments are illustrated in the key.

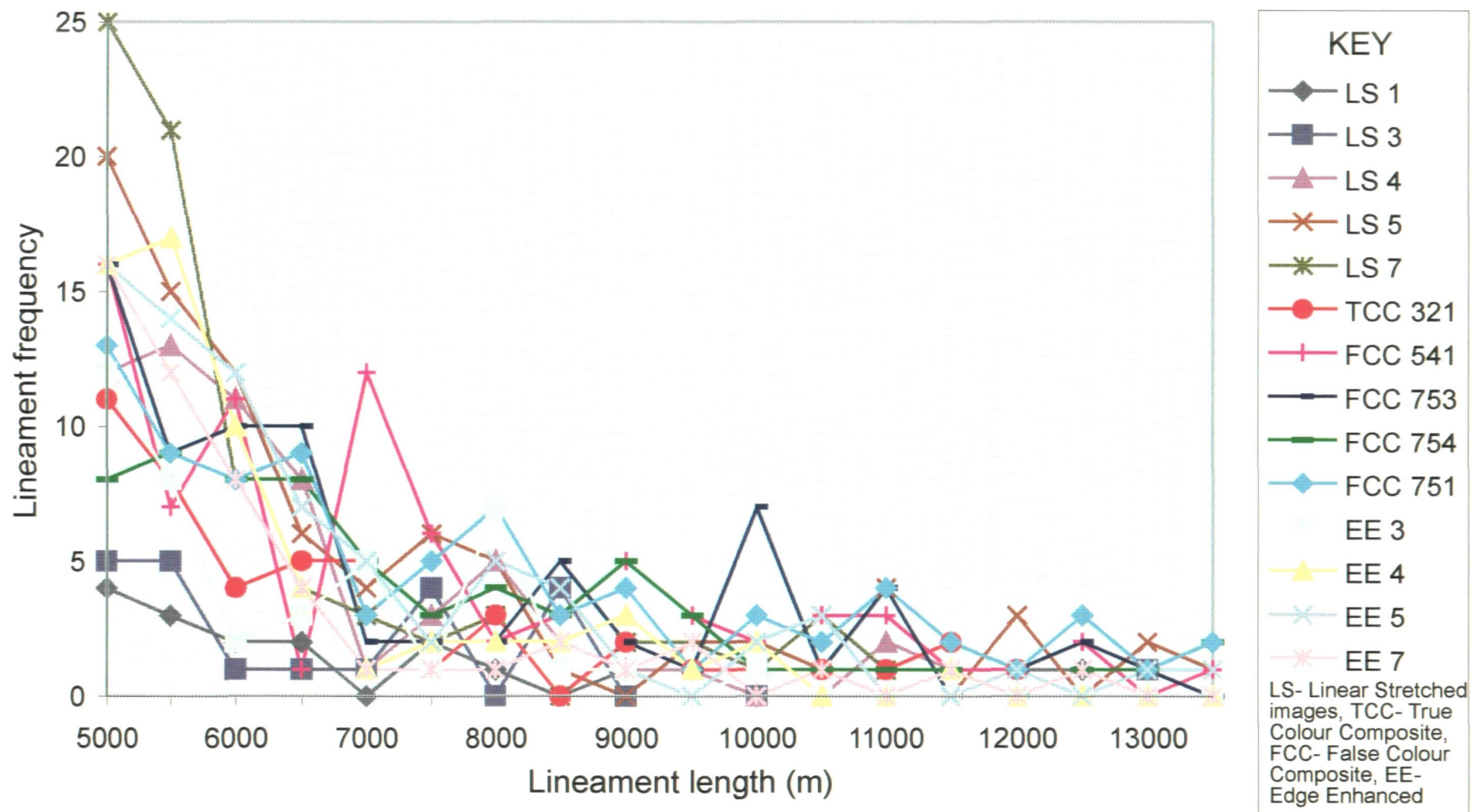


Fig. 3.26. Plot illustrating the effect of image enhancement technique and band number on the frequencies of lineaments between the lengths of 5000m to 13000m for lineaments interpreted from images of scene 1. The enhancement techniques and band numbers used for the interpretation of lineaments are shown in the key.

As the frequencies of longer lineaments are similar, this indicates that the higher frequencies gained from interpreting lineaments from edge enhanced images were not derived from longer lineaments.

The degree of positive skewness was analysed by Fisher's measurement of skewness. The relative frequency of shorter lineaments can be correlated to values obtained from the measurements of skewness: high frequencies produced values of ~ 4.1 (for lineament populations interpreted from edge enhanced images); low frequencies produced measurements of ~ 2.6 (for lineament populations interpreted from linear stretched images); and very low frequencies produced measurements of ~ 1.45 (for lineament populations interpreted from FCC's). The maximum lineament length can also influence the obtained measurement of skewness. For most of the lineament populations the maximum lineament length is $\sim 19000\text{m}$. This relates to a lineament caused by the Brushford fault (see Sections 2.3.5, 4.3.2(iv)). The actual length of the same lineament in the final composite lineament map was 22308m . Analysis of the maximum lineament length for lineaments show that large deviations occurred only in the lineament populations interpreted from images of bands 1 and 3 with a linear contrast stretch applied, which were shorter, and the FCC (7,5,1), which was longer. Bands 1 and 3 had lower maximum lineament lengths because only parts of the fault caused linear feature was interpreted, hence, forming lower measurements of skewness. The long lineament in the FCC (7,5,1) was formed by two long lineaments representing two segments of the same fault forming an outlier and resulting in a higher measurement of skewness not typical of a population interpreted from a FCC. The degree of skewness in a population can therefore be used comparatively to gauge the degree of geological information

obtained by each processing technique. In general the higher degree of skewness the greater the degree of obtained geological information.

Image enhancement applied	Band number	Number of lineaments identified	Maximum lineament length	Fisher's measurement of skewness of lineament lengths
Linear stretch	1	143	12743	2.2
Linear stretch	3	192	15079	2.45
Linear stretch	4	366	18501	2.59
Linear stretch	5	622	21460	2.76
Linear stretch	7	533	19195	2.66
True colour composite	(3,2,1)	154	17887	2.01
FCC	(5,4,1)	207	18078	1.51
FCC	(7,5,1)	223	33897	3.04
FCC	(7,5,3)	195	18748	1.44
FCC	(7,5,4)	211	17819	1.46
Simple (3x3) directional filter	3	2648	18098	3.59
Simple (3x3) directional filter	4	3262	19747	4.13
Simple (3x3) directional filter	5	3477	18537	4.39
Simple (3x3) directional filter	7	2872	19462	4.19

Table 3.3. Statistics of the results of the lineament populations obtained from different image processes and bands.

In summary, the distributions of the lengths of all sample lineament populations are positively skewed and lineaments interpreted from images with linear contrast stretches and directional filters applied are more frequent than lineaments interpreted from FCC's. This is caused by the interpretation of higher frequencies of shorter lineaments and not by fewer longer lineaments. Landsat TM bands 4, 5 and 7 in comparison to TM bands 1 and 3 also produced higher frequencies of shorter lineaments, while band 5 produced the highest frequencies of shorter lineaments. This indicates that the image enhancement processes of linear contrast stretching and directional edge enhancements on images of bands

4, 7 and especially 5, would produce the largest amount of geological information. On this basis, to reduce the amount of time needed to create a lineament map from Cornwall and West Devon (scene 2), lineaments were only interpreted from images of bands 4, 5 and 7 with linear stretches and directional filters applied. To avoid computer memory problems the very large image of West Devon and Cornwall was split into three sub-scenes: West Cornwall (scene 2a); North-East Cornwall (scene 2b); and (scene 2c) South-East Cornwall and South Devon (Fig. 3.21). Scene 2, when mentioned in the remaining sections, therefore, refers to the sub-scenes 2a, 2b and 2c.

The lineament interpretation of each individual image took up to a day (stage 2, Fig 3.22), a large amount of time therefore is needed to complete a composite lineament map of image 1. It was found that lineaments which did not form lineament zones were predominantly composed of lineaments interpreted from images of bands 1 and 3 (see above). Hence, a composite lineament map of scene 2 was instead 'built up' by extending an initial lineament map (Fig. 3.27), thus reducing the time taken to interpret a scene. Analysis of the lineament populations identified from scene 1 suggested that images in band 5 yielded the highest number of lineaments and were proportionally the longest. Consequently, lineaments interpreted from an image of band 5 with a linear contrast stretch applied was used to provide the initial lineament map for scene 2. Linear contrast stretched and directionally enhanced images of bands 4, 5 and 7 were then superimposed over the base map allowing further lineaments to be added or existing lineaments to be modified (increased in length). To ameliorate any bias in the lineament trends which could be formed by directional filters (Professor D. Sanderson, pers. com. 1994) the base lineament map was used as a guide during the interpretation of directionally enhanced images.

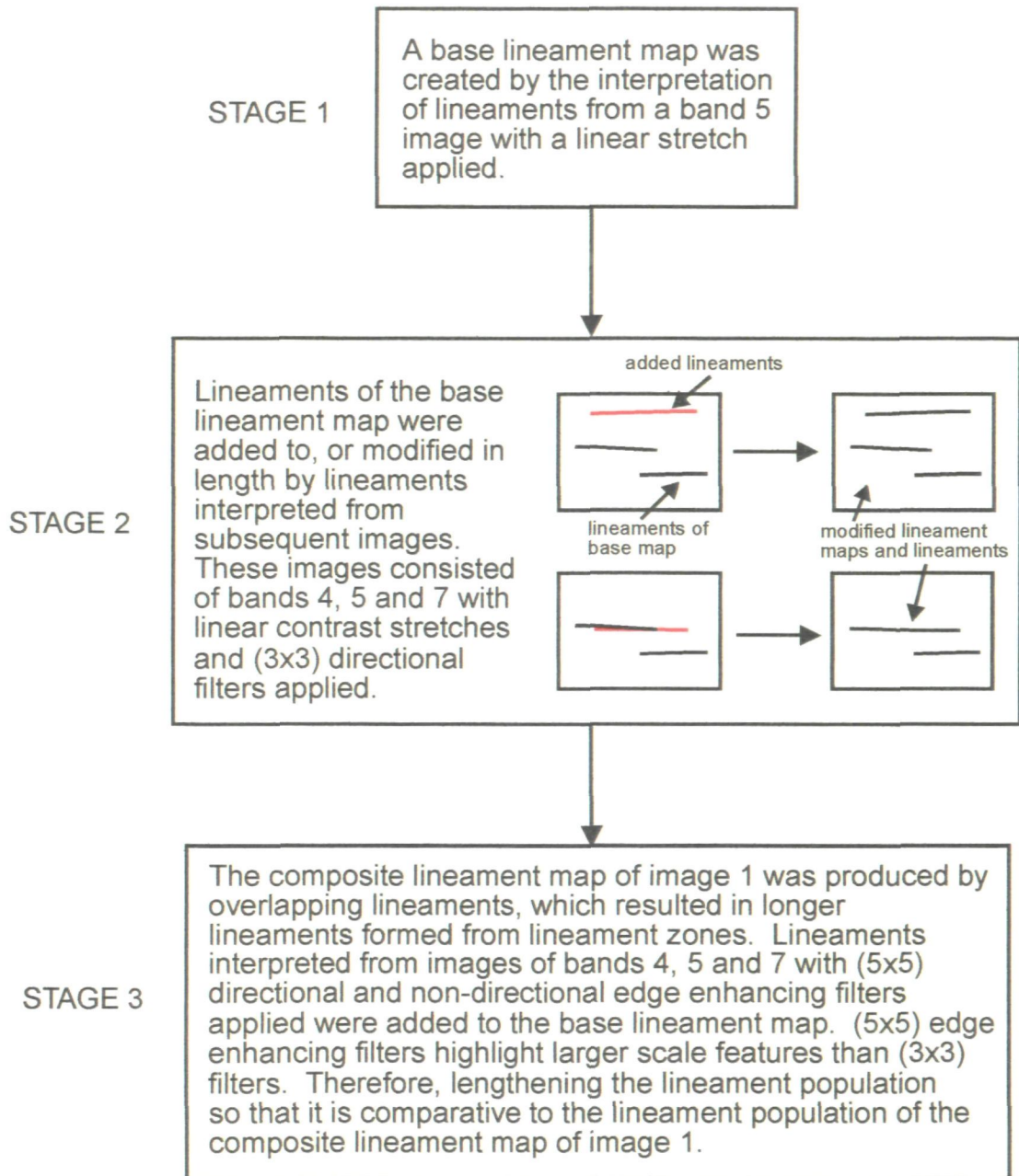


Fig. 3.27. The stages undertaken to form the composite lineament map of scene 2.

To avoid re-interpreting images of scene 1, the lineament maps from scene 1 were compared to scene 2 to identify any differences in the lineament populations. The construction of the composite lineament map of scene 1 produced longer lineaments by amalgamating lineament zones into lineaments. To compensate for this in scene 2, lineaments were interpreted from images enhanced with 5x5 directional and non-directional filters. Larger filters have the effect of enhancing larger scale features while linear features smaller in scale become merged together, hence, lineament length is extended (Section 3.3.3) (Fig. 3.15c). As lineaments interpreted from lineament zones in scene 1 consisted of lineaments predominantly identified from bands 4, 5 and 7, similar to the bands used for scene 2, the effect of lengthening lineaments by forming the composite lineament map of scene 1 were compensated for by using image processing techniques in scene 2. The lineament populations of the two scenes therefore should have similar properties irrespective of the two lineament analysis methods used.

3.7 Combining overlapping lineaments maps interpreted from images of Cornwall and Devon

The result of analysing an area which is covered by different satellite passes or separate sub-scenes (Fig. 3.21) is that a higher density of lineaments may be generated due to overlapping of separately interpreted lineament maps. Hence, overlapping images can create duplicate lineaments with analogous length and trend from single geomorphological features. Visual analysis of the images and lineament maps of the different scenes showed that displacements may occur between the same linear features on different images. This was caused by small inaccuracies in the geometric correction of the images (see

Section 3.3.1). When no displacement occurred between the lineament populations duplicate lineaments were re-digitised as single lineaments. Displaced duplicated lineaments could, however, be confused as representing two different linear features with similar azimuths and lengths. Analysis of both images and the relative spatial displacements of surrounding lineaments were utilised to identify related displaced duplicated lineaments. Related displaced duplicate lineaments were corrected by visually re-digitising the lineaments as a lineament which best described the displaced lineaments. This was achieved by visually estimating the differences in the lineament displacements.

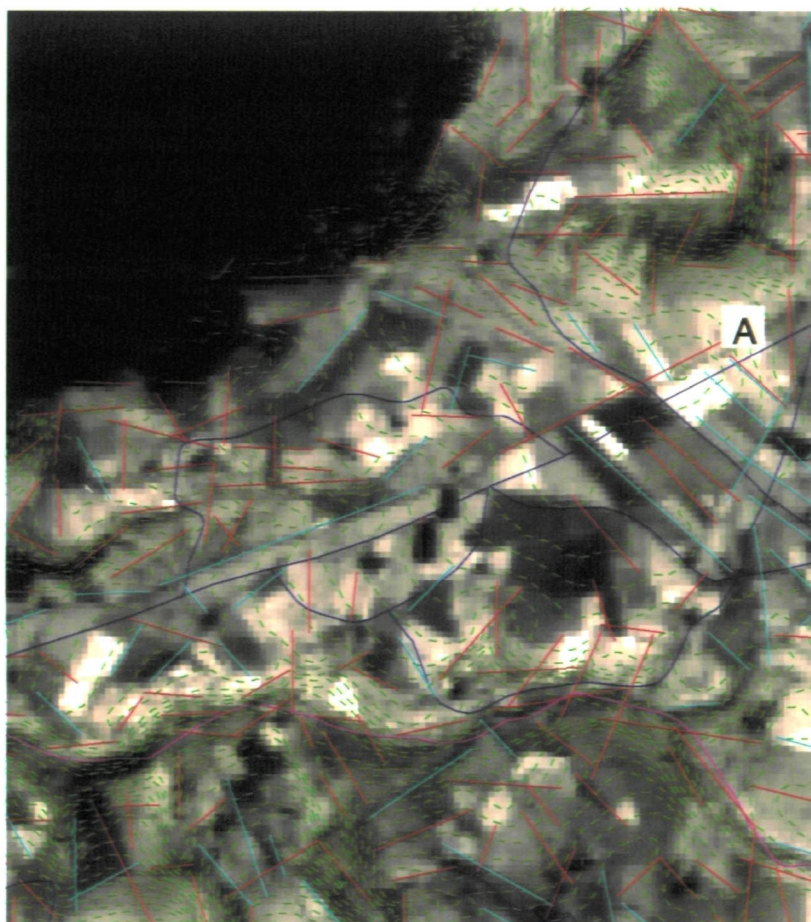
3.8 Image processing techniques of higher resolution images

Scene 3 (Fig. 3.21) covering a small area of North Cornwall was examined in order to investigate the effects of increasing resolution on lineament analysis. For the area, the 150m resolution lineament map of scene 2b created during the regional lineament analysis was compared with those interpreted at 120m, 90m, 60m and 30m. Images with resolutions of 120m, 90m, and 60m were formed by degrading 30m resolution images of scene 3 (see Section 3.3.2). Anthropogenic features within SW England become visually apparent in images with resolutions higher than 150m (see Section 3.4). Landsat TM band 4 images in comparison to bands 5 and 7 exaggerate the visual impact of anthropogenic features (Drury 1986). Therefore with high resolution Landsat TM images lineaments were not interpreted from this band. Lineament maps of North Cornwall were interpreted by the same processing techniques and lineament analysis methods used for compiling lineament maps of scene 2 (Section 3.6).

3.8.1 Knowledge based rules for the removal of anthropogenic lineaments from lineament maps

In 150m resolution images only linear features relating to natural objects are visible using the image processing techniques described in Section 3.6. Increasing image resolution has the effect of exaggerating the visual impact of anthropogenic features. To obtain a sample of lineaments that are more likely to be related to geomorphological features, an additional step in the processing technique was applied. As described in Section 2.6.1, bedrock geology can form topographic features from which lineaments may be interpreted. Within the study area there is sufficient variance in relief to allow comparison between lineament maps and topography. Using this information two knowledge based rules were devised to determine which lineaments were interpreted from anthropogenic features:

(i) Lineaments that show little relationship to topographic features and a strong relationship to anthropogenic features are considered to be formed by anthropogenic features. To identify lineaments within the lineament map which were caused by infra-structure, digitised road and elevation maps were superimposed over the final lineament maps at each resolution using a GIS. Lineaments identified as part of the infra-structure that cross-cut topography were identified and removed. Images with a resolution of $\leq 120\text{m}$ were also found to contain lineaments relating to field boundaries. To identify the contribution these made to the lineament maps, lineament maps were compared to contour maps of elevation data, and the highly visible field patterns on a 30m resolution image in Landsat TM band 4 (Fig. 3.28). Lineaments that were found to correlate to identifiable field boundaries but not topography were removed from the maps (Fig. 3.29a).



- 10m elevation contours
- Main road network
- Main river system
- Original lineament pattern
- Corrected lineament pattern



0Km 1Km

Fig. 3.28. Example of the process used in the removal of anthropogenic features in the lineament pattern interpreted from 30m resolution, Landsat TM images of North Cornwall. Lineaments interpreted as anthropogenic features are identified by the spatial correlation to objects in the background image and the digitised road network. The background image is a 30m resolution, linear stretched band 4 TM image. The lineament highlighted as A, indicates the problem in determining if the feature interpreted represents an anthropogenic or natural object, caused when both have similar trends.

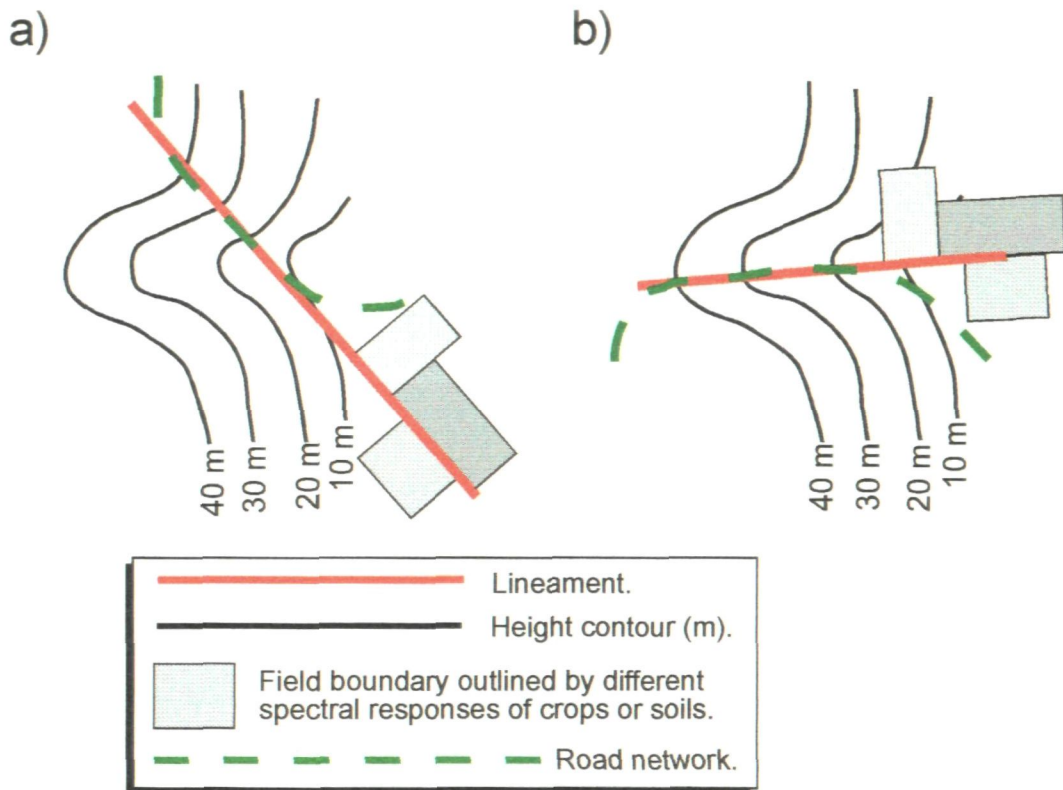


Fig. 3.29. Cartoon diagram showing the identification of anthropogenic related lineaments, and geological related lineaments. Diagram a) shows lineaments which were found to be caused by anthropogenic linear features, and cross-cut relief. These lineaments were removed from the lineament population. Diagram b) shows a lineament which could have been caused by relief or anthropogenic linear features, and hence would remain in the lineament population.

(ii) Anthropogenic linear features may, however, also follow natural geomorphological features such as crests and valleys, therefore it may be difficult for the analyst to determine if the interpreted linear features are caused by anthropogenic or geomorphological features. Consequently, lineaments that possessed both properties but had dissimilar lengths to the anthropogenic features suggesting dissimilar causes were included in the final lineament maps (Fig. 3.29b).

The numbers of lineaments interpreted to relate to anthropogenic features and therefore removed from the lineament sample populations are shown in Fig. 3.30. Increasing numbers of lineaments relating to anthropogenic features were identified from higher resolution images. The visual impact of anthropogenic features in images with a resolution of 150m is negligible as denoted by the flat trend to the graph in Fig. 3.30.

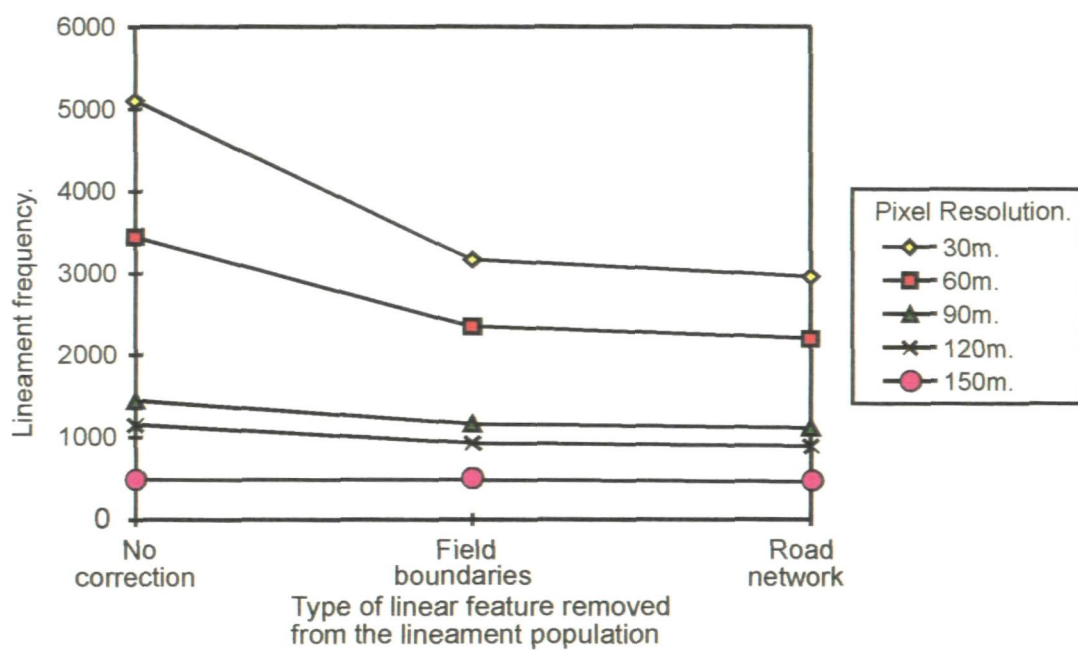


Fig. 3.30. Line graph illustrating the effect image resolution and linear anthropogenic features have on the number of lineaments in the final composite lineament maps of North Cornwall.

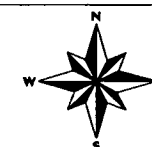
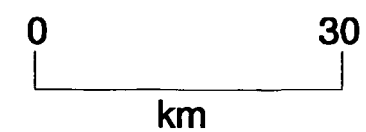
3.9 Regional lineament patterns across SW England

A final compilation regional map of lineaments interpreted from images with a resolution of 150m is shown in Fig. 3.31. The total number of lineaments interpreted was 6482, with a total lineament length of 13413409m giving an average length of 2069m. A frequency/length plot forms a positively skewed distribution (Fig. 3.32). Using Fisher's measurement of skewness the distribution produces a value of 3.65 and suggests higher frequencies of smaller lineaments in the population.

A rose diagram illustrating the frequency of lineament trends (Fig. 3.33) suggests four main lineament trends; a dominant E/W trend and three relatively minor sub-trends along N/S, NE/SW and NW/SE azimuths. Petals trending N/S and E/W are observed to have small azimuth arcs, while NE/SW and NW/SE trending petals have broader distributions. Within this study lineaments divided from a lineament population using systematic division boundaries (e.g. rose diagrams) are termed *lineament groups*.



Fig. 3.31. Lineament map interpreted from 150m resolution Landsat TM images of SW England.



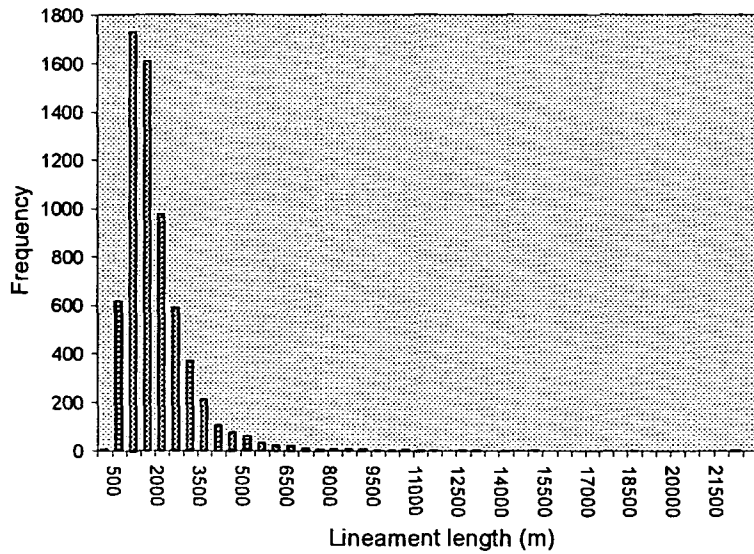


Fig. 3.32. Graph showing the frequency distribution of the length of lineaments interpreted from images of SW England.

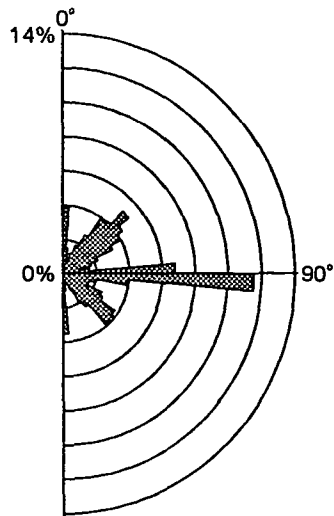


Fig. 3.33. Rose diagram illustrating the trends of lineaments (per 5° intervals) interpreted from images of SW England.

Different areas of SW England have undergone different geological histories forming lithotectonic domains with different lithotectonic trends (see Chapter 2). To be able to analyse the spatial distributions of lineaments within the different lithotectonic domains it is therefore necessary to sub-divide the regional lineament map. The regional lineament map was sub-divided into $(20\text{km})^2$ cells. Cells which were only partly-filled or contained low numbers of lineaments were combined, this resulted in the division of the regional lineament map into 39 cells. The trends of lineaments within each cell were identified by rose diagrams (Fig. 3.34). The rose diagrams showed that the four main lineament trends (E/W, NE/SW, NW/SE and N/S) identified in Fig. 3.33 have a regional distribution. However, it may be observed that one or more of these four lineament groups may be more, or less dominant (e.g. cell 15). Other cells can show complex trends (e.g. cell 22 centred on the Dartmoor granite); where the typically four large major lineament trends (E/W, NE/SW, NW/SE and N/S) are reduced in size, and are combined with multiple smaller lineaments trends.

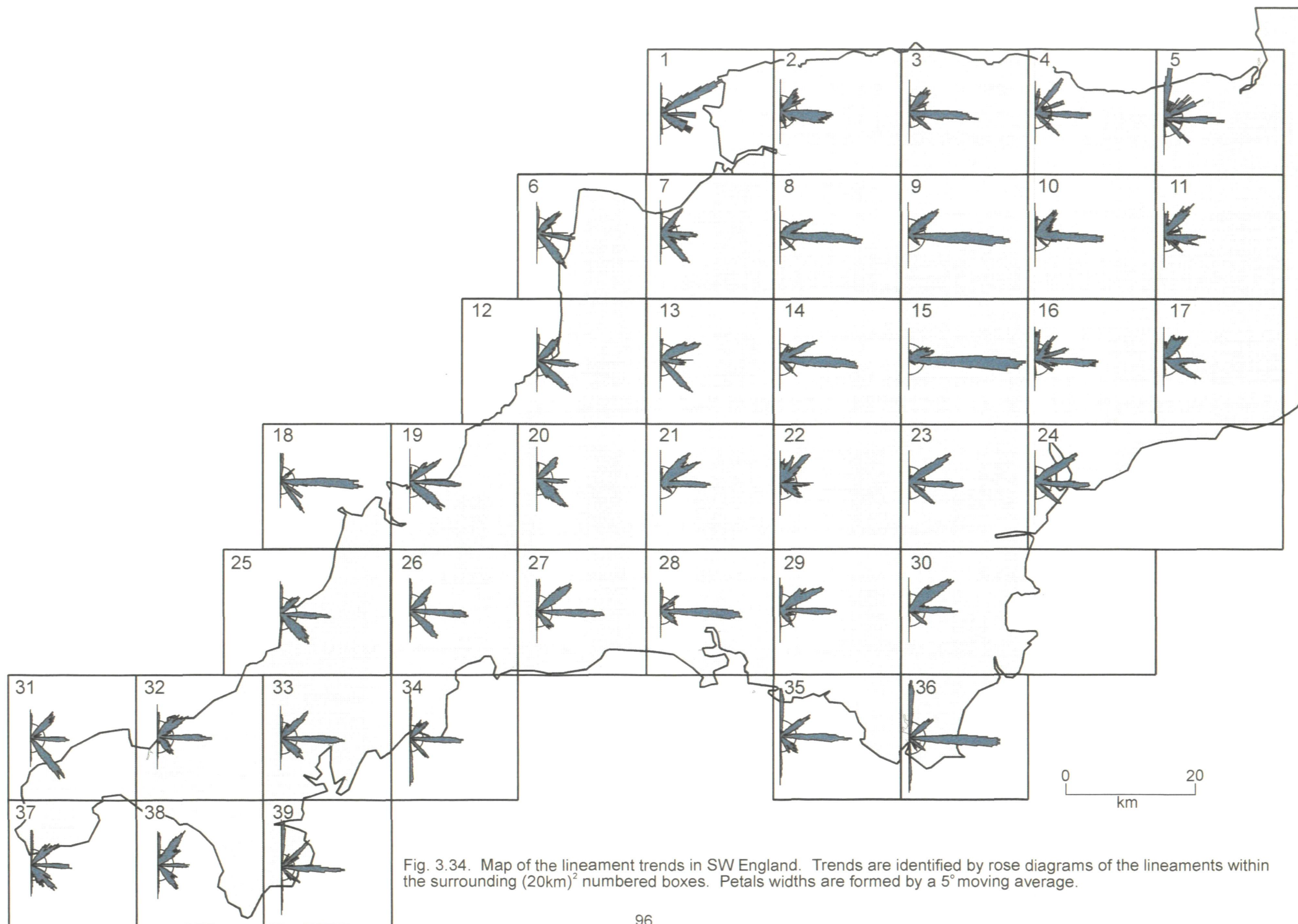


Fig. 3.34. Map of the lineament trends in SW England. Trends are identified by rose diagrams of the lineaments within the surrounding $(20\text{km})^2$ numbered boxes. Petals widths are formed by a 5° moving average.

Furthermore, in some areas extra trends may be observed (e.g. cell 4 to 070°). In order to establish the geological significance of these variations from an arbitrary grid structure, adjacent cells with similar attributes (petal magnitude and trends) were grouped together into larger geographical sub-areas (Table 3.4). This shows that similar lineament patterns can be obtained from adjacent cells up to an area of $(100\text{km})^2$.

These results suggest that the regional lineament map could be divided into different lineament groups by analysis of the lineament trends. However, rose diagrams only show broad differences in lineament trends and results in obscuring minor trends. Also the arbitrary division of data may result in a geologically insignificant division of data when a boundary between different lineaments caused by dissimilar geological structures lies within a lineament group. Differences in the trends of lineaments throughout the region and the disappearance of some of the major trends in the cells also suggests that directional filters do not produce a bias in lineament trends. This is because a consistent distribution of lineaments trending to the E/W, N/S, NE/SW and NE/SW, corresponding the filter directions would be expected across SW England.

Area of SW England covered	Box numbers	Relative magnitudes of the four major lineament trends				Identifiability of lineament trends	Extra lineament trends
		E/W	N/S	NE/SW	NW/SE		
South Devon	35,36	Large	Large	Small	Small	Good	None
South coast of Cornwall	34,39	Medium	Large	Small	Small	Good	None
South Cornwall	25,26,32,33,38	Medium	Medium	Medium	Small-Medium	Good	None
Lands' End	31,37	Medium	Medium	Medium	Large	Good	To 160°
Padstow (west)	18	Large	Medium	Small	Large	Good	To 157°
Whitsand Bay	27,28	Large	Medium	Small-Medium	Small	Good	None
South East Devon	23,24,29,30	Medium	Small	Large	Small	Good	To 40°
Milton Abbot	21	Medium	Small	Large	Small	Medium	To 60°
Padstow (east)	19	Medium	Medium	Medium	Large	Good	To 40°
Dartmoor	22	Small	Small	Medium	Small	Poor	To 22°
North Cornwall	6,7,12,13,20	Small-Medium	Medium	Medium	Large	Good	To 41°, 70°
Croyde	1	Small	Medium	Large	Small	Good	To 120°
North Devon	2,3	Large	Small	Small-Medium	Small	Good	To 110°
Chulmleigh	8,9,10,14,15	Very large	Not present-Small	Small-Medium	Not present-Small	Good	To 70°
Brendon Hills and Cullompton	4,16	Large	Medium	Medium	Small-Medium	Good	To 70°
Quantock Hills	5	Large	Large	Medium	Medium	Good	To 70°
Blackdown Hills	11,17	Medium	Medium	Medium-Large	Small	Good	To 20°, 110°, 120°

Table 3.4. Table indicating regions (identified from rose diagrams in Fig. 3.37) of SW England which possess similar lineament trends.

3.10 Lineament populations of North Cornwall

To investigate the effect of resolution on the lineament populations of North Cornwall a series of composite lineament maps were interpreted of the area from images with resolutions of 150m, 120m, 90m, 60m, 30m. These maps are shown in Figs. 3.35, 3.36, 3.37, 3.38 and 3.39, respectively. A basic statistical treatment of the lineament populations suggests a simple relationship between number of lineaments, lineament length and resolution (Table 3.5).

Image resolution (m)	Number of lineaments	Total lineament length (m)	Average lineament length (m)
150	447	764831	1711
120	889	894248	1005
90	1114	1103005	990
60	2195	1484639	676
30	2957	1285910	434

Table 3.5. Statistics of lineament populations interpreted from TM images of North Cornwall.

In general, with increasing image resolution the number of lineaments interpreted increases, whilst the mean lineament length decreases. The total length of the lineaments interpreted, however, increases with increasing image resolution to 60m, and then drops with the 30m resolution population. These statistics can suggest that either a greater amount of geological information was obtained as more lineaments were interpreted, or a smaller amount of geological information was obtained as the mean lineament length decreased. Areas within the 30m resolution lineament map contain relatively low lineament concentrations where lineaments were previously identified in lower resolution images. This may be further evidence that the processes used to identify lineaments have produced smaller amounts of geological information.

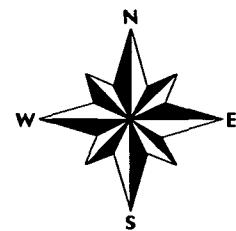
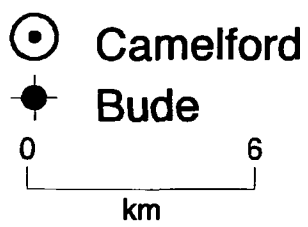
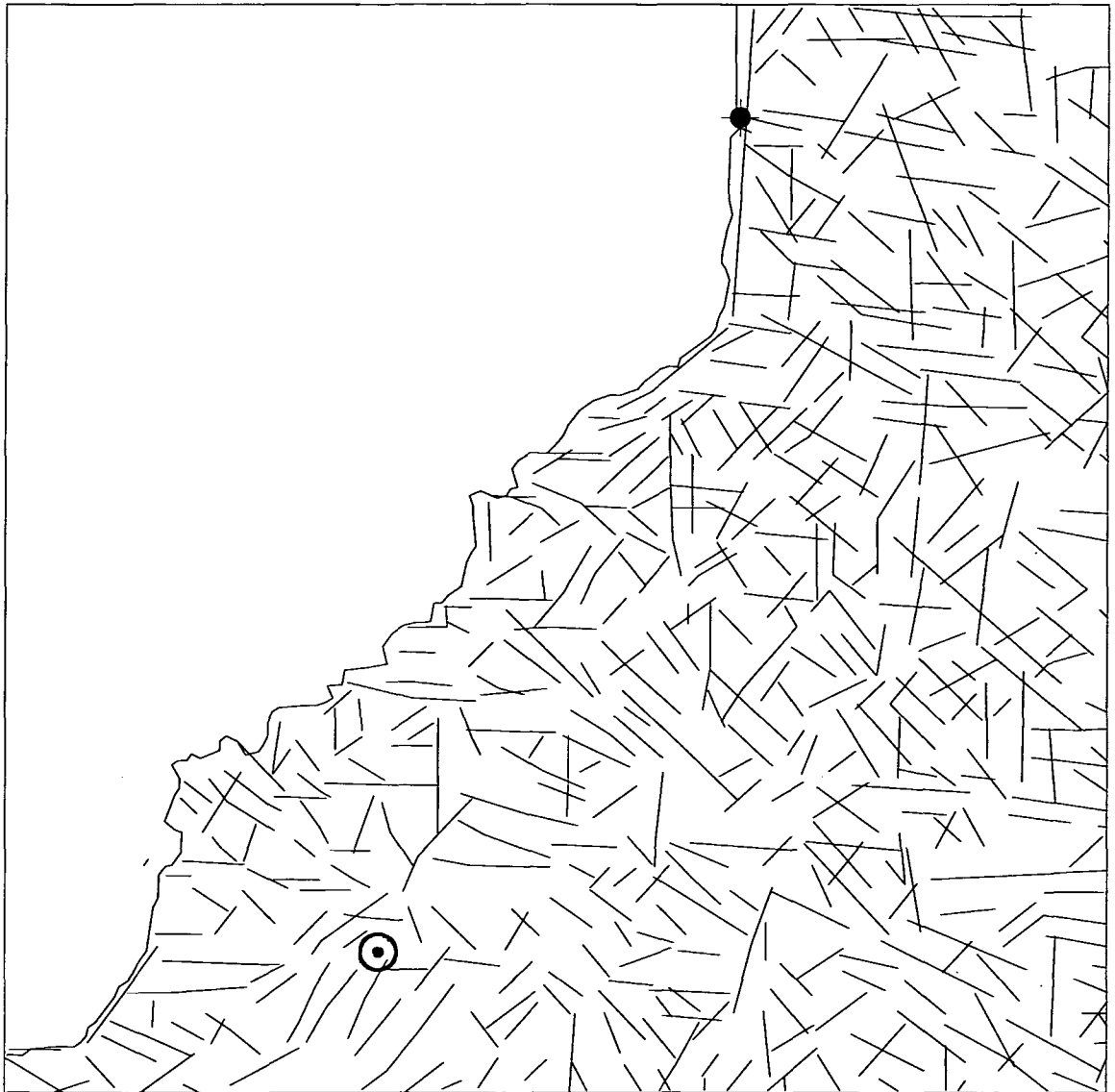


Fig. 3.35. Lineament map interpreted from 150m resolution Landsat TM images of North Cornwall.

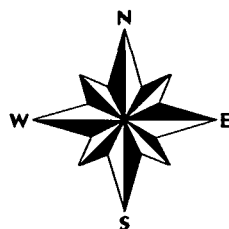
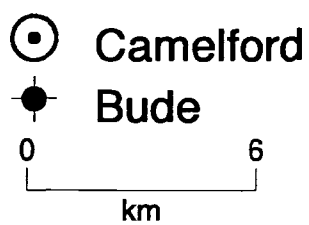
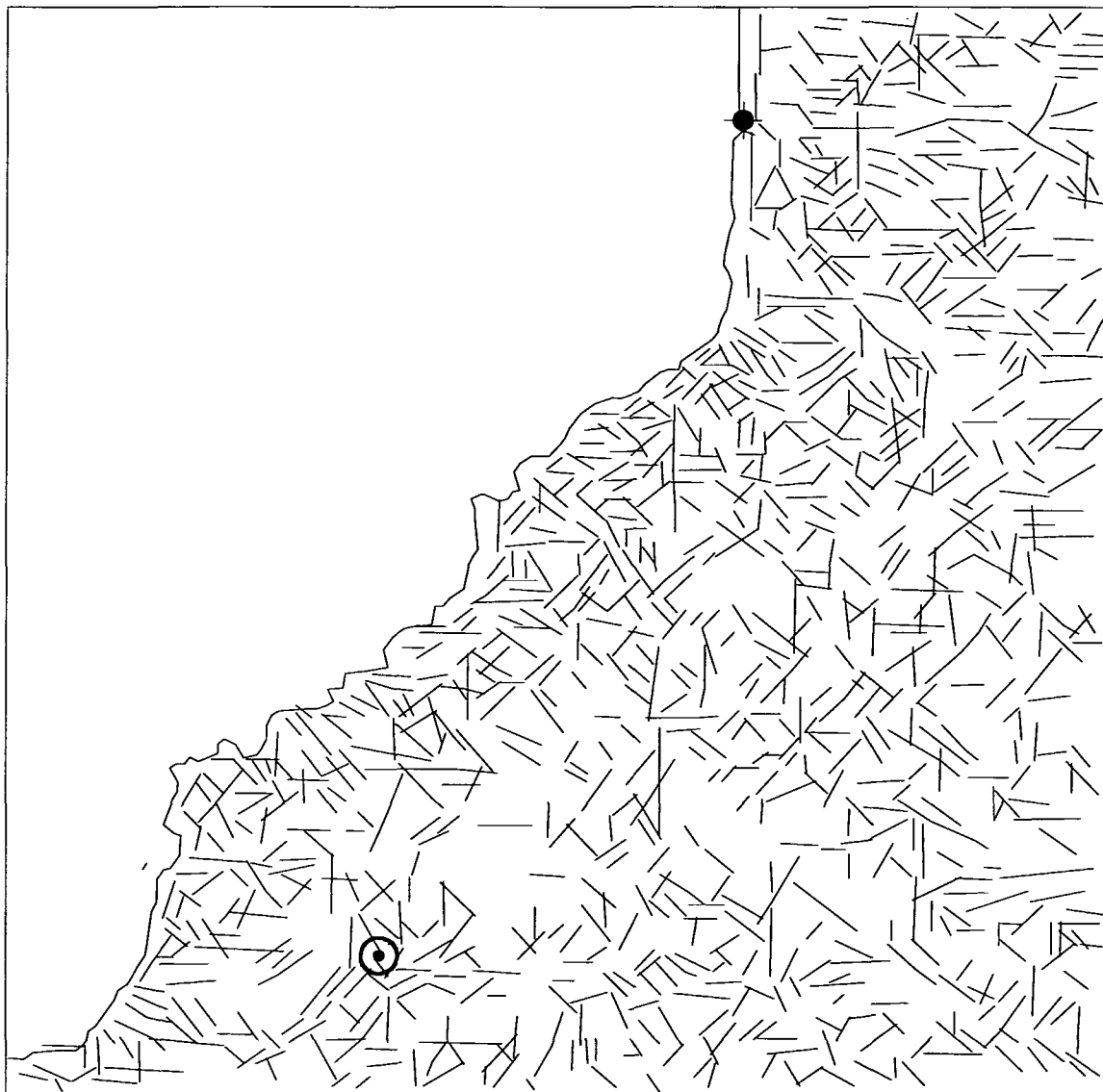


Fig. 3.36. Lineament map interpreted from 120m resolution Landsat TM images of North Cornwall.

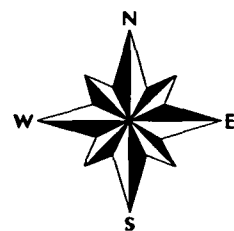
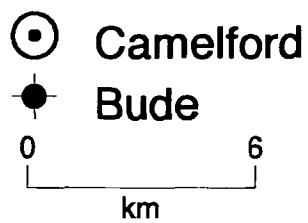
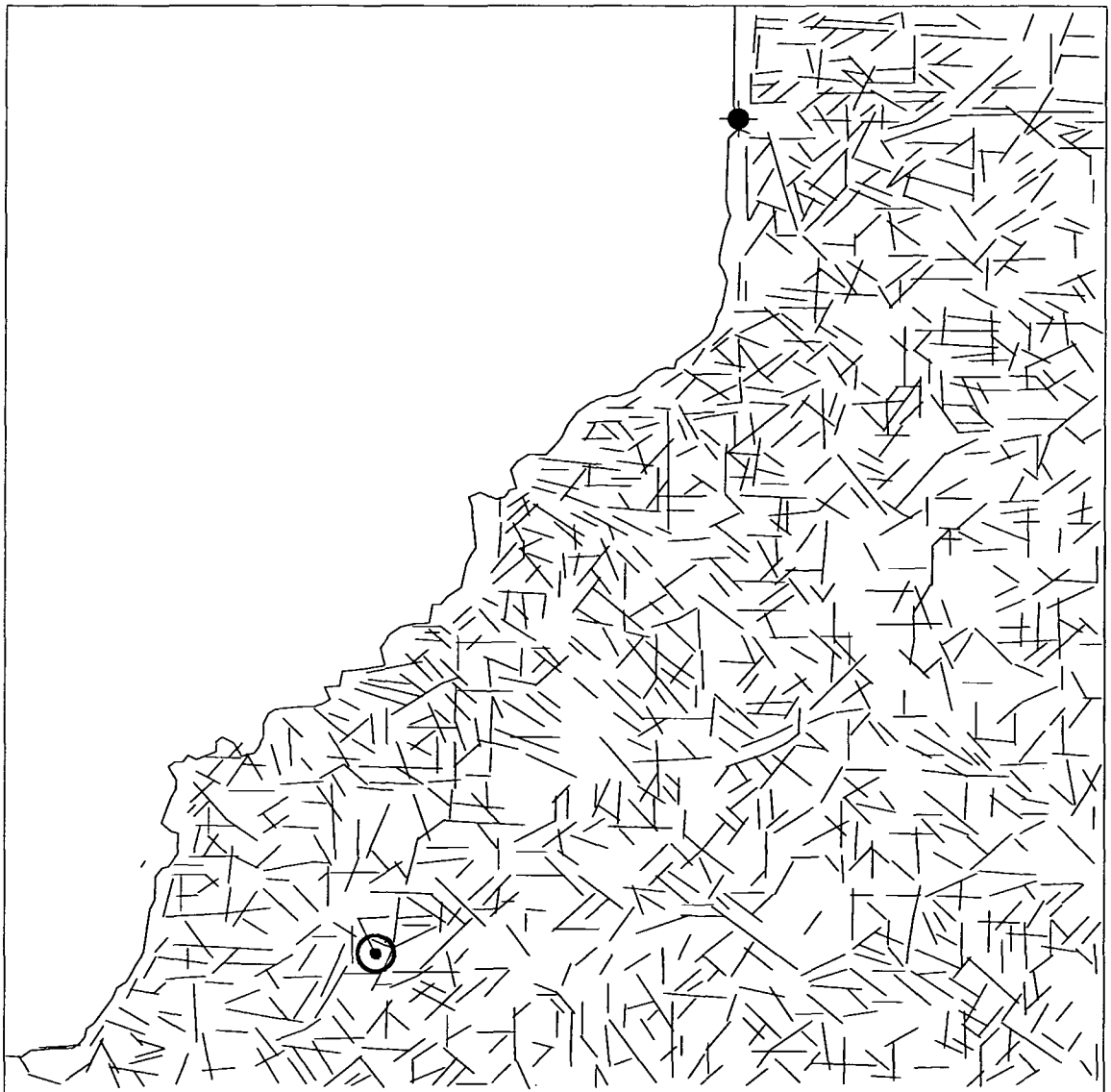


Fig. 3.37. Lineament map interpreted from 90m resolution Landsat TM images of North Cornwall.

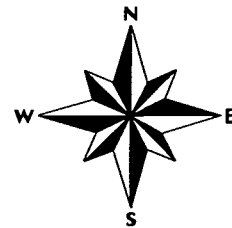
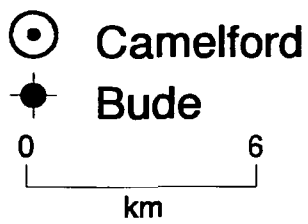
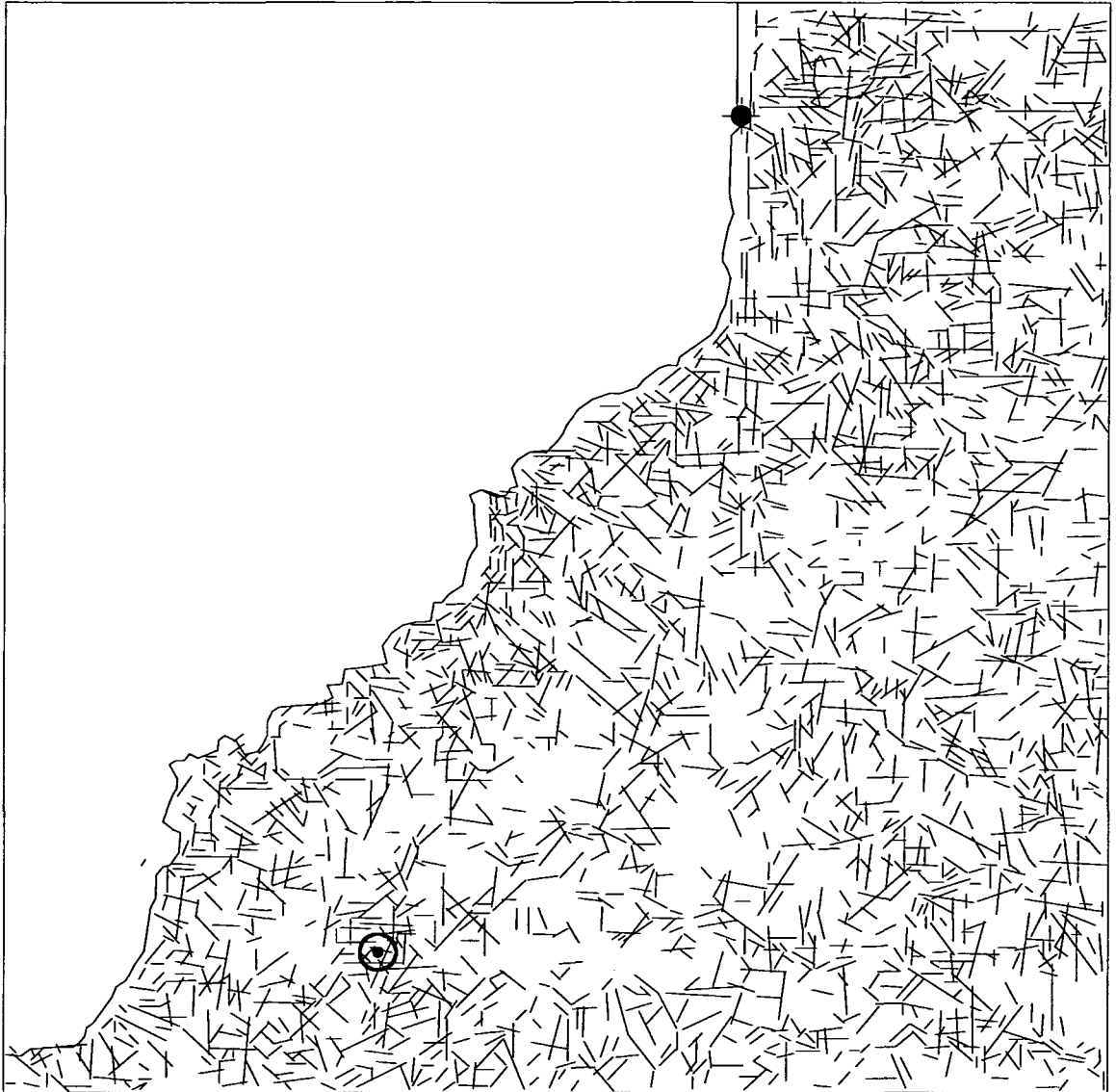
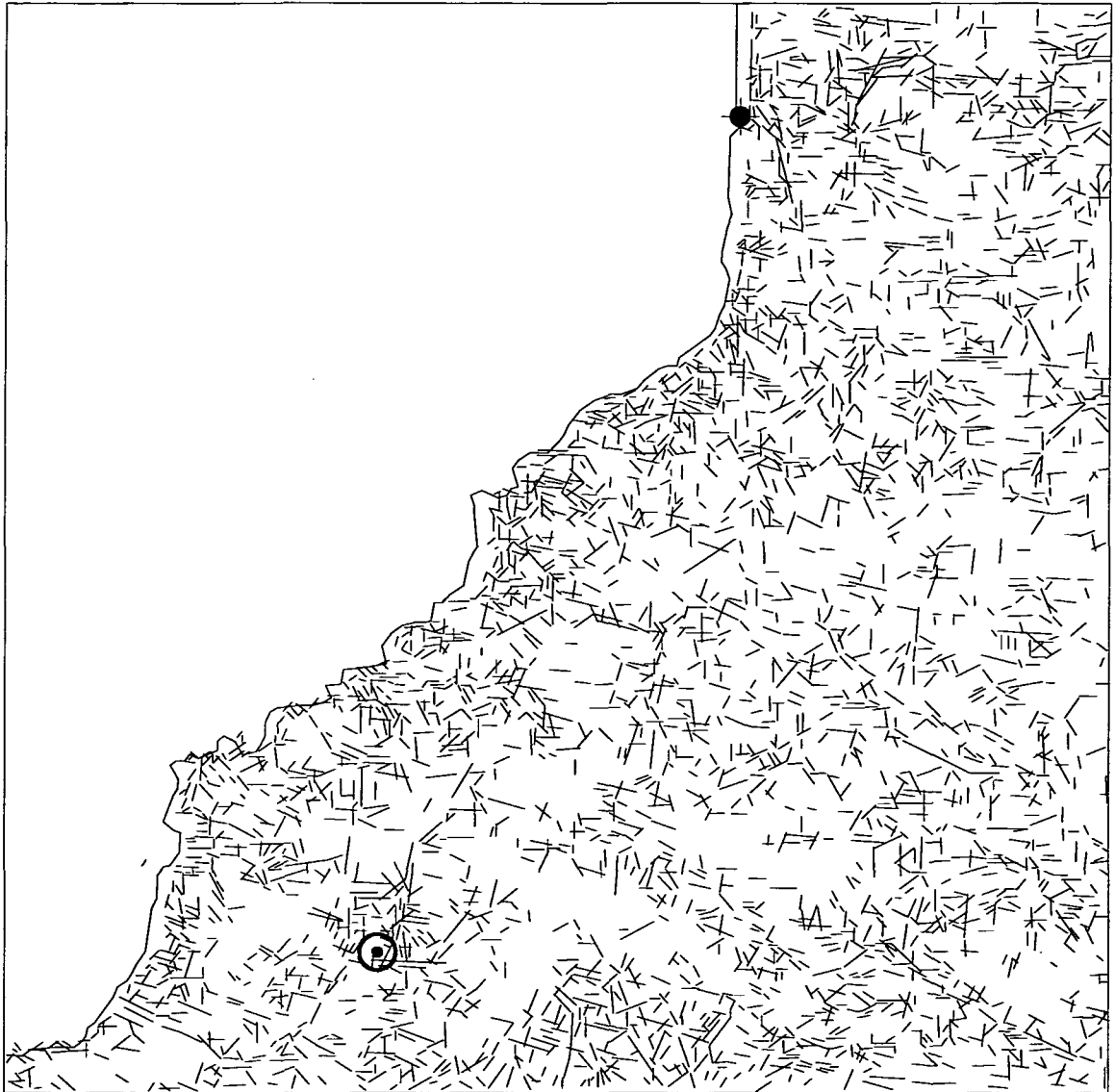


Fig. 3.38. Lineament map interpreted from 60m resolution Landsat TM images of North Cornwall.



⊙ Camelford

● Bude

0 6
km

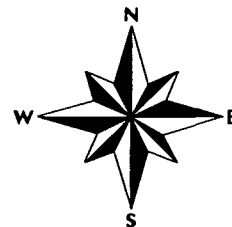


Fig. 3.39. Lineament map interpreted from 30m resolution Landsat TM images of North Cornwall.

Furthermore, relatively similar results have been obtained for the mean lineament length for lineament populations interpreted from images at resolutions of 120m and 90m, where only small differences can be observed.

The effect of increasing image resolution is that smaller differences in reflected EMR are identifiable (see Section 3.4). Therefore, with high resolution images, small as well as large lithotectonic features may be identified. As a result the number of lineaments interpreted at each resolution increases. The mean length of the lineament populations also shows a decrease, the following explanations are possible causes for these relationships:

(i) Small scale geomorphological features become visible in high resolution images which are related to a large scale lithotectonic feature observable in low resolution images, e.g. a large scale fault zone to small scale fault segments. In such a geological example, it may explain how the longest lineaments evident in low resolution become shorter with increasing image resolution. In low resolution images the reflected EMR from numerous similarly trending linear geomorphological features in a fault zone may be combined forming a single long lineament. However, with increasing image resolution the differences in reflected EMR may become discernible forming numerous multiple shorter lineaments. An alternative geological possibility of how longer lineaments become shorter is that in higher resolution images cross-cutting relationships (e.g. E/W trending lithological differences and NW/SE trending faults of North Cornwall) may become identifiable causing the truncation of lineaments representing the earlier lithotectonic feature.

(ii) By the sampling of shorter 'new' geomorphological features produced from scale limited linear lithotectonic features which were previously not observable in low resolution images.

(iii) The 'part-healing' of a geomorphological expression, such as scarp degradation, resulting in the level healed areas producing lower differences in EMR reflection. Low resolution images merge the reflected EMR therefore only large affected areas are observable at such resolutions. Furthermore, the control on the geomorphological expression by small scale lithotectonic features is likely to be relatively weaker in comparison to large scale structures, therefore the part-healing of these features is also more probable on geomorphological features in high resolution images. The effect of the part-healing of linear geomorphological features is that multiple shorter lineaments with similar trends can be interpreted, instead of a single longer lineament.

(iv) The inclusion of lineaments interpreted from smaller linear anthropogenic features in a lineament map. In SW England these anthropogenic features are only observable in images with resolutions above 150m. Most of these linear features, however, have been removed from the lineament maps in the process detailed in Section 3.8.1, hence the effect from anthropogenic features can only be minimal.

Frequency distributions of lineament length over the range of image resolutions are illustrated in Fig. 3.40. All the distributions are positively skewed, Fisher's measurement of skewness of the populations produces values of 2.17, 1.7, 1.57, 1.93 and 2.11 for resolutions of 150m, 120m, 90m, 60m and 30m, respectively.

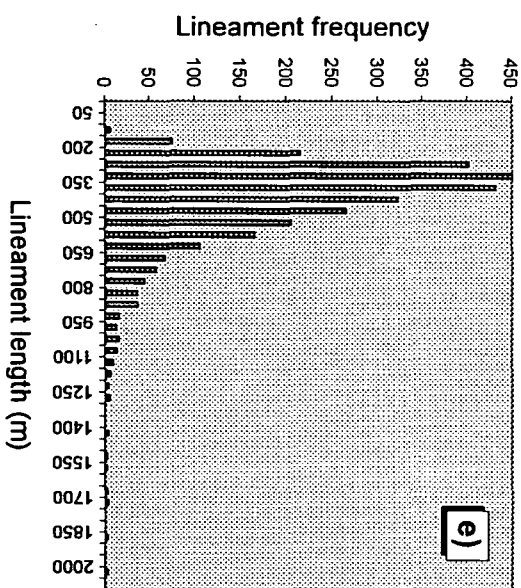
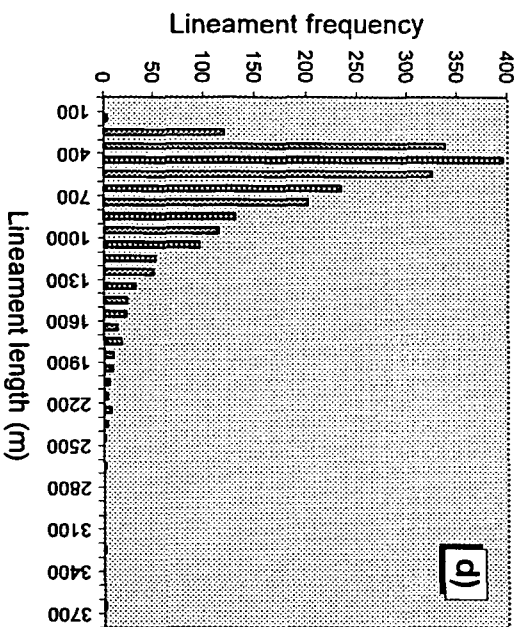
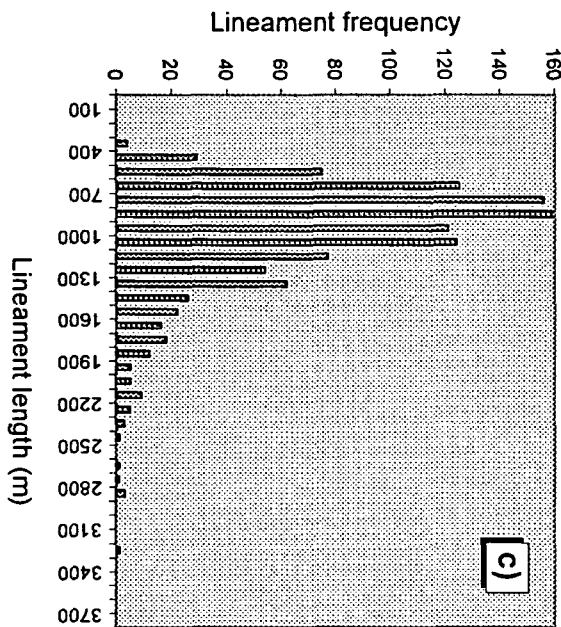
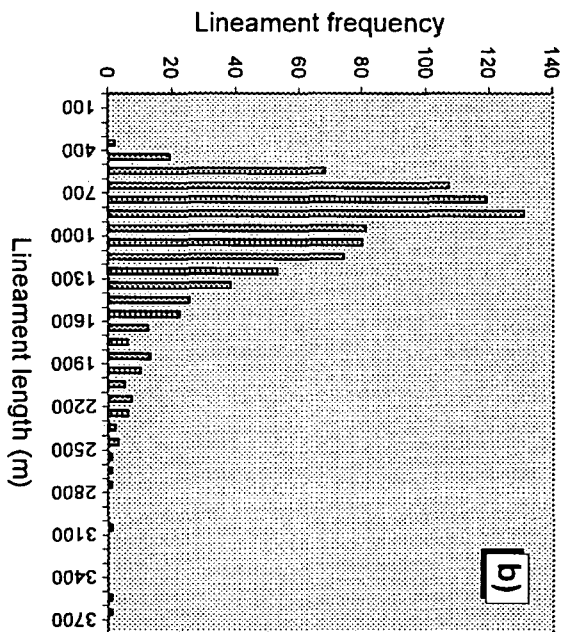
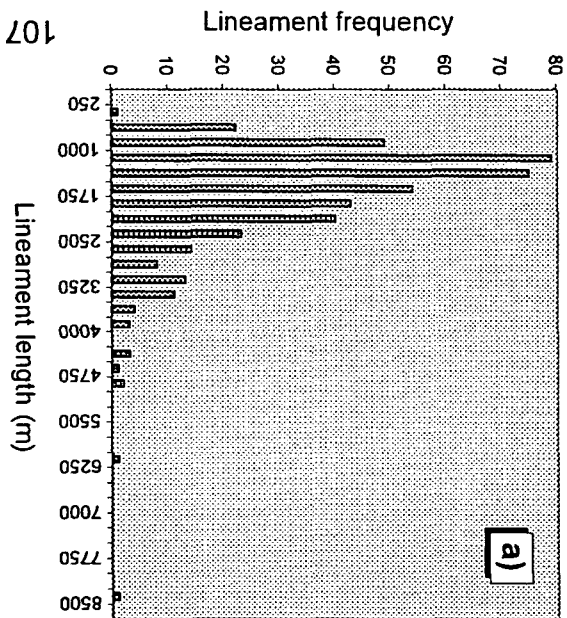


Fig. 3.40. Histograms showing the distribution of lineament lengths interpreted from satellite images of North Cornwall over a range of resolutions, a)=150m, b)=120m, c)=90m, d)=60m and e)=30m.

Positively skewed distributions are obtained for frequency/length distributions from all the lineament populations. These distributions suggest that there are relatively few long linear lithotectonic features to numerous short linear lithotectonic features. The map-scale of images from which these lithotectonic features are interpreted is within the scale range of linear lithotectonic features within SW England (which goes down to the micro-scale, e.g. cleavage), therefore if the scale range of the images were extended, even more shorter lineaments would be interpreted. These lineaments are not interpreted due to a truncation effect caused by under-sampling of short lineaments, a problem common to many remotely sensed sample populations (e.g. Einstein & Beacher 1983, Pickering *et al.* 1995). Truncation occurs when the resolution limit of the image is approached causing short linear geomorphological features to become indeterminable, and therefore a reduction in the frequency of short lineaments.

The effect of resolution on lineament trends is shown in Fig. 3.41. In all the lineament populations, a sharp major E/W, and a sharp relatively minor N/S lineament trend are observed (Fig 3.41). Two further relatively minor lineament trends to the NE/SW and NW/SE exist in the lineament populations interpreted from images with 150m, 120m and 90m resolutions. However, at higher resolutions these degrade into multiple sub-trends ranging between N/S and E/W. These results again suggest that directional filters have little influence on the trends of lineament groups as a consistent distribution of lineaments trending to the E/W, N/S, NE/SW and NW/SE, correlating to the enhanced directions within the images over the resolution range, would be expected.

The rose diagrams suggest that the geological information obtained (identified as new trends) from the lineament maps is similar for resolutions of

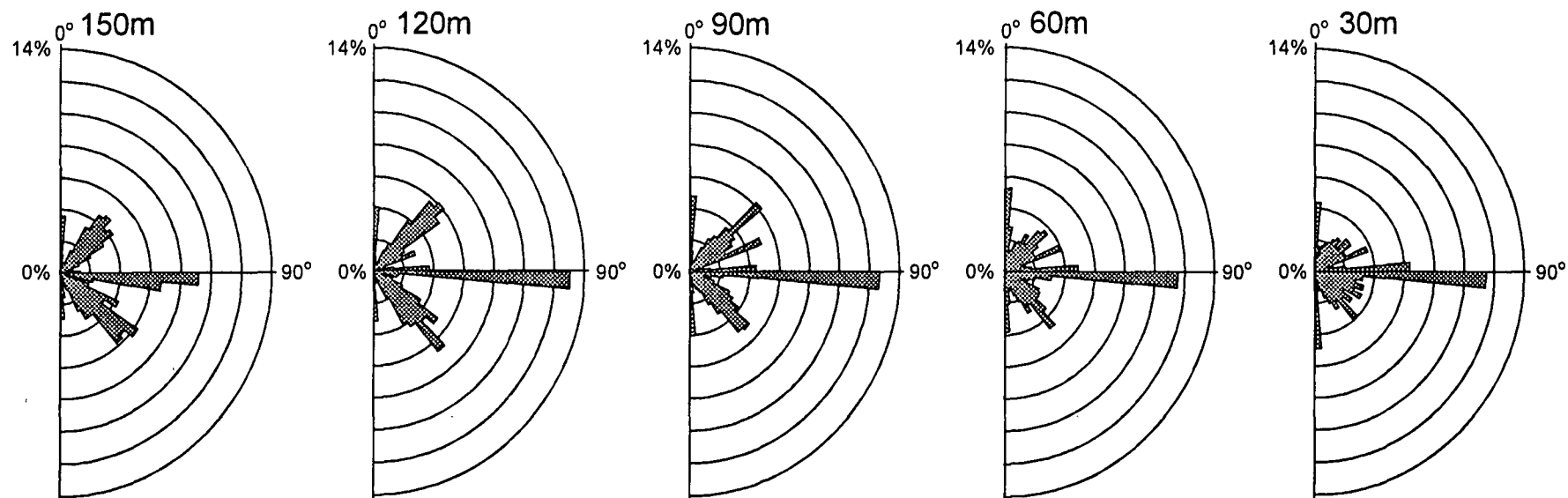


Fig. 3.41. Series of rose diagrams showing the trends of lineaments groups (with a 5° range) interpreted from images of North Cornwall with resolutions of 150m to 30m.

150m, 120m and 90m, however, different lineament trends were found within the lineament maps from images with resolutions of 60m and 30m. This could occur in the higher resolution images because large scale lithotectonic features may possess complex internal zones which become observable in the larger map-scale images (e.g. fault zone). Alternatively, 'new' scale limited lithotectonic features may be observed within the images which possess different trends. As most of the anthropogenic caused lineaments have been removed from the populations, it is unlikely that the large increase in lineament complexity is caused by such features.

In summary, the degree of geological information obtained from North Cornwall increases with increasing image resolution. The lithotectonic features interpreted as lineaments from images with 150m, 120m and 90 resolutions are similar as suggested by the rose diagrams. The similarity, however, between the lineament maps obtained from image resolutions of 120m and 90m (as described by the statistics in this section) is much greater, suggesting that the relative increase in geological information between these two resolutions is low. A diversification in the lineament trends identified in the rose diagrams of the 30m and 60m lineament populations suggest that lineaments are identified from either increasingly complex trends of previously identified linear lithotectonic features or different 'new' linear scale limited lithotectonic features. Low concentrations of lineaments, however, can occur within areas of these lineament maps suggesting that increases in the geological information can only be obtained only from parts of these images.

3.11 The effect of pixelated images on lineament analysis

Analysis of the frequency/azimuth distributions of the lineament populations of North Cornwall and SW England suggest anomalous peaks and troughs (Figs. 3.42, 3.43), particularly around 000° and 090° (Fig. 3.44a, c), but also occurring at 045° (Fig. 3.44b) and 135° . The frequency/azimuth distributions in Figs 3.42, 3.43 have used bin values of 1° . The effect of using a 1° bin value is to hide the actual frequency/azimuth distribution by smoothing the anomalies into single peaks and troughs as identified in the distributions illustrated in Figs 3.44a, b, c. Decreasing the bin value to 0.5° illustrates that the actual frequency/azimuth distribution of the populations is an internal anomalous sharp peak flanked by two troughs (Fig. 3.44d). This indicates that lineaments which trend $<\pm 2^{\circ}$ to 090° have been interpreted as trending at 090° , forming the two troughs and anomalous peak (Fig. 3.45). This small change in lineament trend therefore also occurs for lineaments trending approximately $<\pm 2^{\circ}$ to 000° , 045° and 135° .

Lineaments were interpreted from pixelated images. The contrast in reflected EMR from a linear geomorphological feature trending within $<\pm 2^{\circ}$ to 000° , 045° , 090° and 135° may therefore fall within the square dimensions of the visible pixels (Fig. 3.46a). Consequently, the near sub-parallel lineaments would be '*dragged*' towards and be interpreted with trends of 000° , 045° , 090° and 135° . For linear geomorphological features trending $>\pm 2^{\circ}$ to 000° , 045° , 090° and 135° neighbouring pixels can detect the contrast in reflected EMR (Fig. 3.46b), resulting in accurately interpreted lineaments.

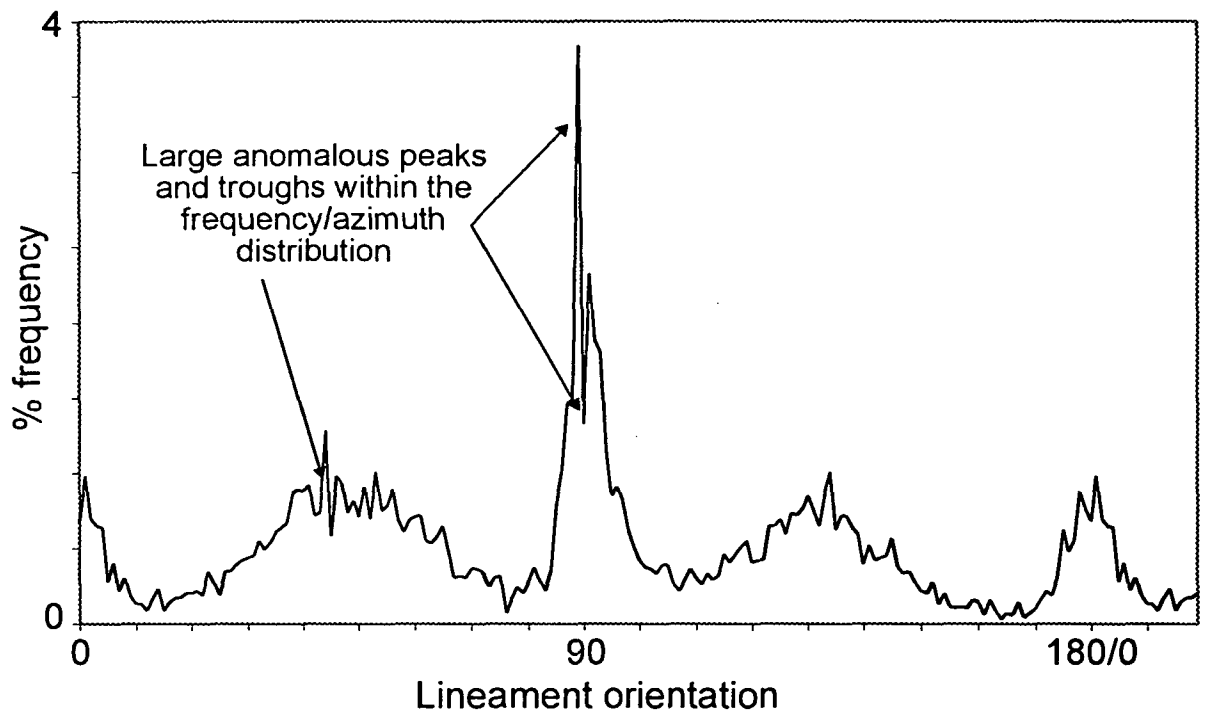


Fig. 3.42. Chart showing the frequency/azimuth distribution for the regional lineament population, interpreted from Landsat TM images of SW England at a pixel resolution of 150m. Highlighted are anomalous peaks and troughs within the distribution.

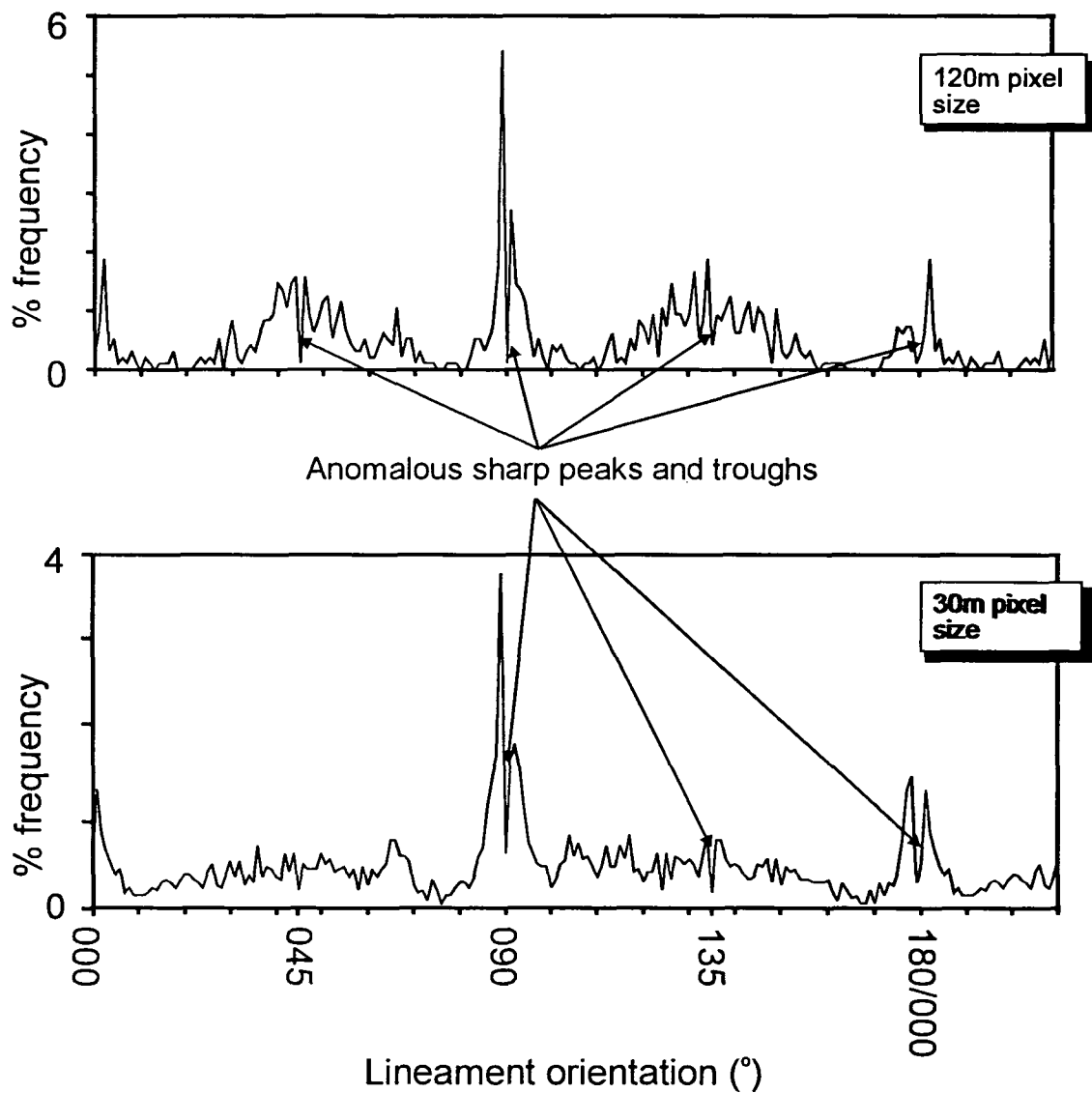


Fig. 3.43. Charts showing examples of the frequency/azimuth distributions of lineament populations interpreted from Landsat TM images of North Cornwall. Highlighted are anomalous peaks and troughs that are visible within the distributions.

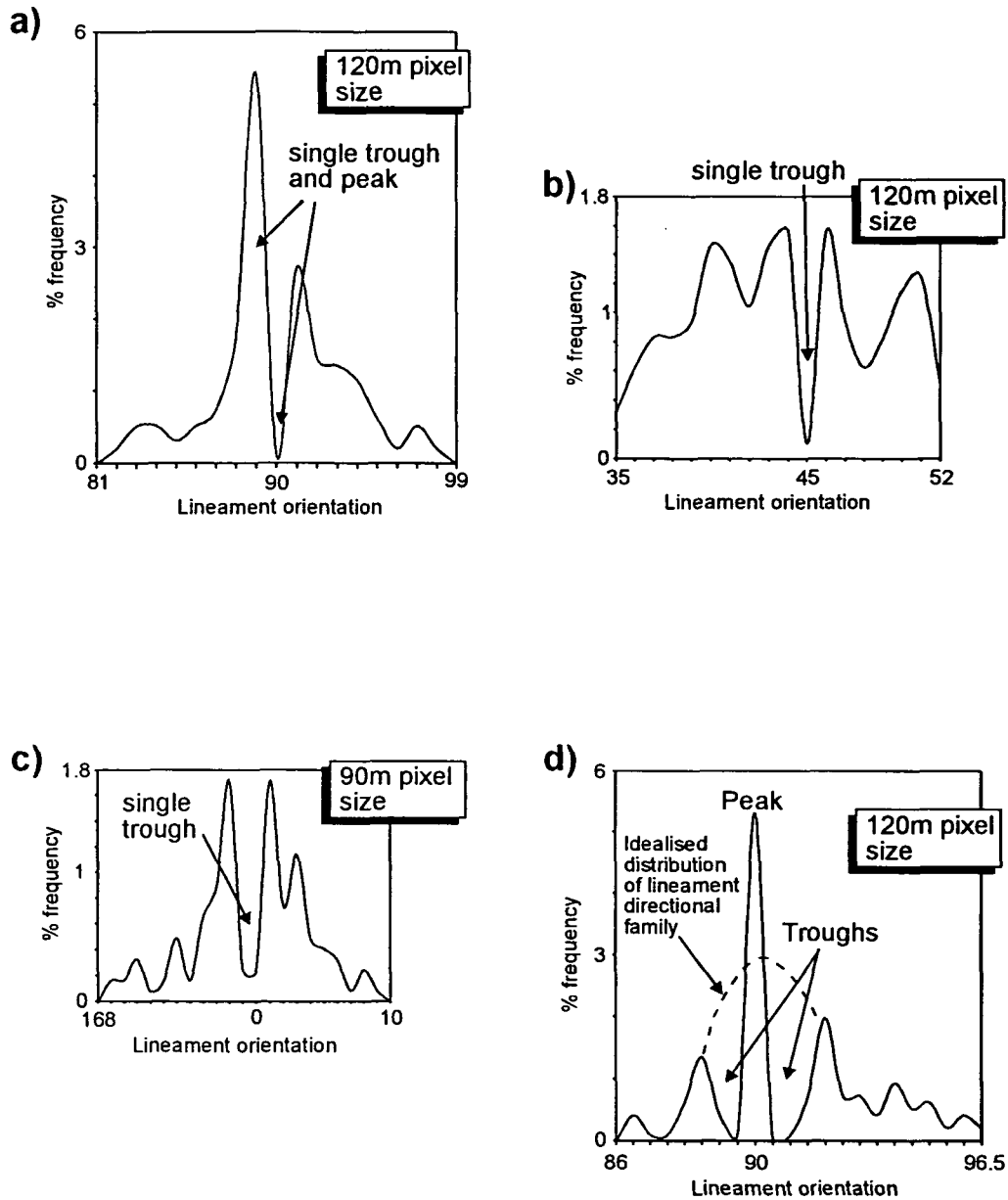


Fig. 3.44. Four detailed smoothed frequency/azimuth graphs illustrating the typical anomalous sharp peaks within the lineament populations interpreted within this study. Graphs a), b) and c) have bin values of 1° and graph d) a bin value of 0.5°. The change in the graphs bin value alters the anomalies from single trough and/or peak to two troughs and a peak.

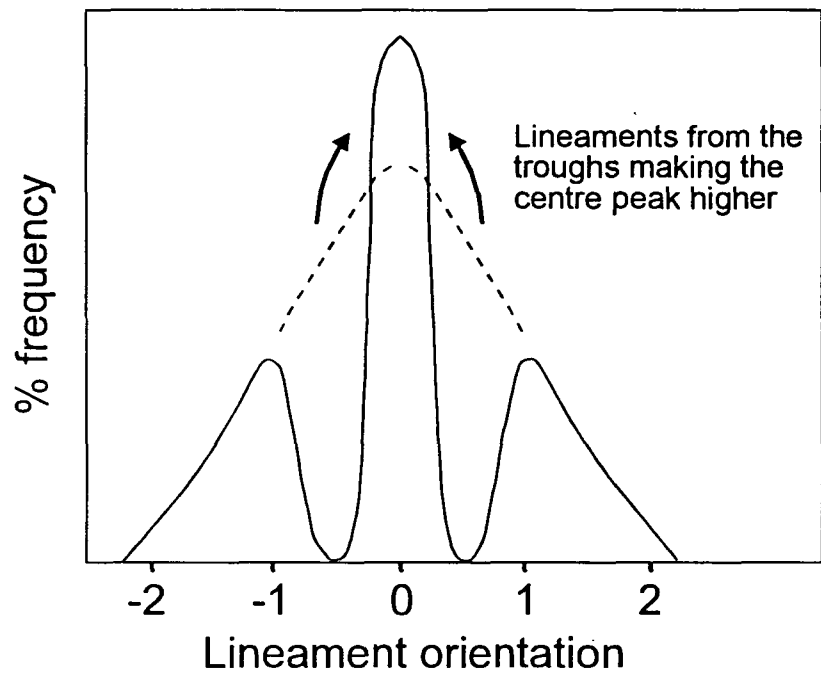
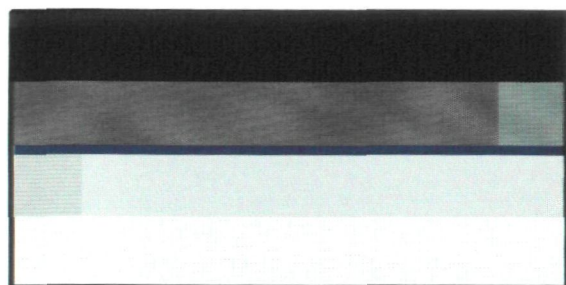
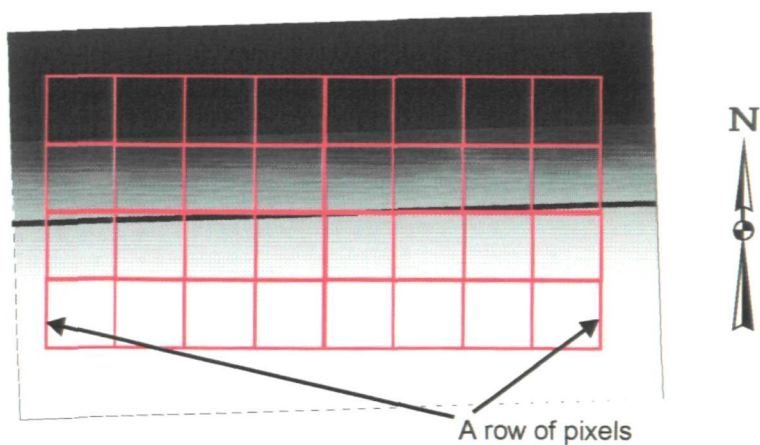


Fig. 3.45. Idealised diagram showing the effect of the 'dragging inwards' of lineaments, in this case upto 1° in azimuth either side to the centre peak, producing two troughs.

a)



b)

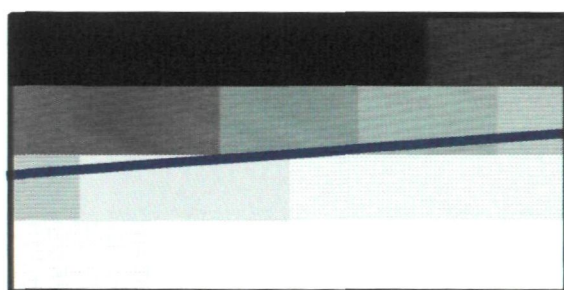
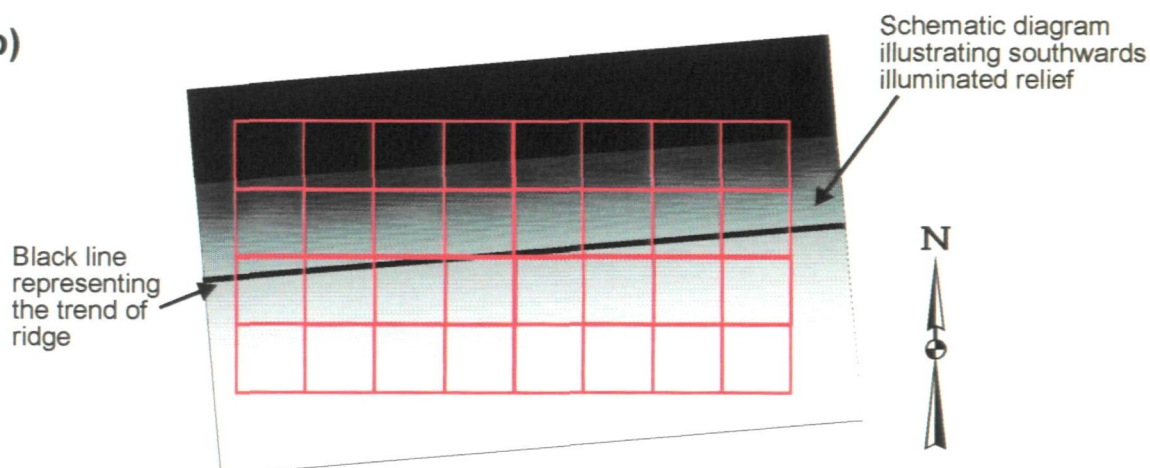


Fig. 3.46. Schematic diagram illustrating how a slight change in the trend of a geomorphological feature can effect the orientation of an interpreted lineament. In a) and b) the gradational shaded rectangles represent plan diagrams of ridges illuminated from the south which trend towards 088° and 085° , respectively. Overlying are red squares representing the area covered by pixels in an image. Below these diagrams are black, grey and white shaded squares representing the same pixels in an image, black to white indicating low to high degrees of reflected EMR. In a) the difference in reflected EMR is only evident across two rows, the result is the interpretation of an E/W trending lineament, illustrated as a blue line. However, in b) the difference in EMR is identified in all four rows, resulting in the interpreted lineament (blue line) possessing the same trend as the geomorphological feature.

Analysis of the frequency/azimuth distributions of high frequency lineament populations interpreted in this study, the 30m resolution lineament population of North Cornwall and the lineament population of SW England, has identified more, but smaller, anomalous sharp peaks and troughs. These anomalous peaks can also be formed by lineament dragging, however. The trends of these small sharp peaks are towards 026.5°, 033.8°, 056.2°, 063.4°, 116.5, 123.8 and 153.8. Lineament dragging was found to occur in directions which lineaments are formed from linear sequences of pixels (e.g. vertical and horizontal). These linear sequences of pixels therefore can be described by their pixel pattern; the ratio between the number of pixels highlighted in a row and the number of pixels highlighted in a column in the image pixel matrix. For a lineament trending to 045° this would produce a row/column ratio of 1:1 (Fig. 3.47a). These extra anomalies therefore reflect linear sequences of pixels formed by stepped pixel patterns, e.g. the anomaly trending towards 026.5° correlates to a row/column ratio of 1:2 (Fig. 3.47b, c, d).

Analysis of the distributions containing the sharp anomalous peaks by plotting trend against length showed a central linear segment comprising of the dragged lineaments surrounded by regular spaced, multiple, upwards concave curved data concentrations, which are symmetrical across the central segment (Fig. 3.48). However, within high frequency populations data were also found between the upwards curved concentrations (Fig. 3.49). These curved distributions were also found in the lineament population obtained only from a linear stretched image of band 5 (Fig. 3.50), suggesting that the anomalies are not caused by directional filters.

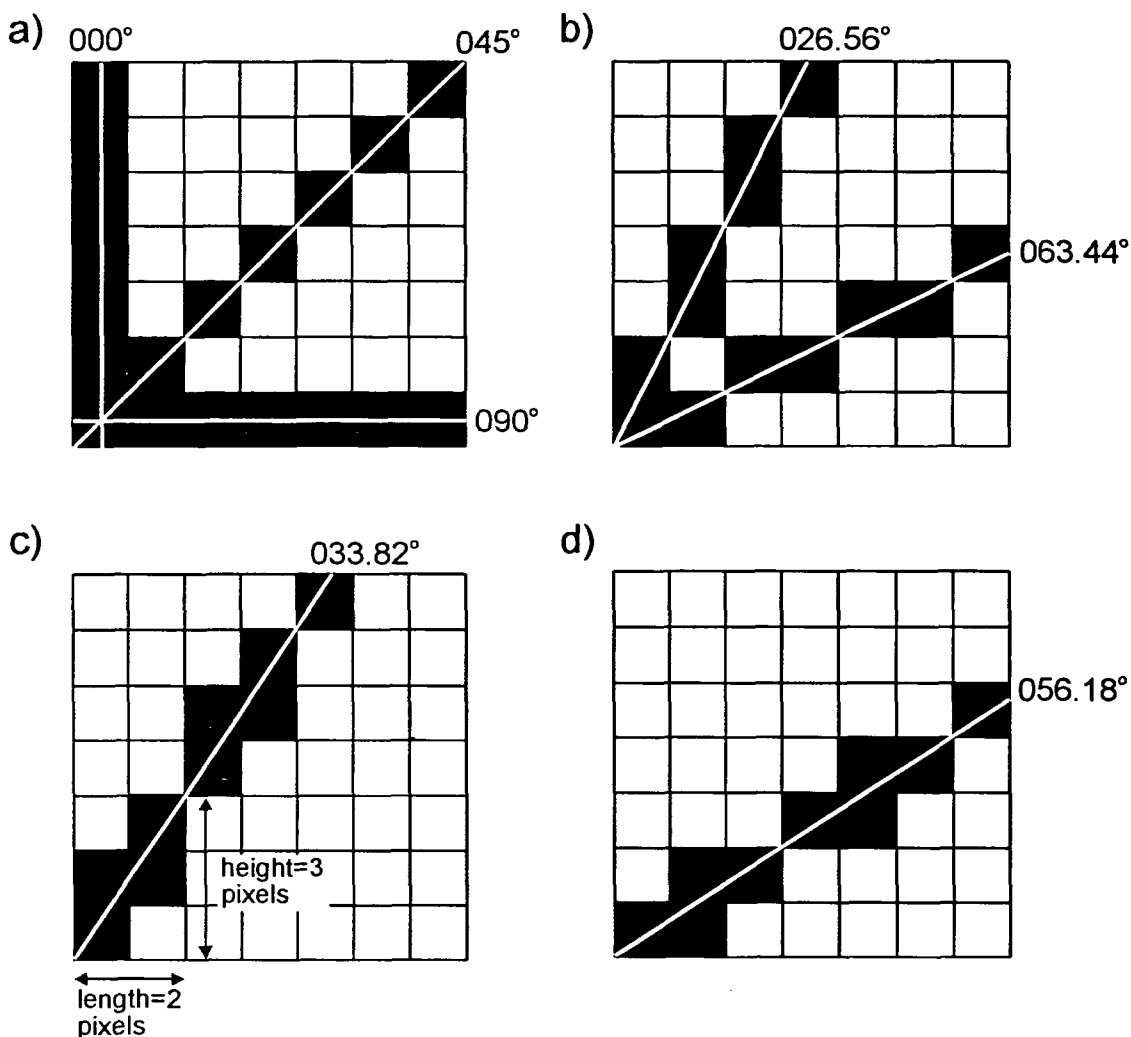


Fig. 3.47. Schematic diagrams illustrating how the trends of anomalous sharp peaks in frequency/azimuth distributions formed by the 'dragging' of lineaments around the lineament trends of lineaments formed from linear sequences of pixels (shown as squares) in an image (represented by the grid). In a) vertical, diagonal and horizontal highlighted pixels form anomalous lineament peaks towards 000° , 045° and 090° , respectively. Other linear sequences of pixels can be identified in the pixel matrix forming slopes of b) 1:2 and 2:1, c) 2:3 and d) 3:2 resulting in possible sharp anomalous peaks towards 026.56° , 63.44° , 33.82° and 56.18° , respectively.

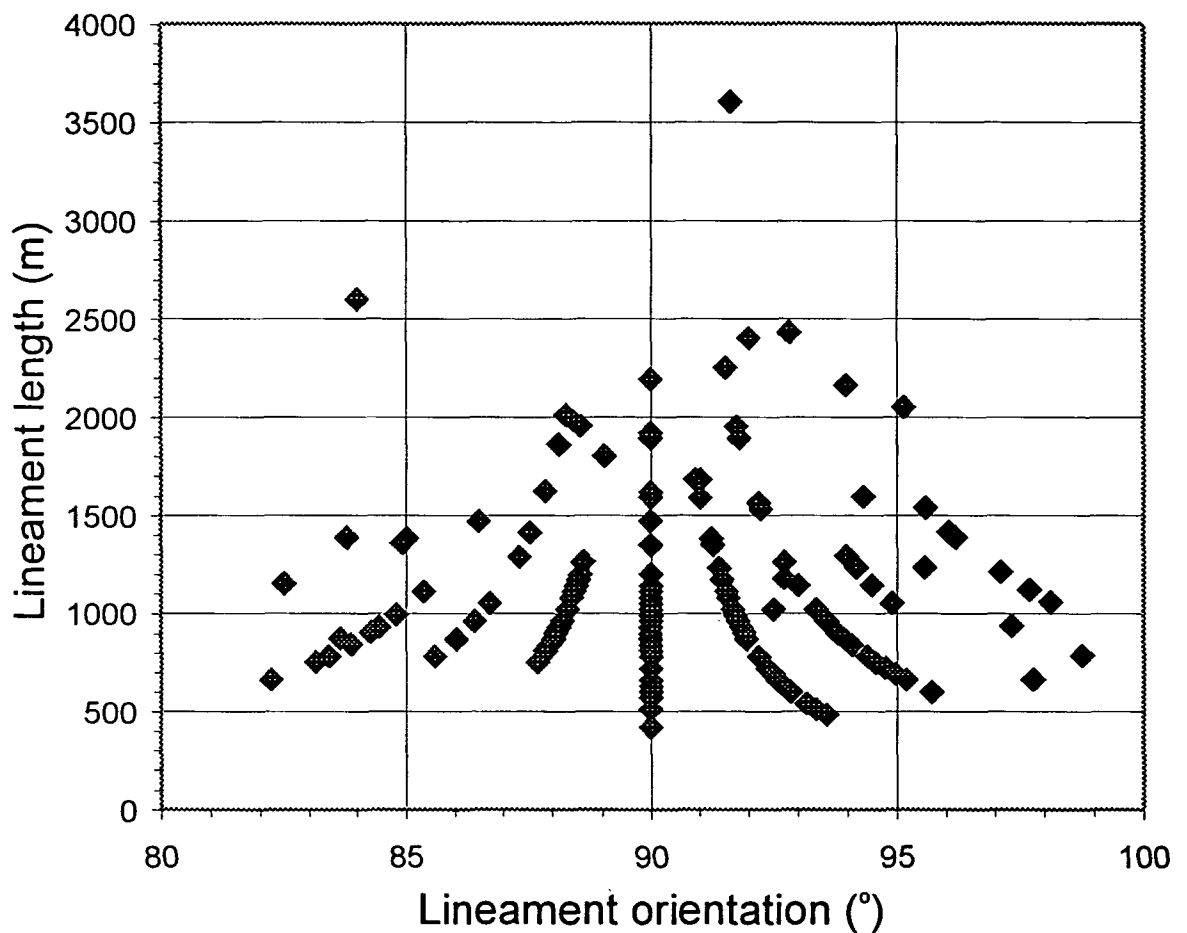


Fig. 3.48. An example of the curved pattern is obtained in the lineament length/ orientation distributions of all the interpreted lineament populations in this study. In this graph the data is taken from the 120m resolution lineament population of North Cornwall. The typical pattern are a series of symmetrical curves of concentrated data points. At the centre of the curves the data concentrates as a vertical linear line previously found to be caused by lineament dragging.

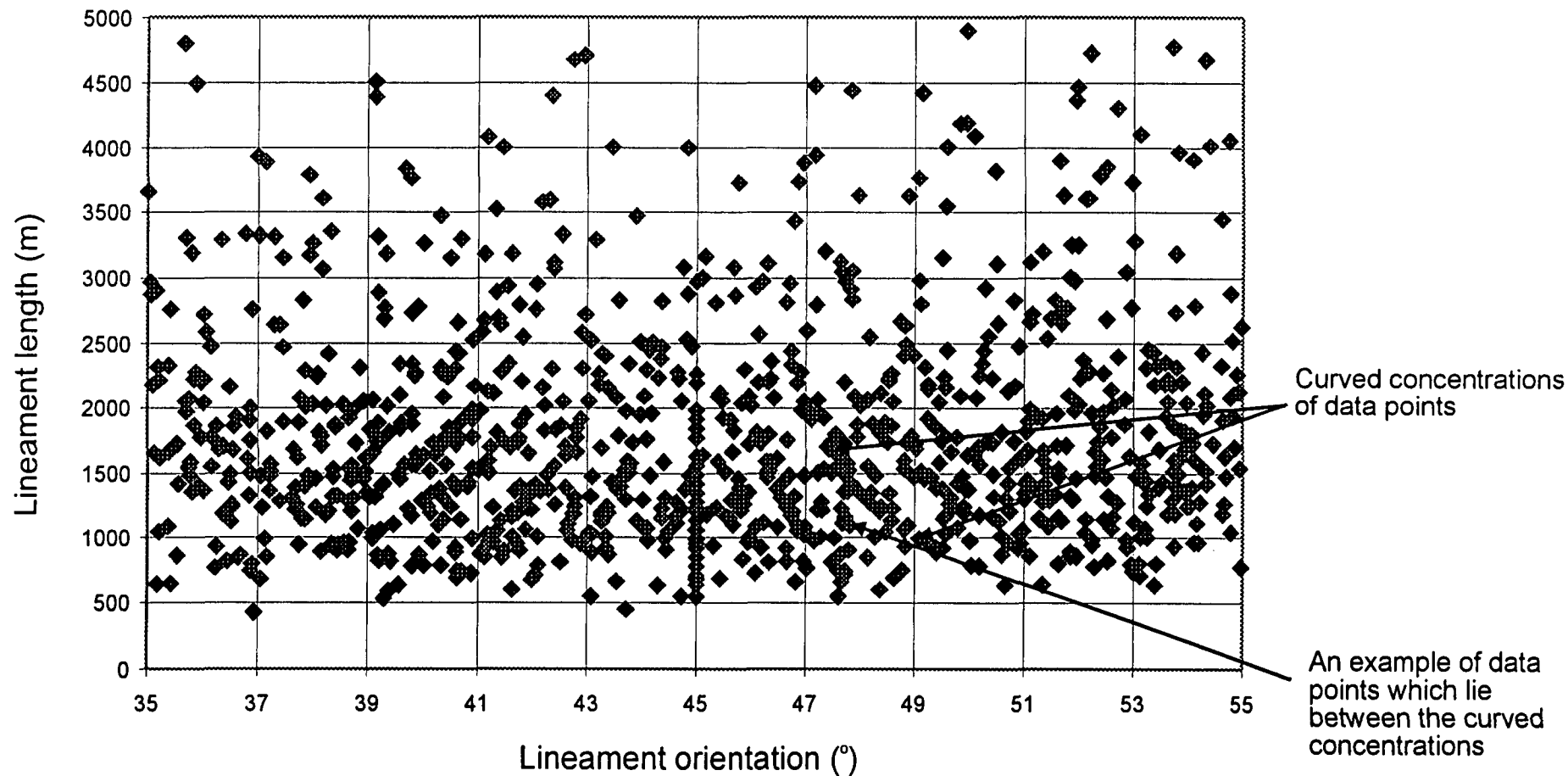
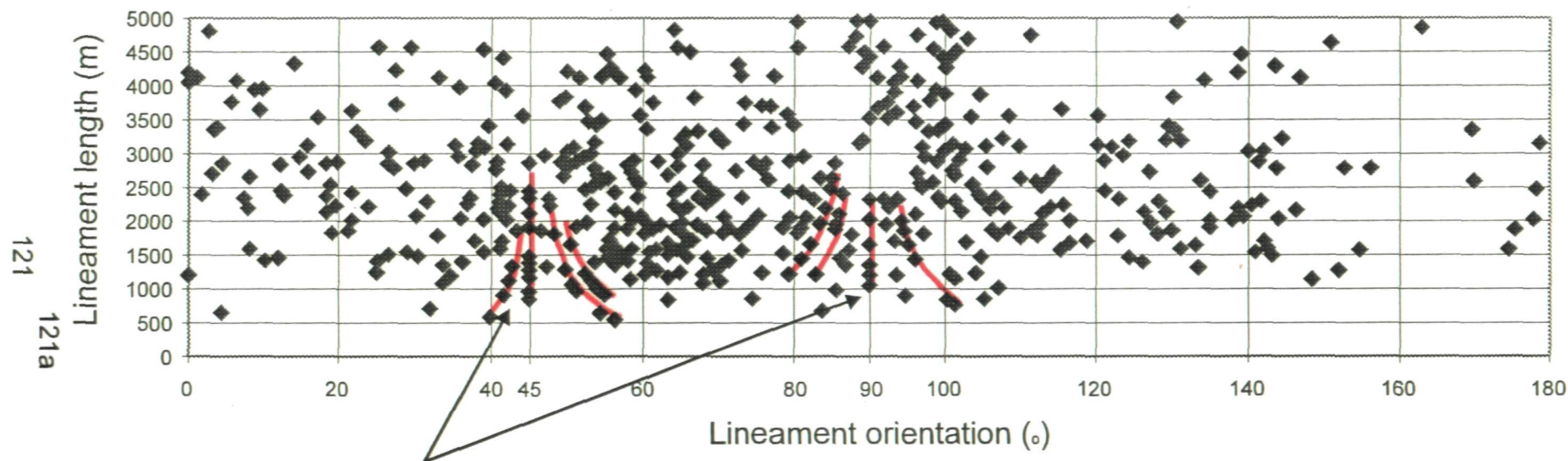


Fig. 3.49. A chart illustrating the curved concentrations of data in the lineament length/orientation distribution for the SW England lineament population. The higher numbers of lineaments within this population ($n=6482$) suggest that data can fall between the curved concentrations.



Relatively distinct central lines on 045° and 090°
surrounded by poorly defined curved concentrations
highlighted in the overlay

Fig. 3.50. A chart of the lineament length/orientation distribution of lineaments interpreted from a linear stretched TM band 5 image of Devon and Somerset (image 1). Evident within the distribution are curved concentrations of data points suggesting that the cause of these anomalies are not directional filters.

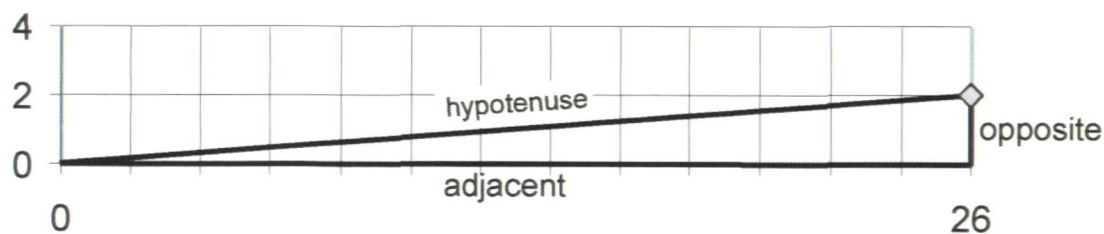
The concentration curves indicate that with increasing lineament length the lineaments trend towards the anomalous peak or central segment. This was tested by plotting on a graph a series of lines which originate from the origin and are fixed in height along the y-axis. Regularly extending the length of the line along the x-axis therefore results in decreasing slope angle and longer lines (Fig. 3.51a). Dropping vertical lines from the sloping lines to the x-axis results in a series of triangles; where the hypotenuse is the sloping line, the opposite is the vertical line between the x-axis and the hypotenuse and the adjacent is the distance along the x-axis to the opposite line (Fig. 3.51b). Using the trend 090° as the adjacent line (or x-axis), sub-parallel lineaments would therefore form the hypotenuse. By interpreting a series of lineaments with a constant opposite length, such curved distributions could therefore be obtained.

The interpretation of lineaments from pixelated images was achieved by visually estimating the trend and length from linear patterns of pixels, therefore for similar patterns the interpreted lineament will possess analogous length and trend. Due to the pixelated images a relatively low number of pixel patterns can form linear sequences of pixels and the pixel pattern formed is dependant upon the original trend of the interpreted geomorphological feature. In the case of E/W trending lineaments a change in lineament pattern can be achieved when: (i) the pixel pattern reflects a near-parallel trending geomorphological feature, consisting of longer sequences of E/W trending pixels and a short sequence of E/W trending pixels in the next pixel row (Figs. 3.52a, b); and (ii) the pixel pattern reflects a sub-parallel geomorphological feature, consisting of even sequence of E/W trending pixels across two pixel rows (Figs. 3.52c, d). Accurate digitising of these pixel patterns would form different constant opposite lengths depending on the pixel pattern type.

a)



b)



c)

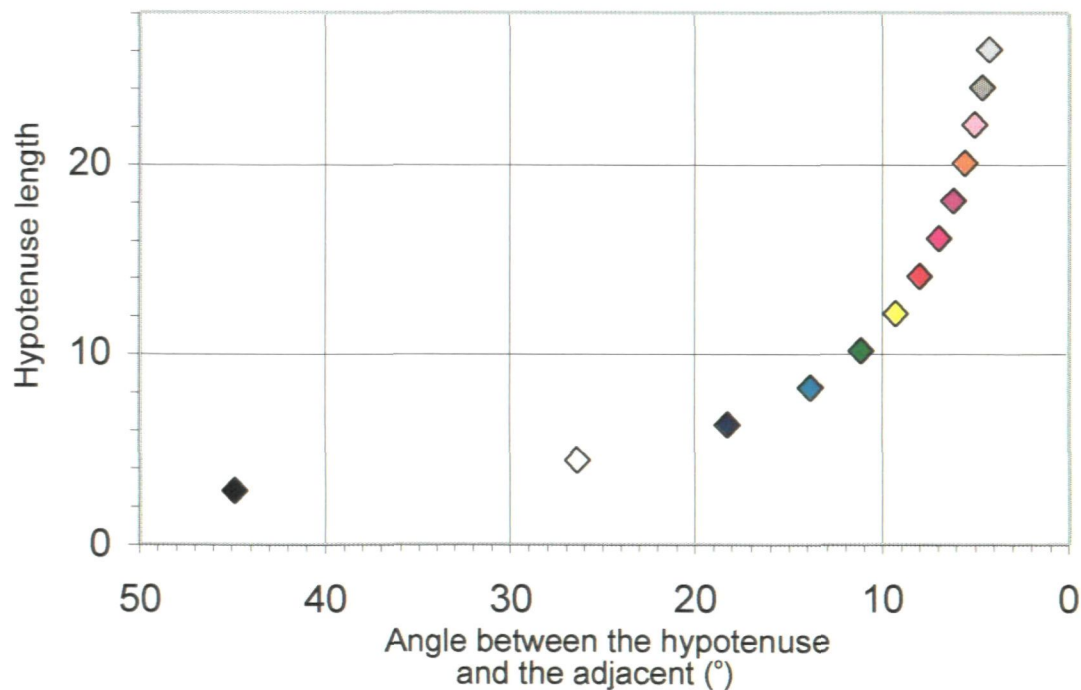


Fig. 3.51. A series of graphs illustrating how a curved length/orientation distribution can be formed by a consistent change to a lines slope and length. Graph a) shows a series of lines constructed from the origin to colour-coded points which are restricted on the y-axis and extended along the x-axis. Each line therefore forms a right-angled triangle to the x-axis, as illustrated in b). In c) the angle from the x-axis for each of the colour-coded lines are plotted against their hypotenuse lengths, forming a curved distribution.

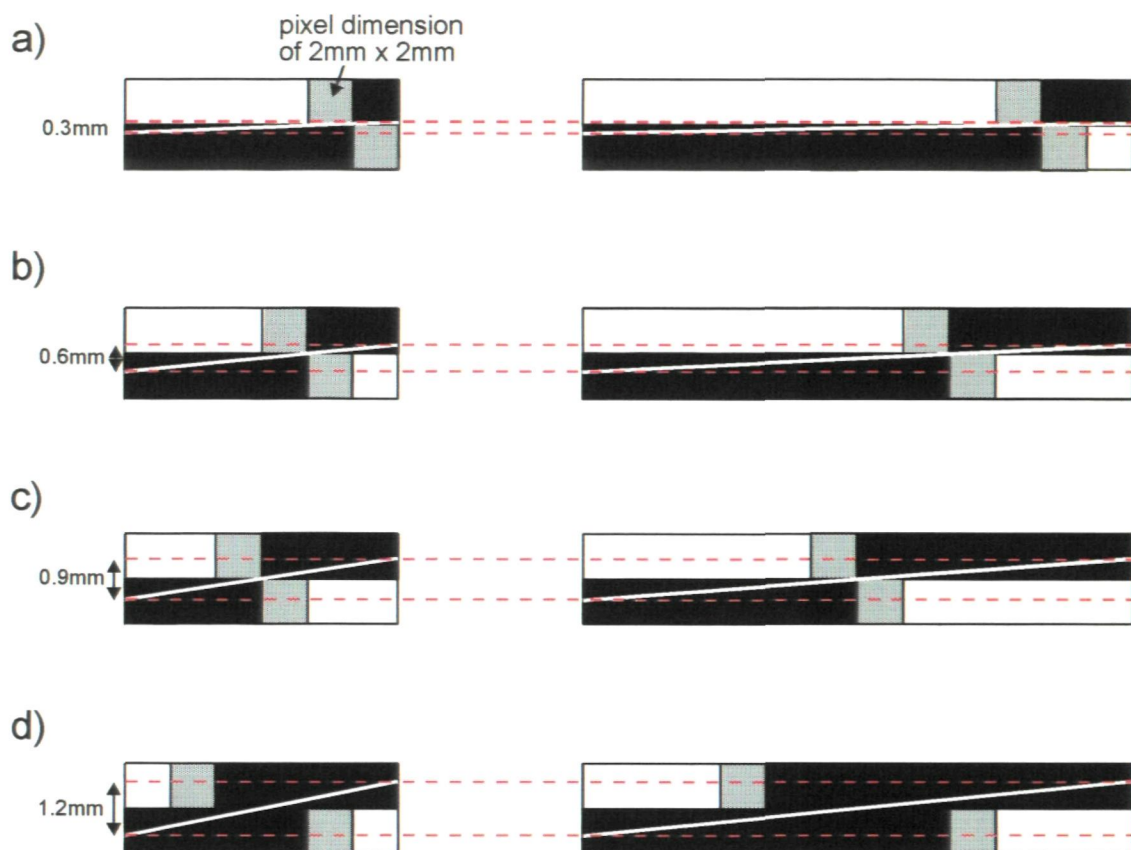


Fig. 3.52. A series of cartoon diagrams illustrating how the opposite length constant can be obtained from similar pixel patterns irrespective of lineament length. For a), b), c) and d) the pixel patterns produce constants of 3mm, 6mm, 9mm and 12mm. The constants are different because the trends of interpreted lineaments (white lines) are weighted towards the longest linear pixel sequence, as shown in a) and b). Linear pixel sequences of equal length can form different constants when c) linear pixel sequences do not overlap and d) when linear pixel sequences overlap.

Extending the patterns in length (reflecting longer geomorphological features) results in longer lineaments that increasingly trend closer to 090° . Analysis of the concentration curves in the 90m resolution lineament population of North Cornwall suggest the constant opposite lengths needed to form these distribution curves are 3mm, 6mm, 9mm and 12mm. Such constant opposite lengths are typical of the lineament patterns described in Fig. 3.53.

The greatest control on these curved distributions is the estimated pixel trend imparted by the finite number of pixel patterns. Each concentration curve reflecting a different pixel pattern. Therefore, the degree of error in the trends of lineaments is half of the difference in lineament azimuth between two neighbouring concentration curves. Thus, the maximum degree of error imparted to lineaments of the 90m resolution lineament population of North Cornwall with the lineament range of 080° to 100° is only $\sim 1.4^{\circ}$ (Fig. 3.54).

3.12 Discussion

The lineament maps of SW England and North Cornwall were interpreted from pixelated images. In low resolution images the advantage was that this allowed lineaments to be mapped from images at a larger map-scale while the effect of anthropogenic features were negated (150m) or minimised (120m to 90m). Similar processes were used for higher resolution images (60m to 30m) to allow a direct comparison between the images. Generally, lineaments are interpreted from images in which the pixels are not discernible (e.g. Drury 1986, Smithurst 1990). The effect of using images in which pixels shapes are identifiable is the preferential interpretation of lineaments which trend towards linear sequences of pixels. This imparts an error of up to $\pm 2^{\circ}$ in the lineament orientation, producing sharp anomalous peaks in the frequency/azimuth

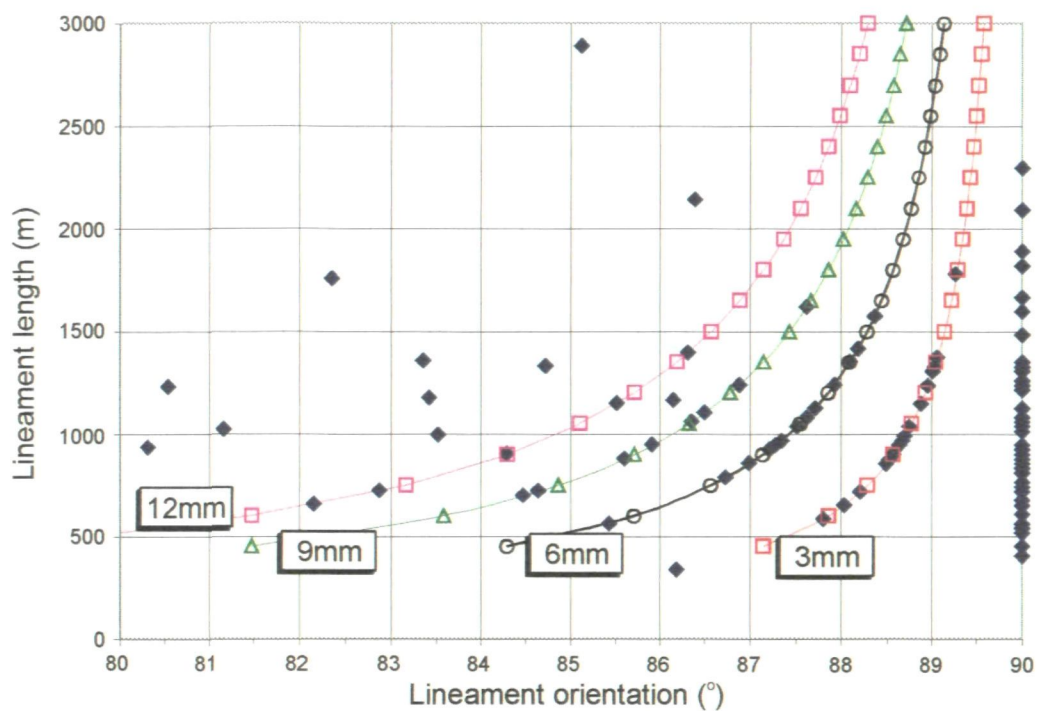


Fig. 3.53. A chart illustrating the distribution of lineament length/orientation for the 120m resolution lineament population of North Cornwall (blue diamonds). The data are found to form multiple curved concentrations, calculated from these curves are the constant opposite lengths of 3mm, 6mm, 9mm and 12mm. These dimensions closely match the constant opposite dimensions of the pixel patterns which form sub-parallel E/W trending lineaments.

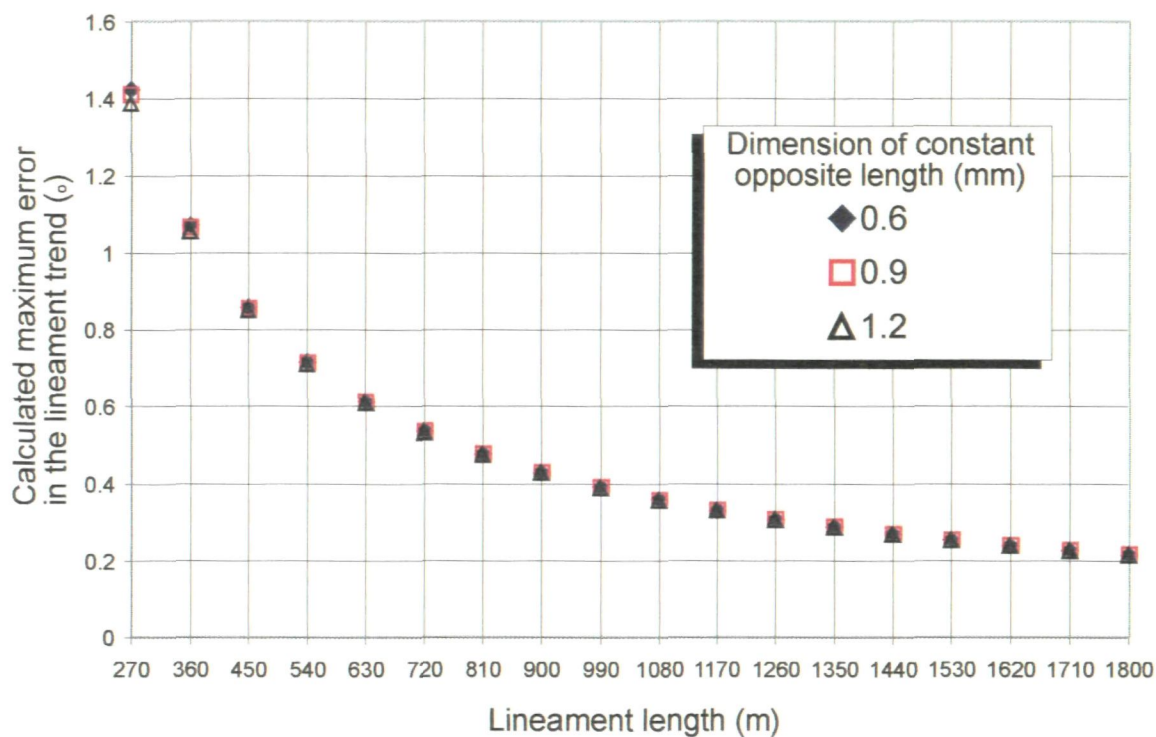


Fig. 3.54. A chart showing the calculated maximum error in the trend of an interpreted lineament within the lineament range of 080° to 100° from the 90m resolution lineament population of North Cornwall. With increasing length the degree of error decreases.

distributions of the lineament populations. Furthermore, smaller errors in lineament orientation of $\sim 1.4^\circ$ are found in lineaments which are sub-parallel to the sharp anomalous peaks. Increasing the pixel screen size to increase the image resolution therefore can cause a small degree of error when interpreting some lineaments. This error can be removed from the lineament populations by reducing the pixel size, the effect of reducing the pixel size. The effect of this, however, is to reduce the degree of geological information interpreted from the images. Consequently, if a very small degree of error imparted to some lineament trends is acceptable it is possible to interpret lineaments from pixelated images.

The major E/W lineament trends and N/S and NW/SE and NE/SW sub-trends identified in the lineament maps have also been shown not to be caused by directional filters, therefore, lineament trends are suggested to only relate to linear lithotectonic trends of SW England. Although the lithotectonic trends in SW England can change depending on the lithotectonic domain, the main lithotectonic trends identified in Chapter 2 are E/W, NE/SW, NW/SE and N/S. A geological interpretation may therefore explain the major lineament trends (see Chapters 4 and 5).

Previous work mapping lineaments in SW England has shown the geological causes of lineaments to be faults, joints and lithological differences (Moore & Camm 1982, Whittle *et al.* 1983, Smithurst 1990). The areas mapped from Landsat MSS images in these earlier studies concentrated more on mineralogical mapping and covers an area to the west of Exeter and south of Bude, at map-scales between 1:50000 and 1:250000 (Moore & Camm 1982, James & Moore 1985). Smithurst (1990) has used Landsat TM images to identify structural trends in SW England at scales of approximately 1:250000.

Lineaments identified by Smithurst (1990) from SW England trend to the

NNW/SSE to NW/SE, NE/SW, and E/W. At such a map-scale only major lithotectonic features may be identifiable in an image. The lithotectonic features identified by Smithurst (1990) to form lineaments are E/W folds and corresponding E/W striking lithological differences, and NW/SE and NE/SW regional faults. Absent from Smithurst's (1990) lineament maps are N/S trending lineaments. Lithotectonic features within SW England with such N/S trends are predominantly fractures associated with the formation of Permo-Triassic basins round the Cornubian massif (Scrivener *et al.* 1994), a set of relatively minor geological structures in comparison to the other main lithotectonic trends. It is probable that the large difference in image map-scales therefore may account for the non-identification of these relatively minor features. The regional lineament map (Fig. 3.31) of lithotectonic trends interpreted at a map-scale of 1:75000, is therefore not only an improvement in the area mapped, but also a map-scale which has resulted in the identification of new lineament trends.

Increasing the image resolution for images of North Cornwall has produced more frequent and shorter lineaments, resulting in an increase of complexity in the lineament trends. However, with higher image resolutions anthropogenic features become visually apparent within the images. The statistical analysis used to identify trends in the lineament populations have not identified any relationship within the lineament populations which can be attributed to the effect of anthropogenic features within the images. Visual analysis of the lineament maps, however, shows that for maps interpreted from 60m and particularly 30m image resolutions areas of North Cornwall can become devoid of lineaments. This may suggest that these areas are absent of linear lithotectonic features. Alternatively, it may be caused by areas that are visually dominated by anthropogenic features which correlate to relatively flat topographic areas. As these lineaments are

removed from the lineament maps (following the processes described in Section 3.8.1) it forms areas with low lineament concentrations. Lineaments interpreted from lower resolution images are found to cross-cut such areas of low lineament density. This suggests therefore that linear lithotectonic features are present within these low lineament density areas. Consequently, it is probable that the process used to remove anthropogenic features from the lineament maps of North Cornwall was successful in images with resolutions up to 90m, can mostly work in images with 60m image resolutions and can fail in parts of images with 30m resolutions.

3.13 Conclusions

(i) From the available satellite sensors, Landsat TM images were the most suitable for lineament analysis of SW England because they covered the largest area of SW England and possessed a higher range of available bands, of which band 5 suppressed anthropogenic features.

(ii) Landsat TM bands 4, 7, and particularly band 5, in comparison to bands 1, 2 and 3 yield significantly higher numbers of lineaments from low resolution (150m) images in the temperate agricultural temperate terrain of SW England. Increasing the image resolution produces an increase in anthropogenic features interpreted from images of all TM bands, particularly in band 4. Hence, for an area such as SW England with well developed agricultural practices and infrastructure, TM band 4 should not be considered for lineament analysis for images with resolutions of <90m.

(iii) Directionally enhanced images in comparison to FCC's and linear stretched images increased the number of shorter lineaments while similar numbers of longer lineaments were identified. It is concluded that directional

filters are useful aids in increasing the degree of geological information obtained from images in temperate agricultural regions.

(iv) Higher image resolutions increase the degree of geological information obtained from the images. However, unwanted smaller scale anthropogenic features become visible in images with resolutions $\leq 120\text{m}$.

(v) A low image resolution of 150m virtually removes the effect of anthropogenic features present in high resolution images of temperate agricultural terrains. Consequently images at map-scales of 1:75000 can be interpreted, thus providing a greater degree of geological information. On this basis, the optimum image resolution for interpreting lineaments from SW England is 150m. In other terrains this optimum resolution will be controlled by the size of the anthropogenic features.

(vi) Four main lineament groups are common to images of SW England and North Cornwall interpreted at images resolutions of 150m, 120m and 90m: a major E/W trend; and minor trends to the N/S, NE/SW and NW/SE. These major trends change in prominence throughout SW England, although geographical domains/sub-areas have been identified to possess distinctly different trends.

(vii) In the lineament populations interpreted from 60m and 30m images of North Cornwall the minor trends to the NE/SW and NW/SE are seen to diverge and become more complex. The four main lineament trends identified from lower resolution images are not caused by directional filters and interpreting pixelated images as such trends would be evident in all the lineament populations. The causes of this divergence are considered to be the identification of either more complex lithotectonic features related to features already identified, or the identification of scale limited linear lithotectonic features.

(viii) The statistical analyses used have not identified how effective the method developed to identify anthropogenic-related lineaments is in the removal of such features from lineament maps interpreted from images with resolutions <150m. Visual analysis of the lineament maps, however, suggests that the processes developed were successful for images of North Cornwall with resolutions of 120m and 90m, and were decreasingly effective for images with resolutions of 60m and 30m. The statistical analyses do suggest that the geological information obtained increases from resolutions of 150m to 120m, a smaller increase in information from 120m to 90m, which again increases with a change in resolution from 90m to 60m. Contrasting evidence was obtained for the lineament population interpreted from image resolutions of 30m.

(ix) Pixelated images designed to reduce the effect of anthropogenic features can cause small directional errors to be imparted to lineaments (maximum of $\sim 2^\circ$) which are sub-parallel or parallel to linear sequences of pixels.

Chapter 4 Geological interpretation of the lineament patterns of SW England

4.1 Introduction

SW England has undergone a complex geological history including multi-phase deformation (Chapter 2). The effect of repeated deformation is that different lithotectonic features may have similar trends. Therefore, lineaments interpreted from different lithotectonic features may possess analogous trends (*lineament mixtures*). Dividing the lineament population into lineament groups may combine different lineament characteristics related to the dissimilar lithotectonic features. Consequently, to determine if the lineament population could be divided into lineament groups the populations lineament patterns are analysed. Lineament patterns should reflect the type of lithotectonic feature interpreted and the localised geological history (e.g. local primary lithotectonic features cross-cut by later faults). In this Chapter the lineament patterns of the main lineament trends (E/W, NE/SW, NW/SE and N/S) are therefore described, and the patterns identified used to predict the lithotectonic origin. The suggested lithotectonic features are then compared to published data (particularly geological maps). Furthermore, the characteristic lineament patterns found in the analysis of the main lineament trends are then used to imply the geological causes of minor lineament patterns.

In comparison to the coastal regions the geology of the inland region of SW England is less well known due to a covering of superficial deposits. The identified lineament patterns are therefore used to: (i) suggest new lithotectonic features within SW England; and (ii) further delineate geographically the broad

lineament trends identified by statistical methods in Chapter 3. Within this study pixelated images were used to remove the effects of anthropogenic features, thus allowing the images to be interpreted at a map-scale of 1:75000. This Chapter therefore also assesses the effect of pixelated images in identifying the regional geology of SW England.

4.2 Characteristic lineament patterns of the four main lineament groups

It has been shown in Section 3.9 that lineaments of the four main lineament trends (E/W, NE/SW, NW/SE and N/S) can occur throughout SW England. However, the dominance of these trends can change. These characteristics, as well as other sub-trends, suggests an overall complex lineament pattern. The common characteristic lineament patterns of the four main lineament trends are therefore initially described, achieved by a simple visual analysis of their properties of: relative lineament lengths; lineament density; the area covered by similarly trending lineaments; and cross-cutting lineaments.

4.2.1 E/W trending lineaments

(i) Large areas in SW England (e.g. central Devon) contain occasionally relatively long E/W lineaments which are typically extended further by other close spatially correlated lineaments, forming *continuous lineaments* (Fig. 4.1a). However, these areas do contain shorter E/W lineaments which are also spatially correlated. These shortened lineaments generally abut onto cross-cutting lineaments (Fig. 4.1b, 4.2a), as a result zones of E/W lineaments can be compartmentalised by the cross-cutting lineaments (Fig. 4.1c).

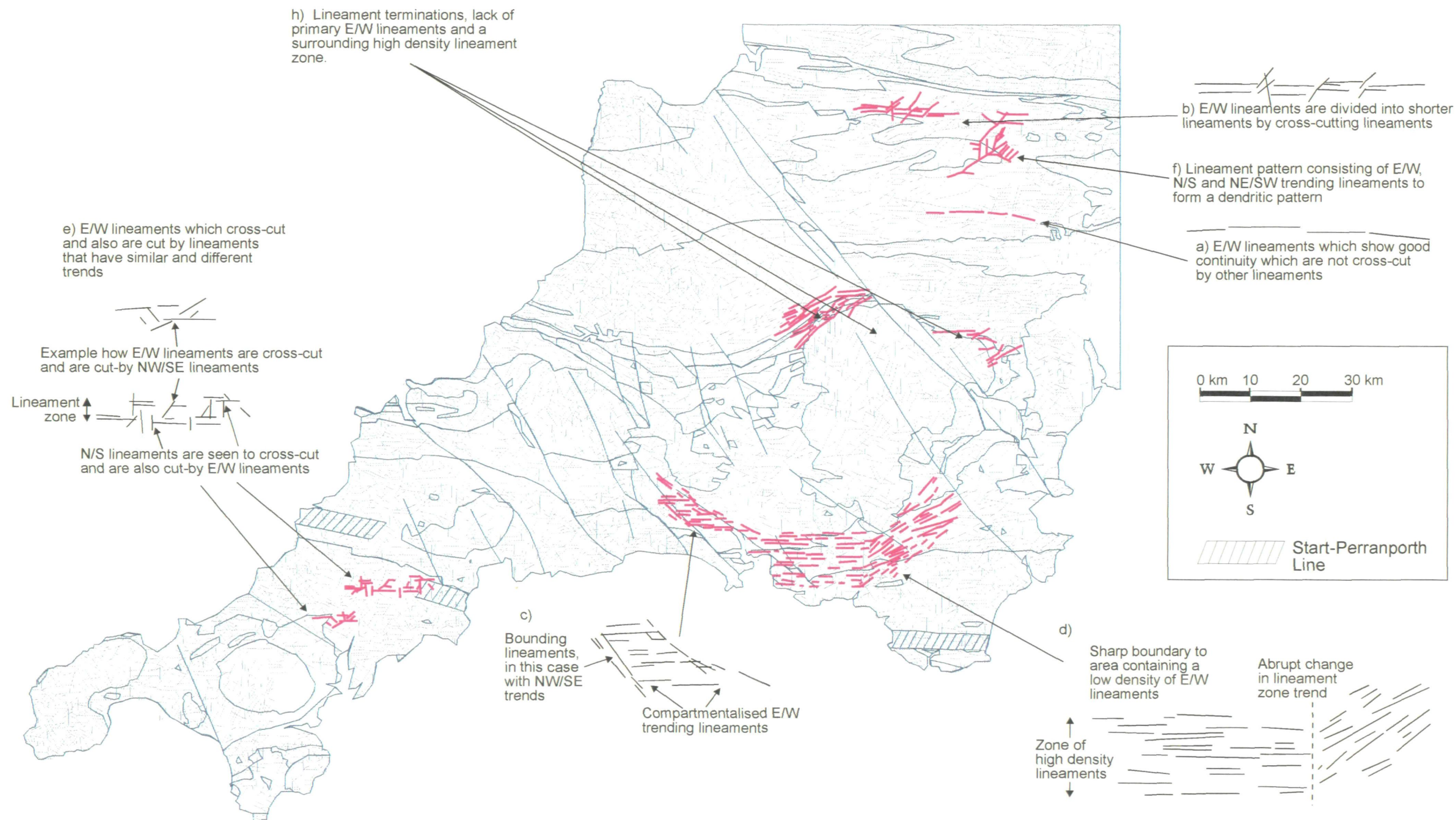
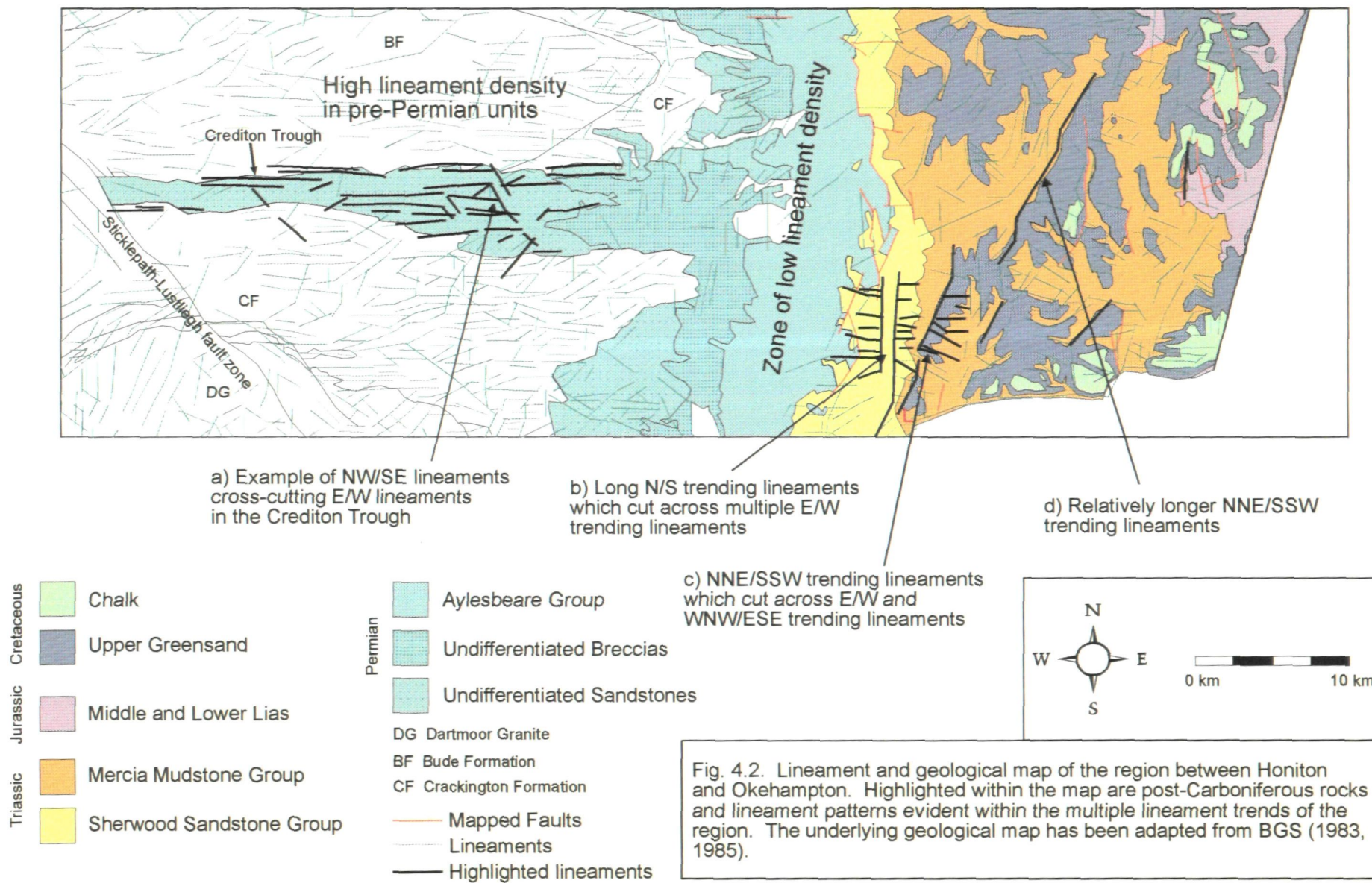


Fig. 4.1. Lineament map illustrating the different E/W trending lineament patterns in SW England. Such E/W lineament patterns are displayed as red lineaments which are fully described by a series of captions.



(ii) E/W lineaments are also found to form dense zones of lineaments, with a more localised distribution of up to 15km² in width and 20km in length (Fig. 4.1d). Within the zones lineaments are found to form continuous lineaments, lineaments which possess discordant trends within the zones tend to cross-cut the continuous lineaments. These zones are also found to be able to abruptly change in trend (Fig. 4.1d). Outside the wide lineament zones patterns tend to differ greatly.

(iii) E/W lineaments can also form zones up to ~4km in width consisting from 1 to 5 lineaments (Fig. 4.1e). The length of these particular zones, however, can be difficult to determine due to the complex nature of the lineament patterns. Within these zones lineaments tend to have a lower maximum length and show low and high lineament continuity. Lineaments within the zones are seen to cross-cut and be cross-cut by ENE/WSW, NE/SW, N/S, NW/SE lineaments, consequently these lineaments tend not to be compartmentalised. The area of SW England in which these patterns occur is generally restricted to South Cornwall (Fig. 1.1).

(iv) E/W lineaments can also be found to terminate in a curvilinear line running northwards from Exeter (Fig. 4.2). These E/W lineaments, however, are not cross-cut by other discordant lineaments. Correlating to the termination of these E/W lineament is an area of very low lineament density.

4.2.2 NW/SE lineaments

NW/SE lineaments in SW England tend to form highly visible thin lineament zones which have a regional distribution (Fig. 4.3). Predominantly, lineaments are short in length relative to the lineament zone and can show continuity to neighbouring lineaments. The width of the lineament zone may

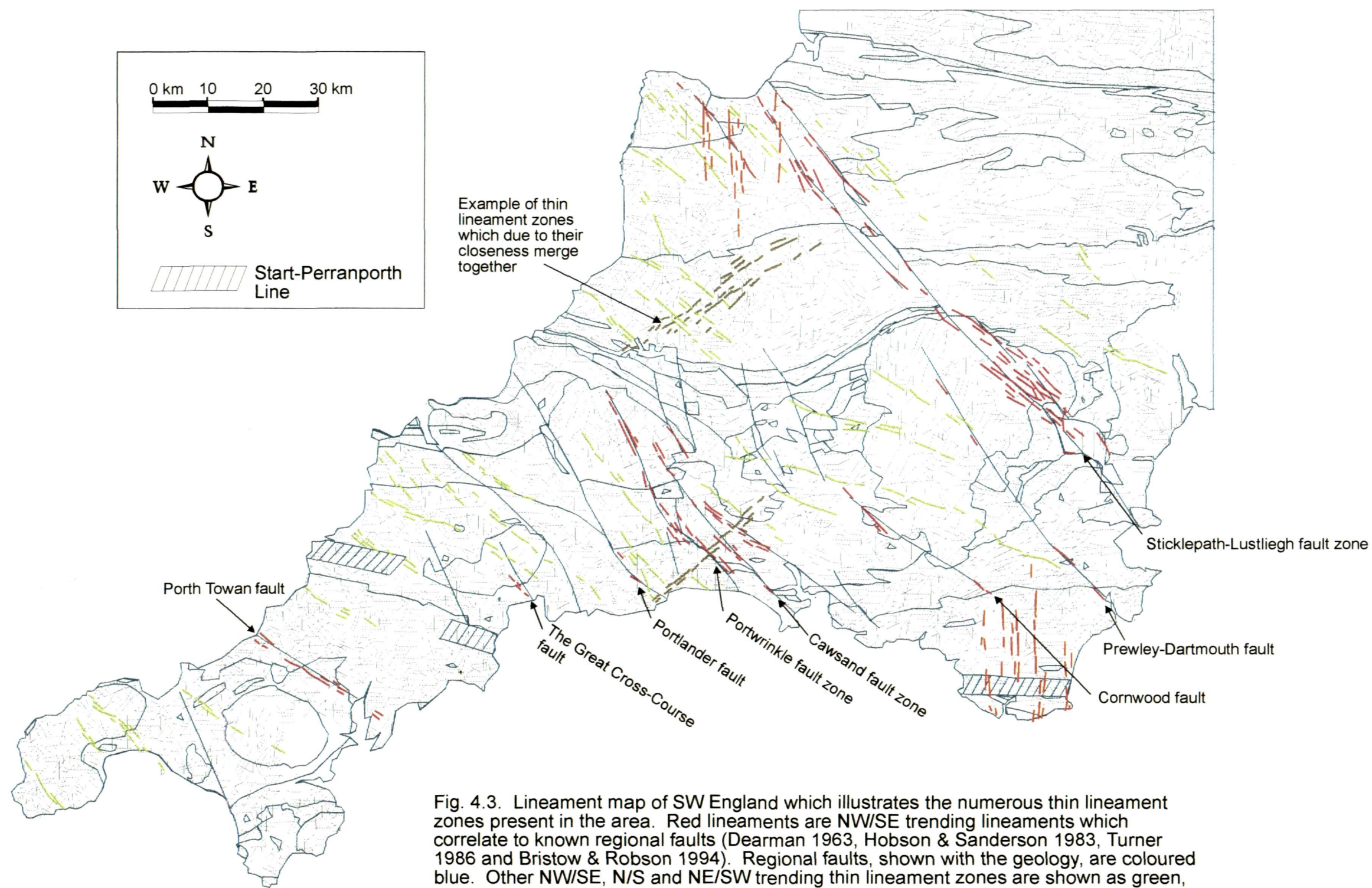


Fig. 4.3. Lineament map of SW England which illustrates the numerous thin lineament zones present in the area. Red lineaments are NW/SE trending lineaments which correlate to known regional faults (Dearman 1963, Hobson & Sanderson 1983, Turner 1986 and Bristow & Robson 1994). Regional faults, shown with the geology, are coloured blue. Other NW/SE, N/S and NE/SW trending thin lineament zones are shown as green, orange and brown lines, respectively.

be described by a single lineament, or multiple lineaments which are parallel or partly overlapping. Over distance, slight changes in lineament orientation can produce curvilinear lineament traces. NW/SE lineaments tend to predominantly cross-cut and compartmentalise E/W trending lineaments, can cross-cut NE/SW lineaments and are typically cross-cut by N/S trending lineaments.

4.2.3 NE/SW trending lineaments

(i) NE/SW lineaments can form thin lineament zones, which apart from being more linear have analogous lineament patterns and distributions to the NW/SE trending lineament zones (Fig. 4.3). These regionally distributed lineament zones, however, are not as visually dominant in the lineament map. NW/SE lineaments within these zones predominantly cross-cut E/W lineaments, can cross-cut NW/SE lineaments and are generally cross-cut by N/S lineaments.

(ii) NE/SW lineaments may form lineament zones that have similar characteristics to those described in Section 4.2.1(iii) (e.g. South-West Devon) (Fig. 4.1d), i.e.: wide zones; high density of lineaments; continuous lineaments; abrupt changes in trend by the lineament zone; distinctly different lineaments trends within the zone compared to outside the zone; lineaments which possess dissimilar trends within the zones tend to cross-cut the lineament zone; and are localised in extent.

(iii) Distinctly different characteristics can be observed for NE/SW trending lineaments in South Cornwall. Short and long lineaments in the area are seen to be cross-cut by and cross-cut E/W, NW/SE and N/S lineaments (4.1e). These lineaments can show good continuity but as they are usually cross-cut they can be disjointed.

4.2.4 N/S trending lineaments

N/S trending lineaments form thin lineament zones of up to ~40km in length (Fig 4.3), similar to those identified in Section 4.2.2. Typically they cross-cut all other discordant major lineament trends.

4.2.5 Analysis of common lineament patterns

(i) Cross-cut E/W lineaments

E/W lineaments can be cross-cut by all other major lineament trends (Fig 4.1a), suggesting that they are relatively early lithotectonic features. The early lithotectonic lineaments can also have a continuous nature and occur over large areas, typical of tilted strata (similarity in trend and the length of outcrop, however, is dependant on the deformation history). Thus these lineament patterns suggest a primary lithotectonic feature. The occurrence of such lineament patterns is typically found in the Culm Basin of central Devon, an area dominated by E/W trending inter-bedded sandstone, siltstone and mudstone units (see Section 2.3.4). Further examples of E/W lineaments are found to be compartmentalised by cross-cutting lineaments (Fig. 4.1c), similar origins are therefore suggested for these lineaments. Differences between lineament characteristics of cross-cut E/W lineaments illustrated in Fig. 4.1b and non-cross-cut lineaments shown in Fig. 4.1a are small. Non-cross-cut continuous lineaments are therefore interpreted as representing similar E/W trending lithological differences.

(ii) NW/SE, NE/SW and N/S lineament zones

The cross-cutting discordant lineaments to the E/W lineaments (*primary lineaments*) trend either to the NW/SE, NE/SW and N/S. The characteristics are

that they can form thin lineament zones and are relatively long, linear features. Geological structures that typically possess such properties are steeply dipping faults (Section 2.6.1(iii)). Comparison between the regional major NW/SE lineament zones and known dextral faults in SW England (Fig. 4.3) shows a good correlation. This suggests a relationship between NW/SE lineament zones and NW/SE fault zones. On this basis it can be inferred that similar NE/SW and N/S thin lineament zones are characteristic of NE/SW and N/S fault zones. The less extensive NE/SW lineament zones can be explained by the sub-ordinate set of NE/SW sinistral strike-slip faults (Freshney *et al.* 1979b, Edmonds *et al.* 1985) and N/S lineament zones to a N/S fracture set (Scrivener *et al.* 1994). Simplistically NW/SE and NE/SW lineament zones can be found to cross-cut each other. However, N/S lineament zones generally cross-cut NW/SE and NE/SW lineaments suggesting that NW/SE and NE/SW fault zones are coeval and are post-dated by N/S fault zones. Anomalous cross-cutting relationships suggest a different formation sequence. However, such anomalous lineament relationships can also be formed by fault reactivation identified to have occurred within SW England (Holloway & Chadwick 1986).

Evidence for the existence of major NW/SE trending strike-slip fault zones in SW England is considered to be unequivocal, e.g. 2km dextral displacement of the Dartmoor granite by the SLFZ (Bristow & Robson 1994, Holloway & Chadwick 1986). Lineaments of these fault zones are therefore ideal for further analysis because the geological causes are known. Due to the low outcrop exposure within SW England some of the previous mapping of these NW/SE dextral faults has been in part dependant on their topographic expression. A high proportion of lineaments interpreted from the satellite imagery correlate to linear topographic features. Consequently, such lineament zones may relate to unproved, although

mapped, geological features. As all the lineament zones identified have lineament patterns characteristic of mapped fault zones, it is therefore considered that such linear features identified by the lineament zones are most likely to be faults.

Initial comparison between mapped fault zones and lineament zones identified in this study indicates lineament zones can be discontinuous (e.g. lineaments corresponding to the fault strands of the SLFZ, Fig. 4.3). Consequently, lineament fault zones need to be extrapolated in some cases. The lineament zone reflecting the SLFZ can also change in thickness from a single lineament to multiple lineaments. The widest lineament zone within SW England is up to 6km within the Dartmoor granite suggesting a similar thickness to the SLFZ. Not all fault zones, however, show a lineament expression. Such cases are the Prewley-Dartmouth wrench fault, the high angle tear faults between Dartmoor and Bodmin Moor, and the normal Looe Valley fault (Fig. 4.3).

Lineaments of the Sticklepath-Lustliegh, Portwrinkle and Porth Towan fault zones are highlighted in Fig. 4.4. The Porth Towan fault produces lineaments that have a maximum trend towards 135° , in comparison the northern section of the Portwrinkle fault trends towards 150° . Lineaments derived from the Portwrinkle and SLFZ show a change in trend northwards with lineaments swinging from a NW/SE trend to a NNW/SSE trend. Such lineaments can therefore be characterised as typically possessing a NW/SE trend, however, lineament trends can change along and also between lineament zones.

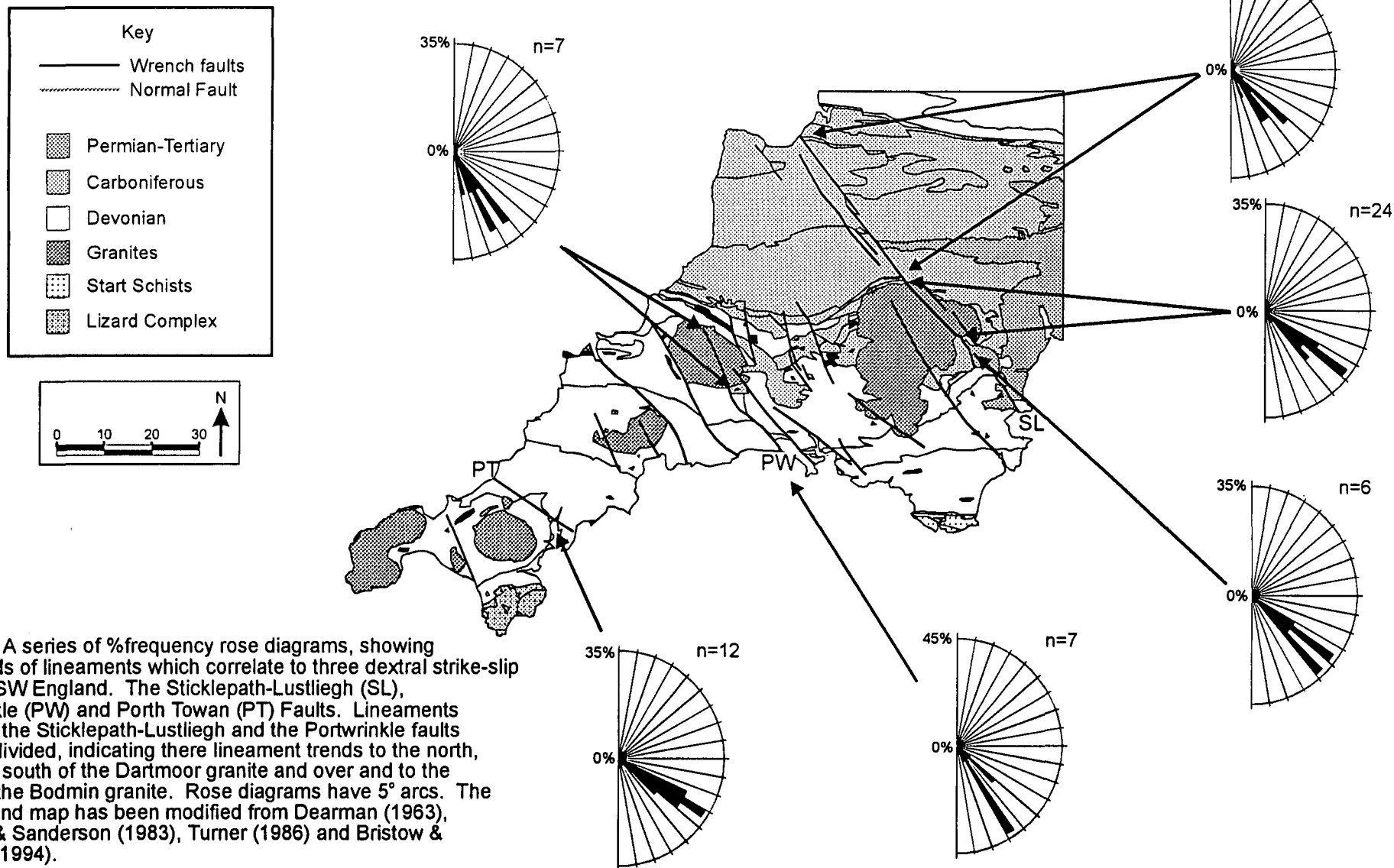


Fig. 4.4. A series of %frequency rose diagrams, showing the trends of lineaments which correlate to three dextral strike-slip faults in SW England. The Sticklepath-Lustliegh (SL), Portwrinkle (PW) and Porth Towan (PT) Faults. Lineaments following the Sticklepath-Lustliegh and the Portwrinkle faults are sub-divided, indicating their lineament trends to the north, over and south of the Dartmoor granite and over and to the south of the Bodmin granite. Rose diagrams have 5° arcs. The background map has been modified from Dearman (1963), Hobson & Sanderson (1983), Turner (1986) and Bristow & Robson (1994).

Average lineament lengths formed from the above faults located in the granite and sedimentary rocks of SW England are shown in Table 4.1, suggesting that lineaments interpreted from a granite are longer.

	SLFZ north of the Dartmoor granite	SLFZ south of the Dartmoor granite	Portwrinkle fault zone	Porth Towan fault zone
Average length of lineaments crossing sedimentary rocks (m)	2470	1902	1975	1836
Average length of lineaments crossing granites (m)	3062		2442	2442

Table 4.1. The average length of lineaments formed by three major fault zones within SW England.

In a uniform rock, fault length has a relationship with the degree of stress applied, with increasing stress corresponding to longer faults (Walsh & Watterson 1988a). Assuming a similar stress field across these NW/SE fault zones, differences in fault length could be related to the rock type. Accommodation of stress in these upper crust granites would predominantly occur as brittle deformation. Rock material properties, particularly higher values of shear modulus can increase the length of faults (Walsh & Watterson 1988a). The shear modulus of the sediments of the Culm deposits are ~1 GPa for mudstones (C.Morris pers. com. 1985, in Walsh & Watterson 1988a), 1-15 GPa for shales and 1-40 GPa for sandstones (Selby 1993), hard sandstones in coal fields have a shear modulus of ~12 GPa (C.Morris pers. com. 1985, in Walsh & Watterson 1988a). Granites, however, have a higher shear modulus of 15-50 GPa (Selby 1993). Relatively softer pelitic and arenitic sedimentary rocks of SW England therefore may allow a greater proportion of the stress applied to be accommodated as ductile deformation and consequently forming smaller fault lengths. Alternatively, fault-line scarps (Chapter 2.5.2) may have been healed

within sedimentary strata. Scarps of these relatively softer rocks would in comparison to granites be preferentially eroded, resulting in a less pronounced geomorphological feature. Lineaments therefore reflect this and as a consequence may not be interpreted from images or be shortened. Lineaments in the mapped lineament zones can also show close continuity suggesting a single fault segment, however, by partial healing of the fault-line scarp multiple shorter lineaments could instead be produced.

(iii) High density wide E/W and NE/SW lineament zones

This lineament pattern, although forming a lineament zone, can be differentiated from lineament zones reflecting high-angle faults by the wider areas of high lineament density and continuous lineaments. The abrupt linear change in lineament density and patterns outside the high density zone suggests a sharp distinct change in geological trend and strike. Possible geological structures which could produce such a change are unconformities, igneous intrusions and thrust belts. The strong parallel nature of the lineament zone means that it is unlikely that such features are formed by most igneous intrusions, apart from large dyke swarms. An unconformity, exposing different rocks could produce such lineament trends. However, angular unconformities generally have a curvilinear trace controlled by topography. It is more likely that the wide lineament zone indicates the presence of high angle thrust faults. A sharp change in lineament trend can be formed across a leading fault, with high densities of similarly trending lineaments produced because in thrust zones bedding is often parallel to the thrust strike and folds carried along the thrusts have analogous symmetry (described in Section 2.6.1(iii)).

Mapped areas of SW England in which lineaments have been found to form wide lineament zones are South Devon (southern zone) and West Devon/East Cornwall (northern zone) (Figs. 4.5, 4.6). N/S lineaments in the areas covered by Figs. 4.5 and 4.6 form thin lineament zones and are considered to be formed in this study by a late N/S fracture (Scrivener *et al.* 1994) (see Section 4.2.5(ii)). Therefore, to allow a better visual interpretation, N/S trending lineaments have been removed from these lineament maps. The basic sedimentology and tectonic history of areas of Devon and Cornwall deformed by thrust tectonics is discussed in Sections 2.3.3 and 2.3.4. Extensive work by various authors (e.g. Isaac *et al.* 1983, Selwood *et al.* 1984, Turner 1986, Selwood & Thomas 1986a) has revealed a complex sedimentology and tectonic history, the basic lithotectonic maps of which are also shown in Figs. 4.5, 4.6.

In the southern zone lineaments trend E/W around Plymouth to NE/SW south-east of Dartmoor. These reflect the lithotectonic trends of the E/W trending Plymouth - Dartmouth Unit and Saltash Unit, ENE/WSW trending Totnes Unit and NE/SW trending Islington and Liverton Unit, Kate Brook Unit and the northern parts of the Southern Unit (Fig. 4.5). In the northern section an arcuate trend to a wide lineament zone can be identified, changing from: ENE/WSW to the north of the Dartmoor granite; NE/SW north-east of the Dartmoor granite; E/W between the Dartmoor and Bodmin granites; WNW/ESE north-east of the Bodmin granite and E/W north of the Bodmin granite. These lineaments also closely follow the outcrop traces of the lithotectonic units of this area (Fig. 4.6). In SW England these lineament patterns can suggest and follow the unique lithotectonic trends of the central SW England thrust belt. However, only broad delineation of the structural zones can be achieved.

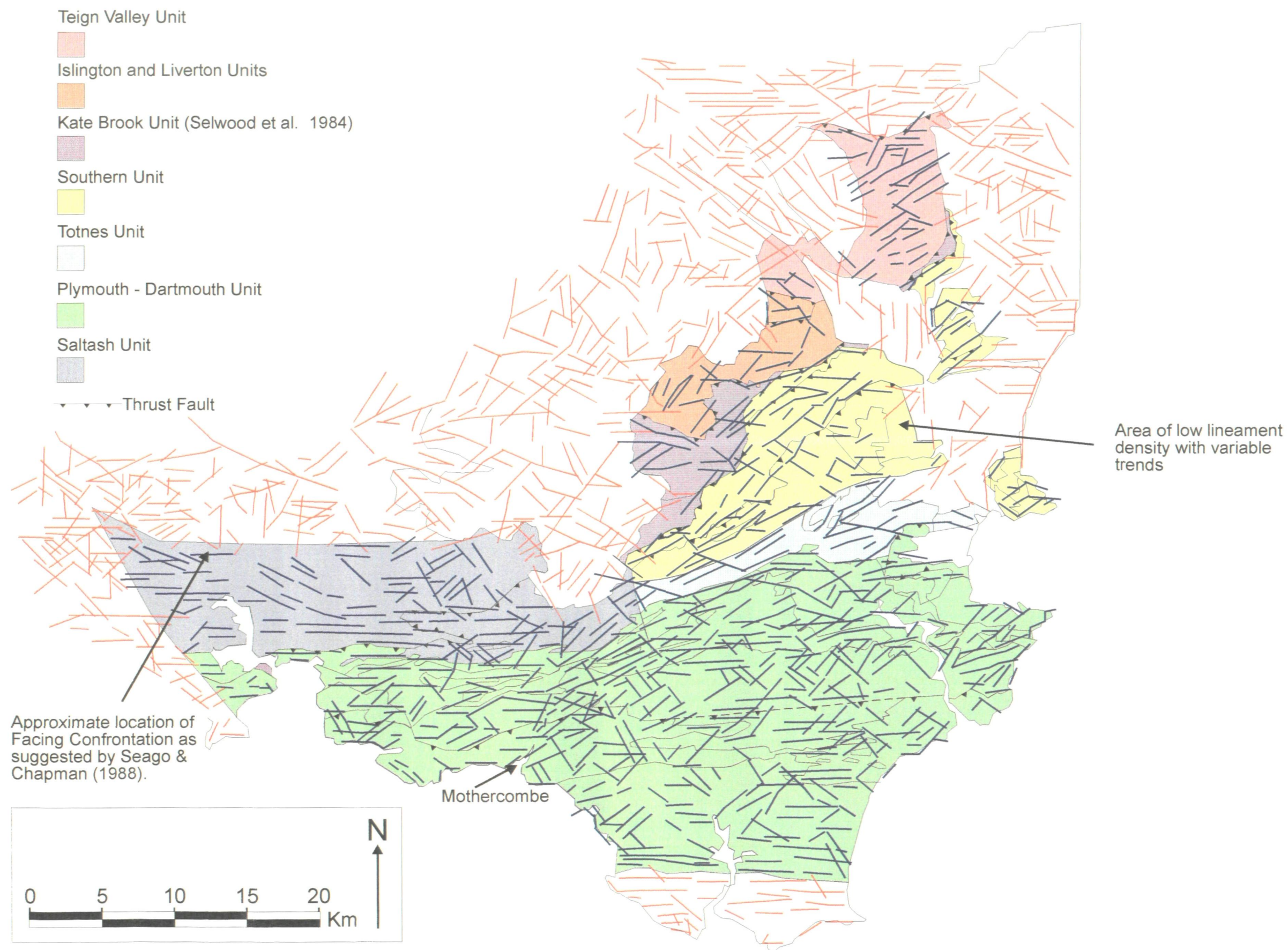


Fig. 4.5. Lineament map of South Devon underlain by mapped tectonostratigraphic units (redrawn from Turner 1986). In this map lineaments that are interpreted to be formed by late N/S fracturing have been removed.

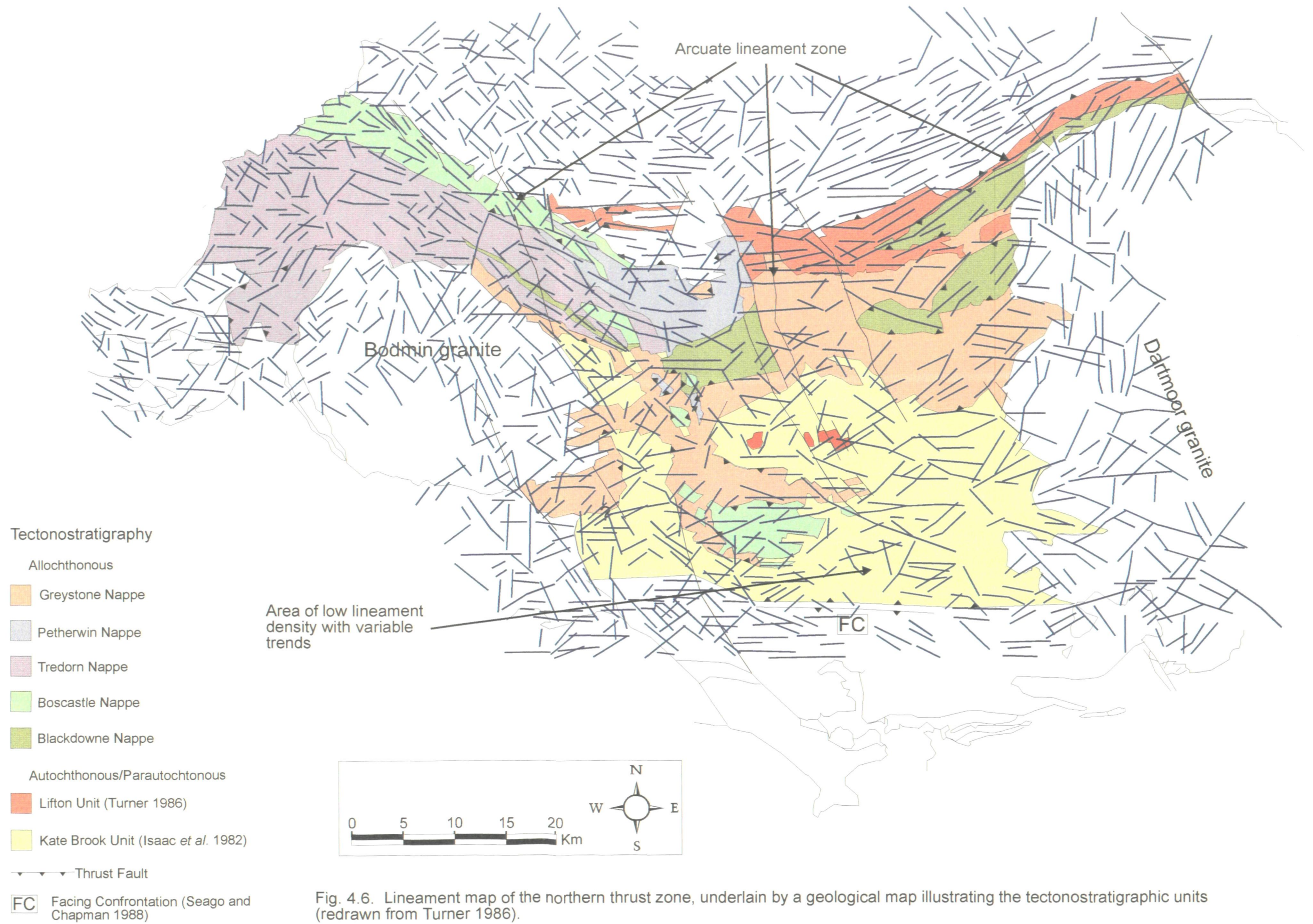


Fig. 4.6. Lineament map of the northern thrust zone, underlain by a geological map illustrating the tectonostratigraphic units (redrawn from Turner 1986).

Areas of anomalous low lineament density with variable trends can also occur within the wide lineament zones (Fig. 4.5). In this area flat lying thrusts form klippen of horizontal bedding and cleavages in the relatively hard rocks of the Ugbrooke-East Ogwell and Torbryan successions to the east of the Southern Unit. Such flat lying structures tend to produce topographically controlled curved outcrop traces reflected in a lower concentration of lineaments and a more variable trending lineament pattern, this suggests that the lineament analysis described in Chapter 3 can be sensitive to more localised lithotectonic trends.

Sharp delineating boundaries between high and low lineament densities can be identified at the edges of the wide lineament zones. These boundaries demark the area of the thrust belt. In the northern zone this correlates to the boundary to the Culm Basin. However, in the southern section an ~E/W trending boundary can be located to the north of Plymouth (Fig. 4.5). This boundary spatially corresponds to the Facing Confrontation at Cargreen between northward facing (southern zone) and southward facing (northern zone) as suggested by Seago & Chapman (1988) (Fig. 4.7). To the north of this zone a low lineament density with variable trends is typical of flat lying structures as previously identified near Newton Abbot. Such lithotectonic trends are found within this part of the northern zone, known as the Kate Brook Unit (Isaac *et al.* 1983). Although lineament patterns cannot be used to identify fold facing directions, such a change in lineament pattern implies major changes in lithotectonic trends, as would be expected when crossing a leading edge thrust, and therefore the suggested Facing Confrontation. An absence of a delineating change in lineament pattern occurs to the east of the southern section where there is a continuation of the lineament pattern into the Permian cover, east of the Teign Valley Unit (Fig. 4.5).

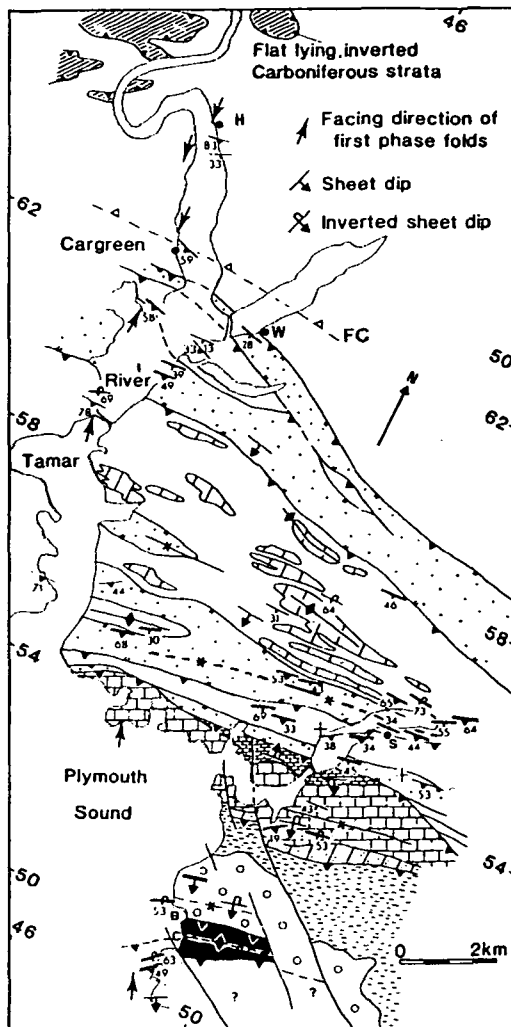
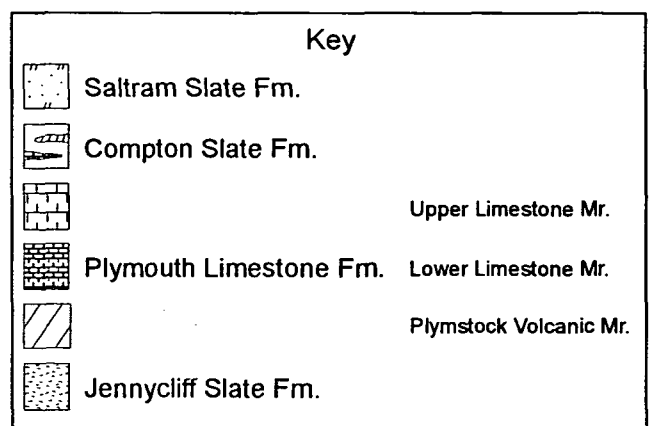
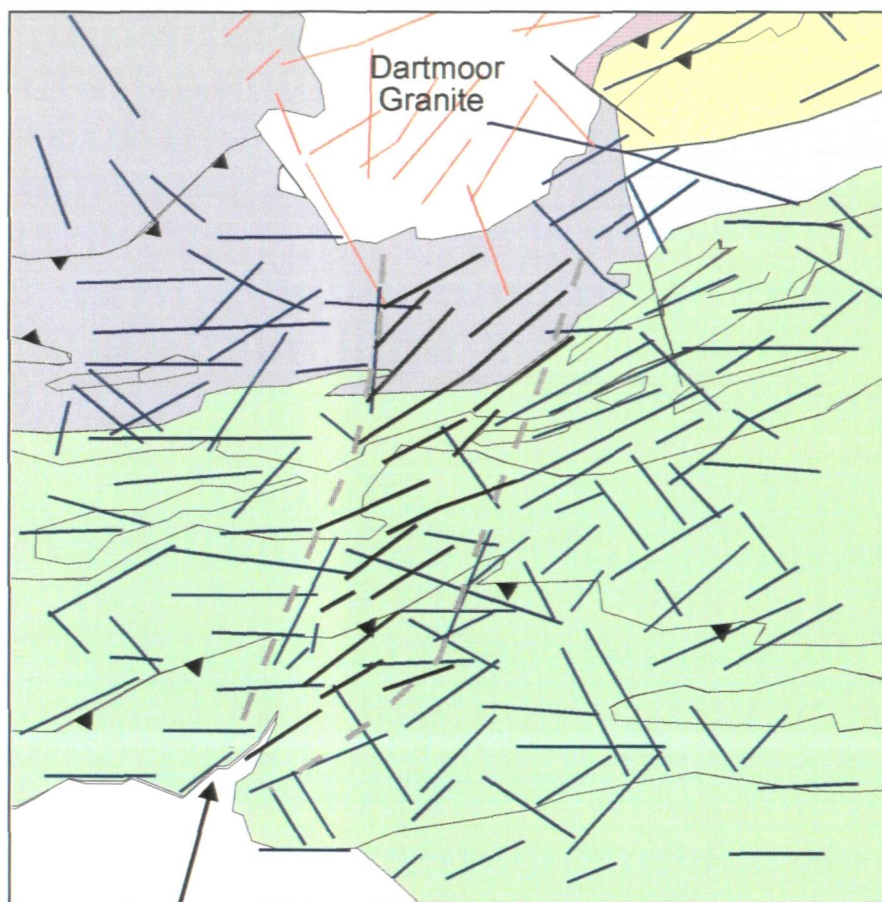


Fig. 4.7. Geological map illustrating the structure of the area from Plymouth Sound to Cargreen. Southwards from the Facing Confrontation (FC) are a series of NW/SE to E/W trending thrusts, with associated E/W trending outcrop traces and folds (redrawn from Seago & Chapman 1988).



This may suggest a reflection in the Permian cover of the underlying geology and hence a continuation of the underlying southern zone to the east.

Trending to the NNE from Mothercombe Bay (in South Devon) is a zone of ENE/WSW to NE/SW trending lineaments which are anomalous to the E/W lineaments, east and west of this zone (Fig 4.8). Central to this zone are the NE/SW lineaments, which are bounded by the ENE/WSW lineaments. This zone can be differentiated from the lineaments relating to the south Devon thrust sheet by a sharp change in lineament trend, the change in trend forms a linear boundary to this anomalous zone. This change in trend can be identified as a low lineament zone in the lineament density map containing E/W lineaments (Fig. 7.4). Furthermore, this zone is shown to correlate to the end of the NE/SW trending lineaments relating to the NE/SW to E/W arcuate trend of the South Devon thrust zone, this can be observed in the lineament density map Fig. A2.7. From this evidence the anomalous trending lineaments within the zone suggest a localised change in trend to the primary lithotectonic features. In this region Seago & Chapman (1988) have mapped ENE/WSW trending outcrop traces. However, the sharp transitions in lineament trend may suggest that this is a zone of deformation. Translation of the primary foliation across a major NNE/WSW trending sinistral shear zone can produce a similar outcrop trace. Hence this zone may be part of the late Variscan sinistral NE/SW fault pattern. Alternatively the proposed shear zone may be formed synchronous to the NW to NNW thrust sheet emplacement (Chapman *et al.* 1984, Coward & McClay 1983) as lateral or oblique ramps.



Mothercombe

———— NE/SW to ENE/WSW trending lineaments within the anomalous zone

- - - - - Boundary of zone

Kate Brook Unit

Southern Unit

Totnes Unit

Plymouth - Dartmouth Unit

Saltash Unit

Fig. 4.8. Geological and lineament map of South Devon, north of Mothercombe. The map highlights an anomalous zone of ENE/WSW trending lineaments.

(iv) Termination of E/W lineaments by a zone of very low lineament density

A N/S zone of very low lineament density can be identified running northwards from Exeter. Within this zone E/W lineaments identified as primary features within the Culm Basin and also the regional NW/SE, NE/SW and N/S thin lineament zones are greatly reduced in frequency. Lineament terminations along the western boundary of the low density zone were achieved primarily without cross-cutting lineaments, suggesting that it is not a faulted boundary. The zone of low density lineaments may be caused by flat lying lithotectonic features, such as found with areas of klippen. Further evidence for flat lying lithotectonic features is suggested by the curvi-linear boundary of this lineament pattern, as a curvi-linear outcrop pattern can be obtained from topographic control on flat lying features. As the lineament patterns in the area suggest the boundary is not fault related and indicate an absence of high density lineament zones of similarly trending continuous lineaments, it is concluded that the origin of flat lying features therefore is not thrust related. These characteristics can suggest an angular unconformity with the area of low lineament density representing flat lying lithotectonic features of the overlying strata. The absence of thin lineament zones (thought to represent late-Variscan fault zones) therefore implies that these rocks were deposited after this phase of deformation.

The area of low lineament density with variable lineament trends correlates to Permian-Triassic aged sediments ranging in dip (to the East) from 30° to 3° - 6° eastwards across the Exe estuary. These sediments form an angular unconformity to the Variscan deformed Palaeozoic rocks to the west, the curvi-linear boundary (which was identified in the lineament map) relating to the relict topography. A large E/W trending lineament set, however, can be identified in the Crediton Trough (Fig. 4.2). The formation of the Crediton Trough is produced by

steep E/W and ENE/WSW Permian normal faults linked either to normal faulting at Wanson Mouth in North Cornwall (Freshney & Taylor 1971) or a reactivated Variscan thrust (Holloway & Chadwick 1986), producing northward and southward dipping strata. E/W lineaments can cross-cut and also cross-cut by NW/SE and NE/SW trending lineaments. This suggests that the E/W lineaments may be primary features as they are cross-cut. However, the cross-cutting E/W lineaments may also represent post-Permian fault movements. Similarly, some of the NW/SE trending fractures therefore must relate to post-Permian movements. The importance of these E/W lineaments is that apart from whether they are cross-cut by (and hence may be lithological differences or early faults) or cross-cut (later faults) discordant lineaments, the absence of thin lineament zones (typical of fault zones) indicates that their origin can not be identified by their lineament pattern.

(v) Complex lineament patterns of South Cornwall

Lineament trends in South Cornwall are similar to elsewhere in SW England, however, the cross-cutting relationships are far more complex. Lineaments of each major trend can be identified to cross-cut all other lineament trends. This has resulted in an absence of long lineaments and a confusing lineament pattern. The cross-cutting relationships suggest that the area contains a complex fracture pattern which has either undergone multiple-phases of deformation and/or reactivation (see Section 4.2.5(ii)).

The primary lithotectonic trends of South Cornwall are illustrated in Fig. 4.9a. Comparison of the lineament patterns to the cleavage trend which tends to be parallel to lithological strike (Leveridge *et al.* 1990) indicates that only some lineaments may be formed by these primary lithotectonic features (Fig. 4.9b),

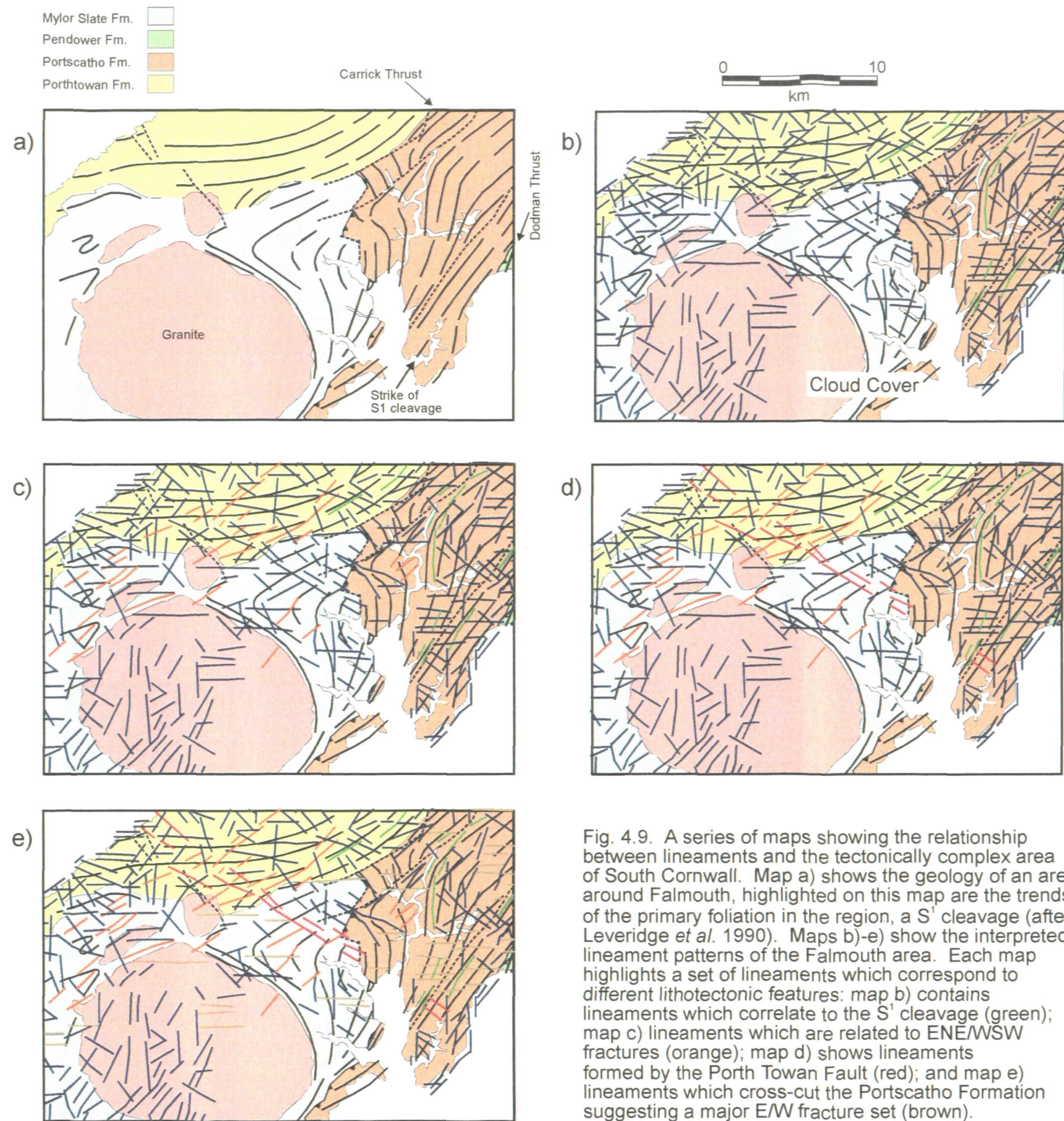


Fig. 4.9. A series of maps showing the relationship between lineaments and the tectonically complex area of South Cornwall. Map a) shows the geology of an area around Falmouth, highlighted on this map are the trends of the primary foliation in the region, a S¹ cleavage (after Leveridge *et al.* 1990). Maps b)-e) show the interpreted lineament patterns of the Falmouth area. Each map highlights a set of lineaments which correspond to different lithotectonic features: map b) contains lineaments which correlate to the S¹ cleavage (green); map c) lineaments which are related to ENE/WSW fractures (orange); map d) shows lineaments formed by the Porth Towan Fault (red); and map e) lineaments which cross-cut the Portscatho Formation suggesting a major E/W fracture set (brown).

therefore most lineaments can be considered to be formed from fractures as suggested by the cross-cutting nature of the lineaments (Figs. 4.9c, d, e). Due to the change in the primary lithotectonic trends in South Cornwall, NNE/SSW to E/W lineaments can be considered to be formed from primary lithotectonic features and fractures while other lineament trends relate mainly to fractures. Cross-cutting lineament patterns in the region therefore suggest a geological history involving multiple phases of deformation and fault reactivation. Such a history has been suggested to occur (Ratley & Sanderson 1982, Alexander & Shail 1995, Shail & Alexander 1997) and produces complex fracture patterns (Fig. 4.10). The degree of information that can be yielded by such complex lineament patterns, however, is low as different fractures form ambiguous lineaments and cause the primary lithotectonic trends to be masked.

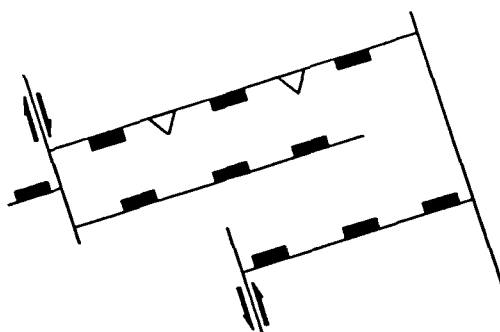
4.3 Characteristics of localised lineament patterns

In this section more localised lineament patterns or lineaments with anomalous trends are described and discussed. Some of the lineament patterns, however, can cover relatively large areas. These patterns have been included in this section because direct comparison to the lineament characteristics in the previous section can be used to determine the geological causes of these more anomalous patterns.

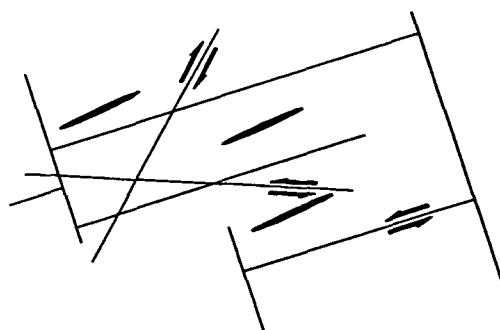
4.3.1 Characteristic lineament patterns

(i) Numerous short E/W lineaments abut at right angles onto single highly-discordant cross-cutting longer lineaments typical of a stream trellis pattern (Figs. 4.2b, c). E/W lineaments are characterised by being relatively short and having

Stephanian to
Early Permian



Early to Late
Permian



Late Permian
to Triassic

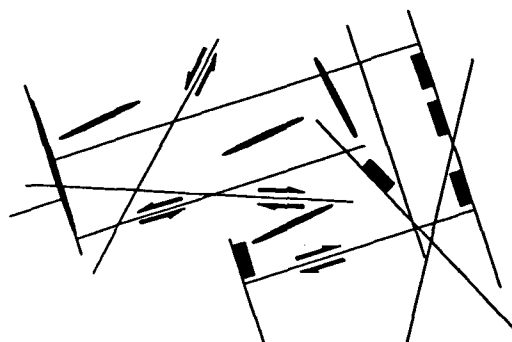
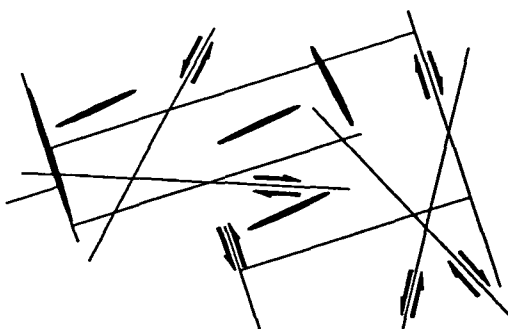


Fig. 4.10. An example of how multiple fracture trends and fault reactivation can create a complex fracture pattern in the Lizard Complex, South Cornwall (redrawn from Shail & Alexander 1997).

similar lengths. The area covered by this lineament pattern in SW England pattern is restricted to East Devon and West Somerset.

(ii) Dendritic lineament patterns in central Devon formed from NE/SW, E/W, N/S and NW/SE lineaments (Fig. 4.1f).

(iii) E/W trending lineaments which can be cross-cut by discordant lineaments showing closures (Fig. 4.11a, b, c)

(iv) In North Devon, E/W to WNW/ESE lineaments can be extremely long. It is found that these relatively few lineaments are inter-connecting, and in part, are discordant to the 'primary' lineaments (Fig. 4.11d). Generally these lineaments are not cross-cut by discordant thin lineament zones.

(v) Large curvatures to thin lineament zones changing in trend from WNW/ESE to NNW/SSE (Fig. 4.11e)

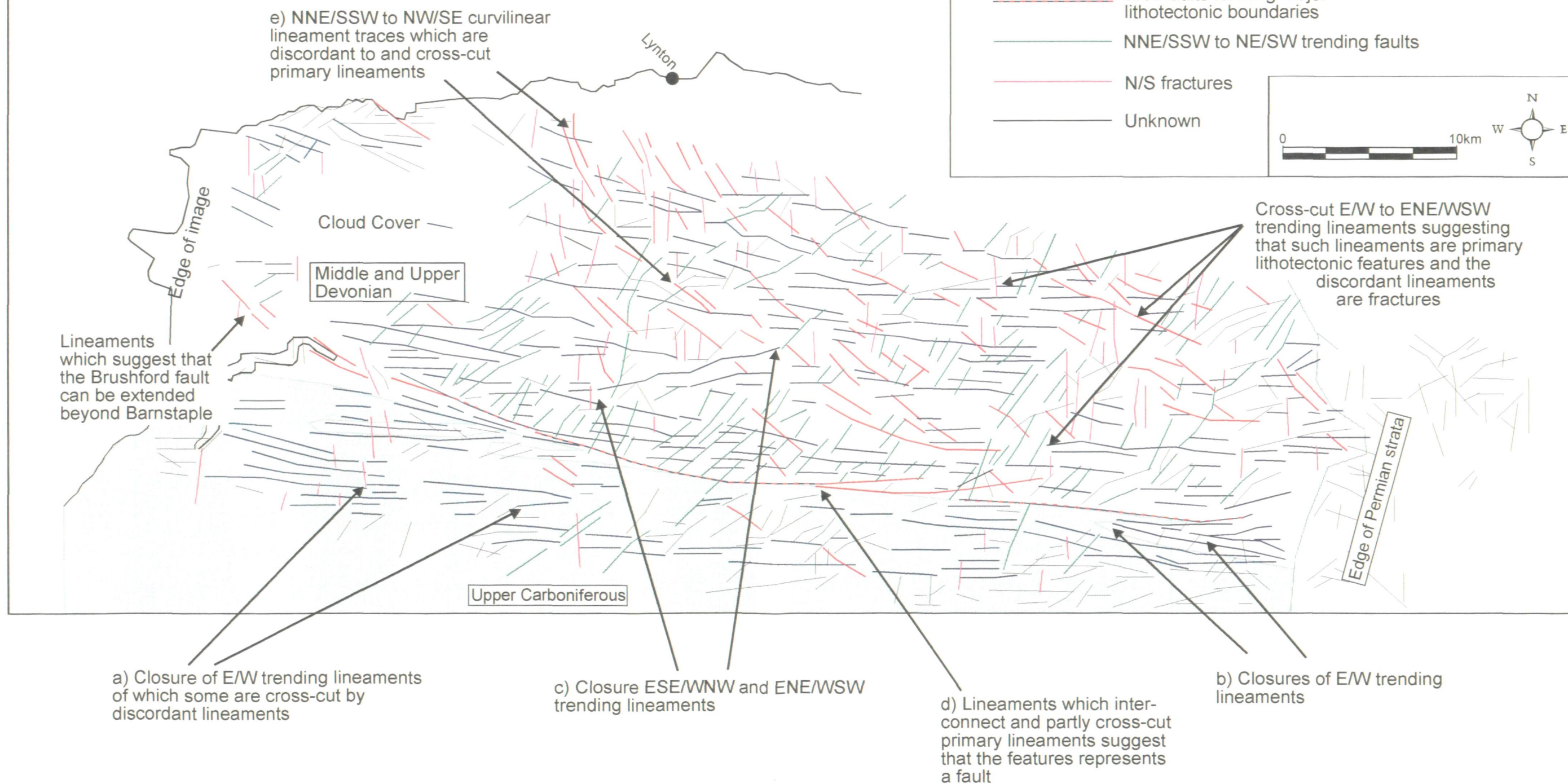
(vi) A localised area of central and South Devon show an absence of primary lineaments, i.e. no continuous lineaments apart from thin lineament zones. Around the edges of this area the E/W to ENE/WSW primary lineaments that can be identified are terminated. However, these are not bounded by discordant lineaments (Fig. 4.1h). Relative to surrounding areas, visual estimation of the lineament density of these localised areas is low.

4.3.2 Geological analysis of the characteristics in localised and anomalous lineament patterns

(i) Trellis lineament pattern

The trellis lineament pattern of Fig. 4.2b and c is the reflection of the local stream pattern typically controlled by scarp dip slopes where the long lineaments reflect the strike of the regional dip and the short discordant streams can indicate the regional dip direction. The lineament pattern in Fig. 4.2b can only suggest the

Fig. 4.11. Lineament map of North Devon illustrating lineament closure patterns (a, b, c), inter-connecting long E/W lineaments (d) and curvilinear NW/SE to NNW/SSE lineament traces (e). The lineament map has been colour coded to show how specific lineament characteristics relating to known lithotectonic features identified from lineament patterns in SW England (highlighted by surrounding captions) can be extrapolated in larger areas. The geological causes of lineaments are shown in the key to the right.



strike of the regional dip (N/S). However, in Fig. 4.2c the discordant lineaments occur only to the ESE of the NNE/SSW trending long lineament reflecting a shallowly dipping dip slope (illustrated in Fig. 2.5), therefore suggesting a regional lithological strike of NNE/SSW which dips at relatively shallow angle to the ESE. The regional dip of the Mesozoic strata in the region is at shallow angles to either the E or ESE indicating that these lineament patterns relate to scarp slope morphology, with the longer NNE/SSW lineaments relating to Upper Greensand scarps (Fig. 4.2c, d).

A possible structural control may be also be involved with the E/W and ESE/WSW trending lineaments in the region. E/W trending lineaments may be the western extension of the large E/W trending, Isle of Wight - Purbeck flexure, or possible reactivation of the underlying structural trends in the Variscan basement. Lineaments trending to the ENE/WSW may also be influenced by a late Cenozoic, meso-fracture pattern (Bevan & Hancock 1986). However, this control cannot be identified from the lineament map.

(ii) Dendritic lineament pattern

Dendritic lineament patterns in East Devon (Fig. 4.1f) probably reflect dendritic stream patterns. NE/SW and N/S (Fig. 3.10) trending stream patterns suggest that the E/W lithological control on the geomorphology and hence lineament patterns in this localised area can be reduced by the cross-cutting streams. These lineament trends, however, may be partially controlled by the regional fracture systems or be related to a drainage system influenced by the former Cretaceous cover (Embleton 1984) (see Section 2.7). Again, this can not be confirmed from the lineament map.

(iii) Closure of E/W trending lineaments

E/W trending lineaments, previously identified as primary features in Section 4.2.5, can show a tight closure pattern. Closure of lineaments can be interpreted to reflect the presence of folds, a tight closure therefore suggesting a tight fold closure. The area in which these lineaments are located lies within the Culm Basin, an area deformed by E/W trending folds (see Section 2.3.4). The lineament closure in the Upper Devonian is less well defined and consists of WNW/ESE and ENE/WSW trending lineaments. The WNW/ESE lineament set in this region can be interpreted as primary lithotectonic features as they are regularly cut by discordant lineaments and form continuous features. To this, the ENE/WSW localised lineament trend is anomalous. Geological maps of the region, however, show that located within this area are the small scale folds of the Bray Valley Syncline and Anticline (Edmonds *et al.* 1985) (Fig 4.12) in which WNW/ESE trending strata are folded into ENE/WSW trending strata. These lineament patterns suggest that the lineament analysis can identify localised structures within SW England.

(iv) Inter-connecting lineaments which cross-cut 'primary' lineaments

These lineaments although being sub-parallel to lineaments identified as primary features can be found to cross-cut these features, suggesting that at least in part they are a series of fault segments. As these lineaments are rarely cross-cut by discordant lineaments this suggests that they are later in age than the main phase of faulting.

In North Devon the Upper Devonian rocks are bounded to the south by a major E/W trending fault, the Brushford fault (Edmonds *et al.* 1985) or the Cranborne-Fordingbridge fault (Lee *et al.* 1990) (Fig. 4.12). The length of the

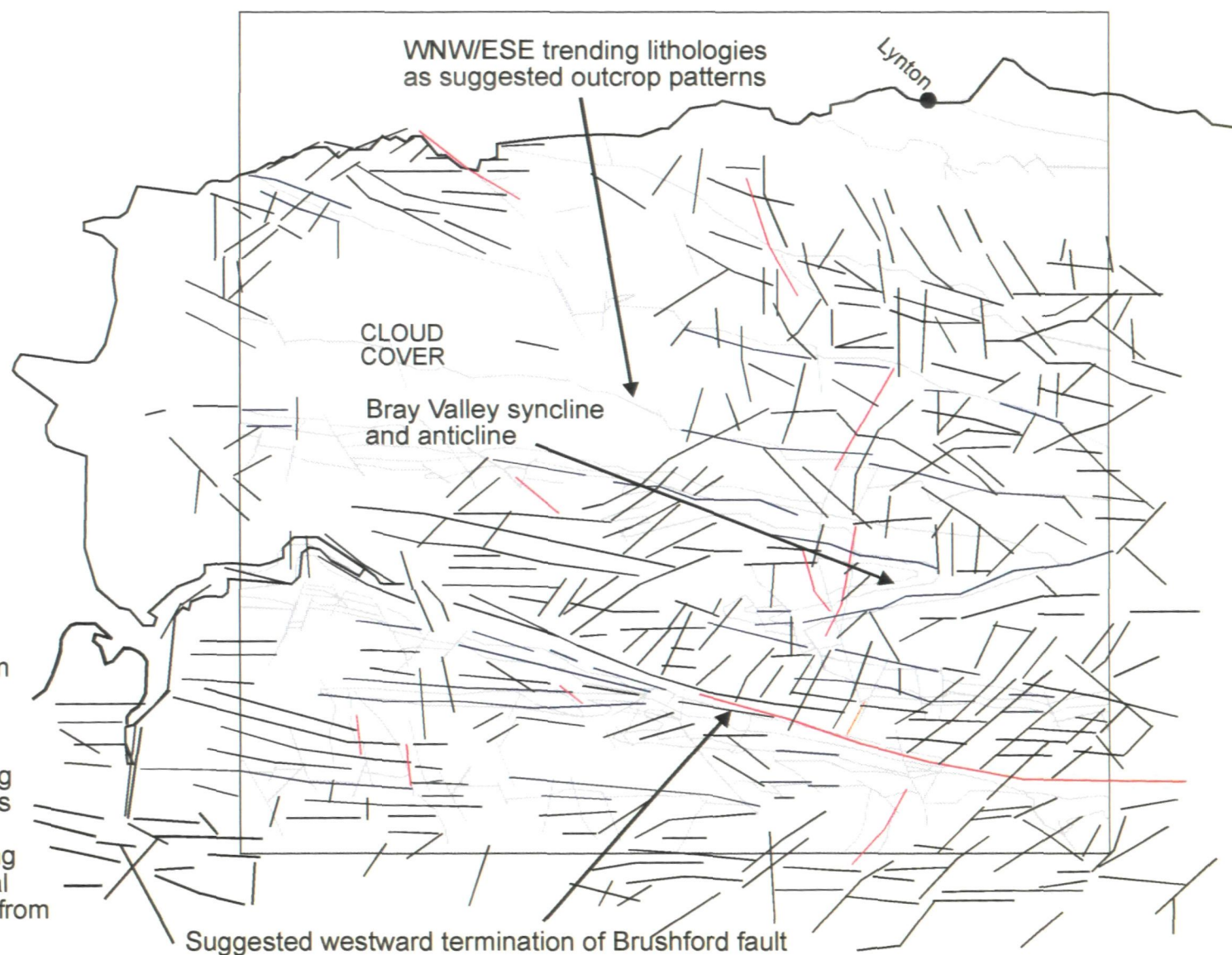


Fig. 4.12 Diagram showing the spatial relationship to the local geology and the geological interpretation of lineaments, from North Devon. Lineaments which are highlighted strongly correlate to linear geological features shown on the underlying geological map. Blue lineaments relate to lithological differences, with red lineaments, cross-cutting faults. The underlying geological map, coloured cyan, is redrawn from Edwards *et al.* (1985).

Brushford fault is mapped by Edmonds *et al.* (1985) to terminate in a major anticline and syncline (Fig. 4.12). Lee *et al.* (1990) identified this feature from combined gravity and aeromagnetic data, and extends the fault to pass through Barnstaple. Analysis of the region by satellite images illustrates that the above curved long lineaments relate to this structure from the Permian sedimentary cover, to Barnstaple. To the west of Barnstaple, extrapolation of the lineament trace suggests a curved change in lineament trend to the NW/SE, hence extending the mapped fault.

(v) Curved thin lineament zones of North Devon

The WNW/ENE to NNW/ESE lineament zones in North Devon typically cross-cut the primary lineaments (Fig. 4.11e). They also show a similarity to regionally extensive NW/SE, NE/SW and N/S lineament zones identified as fault systems (see Section 4.2.5), hence these features are interpreted as fault zones. The change in lineament trend occurs southwards over the region, suggesting that the lineament zones (or interpreted fault zones) sole into the Brushford fault (Fig. 4.13).

Closer analysis of the WNW/ESE trending lineaments, identified previously as primary lithotectonic features, show that some are dextrally offset (Fig. 4.14), further indicating the ~NW/SE lineaments in this region represent a series of fault zones. A high proportion of the 'primary' lineaments cross-cut by the NW/SE trending lineaments within the central area of North Devon, however, possesses an E/W trend (Fig. 4.14). This trend therefore shows an approximate 10° anti-clockwise rotation to the normal WNW/ESE trend of 'lithological' lineaments outside the ~NW/SE lineament zone, and also within the area. A possible

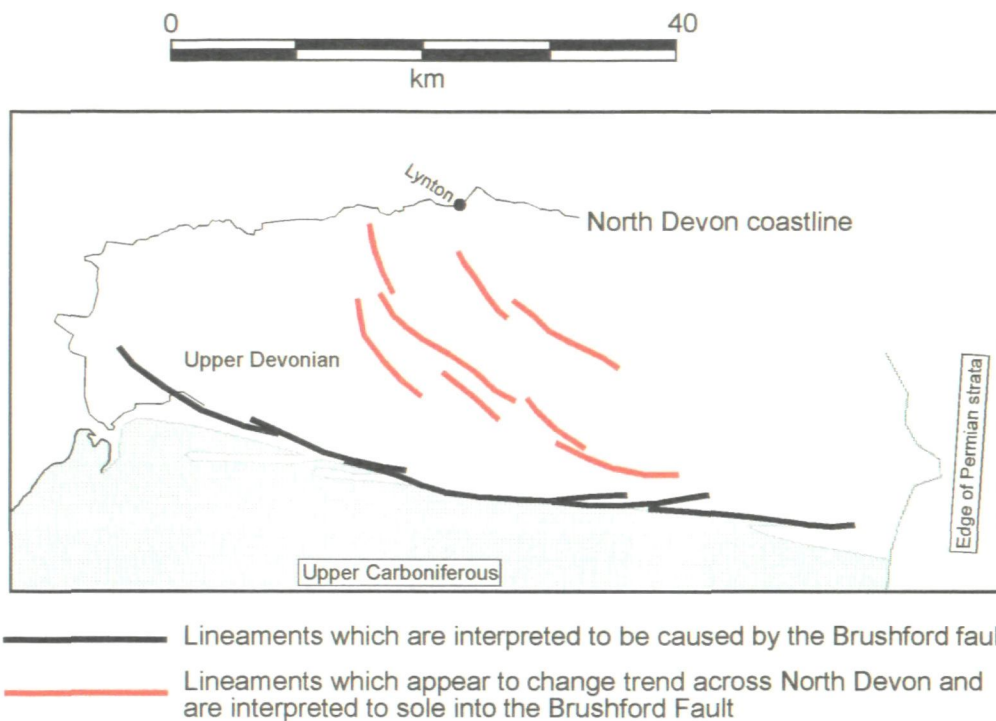
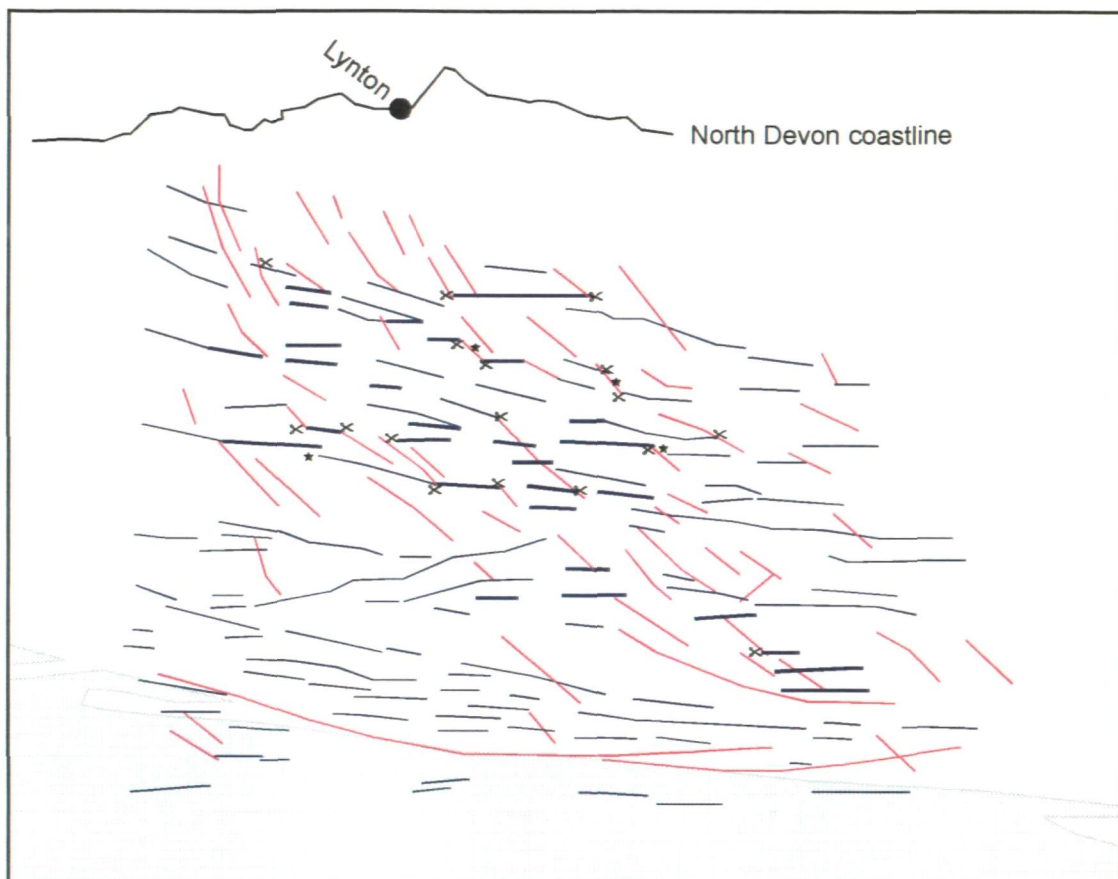


Fig. 4.13. Map covering North Devon showing the trends of major lineaments within the region, interpreted to be related to faults.



- Lineaments interpreted as NW/SE to E/W trending faults
- Lineaments correlating to the lithological outcrop trend
- Lineaments correlating to the lithological outcrop which show a small anti-clockwise rotation
- ★ Lithologic lineaments showing a dextral displacement across lineaments interpreted as cross-cutting faults
- ✕ Lithological lineaments terminating at lineaments interpreted as cross-cutting faults

Fig. 4.14. Lineament map of North Devon showing lineaments which have been found to correlate to the strike of lithology, and cross-cutting NW/SE to E/W trending faults. Highlighted are primary lineaments which may have undergone anti-clockwise rotation.

mechanism for the rotation of such marker beds within fault bounded blocks are block rotation systems.

A domino-type block rotation system which is bounded by dextral NW/SE trending strike-slip faults (Mandl 1987) produces anti-clockwise rotating blocks (Fig. 4.15). This system could be produced by dextral transpression across a major E/W shear zone, in this setting the system bounding fault being the Brushford fault. A dextral transpressive setting is considered by Badham (1982) to have occurred in the Variscides of Europe and by Holdsworth (1989), Jackson (1991) and Mapeo (1992) in the Variscan orogeny of SW England. Schreurs (1994) has produced evidence that antithetic cross-faults which sole into the bounding dextral strike-slip master faults can have a 'Z' sigmoidal shape (Fig. 4.16), similar to the interpreted faults within North Devon. However, the sense of rotation imparted upon the block is clockwise (Fig. 4.16). Block bounding faults have been interpreted to sole into the system bounding faults, in a domino-style block system (Randall *et al.* 1996). Therefore, it is suggested that the change in trend of the ~NW/SE lineaments reflects a change in fault trace as the faults sole in to the Brushford fault, and that block rotation may have occurred in North Devon possibly from dextral transpression.

(vi) Lithological lineament terminations surrounding an area where primary lineaments are absent

Areas which contain low numbers of 'primary' lineaments can be achieved by later complex fracturing (see Section 4.2.5). However, surrounding this localised area of central and South Devon are strong trends of primary lineaments, which can terminate against the area without being cross-cut by discordant lineaments (hence, not cut by faults). The relative lower density of

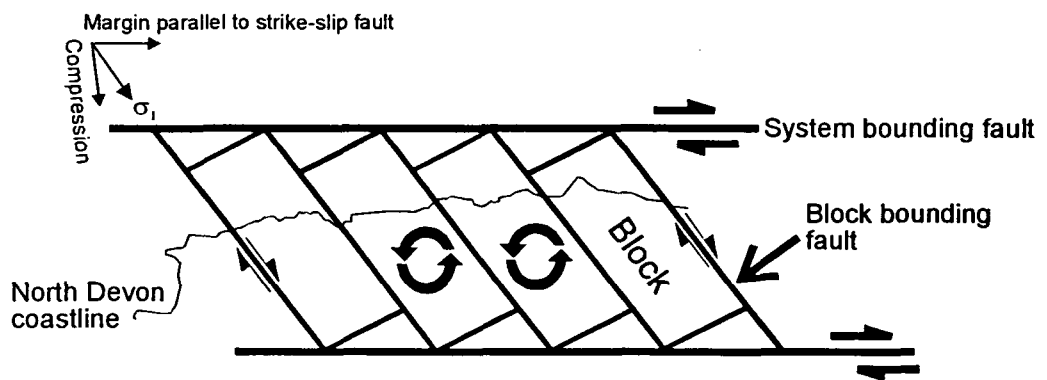


Fig. 4.15. The bookshelf block rotation model of Mandl (1987). Fault bounded blocks have the opposite sense of rotation to the slip movement of the system bounding faults.

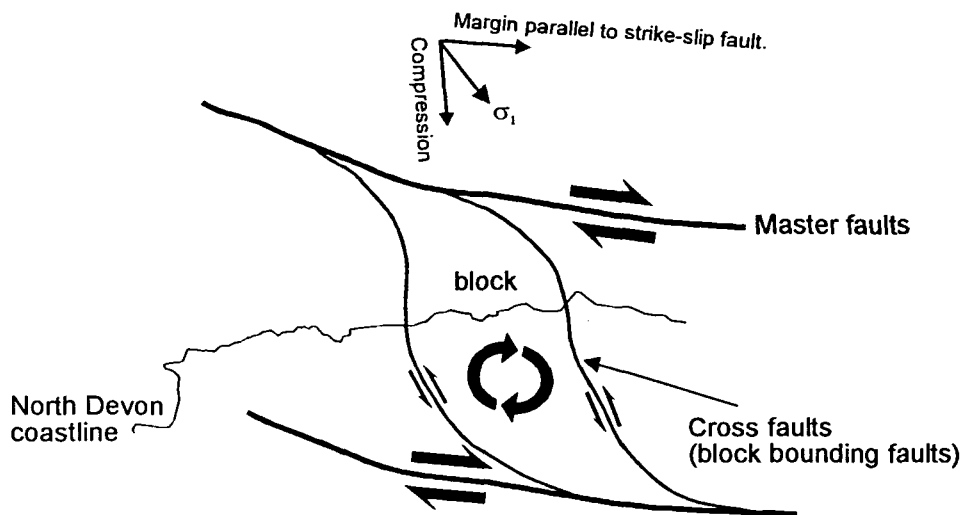


Fig. 4.16. Block rotation model from Schreurs (1994) where the block is rotated in the same direction as the master bounding faults. In this model the cross faults can achieve a sigmoidal shape.

lineaments present within the area, therefore, also suggests that later complex fracturing probably has not masked the 'primary' lineaments. As primary lineaments surround this area in central/South Devon it indicates that either, there is a lack of control on geomorphology by primary lithotectonic features with the area formed from flat lying lithotectonic features (see Section 4.2.5), or in the area there are no primary lithotectonic features. The absence of a faulted boundary indicates that the absence of primary lithotectonic features is not thrust related (klippen). An angular unconformity could therefore explain the change in lineament patterns. However, an igneous body which does not contain a strong foliation can also cause a change in lineament patterns without terminations to primary lithotectonic features. In the case of central/South Devon the intrusion of a granite body, the Dartmoor granite, has caused this lineament pattern. Further granite bodies exist within SW England (see Section 2.4.1), and these granite bodies are difficult to differentiate in the lineament map due to an absence of surrounding primary lineaments. Evidence that this lineament pattern is caused by circular igneous bodies (suggesting a granite intrusion), however, can be obtained from Landsat TM images by analysing FCC's (Fig. 3.16b).

The granites are aged between the Upper Carboniferous and Lower Permian (Darbyshire & Shepherd 1985). This means that the granites have only been deformed by late Variscan and post-Variscan brittle deformation. E/W and ENE/WSW trending mineralised fractures can have similar strikes to strata in SW England. Analysis of lineament trends from the granites therefore avoids confusion with lineaments formed by strata or earlier fractures, found elsewhere in SW England. As lineament patterns produced by the granites were not distinctive from the lineament patterns of the country rocks, lineaments from the granites were identified by direct comparison with geological maps.

Trends of lineaments interpreted from the five main granite bosses are shown in Fig. 4.17 and are summarised in Table 4.2.

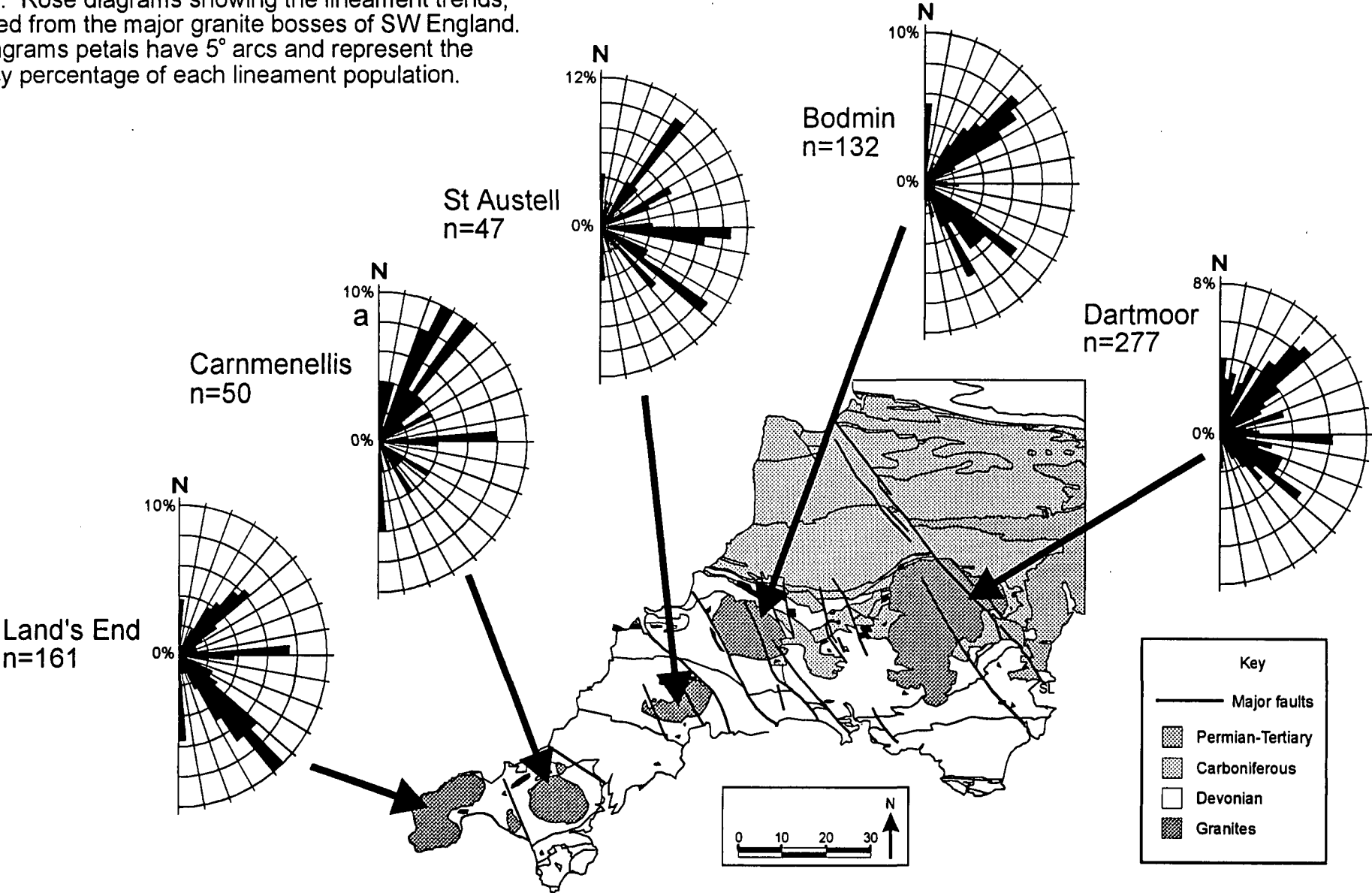
Name of granite	Major lineament group trends, 8%-12% (°)	Medium sized lineament group trends, 4%-<8% (°)	Minor lineament group trends, 0%-<4% (°)
Land's End	130-135	085-090, 030-050	175-005
Carnmenellis	022.5, 035-40, 085-090	175-015, 20-30, 40-45, 60-65, 120-160	
St. Austell	035-040, 90-100, 125-130	175-005, 60-70, 115-120, 135-140	005-030, 140-160
Bodmin	~045	120-155	090
Dartmoor		000-005, 25-30, 35-55, 125-130	70-75, 90-95, 100-105, 110-125, 130-155, 175-180

Table 4.2. Trends of normalised lineament groups (5° intervals) interpreted from the granites of SW England, the trends are split into sizes (major, medium and minor).

These lineament patterns suggest that late fractures in SW England broadly form four main trends E/W, NE/SW, NW/SE and N/S. Hence, lineament groups with E/W and NE/SW trends will contain a mixture of lithotectonic features e.g. E/W trending lineaments caused by lithological differences. Lineaments may also possess anomalous trends e.g. to 025° in the Carnmenellis granite suggesting that late fracture patterns can possess complex relationships, as found in South Cornwall.

Fig. 4.17. Rose diagrams showing the lineament trends, interpreted from the major granite bosses of SW England. Rose diagrams petals have 5° arcs and represent the frequency percentage of each lineament population.

170



4.4 Lineament mixtures in SW England

The lineament trends, the basic patterns, geological causes and the effected areas identified from the lineament map of SW England which were described in Sections 4.2 and 4.3, are summarised in Table 4.3.

Lineament trends	Characteristic lineament patterns	Suggested geological causes	Order of formation as suggested by lineament patterns	Geographical area covered by lineament pattern
E/W, WNW/ESE	Continuous lineaments, cross-cut by thin lineament zones	Lithological differences	1	Central Devon, North Cornwall, North Devon
E/W, ENE/WSW, NE/SW	Wide high density lineament zones of continuous lineaments, zone can change in trend	Thrust belts	1	South Devon, West Devon, East, Cornwall, North Cornwall
E/W, ENE/WSW, NE/SW	Masked by complex lineament patterns reflecting late fractures	Lithotectonic differences	1	South Cornwall
E/W, WNW/ESE, ENE/WSW	Lineament closures	Folding	2	Localised areas in central Devon and North Devon
none	Late fracture patterns, termination of primary lineaments	Massive igneous intrusions (granites)	at least 2	Central Devon, East Cornwall, South Cornwall, South-West Cornwall
NW/SE, NE/SW	Thin, long lineament zones	Fault zones	at least 3, as may be reactivated	Regional
E/W	Lineaments, which cross-cut discordant lineaments identified as fault zones and are present in the granite bodies	Faults	at least 3, as may be reactivated	Regional

NW/SE, NE/SW, E/W, NNE/SSW, ENE/WSW, WNW/ESE	Complex lineament patterns where lineaments are short as all lineaments trends are cross-cut by other lineament trends	Fractures, including fault zones	at least 3, as may be reactivated	South Cornwall
N/S	Thin lineament zones	Fractures and fault zones	at least 4, as may be reactivated	Regional
NW/SE, E/W	Interconnected long lineaments	Brushford fault	5	Localised in North Devon
None	Absence of lineaments, curved boundary to low lineament zone	Angular unconformity	5	East Devon and West Somerset
N/S, NNE/SSW, E/W	Trellis lineament pattern	Trellis stream pattern controlled by lithological differences	6	Localised in East Devon
NW/SE, NE/SW, N/S	Dendritic lineament patterns	Dendritic stream patterns	Recent	Localised in Central Devon

Table 4.3. Summary of the lineament characteristics identified from the lineament map of SW England.

The lineaments of the major lineament groups to the E/W and NE/SW can therefore have multiple significant geological causes e.g. for E/W lineaments this could either be lithological differences, thrust zones or late fractures. Further analysis of these lineament characteristics in these lineament groups will therefore contain properties typical of the different lineament patterns. This suggests that the division of lineaments by lineament groups is not sensitive enough to differentiate between different geological causes and that analysis of:

(i) the inherent scaling relationships would be an amalgamation of different lithotectonic features;

and (ii) lineament density maps would suggest lineament concentrations comprising different lithotectonic features.

Furthermore, division of the lineament map by lineament patterns alone would also be unsuccessful as either not all lineaments follow the typical lineament patterns (Fig. 4.11) and hence are unidentifiable, or the geological causes of some lineaments can be ambiguous (e.g. E/W primary or fault caused lineaments of the Crediton Trough, see Section 4.2.5(iv)). Analysis of lineament length would also produce inconsistent results. As shown in SW England the majority of lineaments are cross-cut by later faults or are reactivated in conjunction with other fractures, hence the length of most lineaments reflect the spacing of the cross-cutting fracture set. Therefore, in SW England analysis of lineament length can only be applied to late geological features where other fault sets have not been reactivated to a great extent, e.g. NW/SE lineaments in central Devon.

4.5 Lineament analysis of SW England

Lineament patterns within the lineament map of SW England have been demonstrated to be able to differentiate between geological causes and age of formation from which a geological history of the region has been suggested, similar to that described in Chapter 2. The characteristic lineament patterns are summarised in Table 4.4. Furthermore, it has been shown that smaller scaled localised lithotectonic trends can be identified from the map, e.g. displaced primary lineaments in North Devon. The lineament analysis of 1:75000 scale, low resolution images (see Chapter 3), can therefore reduce the effect of

anthropogenic features inherent in temperate agricultural terrains while still retaining enough sensitivity to be able to identify small scale features.

Lithotectonic feature	Lineament pattern characteristic
Bedding	<p>(i) Lineaments follow outcrop strike by forming multiple lineaments with similar trend which do not overlap (referred to as continuous lineaments).</p> <p>(ii) Lineament patterns may also resemble a trellis stream pattern of a long lineament cross-cutting perpendicular shorter lineaments. The shorter lineaments relating to the direction of dip.</p> <p>(iii) These primary lineaments are cross-cut by later high angle fracture systems and hence may be compartmentalised by lithotectonic features.</p>
Folding	<p>(i) Lineament pattern outline resembles the outcrop pattern of a fold.</p> <p>(ii) Such lineaments typically have bedding pattern characteristics.</p>
High angle fault zones	<p>(i) May form long lineament zones.</p> <p>(ii) Lineaments within the zone are shorter relative to the lineament zone length.</p> <p>(iii) Lineaments within these zones typically overlap, in extreme cases up to 6 lineaments.</p> <p>(iv) Lineaments may inter-connect.</p> <p>(v) Lineaments cut-across and hence terminate or compartmentalise primary lineaments.</p>
Reactivation of multiple fracture sets	<p>(i) Forms complex patterns from which the order of formation is difficult to determine.</p> <p>(ii) Typically lineaments are shortened relative to other fractured regions due to fracture reactivation.</p>

Thrust Zone	<p>(i) Abrupt changes in lineament density and trend correlating to the leading edge thrust fault.</p> <p>(ii) In areas of steeply dipping thrust zones lineaments have relatively high densities and possess similar trends. These trends can change over distance.</p> <p>(iii) In areas with flat lying thrusts (klippen) lineaments have variable trends and low densities.</p> <p>(iv) Lineaments are cross-cut by later fracture sets.</p>
Igneous intrusion (granite)	<p>(i) Lack of primary lineaments within the intrusion.</p> <p>(ii) Primary lineaments terminate at the edge of the intrusion.</p> <p>(iii) Lineaments within the intrusion typically have fracture characteristics.</p>
Major angular unconformity	<p>(i) Changes in lineament trend and density over the unconformity boundary</p> <p>(ii) This change in lineament pattern may appear similar to the patterns described for thrust zones, however, thrust zones typically possess lineaments relating to leading edge thrust faults.</p> <p>(ii) Boundary to unconformity maybe curved reflecting local topography.</p> <p>(iii) Internal area typically possesses lineaments which show bedding pattern characteristics.</p>

Table 4.4. Summary of the lineament pattern characteristics from which different lithotectonic features in SW England were interpreted.

4.6 Conclusions

(i) Different lineament patterns can be identified from the lineament map of SW England. Characteristics of the lineament patterns can identify which lithotectonic features caused the lineament patterns.

(ii) Lineament patterns interpreted from SW England can be used to differentiate and delineate different lithotectonic zones.

(iii) The main lithotectonic causes of the four major lineament groups in SW England have been identified, for: (a) E/W lineaments as lithological differences, thrust zones, folds and faults; (b) NE/SW lineaments as thrust zones, unknown fractures and strike-slip faults; (c) NW/SE lineaments as strike-slip faults fractures and some unknown fractures; and (d) N/S lineaments as unknown fractures.

(iv) Dividing the regional lineament population into lineament groups could lead to these subsets containing lineament mixtures. Therefore, this method of dividing the regional lineament population may be too insensitive.

(v) The lengths of the majority of primary lineaments mainly reflect the spacing of discordant cross-cutting fractures (e.g. N/S, NW/SE and NE/SW fault zones) or reactivated fractures and not their undeformed lengths.

(vi) A comprehensive regional scale geological history was obtained from the lineament map. This suggests that lineament analysis of 1:75000 scale, pixelated low resolution images are ideal for the regional lineament analysis of temperate agricultural terrains and in SW England the inland extrapolation of the coastal geology.

Chapter 5 Effect of resolution on the interpreted lineament populations

5.1 Introduction

The optimum image resolution for a regional lineament analysis in SW England was identified in Section 3.4 to be 150m, and from these images a regional lineament map has been interpreted. Increasing the image resolution, however, was found to have a profound effect on the frequency, size and directional trends of lineaments interpreted from Landsat TM images of North Cornwall (Chapter 3). Smaller objects can become visible in an image with increasing image resolution (Woodcock & Strahler 1987). Therefore, a lineament map interpreted from higher resolution images may contain either scale invariant lithotectonic features (e.g. Heffer & Bevan 1990) or 'new' smaller scale limited lithotectonic features which begin to fall within the observation threshold of the image resolution. Hence, lineament maps of North Cornwall interpreted from higher resolution images may contain relatively higher degrees of geological information than the regional lineament map.

The main aim of this Chapter is to identify the geological causes of lineaments to allow an assessment of the possible extra geological information gained by increasing image resolution and hence what information is missing from the low resolution lineament map of SW England. However, as shown in Section 3.4, increasing the image resolution increases the visual impact of anthropogenic features. The high resolution images of North Cornwall were cleaned of these anthropogenic features by the use of simple knowledge-based rules (see Section 3.8.1). Therefore, one aim of this research is to further identify the effect that

anthropogenic features have on high resolution large scale images in temperate agricultural terrains.

The geology of North Cornwall consists of Lower Devonian to Upper Carboniferous basin sediments. These have been deformed either by part-synchronous or post-depositional thrusts and folds forming a series of nappes (Section 2.3.3) and the Culm Synclinorium (Fig. 5.1) (see Section 2.3.4). Post-dating the main episode of thrusting is the intrusion of the Bodmin granite, followed by cross-cutting NW/SE and NE/SW trending faults and N/S fractures (Fig. 5.1) (see Section 2.5).

To investigate which type of geological features relate to lineaments interpreted at different resolutions Landsat TM images of North Cornwall were interpreted over a range resolutions from 30m to 150m (Section 3.3.2). Three sub-areas Cambeak, Bridgerule and Laneast (Fig. 5.1) are used to analyse the changes in lineament trends, spatial distributions and patterns. These areas were chosen as they contain the main lithotectonic features in North Cornwall (e.g. WNE/ESE trending nappes in Laneast, E/W trending lithological differences and NE/SW, NW/SE and N/S fractures in Cambeak and Bridgerule). Furthermore, to identify how small scale rock mass properties can form lineament patterns, planar structures were sampled from the coastal cliff section between the Rusey and Strangles cliffs.

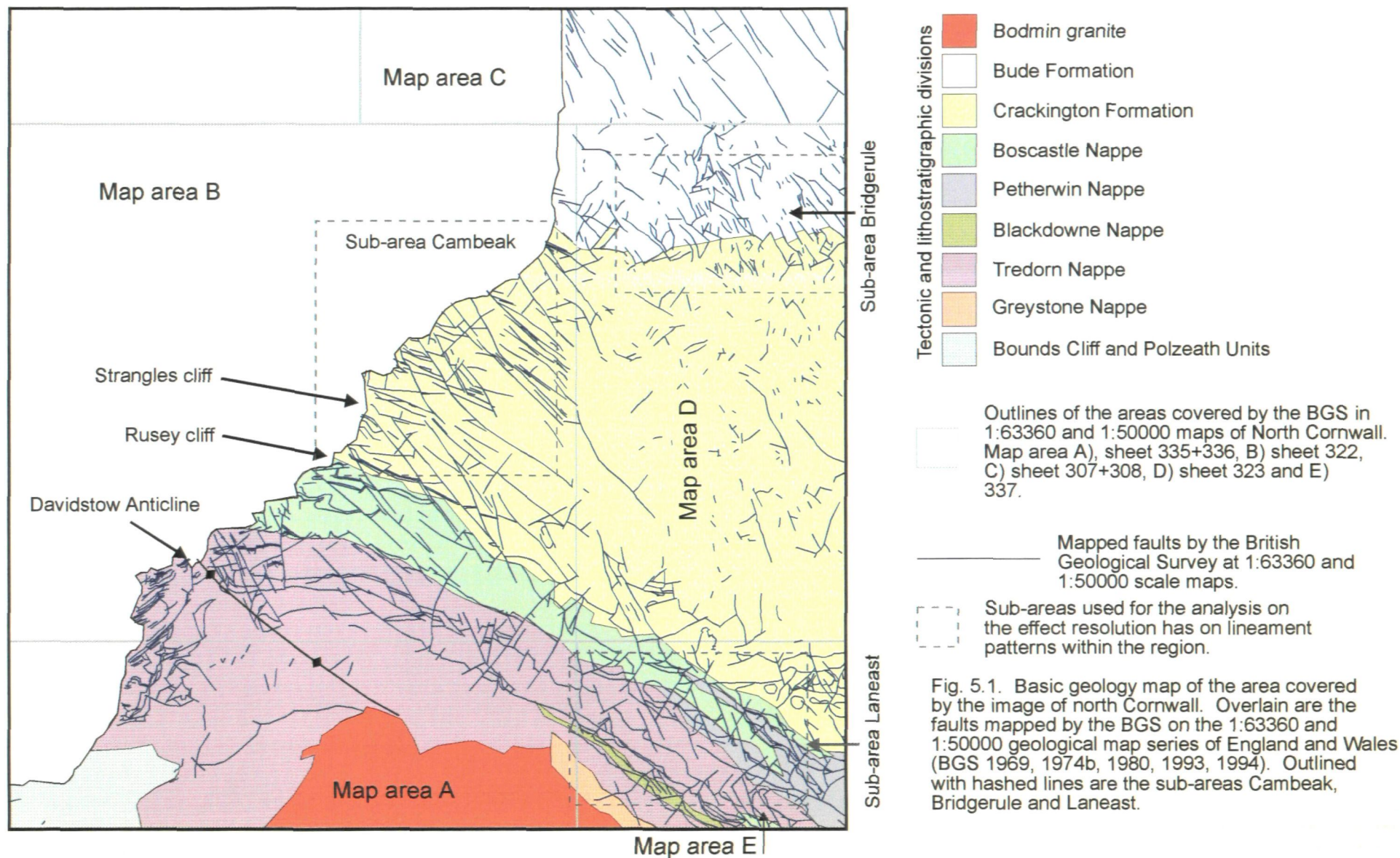


Fig. 5.1. Basic geology map of the area covered by the image of north Cornwall. Overlain are the faults mapped by the BGS on the 1:63360 and 1:50000 geological map series of England and Wales (BGS 1969, 1974b, 1980, 1993, 1994). Outlined with hashed lines are the sub-areas Cambeak, Bridgerule and Laneast.

5.2 The effect of resolution on lineament analysis in the sub-area Cambeak

5.2.1 Lineament maps

Lineament maps and trends (described as a series of rose diagrams) over the resolution range of the sub-area Cambeak are illustrated in Fig. 5.2.

However, for the analysis of the relative frequency percentage of lineaments in lineament groups clearer results were obtained by comparing the data using a line chart (Fig. 5.3). Fig. 5.3 illustrates that the relative frequency percentages of all the lineament groups form complex patterns, therefore only the main lineament trends of the sub-area were analysed:

(i) The highest frequency percentage of lineaments occurs for E/W lineaments. With increasing image resolution there is a fall in the frequency percentage. However, very similar frequencies were obtained for the populations obtained from images with resolutions of 120m, 90m, and 60m.

(ii) For N/S lineament groups the highest frequency percentage was obtained from the 150m lineament population while the lowest were identified from the 120m lineament population.

(iii) NE/SW lineament groups show high frequency percentages for populations interpreted from image resolutions of 150m and 120m (~12%), becoming lower for image resolutions of 90m and 60m (~4.5%).

(iv) For NW/SE lineament groups the highest frequency percentage was obtained for the 60m population (~6.5%), and falls with decreasing resolution.

(v) Similar results were obtained for NW/SE and NE/SW lineament groups for lineaments interpreted from 30m resolution images (~3%); the NW/SE and NE/SW peaks evident in the lineament groups from lower image resolutions become merged with the lineament groups $\pm 10^\circ$ to the NW/SE or NE/SW.

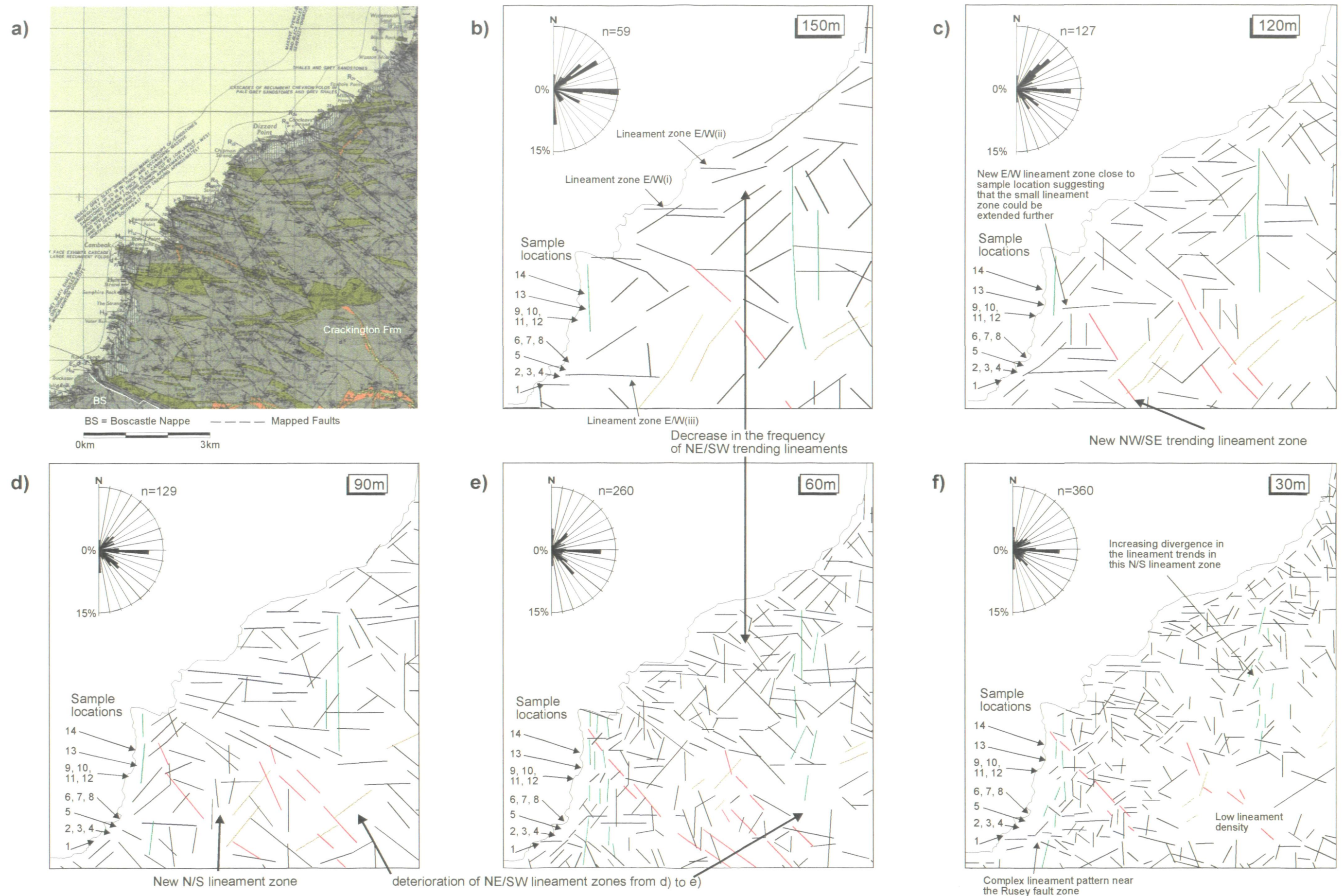


Fig. 5.2. A series of maps covering the sub-area of Cambeak showing a) the geology and b)-f) the lineaments maps interpreted from Landsat TM images at 150m, 120m, 90m, 60m and 30m resolutions. Lineament trends from each population are shown as rose diagrams to the left of each map. Located on the maps are the sample locations used to analyse the rock mass properties of the Rusey and Strangles cliffs. Different lineament trends are highlighted: blue for E/W trending lineaments; green for N/S trending lineaments, brown for NE/SW trending lineaments and red for NW/SE trending lineaments. Map a) has been modified from BGS (1969) 1:63360 scale, sheet 332.

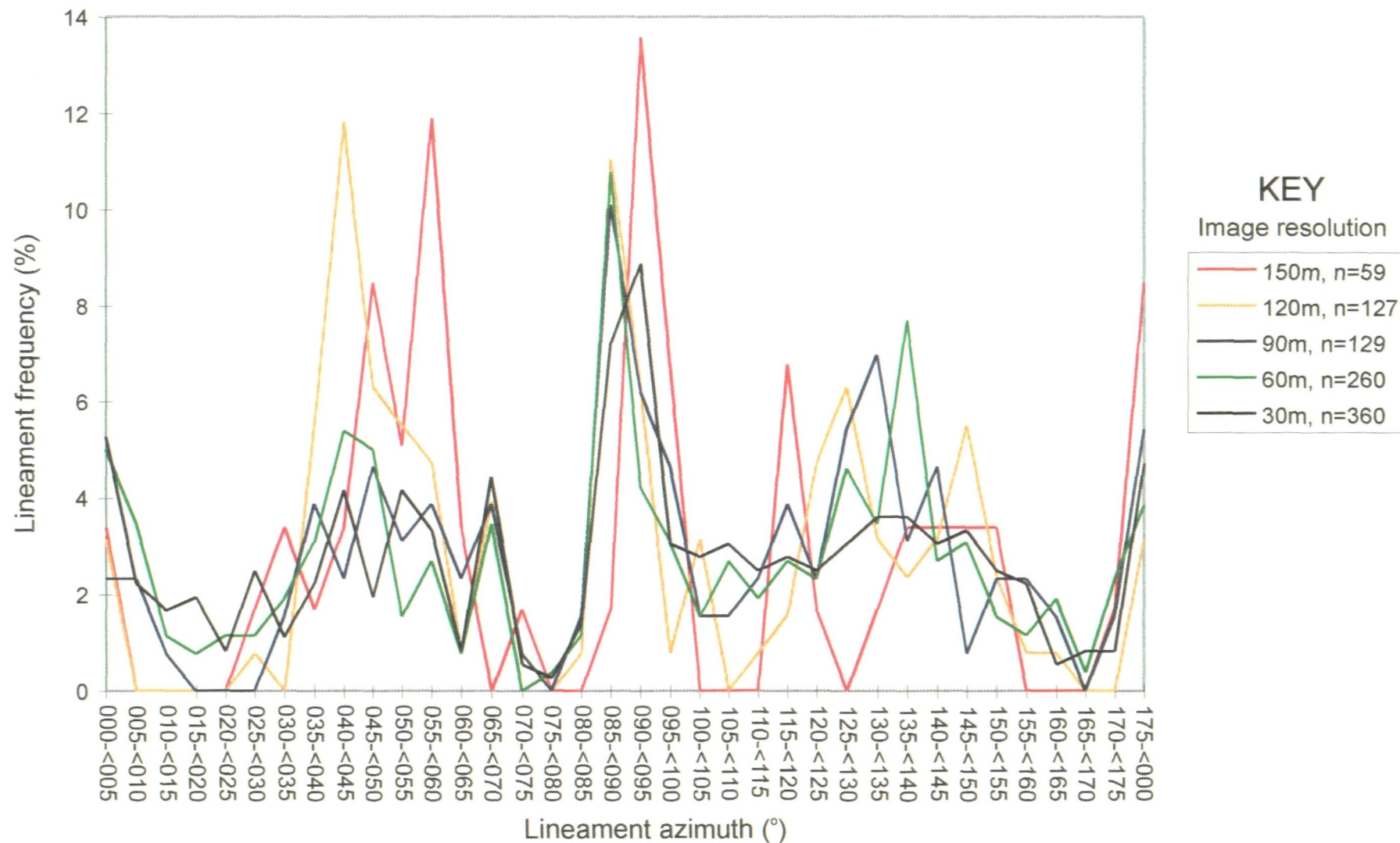


Fig. 5.3. Line chart showing the frequency percentage of lineaments (in 5° lineament groups) over the resolution range of 150m to 30m (see key) for the sub-area of Cambeak.

In the 30m resolution lineament population this results in a lower frequency percentage than the respective 60m lineament population.

The relative maximum peaks between the lineament populations at each resolution can, however, be affected by lineaments interpreted from higher resolution images possessing sub-trends other than the four main lineament trends evident in the lower resolution lineament populations. These extra lineaments in the higher resolution images therefore decrease the frequency percentage peaks of the four main trends as the frequency percentage of the whole population is calculated. Hence, the E/W, N/S and NE/SW frequency percentages in the 150m resolution population may in comparison to the other lineament populations be artificially high.

The lineament patterns of the four main lineament trends in the lineament map can also show distinct differences between each lineament trend and across the resolution range (Fig. 5.2):

(i) Three E/W lineament zones are identified across the resolution range, these lineament zones display different lineament patterns, E/W(i) is typically cross-cut by all other lineaments (suggesting a primary feature) while E/W(ii) and E/W(iii) can cross-cut the other lineament trends. The lineament zones can be identified over the resolution range and with increasing resolution new E/W trending zones can be interpreted (e.g. Fig 5.2c).

(ii) N/S lineaments form long lineament zones over the resolution range, with increasing image resolution new lineament zones can be identified (e.g. Fig. 5.2d). Typically they cross-cut most other lineaments.

(iii) NE/SW lineament zones can be found to either be cross-cut or cross-cut other lineament trends. These lineament zones can be identified in the 150m

to 90m resolution lineament maps (Figs. 5.2b, c, d). However, in the 60m and 30m resolution lineament maps these zones become incomplete and intermittent.

(iv) NW/SE lineament zones can be found to cross-cut and also be cross-cut by other lineaments. Increasing the image resolution up to 60m can identify more NW/SE lineament zones (Fig. 5.2c) and extend the lineament zone length. However, NW/SE lineament zones at 60m and especially 30m resolution lineament maps can also degrade forming incomplete and intermittent lineament zones.

(v) Common to all lineament trends with increasing image resolution (particularly 30m) the length of the lineaments decreases (e.g. E/W(iii) in Fig. 5.2f). Also with increasing resolution the trends of lineaments within lineament zones can show greater diversity.

From these results the following general characteristics can be identified: N/S and E/W lineaments can be mapped over the whole resolution range and can increase in frequency with increasing image resolution; NW/SE lineaments increase in frequency in images up to resolutions of 60m; whilst NE/SW lineaments decrease in frequency with increasing image resolution. The effect of resolution on identifying lineaments from geomorphological features is that smaller objects are identified in higher resolution images (Woodcock & Strahler 1987) (see Section 3.4), i.e. large features in low resolution images, small features in high resolution images (Fig. 3.20). Therefore, if the cause of the lineaments was relief and lineament frequency is related to the size of the interpreted geomorphological feature: NE/SW lineaments would be identified from broad large features; E/W and N/S features would be relatively smaller valleys;

and NW/SE lineaments interpreted from the smallest topographic features (as illustrated in Fig. 5.4).

Identified from the lineament maps are areas that possess low lineament densities in higher resolution images. These low density areas did effect NW/SE and NE/SW trending lineaments as these are present in lower resolution images. Areas of low lineament density show a correlation to low variance in relief as described by a topographic map of the area (Fig. 5.4).

5.2.2 Lineament patterns of the Rusey and the Strangles cliffs

The major lithotectonic features mapped within the sub-area Cambeak are E/W lithological differences, E/W faults, NW/SE to WNW/ESE faults and a subordinate NE/SW set of faults (Fig. 5.2a). However, the lineament maps previously discussed suggest that more lithotectonic features exist than is suggested by the geological map (e.g. N/S lineaments). To identify possible geological features in the area which could cause such lineaments, the area between the Rusey and the Strangles cliffs (Fig 5.5) has been sampled to identify planar structures within the rock mass. Table 5.1 describes the lineament patterns closest to the sample location points (Fig. 5.5) over the resolution range. Lineaments, however, were found to occur at least 400m from the digitised coastline, and hence 400m from some of the sample points. The 400m spatial discrepancy can be accounted for by the large cliff sections (Fig. 5.5) which was possibly compounded further by small spatial errors in the geometric correction of the images (see Section 3.3.1).

1 0 1 2 Kilometers

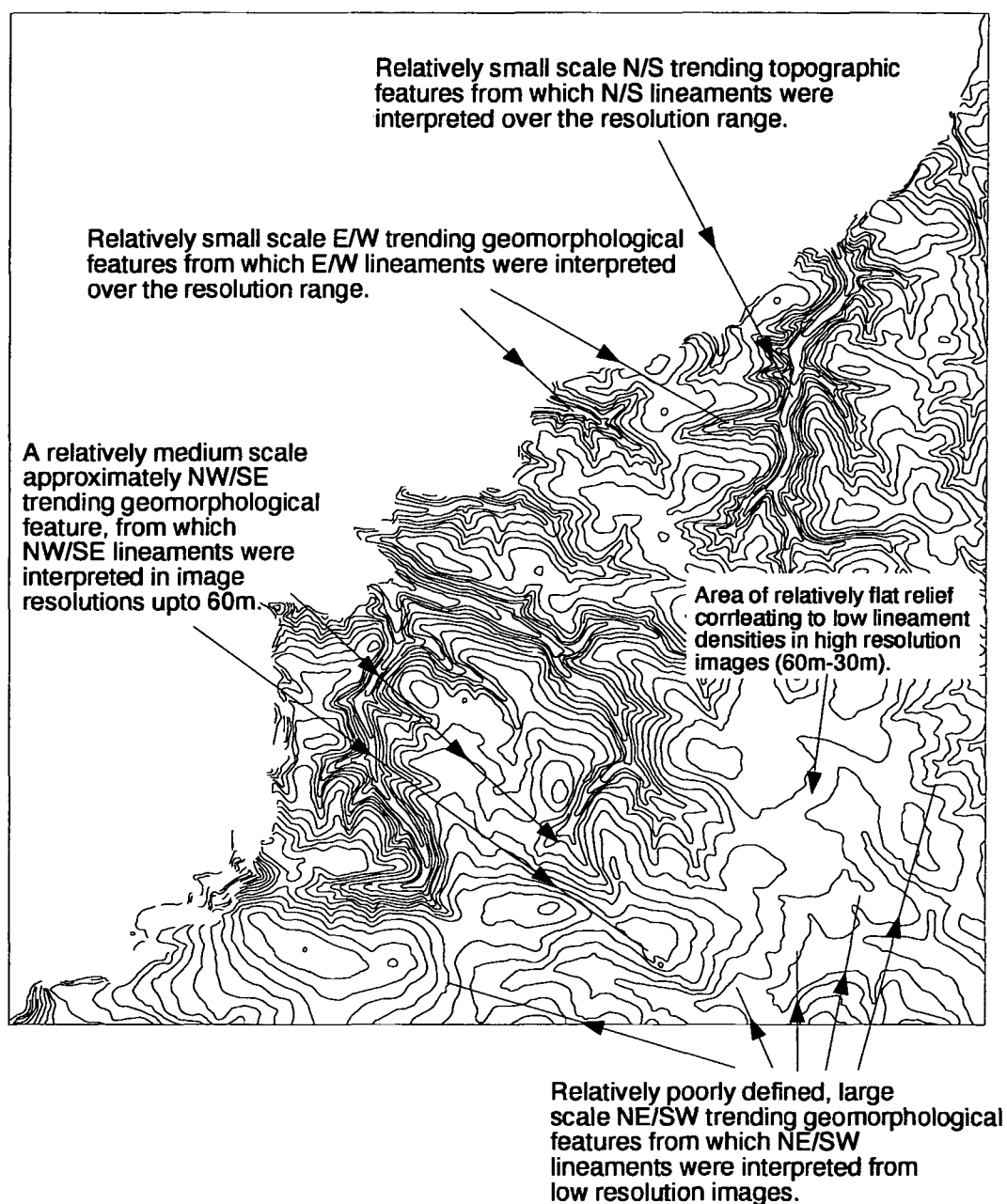


Fig. 5.4. 10m elevation contours illustrating the topographic trends and relative changes in the scale of geomorphological features in the sub-area Cambeak.

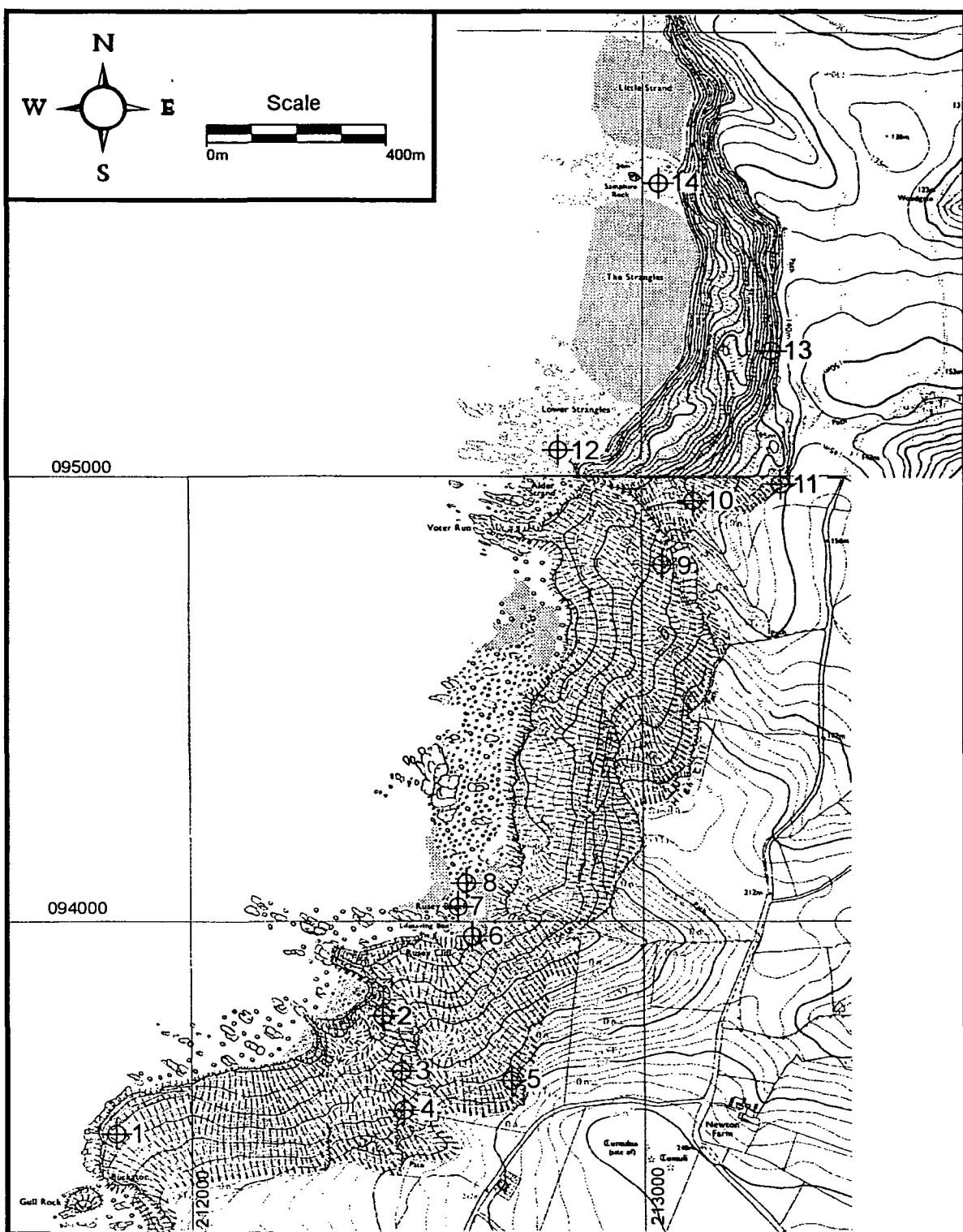


Fig. 5.5. Map showing locations used to sample planar structures from the Rusey and Strangles cliffs.

Sample location number	Lineament trends in the 150m lineament map of the sample area	Lineament trends in the 120m lineament map of the sample area	Lineament trends in the 90m lineament map of the sample area	Lineament trends in the 60m lineament map of the sample area	Lineament trends in the 30m lineament map of the sample area
1	000°, 090°	040°	040°	030°, 090°	090°
2	090°	040°	118°	045°, 090°, 131°, 110°	051°, 090°, 114°
3	090°	040°	118°	045°, 090°, 131°, 110°	051°, 090°, 114°
4	090°	040°	118°	045°, 090°, 131°, 110°	051°, 090°, 114°
5	090°	040°, 090°	118°	045°, 090°, 131°, 110°	051°, 090°, 114°
6	033°, 090°	040°, 090°	038°, 092°	047°, 090°	021°, 130°
7	033°, 090°	040°, 090°	038°, 092°	047°, 090°	021°, 130°
8	033°, 090°	040°, 090°	038°, 092°	047°, 090°	021°, 130°
9	000°	000°, 090°	005°, 050°	042°	042°
10	000°	000°, 090°	005°	042°	042°
11	000°	000°, 090°	005°	042°	042°
12	000°	000°	005°	000°	000°
13	000°	000°	005°	000°	000°
14	000°	000°	005°	000°	000°

Table 5.1. Effect of resolution on lineament trends identified from the sample area of the Rusey and Strangles cliffs.

These results show that in some sample locations the same trending lineaments occur over the whole resolution range e.g. only N/S lineaments occur in locations 12, 13 and 14. However, for the majority of sample locations lineaments with different trends occur over the resolution range. Apart from the possible causes of lineament differences identified over the whole sub-area, further causes can be identified for these differences at a local scale:

(i) anomalous lineaments: the occurrence of an anomalous lineament trend in a single lineament map may be produced by inconsistent lineament interpretation, e.g. locations 9, 10 and 11 where E/W lineaments have only been found to occur near the sample location in the 120m resolution lineament map (Fig. 5.2c). In the 90m, 60m and 30m lineament maps E/W lineaments with

similar characteristics occur further inland, hence suggesting that these features exist but have not been consistently interpreted.

(ii) change in lineament trends: an increase in image resolution resulting in different lineament trends being interpreted. In the cases of sample locations 9, 10 and 11, with increasing resolution the dominant N/S lineament trend in the low resolution images becomes separated by a smaller zone of ~NE/SW trending lineaments (Figs. 5.2e, f). Hence, only at high image resolutions could such smaller zones be identified.

5.2.3 Relationships between the lineament patterns and large scale lithotectonic features

The effect of resolution on lineament populations has been previously suggested to highlight different geomorphological features (Section 5.2.1). This section describes the major lithotectonic features identified from published data and attempts to relate them to the lineament patterns identified from the Cambeak sub-area. The sub-area of Cambeak covers the Boscastle Formation (part of the of the Boscastle Nappe) and the Crackington Formation, separated by the Rusey fault zone. The Boscastle Formation mainly consists of sandstones inter-bedded with mudstones, whereas the Crackington Formation mainly consists of sandstone units inter-bedded with argillites (Thomas 1988).

E/W lineaments have been shown within the Culm Basin to be caused by such E/W trending lithological differences (see Section 4.2.5), where the characteristics are that they are cross-cut by lineaments relating to later cross-cutting fractures. In the sub-area Cambeak E/W lineament zones possess such characteristics therefore also suggesting that they represent such features (Section 5.2.1). The tectonic deformation of the Culm Trough is

considered to be produced by NNW compression producing a series of E/W to ENE/WSW trending folds which form E/W to ENE/WSW outcropping lithological units along the North Cornwall coast that dip to the north and south at low to high angles (e.g. Freshney *et al.* 1979b). Zones 2, 3 and 4 of the Sanderson & Dearman (1973) fold classification lie within the Culm Basin, describing a change in fold attitude from upright around Bude, to inclined and recumbent folds between Millook Haven and Crackington Haven formed by an overfold structure (see Section 2.3.4). Lineaments suggesting fold closures have been interpreted from the northern area of the Culm deposits (see Section 4.2.5). However, an absence of further fold lineament patterns means that the change in fold style was not identified by lineament analysis. The overfold structure has been thought to have moved southwards over the Rusey fault zone, which with other numerous northerly dipping thrusts were reactivated as normal faults, extending the recumbent fold limb of the overfold north of Rusey (Freshney *et al.* 1972).

The lineament characteristics relating to faults identified in Section 4.2.2 are the formation of thin lineament zones which cross-cut primary lineaments, and the lineaments themselves can overlap. Such characteristics have been found to occur for N/S, NW/SE, NE/SW and E/W lineament zones (Section 2.3.1). Mapeo (1992) confirms that late Variscan faults in North Cornwall can possess similar trends with WNW/ESE and E/W trending oblique-slip faults, a smaller set of dip-slip faults with NNW/SSE and N/S trends and strike-slip faults with sinistral and dextral movements trending either to the NW/SE and E/W. Furthermore, Freshney *et al.* (1972) has identified a set of normal E/W faults within the region. Faulting within the region as interpreted by British Geological Survey (1969, 1974b, 1980, 1993, 1994) in Fig. 5.1. suggests that the extent of faulting estimated is more dependant upon the age of the mapping. However, broad

tends can be interpreted in the sub-area Cambeak with NW/SE to NNE/SSW faults and a subordinate set of NE/SW faults.

In summary, the main lithotectonic features in the sub-area correlate to the characteristic lineament patterns identified from lineament zones in Chapter 4 and in the sub-area Cambeak, suggesting common causes. However, the geological maps of the area are not able to explain certain lineament patterns, e.g. the existence of greater numbers of NE/SW lineaments in the low resolution lineament maps or how small changes can occur with increasing image resolutions. Therefore, additional lithotectonic features not previously identified in the literature may be the cause for such anomalous trends.

5.2.4 Relationships between lineament patterns and small scale lithotectonic features

Lithotectonic features not fully described in the published data are the localised small scale planar structures within the rock mass. To identify the trends of the foliations of the sub-areas rock mass, the area was investigated by line-sampling in the locations illustrated in Fig. 5.5. To avoid a sample-bias in one direction locations were favoured where samples could be conducted in multiple directions. For each location the data obtained is described by stereograms. Location 1 lies within the Boscastle Formation of the Boscastle Nappe. To the north of location 1, locations 2, 3 and 4 lie within or close to the Rusey fault zone. The remaining locations are within the Crackington Formation:

(i) Location 1 (Fig. 5.6). In this exposure the Boscastle Formation consists of a mudstone which contains a slaty cleavage dipping 30/029. Two vertical to sub-vertical joint sets were observed which trend N/S to NNE/SSE and NE/SW (Fig. 5.6b).

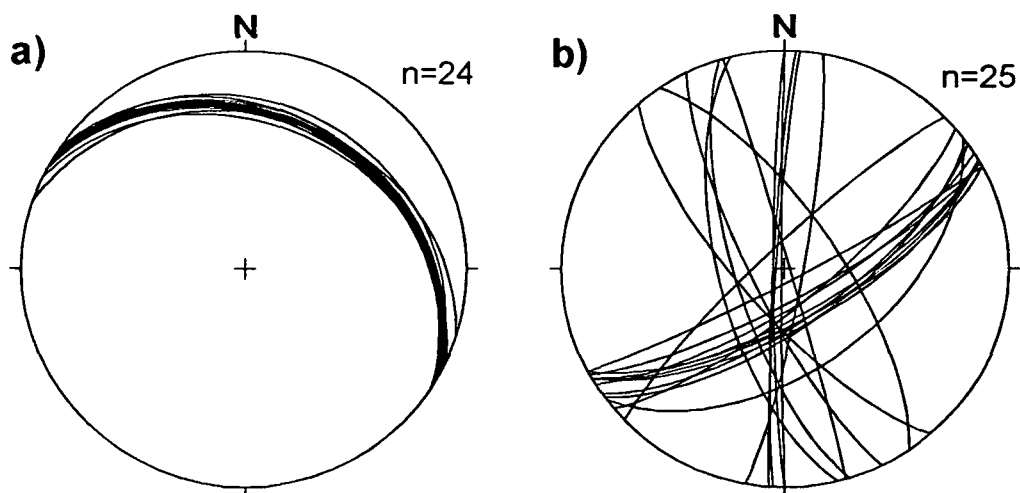


Fig. 5.6. Geometries of the planar structures from location 1: a) a pervasive cleavage; and b) jointing on equal area stereograms. Data were sampled by line transects with trends 10/050 and 24/002.

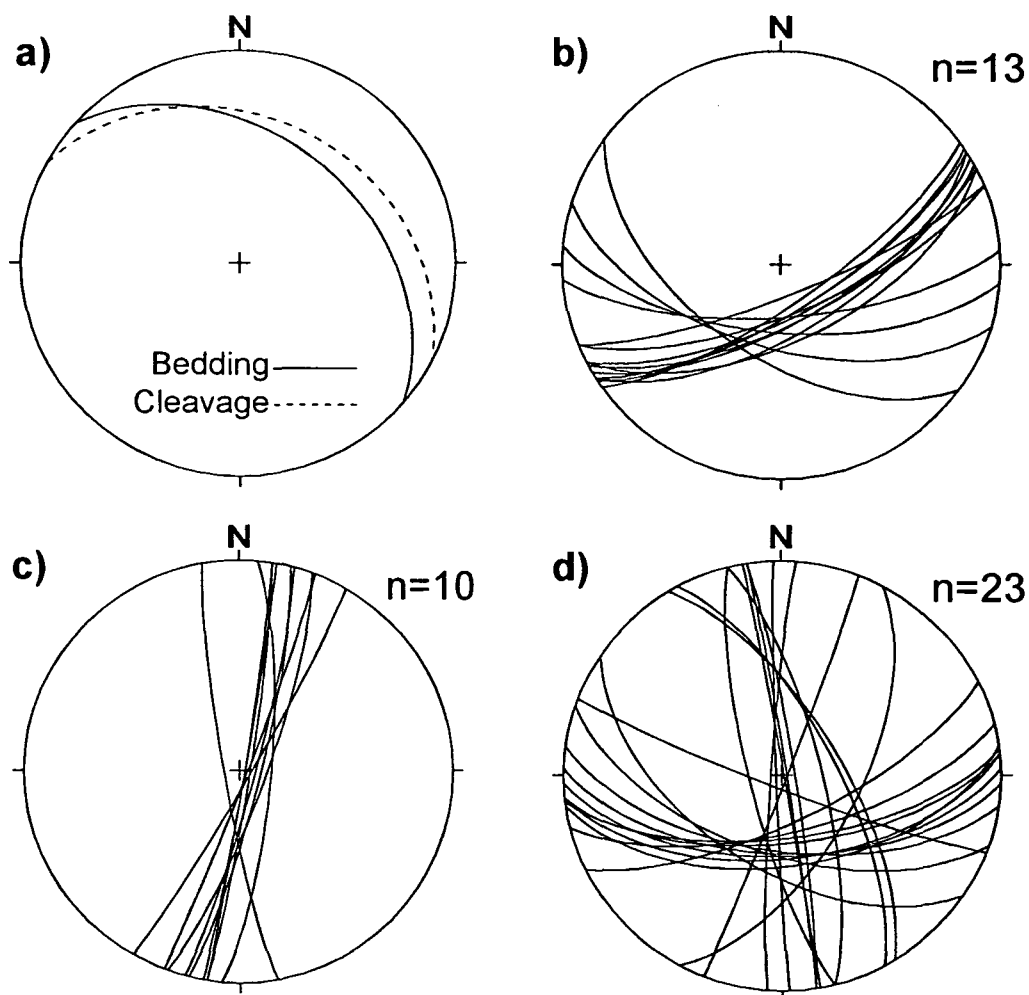


Fig. 5.7. Series of stereograms containing data interpreted from a) and b) locations 2, c) location 3 and d) location 4. Plot a) illustrates the bedding and cleavage to the north of the Rusey fault zone. Plots b) and c) comprises of joint data while plot d) contains sets of unknown fractures. Data were collected by a series of line transects trending 79/244 and 29/349 at location 2, 10/294 at location 3 and 06/253 and 25/008 at location 4.

(ii) Locations 2, 3 and 4 (Fig 5.7). The northwards dipping Rusey fault was observed as a black brecciated fault rock containing predominantly shales with a few sandstones horizons. To the north of the fault zone the inter-bedded sandstone and mudstone rock mass exhibits strong jointing. At location 2 the typical attitudes of the bedding plane is 041/40 and contains a pervasive bedding parallel cleavage. Three later joint sets are observed within the area, a vertical N/S striking joint set with similar trending faults and steeply southwards dipping sets with E/W or ENE/WSW trends.

(iii) Location 5 (Fig 5.8). These inter-bedded mudstones and fine sandstones (between 5cm and 20cm in thickness) are highly fractured. Jointing within the rock mass appears to have two sets, a moderate to steeply dipping set which dips towards the south-east and a more shallowly dipping set with dip directions to the north-west. Within this location the cleavage typically strikes ENE/WSW and possesses moderate dips.

(iv) Locations 6, 7 and 8 (Figs. 5.9, 5.10, 5.11). In this area the inter-bedded mudstones, siltstones and fine grained sandstones show a range in bedding thickness from 2 to 12 cm. Bedding has a mean dip direction of 003° and a dip of 34°. A cleavage is present in the finer grained rocks and has an average dip direction and dip of 027/37. However, the cleavage trend can change from E/W to NNE/SSW and dip from sub-horizontal to steep. The strike of the joint pattern at location 6 shows a large distribution, approximating to a N/S strike and dips changing from moderate to vertical. At locations 7 and 8, a strong vertically dipping N/S joint set is observed of which some joints have been infilled with quartz. In locations 7 and 8 a minor ENE/WSW trending joint and vein set has been identified, typically these joints and veins have steep to vertical dips.

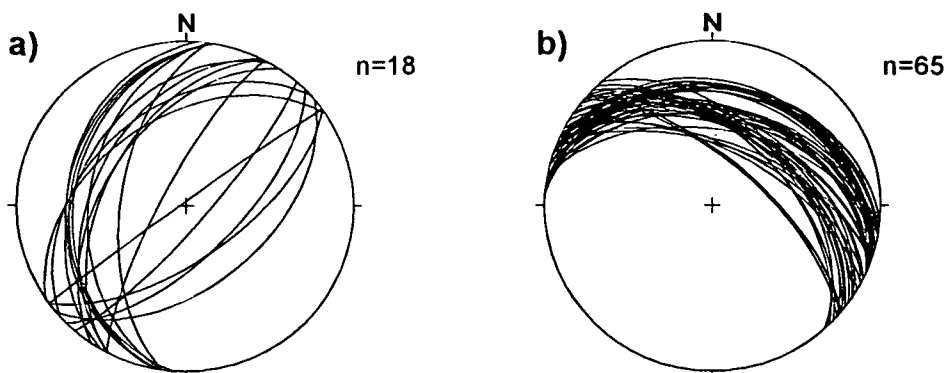


Fig. 5.8. Stereograms of a) jointing and b) cleavage obtained from location 5. Data were obtained from a line transect trending 00/012.

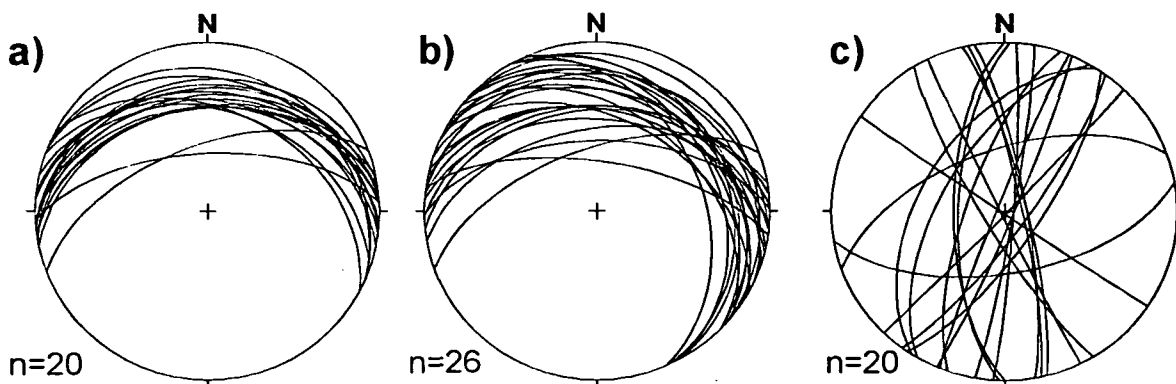


Fig. 5.9. Series of equal area stereograms containing planar discontinuities present at location 6: a) bedding surfaces; b) cleavage; and c) jointing. These data were collected from three line transects trending 10/214, 15/250 and 10/245.

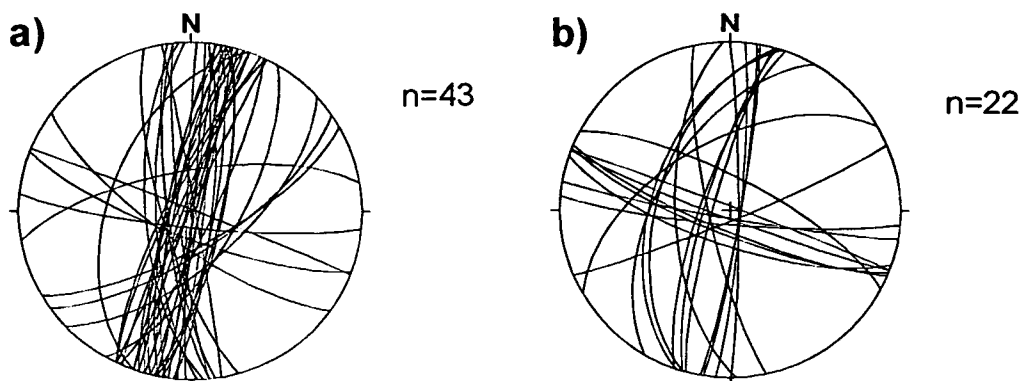


Fig. 5.10. Geometries of a) jointing and b) veining obtained from location 7 on equal area stereograms. Data were obtained from a line transect trending 04/321 on a bedding surface 009/01.

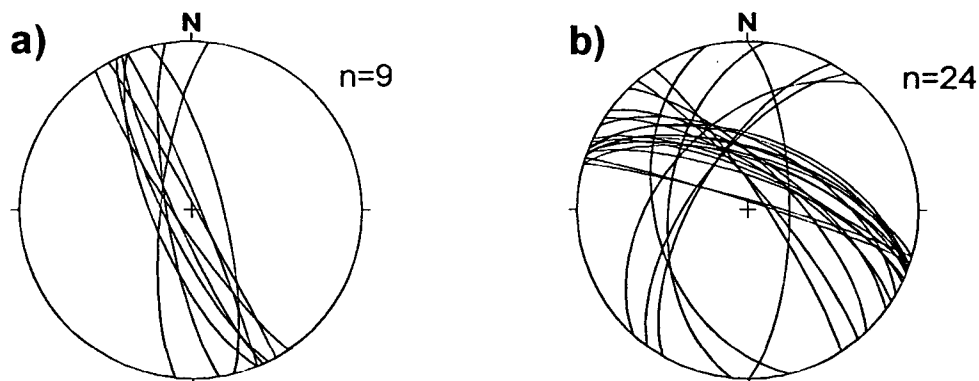


Fig. 5.11. Stereograms of a) jointing and b) veining from location 8. Sampling of the data was by a line transect trending 04/90 on a bedding surface dipping 174/25.

(v) Locations 9 and 10 (Fig. 5.12) contain mudstones and siltstones showing three different sets of joints. All three joint sets are steep to vertically dipping and have maximum trends to the N/S, E/W and NE/SW.

(vi) Location 11 (Fig. 5.13). The main lithologies are mudstones and siltstones, inter-bedded with fine to coarse sandstones up to 1m in thickness. Bedding planes from this ENE/WSW transect strike E/W and dip to the north at 45°. A joint set trending NNE/SSW cuts across the bedding with steep to vertical dips.

(vii) Location 12 (Fig. 5.14). Within this location mudstones with few inter-bedded sandstones dominate. Bedding planes which trend WNW/ESE are folded forming an upright fold which is open and gently inclined to the west-north-west. The cleavage recorded at this location contrasts with this fold by shallowly dipping to the north, hence suggesting that it is unrelated. Recorded joints show a general NNE/SSW strike, however, the direction of dip occurs to the west-north-west and east-south-east, and dip changes from vertical to shallow.

(viii) Location 13 (Fig. 5.15). Around location 13 the lithologies consist mainly of mudstones inter-bedded with sandstones which can be up to 40cm in thickness. This sequence has been folded into horizontal plunging close recumbent folds. In these folds bedding and cleavage planes on the major fold limb dip moderately to the north-north-east and bedding planes on the subordinate limb at low angles to the west. A dominant joint set occurs at this location which strikes N/S and has steep to vertical dips.

(ix) Location 14 (Fig. 5.16). At the base of the Strangles cliff the main lithologies are mudstones to fine siltstones with inter-bedded sandstones. Bedding planes at Location 14 dip at moderate angles to the south-south-west and a cleavage at near-horizontal dips to the south-south-west.

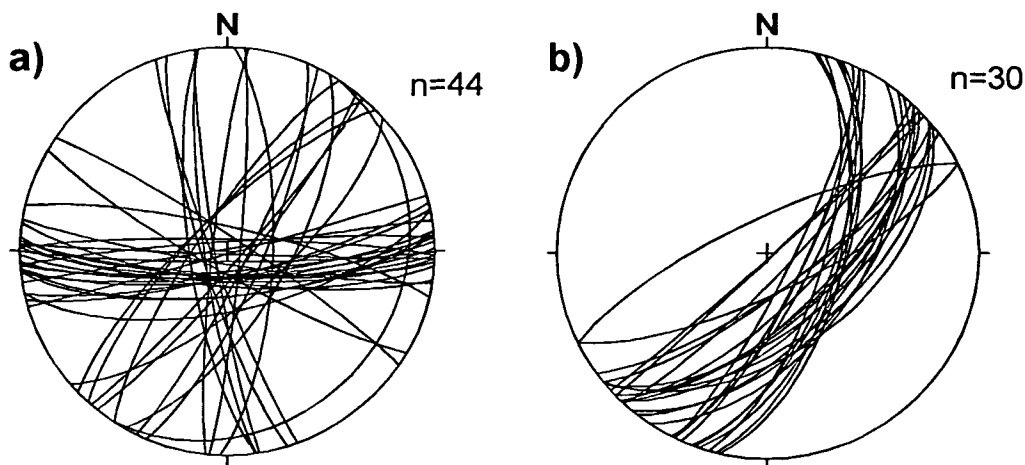


Fig. 5.12. Equal area stereograms of jointing obtained from a) location 9 and b) location 10. Each data set were obtained from line sections trending 00/115 and 12/288 for locations 9 and 10, respectively.

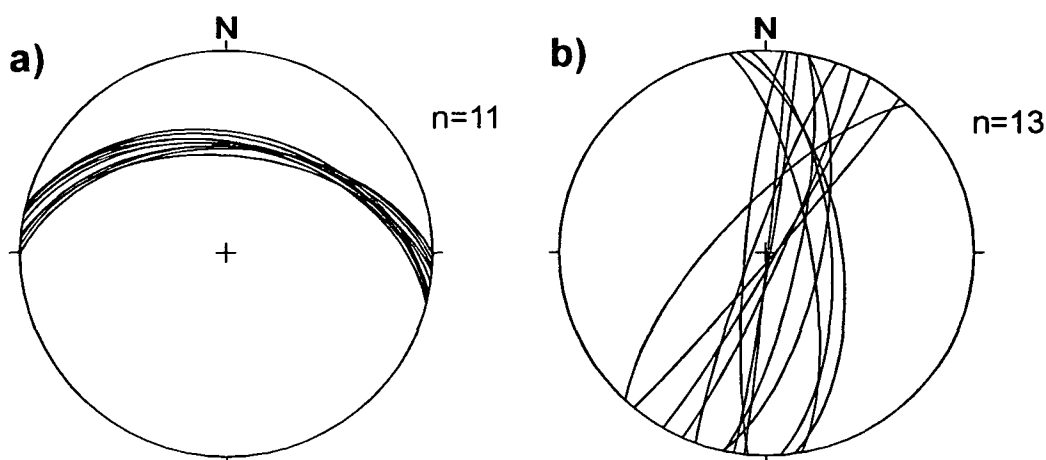


Fig. 5.13. Data from location 11 displayed on equal area stereograms: a) bedding planes; and b) jointing. Data were sampled from a line transect trending 18/296.

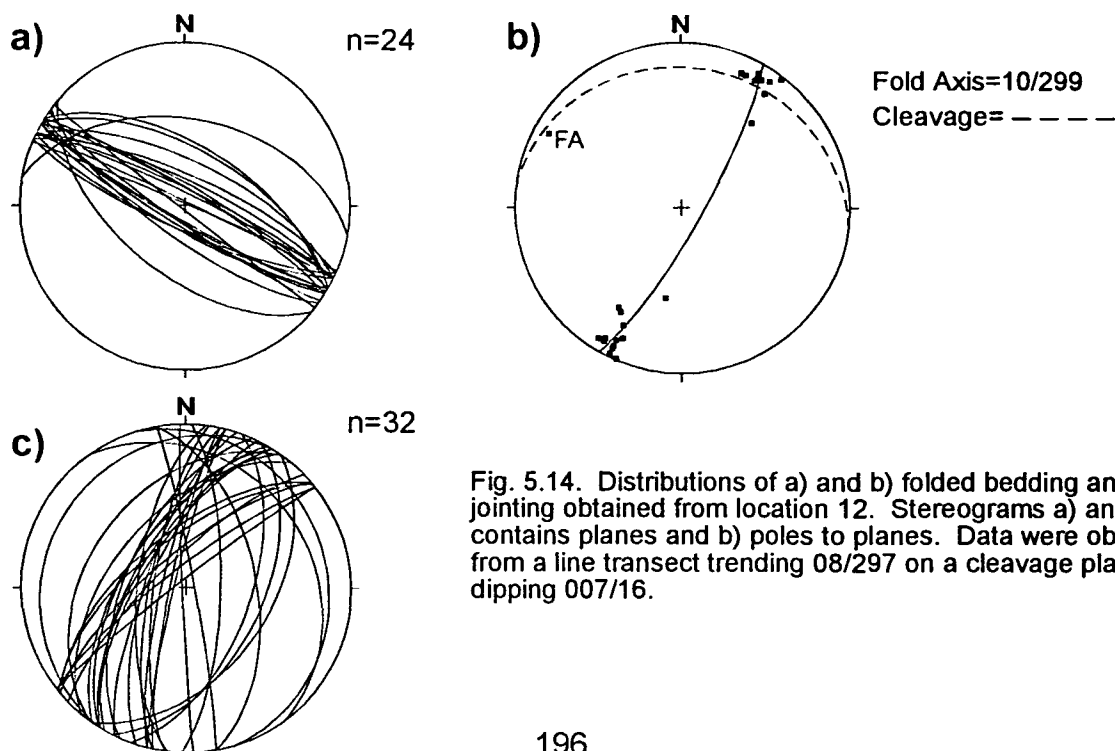


Fig. 5.14. Distributions of a) and b) folded bedding and d) jointing obtained from location 12. Stereograms a) and c) contains planes and b) poles to planes. Data were obtained from a line transect trending 08/297 on a cleavage plane dipping 007/16.

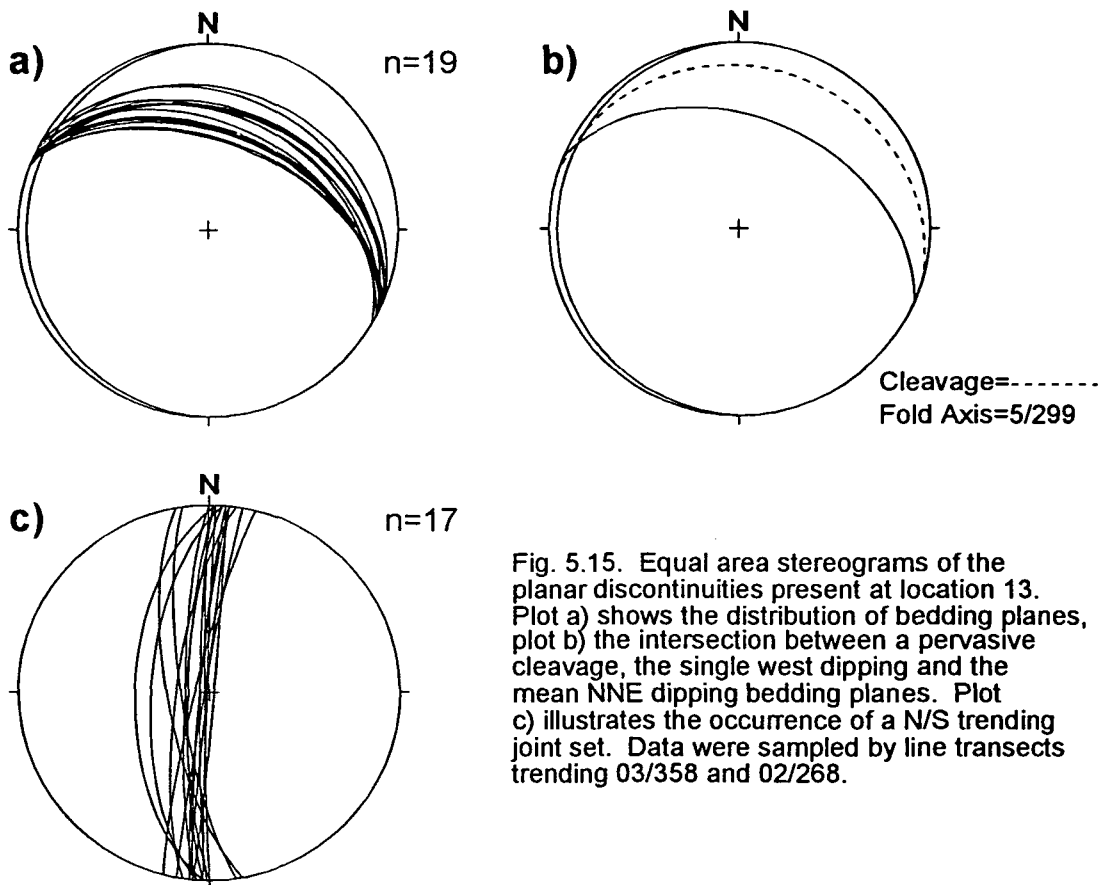


Fig. 5.15. Equal area stereograms of the planar discontinuities present at location 13. Plot a) shows the distribution of bedding planes, plot b) the intersection between a pervasive cleavage, the single west dipping and the mean NNE dipping bedding planes. Plot c) illustrates the occurrence of a N/S trending joint set. Data were sampled by line transects trending 03/358 and 02/268.

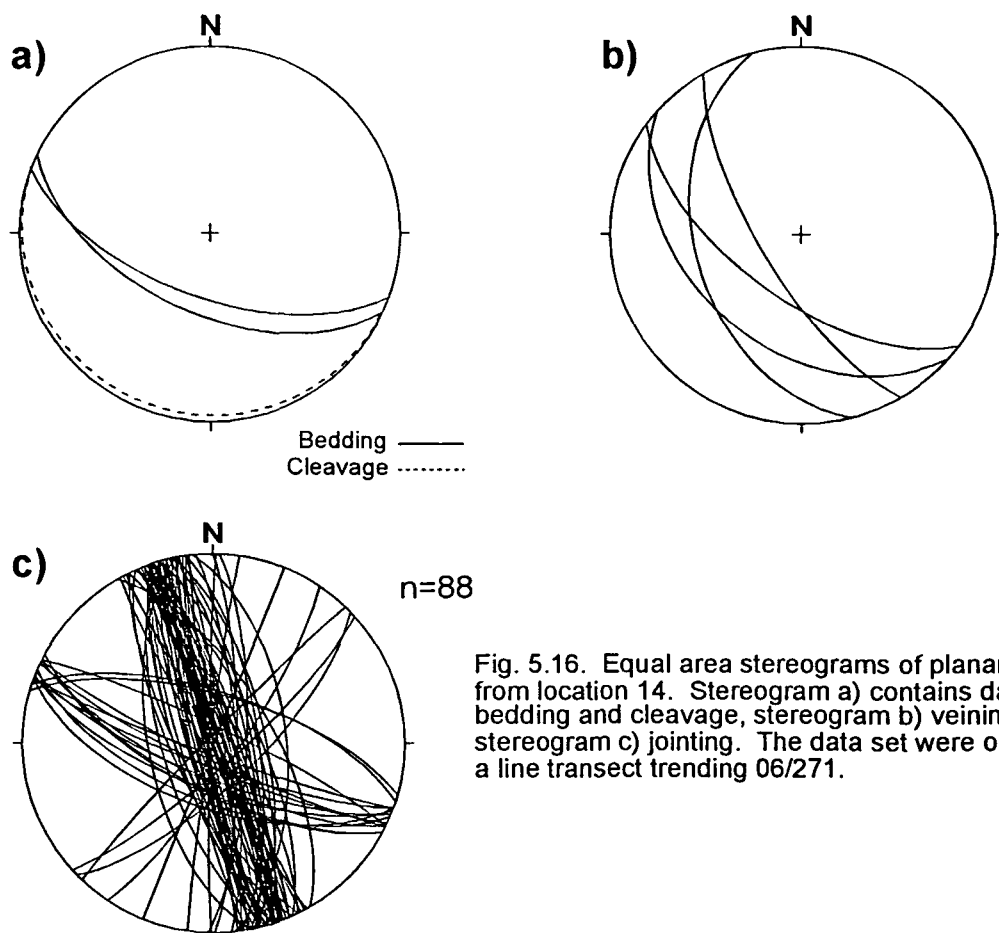


Fig. 5.16. Equal area stereograms of planar data obtained from location 14. Stereogram a) contains data of the areas bedding and cleavage, stereogram b) veining and stereogram c) jointing. The data set were obtained from a line transect trending 06/271.

Veining present within the line transects was seen to strike NW/SE with moderate to steep dips to the south-west. Two dominant joint sets were observed within the transects, a major NNW/SSE striking set and a subordinate WNW/ESE striking set. Both joint sets possessed steep to vertical dips and dipped to the east-north-east or west-south-west and north-north-east or south-south-west, respectively.

These data are summarised in Table 5.2. Only included in the table are planar discontinuities which have greater than shallow dips, as the outcrop strike of sub-horizontal foliations are controlled by topography and is therefore likely to have a smaller impact on the lineament map (i.e. as produced by klippen, see Section 4.2.5(iii)).

Sample location number	Strike of bedding if identifiable	Strike of cleavage if present	Strike of joint and vein sets if present
1	no data	WNW/ESE	N/S to NNW/SSE, NE/SW
2	NW/SE	NW/SE	ENE/WSW
3	no data	no data	N/S
4	no data	no data	N/S, E/W
5	no data	ENE/WSW	N/S to NE/SW
6	E/W	ENE/WSW	NNW/SSE to N/S, E/W
7	E/W	ENE/WSW	N/S, ENE/WSW
8	E/W	ENE/WSW	NNW/ESE, ENE/WSW
9	no data	no data	N/S to NE/SW, E/W
10	no data	no data	NNE/SSW to NE/SW
11	E/W	WNW/ESE	NNE/SSW
12	WNW/ESE	E/W	NNE/SSW
13	WNW/ESE, N/S	WNW/ESE	N/S
14	WNW/ESE	no data	NNW/SSE, WNW/ESE

Table 5.2. The strike of the major shallow to vertical dipping planar discontinuities in the Rusey and Strangles cliffs.

Faults mapped within the area are shown in Figs. 5.17 and 5.18. Fault trends identified suggest that the main trends strike NW/SE and E/W. Sub-ordinate trends occur to the NE/SW and N/S. Faults which trend NW/SE are

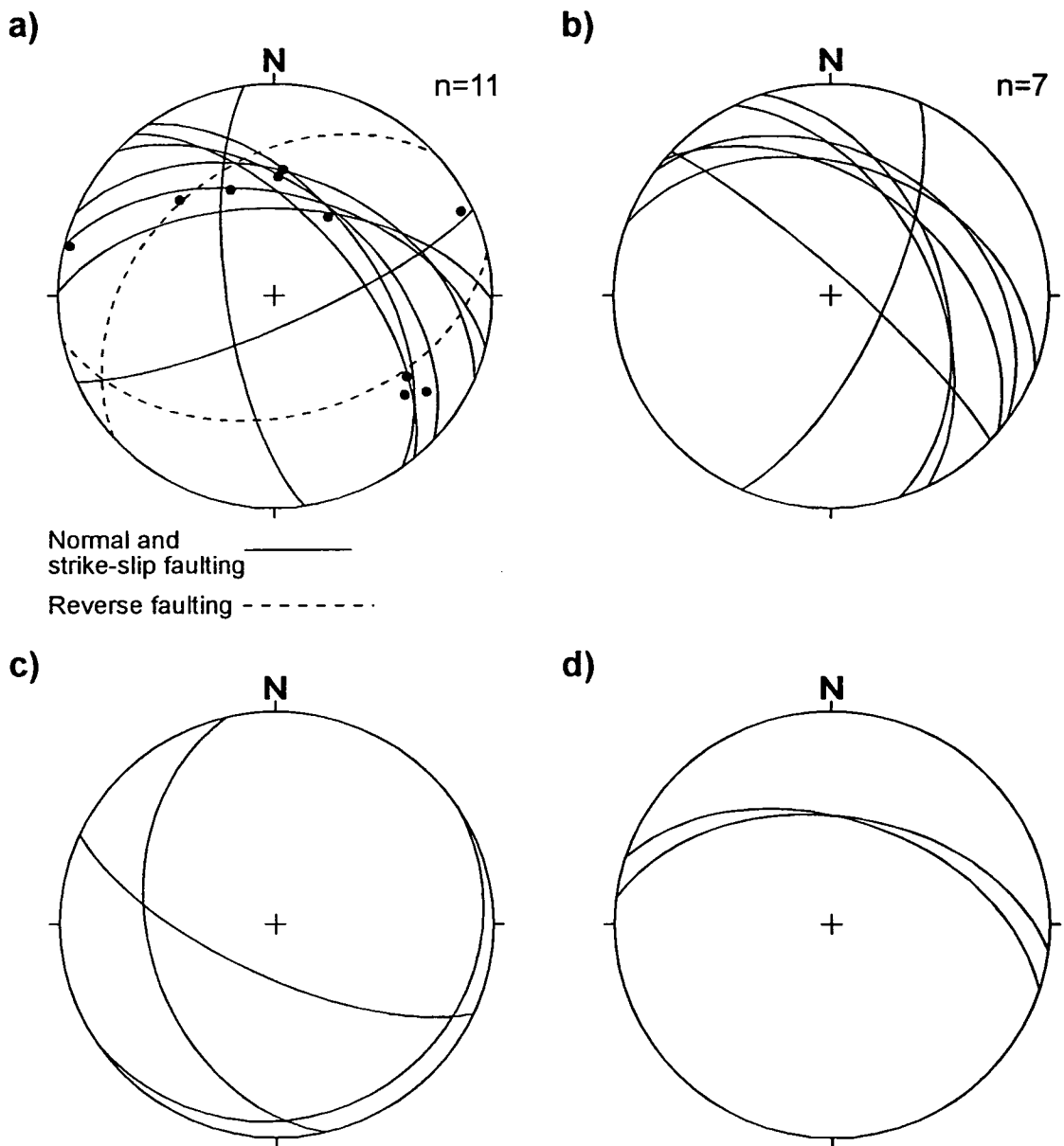


Fig. 5.17. Series of stereograms showing the trends of faults interpreted from the Rusey and the Strangles cliffs. Stereogram a) contains fault data which possessed fault-slip indicators, reverse faults are shown with a hashed line. Stereograms b) and c) show the distributions of faults with apparent normal and reverse movements, respectively. Plot d) shows the trends of faults identified from the Rusey fault zone with unknown directions of movement.

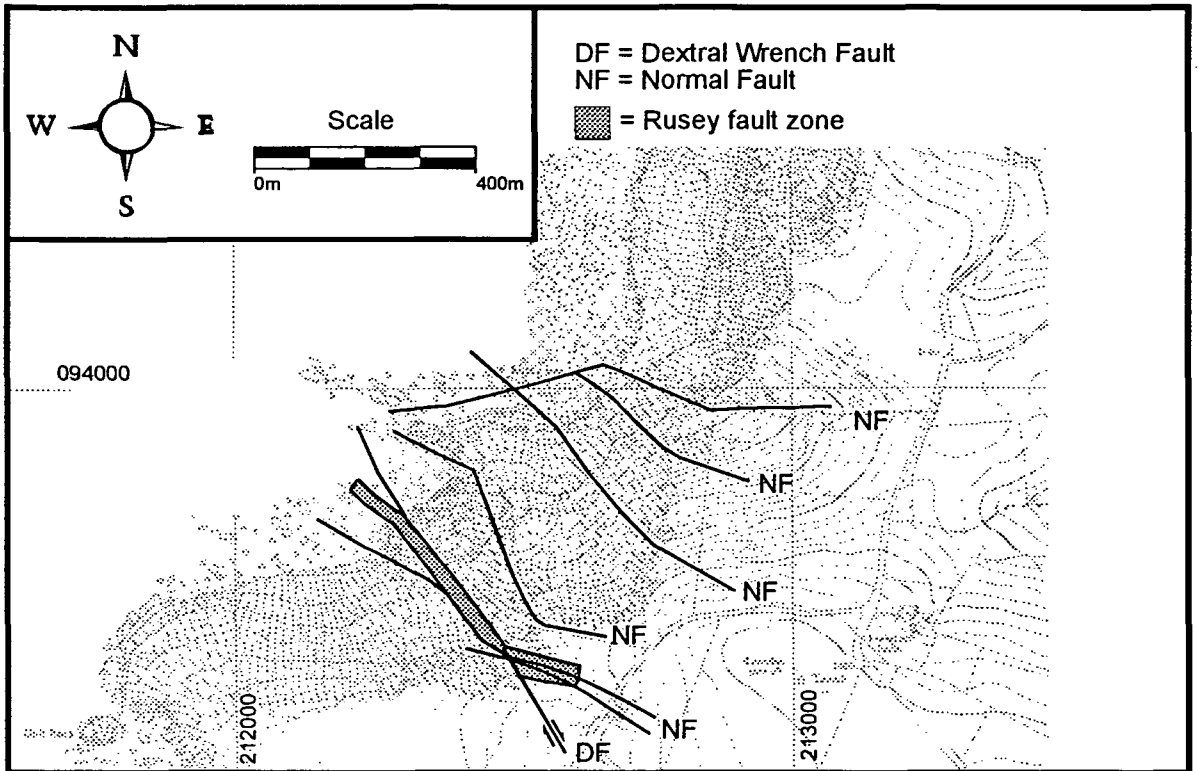


Fig. 5.18. Map of the major faults around Rusey cliffs. Based on Freshney *et al.* (1972), unpublished work by Lister (1989) and the authors own observations.

seen to have a mainly oblique-slip normal displacement, with dextral and sinistral components of movement. NE/SW to ENE/WSW trending faults were found to occur as sinistral strike-slip faults and reverse dip-slip faults. Faults interpreted from the Rusey fault zone typically dip to the north-north-east at moderate angles.

To identify if the lineament patterns (Table 5.1) around the Rusey and Strangles cliffs are controlled by these planar structures (Table 5.2) the trends from each dataset are compared:

(i) Sample locations 9-14. N/S lineaments have been identified in most of these sample locations and over the resolution range. Correlating to this strong lineament trend is a pervasive N/S fracture set identified at the majority of sample locations. However, for the higher resolution images (60m and 30m) in sites 9, 10, 11 a small zone of NE/SW lineaments occur. Within these areas the fracture set ranges from the strong N/S trend to a weaker NE/SW trend, suggesting that in higher resolution images smaller fracture sets can be interpreted.

(ii) Sample locations 6, 7 and 8. In these sample locations the dominant lineament trends are E/W and NE/SW. E/W lineaments could be explained by the E/W trending bedding. However, within this location an E/W trending normal fault produces a marked topographic expression (Fig. 5.18). From this feature the E/W lineament zone E/W(iii) (Fig. 5.2) is interpreted and forms the E/W lineaments in these locations. Furthermore, the absence of N/S lineaments may suggest that this prominent topographic feature masks the major N/S fracture set present in the majority of the sample area. Line sampling in these locations, however, could not identify a planar structure which could cause the NE/SW lineament set.

(iii) Sample locations 2, 3, 4 and 5. Lineament patterns in these locations change with an increase in image resolution, and in high resolution images they comprise of multiple lineament trends. These locations cover the area close to

and within the structurally complex Rusey fault zone, a zone comprising of different planar trends. Therefore, it is suggested that with increasing image resolution these structures become apparent by forming a complex lineament pattern.

(iv) Sample location 1. This location again shows variable lineament trends with increasing image resolution from E/W, NE/SW and N/S lineaments. These lineaments, however, could relate to WNW/ESE, N/S and NE/SW planar structures. Therefore, it is again suggested that with increasing image resolution these structures become apparent by forming a complex lineament pattern.

5.2.5 Discussion of the effect of resolution on lineament analysis of the sub-area Cambeak

The lineament characteristics of the four main lineament trends were found to change with increasing image resolution. The increase of E/W, N/S and NW/SE lineaments, including the appearance of 'new' lineament zones, suggest that with higher image resolutions of up to 60m the geological information increases. Correlating to an increase in information for E/W and NW/SE trending lineament groups are similar or higher frequency lineament percentages (Fig. 5.3). Such a frequency percentage pattern may therefore be a rapid indication of an increase in geological information with increasing image resolution. However, the frequency of NE/SW lineaments decreased with increasing image resolution and the frequency percentage of N/S lineaments were random with increasing resolution suggesting that this effect is not applicable to all lineament trends. Consequently, the overall effect of increasing image resolution is to change the characteristic lineament pattern in the lineament maps.

These lineament pattern changes were attributed to the size of geomorphological features present within the sub-area.

Analysis of the lineament patterns in Cambeak and those identified from the regional lineament map of SW England suggest similar geological causes for the main lineament trends. However, with increasing image resolution the change in lineament patterns cannot be totally explained by these major lithotectonic causes. Correlation between the planar structures in the rock mass and localised lineament trends show that fractures can form lineaments in low and high resolution images, particularly evident for N/S lineaments. It was identified that lineaments in lineament zones show an increase in diversity with increasing image resolution. This is attributed to the identification of sub-sets of smaller, very localised fracture sub-sets (sample areas 9, 10, 11), hence, again indicating that greater amounts of geological information are obtained from higher resolution images. However, this extra information may not be always used to suggest the localised planar structures within the rock mass as either these can be masked by major lithotectonic features (e.g. an E/W trending normal fault at locations 6, 7 and 8) or produce confusing lineament patterns comprising of multiple lineament trends as formed in complex geological areas (e.g. Rusey fault zone).

Published data indicates that NE/SW strike-slip faults are sub-ordinate to NW/SE faulting within North Cornwall. However, in low resolution images of the sub-area Cambeak there are higher numbers of NE/SW lineaments some of which were found to possess fault zone characteristics. The causes of these lineaments were not identified but it is suggested either that the degree of NE/SW faulting in the geological maps of the sub-area is underestimated or an unidentified NE/SW fracture set exists.

Lineament lengths in fault zones in higher resolution images increasingly become shorter. The main explanations (see Section 3.10) for the causes of smaller lineaments are: the interpretation of new smaller structures related to a previously identified major structure with a scale range across the resolution range of the interpreted images; interpretation of entirely new features; and the part-healing of geomorphological features. New geomorphological features related to major lithotectonic features and new lithotectonic features were interpreted from the lineament maps of the sub-image of Cambeak, hence indicating that the decrease in lineament length with increasing image resolution is in part related to such lithotectonic features. However, these shorter lineaments populations could still be shortened further by part-scarp healing (see Sections 3.10(iii), 4.2.5(ii)).

5.3 The effect of resolution on lineament analysis in the sub-area Bridgerule

5.3.1 Lineament maps

The 150m to 30m resolution lineament maps of the sub-area Bridgerule are shown in Fig. 5.19. Fig. 5.20 illustrates the frequency percentage of these lineament groups, the main lineament trends possess the following patterns:

(i) The major E/W lineament peak interpreted from the 150m resolution image is centred on the 095°-100° lineament group. The E/W lineament groups interpreted from images with resolutions of 120m to 30m are centred on the 085°-090° lineament group, suggesting an anti-clockwise rotation of lineaments. The frequency of the ~E/W trending lineament group generally decreases from 15.7% to 8% with increasing image resolution up to 60m. However, a sharp rise is identified in Fig. 5.20 for the frequency percentage of the lineament population interpreted from 30m resolution images.

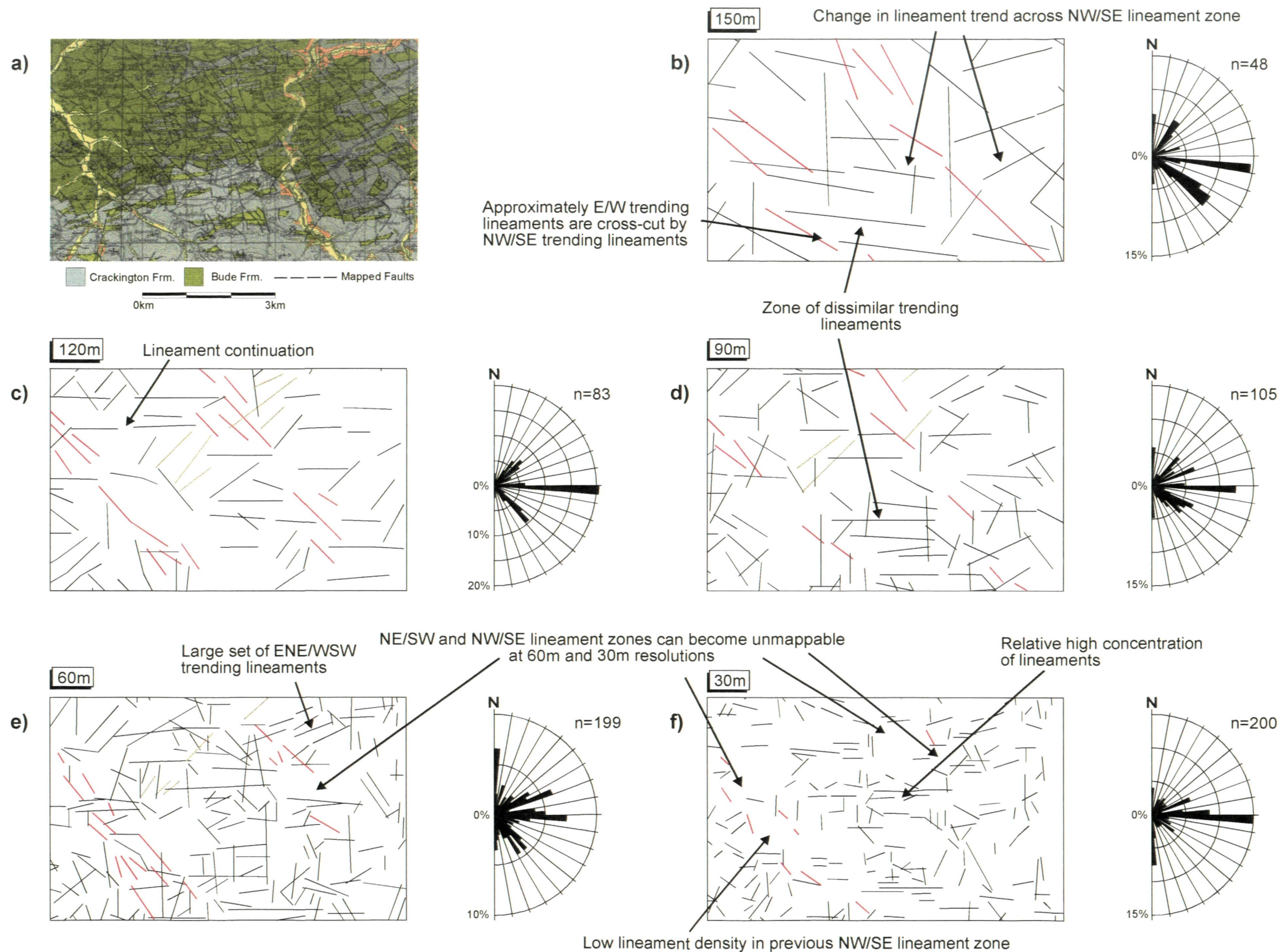


Fig. 5.19. Maps of a) geology, reprinted from the 1:50000 scale BGS (1974b) sheet 323 and b) to f) lineaments of the sub-area Bridgerule. Lineaments have been interpreted from TM images with resolutions of 150m, 120m, 90m, 60m and 30m. Rose diagrams to the right of each map show the lineament trends in each population. Lineaments coloured red and brown form thin lineament zones and are interpreted to be caused by NW/SE and NE/SW trending faults, respectively.

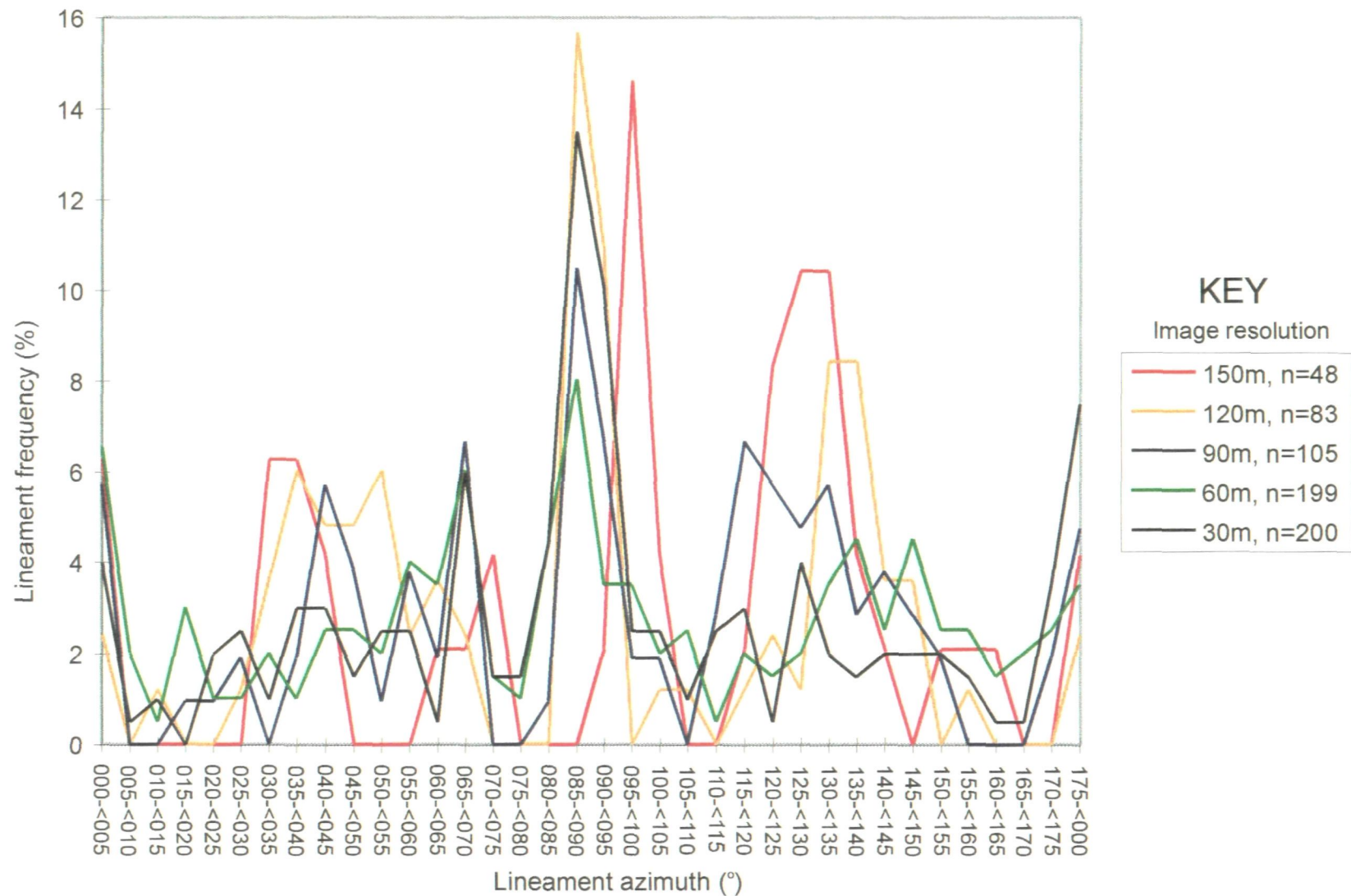


Fig. 5.20. Line chart illustrating the frequency percentage of lineaments (in 5° lineament groups) over the resolution range of 150m to 30m (see key) for the sub-area of Bridgerule.

(ii) The effect of image resolution on the frequency percentages of N/S lineaments is not easily identifiable. However, in general higher resolution populations have the highest values.

(iii) The frequency percentage of NW/SE trending lineament groups lowered with increasing image resolution, changing from 10.5% for the 150m resolution lineament population to 1.7% for the 30m resolution lineament population.

(iv) The effect of resolution on NE/SW lineament groups is similar to that of NW/SE lineament groups, as the frequency percentage falls with increasing image resolution from ~6.1% (150m) to ~2.2% (30m).

(v) Another major lineament sub-set can be identified between 065° to 075° (the frequency percentage values of this sub-set is 2% higher than the relevant sub-set in sub-area Cambeak). The effect of increasing resolution on these lineament groups is for their frequency percentage to increase from ~3% to ~6%.

The decrease in percentage frequency of NW/SE and NE/SW lineament zones can be identified in the lineament maps (Fig. 5.19) by becoming unmappable in the higher resolution maps (60m and 30m), whereas N/S, E/W and ENE/WSW lineament zones can still be identified in higher resolution images (Fig. 5.20e, f). Lineament density in the sub-area Bridgerule generally shows a decrease from the 60m to the 30m lineament map. Small areas in the sub-area Bridgerule, however, can possess relatively high lineament density, typically consisting of E/W lineaments. Conversely, areas occupied by NW/SE and NE/SW lineaments in low resolution lineament maps can show areas of relatively very low lineament density in the 30m resolution lineament map (Fig. 5.20f), reflecting the decrease in frequency percentage of lineaments with this trend.

Analysis of the topography within the sub-area (Fig. 5.21) suggest that relative high lineament densities correlate to marked topography.

5.3.2 Lineament patterns and lithotectonic trends in the sub-area Bridgerule

The sub-area Bridgerule consists of inter-bedded sandstones and mudstones of the Upper Carboniferous Crackington Formation and Bude Formation (distinguishable from the Crackington Formation by thick sandstone groups) (Freshney *et al.* 1979b). In all of the lineament maps the E/W and the ENE/WSW lineaments trends are typically cross-cut by the other main lineament trends. Furthermore, some of the E/W lineaments show continuity typical of lineaments caused by lithotectonic differences (see Section 4.2.1(i)). As described in Sections 2.3.4 and 5.2.3 the Culm deposits have undergone folding to form E/W outcrop trends. A sub-trend to the main E/W fold trend is to the ENE/WSW in the north-east of the sub-area Bridgerule, similar in trend to the large periclinal folds identified in the region of Chulmleigh (Freshney *et al.* 1979a). Except for the 120m lineament population (Fig. 5.20c) ENE/WSW lineaments are particularly dense within this area. The absence of these ENE/WSW lineaments within this small area may be due to visual lineament interpretation, consequently a degree of error may occur in the interpretation of lineaments. This can occur particularly for lineaments which are interpreted from less distinct linear features within an image.

Cross-cutting the primary lineaments are NW/SE, NE/SW and N/S, the latter typically cross-cutting the NW/SE and NE/SW lineaments as well. Cross-cutting lineament relationships suggest that these lineaments are a series of fractures as suggested by published data (Sections 2.5) and ground surveying (see Section 5.2.4).

1 0 1 2 Kilometers

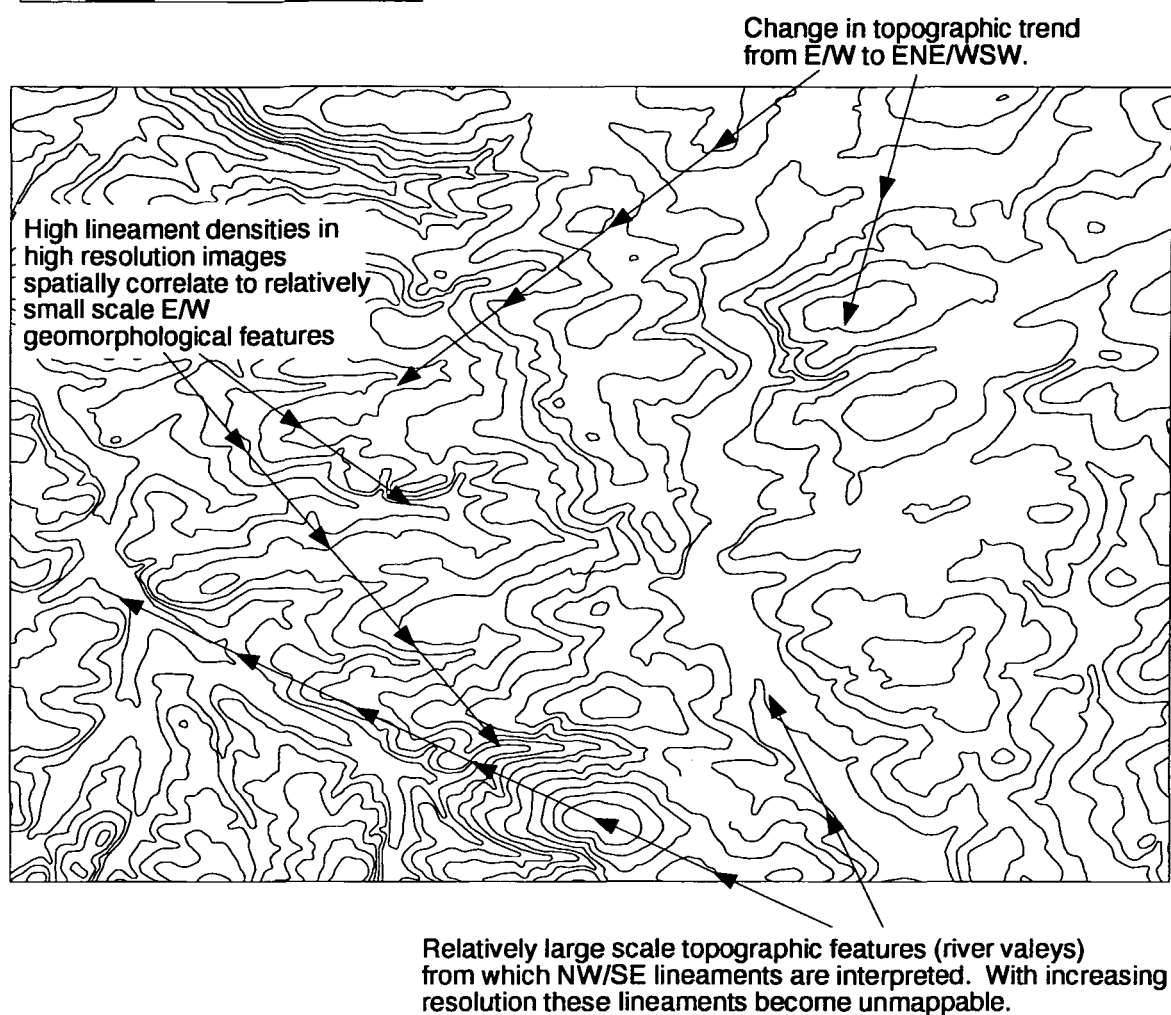


Fig. 5.21. 10m elevation contours illustrating the topographic trends and relative changes in geomorphological scale in the sub-area Bridgerule.

5.3.3 Discussion on the effect of resolution on lineament analysis in the sub-area Bridgerule

Similar to the sub-area Cambeak the major lithotectonic features of the Culm Basin have been identified from the lineament map. Of these the NW/SE and NE/SW lineaments become unmappable in images with 60m and 30m resolutions as larger geomorphological features within the images become less apparent. This suggests the geological information increases with resolution and falls in image resolutions of 60m and 30m. However, subtle differences in the lineament characteristics have been found between the two lineament maps. An extra lineament trend to the ENE/WSW over the whole resolution range was identified and related to a change in the trend of folding within the sub-area, hence suggesting that ~E/W lineaments which show continuity are caused by lithological differences.

A purely geological cause has not been found for the anomalous clockwise rotation of E/W lineaments (from the lineament groups of 095°-100° to 085°-090°) between the image resolutions of 150m and higher (Section 5.3.1). These lineaments have apparent characteristics of primary features indicating lithotectonic causes, an explanation which satisfies the E/W trending lineaments of the lineament maps between 120m and 30m. As illustrated in Fig. 3.20 increasing the image resolution allows the identification of smaller features. Hence, lineaments interpreted from low resolution images may be the result of the combined EMR reflectances from displaced primary features. Therefore, in low resolution images 085°-090° trending lithological units could be interpreted to trend towards 100° by the dextral displacement of E/W primary features on NW/SE trending strike-slip faults, the smaller faults of which are below the observation threshold of the low resolution images (Fig. 5.22a).

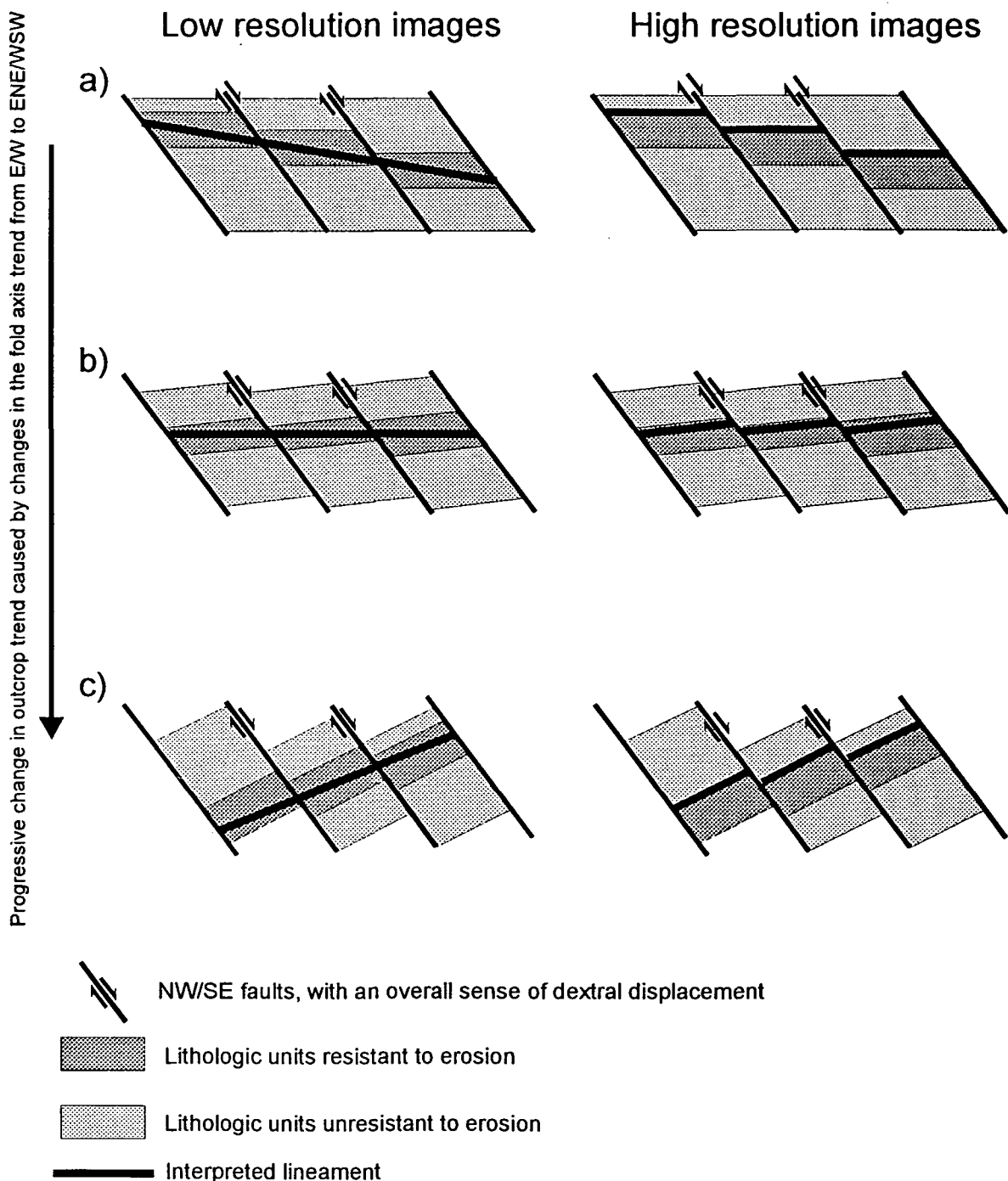


Fig. 5.22. Schematic diagram of how lineament trend and length can alter with a change in image resolution in the sub-area Bridgerule. Lineaments interpreted from low and high resolution images are shown in the diagrams on the left and right, respectively. Each diagram contains displaced lithologic units with trends between E/W to ENE/WSW and are bounded by NW/SE dextral strike-slip faults. Diagram a) illustrates how lineaments which trend towards 110° can be obtained from low resolution images, while in high resolution images the same primary features produce shorter E/W lineaments. Diagram b) shows the effect of only a small change in outcrop trend by forming approximately E/W lineaments in low resolution images, and shorter lineaments trending towards 080° in higher resolution images. Diagram c) shows how the trend of lineaments in the low resolution images become more accurate to the outcrop trends when the outcrop trends of the lithologic units are more perpendicular to the trends of the bounding faults, in high resolution images these lineaments become shorter.

However, with increasing image resolution the E/W primary features and smaller faults begin to fall within the image observation threshold and hence shorter E/W lineaments are interpreted. Furthermore, ENE/WSW trending primary lineaments were found to have higher frequency percentages with increasing image resolution. Therefore, using a similar process the increase of these lineaments may be caused by the differentiation of smaller ENE/WSW trending geomorphological features which previously may not have been identified or were identified as a different trend (Figs. 5.22b, c). Thus low resolution images could contain lineaments that may not suggest the actual geological relationship. Hence the accuracy of a lineament map may increase with increasing image resolution.

5.4 The effect of resolution on lineament analysis in the sub-area Laneast

5.4.1 Lineament maps

The 150m to 30m resolution lineament maps and rose diagrams of the sub-area Laneast are illustrated in Fig. 5.23. The effect of resolution on the frequency percentage of lineaments in lineament groups are shown in Fig. 5.24. The following relationships of the main lineament trends were identified:

- (i) E/W lineaments increase in frequency with increasing image resolution from 4.6% to 12.4%.
- (ii) The effect of resolution on the frequency of N/S lineaments is less clear. However, generally with increasing image resolution the frequency of lineaments increases.
- (iii) NW/SE and NE/SW lineaments have similar characteristics with the peak trend changing by $\pm 10^\circ$ over the resolution range and with increasing resolution giving a decrease in frequency percentage.

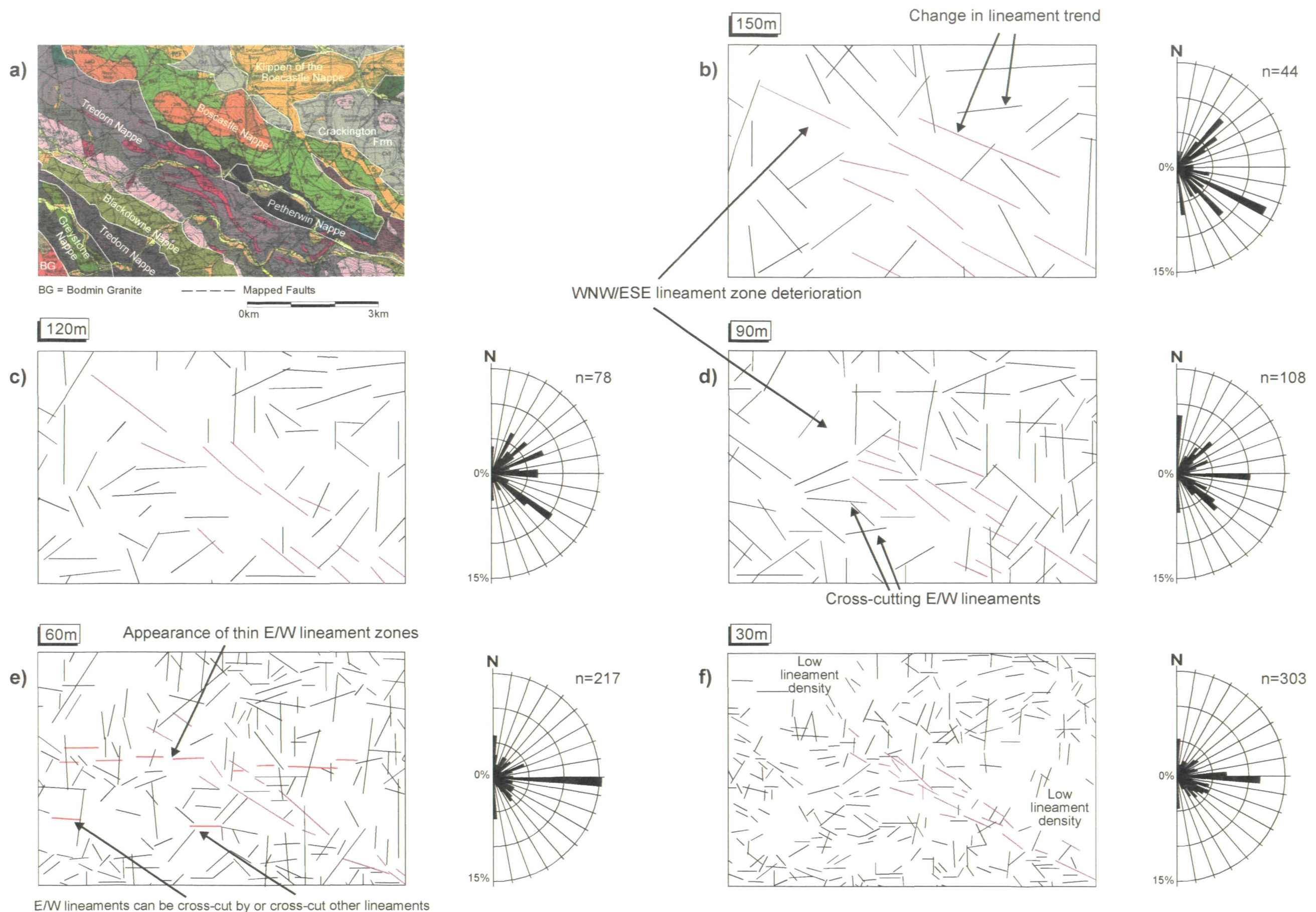


Fig. 5.23. Six maps illustrating a) the geology, modified from the 1:50000 scale BGS (1993) sheet 337, and b)-f) lineaments interpreted from TM images of the sub-area Laneast. The resolution of the interpreted images are shown above each map. Lineament trends within each map are depicted to the right by a series of rose diagrams. Lineaments highlighted in purple change in character with increasing resolution from a broad lineament zone to a thinner lineament zone.

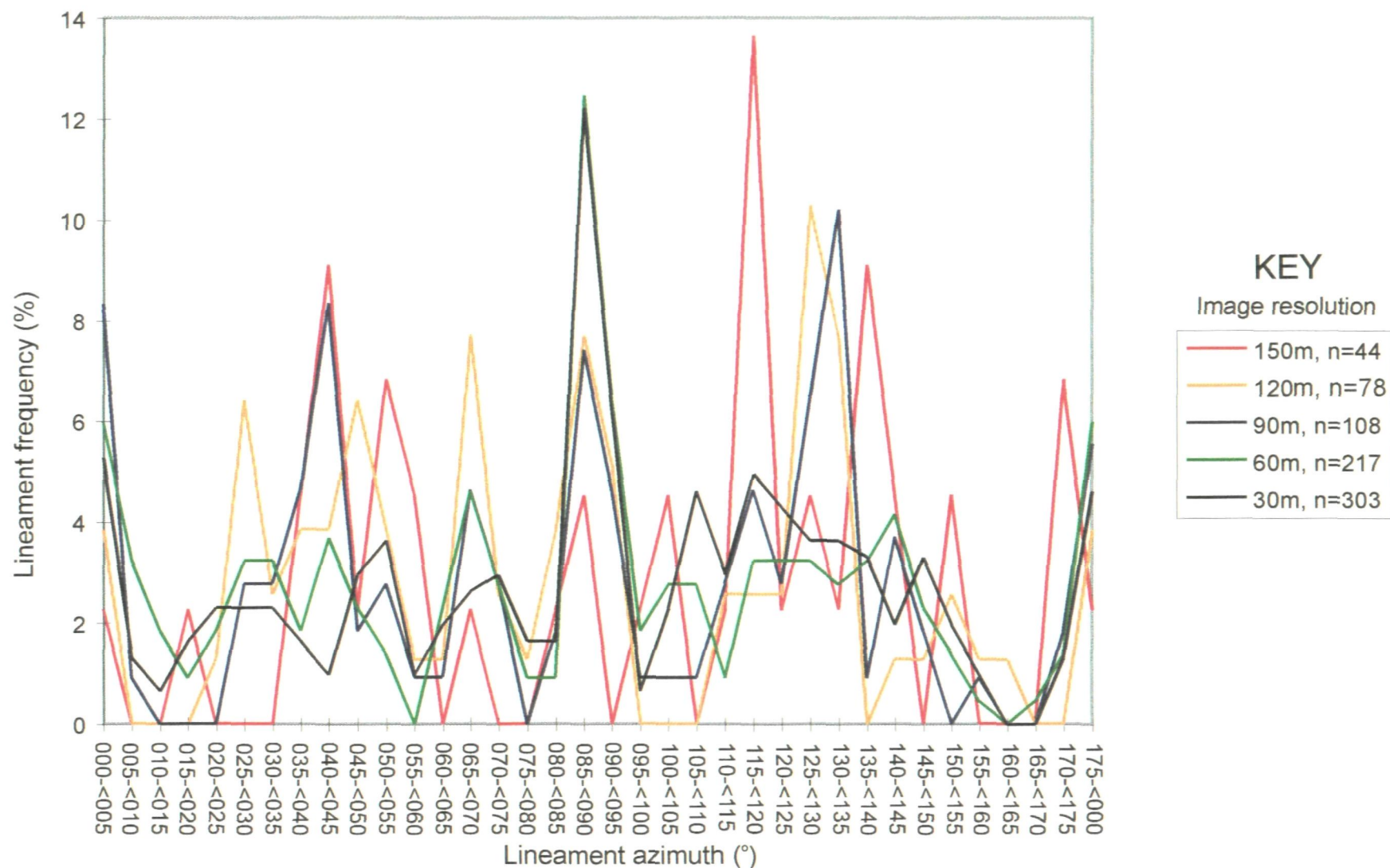


Fig. 5.24. Line chart showing the frequency percentage of lineaments (in 5° lineament groups) over the resolution range of 150m to 30m (see key) for the sub-area of Laneast.

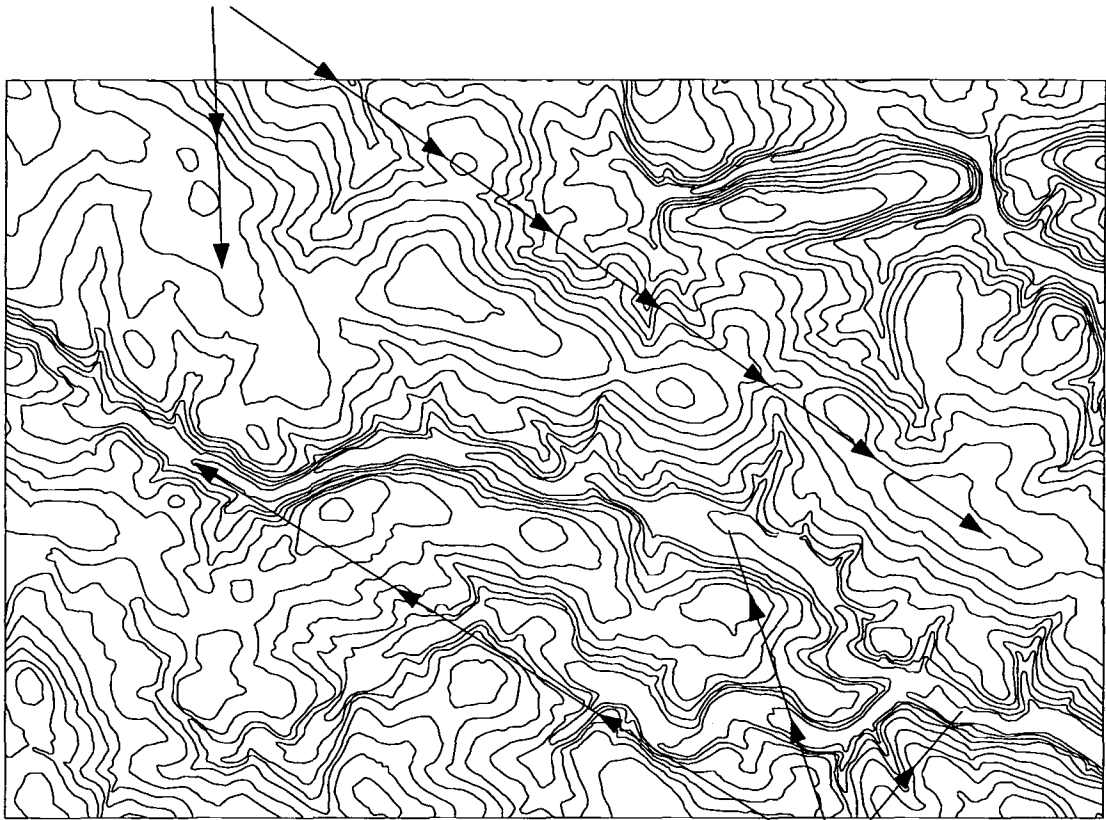
(iv) An additional peak in lineament frequency (13.7%) was identified at 120° in the 150m resolution lineament map. With increasing resolution the lineament frequency falls sharply to ~4%.

In comparison to the sub-areas Cambeak and Bridgerule there is an absence of E/W lineaments in the lowest resolution images and a wide WNW/ESE trending lineament zone. This wide lineament zone is apparent particularly in the 150m resolution image. With increasing image resolution the length and width of this zone decreases eventually forming two thin zones (Figs. 5.23e, f). However, these zones are still discernible from the more complex lineament patterns of the higher resolution lineament populations. Located around this WNW/ESE lineament zone are low lineament density areas in the high resolution lineament map (Fig. 5.23d, e, f). Comparison with the relief of the area indicates that the difference in lineament density of this lineament zone is related to a WNW/ESE topographic trend, the higher lineament density area to a sharp topographic low (valley) and the low lineament densities to broad topographic highs (ridge) (Fig. 5.25).

5.4.2 Lineament patterns and lithotectonic trends in the sub-area Laneast

The lineament maps of the sub-area Laneast over the resolution range show an ENE/WSW trending lineament zone which contrasts against E/W lineaments to the north-east of the lineament map. Generally these ENE/WSW lineaments are cross-cut by N/S, NE/SW, NW/SE and in higher resolution images E/W lineaments, suggesting they are primary lithotectonic features. The lineament characteristics in the low resolution lineament maps (a sharp change in lineament characteristics outside the zone, and a wide dense set of primary lineaments which are cross-cut by later features) reveal that these lineaments

Relative large scale topographic highs (ridges) which cause low lineament densities from high resolution (90m-30m) images.



Relative small scale topographic lows (valleys) which cause high lineament densities from high resolution (60m and 30m) images.

Fig. 5.25. 10m elevation contours in the sub-area Laneast illustrating the relative changes in the scale of geomorphological features.



represent a thrust zone. The WNW/ESE lineament zone correlates to the WNW/ESE main lithotectonic trend in the sub-area Laneast, the Boscastle, Tredorn, Petherwin, Blackdowne and Greystone Nappes, or the bedding and cleavage within the nappes which are generally parallel to sub-parallel to the thrusts (Warr 1989). Within the high resolution lineament maps, however, the characteristic lineament pattern of a thrust zone can not be identified within the lineament maps as the WNW/ESE lineament zones become more akin to individual fault zones.

Located to the north-east of the WNW/ESE lineament zone in the 150m resolution images are ~E/W lineaments. These lineaments follow the Crackington Formation and the overlying klippen of the Boscastle Nappe. However, with increasing image resolution the frequency of E/W lineaments has been found to increase and are visible throughout the lineament map. These E/W lineaments can form thin lineament zones (Fig. 5.23e) which can be cross-cut and cross-cut the other major lineament trends (Fig. 5.23d, e), therefore suggesting that these higher resolution E/W lineaments represent a smaller scale fracture set (as found elsewhere within the regional lineament map of SW England, Table 4.2) only visible in <120m resolution images.

5.4.3 Discussion on the effect of resolution on lineament analysis in the sub-area Bridgerule

In the sub-area Bridgerule resolution has the effect of either highlighting or masking the area's major lithotectonic feature, a series of WNW/ESE trending nappes. Analysis of the topographic features formed from these nappes show that they are mainly large scale features and hence are preferentially interpreted from low resolution images. As a result in the 90m, 60m, and 30m lineament

maps geological information is lost. Furthermore, the characteristic lineament pattern of thrust zones in high resolution lineament maps becomes similar to individual fault zones suggesting that thrust zones may not be identifiable in high resolution images.

In comparison, with increasing image resolution a new lithotectonic feature, an E/W fracture set apparent elsewhere in SW England, has been identified. The appearance of this feature from only a small resolution increase suggests that it may be difficult to predict the trends of small scale lithotectonic features from low resolution images. These results again suggest that the visibility of lithotectonic features is dependant upon the scale of the related geomorphological feature, hence for large scale features the geological information decreases with increasing resolution and for small scale features information increases with increasing image resolution.

5.5 Discussion on the effect of resolution on images of North Cornwall and the extrapolation of the regional lineament map

It has been found in the sub-areas Cambeak and Laneast that large scale geomorphological features are more prominent in low resolution images. Large scale geomorphological features in North Cornwall form flat topped ridges (WNW/ESE features in the sub-area Laneast) or broad valleys (NE/SW features in the sub-area Cambeak). Therefore these large scale features have small but continuous changes in relief, and the effect of increasing the image resolution on the EMR reflected from these features is for the difference in reflected EMR for each neighbouring pixel to be lowered. Hence, this reduces the visibility of large scale features and lowers the frequency of lineaments interpreted from such features, e.g. NE/SW lineaments in the sub-area Cambeak and WNW/ESE

lineaments in the sub-area Laneast. This effect was found to occur between the 150m and 120m resolution lineament maps and therefore it is suggested that for the identification of thrust zones from Landsat TM images of SW England the image resolution should be decreased to 150m. Increasing the image resolution further yields less geological information and changes the characteristic thrust zone lineament pattern.

For smaller scale geomorphological features an increase in image resolution can yield more information (e.g. more fault controlled NW/SE lineament zones in Cambeak), to the extent that new lithotectonic features were identified (e.g. E/W fractures in the sub-area Laneast and minor fracture trends in the sub-area Cambeak). This increase in information was found in images with resolutions up to 60m. Above this resolution small areas of very low lineament densities were found. These low lineament densities were correlated to relatively level relief. In these areas the relatively level relief would mean that fewer lineaments would be interpreted initially. However, in areas of high resolution images with small changes in slope angle the major controls on the reflected EM radiation are the anthropogenic features which mask the geomorphological structure (see Section 3.4) (Fig. 3.4). Furthermore, less spatial control would be exerted on the location of field boundaries and infra-structure and hence following the knowledge based rules devised in Section 3.8.1 (that lineaments be removed from the lineament map if they spatially correlate to an anthropogenic feature which is not controlled by a geomorphological structure) this effect is compounded. As a result even less lineaments are interpreted from high resolution images in areas containing small changes in slope angle.

Generally E/W and N/S lineaments were less affected by anthropogenic features in high resolution images. The causes of these lineaments were large

and small scale ridges and valleys, consequently the smaller changes in relief were still identifiable in the high resolution images. Therefore, for lithotectonic features represented by such lineament trends further geological information maybe obtainable in higher resolution images.

As a result of the combined effects of the different scale geomorphological features and anthropogenic features, increasing the image resolution has resulted in different lineament patterns. Missing from the regional lineament map are relatively minor sets of small scale structures. However, major sets are identifiable e.g. N/S jointing in North Cornwall. Therefore, to sample the more minor structures an increase in image resolution is needed. A general increase in the accuracy and geological information (including new lineament zones) of the major lithotectonic features in SW England were obtained with an increase in image resolution. However, no new major features were identified, indeed the visual impact of the thrust zone in the sub-area Laneast decreased. Therefore, it is suggested that for the regional lineament analysis of SW England an image resolution of 150m was appropriate.

5.6 Conclusions

(i) Increasing the image resolution generally resulted in greater amounts of geological information of the major lineament trends (E/W, N/S, NE/SW and NW/SE) being interpreted. The frequency of the major lineament trends, however, were found to decrease at different higher image resolutions; E/W and N/S lineaments were visible in the 30m resolution images whereas NE/SW and NW/SE lineaments became unmappable in the 60m and 30m resolution images. This difference is caused by the scale and morphology of the interpreted geomorphological features.

(ii) The effect of anthropogenic features within the images caused areas in the interpreted 60m and 30m resolution lineament maps to be devoid of lineaments, relative to lineament maps of lower resolution images. Lineament loss was enhanced in areas where only minor changes in slope occurred.

(iii) Lineaments which are related to small scale linear geological features can result in incorrectly interpreted obliquely trending lineament patterns when analysed in low resolution images.

(iv) Increasing image resolution results in the change of the characteristic lineament pattern of a thrust zone to that of a series of high-angle fault zones and a loss of geological information. Therefore, thrust zones should be mapped from low resolution images.

(v) The N/S trending set of major planar structures in the rock mass were found to cause lineaments in the regional lineament map. Minor planar structures, however, can only be identified in higher resolution images (NW/SE fractures at sample locations 9, 10, 11 and 12, sub-area Cambeak). Furthermore, new lineaments zones related to lithotectonic structures identified in low resolution images were interpreted from higher resolution images (E/W lineaments in the sub-area Cambeak). Therefore, with increasing image resolution more geological features were identified to cause lineaments within the images. The complexity of the geology interpreted is therefore linked to resolution.

(vi) Increasing the image resolution from 150m, however, has not resulted in the identification of large numbers of 'new' major lithotectonic structures, therefore such an image resolution is the optimum resolution for regional lineament analysis. Therefore, to analyse in more detail all the major lithotectonic structures and new minor structures image resolution can be increased up to 60m.

Chapter 6 Differentiating lineament directional families using cluster analysis

6.1 Introduction

In SW England and North Cornwall lineaments were interpreted to reflect the surface expression of different lithotectonic features possessing dissimilar trends (Chapters 4, 5). Usually rose diagrams are used for the analysis of lineament trends (e.g. Smithurst 1990), however, the division of lineaments from SW England and North Cornwall into lineament groups (the arbitrary division of data) only identified the broad main lineament trends of the major lithotectonic features. Therefore, to analyse the characteristics of lineaments related to all the lithotectonic features represented within the lineament maps identified in this study, the lineament populations need to be more discriminatively (where the limits of the trends of each lithotectonic set are identified) and sensitively (where smaller lithotectonic sets are identified) divided into lineament directional families (Hardcastle 1995).

Lineament directional families have an irregular frequency/azimuth distribution formed by a series of peaks and troughs which when arithmetically smoothed forms an apparent bell-shaped distribution (Wise *et al.* 1985, Hardcastle 1995). Furthermore, in areas such as SW England where repeated geological processes have been operative, complex lineament frequency/azimuth distributions often comprising mixtures of overlapping lineament directional families are more typical (Figs. 6.1, 6.2). The identification of lineament directional families by minima between overlapping directional families may therefore be complicated by either, in phase peaks and troughs accentuating, or out of phase masking, localised minima in the data.

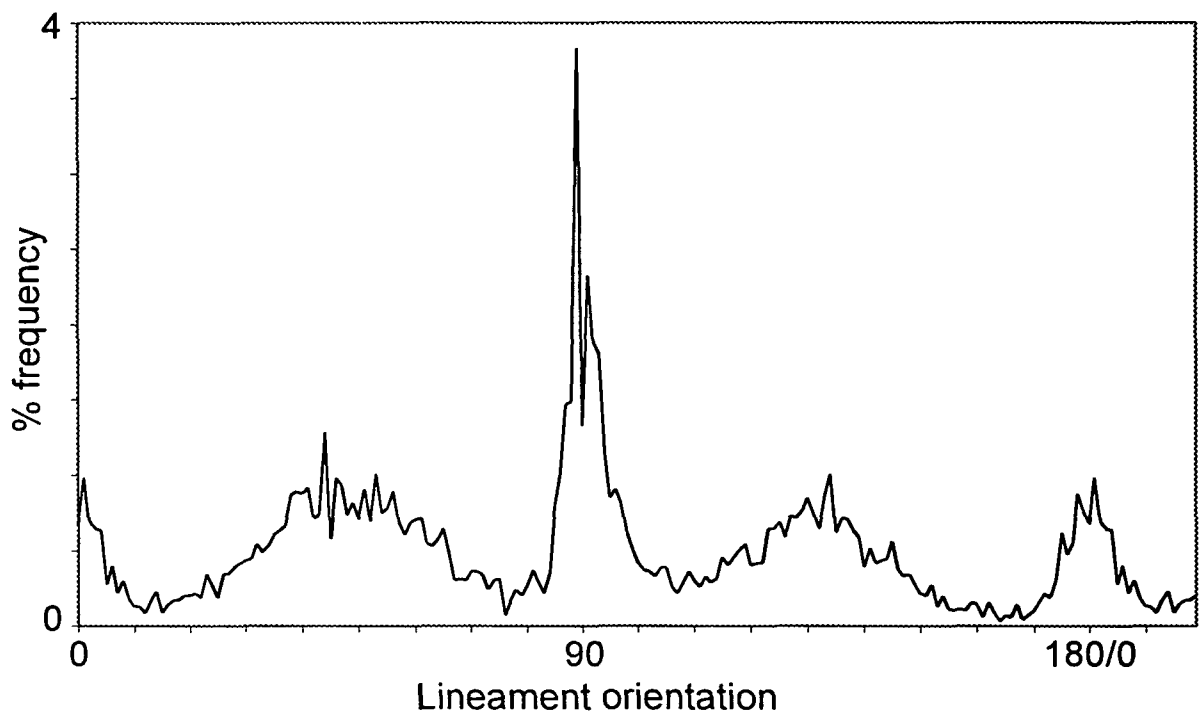


Fig. 6.1. Chart illustrating the frequency/azimuth distribution for the regional lineament population, interpreted from Landsat TM images of SW England at a pixel resolution of 150m.

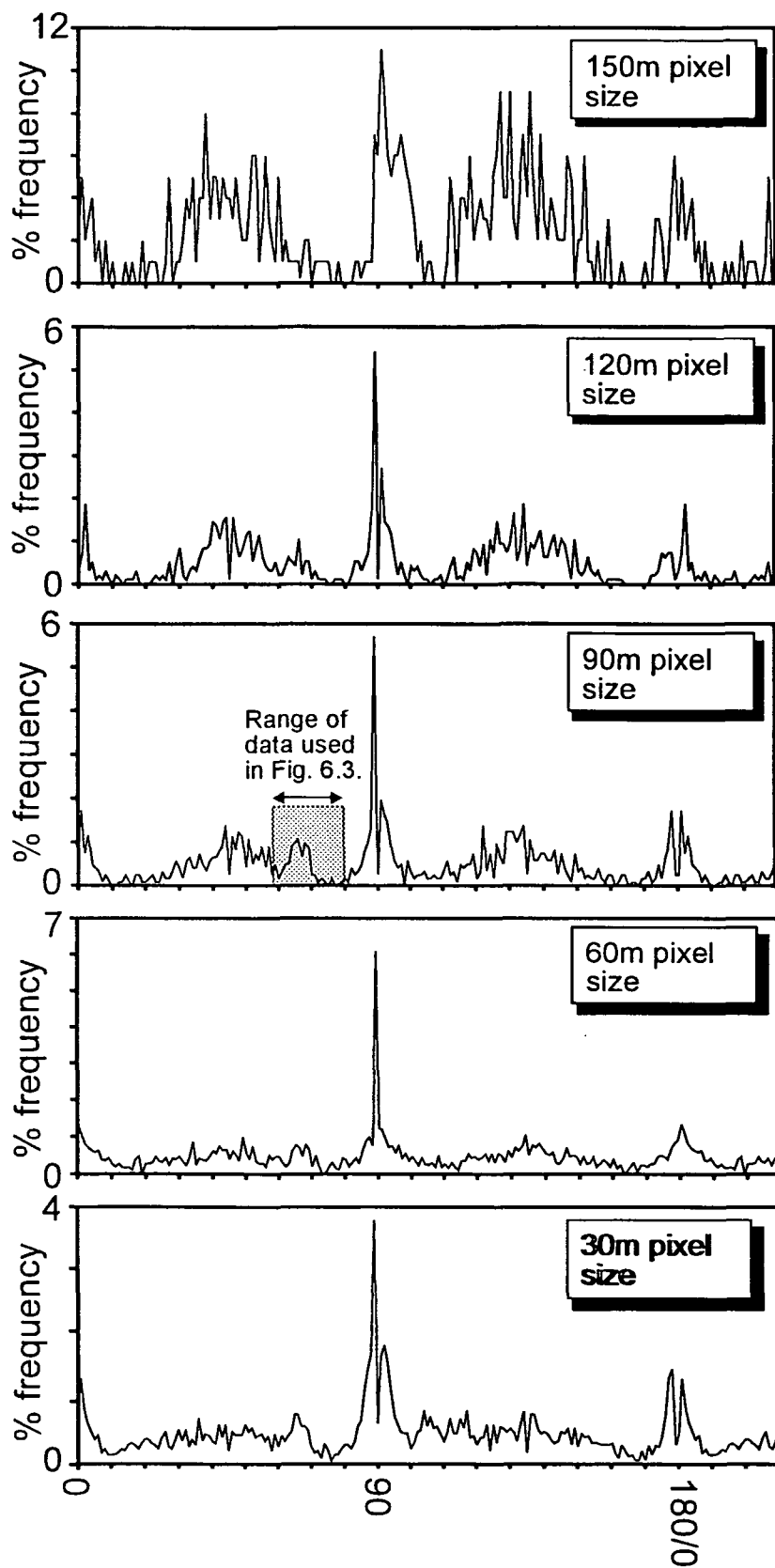


Fig. 6.2. Charts illustrating the frequency/azimuth distributions of lineament populations interpreted from Landsat TM images of North Cornwall with resolutions of 150m to 30m.

A variety of cluster algorithms and methods have been used in order to divide multivariate data into groups that reflect each of the variables. As lineament length of a lithotectonic feature is greatly influenced by later cross-cutting structures in SW England lineament data are only clustered on the basis of a single variable, lineament orientation. Edges of clusters correspond to marked minimum in the lineament frequency/azimuth distribution and are used to define lineament directional families. The effects of different cluster algorithms and methods are also explored on the final groupings of data.

In Chapter 5, increasing image resolution was found to effect the geological information within the lineament maps by either identifying new small scale lithotectonic features related to previously mapped, large scale lithotectonic features, or identifying entirely 'new' scale limited lithotectonic features. The effect of changing resolution on the nature of the lineament directional families derived from the cluster analysis is also examined.

6.2 Description of the lineament frequency/azimuth distributions

Line graphs showing distributions of lineament frequency/azimuth (Figs. 6.1, 6.2) indicate that concentrations of lineament orientations can occur in populations interpreted from images of different resolutions and areas. Within any individual concentration lineament orientation (Fig. 6.3) an irregular pattern of peaks and troughs is seen. These describe an overall bell-shaped curve with distinct maxima flanked by two minima, which according to Hardcastle (1995) defines a directional family. Similar irregularities in lineament frequency/azimuth charts have been obtained by Wise *et al.* (1985) for topographic lineaments, and Conradsen *et al.* (1986) for lineaments interpreted from images.

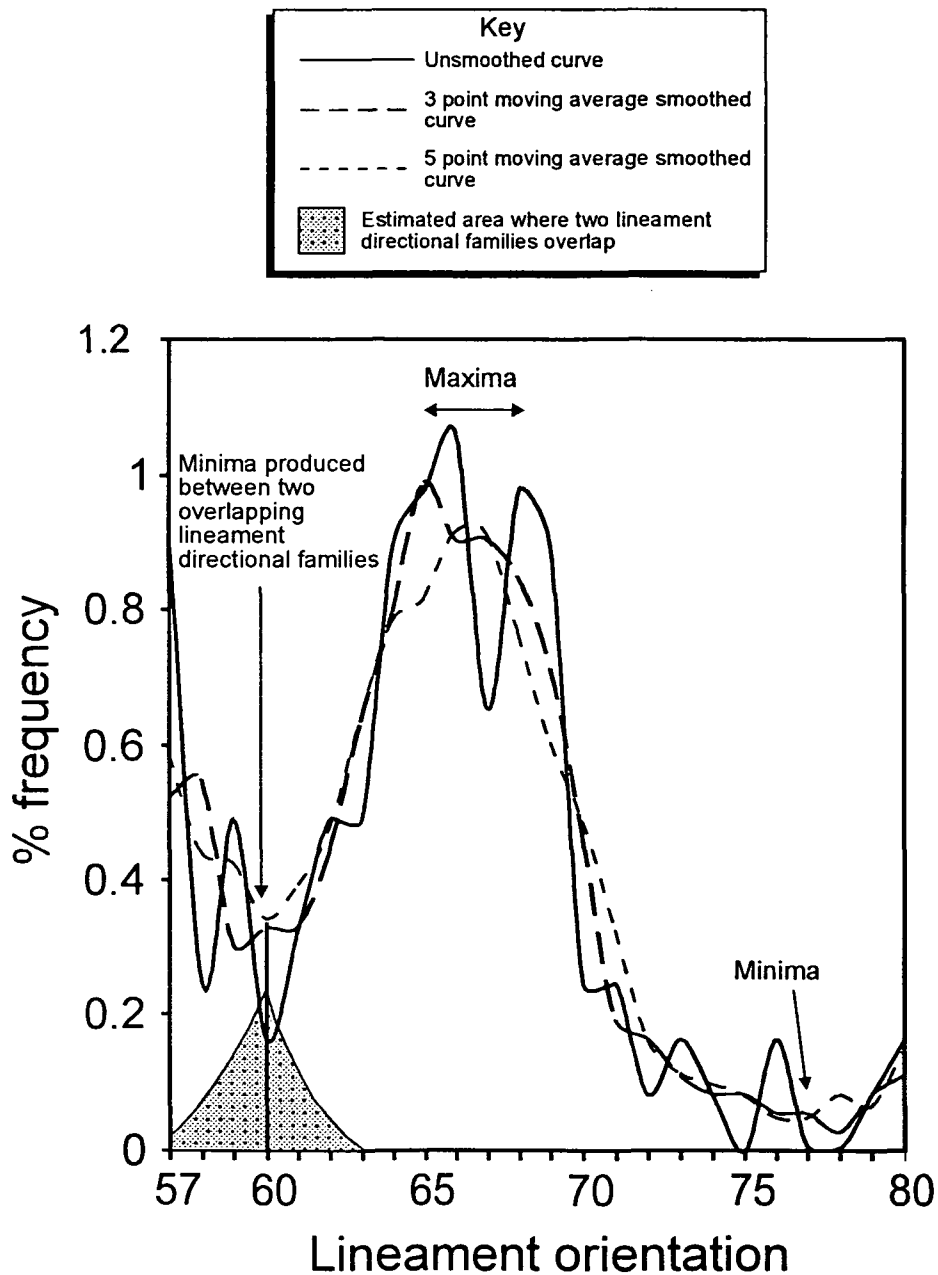


Fig. 6.3. Chart illustrating the frequency/azimuth distribution of a bell-shaped lineament directional family interpreted from the 90m lineament population of North Cornwall. The hashed lines show data that has been smoothed, and suggests that the distribution at 60° consists of two overlapping lineament directional families.

6.2.1 Lineament directional families and normal distributions

Wise *et al.* (1985) and Hardcastle (1995) smoothed their irregular frequency/azimuth data with two-passes of a moving 10° average filter, producing multi-modal distributions. Gaussian curves were then fitted over the smoothed curves thus identifying the bell-shaped lineament directional families. Similar results can be obtained from some of the data presented (Fig. 6.3) where the smoothed data describes an apparent bell-shaped curve consisting of two minima and a maxima.

Furthermore, overlapping lineament directional families can form multi-modal distributions (Wise *et al.* 1985, Hardcastle 1995) (Fig. 6.3). The formation of either a uni-modal or bi-modal distribution by mixtures of normal distributions is illustrated in a series of graphs (Fig. 6.4), where m is the mean of the normal distribution and s is the standard deviation. Figs 6.4a and 6.4b, show uni-modal distributions produced from two normal distributions. Increasing the difference in the means of the two normal distributions as shown in Figs. 6.4c and 6.4d, results in bi-modal distributions. In Fig. 6.4e a distribution which contains one significant peak is produced from 3 normal distributions which have different distances between the mean and standard deviation. These distributions suggest that uni-modal and bi-modal distributions can be obtained by various combinations of any of the above components. This clearly presents a problem when trying to describe individual distributions with best-fit Gaussian curves.

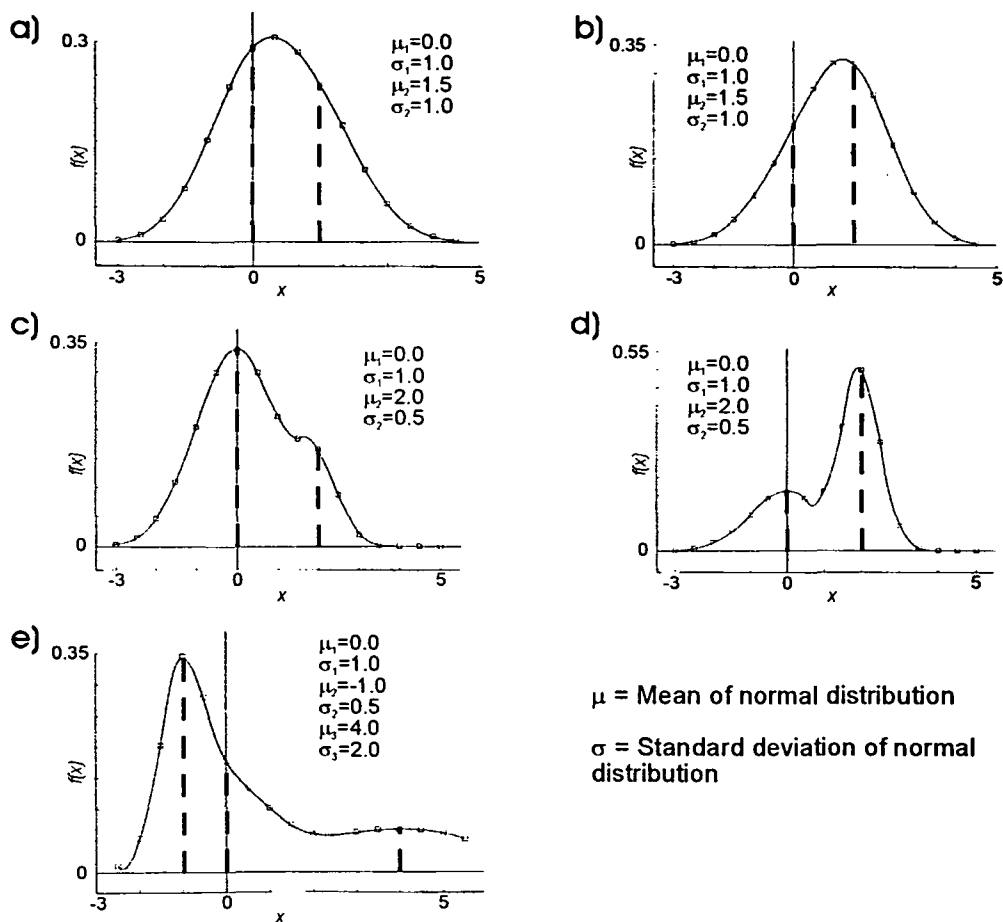


Fig. 6.4. Unimodal and bi-modal distributions produced by mixtures of normal distributions. Diagrams a), b), c) and d) are mixtures of two normal distributions and diagram e), a mixture of three normal distributions (redrawn after Everitt & Hand 1981).

6.3 Previous research in the identification of lineament directional families

Wise *et al.* (1985) devised methods for dividing multi-modal lineament family mixtures by automatically fitting Gaussian curves to 10° smoothed frequency/azimuth distributions. Applying two passes of a 10° running average filter on the data, however, may mask small frequency/azimuth distributions due to the smoothing of smaller peaks and troughs of minor directional families. Furthermore, to fit Gaussian curves over the data the trends of lineaments in the lineament directional families must form bell-shaped curves or normal distributions. The trends of lineaments representing small and large scale lithotectonic features interpreted from images of SW England can be found to change over distance, including lineaments interpreted from:

- (i) the thrust and fold belt of South Devon (southern zone) and West Devon/East Cornwall (northern zone) (see Section 4.2.5(iii));
- (ii) major NW/SE trending fault zones (e.g. SLFZ) (see Section 4.2.5(ii));
- and (iii) lineaments following fold closures (see Section 4.3.2(iii)).

The lineaments related to these lithotectonic structures are likely therefore to produce skewed frequency/azimuth distributions, hence causing problems in the fitting of Gaussian curves. A further problem suggested by Wise *et al.* (1985) is that the technique may not be able to separate closely spaced lineament directional families, as previously indicated in Section 6.2.1.

An alternative method for dividing lineament populations by orientation is described by Conradsen *et al.* (1986); by identifying deviations caused by minima and maxima in a smoothed frequency/azimuth distribution from a base-line sinusoidal curve calculated for the entire distribution. Multiple peaks in the data therefore require the fitting of multiple sinusoidal curves. Therefore, this

technique would not be suitable for the complex multi-modal data identified in this study as overlapping normal distributions would not be separated.

In conclusion, both the Wise *et al.* (1985) and Conradsen *et al.* (1986) methods for the identification of lineament directional families require a degree of smoothing of the frequency/azimuth data beyond that already imposed on the data by using a fixed bin-range in the analysis. In a poly-deformed terrain such as SW England it was considered that this may result in the removal of geological significant peaks emanating from unequal mixing of two normally distributed lineament subsets. Hence, it was considered that each of these techniques may underestimate the actual number of lineament families present in the total lineament population. Furthermore, the technique of Wise *et al.* (1985) require identification of normally distributed components in the frequency/azimuth curve and these have been shown to be difficult to identify (Fig. 6.4). Consequently, a technique is needed which does not require smoothing of the data or relies on identifying normal distributions in the data. A further requirement is that the technique must be able to cope with complex multi-modal distributions and ignore sharp anomalous peaks found to be present within the data (see Section 3.11).

6.4 Cluster analysis

6.4.1 Introduction

Anderberg (1973) suggests that a cluster algorithm can assemble data with measurable degrees of similarity into groups which prior misconceptions and ignorance might otherwise preclude. Therefore, measured similarities (usually multi-variate) are high among members of the same group but are low among members of different groups. Hence, a cluster analysis of the lineament data obtained from SW England might group data on the basis of similar azimuth,

length, degree of cross-cutting lineaments and proximity to other lineaments. Although all of the measurable properties of the lineaments could be used to determine clusters it was decided to cluster the data by only measuring the similarity of lineament azimuth as:

(i) lineament patterns can be similar from different lithotectonic origins (see Section 4.4);

(ii) lineament length for many lineaments is dependant on the spacing of cross-cutting lithotectonic features (Section 4.4);

and (iii) the number of cross-cutting lineaments and lineament proximity would be difficult to automatically measure in ARC/INFO.

Clustering procedures group data by measuring either the distances between or the absolute values of differences, or the similarity of cases and clusters. The difference between the two measurements are that similarity measures values between 0 and 1, distance measures any positive value. Therefore a distance measure was used in the cluster analysis of lineament orientation. The method of cluster analysis can also effect the order (or step) at which each case or cluster is combined. Since the exact type of cluster analysis used could change the lineament directional boundaries obtained, agglomerative hierarchical clustering techniques and a non-hierarchical method were considered and the results evaluated.

Typically cluster analysis is applied to high numbers of multi-variate data. Cluster analysis of the single-variant lineament orientation to obtain lineament directional families therefore may be argued to be an inappropriate use of the technique. However, the inter-lineament orientation distance values are the same as a distance matrix (a matrix formed from the inter-individual distances in the raw

data) formed by multi-variate cluster analysis. Therefore cluster analysis was considered to be suitable for the analysis of the inter-individual distances of lineament orientation.

Using the statistical software SPSS for Windows (Release 5.0, 1992), two methods of cluster analysis were considered for the grouping of lineament orientation, hierarchical agglomerative and iterative-partitioning. Both of these methods separate the lineament orientation data into larger groups in a series of steps (agglomerations) initially from cases (single bits of data) into broader clusters, until finally no further divisions need to be achieved (forming groups or final clusters). The main difference between the two techniques is that unlike the hierarchical agglomerative methods, the iterative-partitioning method can reassign a case to another class after the case has already been provisionally assigned to a class.

6.4.2 Cluster processing using hierarchical methods

During hierarchical agglomerative clustering clusters of data are formed by grouping individual cases into progressively fewer and larger clusters. Initially, therefore, all cases (individual data points) are treated as separate clusters. The first stage of the process involves grouping the two most similar cases together, forming a cluster. Subsequently, either a third case is assigned to this cluster or a new cluster is formed from two other cases. Existing clusters or cases are combined progressively in this way until a single cluster is formed. Consequently, once formed, clusters may not be split at later stages in the process.

Which cases are grouped into clusters, or which clusters are grouped into larger clusters, is determined by the measure of distance. The squared Euclidean

distance measures the distance between two items, X and Y, as the sum of the squared differences between the values for the items:

$$\text{Distance } (X,Y) = \sum_i (X_i - Y_i)^2 \quad (\text{equ. 6.1})$$

The value of using this distance measure is that the differences between values are weighted and hence may readily differentiate between closely spaced clusters.

Two clustering methods were tested: the centroid and median methods. The centroid method calculates the inter-cluster distances as the distance between the means of all the variables (in this study, the means of the lineament orientation) of two combined clusters. Hence, groups with the smallest differences between their centroids or cases are joined first. This method can, however, introduce a bias in the placing of a new centroid, since when two clusters (A and B) are dissimilar in size ($A > B$), the combined cluster (A+B) has a centroid weighted proportionally towards the largest cluster. The bias of each new centroid to the larger cluster is considered to be a disadvantage by Everitt (1980) since smaller valid clusters may be joined to larger clusters. Alternatively, the bias would potentially improve the cluster divisions in the data by attracting clusters to the larger and more significant concentrations. This is identified by comparison to a second clustering method, the median method. Identical in all facets except that any two clusters, when combined, are given equal weight.

6.4.3 Results of the hierarchical clustering methods

The viability of the clustering technique in distinguishing lineament directional families was tested using azimuths of lineaments identified from the 150m resolution lineament population of North Cornwall. This population was

selected for the pilot study because it contained the most simplistic frequency/azimuth distribution related to the geologically least complex sample. The absence of complex lineament patterns has allowed the relationship between different lineament trends and dissimilar lithotectonic features to be more accurately identified (summarised in Section 4.4, Chapter 5). Therefore, an evaluation of the clustering methods can be achieved by comparing identified lineament directional families from different clustering methods to known lithotectonic trends.

Dendograms are used to illustrate the order in which cluster were combined from each clustering method (Fig. 6.5). At each agglomeration, a cluster difference coefficient is calculated: the centroid cluster difference coefficient is calculated by averaging each of the clusters to be joined and squaring the difference; and the median method by the average between the averages of the two clusters to be joined (therefore equal weighting) and squaring the difference. These results are shown in Tables 6.1 and 6.2.

6.4.4 Discussion and interpretation

Small cluster distance coefficients suggest that similar clusters are being combined, while large coefficients suggest dissimilar clusters are being combined. The cluster distance coefficient can, therefore, be used to determine the optimum number of clusters present within the data. Initial agglomeration will combine similar clusters producing small increases in the cluster distance coefficient. A large increase therefore suggests that dissimilar clusters are being combined. At this point the agglomeration procedure should be stopped (SPSS Inc. 1988). The coefficient difference (expressed as a coefficient ratio) at each agglomeration step

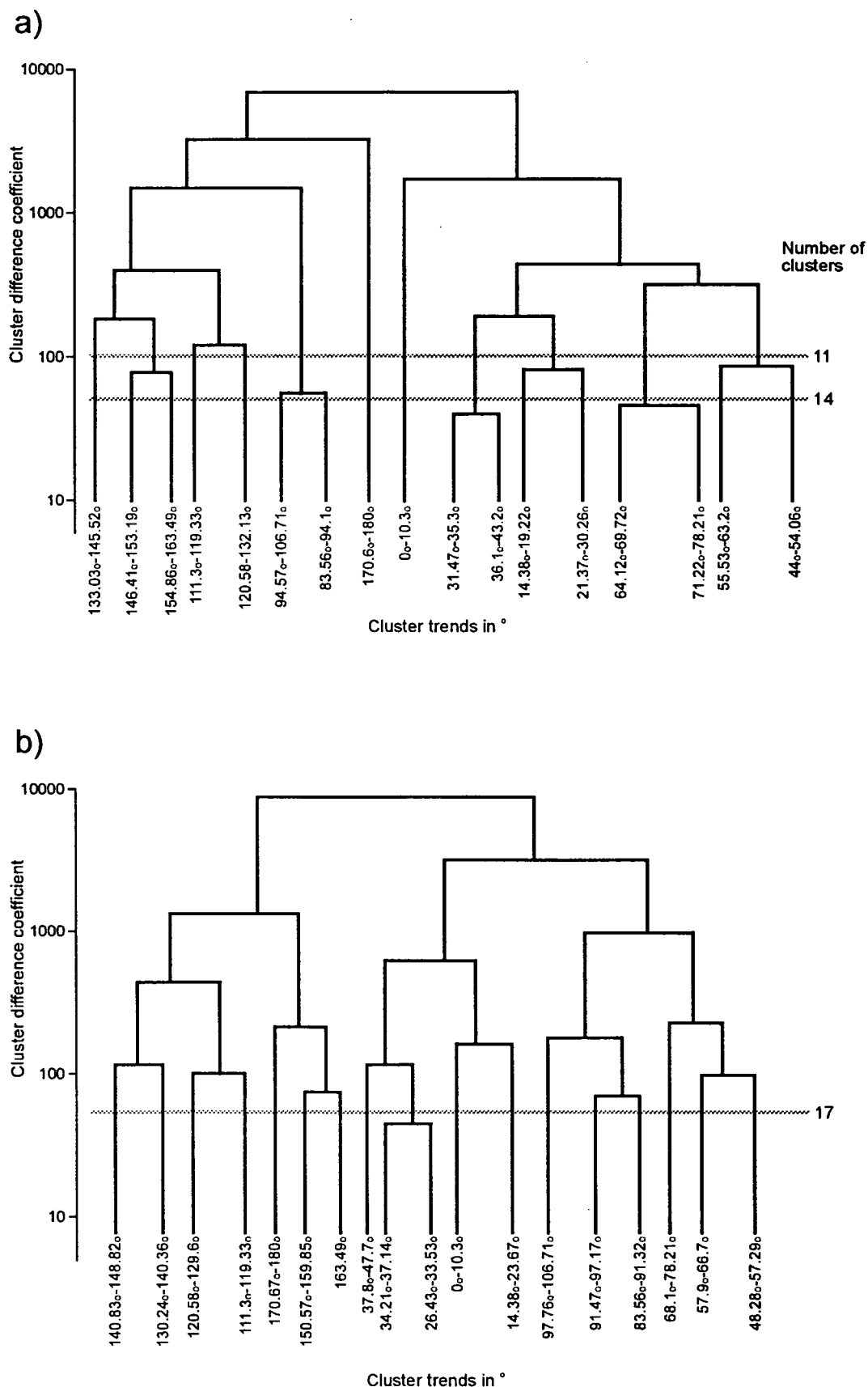


Fig. 6.5. Dendograms illustrating the fusion history of clusters in the later stages of a) centroid, and b) median hierarchical clustering of the 150m resolution lineament population of North Cornwall. Marked on in light grey are the cluster solutions suggested by large jumps in the cluster difference coefficient ratio.

is shown in Tables 6.1 and 6.2, for the centroid and median methods, respectively.

Agglomeration stage	Number of clusters	Cluster difference coefficient	Coefficient ratio
446	2	6946.14	2.13
445	3	3252.2	1.83
444	4	1774.28	1.20
443	5	1476	3.36
442	6	439.37	1.11
441	7	395.58	1.26
440	8	313.03	1.62
439	9	192.73	1.06
438	10	182.36	1.49
437	11	122.27	1.41
436	12	86.87	1.05
435	13	82.88	1.06
434	14	78.35	1.38
433	15	56.74	1.23
432	16	46.3	1.15
431	17	40.23	1.05
430	18	38.2	

Table 6.1. Cluster difference coefficients (expressed as a ratio) obtained from the hierarchical centroid cluster analysis of the lineament population interpreted from 150m resolution images of North Cornwall.

Agglomeration stage	Number of clusters	Cluster difference coefficient	Coefficient ratio
446	2	8984.2	2.84
445	3	3158.08	2.37
444	4	1332.4	1.38
443	5	966.82	1.56
442	6	619.615	1.42
441	7	435.75	1.92
440	8	227.28	1.08
439	9	211.4	1.17
438	10	180.9	1.11
437	11	162.31	1.41
436	12	115.2	1.06
435	13	108.2	1.08
434	14	100.15	1.02
433	15	98.14	1.32
432	16	74.32	1.07
431	17	69.63	1.55
430	18	44.78	1.14
429	19	39.25	

Table 6.2. Cluster difference coefficients (expressed as a ratio) obtained from the hierarchical median cluster analysis of the lineament population interpreted from 150m resolution images of North Cornwall.

Using an increase in cluster ratio of ~ 1.4 as an arbitrary value for stopping the agglomeration of clusters the clustering process may be stopped after stage 433, or 437 for the centroid method and after stage 430 for the median method.

The cluster distributions produced by the centroid and median methods at the stages identified above are illustrated in Fig. 6.6. The number of clusters is effectively one less than identified during agglomeration stages as the cluster concentration centred from $0/180^\circ$ is divided in the analyses. Therefore, for the 150m lineament population of North Cornwall the centroid method suggests that there are either 13 or 10 lineament directional families and the median method suggests there are 16 directional families. To identify which division of data is the most geological realistic the clusters are compared to the lineament frequency/azimuth distribution of the 150m resolution lineament population. In this study a poor division of the data was considered to have occurred if:

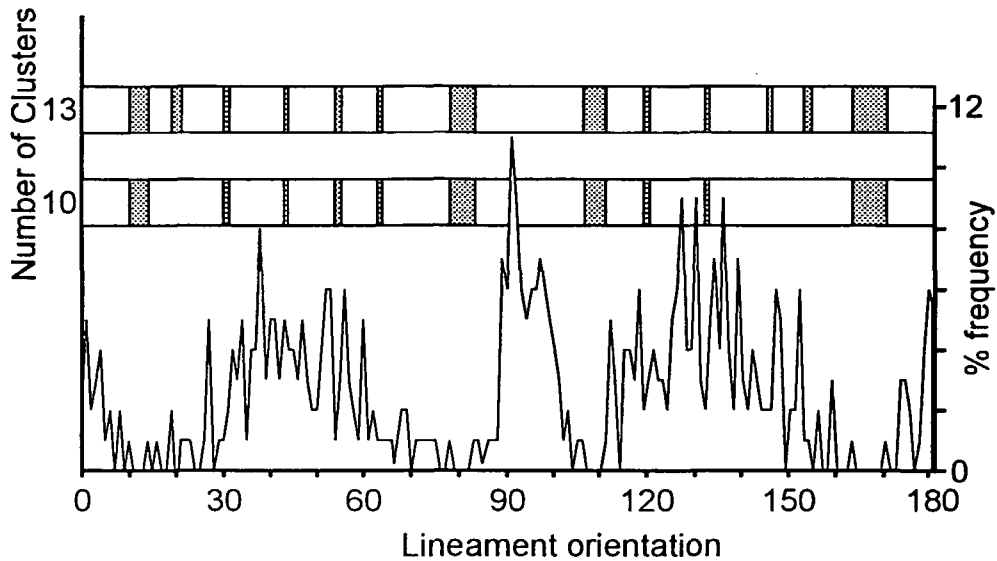
- (i) the E/W peak in the lineament frequency/azimuth distribution of the 150m resolution lineament population is divided as this peak is considered to be formed dominantly by similarly trending lithotectonic features (Chapter 5);

- (ii) the high concentrations of lineaments in the frequency/azimuth distributions are divided by the cluster analysis, such concentrations can be found between 050° and 063° ;

- and (iii) the anomalous sharp peaks and troughs identified in Section 3.11 repeatedly form boundaries to the clusters.

Cluster divisions at the anomalous troughs along azimuths 045° and 135° are not considered to be an artificial division when the larger anomalies which trend to 090° and $0/180^\circ$ are not divided, because cluster analysis will identify the

a)



b)

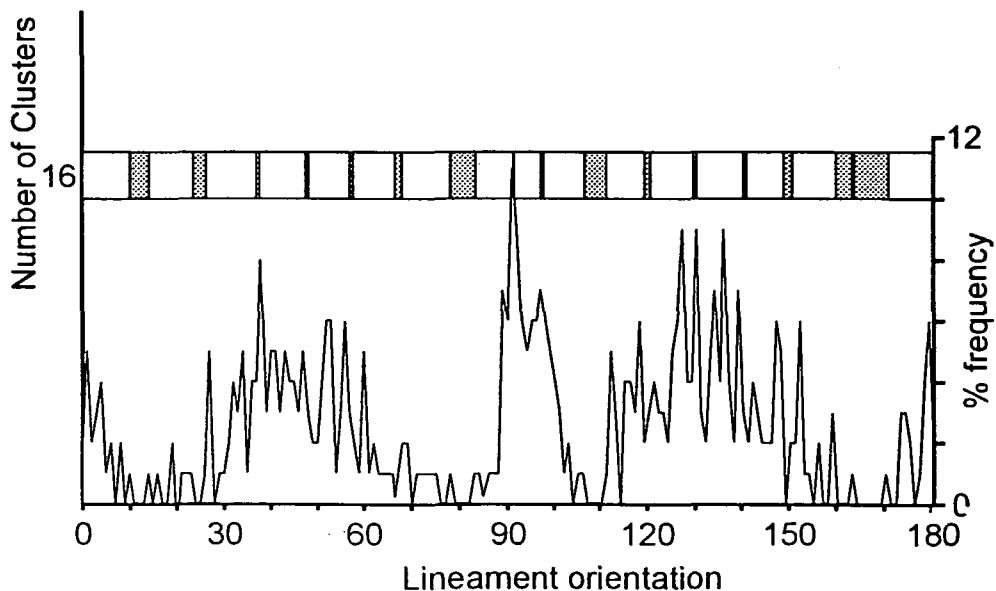


Fig. 6.6. These diagrams show the trends of suggested lineament families identified by the a) centroid and b) median agglomerative hierarchical clustering methods from lineaments of the 150m resolution lineament population of North Cornwall. The white zones within the bar charts shows the trends of identified clusters which are placed above lineament frequency/azimuth line graphs of the lineament population.

largest inter-cluster distances first. Therefore, it is likely in these cases that the smaller anomalous troughs possess the same trend as a minima in the data related to either the boundaries of a lineament directional family, or overlapping lineament directional families. Closely spaced clusters are also considered not to be indicative of a poor division of data as these distributions may relate to overlapping lineament directional families.

Initial visual analysis of the obtained solution from the median method indicates that this method has overdivided the data forming a poor visual match; as the E/W major lineament trend has been divided into 3 clusters, and that single frequency/azimuth concentrations have been divided into 2 clusters (e.g. between 050° and 063° at 54°). The centroid method produced a better visual match; the E/W lineament trend was not divided. However, in both solutions the lineament concentration between 050° and 063° was divided at 54° . Furthermore the 10 cluster solution may have oversimplified the data between the lineament trends of 132° and 153° .

From these results the visual analysis of the cluster solutions has shown that although the best method for cluster analysis of lineament trends to identify lineament directional families is probably the centroid method, the obtained solutions were found to poorly match the expected lineament directional family distributions. This may be because the hierarchical methods make only one pass through the data and consequently a poor initial partition cannot be revised in later steps of the process (Everitt 1980). Furthermore, the agglomerative hierarchical method requires significant amounts of computing processing and base memory for large data sets. Above 450 bits of data the hierarchical cluster analysis programme rapidly exceeded available computing facilities. Therefore agglomerative hierarchical cluster analysis could not be used to identify lineament

directional families for the majority of lineament populations in this study. These results, however, suggest that clustering by the centroid method may produce a good division of data if the clustering technique used can: (i) correct a poor initial partition; and (ii) has the ability to process very large data sets (up to 6482 for the lineament population of SW England).

6.4.5 Cluster processing using an iterative partitioning method

Iterative partitioning methods separate data into a number of user specified clusters, or k clusters. The iterative partitioning method used to divide lineament orientation into lineament directional families is the k -means clustering method (SPSS Inc. 1990). To obtain k clusters the data is initially partitioned into k temporary cluster centres, achieved by a serial partition of the first k cases (MacQueen 1967). To these initial k temporary cluster centres further cases are processed by nearest centroid sorting (Anderberg 1973), using the distance measure of squared Euclidean distance.

Depending on the lineament orientations of the first k data points a final cluster or lineament directional family may be over-divided if there is a bias in the k data points to this cluster. Therefore, the lineament orientation data is randomised before clustering. However, poor and good separations of data were obtained as biases still occurred in the randomised initial k data points. To obtain a good solution the analysis was repeated on differently randomised data sets. To distinguish between poor and good separations the results are tested by a descriptive ratio of the between-cluster mean square (the mean of the squared differences in distances between cluster centres) and the within-cluster mean square (the mean of the squared differences in distances between cases within a

cluster). Large ratios are associated with a good separation of clusters. The best divisions were found to contain these values and hence the randomised data which formed the largest ratios were selected for the final cluster solution.

To obtain a final cluster solution the *k*-means cluster analysis uses nearest centroid sorting (Anderberg 1973) to iteratively converge the temporary cluster centres to the concentrations in the lineament frequency/azimuth distributions. This migration of the cluster centres is accomplished by:

(i) Step one. Addition of new cases are assigned to the nearest temporary cluster centres, revised cluster centres are then calculated from the mean of each cluster (Fig. 6.7). This process continues until the all data has been added.

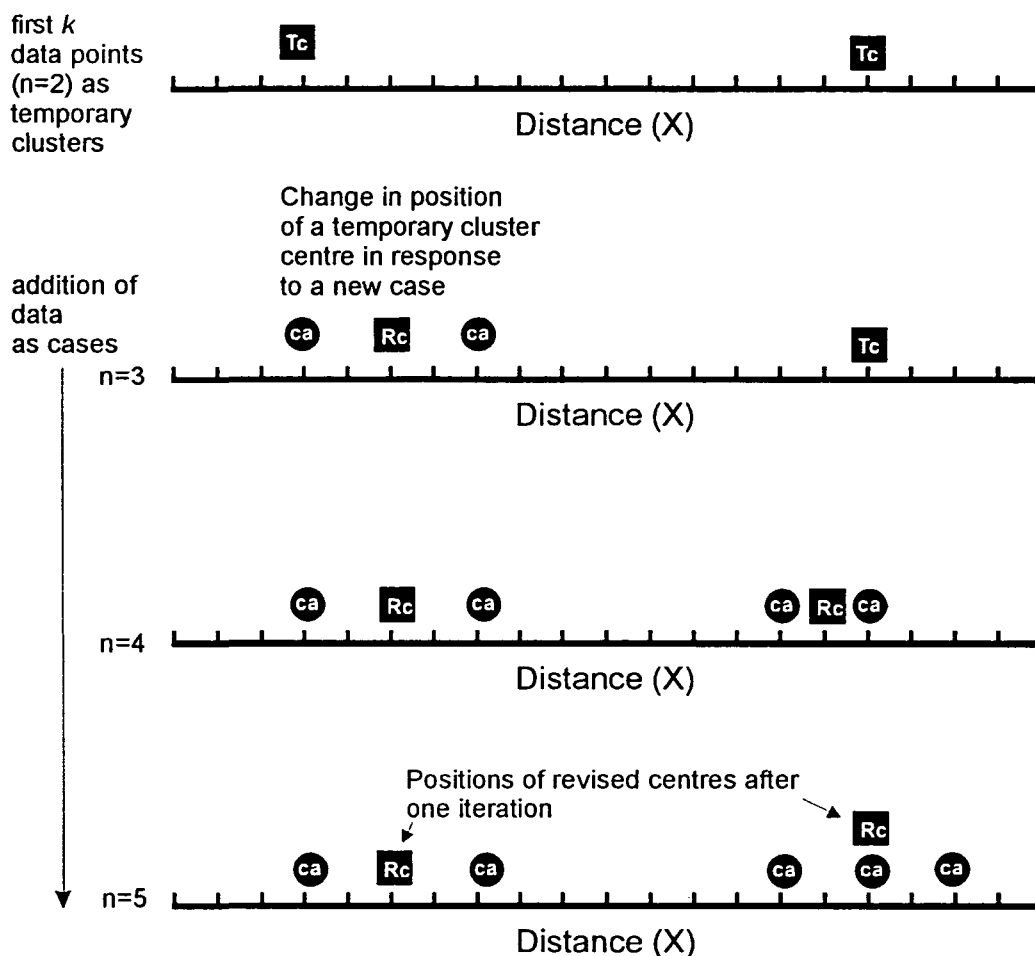
(ii) Step two. Step one is repeated with the last revised temporary cluster values if the change in distance of the last revised cluster centres is greater than the set minimum distance (Fig. 6.7) (in this study the minimum distance was set at 0.01). When the minimum distance is less than the set value the temporary cluster centres become the final cluster centres.

(iii) Step three. The data is reassigned to the closest final cluster centres.

6.4.6 Results of the *k*-means clustering method

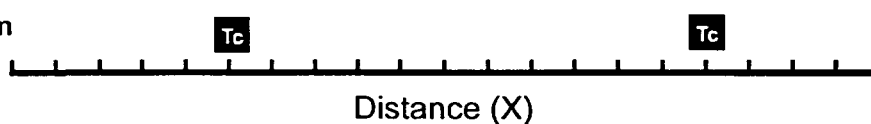
The *k*-means clustering method was initially tested on the azimuths of the 150m resolution lineament population of North Cornwall for the same reasons as suggested in Section 6.4.4. The best cluster solution for *k* clusters is identified by a descriptive ratio. However, the number of clusters in a solution is dependent on the initial choice of *k*. Unlike the hierarchical clustering methods a descriptive ratio cannot be used to determine the number of clusters which forms the

1st Iteration



As the distance moved by the revised centres relative to the initial temporary cluster centres is greater than the analyst specified minimum value the process is repeated with the final revised centres as the initial temporary cluster centres.

2nd iteration



Tc=temporary clusters
Rc=revised centres
ca=cases

Fig. 6.7. Schematic diagram describing the procedure used by the iterative k -means cluster analysis to identify final cluster centres.

best separation of data. This is because the randomised data necessary for the best separation of data in the *k*-means method for the solution at different numbers of clusters result in changes in the descriptive ratios for each *k* cluster solution.

Techniques which can test the significance of the *k* clusters present (e.g. Beale 1969, Wolfe 1970) have been discussed by Everitt (1980), and who concludes that no satisfactory test has been identified. Therefore for the 150m resolution lineament population a range of *k* (9, 10, 11 and 13) cluster solutions was obtained (Fig. 6.8).

6.4.7 Discussion and interpretation

A range of cluster solutions were identified for the 150m resolution lineament population of North Cornwall, and visual assessment was used to determine the most suitable number of clusters for each solution. The visual assessment was based on the hypothesis that cluster boundaries were compared to the concentrations of data in lineament frequency/azimuth distributions (see Section 6.4.3), identical to the method used in the hierarchical clustering process.

Initial analysis of the 13 and 11 cluster solutions suggests that these solutions have overdivided the data, forming a poor visual match; as the E/W and N/S major lineament trends have been divided into 2 clusters. Furthermore, the 9 cluster solution may have oversimplified the data between the lineament trends of 125° and 164°. The 10 cluster solution produced a better visual match: the E/W lineament trend was not divided; and the boundaries of the cluster solutions correspond to major minima in the frequency/azimuth distribution.

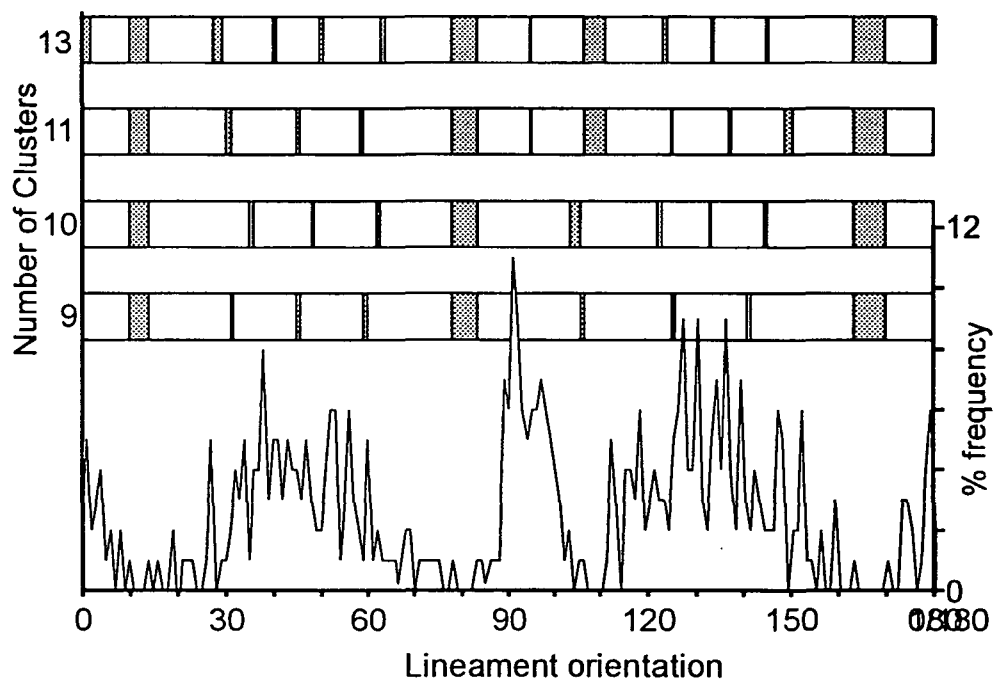


Fig. 6.8. This diagram shows the distribution of lineament families suggested by the *k*-means cluster procedure using the nearest centroid sorting technique. The distributions which are indicated by the bar charts are for 9, 10, 11 and 13 cluster solutions.

6.4.8 Application of k-means clustering to other lineament populations

The cluster solutions for lineament populations identified from images of North Cornwall and SW England are shown in Fig. 6.9. As discussed previously, solutions have been identified from a range of cluster numbers. Lineament populations of North Cornwall were interpreted to have 12, 13, 20 and 22 clusters for resolutions of 120m, 90m, 60m and 30m, respectively, and for lineaments from images of SW England a solution containing 26 clusters has been obtained. Therefore, for the lineament populations in this study, increasing the image resolution or area also increases the number of lineament directional families, leading to the interpretation of more lithotectonic features.

Cluster solutions for the 30m resolution lineament population of North Cornwall and the 150m lineament population of SW England contain cluster divisions corresponding to the sharp anomalous peaks caused by pixelated images (see Section 3.11). Cluster solutions which include divisions with these trends are considered to be inaccurate. However, with high image resolutions and images of large areas the frequency of lineaments increases, clearly defining in the lineament frequency/azimuth distributions more minor minima. Consequently in the frequency/azimuth distributions, the sharp anomalies produced by 'lineament dragging' (see Section 3.11) are more prominent. Hence, the *k*-means clustering process identified these anomalies as cluster boundaries. Thus, to obtain a meaningful solution, solutions with these cluster divisions were considered, however, the cluster boundaries relating to such anomalies were discounted.

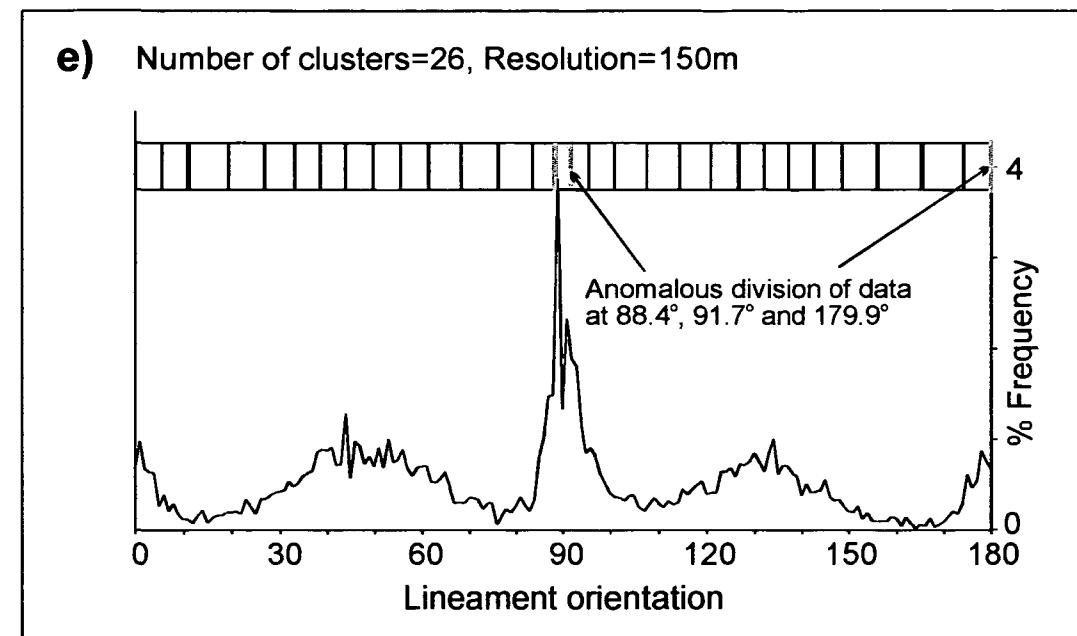
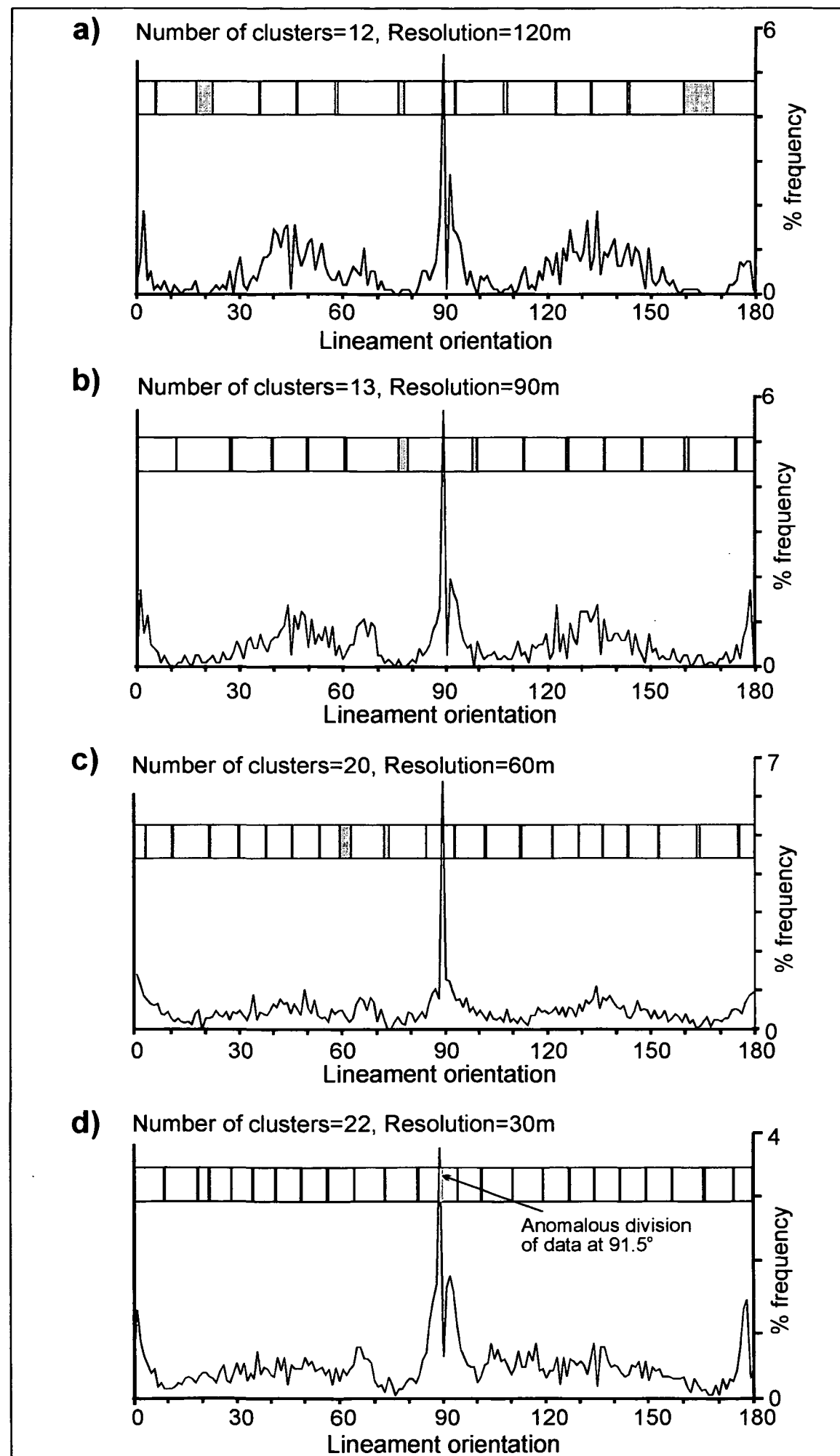


Fig. 6.9. Results from the division of lineament orientation by the *k*-means clustering process. Diagrams a), b), c) and d) are for lineaments interpreted from images of North Cornwall at pixel resolutions of 120m, 90m, 60m and 30m, respectively. Diagram e) is the result for lineaments interpreted from images of SW England, at pixel resolution of 150m. Above the frequency/azimuth graphs are white blocks which show the obtained cluster divisions. Grey lines within a white block indicate where the clustering process has selected a division which correlates to localised anomalies in the data, caused by pixelated images.

6.5 Image resolution, image size and lineament directional families

6.5.1 Mixtures of lineament families

Increasing the image resolution and image size results in higher numbers of lineament directional families being identified. Analysis of distributions resulting from mixtures of known normal distributions can suggest that minima in the lineament frequency/azimuth curves can be formed by the overlapping of normally distributed lineament directional families (Figs. 6.3, 6.4). This probably occurs for all the lineament populations, however, with higher numbers of lineament directional families identified the likelihood that overlapping lineament families occurs increases. Analysis of such overlapping lineament directional families (e.g. density maps) therefore may show a geological characteristic of neighbouring lineament directional families, and this characteristic could increase with increasing image resolution and area.

6.5.2 Resolution

With increasing resolution linear geological features are visible across the resolution range and hence would form *continuous* clusters. However, smaller scale linear geological features can become visible within the images (Chapters 3 and 5), conversely lineaments with particular trends (such as NW/SE trending lineaments caused by faults) can become less distinct (Chapter 5). Therefore clusters representing changing geological features may also change with increasing image resolution (Fig. 6.10):

(i) Developing clusters occur along trends where previously no lineaments were identified at lower resolutions. Developing clusters occur in the 90m resolution data at 170° and in the 60m resolution data at 78° (Fig. 6.11a).

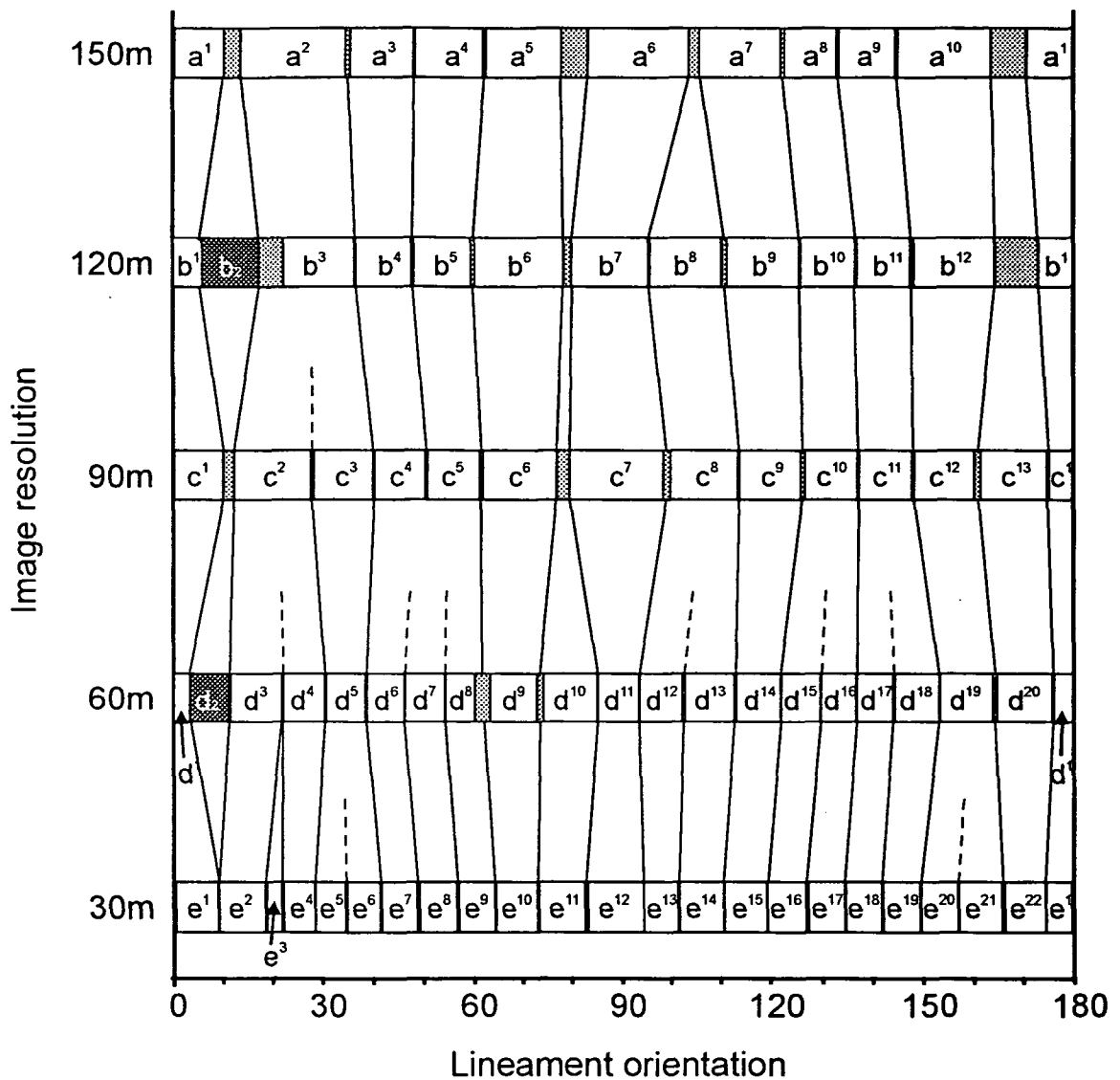
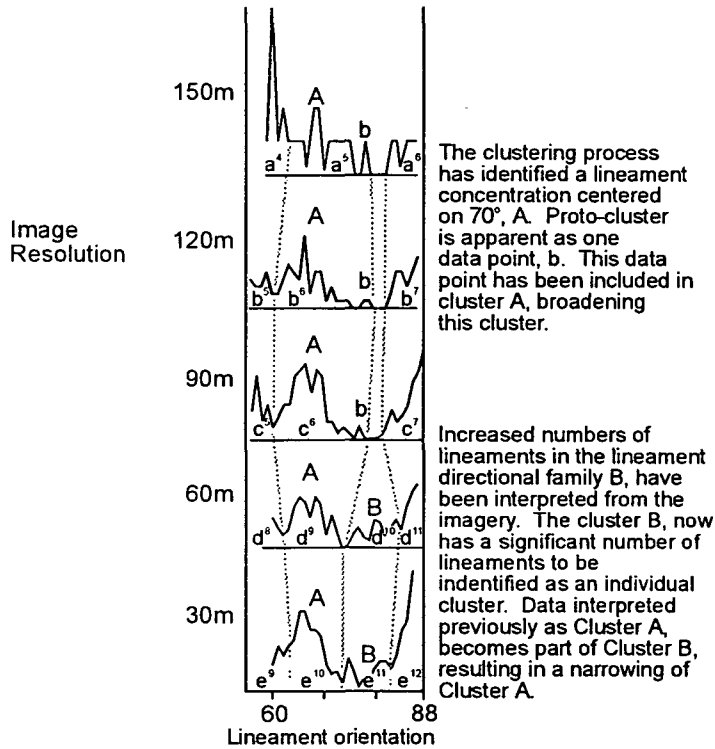


Fig. 6.10. Distribution of clusters, correlating to high concentrations of lineaments, which were interpreted from imagery with a pixel resolution range of 150m to 30m. The diagram shows the trends of clusters which are persistently identified throughout the pixel range (solid lines), and clusters which diverge with increasing pixel resolution (hashed lines). Clusters which are anomalous compared to corresponding trends observed at all resolutions, are shown as dark grey squares. Light grey squares correlate to azimuth ranges within the datasets which are devoid of lineaments.

a)



b)

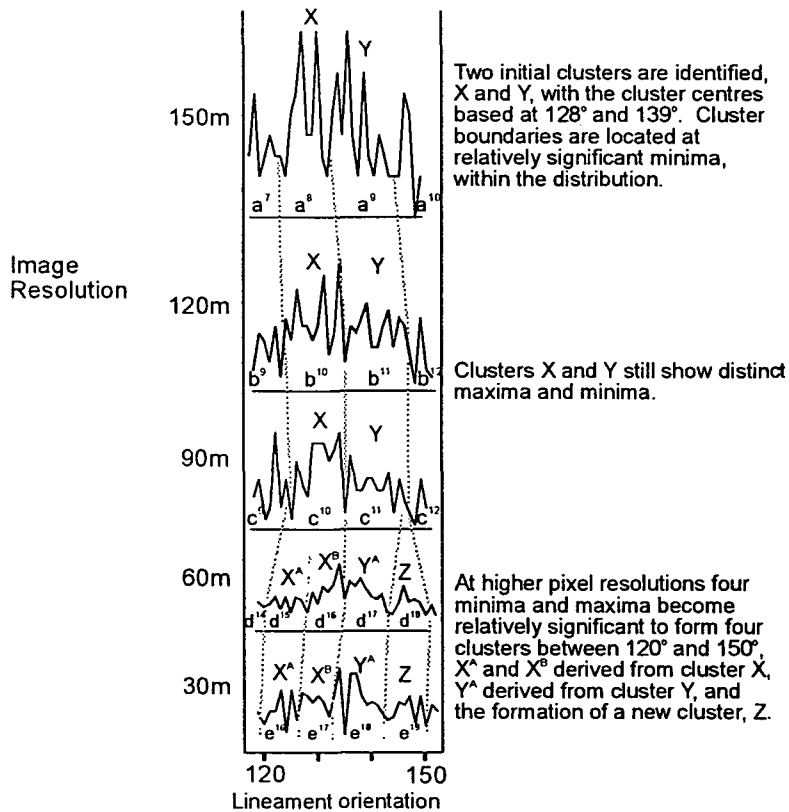


Fig. 6.11. Depicted are relationships of how clusters distributions evolve with increasing pixel resolution. Sequence a) shows the formation of a cluster (B), as greater numbers of lineaments form a significant concentration of data. The series of line graphs in sequence b) show a 'parent' cluster forming two sub-clusters when relative maxima and minima within the data become more significant. Each cluster is labelled in accordance with the lineament directional families in Fig. 6.10.

These clusters occur as small, scale limited, lithotectonic features fall within the observation threshold of the higher resolution images.

(ii) Dividing clusters are continuous clusters which at a higher image resolution becomes identified as two or more individual clusters (Fig 6.11b). The identification of the two clusters occurs when the relative magnitudes of the normal distributions of the lineament directional family increase to form two distinct maxima. This can occur by the formation of a developing cluster whose distribution overlaps an initial continuous cluster, so that two maxima appear with increasing resolution. Alternatively, two independent clusters may have been interpreted as a continuous cluster at low resolutions. At low image resolutions irregularity of the frequency/azimuth distribution is greater. Hence, overlapping data produces complex patterns in which distinct maxima and minima are often absent. With higher resolution images the number of lineaments identified increases, smoothing the data producing more distinct maxima and minima.

(iii) Absent clusters, clusters which are missing from lineament populations interpreted over the resolution range. Two clusters located between 3° to 17° (b^2) and 2° to 11° (d^2) for the cluster solutions for 120m and 60m, respectively, show a poor correlation to the directional trends of clusters of data in the 150m, 90m and 60m solutions (Fig 6.10). The magnitude of these anomalous clusters is relatively small compared to the neighbouring cluster centred at $000^\circ/180^\circ$ (Fig. 6.11b). Overlapping of normal distributions of this type where relative magnitudes are markedly different and the mean of the normal distribution are close, results in the maxima of the smaller normal distribution being reduced (Figs 6.4a, b). Therefore absent clusters in the data obtained from images with 150m, 90m and 30m resolutions are interpreted to be an effect of masking by the closely overlapping, relatively larger magnitude clusters of data. A small increase in distance between

the means of the normal distributions results in the identification of the large magnitude cluster and the small magnitude cluster (Figs. 6.4c, d). The *k*-means cluster analysis therefore may not separate concentrations of lineament orientations if the mean concentrations (centroids) of clusters are close and the relative magnitudes are different.

6.6 Number of clusters

Several solutions, each with different number of clusters, can be obtained from the cluster analysis of the lineament data. Changing the number of clusters will, however, increase or decrease the number of lineaments identified in each individual lineament directional family. A suitable method for determining the accuracy of each solution has not been determined, and thus the final selection is subjective (see Section 6.4.6). By analysing known geological distributions and comparing to the cluster solutions, some insight into the validity of each cluster solution may be gained.

From low resolution images (e.g. 150m) of North Cornwall, three lineament directional families were obtained trending between 122° and 163°. These lineament directional families have a range in trends of 10°, 11°, and 20°. Late Variscan, dextral strike-slip faults trend between 120° and 160° in North Cornwall and regionally across SW England (e.g. Dearman 1963, Mapeo 1992). It is possible that these divisions are therefore accurate, being formed by different episodes of faulting within a similar stress regime.

With higher resolutions the number of clusters between the trends of 120° and 160° increases because minima and maxima within the frequency/azimuth distributions become relatively more distinct. The higher number of clusters identified causes a fall in the size of the cluster directional range as the lineament

directional families overlap (see Section 6.5.1). Cluster ranges in the 30m lineament population typically falls to 8° , with a maximum of 10° . In North Cornwall, Mapeo (1992) also describes sets of normal and reverse faults within the broad NW/SE structural trend. The higher frequencies of clusters therefore can be explained that with increasing resolution, minor fault populations may begin to fall within the observation threshold of the image or that the data are over-divided.

Increasing the image area also results in an increase in the number of lineament directional families identified; 10, 12, 13, 20 and 22 lineament directional families for the lineament populations interpreted from 150m, 120m, 90m, 60m and 30m resolution images, respectively. Analysis of the basic lineament statistics suggest that the geological information in the lineament populations increased between 150m and 120m, a small rise from 120m to 90m, and a large increase from 90m to 30m (see Section 3.10). The obtained number of lineament directional families suggesting the degree of geological information (increasing number of lineament directional families indicate a higher degree of geological information) interpreted, correlate to these statistical observations. Therefore, the identified number of clusters may approximately be accurate.

The number of lineament directional families identified for the lineament population of SW England is 26, a high number in comparison to 10 lineament directional families obtained from the equivalent resolution lineament population of North Cornwall. In this case, higher numbers of lineament directional families can be explained by the larger area covering different lithotectonic features with distinct trends or that again the data are over-divided.

6.7 Discussion

It has been shown in this study of separating lineament populations into lineament directional families by lineament orientation that the iterative *k*-means cluster analysis identified the most geological realistic division. Although the technique occasionally is not able to separate concentrations of data which are closely spaced and have different magnitudes. The determination of the number clusters in a solution by this method, however, is subjective but can be explained in geological terms (Section 6.6). Hierarchical cluster methods use a cluster difference coefficient to indicate when the clustering process should be completed. In comparison to the median method, the centroid method was found when using the hierarchical clustering technique to produce the most geologically realistic cluster solution. SPSS Inc. (1988) suggests that such hierarchical clustering techniques, using the cluster difference coefficient, can indicate the number of clusters to be identified by the *k*-means cluster analysis (e.g. identical number of clusters were identified by the centroid sorted hierarchical cluster analysis and the *k*-means cluster analysis for the 150m lineament population of North Cornwall). Hence, using the number of clusters identified by the centroid sorted hierarchical cluster analysis could remove the subjectivity from the *k*-means cluster analysis. Unfortunately, hierarchical cluster analysis programme rapidly exceeded available computing facilities to allow this method to analyse lineament populations other than the 150m resolution lineament population of North Cornwall. Recent advances in computing processing power, however, may allow such analysis to occur, therefore removing the subjectivity from *k*-means cluster analysis.

Increasing the image resolution or image area was found to increase the number of interpreted clusters. For the 30m resolution lineament population of

North Cornwall and the SW England lineament population, the very high numbers of identified clusters will probably result in overlapping lineament directional families. Hence, the lineament characteristics of the overlapping directional families will be mixed. To reduce the degree of overlapping a lower number of lineament directional families may need to be sampled from the images.

Therefore, for SW England this could be achieved by initially dividing the regional lineament population into sub-areas and hence smaller sample sizes, reducing the possibility of sampling large numbers of different lineament directional families. For the high resolution lineament populations of North Cornwall reducing the sample area would only affect very localised lineament directional families. From the analysis of lineament patterns of North Cornwall (Chapter 5) lineaments in the lineament directional families which form maxima and minima in the lineament azimuth/frequency distributions (e.g. ~NW/SE trending lineaments interpreted to relate to ~NW/SE trending faults) typically occur throughout the area.

A 'perfect' lineament directional family is considered to represent a group of related geological features formed during a single geological event. The identification of higher numbers of lineament directional families, therefore suggests that a wider range of geological features have become observable in the images. Consequently, the complexity of geological data interpreted from the images will be increased. This supports the previously held assertion that the complexity of the geology interpreted is linked to image resolution (Section 5.6).

6.8 Conclusions

(i) Hierarchical agglomerative clustering, using centroid and median sorting and the squared Euclidean distance measure, produced differing solutions(due to

the sorting technique). The most geological realistic solution was identified by the centroid method.

(ii) *k*-means clustering, using nearest centroid sorting produced more viable solutions. Advantages of *k*-means clustering over the tested hierarchical agglomerative clustering methods are the relative quickness and the greater amount of data the method is able to handle. However, the number of clusters identified is subjective.

(iii) The subjectivity in the *k*-means clustering technique can be removed by using the centroid sorting hierarchical cluster method to identify the initial number of clusters. Above 450 bits of data the hierarchical cluster analysis programme rapidly exceeded available computing facilities. This could change with increased computing power.

(iv) The number of lineament directional families identified by *k*-means cluster analysis increases with higher resolution images and greater image size. This indicates that higher image resolutions increase the visibility of smaller features, and that a larger image area will sample a greater variety of linear features if the bedrock geology is heterogeneous.

(v) High numbers of lineament directional families reduces the orientation range of the lineament directional families below the natural range expected for lithotectonic features, such as faults. This suggests that either the technique over-divides the lineament population or if a true reflection of the number of geological features was obtained, the lineament directional families increasingly overlap. Therefore the purity of each lineament directional family may decrease with increasing image resolution or image size, as more lineament directional families are identified.

(vi) The change in the number of lineament directional families in lineament populations from increasing image resolutions is caused by the continuous interpretation of lineament directional families or new lineament directional families. New lineament directional families can either divide from existing lineament directional families (dividing lineament directional families) or become apparent with increasing image resolution (developing lineament directional families).

Chapter 7 Geological analysis of lineament directional families in SW England

7.1 Introduction

The main aims of this Chapter are:

(i) To examine how the extent of individual lithotectonic domains within SW England may be resolved. As suggested in Section 4.4, dominant lineament trends can vary from one lithotectonic domain to another across SW England. These domains can be regional or localised in distribution and so far in this study the exact boundaries of each lithotectonic zone have not been identified. This is because lineaments do not always exhibit lineament patterns from which the geological cause can be identified. Thus, the delineation of lithotectonic zones based only on lineaments which display particular patterns in SW England may lead to a degree of subjectivity. Construction and analysis of regional density maps of lineament directional families (therefore based on lineament trend) may accurately resolve the extent of individual lithotectonic domains within SW England when areas of high lineament density are correlated with particular lineament patterns related to specific geological features.

(ii) To analyse the methods used to obtain, and examine the scaling relationships of, NW/SE trending lineaments (considered to relate mainly to faults) from North Cornwall and SW England. Over the last ten years, remotely sensed data, e.g. seismic surveying, has increasingly been used to sample and estimate the scaling relationships of fault populations (e.g. Fossen & Rornes 1996). Seismic profiles sample fault populations at a small map-scale and knowledge of scaling relationships allow predictions to be made about the fault population

below the limit of seismic resolution (typically 30m). To improve accuracy, remotely sensed samples are often combined with information about the fault populations gained at an outcrop-scale (e.g. Heffer & Bevan 1990, Yielding *et al.* 1992, Pickering *et al.* 1994). For sea-based, seismic interpreted, large scale fault datasets, information about the fault populations at an outcrop scale is typically obtained either by analysing well cores (Heffer & Bevan 1990, Yielding *et al.* 1992) or related land based outcrops (Pickering *et al.* 1994). The drawbacks of such datasets are that the information yielded may not be representative of the whole sample area. Similar procedures have not been attempted from satellite images where scale can easily be altered without necessarily re-sampling the field area. However, in SW England the effect of anthropogenic features within the images have been mitigated in this study by decreasing image resolution. Decreasing image resolution has the same effect as image map-scale on sampled fault populations since low resolution images (similar to small map-scale images) sample larger scale lithotectonic features. Therefore, by changing the pixel resolution comparison of power-law distributions of populations sampled at different map-scales can be made without changing the sampling technique. In order to be able to examine the effect of resolution on the scaling relationships of fault related lineament populations Landsat TM images of North Cornwall have been interpreted over a range of image resolutions (see Section 3.3.2). Furthermore, the successful identification of scaling relationships in lineaments related to faults means that an estimation of a lineament population in higher image resolutions can be achieved from lower resolution images. This circumvents the need to use high resolution images to sample small scale lithotectonic structures, consequently reducing the time taken for such an analysis.

To achieve these aims the lineament subsets need to contain lineaments related to a single type of lithotectonic feature, as different lithotectonic features may have dissimilar characteristics (different lineament patterns, lineament length, lineament spacing and spatial distribution). In Chapter 6 the lineament populations of SW England and North Cornwall have been divided into lineament directional families by *k*-means cluster analysis, based on similarity of lineament trends. Lineaments in each lineament directional family are ideally formed from a geologically 'pure' population (lineaments are related to the same type of lithotectonic feature). Under these circumstances the centre of the lineament directional family is centred on the peak trend of the lithotectonic features and the variance in lineament trend correlates to the natural variance in the trends of the lithotectonic features. Characteristics of length, spacing and density in closely neighbouring lineament directional families (families that have near similar trends), therefore, may be similar if the peak trend of the interpreted lithotectonic feature changes, for example, with time. Alternatively, such similarity could occur if the natural variance in the trends of different lithotectonic features overlap resulting in lineaments which possess similar trends being related to different lithotectonic features. Neighbouring lineament directional families interpreted from such populations will contain lineaments related to mixed lithotectonic features, referred to in this study as mixed lineaments. Dissimilar lineament characteristics, however, can be produced from different lithotectonic features with slight changes in trend.

Three approaches have been adopted to help identify whether the *k*-means iterative cluster analysis adequately identifies pure lineament directional families:

(i) The analysis of lineament patterns and characteristics between neighbouring lineament directional families (dissimilarity suggests different lithotectonic features and hence pure lineament directional families).

(ii) The analysis of the scaling relationships of lineaments related to NW/SE faults separated by different methods into lineament subsets with dissimilar azimuthal ranges to identify which produces evidence of mixed fault populations. Due to the periglacial head and vegetation coverage of SW England masking the direct geological interpretation of faults, lineaments related to faults were sampled from the lineament populations by: (a) using lineament patterns to allow a direct identification of lineaments related to the Sticklepath-Lustliegh fault zone; and (b) indirectly by identifying the lineament trends within the lineament patterns and using the separation methods of rose diagrams and lineament directional families to determine lineament subsets relating to NW/SE trending faults.

(iii) Analysing the scaling relationships of neighbouring lineament directional families which consist of lineaments related to NW/SE faults by combining the lineament directional families to reveal if they produce different scaling relationships which suggest mixed fault populations.

By using these results lineament density maps were compiled from neighbouring (*linked*) lineament directional families which were found to possess similar characteristics and individual lineament directional families which displayed unique characteristics. The possible causes of linked lineament directional families are investigated and their effect on the obtained density maps and their implications on scaling relationships are discussed.

The coverage of superficial deposits upon the bedrock in SW England makes estimation of fault displacement (the typical measure of scale from seismic

profiles) impossible from TM satellite images. Therefore, the successful sampling method (either by rose diagrams or *k*-means cluster analysis) was used to identify the effect of image resolution on the scaling relationships of other measures of fault scale identifiable from the TM images, namely lineament length and spacing.

7.2 Characteristics of lineament directional families identified from SW

England

The 26 lineament directional families identified from the lineament population of SW England by the *k*-means cluster analysis (Chapter 6) are illustrated in Fig. 7.1. The high number of almost contiguous lineament directional families increases the probability of overlap between neighbouring families (see Section 6.5.1) resulting in lineament mixtures. The lineament directional families identified from the overall lineament map of SW England have smaller azimuth ranges in comparison to those identified from equivalent (150m) resolution images of the North Cornwall sub-area. As the North Cornwall lineament data clearly represents a sub-set of the total lineament data from SW England, at least some lineament directional families would be expected to have similar azimuthal ranges. Increased overlapping of lineament directional families in the SW England lineament population (reflecting sampling of a heterogeneously distributed bed-rock geology) may explain such a reduction. Alternatively, it might be suggested that the lineament population has been over-divided (see Section 6.6). Therefore, the lineament characteristics of neighbouring lineament directional families are analysed to identify if they are similar and the causes of the similarity are geological.

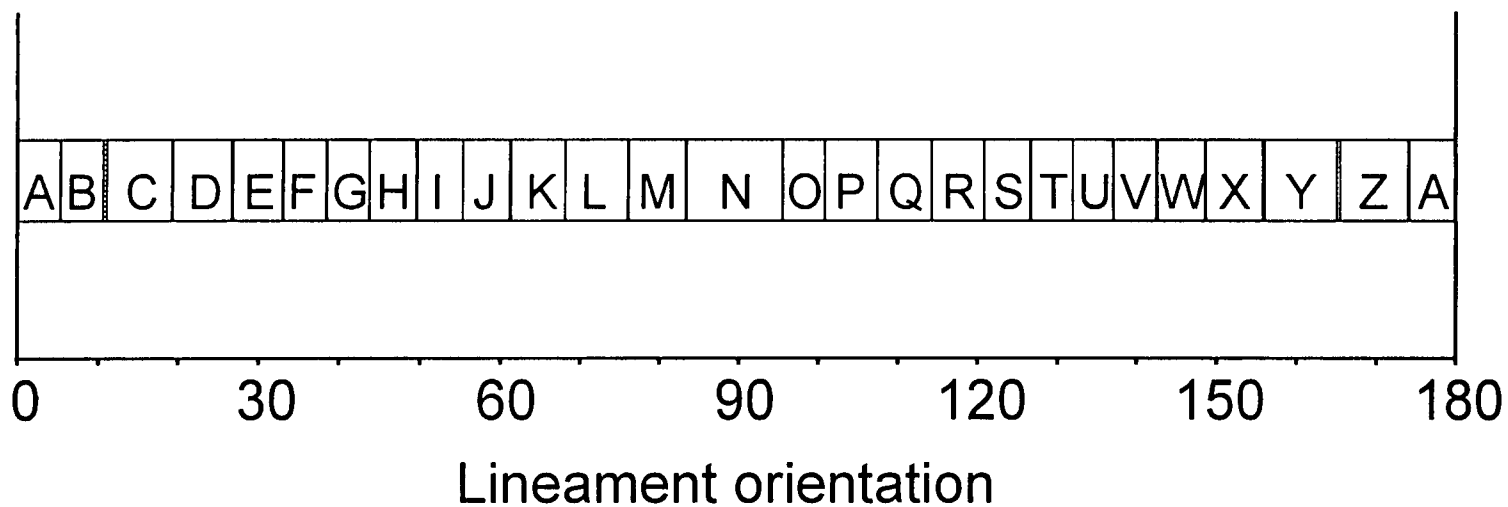


Fig. 7.1. Diagram showing the azimuth ranges of lineament directional families (represented as boxes) identified from SW England. Each lineament directional family has been labelled with a letter.

7.2.1 Analysis of characteristics of neighbouring lineament directional families

Preliminary visual analysis of lineament directional families with different trends identified from the regional population typically showed large spatial and lineament pattern differences. Such lineament directional families generally relate to dissimilar geological features (e.g. E/W lineaments relating to primary lithotectonic features and NW/SE lineaments relating to cross-cutting faults). However, some of the neighbouring lineament directional families were found to possess similar characteristics (similar spatial distributions and lineament patterns). To analyse if the causes of the similar lineament directional families is geological and not by over-division of the population the similar lineament characteristics of the neighbouring lineament directional families U, V and W and C, D and E are examined in greater detail (Fig. 7.1).

The lineament directional families U, V and W (Fig. 7.2) cover the azimuthal range from 132° to 148°. Lineaments within this azimuthal range express a lineament pattern characteristic of faults and are interpreted in Section 4.2.5(ii) to be predominantly related to the regionally distributed dextral strike-slip fault set. The lineaments have similar spatial distributions and possess good linearity (the trace of the geological feature formed by linking lineaments) between lineaments and low numbers of lineament intersections (cross-cutting lineaments suggesting different lithotectonic features). In localised areas of SW England, lineaments from each lineament directional family may cluster (Fig. 7.2), suggesting that these lineament directional families are linked. The dominant trend, however, varies locally. Faults are rarely uniformly linear, an example of such behaviour is the large variances in fault trend (Schreurs 1994) where 'Z' sigmoidal shaped antithetic cross-faults are formed within master bounding

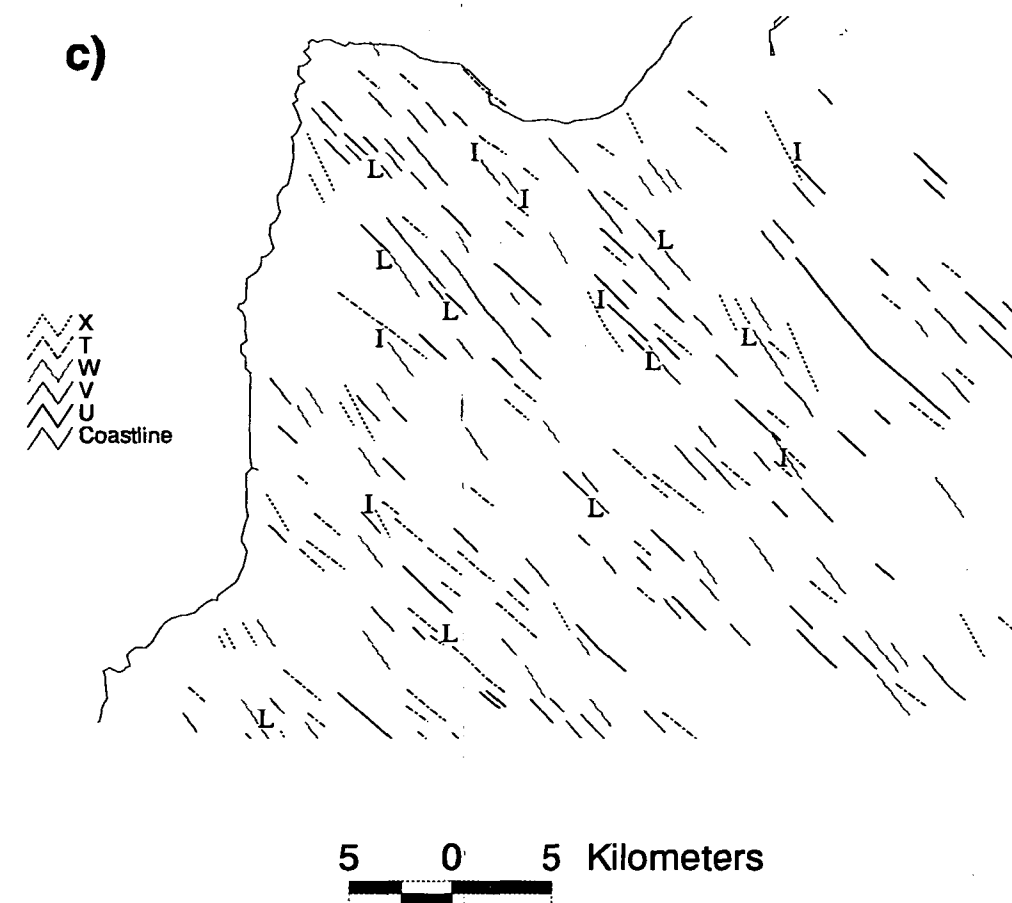
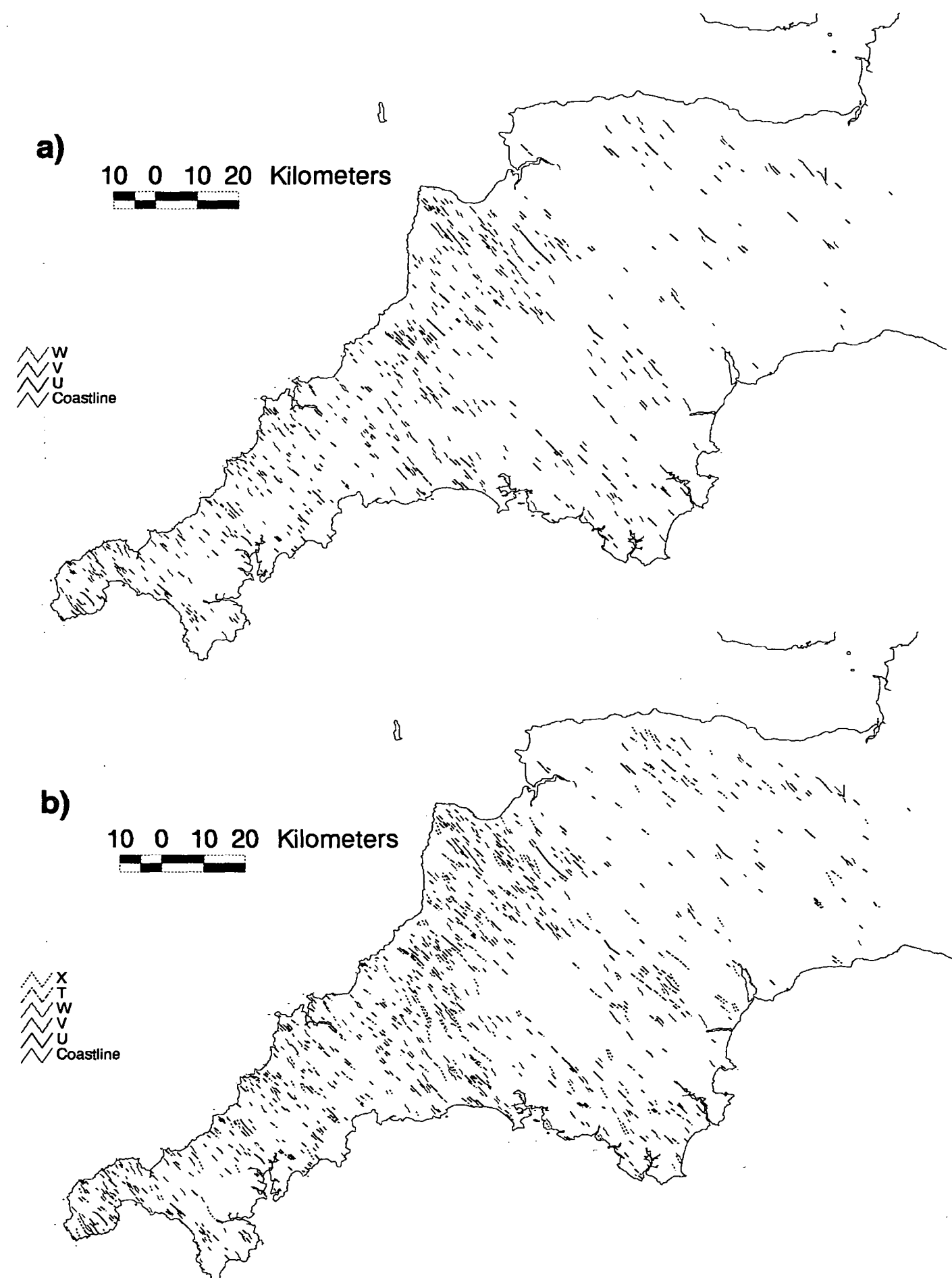


Fig. 7.2. Lineament maps of SW England comprising of lineaments which have been divided into the lineament directional families T, U, V, W and X. Map a) contains lineaments from the linked lineament directional families U, V and W, while map b) contains lineaments of the linked families U, V, W and X and un-linked families T and X. Map c) highlights the area of North Cornwall and shows lineaments which intersect (I) and possess linearity (L) with neighbouring lineament directional families.

faults (as suggested in Section 4.3.2(v) to have occurred within North Devon). Hence slight curvatures in such large faults and subtle changes in fault trend throughout the region may account for multiple lineament azimuth concentrations between 132° to 148°. Therefore, although a single geological cause was identified for NW/SE trending lineaments multiple directional families were identified.

The similarity of the spatial distributions of the lineament directional families C, D and E (Fig. 7.3a) suggest that these directional families may also be linked to a single, slightly variable, geological structure. However, the lineament patterns identified from these lineament directional families indicate the actual geological significance to be: (i) NNE/SSW trending lithological differences in East Devon and West Somerset (Section 4.3.2(i)); (ii) in Devon and East Cornwall fractures within the Dartmoor granite (see Section 4.2.5(ii)); and lithological differences and fractures in South Cornwall (Section 4.2.5(v)). Within each of these areas lineaments of the directional families C, D and E may contribute to the local lineament pattern. Minor changes in the main trends of the three lithotectonic features will result in multiple concentrations in lineament orientations correlating to the C, D and E lineament directional families. Therefore, different geological causes which possess overlapping lineament trends identified as multiple lineament directional families can also form linked lineament distributions.

These results therefore suggest that *k*-means cluster analysis has not over-divided the population, but linked lineament directional families correspond to peak concentrations in the frequency/azimuth distributions formed from overlapping lithotectonic features. Mixing of overlapping lineament directional families can be reduced by lowering the geological information sampled

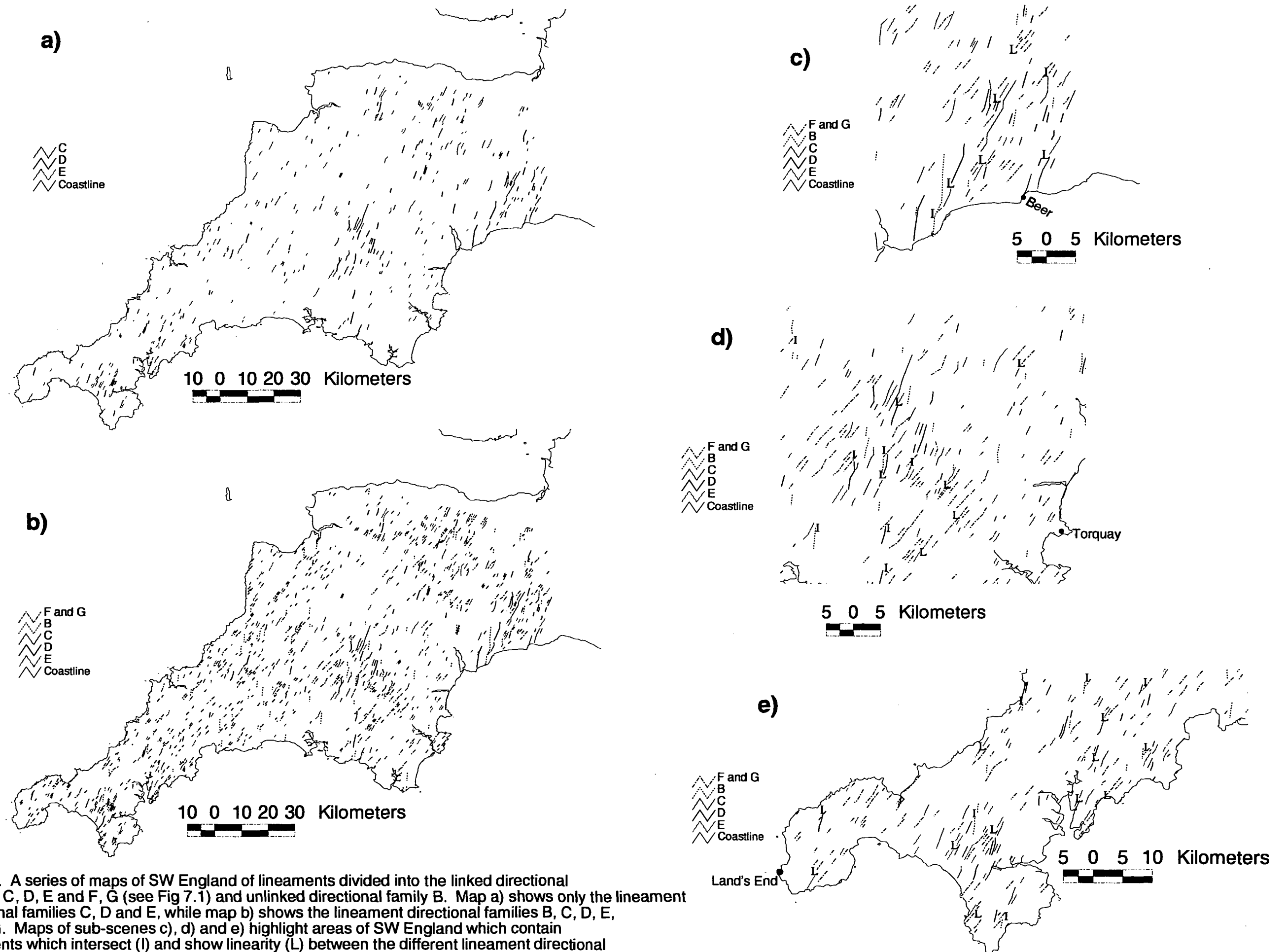


Fig. 7.3. A series of maps of SW England of lineaments divided into the linked directional families C, D, E and F, G (see Fig 7.1) and unlinked directional family B. Map a) shows only the lineament directional families C, D and E, while map b) shows the lineament directional families B, C, D, E, F and G. Maps of sub-scenes c), d) and e) highlight areas of SW England which contain lineaments which intersect (I) and show linearity (L) between the different lineament directional families.

from images. This could be achieved in two ways, either by reducing the image area (see Section 6.6) or interpreting smaller scale images. Alternatively, this could be avoided by relating each spatially different lineament concentration formed from linked or single lineament directional families to the lineament patterns identified in Chapter 4. Therefore, from such identified lineament concentrations the related lithotectonic features and their lithotectonic domains can be delineated.

To identify the number of linked lineament directional families the characteristics of all the lineament directional families were examined. Intersecting lineaments and dissimilar spatial characteristics (suggesting different geological causes) were used to determine un-linked lineament directional families. Addition of the neighbouring lineament directional families T and X to U, V and W, and B to C, D and E, produced higher numbers of intersecting lineaments and different spatial distributions, suggesting the neighbouring lineament directional families are un-linked (Figs. 7.2b, c, 7.3c, d, e). Furthermore, the lineament directional families T, X and B exhibit poor linearity with the neighbouring linked lineament directional families U, V, W and C, D, E, respectively. This again indicates the neighbouring lineament directional families T, X and B are un-linked to the families U, V, W and C, D, E, respectively (Figs. 7.2b, c, 7.3c, d, e). Further evidence can be found to determine linked lineament directional families by comparing two neighbouring linked lineament directional families, C, D and E to F and G. As illustrated in Fig. 7.3 the lineament directional family F shows characteristics more similar to G than E. The obtained linked and un-linked lineament directional families for the lineament population interpreted from images of SW England are shown in Table 7.1.

Lineament directional families	Relative estimation of the frequency of intersecting lineaments	Relative estimation of linearity between lineaments	Visual estimation of the spatial similarity of lineaments
B, C	Medium	Poor	Medium
C, D	Low	Good	Good
C, D, E	Low	Good	Good
E, F	High	Poor-Medium	Poor
F, G	Low	Good	Medium-Good
F, G, H	Low	Good	Poor-Good
H, I	Low	Good	Good
H, I, J	Medium	Medium-Good	Medium-Good
J, K	Low	Good	Good
J, K, L	Medium	Poor	Poor-Good
L, M	Low	Medium	Poor
M, N	Medium	Good	Good
N, O	Medium	Poor-Good	Poor
N, O, P	High	Medium	Poor
O, P	Very Low	Good	Good
O, P, Q	High	Poor	Medium
P, Q	Low	Medium	Medium
Q, R	Low	Medium	Medium
R, S	Very Low	Good	Good
R, S, T	Medium	Medium	Poor-Good
S, T	Low	Poor-Medium	Medium
T, U	Low	Medium	Poor
U, V	Low	Good	Good
U, V, W	Low	Good	Good
W, X	Low	Poor-Medium	Medium
X, Y	Low	Good	Good
Y, Z	Medium	Poor	Poor
Z, A	Low	Good	Good
A, B	Medium	Medium	Poor

Table 7.1. Results of the visual analysis on the number of lineament intersections, degree of linearity, and spatial similarity of combined lineament directional families. Combinations of lineament directional families which are suggested to be linked are highlighted.

7.3 Density maps of lineament directional families identified from SW

England

7.3.1 Construction of lineament density maps

Analysis of the densities of lineament length, frequency or intersections have been used to obtain information on either geological history (e.g. Sawatzky & Raines 1981) or fractures (Greenbaum 1985, Qari & Sen 1994, Mostafa & Qari 1995). To obtain information on the distribution of the major lithotectonic domains in SW England density maps of lineament frequency and total lineament length were compiled. Analysis of lineament intersections provides greater information on the density of connecting fractures (Mostafa & Qari 1995) and were not used because they will yield less information on lithotectonic domains. Individual density maps were constructed for single (non-linked) and linked directional families (Table 7.1) using the GIS ARC/INFO (Appendix 1). The area of SW England was initially divided by a computer generated grid consisting of 5km^2 cells. The compiled lineament maps of SW England were used to calculate lineament frequency and length per 5km^2 cell within the grid. A surface map for each variable was modelled by converting the data into triangulated irregular networks (TIN). Each TIN comprises a sheet of non-overlapping connected triangles based in this case on regularly spaced nodes, with x and y geographic co-ordinates and z values (z in this study represents lineament frequency or total lineament length per 5km^2). The TIN surface modelling technique was used as a surface map constructed by a series of triangles is sensitive to areas containing complex concentrations (Burrough 1986), and therefore considered to contain enough accuracy for this regional investigation. Each density map was normalised relative to the highest cell concentration obtained

from all maps of a particular type (frequency or length), using the programme ARC/VIEW.

7.3.2 Lineament density maps of SW England

The maximum density of lineament frequency was found to be $15/5\text{km}^2$ and lineament length $25\text{km}/5\text{km}^2$, in both cases relating to combined lineament directional families M and N. Maximum density values for several other lineament directional families were much lower (e.g. Fig. A2.13). To exaggerate the more subtle differences in the lineament densities of these directional families the contour intervals up to $8/5\text{km}^2$ (lineament frequency) and $12.48\text{km}/5\text{km}^2$ (lineament length) are reduced, in effect stretching the lower density lineament density maps. Surface modelling of the lineament density in the coastal regions of all lineament density maps display lower lineament density values since large portions of the 5km^2 cells contained the sea and were devoid of lineaments. This was accounted for in the interpretation of the lineament density maps.

To illustrate the value of this form of lineament analysis, the lineament density maps of linked lineament directional families M, N (Fig. 7.4) and U, V, W (Fig. 7.5) are discussed further. Lineament density maps constructed for the remaining lineament directional families identified from SW England are within Appendix 2.

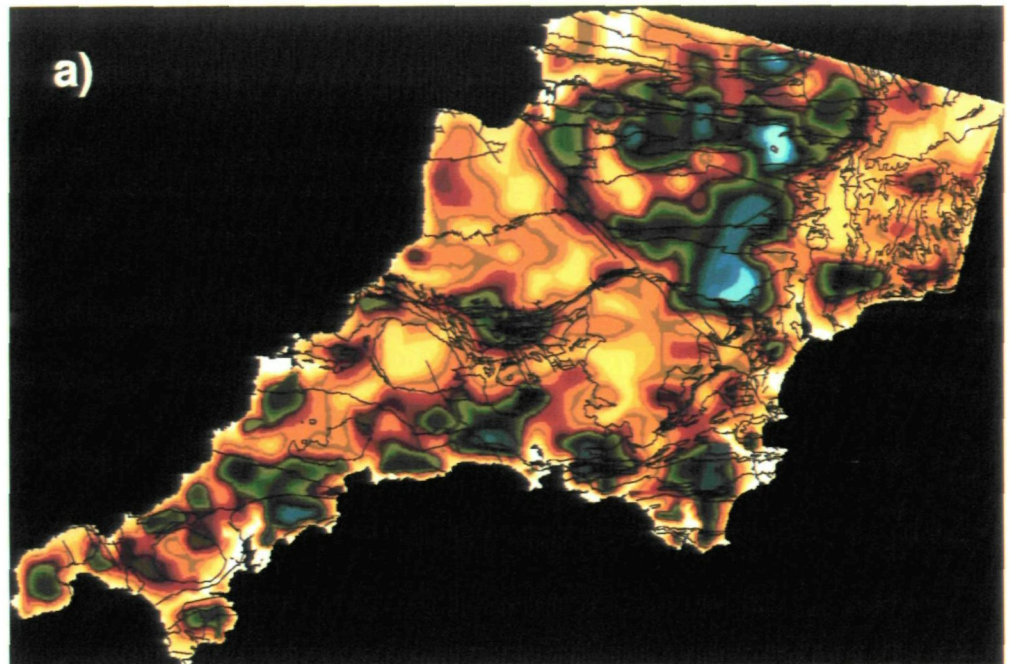
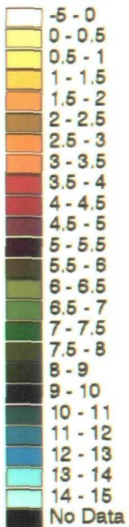
7.3.2.a E/W lineaments (families M and N)

Similar high lineament densities for both variables (length and frequency) are apparent throughout SW England (Fig. 7.4), however, particular characteristics can be determined:

KEY

Outline of the
geology of SW
England

Lineament
frequency/
5km grid



KEY

Outline of the
geology of SW
England

Lineament
length/
5km grid

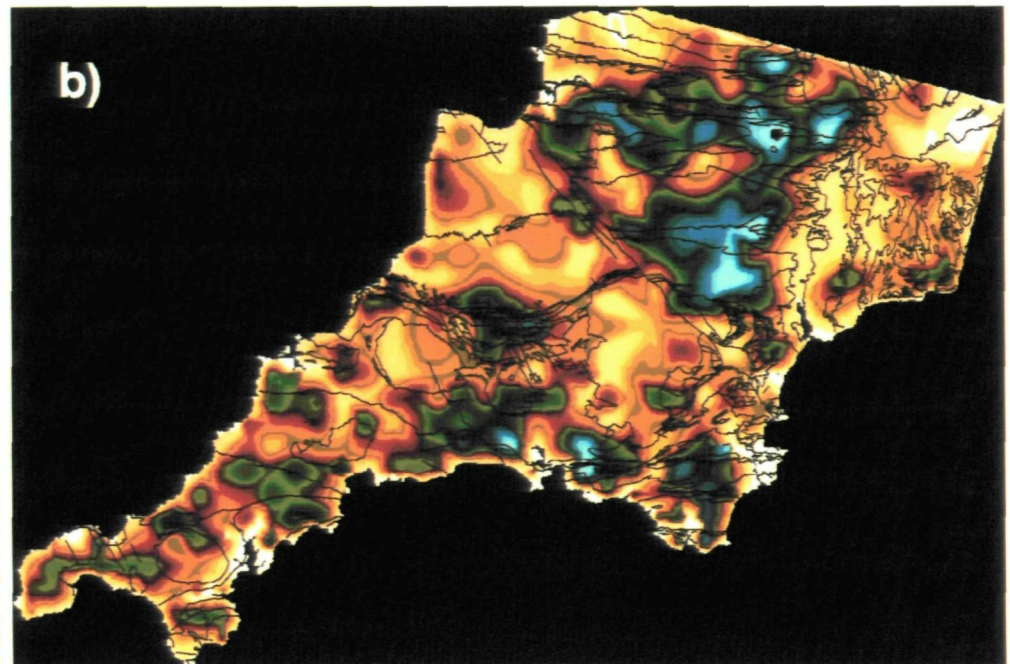
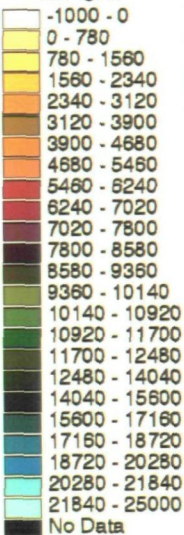
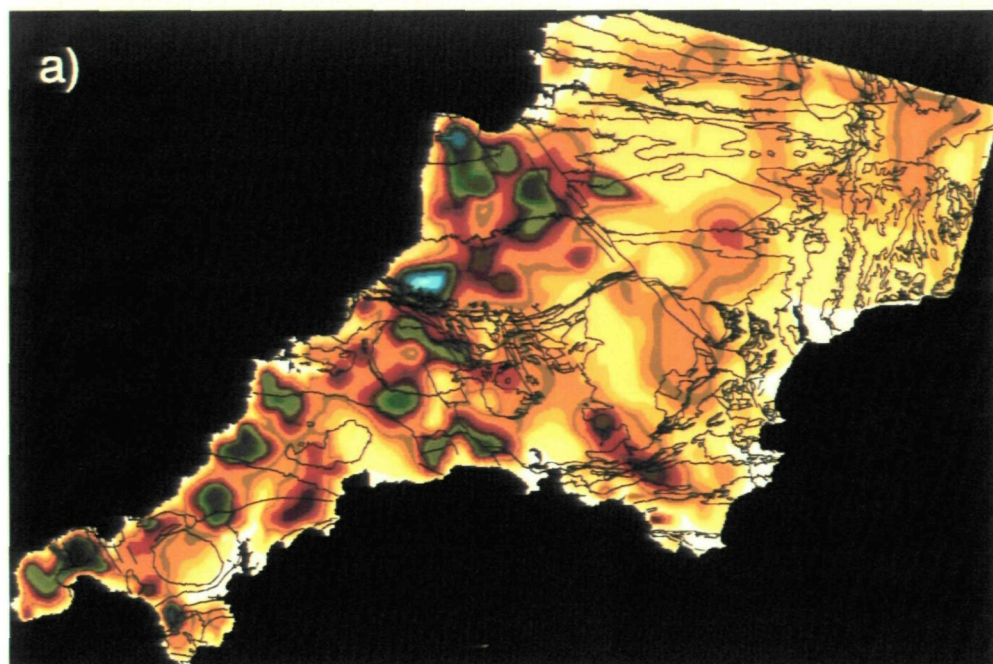
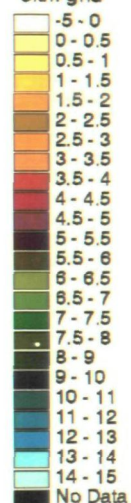


Fig. 7.4. Density maps of a) the frequency and b) length of lineaments separated into the lineament directional families M and N. Lineaments were interpreted from Landsat TM images of SW England.

KEY

Outline of the
geology of SW
England

Lineament
frequency/
5km grid



KEY

Outline of the
geology of SW
England

Lineament
length (m)/
5km grid

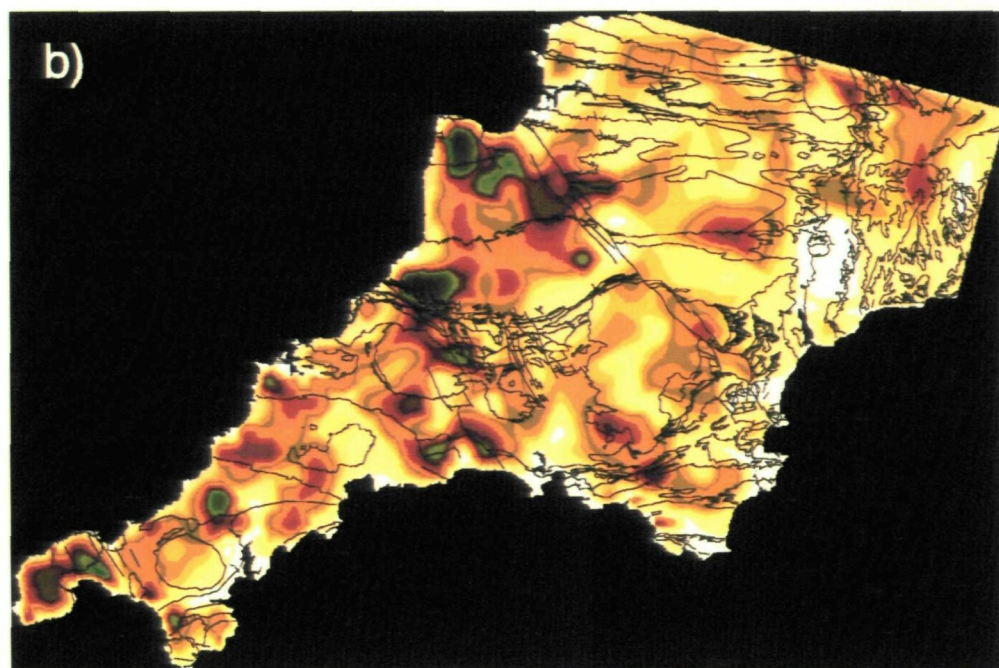
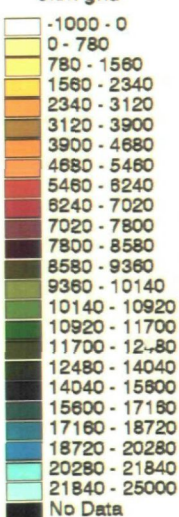


Fig. 7.5. Density maps of a) lineament frequency and b) length of lineaments of the linked lineament directional families U, V and W (Fig. 7.1). Lineaments were interpreted from Landsat TM images of SW England.

(i) In the area of South-East Cornwall the high lineament length density zone is indented with low lineament length densities (Fig. 7.4b), these indentations are not apparent in the lineament frequency density map (Fig. 7.4a).

(ii) In the area of central Devon, within the Culm Basin densities of both lineament variables are relatively much higher to the east of the SLFZ. Although, small areas of low and medium lineament densities can occur to the east and west of the SLFZ, respectively.

(iii) The western boundary of the high lineament length density in the east of the Culm Basin is comparatively more linear.

7.3.2.b NW/SE lineaments (families U, V and W)

In comparison to the E/W trending lineaments NW/SE lineaments possess the following characteristics:

(i) High lineament densities of NW/SE lineaments cover a relatively smaller area of SW England, but are particularly prevalent along the north coast of SW England.

(ii) The occurrence of high densities of NW/SE lineaments in the Culm Basin is to the west of the SLFZ. Although, high lineament densities can occur to the east of the SLFZ these areas correlate to low E/W lineament densities.

7.3.3 Discussion

Lineament densities identified for the directional families M, N suggests that a high concentration of E/W lineaments occurs across SW England (Fig. 7.4). In the area of South Cornwall, the lineament patterns indicate that they generally represent a series of re-activated fractures (Section 4.2.5(v)). The lineament

density maps of this area suggest that the E/W lineaments of this area can form high lineament densities northwards to the St. Austell granite and eastwards into South-East Cornwall and South Devon. In South-East Cornwall (Plymouth area) and South Devon the lineament patterns were interpreted to be related to lithotectonic features of the South Devon thrust zone. Therefore, although information on the spatial extent can be identified by the density maps, it may be difficult differentiating between different lithotectonic domains without analysing the relevant lineament patterns.

In the area of South-East Cornwall the lineament pattern indicates that E/W lineaments (lineament directional families N, M) are cross-cut by later NW/SE lineaments, related to NW/SE trending major faults (e.g. Portwrinkle fault zone) (see Section 4.2.5(ii), Fig. 4.4). Therefore, for the two variables analysed in the local area around major faults, 'primary' lineaments are increased in number and shortened in length as they are split by the later cross-cutting faults. This explains the indentations in the high length density of the primary E/W lineaments, which are not present in the lineament frequency map. The different density maps can therefore identify the local geological history. More importantly, however, density maps of lineament length may more accurately identify lithotectonic domains which are fault bounded, because the boundary of the high lineament length density will in comparison to lineament frequency closely follow the bounding fault.

Lineament density of NW/SE and E/W trending lineaments differ within the Culm Basin across the SLFZ. Lineament patterns across the Culm Basin indicate E/W to ENE/WSW lineaments represent a primary lithotectonic feature, probably tilted (by folding) bedding (see Sections 4.2.5(i), 4.3.2(iii)). Therefore, the change in lineament density may be related to differences in the trend of the interpreted

E/W to ENE/WSW trending primary features. However, the area occupied by the primary ENE/WSW lineaments is relatively small and may not account for this large decrease in lineament density. The lineament patterns exhibited by lineaments within the lineament directional families U, V, W indicate faulting to be the related lithotectonic feature (see Section 4.2.5(ii)). The occurrence of faults has been shown previously to reduce the number of primary lineaments interpreted from the images. Therefore in the Culm Basin of the area of North Cornwall the high density faulting (as suggested by the density map, Fig. 7.5) obscures the E/W trending primary lithotectonic features. Low lineament densities of the lineament directional families M N, however, can also be identified in the Culm Basin east of the SLFZ. Correlating to these areas are high densities of the lineament directional families U, V, W. Again obscuring of E/W lineaments by NW/SE trending lineaments is envisaged. As the change in lineament density occurs across the SLFZ, this may suggest that this fault is a major bounding fault for a tectonic domain. Furthermore, as lineament length is more affected by bounding faults, the linear western boundary of the high E/W lineament length in the Culm Basin indicates the SLFZ is a bounding fault.

These results suggest the boundary to the high density faulting appears to be related to the SLFZ. However, further major NW/SE trending lineaments can be identified to the east of the SLFZ. This indicates that although the SLFZ appears to be a bounding fault, this major fault zone may be linked to other large NW/SE trending fault zones cross-cutting through the Culm Basin.

The analysis of lineament length and frequency density maps of the lineament directional families N, M and U, V, W suggests that the method used to construct density maps of SW England can accurately represent prevailing structural and lithological trends within the region. Furthermore, the density maps

aid in the more complex task of differentiating local and regional changes in trend and the boundaries of domains with differing trends. The methods used to construct density maps therefore can resolve the extent of lithotectonic domains within SW England. To obtain a more complete analysis the density maps of all other lineament trends also need to be considered. The geological history of an area may also be obtained from lineament density maps, however, this information is more readily accessible by analysing lineament patterns (Chapter 4). For some lithotectonic features, however, the azimuthal range in lineaments related to the lithotectonic features is greater than the relevant lineament directional families (e.g. the lineament zone relating to the South Devon thrust belt have azimuthal ranges of E/W to NE/SW). Consequently, the high lineament densities correlating to such a feature will appear in multiple density maps consisting of lineaments covering the azimuthal range of such a feature. Therefore, to identify the structural and lithological domains related to variably trending lithotectonic features (e.g. the South Devon thrust and fold belt), multiple density maps of lineaments covering the range in trends will need to be analysed. Alternatively, developing the cluster analysis technique to include multi-variate data (e.g. spatial distribution of lineaments), thus becoming less sensitive to changes in lineament trend may form lineament directional families which relate to such features.

7.4 Scaling relationships of lineaments

Analysis of populations comprising of different lithotectonic features would produce scaling relationships reflecting the different lithotectonic features. Therefore, within this study it is necessary to identify populations of lineaments which reflect single lithotectonic features, in this case faulting. NW/SE trending

lineaments are considered to be most reliable on the basis of: (i) lineament patterns reflecting the cross-cutting nature of NW/SE trending wrench faults (see Section 4.2.5(ii)); (ii) analysis of lineaments in an area comprising of NW/SE wrench faults (North Cornwall); and (iii) a high density of NW/SE trending lineaments reflecting this area (see Section 7.3.2.b). To analyse the scaling relationships of the NW/SE trending fault-related lineaments, subsets of data have been separated from the total lineament data set using several methods: (i) direct comparison to geological maps to identify which lineament zones correspond to mapped faults; and (ii) indirectly by identifying the trends in the lineaments patterns which express fault-related characteristics and using rose diagrams to identify lineament groups and cluster analysis to identify lineament directional families related to such features.

Numerous authors have identified power-law distributions in fault populations based on a variety of scaling attributes including fault length (Heffer & Bevan 1990, Yielding *et al.* 1992, Watterson *et al.* 1996), fault displacement (Jackson & Sanderson 1992, Peacock & Sanderson 1994, Needham *et al.* 1996) and fault spacing (Gillespie *et al.* 1993). In these analyses a variety of cumulative frequency-size plots are commonly used to make an assessment of the type of population distribution. Power-law, negative exponential, log-normal and normal are the most common distributions considered (e.g. Gillespie 1993). This approach is used in this study in order to assess the nature of distribution of lineament subsets identified from images of North Cornwall and SW England. Examples of power-law, log-normal and negative exponential distributions are illustrated in Fig. 7.6. Visual comparison was used to identify which type of cumulative frequency-size distribution best fitted the lineament data for each subset in this study.

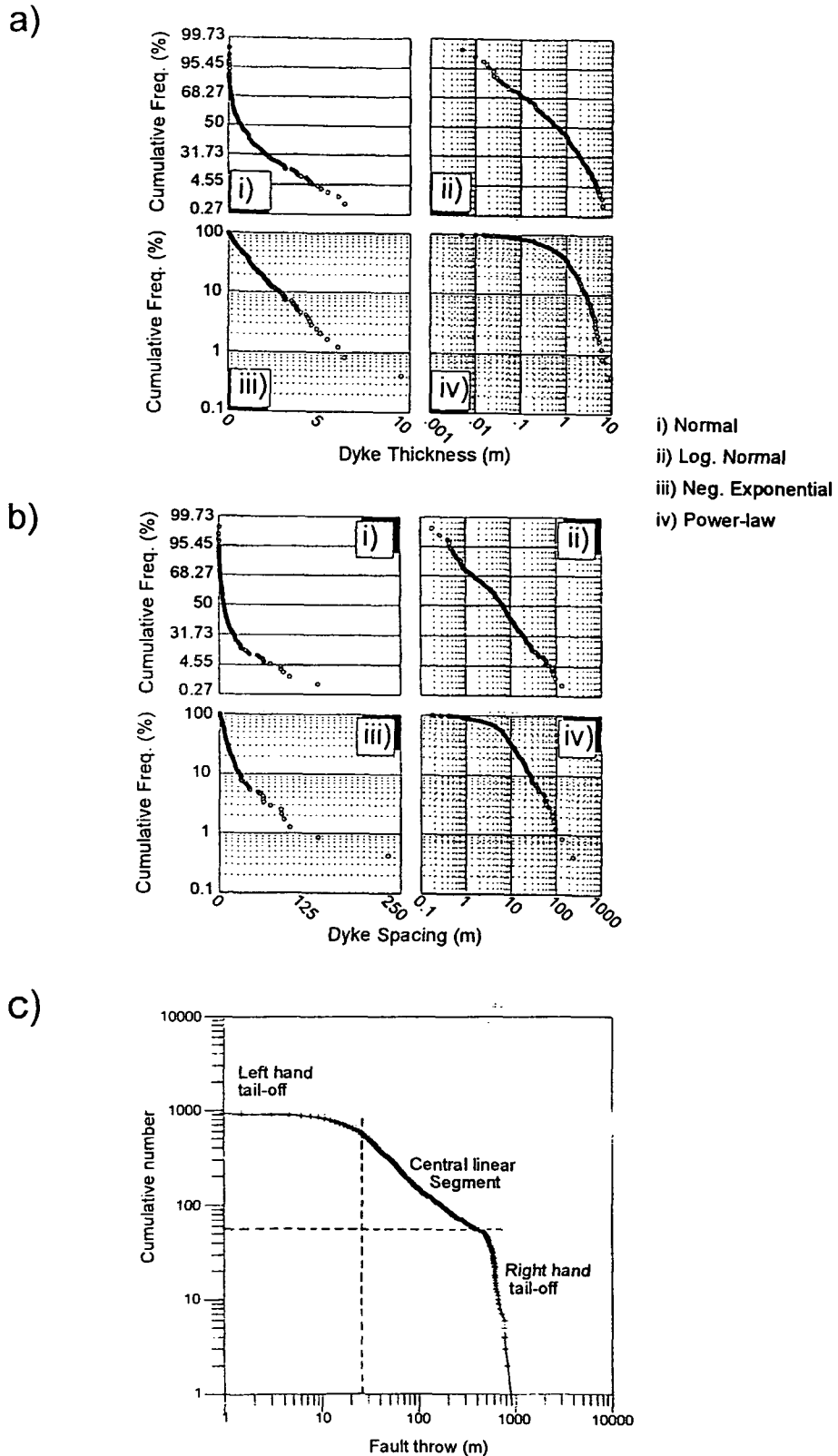


Fig. 7.6. Examples of different scaling relationships. In the case of: a) dyke thickness has either log-normal or negative exponential distributions; b) dyke spacing has a log-normal distribution; and c) fault throw has a power-law distribution. The cumulative frequency-size plot of fault throw illustrates the effect of sampling biases on a power-law distribution. In this case the right hand segment is produced by the effect of closely spaced multi-line sampling and the left hand segment is produced by the lower limit of seismic resolution. Plots a) and b) were redrawn from Jolly & Sanderson (1995) and plot c) modified from Yielding *et al.* (1992).

7.5 Analyses of lineaments related to the SLFZ

Within SW England only the SLFZ is large enough to allow sufficient lineaments ($n > 20$) to be interpreted from low resolution images for a simple analysis of the fault zones scaling relationships (Fig. 7.7). Although the SLFZ is a major fault within SW England, the related lineament zone is too narrow to measure lineament spacing therefore only lineament length was determined for the purpose of analysing scaling relationships in the fault zone. The selected lineaments ranged in trend between 120.1° to 158.6° . As illustrated in Table 4.1 lineament length is shorter within the Variscan country rocks than the igneous Dartmoor granite. To investigate if these differences can effect scaling relationships in the SLFZ, lineaments were further sub-divided into lineament populations either from the Dartmoor granite or the country rocks (Fig. 7.7). To avoid a type B sampling bias (lineaments which cut across the sample area boundary are shortened causing an under-estimation in the larger scale lineaments; Pickering *et al.* 1995) in the subset identified from the granite lineaments which were contained or mostly-contained within the area sampled were retained, however, lineaments which were only partially contained within the sample area were omitted.

7.5.1 Results

The cumulative frequency-size curves were best described by a power-law distribution for lineaments imaged from the SLFZ and the SLFZ within the Dartmoor granite and the Culm basin. These curves are shown in Figs. 7.8a, b, c. The sampling biases *truncation* and *censoring* can alter the slope of a straight-line power-law population curve (Einstein & Baecher 1983, Pickering *et al.* 1995) (Fig. 7.6c). To obtain an un-biased D -value the slope of the central segment of the

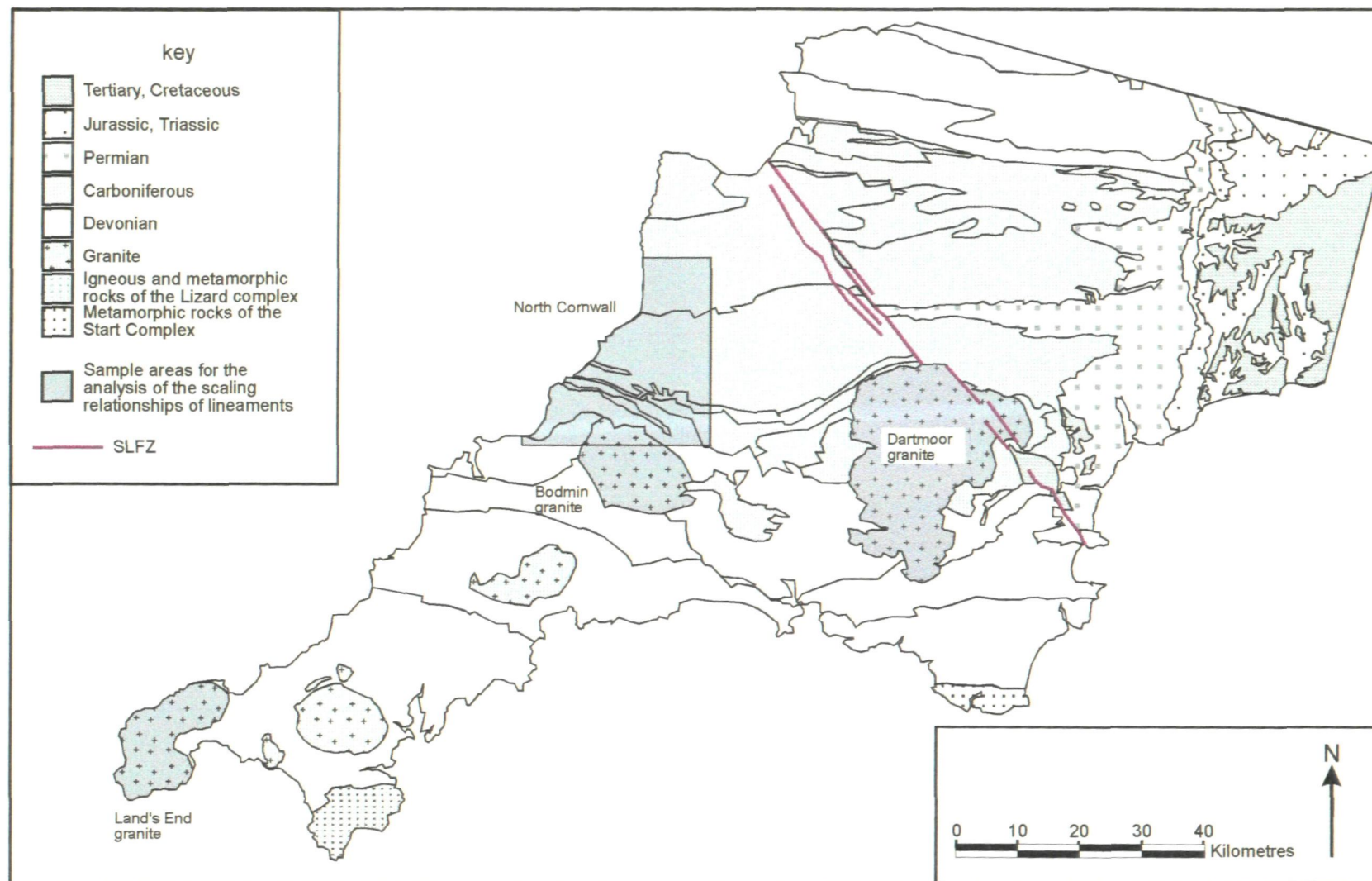


Fig. 7.7. Map showing the lineament sample areas used in the analysis of lineament scaling relationships.

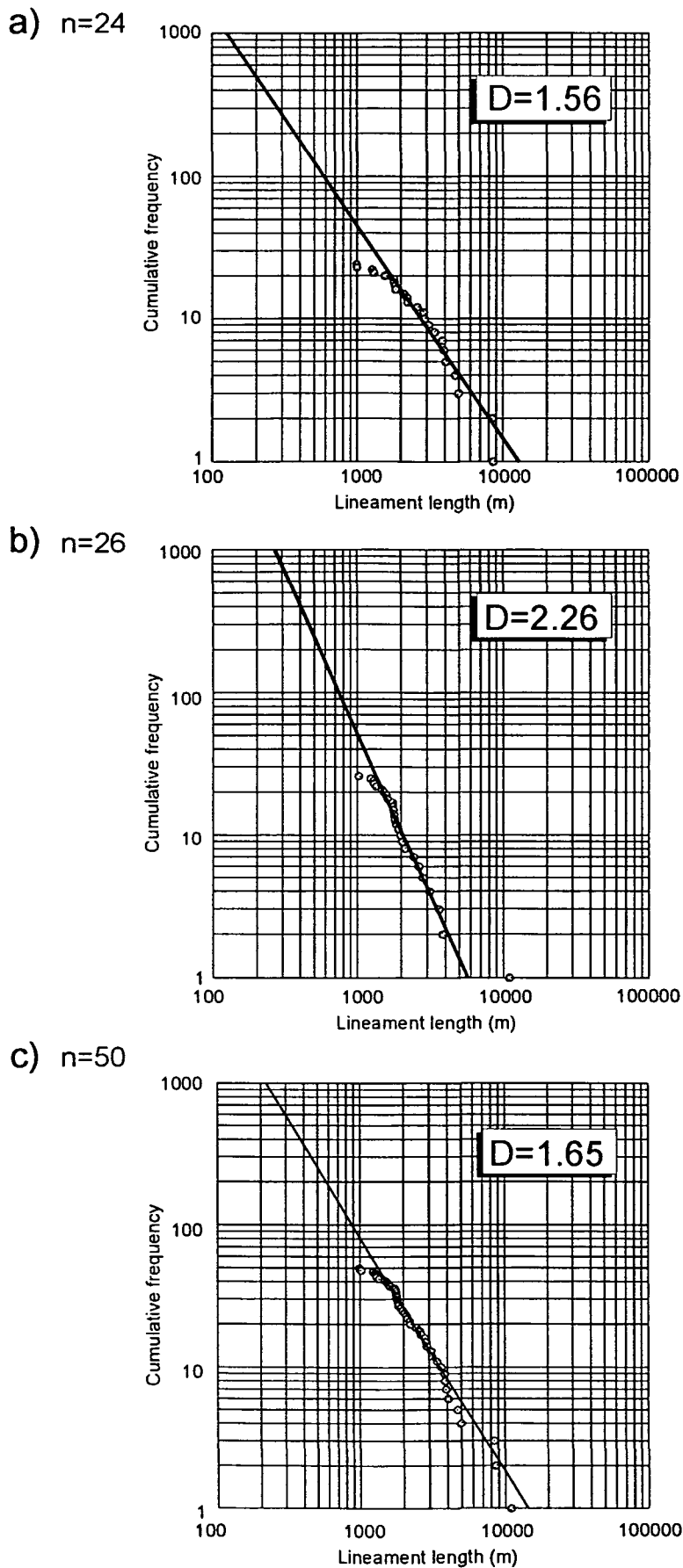


Fig. 7.8. Cumulative frequency-length plots illustrating the power-law population curves of lineaments interpreted from images of SW England. Plot a) shows the distribution obtained from lineaments following the SLFZ through the Dartmoor granite, plot b) lineaments which follow the SLFZ through the country rocks and plot c) the combined populations.

population curves were measured. Data points which formed the central segment of the population curve were visually identified and a line fitted (the slope of the line being the D -value) using the least squares method.

Fault zone and area sampled	Number of lineaments	D -value obtained	68% confidence limit of the sample D -value
SLFZ in the Dartmoor granite and Culm Basin	50	1.65	± 0.48
SLFZ in the Dartmoor granite	24	1.56	± 0.82
SLFZ in the Culm Basin	26	2.26	± 0.93

Table 7.2. Obtained D -values from power-law distributions of lineaments caused by fault segments within the SLFZ. The 68% significance range of the possible error for each D -value is also given.

The central segments of the obtained power-law distributions of the tested lineament sub-sets were found to be ≤ 1 -order of magnitude and contained < 100 data points. Fault populations which are interpreted as possessing significant power-law distributions typically have a range distributions in the linear segment from 1 to 2-order of magnitudes (e.g. Jackson & Sanderson 1992, Yielding *et al.* 1996). In populations which contain low numbers of data points and a small size range, the degree of error when fitting a line to a linear central segment curve becomes higher. An assessment of the degree of confidence in a D -value was empirically derived by Pickering *et al.* (1995), where there is an approximate relationship between the standard deviation of a sample D -value distribution, sample size and the population D -value:

$$D \geq 1: \quad \sigma = kD \sqrt{\frac{1}{\text{sample size}}} \quad (\text{equ. 7.1})$$

$$D < 1: \quad \sigma = k \sqrt{\frac{D}{\text{sample size}}} \quad (\text{equ. 7.2})$$

k has been found to possess a value of 1.9 for the cumulative frequency analysis method with a sample size of 1 order of magnitude (table 1, Pickering *et al.* 1995). Therefore this value of k is appropriate for most of the power-law distributions tested, the estimate obtained of the standard deviation of a sample D -value distribution is equal to the 68% confidence limit. For samples with a sample size of <1 order of magnitude the confidence limit is lower than the actual confidence limit range, because with decreasing sample size k increases. K values of sample sizes of <1 order of magnitude have not been calculated by Pickering *et al.* (1995). The degree of confidence in the D -values obtained from the SLFZ are summarised in Table 7.2.

7.5.2 Discussion

Spatially distributed geological data can be sampled by traverses (1-dimensional), through area (2-dimensional) or by volume sampling (3-dimensional). D -values of 1 from line sampling indicate self-similarity, while self-similar populations from areas and volumes have D -values of 2 and 3, respectively. Self-similarity suggests that a population is geometrically the same over a range scales. However, a change in geometric magnitude over a range of scales is known as *self-affinity*. Self-affine distributions in 1D sampled populations typically have $D \neq 1$, in 2D populations $D \neq 2$, and in 3D populations, $D \neq 3$ (Jackson & Sanderson 1992).

The sampling of the lengths of lineaments from a map is a 2D analysis. The power-law distribution obtained therefore suggests that lineament length from the SLFZ has a self-affine fractal distribution ($D=1.65$). However, due to the large possible errors in the D -value (± 0.48) there is little confidence in the suggested

self-affine behaviour. Division of this data into lineaments from the SLFZ in the Dartmoor granite and Culm basin forms two different D -values of $1.56 (\pm 0.82)$ and $2.26 (\pm 0.93)$, also indicating self-affine fractal distributions. Again, the possible errors in the D -value indicates there can be little confidence in the suggested self-affine behaviour.

As fault length has been found to form power-law distributions in other fault populations (e.g. Watterson *et al.* 1996) a power-law distribution from lineaments formed from faults in a fault zone is not unexpected. Estimations of the fractal dimension of these lineaments, however, is less reliable as shown by the possible variance of D . These results, however, indicate that power-law distributions can be obtained from lineaments from pixelated images.

The large errors estimated for the D -values obtained from lineaments in the Culm Basin and the Dartmoor granite subsets suggest that they are not significantly different. It has been found, however, that lineaments interpreted from the Dartmoor granite are generally longer than the lineaments interpreted from the Culm basin (Table 4.1). This difference has been attributed to either a difference in the shear modulus between sedimentary rocks and granites or partial fault-line scarp healing in the sedimentary rocks causing sub-division of lineaments (see Section 4.2.5(ii)). Consequently, although the D -values of the two subsets cannot be statistically proven to be dissimilar due to low numbers of data, the difference may be real. The results would therefore show that the type of rock a fault zone propagates through may affect the scaling relationships of interpreted lineaments. The different scaling relationships, however, are not necessarily distinguishable once subsets are combined.

7.6 Analyses of lineaments divided into lineament groups

The length of lineaments related to a known fault has been shown to best approximate a power-law distribution. This section analyses the effect on the scaling relationships of larger subsets identified as major peaks in rose diagrams (lineament groups) from the overall lineament population of SW England. The characteristic lineament pattern of these lineament groups indicate that they are, at least in part, fault related (Section 4.2.5(ii)). Lineaments were sub-sampled from the granite hosts following the same procedure used to avoid type B censoring biases described above (Section 7.5). The sample areas (Fig. 7.7) are from granites which possess high numbers of NW/SE lineaments, the azimuth ranges of the lineament groups are shown in Table 7.3.

Sample area from which lineaments were interpreted	Method used to identify lineaments	Azimuth ranges of lineaments	Lineament property analysed
Bodmin granite	Rose diagrams	118.2° to 163.4°	Length
Land's End granite	Rose diagrams	115.6° to 162°	Length
Dartmoor granite	Rose diagrams	106.4° to 154.4°	Length

Table 7.3 Azimuth ranges of the lineament groups sampled from granites within SW England.

7.6.1 Results

The types of cumulative frequency-lineament length curves which best fit to lineaments of the lineament groups of the Bodmin granite, the Dartmoor granite and the Land's End granite are shown in Table 7.4. The scaling relationships of lineament length for these lineament groups are illustrated in Figs. 7.9, 7.10.

Sample area of lineament group	Type of size-frequency distribution interpreted to fit the lineament group	<i>D</i> -value of power-law	68% confidence limit of the sample <i>D</i> -value
Bodmin granite	Log-normal (Fig. 7.9a)		
Dartmoor granite	Power-law (Fig. 7.9c)	2.42	±0.76
Land's End granite	Segmented power-law forming 2 <i>D</i> -values (Fig. 7.10)	1.33 2.92	±0.39 ±1.3

Table 7.4. Table showing the types of cumulative frequency-size curves interpreted for the lineament groups sampled from SW England. If a power-law distribution was obtained, the *D*-value and an estimation of confidence is given.

7.6.2 Discussion

The results obtained suggest a range of distributions can be identified from supposed fault-related lineaments along selected trends. The probable cause of these differences is considered to be sampling of multiple fracture sets:

(i) The estimated *D*-value obtained for the power-law distribution for the lineament group identified from within the Dartmoor granite suggests a higher *D*-value than that obtained from lineaments only related to the SLFZ within the Dartmoor granite. However, each sub-population contained similar trending lineaments. The degree of significance estimated from the *D*-values between the different lineament subsets may explain this difference. Alternatively, the difference in *D*-values between the lineament group from the Dartmoor granite and lineaments related to the SLFZ therefore could be caused by mixing of other fracture populations with similar trends but different scaling relationships. Within

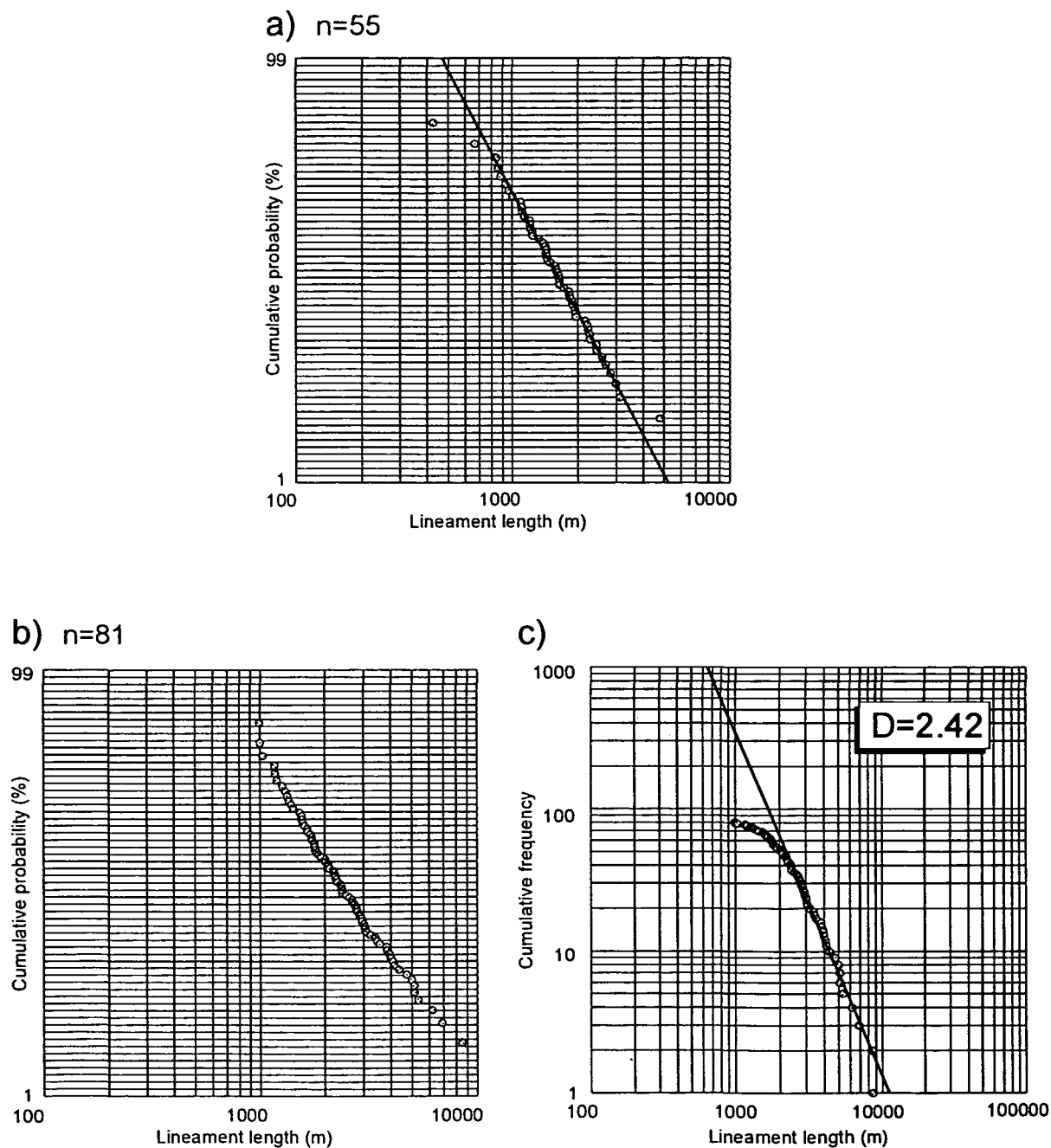
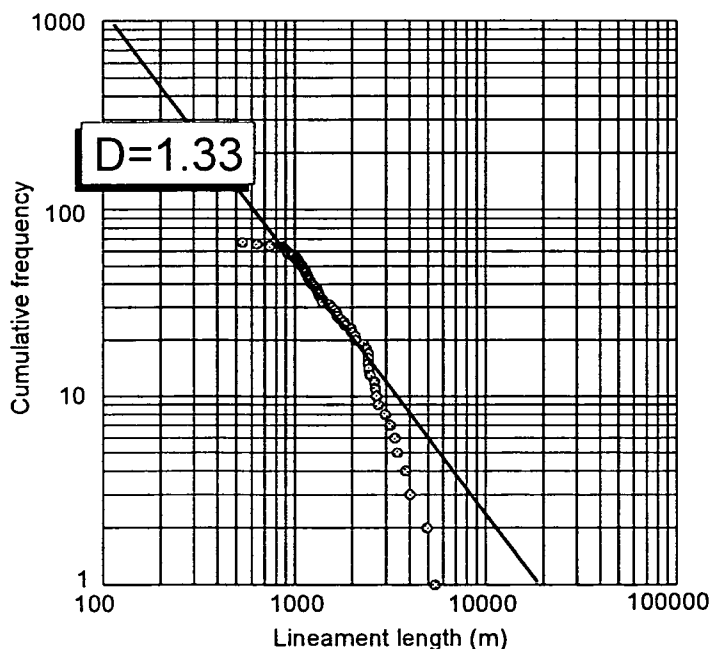
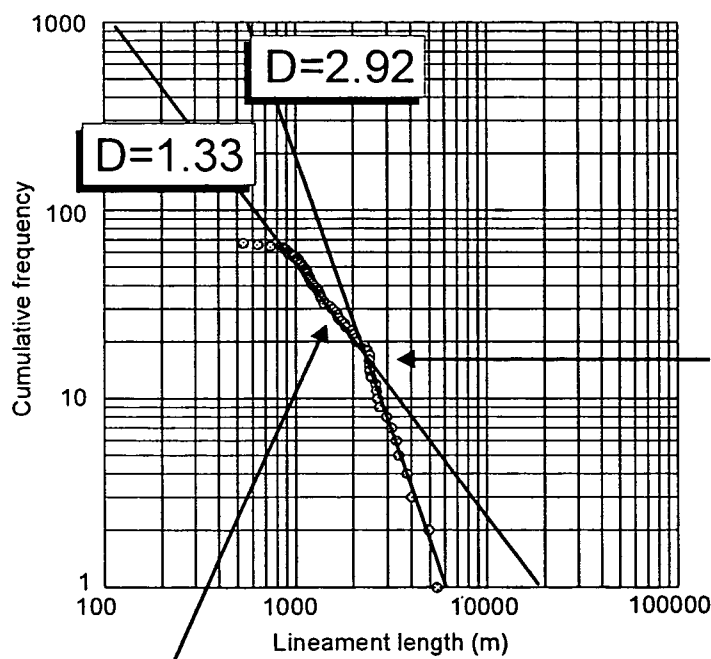


Fig. 7.9. Cumulative frequency-lineament length plots of lineament groups related to faults from the Bodmin (a) and Dartmoor granites (b and c). In these cases data were found to lie on a straight line in a) and c), indicating that lineament length in the Bodmin granite is log-normal and in the Dartmoor granite power-law (assuming the subset is affected by a sampling bias causing left hand tail-off). Data also forms a curved distribution in plot b) suggesting that the Dartmoor granite subset may also be poorly approximated to a log-normal distribution.

a) $n=67$



b) $n=67$



Kink between segments is above the limit of image resolution where left-hand truncation occurs in the SLFZ

Average limit of image resolution where left-hand truncation occurs in the SLFZ

Fig. 7.10. Cumulative frequency-lineament length plots in log-log space of the Land's End granite lineament group, identified from the SW England lineament population. Two different distributions can be interpreted: plot a) illustrating a power-law population curve with a single central segment and a large right-hand tail off; and plot b) a segmented power-law possessing two straight central segments, separated by a sharp kink. This is shown not to be caused by a left-hand tail off.

the granites of SW England other fracture sets have similar trends to the sampled lineaments, for example NW/SE trending joint sets (Edmonds *et al.* 1968, Booth & Exley 1987).

(ii) The cumulative-frequency distribution obtained from the Bodmin granite lineament group (which includes lineaments believed to be related to the Portwrinkle fault zone; see Section 4.2.5(ii), Fig. 4.4) suggests that lineament length within this area exhibits a log-normal distribution. Such a distribution is not typical of fault populations or of fault-related lineaments within the Dartmoor granite. Log-normal distributions may, however, result from multiple power-law populations (Ranalli & Hardy 1990). Therefore, the Bodmin granite lineament group may contain a mixed lineament population relating to multiple fault populations. Alternatively, the majority of lineaments in the Bodmin granite lineament group could be related to other modes of fractures, such as jointing which may form non-power-law distributions (Gillespie *et al.* 1993).

(iii) The population curve of the lengths of lineaments in the lineament group sampled from the Land's End granite can be interpreted to have a large right-hand tail off. As the subset was sampled from an area the bias is not caused by multi-line sampling. The type B sampling effect (as described in section 7.5) or the finite range effect (caused by the very low numbers of the longest faults in a fault population not crossing the sample area) (Pickering *et al.* 1995) may reduce the number of longer lineaments. Typically this causes a curved steepening to the right-hand tail off (Pickering *et al.* 1995). However, the right-hand tail off is linear suggesting that it is not related to sampling biases. Alternatively, this population curve may be explained as a segmented power-law population curve with two different D -values of $1.33 (\pm 0.39)$ and $2.92 (\pm 1.3)$ and a much smaller right-hand tail off (Fig. 7.7b). Although, the calculated error values can indicate

that the obtained D -values are not significantly different, the distinct kink and change of slope in the central section of the curve suggest that the population contains two central segments. Segmented power-law curves have been documented from analysis of fault populations (Fossen & Rornes 1996, Wojtal 1996) and may therefore offer a realistic explanation. At a scale range similar to those studied here, segmented power-law distributions have been linked to the effects of layer-thickness (Wojtal 1994), a property not apparent in the uniform Land's End granite. A simple explanation can not therefore explain the apparent segmented power-law distribution. Segmented power-law population curves, however, can be simplified by dividing the population into smaller subsets (Fossen & Rornes 1996). Therefore, the segmented power-law curve may represent two scale limited fault populations with differing D -values.

The cumulative frequency-size distributions obtained from these supposedly fault-related lineament groups suggest that the subsets contain lineaments that may in fact relate to mixed fracture sets or represent two scale limited fault populations. Therefore, dividing lineament populations in this study by identifying lineaments which possess fault-related lineament patterns and using rose diagrams to select the lineament subsets (lineament groups) forms subsets which probably contain multiple fault sets or mixed fracture sets. Thus, to analyse the scaling relationships of lineaments from SW England a method is needed which can distinguish between sets of near similar trending lithotectonic features. This would also mean that the azimuthal range of the lineament subsets would also decrease relative to those identified within the lineament groups, as it has been identified that lineament groups need to be sub-divided further.

7.7 Analyses of lineaments divided into lineament directional families

The division of lineament populations into lineament directional families results in lineament subsets which in comparison to lineament groups have narrower azimuthal ranges, thus reducing the possibility that a subset contains a mixture of lineaments. The analyses of lineament directional families identified from the lineament population interpreted from images of SW England, however, has shown that for highly geologically complex areas lineament directional families contain lineament mixtures of unrelated lithotectonic features (Section 7.2.1). By decreasing the image area this complexity is lowered leading to less lineament mixing, therefore lineament directional families from the sub-area of North Cornwall are used to analyse the scaling relationships of lineament directional families. The lineament directional families analysed contain lineaments which show lineament patterns characteristic of faults. The trends of these lineament directional families are between 132.5° and 166° (Fig. 7.11). The drawback of reducing the size of the sample area and the azimuthal range of a lineament subset is that the data number is lowered, thus increasing the possible error in the D -value obtained from a power-law distribution.

To analyse the effect of reducing the azimuth ranges the scaling relationships of: (i) combined lineament directional families (which are essentially lineaments groups with smaller azimuth ranges than that identified by rose diagrams); and (ii) individual lineament groups, are investigated. Once analysed, the method which produces subsets of fault-related lineaments that indicate the least mixed lineament subset (i.e. un-segmented power-law distributions) will be used to investigate the effect of resolution on the scaling relationships of subsets of fault-related lineaments.

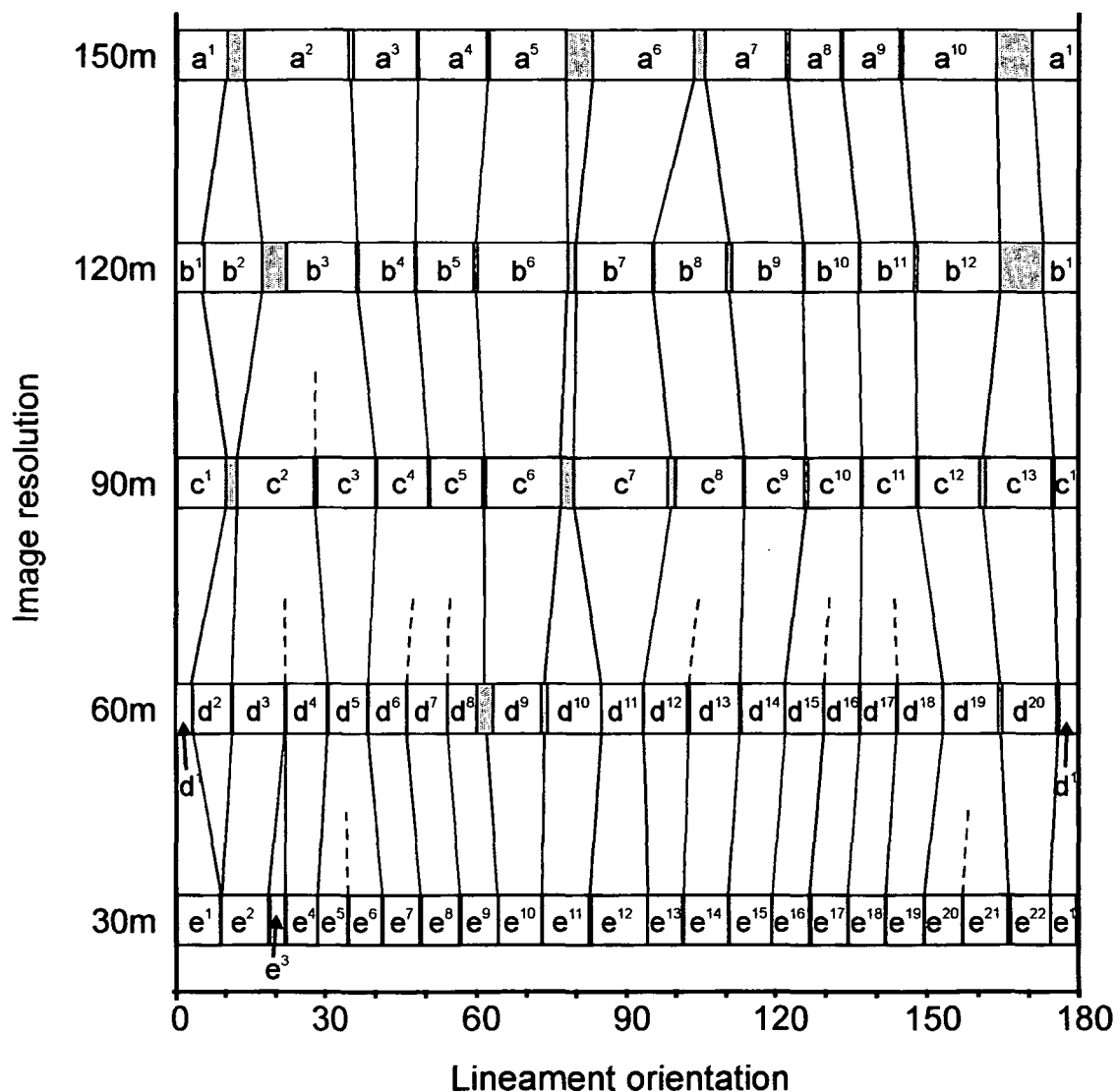


Fig. 7.11. Diagram of the distribution of lineament directional families identified by *k*-means cluster analysis from lineaments interpreted from different resolution images of North Cornwall. The range of lineament trends in the lineament directional families is represented by the width of the boxes, grey areas represent the range of trends which are absent of lineaments. Each lineament family has been labelled and if used in the analysis of the scaling relationships of lineament directional families are highlighted in pale yellow.

As the subsets were obtained from an area the scaling relationships of lineament spacing, as well as lineament length, were analysed. Lineament spacing was sampled by 1D line-sampling using the GIS, ARC/INFO. A series of lines were constructed in ARC/INFO and rotated 90° to the mean lineament trend (Fig. 7.12). Multi-line sampling typically leads to steep right-hand segments in a power-law population curve where the largest fault has been sampled repeatedly, the size of the right-hand segment corresponds to the number of line samples (Yielding *et al.* 1992). Multi-line sampling of lineament spaces with the width of the line sample being smaller than the length of the longest lineament would result in over-sampling of the longer lineaments therefore forming this sampling bias. To avoid the multi-line sampling bias the spacing of the sample lines was longer than the maximum lineament length within the population to be sampled. The distance between lineaments was measured along the sample lines when the sample line crosses two or more lineaments.

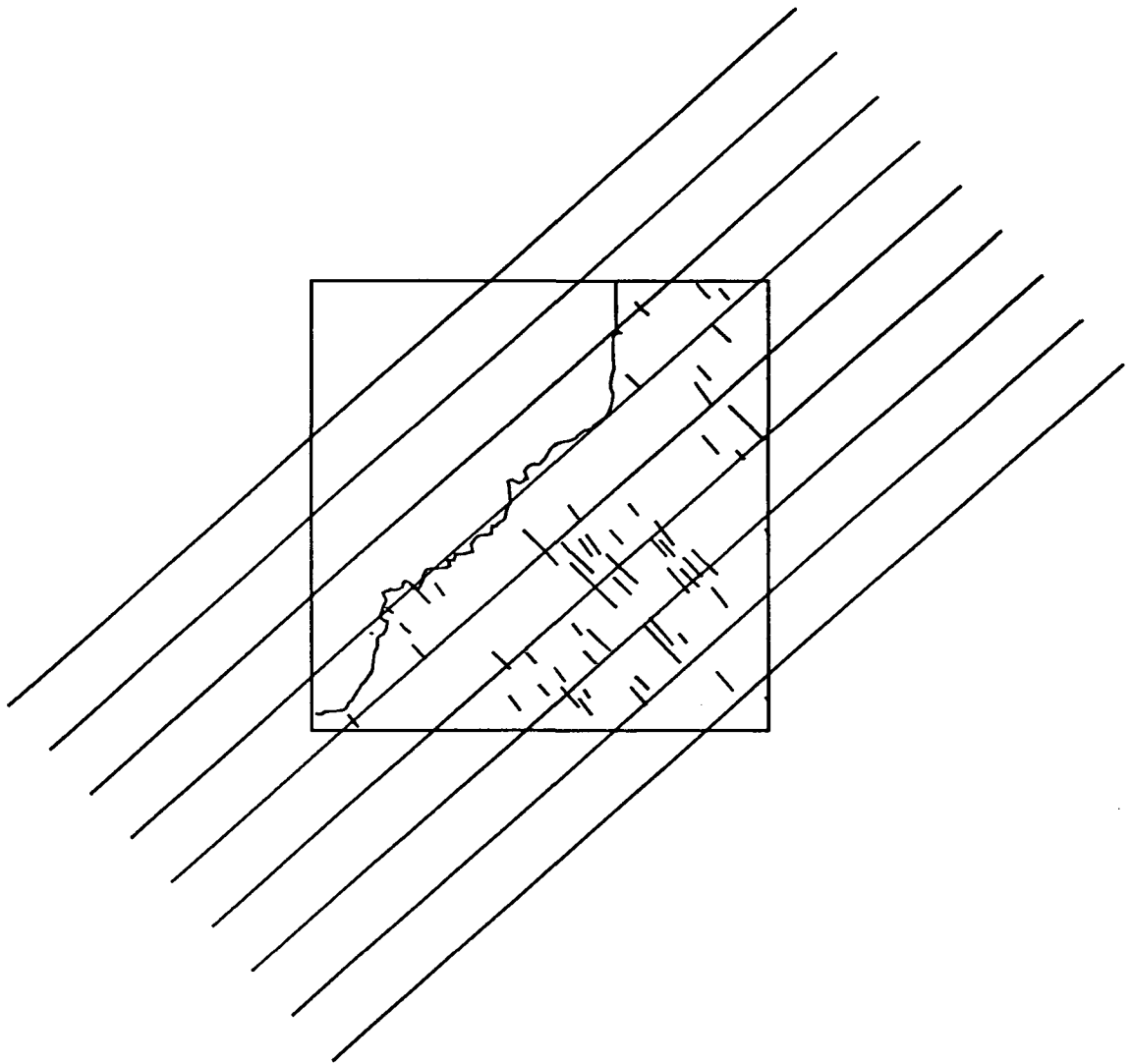


Fig. 7.12. Diagram of the computer generated lines used for line-sampling of lineament spacing of the lineament directional family a^g .

7.7.1 Scaling relationships of combined lineament directional families

To investigate the effect on the scaling relationships resulting from combining lineament directional families, the scaling relationships of all the fault-related lineament directional families (which possess azimuthal ranges between $\sim 132^\circ$ to $\sim 165^\circ$) identified from North Cornwall have been investigated. The combined lineament directional families which yield results useful to this study are described in Table 7.5.

The combined lineament directional families used	Azimuth ranges of lineaments	Lineament property analysed
$a^9 - a^{10}$ (Fig. 7.11)	133.2° to 159.85°	Length
$d^{17} - d^{18} - d^{19}$ (Fig. 7.11)	136.9° to 163.93°	Spacing

Table 7.5. The azimuth ranges of the combined lineament directional families.

Lineament lengths of the combined lineament directional families $a^9 - a^{10}$ and individual lineament directional families a^9 and a^{10} from the 150m resolution lineament population of North Cornwall (Fig. 7.11) are interpreted to form the power-law population curves shown in Table 7.6 and Fig. 7.13.

Lineament directional families used in sample	Can the population be interpreted to form a segmented population curve?	Approximate size range of the straight segment	D-values of straight segments	68% confidence limit of D-values
$a^9 - a^{10}$	Yes (Fig. 7.13a)	1000m-1100m 1100m-1450m	1.89 2.79	± 0.644 ± 0.98
a^9	No (Fig. 7.13b)	1050m-1250m	2.27	± 0.8
a^{10}	No (Fig. 7.13c)	1000m-1120m	2.13	± 0.95

Table 7.6. Table showing the cumulative frequency-size curves interpreted from log-log plots of lineaments of the combined and single lineament directional families a^9 and a^{10} .

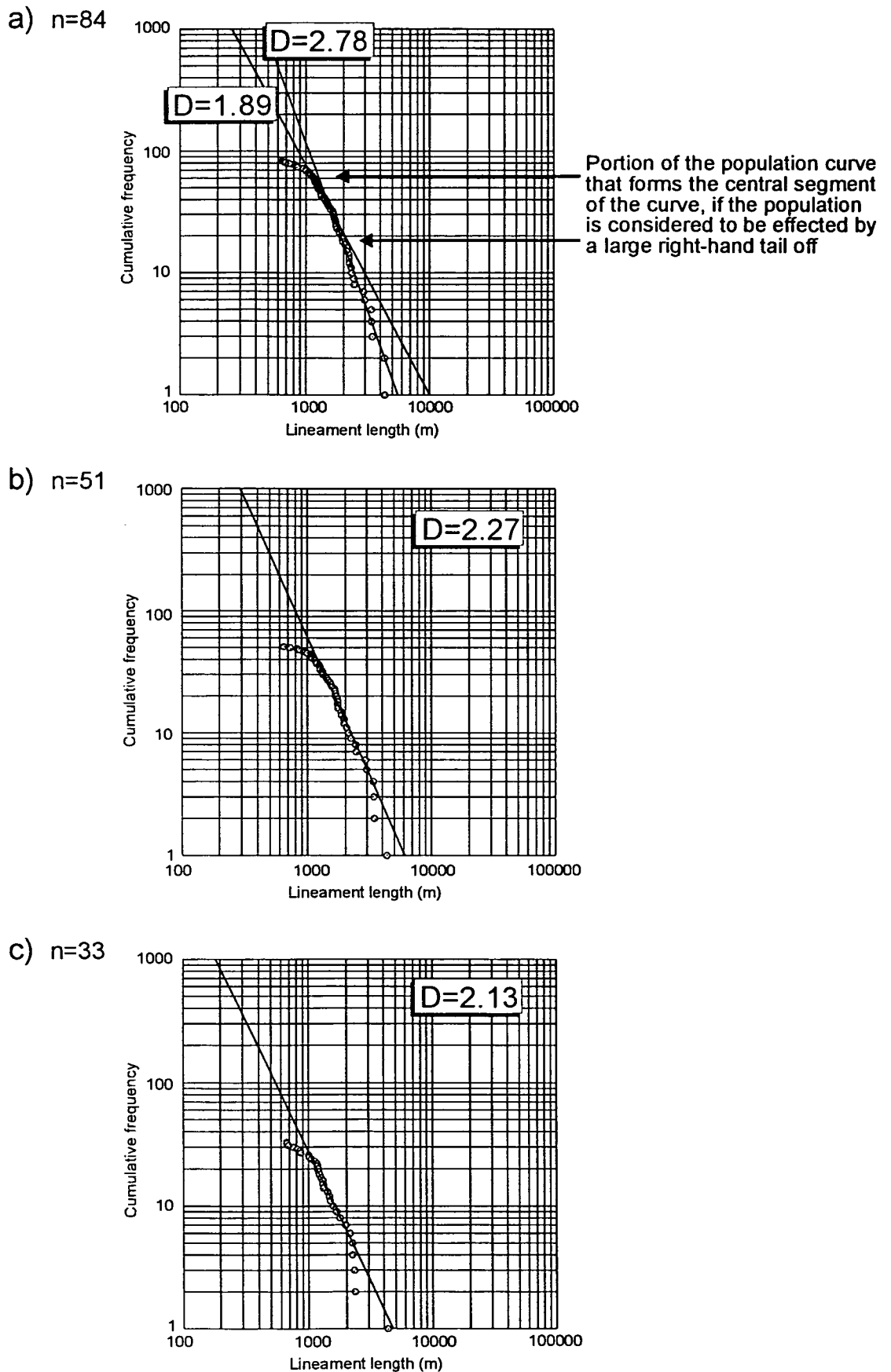


Fig. 7.13. Cumulative frequency-length log-log plots of the lineament directional families a^9 and a^{10} . Plot a) illustrates the population curve of the combined lineament directional families a^9 - a^{10} . This curve could be interpreted in two ways, a power-law distribution which is highly effected by right hand tail off or a segmented population curve. The two central segments of the segmented power-law being separated by a slight kink forming two D -values. Plots b) and c) illustrate the power-law distributions obtained when the constituent lineament directional families are divided into a^9 and a^{10} , respectively.

Lineament spacing was also analysed for equivalent lineament directional families identified at 60m resolution (combined lineament directional families d^{17} - d^{18} and d^{17} - d^{18} - d^{19} and individual lineament directional families d^{17} and d^{18}). The cumulative frequency-size curves obtained are shown in Table 7.7 and Fig. 7.14.

Lineament directional families used in sample	Can the population be interpreted to form a segmented population curve	Approximate size range of the straight segment	<i>D</i> -values of straight segments	68% confidence limit of <i>D</i> -values
d^{17} - d^{18} - d^{19}	Yes (Fig. 7.14a)	700m-1700m 1700m-2800m 2800m-5500m	0.48 0.92 1.74	± 0.29 ± 0.52 ± 0.77
d^{17} - d^{18}	Yes (Fig. 7.14b)	1000m-5000m 4500m-10000m	0.57 2.4	± 0.26 ± 1.14
d^{17}	No (Fig. 7.14c)	1000m-6000m	0.81	± 0.42
d^{18}	No (Fig. 7.14d)	1150m-15000m	0.71	± 0.31

Table 7.7. Table showing cumulative frequency- size curves interpreted from lineaments in the combined and single lineament directional families d^{17} , d^{18} and d^{19} . The data number was too low to identify the scaling relationship for d^{19} .

A segmented power-law distribution was found to best describe the cumulative frequency-size curve for the combined lineament directional families a^9 , a^{10} , formed from linear segments with *D*-values separated by a small kink in the curve. The lineament subset could alternatively be described as an un-segmented power-law, with the population being effected by large amount of right-hand tail off. The large degree of right tail-off necessary to produce this distribution suggests that this explanation is less likely.

Assuming a segmented power-law distribution for the combined lineament directional families a^9 - a^{10} , the confidence limits on the two *D*-values suggest that the obtained slopes are not significantly different. Dividing the combined lineament population into individual lineament directional families,

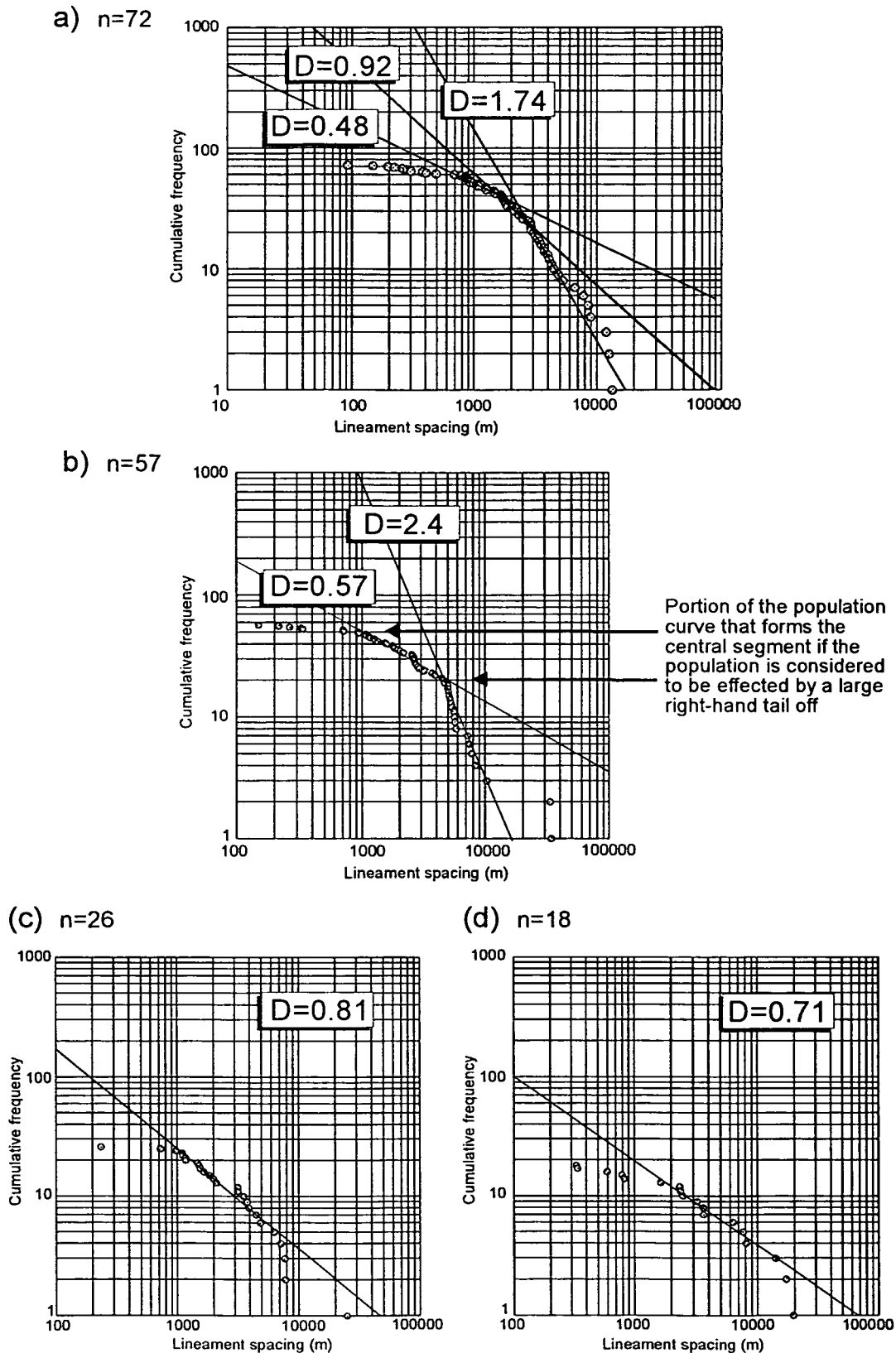


Fig. 7.14. Four cumulative frequency-spacing log-log plots of the lineament directional families d^{17} , d^{18} and d^{19} . Plot a) is of the combined lineament populations d^{17} - d^{18} - d^{19} . This sub-population can be interpreted to form a downwards concave population curve, however, three straight segments can be interpreted within the curve. The D -values of these segments are shown. Plot b) illustrates the population curve obtained from the combined lineament directional families d^{17} - d^{18} . This population curve can be interpreted as either a power-law distribution possessing a large right hand tail-off or a segmented population curve with two straight segments (as shown). Plots c) and d) show power-law distributions obtained from the individual lineament directional families d^{17} and d^{18} , respectively. The population curve of the lineament directional family d^{18} is interpreted to possess a more linear central segment.

however, simplifies this population curve into two separate power-law distributions. This therefore may suggest that the combined lineament directional family $a^9 - a^{10}$ forms a segmented power-law distribution. Changes in the slope of the segmented curve may be caused from differences in the size ranges of the straight segments obtained from the power-law distributions interpreted from the individual lineament directional families. Therefore, each segment within the segmented curve primarily reflects the scaling relationship of the constituent lineament directional families within the relative size range.

The cumulative frequency-size curves of the combined lineament directional families $d^{17} - d^{18} - d^{19}$ and $d^{17} - d^{18}$ can be interpreted to form a non-power-law distribution which describes a downwards convex curve and a power-law distribution which is greatly effected by right-hand tail off, respectively. However, an alternative interpretation is that the populations form three segment and two segment power-law distributions. Reducing the number of combined lineament directional families in the lineament sub-population may therefore decrease the number of identified segments. Furthermore, confidence limits of the 2 segment power-law suggest that there is a significant difference in the estimated D -values. The size ranges of linear central sections of the power-law distributions identified from the constituent lineament directional families were also found to be different. Again, therefore, each segment within the segmented curve may reflect the scaling relationship of the constituent lineament directional families within the relative size range.

Separating the combined lineament directional family $d^{17} - d^{18}$ into the constituent lineament directional families results in the formation of slightly scattered though largely un-segmented power-law distributions. D -values of 0.71 (± 0.42) and 0.84 (± 0.31) are typical of power-law distributions obtained for 1D

sampled data (see Section 7.5.2) (Jackson & Sanderson 1992). The power-law central segment of the d^{17} lineament directional family, however, can be argued to vary in slope, possibly suggesting a segmented power-law. A possible explanation for this variance may be due to lineament mixing between the neighbouring lineament directional families. An increase in the likelihood of lineament mixing increases with larger map-scale images as greater degrees of geological information are sampled. Therefore, a possible effect of degrading the lineament families is that the cumulative frequency-size curves obtained reflect progressive mixing and not true power-law distributions.

Fossen & Rornes (1996) found that segmented population curves could be simplified into single power-law distributions by dividing the faults into sub-populations based on genetic, spatial and geometric criteria. Analysis of combined lineament directional families results in segmented power-law distribution curves, indicating that the subset possesses different fracture subsets. Consequently, this suggests that *k*-means cluster analysis can identify minor subsets within the lineament populations sampled from a small area and that lineament directional families identified from North Cornwall contain a relatively low degree of lineament mixing. Furthermore, in this study the analysis of the scaling relationships of lineaments related to faults should be conducted on lineaments which possess lineament patterns characteristic of faults which are sub-divided into lineament directional families. However, this more subtle analysis lowers the data number further increasing the possible error in *D* or making scaling relationship of the subset unidentifiable (i.e. d^{19}).

7.7.2 Effect of image resolution on the scaling relationships of lineament length

To analyse the effect of image resolution on scaling relationships of lineaments derived from satellite images, cumulative frequency-size distributions obtained for lineament directional families in North Cornwall are assessed at a range of resolutions. To do this, fault-related lineament directional families corresponding to the same fault subset are analysed. Therefore, the 'corresponding' lineament directional families which can be investigated have lineament azimuthal ranges between $\sim 132.5^\circ$ to $\sim 150^\circ$ (a^9 , b^{11} , c^{11} , d^{17} , d^{18} , e^{18} and e^{19}) and $\sim 150^\circ$ to $\sim 166^\circ$ (a^{10} , b^{12} , c^{12} , d^{19} , e^{20} and e^{21}) (Fig. 7.11).

The interpreted cumulative frequency-size curves for the lineament azimuth ranges of $\sim 150^\circ$ to $\sim 166^\circ$ and $\sim 132.5^\circ$ to $\sim 150^\circ$ are described in Tables 7.8a and 7.8b, respectively. Examples of typical cumulative frequency-size curves obtained from the interpretation of lineament directional families a^{10} , b^{12} and c^{12} are illustrated in Fig. 7.15.

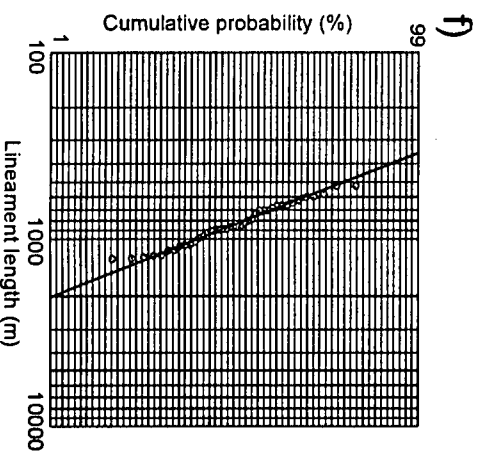
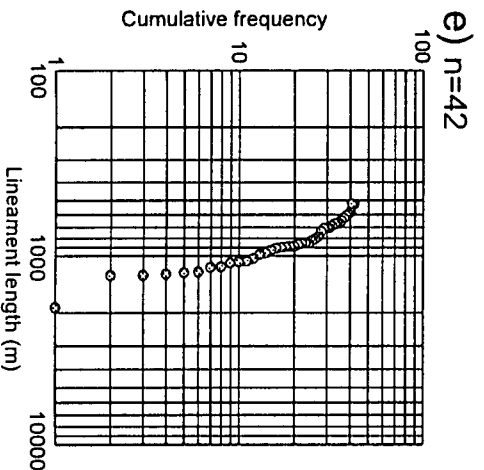
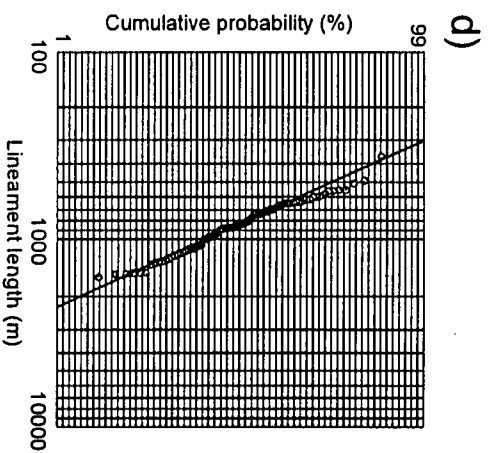
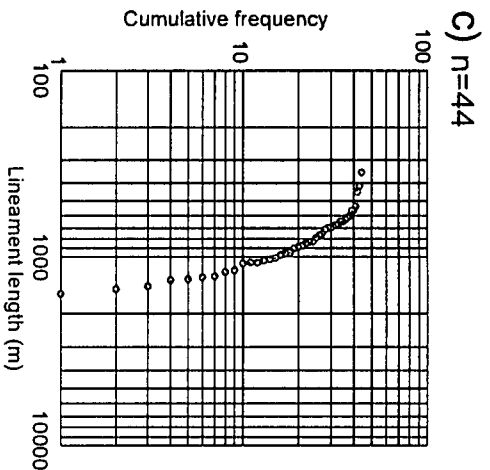
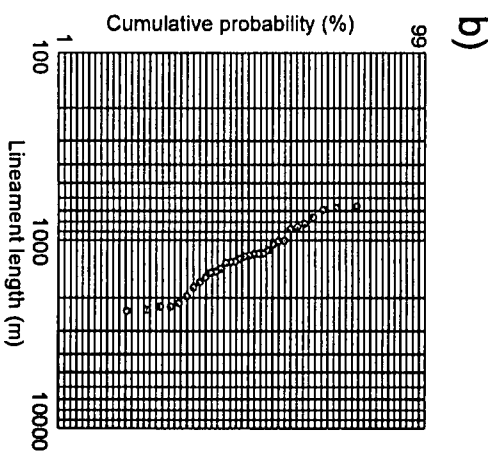
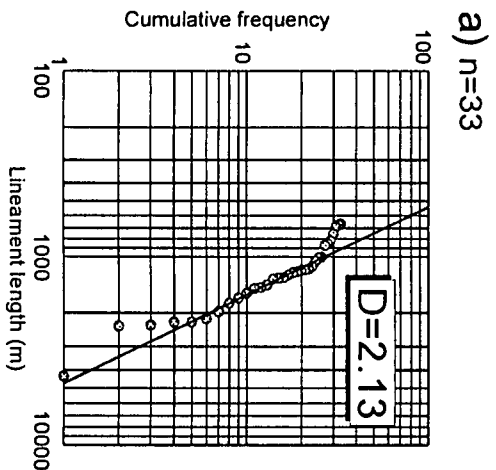


Fig. 7.15. Cumulative frequency-length plots of the lineament directional families a¹⁰, b¹² and c¹², the lineaments of which are interpreted from images with 150m, 120m and 90m resolutions, respectively. All the lineament sub-populations are tested for power-law (a, c, e) and log-normal (b, d, f) distributions. The obtained population curves suggest a change in the type of cumulative frequency-size distribution from power-law, plot a), to log-normal, plots d) and f), with increasing image resolution. This has resulted in an increase in slope of the population curves in the log-log plots b) and c), and a decrease in the maximum lineament length.

(a) Table of results from lineaments in the azimuth range of $\sim 150^\circ$ to $\sim 166^\circ$

Lineament directional family sampled	Image resolution	Type of cumulative frequency-length distribution interpreted	Obtained <i>D</i> -value if a power-law distribution is interpreted with 68% significance range	68% confidence limit of <i>D</i> -value
a ¹⁰ (Fig. 7.15a)	150m	Power-law	2.13	± 0.95
b ¹² (Fig. 7.15d)	120m	Log-normal		
c ¹² (Fig. 7.15f)	90m	Log-normal		
d ¹⁹	60m	Log-normal		
e ²⁰	30m	Log-normal		
e ²¹	30m	Log-normal		

(b) Table of results from lineaments in the azimuth range of $\sim 135^\circ$ to $\sim 150^\circ$

Lineament directional family sampled	Image resolution	Type of cumulative frequency-length distribution interpreted	Obtained <i>D</i> -value if a power-law distribution is interpreted with 68% confidence limit	Average length of lineaments
a ⁹	150m	Power-law	2.27	± 0.8
b ¹¹	120m	Log-normal		
c ¹¹	90m	Log-normal		
d ¹⁷	60m	Log-normal		
d ¹⁸	60m	Log-normal		
e ¹⁸	30m	Log-normal		
e ¹⁹	30m	Log-normal		

Table 7.8. The interpreted cumulative frequency-length curves for lineament directional families identified from the 150m to 30m resolution lineament populations of North Cornwall. Tables (a) and (b) are the results obtained for lineaments divided into lineament directional families which lie between $\sim 150^\circ$ to $\sim 166^\circ$ and $\sim 132.5^\circ$ to $\sim 150^\circ$, respectively.

These results show that increasing the image resolution from 150m to 120m steepens the power-law distribution (Figs 7.15a, c) which is, perhaps, better described as a log-normal distribution (Figs 7.15b, d). Removal of longer lineaments from a power-law population can steepen a power-law distribution (Jackson & Sanderson 1992, Pickering *et al.* 1995). Also the addition of shorter lineaments can steepen a power-law distribution. This indicates that with

increasing image pixel resolution the proportion of longer lineaments decreases and shorter lineaments increases, resulting in a steeper power-law distributions which are best described as log-normal distributions. However, fault lengths in samples taken from images with 150m resolutions and in other fault data sets (e.g. Heffer & Bevan 1990) are interpreted to have cumulative frequency-size distributions that remain power-law. A power-law population curve can be extrapolated over several orders of magnitude, certainly beyond the scale range of the images sampled. Therefore, a change in the scaling relationship of a fault population is unlikely to be the cause for the change in the cumulative frequency-size distribution of the lineament subsets. Two possible non-geological causes can therefore be suggested for this proportional change in the lengths of lineaments in these subsets:

(i) In the lineament populations sampled from the area of North Cornwall lineaments which cross-cut the boundary of the image are shortened. Therefore, a type B censoring bias may affect the power-law distributions obtained from North Cornwall (Pickering *et al.* 1995). However, the area of the region is relatively large in size compared to the length of lineaments sampled and therefore this effect is considered to be minimal and would not preferentially affect subsets identified at high pixel resolutions.

(ii) Interpretation of only parts of a long fault-line scarp could also change the ratio between lineament lengths in the subsets, by forming multiple shorter lineaments. With increasing image resolution localised areas comprising of flat topography become identifiable within the images (Fig. 3.18, see Section 3.4) leading to partial fault-line scarp healing. Low resolution images (150m) merge these localised differences, as a result forming a single long lineament. Increasing the image resolution (120m-30m) lowers the limit of resolution resulting

in the localised flat topographic areas becoming visible within the images and the fault-line scarp being interpreted as multiple shorter lineaments.

Irrespective of this precise cause, the analysis of the scaling relationships of fault-related lineament lengths interpreted from pixelated images of sedimentary rocks in a temperate agricultural terrain is probably best conducted upon images with a resolution greater than 120m. Below this resolution lineament lengths may be influenced greatly by factors other than those related to actual fault length.

7.7.3 Effect of image resolution on the scaling relationships of lineament spacing

Line-sampling to find the population curves of the spacing of lineaments divided into lineament directional families in the azimuth ranges of $\sim 132.5^\circ$ to $\sim 150^\circ$ and $\sim 150^\circ$ to $\sim 166^\circ$ (Fig. 7.11) produced small amounts of data. However, sample numbers obtained for the lineaments directional families between $\sim 132.5^\circ$ and $\sim 150^\circ$ were relatively higher, ranging from 12 to 25. As higher sample numbers increase the degree of confidence in the cumulative frequency-size curves obtained, the scaling relationships of the lineament directional families trending between $\sim 132.5^\circ$ and $\sim 150^\circ$ are therefore investigated.

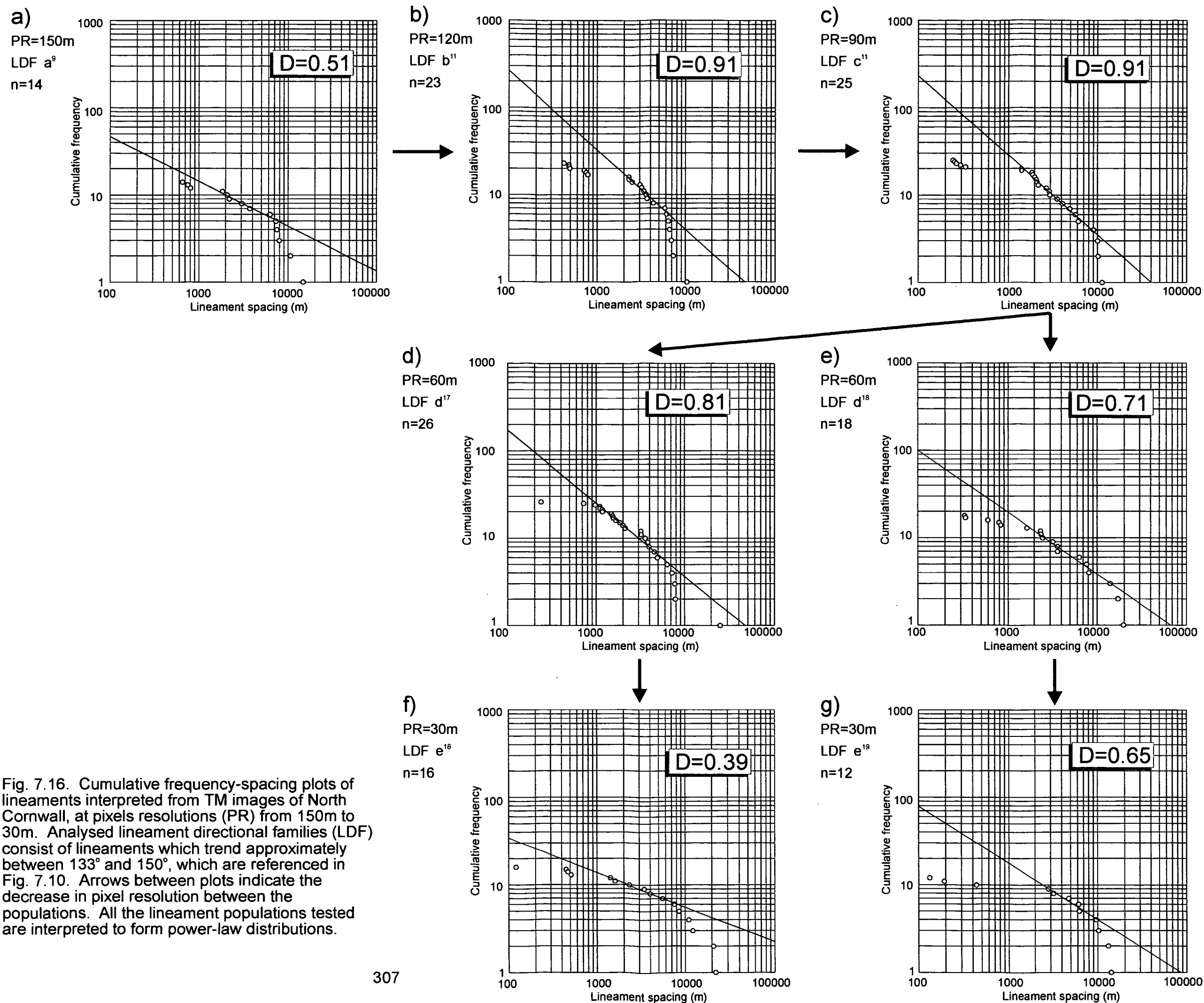
The results are described in Table 7.9 and illustrated in Fig. 7.16.

Lineament directional family sampled	Image pixel size	Number of spacings in sample	Interpreted cumulative frequency-spacing distribution	Approximate size range of central segment	D-value calculated from sample with 68% confidence limit
a ⁹ (Fig. 7.16a)	150m	14	Power-law	2000m-7000m	0.51±0.55
b ¹¹ (Fig. 7.16b)	120m	23	Power-law	2200m-7000m	0.91±0.6
c ¹¹ (Fig. 7.16c)	90m	25	Power-law	1500m-9000m	0.91±0.45
d ¹⁷ (Fig. 7.16d)	60m	26	Power-law	1000m-5000m	0.81±0.42
d ¹⁸ (Fig. 7.16e)	60m	18	Power-law	1500m-15000m	0.71±0.31
e ¹⁸ (Fig. 7.16f)	30m	16	Power-law	1500m-7000m	0.39±0.48
e ¹⁹ (Fig. 7.16g)	30m	12	Power-law	3000m-10000m	0.65±0.68

Table 7.9. The cumulative frequency-spacing curves interpreted from the lineament directional families trending between 132.5° and 150°, which have been identified from the 30m to 150m resolution lineament populations of North Cornwall. Calculated from the obtained power-law distributions are the *D*-values and the *D*-value confidence limits.

The cumulative frequency-size curves for the spacing of lineaments interpreted over the resolution range all suggest power-law distributions. Due to the small sample sizes, however, the power-law distributions obtained from the lineament subsets interpreted from images with resolutions of 150m to 60m and especially 30m, are generally poor. Furthermore, due to the low data numbers the *D*-values obtained are uninterpretable.

Unlike lineament length, however, the interpreted scaling distribution for lineament spacing appears to be unaffected by image resolution. Therefore, whatever the cause of changes in the distribution of lineament length (either a sampling bias or fault-line scarp healing), the cause appears to have little or no affect on lineament spacing. Healing of fault-line scarps will produce topographic effects that either shorten or split lineaments with increasing image resolution.



If the length of lineament which is missing is small the likelihood that a sample line used to identify lineament spacing will intersect this gap is also low. However, the equivalent effect on lineament length is markedly higher. This hypothesis can therefore explain how fault-line scarp healing can affect lineament length and not lineament spacing.

7.7.4 Extrapolating the scaling relationships

Lineament spacing and length have been found to produce power-law distributions across a range of image resolutions. Many samples, however, produce unreliable D -values and poorly constrained power-law distributions due to unacceptably small sample sizes. Hence, extrapolation of the scaling relationships beyond the resolution limit for these power-law distributions will undoubtedly lead to incorrect estimations of the lineament subsets. Increasing the sample size will increase the confidence limits of the interpreted D -value (Pickering *et al.* 1995). A larger sample area would potentially increase the numbers of lineaments in all the sample populations tested in this study. An increase in the sample area to a regional scale also, however, increases lineament mixing (as found for the lineament directional families identified from the lineament population of SW England) causing a degradation of the power-law population curve (Section 7.5.2) or lead to segmented power-laws (as found when lineament directional families representing fault sub-populations were mixed).

Segmented power-laws at distinct image resolutions may suggest that a subset contains different scaling relationships relating to the change in D -value (Fossen & Rornes 1996, Knott *et al.* 1996, Wojtal 1996). Therefore, if a segmented population curve is encountered beyond the sample resolution range this would again give inaccurate estimations of the sample population. This study

indicates that even with minor changes in image scale, segmented power-laws can be identified. The implication of these results for the analysis of the scaling relationships of fault populations is that the D -values obtained may, in some cases, incorrectly estimate the true fault distribution beyond the limit of resolution. However, further rigorous testing with larger datasets is required to improve results.

7.8 Conclusions

(i) Neighbouring lineament directional families identified from lineament populations across SW England were found to possess similar lineament characteristics. This probably reflects lineament mixing rather than over-division of the lineament population. However, by analysing the scaling relationships of lineament directional families interpreted from North Cornwall it was identified that such families possessed dissimilar characteristics. Therefore, the applicability of k -means cluster analysis to accurately define a lineament subset by trend is limited to lineament populations interpreted from images of geologically complex regions with areas smaller in size than the whole of SW England.

(ii) Density maps of the lineament frequency and length of linked lineament directional families provide a useful additional aid to the visual representation of lineaments. Density maps of lineament length were able to specifically identify areas of shortened lineaments related to major cross-cutting faults.

(iii) Linked lineament directional families were found to correlate to known tectonic domains. The density maps reaffirm and, perhaps, increase the importance of the SLFZ in the regional structure of SW England.

(iv) Power-law distributions can be obtained from lineaments interpreted from satellite images, provided the geological nature of the lineaments (e.g. fault-

related) can be determined with confidence. However, confidence limits of estimated D -values obtained in this study are large reflecting low sample numbers. Therefore, for the results in this study the lineament populations should not be extrapolated beyond the limit of image resolution.

(v) Increasing the number of lineaments in the sample reduces the degree of error in the D -values. This can be achieved by increasing the area of the interpreted image. However, sampling lineaments from images at the regional scale results in mixed lineament subsets and a degradation in the obtained cumulative frequency-size distribution.

(vi) The method used to divide a lineament population can greatly affect the cumulative frequency-size distribution obtained. Grouping lineaments related to faults into lineament groups either by rose diagrams or combining lineament directional families results in subsets of mixed lineaments. The degree of mixing may be reduced by using individual lineament directional families.

(vii) The length of lineaments in directional families related to the regional NW/SE to NNW/SSE fault set apparently change from power-law distribution to log-normal distributions as image resolution is increased above 150m. This may be linked to partial fault-line scarp healing.

(viii) Lineament spacing of the same lineament families all form power-law distributions. This may be because the effect of fault-line scarp healing on spacing of these lineament populations is considerably lower.

(ix) Possible segmented power-law distributions are identified from several combined lineament subsets. Segmented power-law distributions were not identified from individual lineament directional families, suggesting that k -means cluster analysis produces a good split to the data as mixing between lineaments related to fault sub-populations, is reduced.

Chapter 8 Conclusions and future work

8.1 Conclusions

Lineament analysis - image processing and lineament identification

(Chapter 3)

Various techniques have been used to reduce the effect of anthropogenic features visible within large map-scale images of a temperate agricultural terrain while enhancing the geological information. From these techniques the following conclusions have become apparent in this study:

(i) The best remotely sensed images available from the NERC archive for lineament analysis in SW England were from the Landsat TM sensor, as they covered the largest area of SW England and possessed a higher range of available bands, of which some suppressed anthropogenic features.

(ii) By decreasing image resolution to 150m the visual impact of anthropogenic features became negligible, hence allowing an increase in image scale to maximise the degree of obtainable geological information. Therefore, on this basis the optimum image resolution for regional lineament analysis in SW England is 150m.

(iii) For low resolution lineament analysis of SW England Landsat TM images of bands 4, 5 and 7 with directional and non-directional filters applied produced the greatest degrees of geological information by increasing the frequency of shorter lineaments.

(iv) Similar bands and processing techniques can be used for interpreting lineaments from higher resolution images (120m, 90m, 60m and 30m). Anthropogenic features become visible in images with resolution of <150m,

therefore, for images with resolutions above 90m the vegetation enhancing band 4 should not be used.

(v) The major lineament trends common in lower resolution images in SW England (150m - 90m) are E/W, N/S, NE/SW and NW/SE. These trends can vary across different domains/sub-areas of SW England.

(vi) The major lineament trends in lineament populations from higher resolution images are different therefore the main lineament trends are not caused by directional filters.

(vii) The geological information in higher resolution images increases in steps, with large increases between 150m to 120m and 90m to 30m and small increases between 120m to 90m. Visual analysis of lineament maps, however, suggests that the knowledge based rules devised to remove anthropogenic features from images with resolutions of <150m may begin to fail in the lineament populations of 60m and 30m.

(viii) Using pixelated images designed to reduce the effect of anthropogenic features causes small directional errors to be imparted to lineaments (maximum of $\sim 2^\circ$) which are sub-parallel or parallel to linear sequences of pixels.

Geological interpretation of the lineament patterns of SW England

(Chapter 4)

(i) Lineament patterns interpreted from the lineament map of SW England suggest different lithotectonic causes, from which different lithotectonic zones of SW England could be delineated.

(ii) The lithotectonic causes of the E/W, N/S, NE/SW and NW/SE trending lineament groups are lithological differences, thrust zones, folds and faults.

Different lithotectonic features possessed similar trends and therefore could form lineament mixtures in lineament groups if the regional lineament population was separated by this method.

(iii) A comprehensive geological history was obtained from the lineament map, suggesting that lineament analysis of pixelated low resolution images of temperate agricultural terrains yield substantial geological information and in SW England the interpretation of the inland geology.

Effect of resolution on the interpreted lineament populations (Chapter 5)

(i) Increasing the image resolution generally resulted in higher degrees of geological information within the interpreted lineament maps from images up to resolutions of 60m. In the 60m and 30m resolution lineament populations the degree of geological information suggested for NE/SW and NW/SE lineaments was lower. This difference is caused by the scale and morphology of the interpreted geomorphological features.

(ii) The effect of anthropogenic features within the images was found to remove lineaments interpreted from the 60m and 30m resolution images. Lineament loss was enhanced in areas with relatively level relief.

(iii) Low lineament resolutions can produce inaccurate lineament patterns from specific lithotectonic structures.

(iv) The scale of the fracture sets within the rock mass can influence at which image resolution the geomorphological expression of these features may form lineaments. The complexity of the geology interpreted is therefore linked to image resolution.

(v) Increasing the image resolution above 150m has not resulted in the identification of large numbers of 'new' major lithotectonic structures. Therefore

such an image resolution is the optimum resolution for regional lineament analysis. To analyse in more detail all the major lithotectonic structures and 'new' minor structures image resolution can be increased up to 60m.

Differentiating lineament directional families using cluster analysis

(Chapter 6)

A new application of the statistical techniques of cluster analysis has been investigated to divide the lineament populations interpreted in this study into lineament directional families. The following conclusions are apparent from this study:

(i) *k*-means clustering, using nearest centroid sorting produced the most geological viable solution, although the number of clusters identified for the final geological solution is subjective.

(ii) The subjectivity in the *k*-means clustering technique can be removed by using the centroid sorting hierarchical cluster method to identify the initial number of clusters. Above 450 bits of data the hierarchical cluster analysis programme rapidly exceeded available computing facilities. This could change with increased computing power.

(iii) The number of lineament directional families identified by *k*-means cluster analysis increases with higher resolution images and greater image size. Thus, higher image resolutions may increase the visibility of smaller features, and larger image areas sample a greater variety of linear features if the bedrock geology is heterogeneous.

(iv) The high numbers of lineament directional families identified from high resolution images of North Cornwall or the large image area of SW England may

be due to over-division of these populations. Alternatively, lineament directional families may overlap.

(v) The change in the number of lineament directional families in lineament populations from increasing image resolutions is caused by continuous (present across the resolution range), dividing and developing (both interpreted with increasing image resolution) lineament directional families.

Geological analysis of lineament directional families in SW England ***(Chapter 7)***

Two methods have been used to further characterise the lineament populations interpreted from North Cornwall and SW England: density maps and scaling relationships. These methods also suggest how geologically realistic is the division of lineament populations into lineament directional families. The following conclusions emerged from this study:

(i) Neighbouring lineament directional families identified from the lineament population from SW England were found to suffer from lineament mixing. Therefore the lineament population was not over-divided by the *k*-means cluster analysis. Lineament mixing can be reduced by interpreting lineaments from the same resolution images of a geologically complex areas by decreasing the image size.

(ii) Linked lineament directional families were found to correlate to known tectonic domains. The density maps reaffirm and, perhaps, increase the importance of the SLFZ in the tectonic evolution of SW England.

(iii) Power-law distributions can be obtained from length and spacing of lineaments identified by their lineament patterns to be related to faulting. However, due to large possible errors in the *D*-values caused by low data

numbers, the extrapolation of power-law distributions obtained in this study beyond the limit of image resolution will lead to incorrect estimations in length and spacing of such fault-related lineament populations.

(iv) Increasing the number of lineaments in the sample will reduce the degree of error in the D -values. This can be achieved by increasing the area of the interpreted image. However, sampling lineaments from images at the regional scale resulted in mixed lineament subsets and a degradation in the obtained cumulative frequency-size distribution.

(v) The method used to divide a lineament population can greatly effect the obtained cumulative frequency-size distribution due to lineament mixing. The least degree of mixing was found to be within individual lineament directional families.

(vi) The scaling relationships for lineament length changed from power-law distribution to log-normal distributions for populations obtained from images with resolutions above 150m. This may be linked to partial fault-line scarp healing.

(vii) Lineament spacing of the same lineament families all form power-law distributions. This may be because the equivalent effect of fault-line scarp healing in these lineaments populations is considerably lower.

(viii) Segmented power-law distributions were identified from the lineament subsets. These were not apparent within individual lineament directional families inferring that k -means clustering produces a good division of the lineament populations by reducing lineament mixing.

8.2 Future work

In this study remote sensing and GIS techniques were combined to aid in the interpretation and analysis of images to investigate the geology within SW England. The GIS allowed the manipulation and analysis of large data sets, simplifying the obtained detailed lineament maps. However, to construct such lineament maps from the initial un-processed images took up to two years. Therefore it is suggested that the geological information gained against the time taken to produce these maps is high for large lineament populations obtained either from small map-scale regional images or an in-depth lineament analysis of large map-scale smaller images. For broad analysis of the regional or localised geology, it may be more time effective to use hard copies of the images, combined with ground truthing.

The analysis of the lineament patterns obtained from the regional lineament population identified previously known geological features, e.g. the SLFZ. However, previously unknown features can be determined. Such an example is the fault network and possible block rotation in North Devon, related to dextral transpression. Future work could involve the analysis of marker beds by palaeomagnetism to determine if block rotation has occurred, although the degree of marker rotation may be below the detectable limit of palaeomagnetism. The increase in geological information obtainable from relatively larger map-scale pixelated low resolution images in comparison to small map-scale high resolution images of a temperate agricultural terrain could be used within the minerals and hydrocarbon industry to identify smaller scale fracture patterns. Within SW England such patterns may identify new metalliferous deposits, although the deposits may not be economically viable.

k-means cluster analysis has been found to produce a good division to the lineament populations obtained within this study, although the final number of lineament directional families is subjective. Further work into cluster algorithms may produce better sub-divisions to the data or the introduction of more powerful computing facilities resolve the subjectivity within the technique. From the analysis of the scaling relationships of lineaments it was found that segmented power-laws were separated by individual lineament directional families. It is therefore considered that clustering techniques could be used to assist in the analysis of scaling relationships of fault populations by determining sub-populations of faults. Such methods are already used to help estimate fault paleostress tensors (Nemcock & Lisle 1995).

Poor confidence limits were typically identified for the *D*-values obtained from the power-law distributions interpreted from lineament directional families of North Cornwall. Therefore, apart from a basic analysis of the effect of resolution on the type of scaling relationships formed, analyses such as extending the obtained distributions could not be attempted. Further work could therefore be attempted on the effect of resolution on lineament populations if larger data sets can be analysed (see Section 7.7.4). Alternatively, larger lineament populations could be interpreted if the sample area consisted of exposed bedrock. This would: (i) increase the scale range of remotely sensed images, e.g. from aerial photography to Landsat TM images, used to identify faulting as the missing anthropogenic features need not be masked by low resolution images; and (ii) allow the identification of outcrop-scale features by the removal of superficial deposits.

References

- Alexander, A.C. & Shail, R.K. 1995. Late Variscan structures on the coast between Perranporth and St. Ives, south Cornwall. *Proceedings of the Ussher Society*, **8**, 398-404.
- Anderberg, M.R. 1973. *Cluster analysis for applications*. Academic Press, Inc., London, 359p.
- Andrews, J.R., Barker, A.J. & Pamplin, C.F. 1988. A reappraisal of the facing confrontation in north Cornwall: fold- or thrust- dominated tectonics? *Journal of the Geological Society, London*, **145**, 777-788.
- Badham, J.P.N. 1982. Strike-slip origins - an explanation for the Hercynides. *Journal of the Geological Society, London*, **139**, 493-504.
- Bagheri, S. & Kiefer, R.W. 1986. Regional geological mapping of digitally enhanced Landsat imagery in the south central Alborz mountains of northern Iran. *Symposium on Remote Sensing for Resources Development and Environmental Management*. Enschede, 555-559.
- Barnes, R.P. & Andrews, J.R. 1986. Upper Palaeozoic ophiolite generation in south Cornwall. *Journal of the Geological Society, London*, **143**, 117-124.
- Beale, E.M.L. 1969. *Cluster Analysis*. Scientific Control Systems Ltd, London.
- Bevan, T.G. & Hancock, P.L. 1986. A Late Cenozoic regional mesofracture system in southern England and northern France. *Journal of the Geological Society, London*, **143**, 355-362.
- Booth, B. & Exley, C.S. 1987. Petrological features of the Land's End Granites. *Proceedings of the Ussher Society*, **6**, 439-446.

Bott, M.H.P., Day, A.A. & Masson-Smith, D. 1958. The geological interpretation of gravity and magnetic surveys in Devon and Cornwall. *Philosophical Transactions of the Royal Society*, **251A**, 161-191.

Bott, M.H.P. & Scott, P. 1964. Recent geophysical studies in South-West England. In: *Present views on some aspects of the geology of Cornwall and Devon*. Royal Geological Society of Cornwall Commemorative Volume for 1964, 26-44.

Bristow, C.M. & Robson, J.L. 1994. Palaeogene basin development in Devon. *Transactions of the Institution of Mining and Metallurgy*, **103**, 163-224.

British Geological Survey. 1969. Boscastle, England and Wales Sheet 322. Solid and Drift Geology. 1:63630. *British Geological Survey, Keyworth, Nottingham*.

British Geological Survey. 1974a. Ivybridge, England and Wales Sheet 349. Solid and Drift Geology. 1:50000. *British Geological Survey, Keyworth, Nottingham*.

British Geological Survey. 1974b. Holdsworth, England and Wales Sheet 323. Solid and Drift Geology. 1:50000. *British Geological Survey, Keyworth, Nottingham*.

British Geological Survey. 1975. Kingsbridge and Start Point, England and Wales Sheet 355 and 356. Solid and Drift Geology. 1:50000. *British Geological Survey, Keyworth, Nottingham*.

British Geological Survey. 1976a. Newton Abbot, England and Wales Sheet 339. Solid and Drift Geology. 1:50000. *British Geological Survey, Keyworth, Nottingham*.

British Geological Survey. 1976b. Torquay, England and Wales Sheet 350. Solid and Drift Geology. 1:50000. *British Geological Survey, Keyworth, Nottingham*.

British Geological Survey. 1977. Plymouth, England and Wales Sheet 348. Solid and Drift Geology. 1:50000. *British Geological Survey, Keyworth, Nottingham.*

British Geological Survey. 1980. Bude, England and Wales Sheet 307+308. Solid and Drift Geology. 1:50000. *British Geological Survey, Keyworth, Nottingham.*

British Geological Survey. 1983. Portland, Sheet 50°N - 04°W. Solid Geology. 1:250000. *British Geological Survey, Keyworth, Nottingham.*

British Geological Survey. 1985. Land's End, Sheet 50°N - 06°W. Solid Geology. 1:250000. *British Geological Survey, Keyworth, Nottingham.*

British Geological Survey. 1988. Bristol Channel. Sheet 51°N - 04°W. Solid Geology. 1:250000. *British Geological Survey, Keyworth, Nottingham.*

British Geological Survey. 1993. Tavistock, England and Wales Sheet 337. Solid and Drift Geology. 1:50000. *British Geological Survey, Keyworth, Nottingham.*

British Geological Survey. 1994. Trevoze Head and Camelford, England and Wales Sheet 335 and 336. Solid and Drift Geology. 1:50000. *British Geological Survey, Keyworth, Nottingham.*

British Geological Survey. 1995. Dartmoor Forest, England and Wales Sheet 338. Solid and Drift Geology. 1:50000. *British Geological Survey, Keyworth, Nottingham.*

Burrough, P.A. 1986. *Principles of Geographic Information Systems for land resources assessment.* Oxford Clarendon Press, Oxford, 194p.

Burton, C.J. & Tanner, P.W.G. 1986. The stratigraphy and structure of the Devonian rocks around Liskeard, east Cornwall, with regional implications. *Journal of the Geological Society, London*, **143**, 95-105.

- Chapman, T.J., Fry, R.L. & Heavey, P.T. 1984. A structural cross-section through SW Devon. *In: Hutton, D.H.W. & Sanderson, D.J. (eds) Variscan Tectonics of the North Atlantic Region*. Special Publications of the Geological Society, London, **14**, 113-118.
- Charman, D.J., & Newnham, R.M. & Croot, D.G. 1996. *The Quaternary of Devon and East Cornwall: field guide*. Quaternary Research Association, London, 224p.
- Chavez, P. 1982. An automatic optimum kernel size selection technique for edge enhancement. *Remote Sensing of the Environment*, **12**, 23-38.
- Childs, C., Walsh, J.J. & Watterson, J. 1990. A method for estimation of the density of fault displacements below the seismic resolution in reservoir formations. *In: Buller, A.T. (ed) North Sea Oil and Gas Reservoirs II*. Graham & Trotman, London, 309-318.
- Conradsen, K., Nilsson, G. & Thyrted, T. 1986. Statistical lineament analysis in South Greenland based on Landsat imagery. *IEEE Transactions on Geoscience and Remote Sensing*, **GE-24** (3), 313-321.
- Coward, M.P. & McClay, K.R. 1983. Thrust tectonics of S Devon. *Journal of the Geological Society, London*, **140**, 215-228.
- Croot, D., Gilbert, A., Griffiths, J., & van der Meer, J. 1996. The character, age and depositional environments of the Fremington Clay Series, North Devon. *In: Charman, D.J., Newnham, R.M. & Croot, D.G. (Eds), The Quaternary of Devon and East Cornwall: field guide*. Quaternary Research Association, London, 14-34.
- Darbyshire, D.P.F. & Shepherd, T.J. 1985. Chronology of granite magmatism and associated minerallisation, SW England. *Journal of the Geological Society, London*, **142**, 1159-1178.

De la Beche, H.T. 1839. Report on the geology of Cornwall, Devon and West Somerset. *Memoirs of the Geological Survey of Great Britain*. Her Majesty's Stationery Office, London, 648p.

Dearman, W.R. 1963. Wrench-faulting in Cornwall and South Devon. *Proceedings of the Geologists' Association*, **74** (3), 265-287.

Dines, H.G. 1956. The Metalliferous Mining Region of Southwest England. *Memoirs of the Geological Survey of Great Britain*. Her Majesty's Stationery Office, London, 795p.

Dobson, M.H. & Rex, D.C. 1971. Potassium - argon ages of slates and phyllites from Southwest England. *Quarterly Journal of the Geological Society, London*, **126**, 465-499.

Drury, S.A. 1986. Remote sensing of geological structure in temperate agricultural terrains. *Geological Magazine*, **123**, 113-121.

Drury, S.A. 1987. *Image interpretation in Geology*. Allen & Unwin, London, 236p.

Durrance, E.M. & Laming, D.J.C. 1982. *The geology of Devon*. University of Exeter Press, 346p.

Edmonds, E.A., Mckeown, M.C. & Williams, M. 1975. British Regional Geology: South-West England. *British Geological Survey, London*. Her Majesty's Stationary Office, London, 138p.

Edmonds, E.A., Whittaker, A. & Williams, B.J. 1985. Geology of the country around Ilfracombe and Barnstaple. *British Geological Survey. Memoir for sheets 277 and 293 NS* 89p.

Edmonds, E.A., Wright, J.E., Beer, K.E., Hawkes, J.R., Williams, M., Freshney, E.C. & Fenning, P.J. 1968. Geology of the country around Okehampton. *Memoirs of the Geological Survey of Great Britain (England and Wales)*, 256p.

Einstein, H.H. & Baecher, G.B. 1983. Probabilistic and Statistical Methods in Engineering Geology, Specific Methods and Examples Part 1: Exploration. *Rock Mechanics and Rock Engineering*, **16**, 39-72.

Embleton, C. 1984. *Geomorphology of Europe*. Macmillan Publishers, London, 465p.

Engel, J.L. & Weinstein, O. 1983. The Thematic Mapper - An Overview. *IEEE Transactions on Geoscience and Remote Sensing*, **GE-21** (3), 258-265.

Everitt, B.S. & Hand, D.J. 1981. *Finite mixture distributions*. Chapman and Hall, London, 143p.

Everitt, B. 1980. *Cluster Analysis*. 2nd Edition, Heinemann Educational Books, London, 136p.

Floyd, P.A., Holdsworth, R.E. & Steele, S.A. 1993. Geochemistry of the Start Complex greenschists: Rhenohercynian MORB? *Geology Magazine*, **130** (3), 345-352.

Fossen, H. & Rornes, A. 1996. Properties of fault populations in the Gullfaks Field, northern North Sea. *Journal of Structural Geology*, **18**, 179-190.

Freshney, E.C., Beer, K.E. & Wright, J.E. 1979a. Geology of the country around Chulmleigh. *Memoirs of the Geological Survey of Great Britain (England and Wales)*, Sheet 309, 69p.

Freshney, E.C., Edmonds, E.A., Taylor, R.E. & Williams, B.J. 1979b. Geology of the country around Bude and Bradworthy. *Memoirs of the Geological Survey of Great Britain (England and Wales)*, 62p.

- Freshney, E.C., McKeown, M.C. & Williams, M. 1972. Geology of the Coast between Tintagel and Bude. *Memoirs of the Geological Survey of Great Britain (England and Wales)*, 92p.
- Freshney, E.C. & Taylor, R.T. 1971. The structure of mid Devon and north Cornwall. *Proceedings of the Ussher Society*, **2**, 241-248.
- Gausman, H.W., Escobar, D.E., Everitt, J.H., Richardson, A.J. & Rodriguez, R.R. 1978. Distinguishing Succulent Plants from Crop and Woody Plants. *Photogrammetric Engineering and remote Sensing*, **44** (4), 487-491.
- Gillespie, P.A., Howard, C.B., Walsh, J.J. & Watterson, J. 1993. Measurement and characterisation of spatial distributions of fractures. *Tectonophysics*, **226**, 113-141.
- Goetz, A.F.H., Rock, B.N. & Lawrence, C.R. 1983. Remote Sensing for Exploration: An Overview. *Economic Geology*, **78** (4), 573-590.
- Greenbaum, D. 1985. Review of Remote Sensing Applications to Groundwater Exploration in Basement and Regolith. *British geological Survey, Remote Sensing and Applied Geophysical Research Group, Keyworth, Nottingham*, 36p.
- Gupta, R.P. 1991. *Remote Sensing Geology*. Springer-Verlag, Berlin, Hiedelburg, New York, 348p.
- Hardcastle, K.C. 1995. Photolineament factor: a new computer-aided method for remotely sensing the degree to which bedrock is fractured. *Photogrammetric Engineering & Remote Sensing*, **61** (6), 739-747.
- Heffer, K.J. & Bevan, T.G. 1990. Scaling Relationships in Natural Fractures: Data, theory, and Application. *Proceedings of the European Petroleum Conference*, **2**, 367-376 (SPE paper No. 20981).

- Hendriks, E.M. 1937. Rock successions and structure in south Cornwall. *Quarterly Journal of the Geological Society*, **93**, 322-367.
- Hendriks, E.M. 1959. A summary of present views on the structure of Cornwall and Devon. *Geological Magazine*, **96**, 253-257.
- Hobson, D.M. 1976a. A structural section between Plymouth and Bolt Tail. *Proceedings of the Geologists' Association, London*, **87**, 27-43.
- Hobson, D.M. 1976b. The structure of the Dartmouth antiform. *Proceedings of the Ussher Society*, **3**, 320-32.
- Hobson, D.M. & Sanderson, D.J. 1983. Variscan Deformation in Southwest England. In: Hancock, P.L. (ed) *The Variscan Fold Belt in the British Isles*. Adam Hilger, Bristol, 108-129.
- Holder, M.T. & Leveridge, B.E. 1986b. Correlation of the Rhenohercynian Variscides. *Journal of the Geological Society, London*, **143**, 141-147.
- Holdsworth, R.E. 1989. The Start-Perranporth line: a Devonian terrane boundary in the Variscan orogen of SW England. *Journal of the Geological Society, London*, **146**, 419-422.
- Holloway, S. & Chadwick, R.A. 1986. The Sticklepath-Lustliegh fault zone: Tertiary sinistral reactivation of a Variscan dextral strike-slip fault. *Journal of the Geological Society, London*, **143**, 447-452.
- Hopper, A.J. 1996. Remote sensing detection of landfill pollutant migration. *Proceedings of the 22nd Annual Conference of the Remote Sensing Society*, 281-289.
- Isaac, K.P. 1981. The Hercynian geology of Lydford Gorge, north-west Dartmoor, and its regional significance. *Proceedings of the Ussher Society*, **5**, 147-152.

Isaac, K.P., Chandler, P., Whiteley, M.J. & Turner, P.J. 1983. An excursion guide to the geology of central South West England: report on the field meeting to West Devon and East Cornwall, 28-31 May 1982. *Proceedings of the Geologists' Association*, **94**, 357-376.

Isaac, K.P. 1985. Thrust and nappe tectonics of west Devon. *Proceedings of the Geologists' Association*, **96** (2), 109-127.

Isaac, K.P., Turner, P.J. & Stewart, I.J. 1982. The evolution of the Hercynides of central SW England. *Journal of the Geological Society, London*, **96** (2), 129-141.

Jackson, R.R. 1991. Vein arrays and their relationship to transpression during fold development in the Culm Basin, central South-West England. *Proceedings of the Ussher Society*, **7**, 356-362.

Jackson, P. & Sanderson, D.J. 1992. Scaling of fault displacements from the Badajoz-Cordoba shear zone, SW Spain. *Tectonophysics*, **210**, 179-190.

James, J.M. & Moore, J.Mc. 1985. Multi-seasonal imagery studies for geological mapping and prospecting in cultivated terrain of S.W. England. *Proceedings of the International Symposium on the Remote Sensing of the environment, Fourth Thematic Conference - Remote Sensing for Exploration Geology. San Francisco, California*, 475-484.

Jolly, R.J.H. & Sanderson, D.J. 1995. Variation in the form and distribution of dykes in the Mull swarm, Scotland. *Journal of Structural Geology*, **17** (11), 1543-1557.

Kirkham, M.B. & Kanemasu, E.T. 1983. Wheat. *In*: Teare, I.D. & Peet, M.M (eds). *Crop water relations*. John Wiley & Sons, New York, 547p.

- Knott, S.D., Beach, A., Brockbank, P.J., Brown, J.L., McCallum, J.E. & Welbon, A.I. 1996. Spatial and mechanical controls on normal fault populations. *Journal of Structural Geology*, **18** (2/3), 359-372.
- Lee, M.K., Pharaoh, T.C. & Soper, N.J. 1990. Structural trends in central Britain from images of gravity and aeromagnetic fields. *Journal of the Geological Society, London*, **147**, 241-258.
- Leibowitz, H. 1953. Some observations and theory of the variation of visual acuity with the orientation of the test objects. *Journal of the Optical Society of America*, **43**, 902-905.
- Leveridge, B.E., Holder, M.T. & Day, G.A. 1984. Thrust nappe tectonics in the Devonian of south Cornwall and the western English Channel. *In*: Hutton, D.H.W. & Sanderson, D.J. (eds) *Variscan Tectonics of the North Atlantic Region*. Special Publications of the Geological Society, London, **14**, 103-112.
- Leveridge, B.E., Holder, M.T. & Goode, A.J.J. 1990. Geology of the country around Falmouth. *Memoir of the British Geological Survey, Sheet 352 (England and Wales)*, 70p.
- Lister, H.T. 1989. Structural evolution of the Rusey fault zone, North Cornwall, and implications for coastal stability. *Unpublished BSc thesis, University of Plymouth*, 112p.
- LLoyd, G.E. & Whalley, J.S. 1986. The modification of chevron folds by simple shear: examples from north Cornwall and Devon. *Journal of the Geological Society, London*, **143**, 89-94.
- MacQueen, J. 1967. some methods for classification and analysis of multivariate observations. *Proceedings of the 5th Berkely Symposium*, **1**, 281-297.

- Mah, A., Taylor, G.R., Lennox, P. & Balia, L. 1995. Lineament analysis of Landsat Thematic Mapper images, Northern Territory, Australia. *Photogrammetric Engineering & Remote Sensing*, **61** (6), 761-773.
- Mandl, G. 1987. Tectonic deformation by rotating parallel faults the "bookshelf" mechanism. *Tectonophysics*, **141**, 277-316.
- Mapeo, R.B.M. 1992. The structure and tectonics of the Bude Formation, North Cornwall, SW England. *Ph.D. Thesis, University of Southampton*, unpaginated.
- Moore, J.Mc. & Camm, S. 1982. Interactive enhancement of Landsat imagery for structural mapping in tin-tungsten prospecting: A case history of S.W. England orefield. *Proceedings of the International Symposium on the Remote Sensing of the environment, Second Thematic Conference - Remote Sensing for Exploration Geology. Fort Worth, Texas*, 727-740.
- Mostafa, M.E. & Qari, M.Y.H.T. 1995. An exact technique of counting lineaments. *Engineering Geology*, **39**, 5-16.
- Needham, T., Yielding, G. & Fox, R. 1996. Fault population description and prediction using examples from the offshore U.K. *Journal of Structural Geology*, **18** (2/3), 155-167.
- Nemcock, M. & Lisle, R.J. 1995. A stress inversion procedure for polyphase fault/slip data sets. *Journal of Structural Geology*, **17** (10), 1445-1453.
- O'Leary, D.W., Friedman, J.D. & Pohn, H.A. 1976. Lineament, linear, lineation: Some proposed new standards for old terms. *Geological Society of America*, **87**, 1463-1469.
- Peacock, D.C.P. & Sanderson, D.J. 1994. Strain and scaling of faults in the chalk at Flamborough Head, U.K.. *Journal of Structural Geology*, **16** (1), 97-107.

- Pickering, G., Bull, J.M. & Sanderson, D.J. 1995. Sampling power-law distributions. *Tectonophysics*, **248**, 1-20.
- Pickering, G., Bull, J.M., Sanderson, D. & Harrison, P.V. 1994. Fractal Fault Displacements: A Case Study from the Moray Firth, Scotland. *In: Kruhl, J.H. (ed.) Fractals and Dynamic Systems in Geoscience*. Springer-Verlag, Frankfurt, 105-119.
- Prost, G.L. 1989. Recognising thrust faults, and exploration implications. *Proceedings of the Seventh Thematic Conference on Remote Sensing for Exploration Geology*, **2**, 1111-1123.
- Qari, M.Y.H.T. & Sen, Z. 1994. Remotely sensed fracture patterns in southwestern Saudi Arabia and qualitative analysis. *Bulletin of the International Association of Engineering Geology*, **49**, 63-72.
- Ranalli, G & Hardy, L. 1990. Statistical approach to brittle fracture in the Earth's crust. *In: Agterberg, F.P. & Bonham-Carter (Eds), Statistical Applications to the Earth Sciences*. Geological Survey of Canada, Papers, 89-9, 255-262.
- Randall, D.E., Taylor, G.K. & Grocott, J.G. 1996. Major crustal rotations in the Andean margin: Paleomagnetic results from the Coastal Cordillera of northern Chile. *Journal of Geophysical Research*, **101**, 15783-15798.
- Rathey, P.R. & Sanderson, D.J. 1982. Patterns of folding within nappes and thrust sheets: examples from the Variscan of Southwest England. *Tectonophysics*, **88**, 247-267.
- Robinson, S.G. 1976. Edge detection by compass gradient masks. *Computer Graphics and Image Processing*, **6**, 492-501.
- Sanderson, D.J. & Dearman, W.R. 1973. Structural zones of the Variscan fold belt in SW England, their location and development. *Journal of the Geological Society, London*, **145**, 789-800.

- Sawatsky, D.L. & Raines, G.L. 1981. Geologic uses of linear-feature maps derived from small scale images. *Proceedings of the 3rd Conference on Basement Tectonics*, 91-100.
- Schowengerdt, R.A. 1983. *Techniques for image processing and classification in remote sensing*. Orlando, Florida: Academic Press, 248p.
- Schreurs, G. 1994. Experiments on strike-slip faulting and block rotation. *Geology*, **22**, 567-570.
- Scrivener, R. C., Darbyshire, D. P. F. & Shepherd, T.J. 1994. Timing and significance of crosscourse minerallisation in SW England. *Journal of the Geological Society, London*, **151**, 587-590.
- Seago, R.D. & Chapman, T.J. 1988. The confrontation of structural styles and the evolution of a foreland basin in central SW England. *Journal of the Geological Society, London*, **145**, 789-800.
- Sedgwick, A. & Murchison, R.I. 1837. Classification of the older stratified rocks of Devonshire and Cornwall. *London and Edinburgh Philosophical Magazine and Journal of Science*, **14**, 241-260 and 354.
- Selby, M.J. 1993. *Hillslope materials and processes*. Oxford University Press, Oxford. 451p.
- Selwood, E.B. 1990. A review of basin development in central South-West England. *Proceedings of the Ussher Society*, **7**, 199-205.
- Selwood, E.B., Edwards, R.A., Simpson, S., Chesher, J.A., Hamblin, R.J.O., Henson, M.R., Riddolls, B.W. & Waters, R.A. 1984. Geology of the country around Newton Abbot. *Memoirs of the British Geological Survey, Sheet 339*, 212p.

- Selwood, E.B., Stewart, I.J. & Thomas, J.M. 1985. Upper Palaeozoic sediments and structure in north Cornwall - a reinterpretation. *Proceedings of the Geologists' Association, London*, **96**, 129-41.
- Selwood, E.B. & Thomas, J.M. 1986a. Variscan facies and structures in central SW England. *Journal of the Geological Society, London*, **143**, 199-207.
- Selwood, E.B. & Thomas, J.M. 1986b. Upper Palaeozoic successions and nappe structures in north Cornwall. *Journal of the Geological Society, London*, **143**, 75-82.
- Shackleton, R. M., Ries, A.C. & Coward M.P. 1982. An interpretation of the Variscan structures in SW England. *Journal of the Geological Society, London*, **139**, 533-541.
- Shail, R.K. 1989. Gramscatho-Mylor facies relationships; Hayle, south Cornwall. *Proceedings of the Ussher Society*, **7**, 125-130.
- Shail, R.K. & Alexander, A.C. 1997. Late Carboniferous to Triassic reactivation of Variscan basement in the western English Channel: evidence from onshore exposures in south Cornwall. *Journal of the Geological Society, London*, **154**, 163-168.
- Siegal, B. S. & Gillespie, A. R. 1980. *Remote sensing in Geology*. Wiley, New York, 694p.
- Smithurst, L.J.M. 1990. Structural remote sensing of South-West England. *Proceedings of the Ussher Society*, **7**, 236-241.
- SPSS, Inc. 1988. *SPSS-X User Guide*. 3rd Edition, 1072p.
- SPSS, Inc. 1990. *SPSS/PC+ Statistics 4.0 for the IBM PC/XT/AT + PS/2*, 273p.

- Tanner, P.W.G. 1985. Structural history of the Devonian rocks south of Liskeard, East Cornwall. *Proceedings of the Ussher Society*, **6**, 155-164.
- Thomas, J.M. 1988. Basin history of the Culm Trough of Southwest England. In: Besley, B.M. & Kelling, G.(eds) *Sedimentation in a Synorogenic Basin Complex: the Upper Carboniferous of Northwest Europe*. Blackie, Glasgow and London, 24-37.
- Turner, P.J. 1985. Stratigraphical and structural variations in the Lifton-Marystow area, West Devon, England. *Proceedings of the Geologists' Association, London*, **96** (4), 323-335.
- Turner, P.J. 1986. Stratigraphical and structural variations in central SW England: a critical appraisal. *Proceedings of the Geologists' Association, London*, **97** (4), 331-345.
- Thornbury, W.D. 1954. *Principles of Geomorphology*. John Wiley & Sons, London, 618 p.
- Walsh, J.J. & Watterson, J. 1988a. Analysis of the relationship between displacements and dimensions of faults. *Journal of Structural Geology*, **10**, 239-247.
- Walsh, J.J. & Watterson, J. 1988b. Dips of normal faults in British Coal measures and other sedimentary sequences. *Journal of the Geological Society, London*, **145**, 859-873.
- Warr, L.N. 1989. The structural evolution of the Davidstow Anticline, and its relationship to the Southern Culm Overfold, north Cornwall. *Proceedings of the Ussher Society*, **7**, 136-140.
- Watterson, J., Walsh, J.J., Gillespie, P.A. & Easton, S. 1996. Scaling relationships of fault sizes on a large-scale range fault map. *Journal of Structural Geology*, **18** (2/3), 199-214.

Wheeler, R.L. 1983. Linesmanship and the practice of linear geo-art: Discussion and Reply. *Geological Society of American Bulletin*, **94**, 1377-1378.

Whittle, R.A., Gutmanis, J.C. & Shilston, D.T. 1983. Using satellite imagery to detect faults. *Ground Engineering*, **16**, No.1, 26-28.

Wilkinson, J.J. & Knight, R.R.W. 1989. Palynological evidence from the Porthleven area, south Cornwall. *Journal of the Geological Society, London*, **146**, 739-742.

Wise, D.U. 1982. Linesmanship and the practice of linear geo-art. *Geological Society of American Bulletin*, **93**, 886-888.

Wise, D.U. 1983. Linesmanship and the practice of linear geo-art: Discussion and Reply. *Geological Society of American Bulletin*, **94**, 1379.

Wise, D.U., Funicello, R., Parotto, M. & Salvini, F. 1985. Topographic lineament swarms: Clues to their origins from domain analysis of Italy. *Geological Society of America Bulletin*, **96**, 952-967.

Wojtal, S. 1994. Fault scaling laws and the temporal evolution of fault systems. *Journal of Structural Geology*, **16**, 603-612.

Wojtal, S.F. 1996. Changes in fault displacement populations correlated to linkage between faults. *Journal of Structural Geology*, **18** (2/3), 265-279.

Wolfe, J.H. 1970. Pattern Clustering by multi-variate mixture analysis. *Multivariate Behavioural Research*, **13**, 33-44.

Woodcock, C.E. & Strahler, A.H. 1987. The factor of scale in remote sensing. *Remote Sensing of Environment*, **21**, 311-332.

Yielding, G., Needham, T. & Jones, H. 1996. Sampling of fault populations using sub-surface data: a review. *Journal of Structural Geology*, **18** (2/3), 135-146.

Yielding, G., Walsh, J. & Watterson, J. 1992. The prediction of small-scale faulting in reservoirs. *First Break*, **10** (12), 449-460.

Appendix 1

Process for constructing lineament density maps

The formation of lineament density maps was conducted with the use of ARC/INFO and essentially proceeded in two stages: the conversion of the lineament map into a grid where the number of lineaments and the total lineament length were counted (stage 1); and the compilation of this output into a graphic form (stage 2).

(i) Stage 1, counting the number or length of lineaments

This programme was written in ARC/INFO Macro Language, in conjunction with Dr K. Morris. The arguments entered are the lineament to be converted (cover), the size of the grid, and the geographical co-ordinates.

```
&args cover gridsize xmin ymin xmax ymax
/* AML to produce lineament density, length and RFI isopleth maps
&sv xstart = %xmin%
&if [exists isofreq.asc -file] &then ; &sys rm -f isofreq.asc
&if [exists isolength.asc -file] &then ; &sys rm -f isolength.asc
&sv numrows = ( %ymax% - %ymin% ) / %gridsize%
&sv numcols = ( %xmax% - %xmin% ) / %gridsize%
&sys ~/iso/createheader isofreq.asc %numcols% %numrows% %xmin% %ymin%
%gridsize%
&sys ~/iso/createheader isolength.asc %numcols% %numrows% %xmin%
%ymin% %gridsize%
&sv filefreq = [open isofreq.asc openstatus -append]
&sv filelength = [open isolength.asc openstatus -append]
&do &while %ymax% > %ymin%
    &sv xmin = %xstart%
    &sv ytop = %ymax%
```

```

&sv ybot = %ytop% - %gridsize%
&do &while %xmin% < %xmax%
    &sv xright = %xmin% + %gridsize%
    &if [exists isoclip -cover] &then; kill isoclip all
    &if [exists templin -cover] &then; kill templin all
generate isoclip
lines
1
%xmin% %ybot%
%xmin% %ytop%
%xright% %ytop%
%xright% %ybot%
%xmin% %ybot%
end
end
q
    build isoclip poly
    clip %cover% isoclip templin line 0.0000000001
    build templin line
    ap
    statistics templin arc
        sum length
    end
    &sv sum1 = [show statistic 1 1]
    reselect templin arc length > 0
    &sv num1 = [before [show select templin arc] , ]
    &if %num1% = 0 &then &do
        &sv num1 = -9999
        &sv sum1 = -9999
    &end
    &sv temp = [write %filefreq% %num1%]
    &sv temp = [write %filelength% %sum1%]
    &lv %sum1%
    &lv %num1%

```

```

q
&sv xmin = %xright%
&end
&sv ymax = %ybot%
&end

```

(ii) Stage 2, Conversion into a graphical output

```

Asciigrid [FN1] [FN2]      (converts the output from the macro into a grid)
Latticetin [FN2] [FN3]     (creates a tin from the grid)
Tinarc [FN3] [FN4] point   (converts the TIN nodes from the grid into points)

```

```

Createtin NAME              (forms a boundary to the TIN)
cover [FN4] point
cover [digitised area of region] poly [digitised area of region]-id 7
END

```

```

Tinlattice NAME [FN5] Quintic (converts a TIN to a lattice by interpolation of
                                mesh points using the bivariate quintic
                                method,
                                the lattice size is 300m and hence the TIN
                                appears graded)

```

```

Tincontour [FN5] [FN6] interval base contour
                                (to obtain contours if neccesary)

```

Appendix 2

Density maps of lineament directional families identified by cluster analysis from the lineament population of SW England (Fig. A2.1).

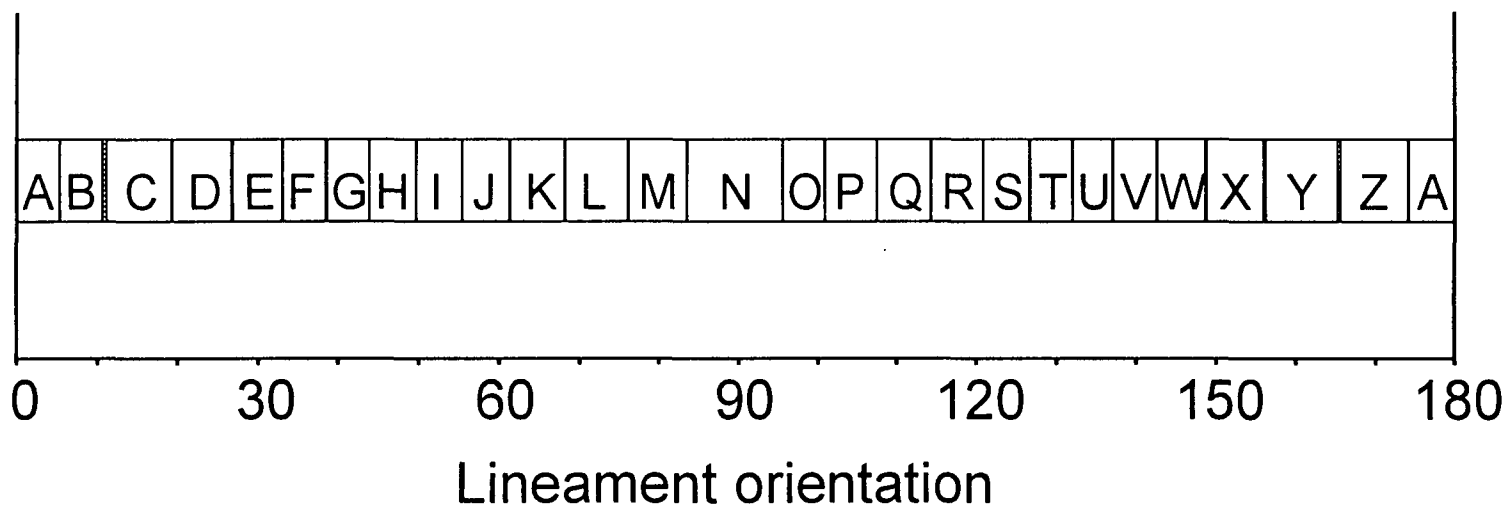
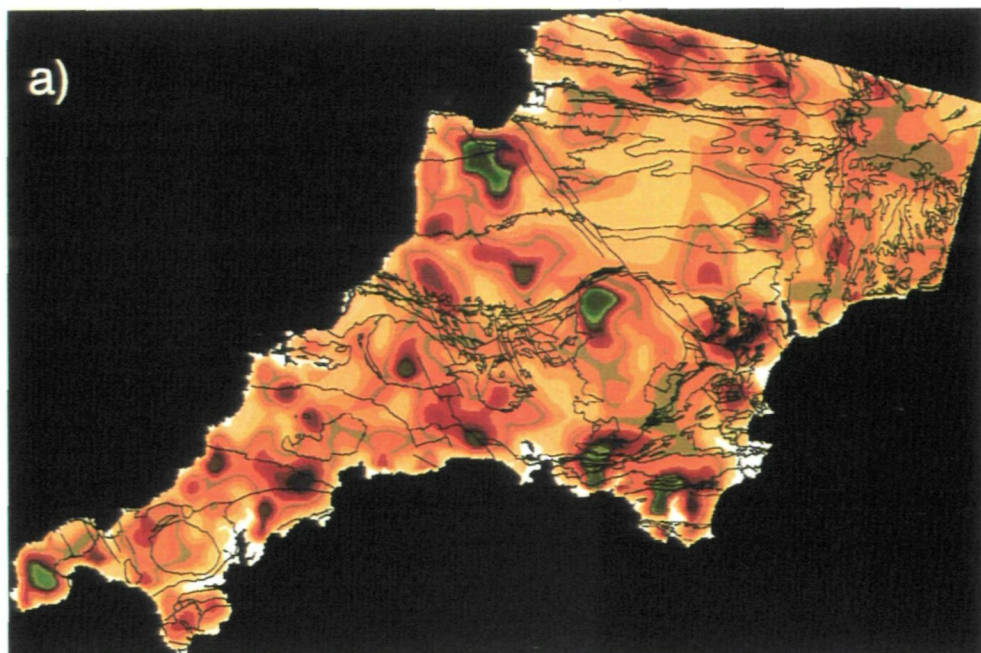
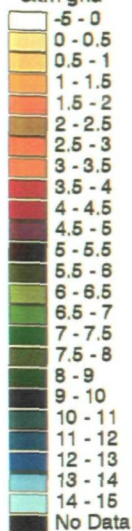


Fig. A2.1. Diagram showing the azimuth ranges of lineament directional families (represented as boxes) identified from SW England. Each lineament directional family has been labelled with a letter.

KEY
Outline of the
geology of SW
England

Lineament
frequency/
5km grid



KEY
Outline of the
geology of SW
England

Lineament
length (m)/
5km grid

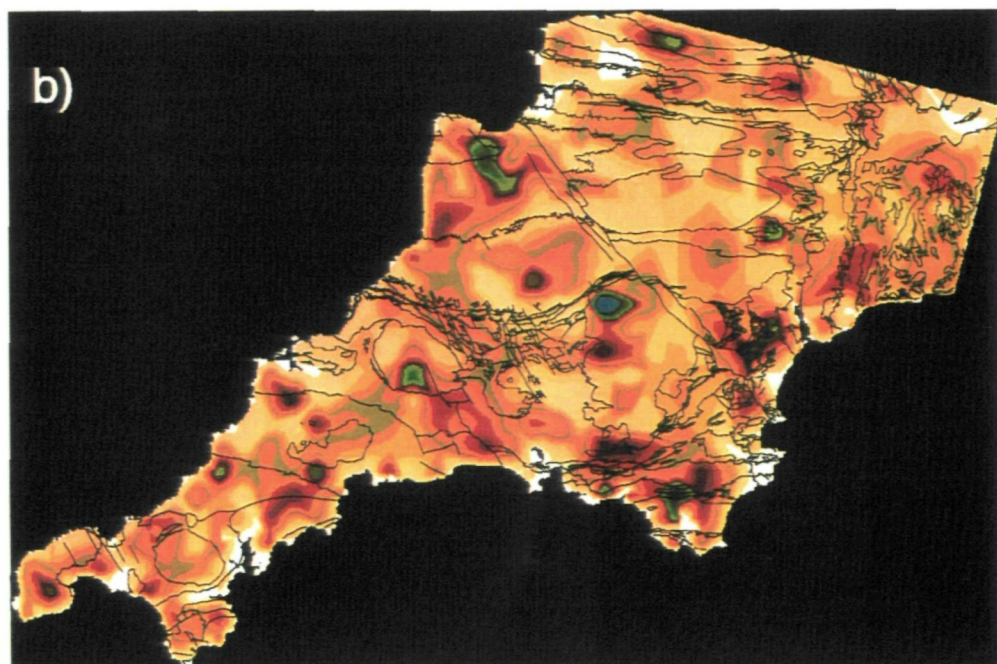
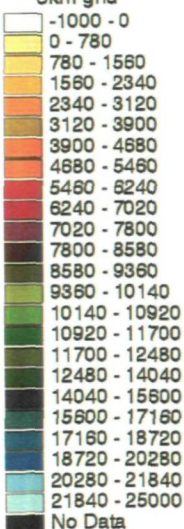
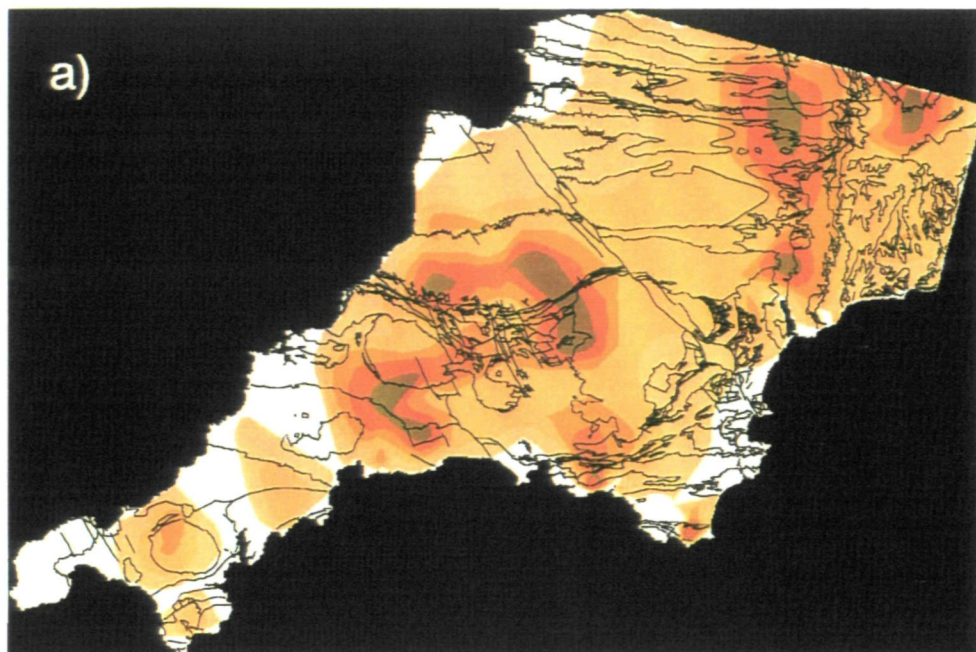
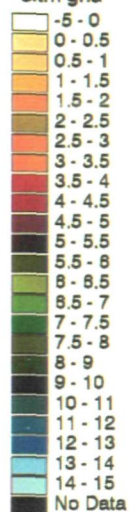


Fig. A2.2. Density maps of a) frequency and b) length of lineaments divided into the lineament directional families Z and A (see Fig. A2.1), from the lineament population of SW England.

KEY
Outline of the
geology of SW
England

Lineament
frequency/
5km grid



KEY
Outline of the
geology of SW
England

Lineament
length (m)/
5km grid

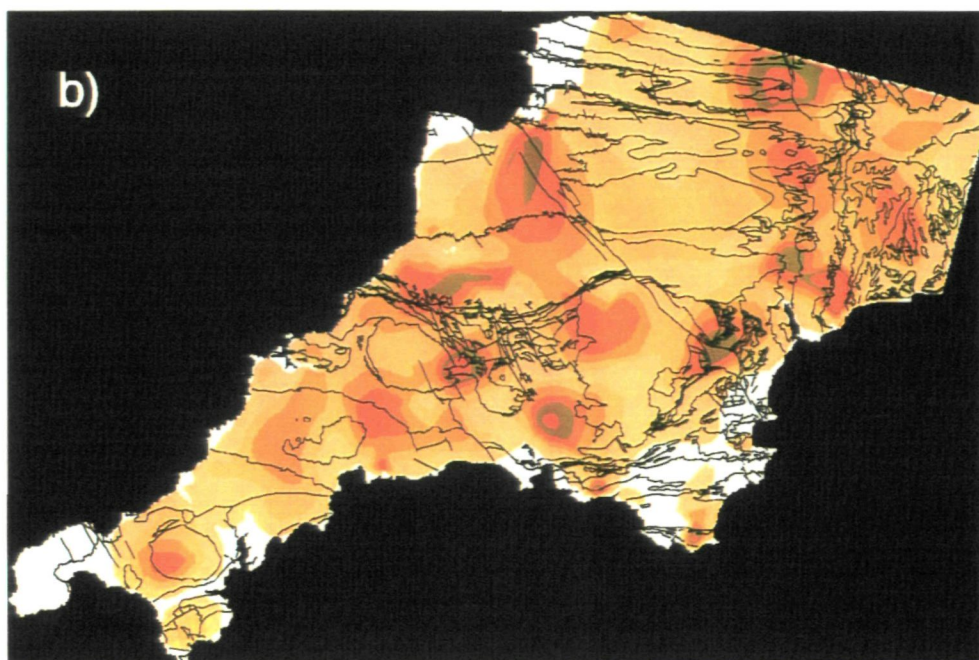
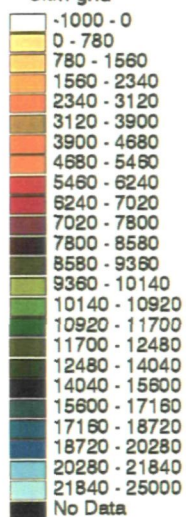
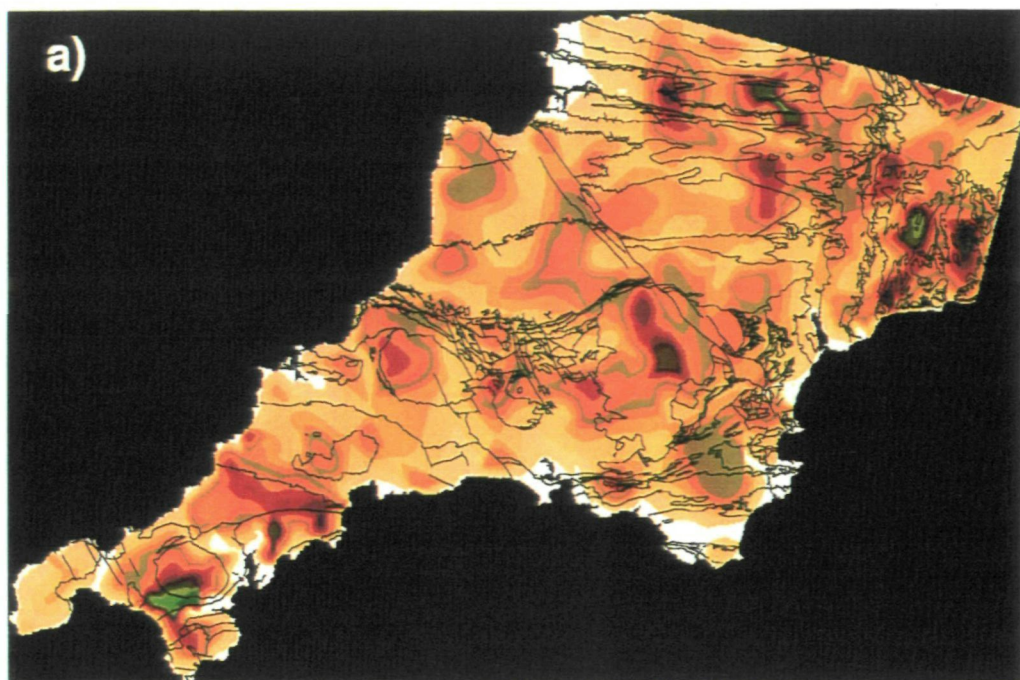
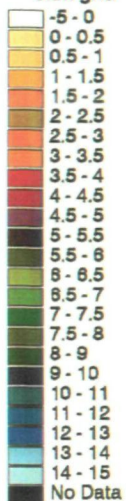


Fig. A2.3. Density maps of a) frequency and b) length of lineaments in the lineament directional family B, a subset of the SW England lineament population.

KEY

Outline of the
geology of SW
England

Lineament
frequency/
5km grid



KEY

Outline of the
geology of SW
England

Lineament
length (m)/
5km grid

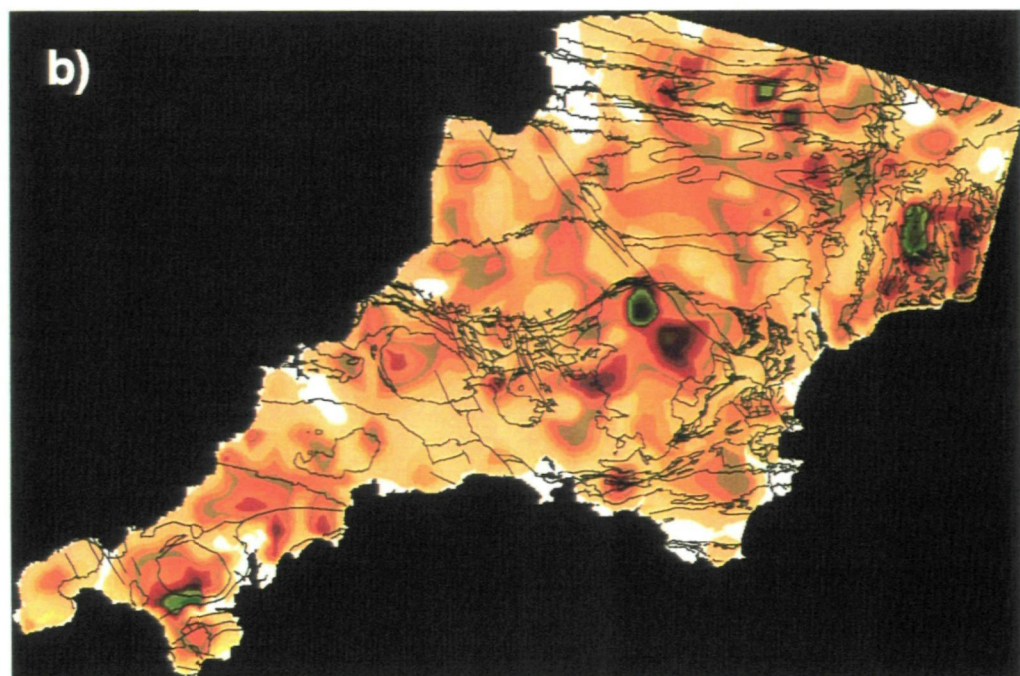
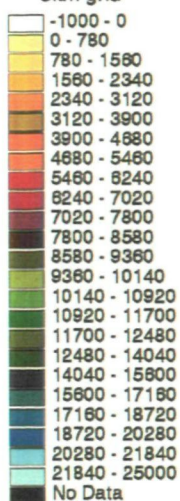
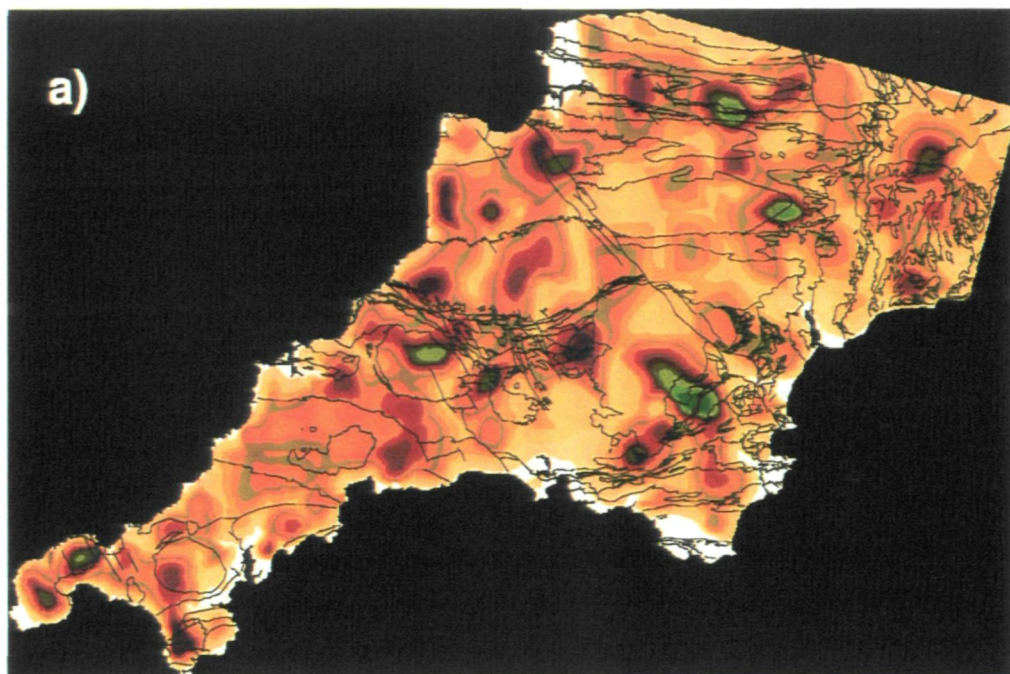
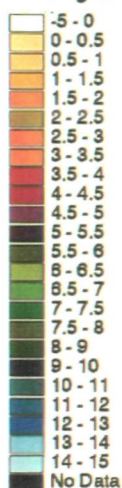


Fig. A2.4. Density maps of a) frequency and b) length of lineaments in the linked lineament directional families C, D and E, subsets of the regional lineament population.

KEY

Outline of the
geology of SW
England

Lineament
frequency/
5km grid



KEY

Outline of the
geology of SW
England

Lineament
length/
5km grid

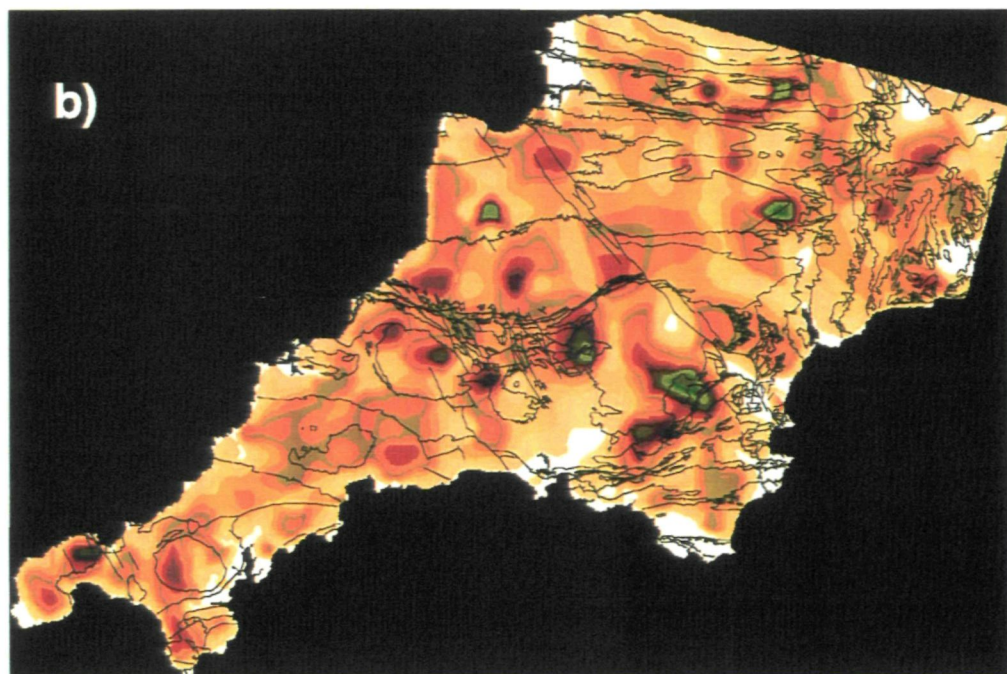
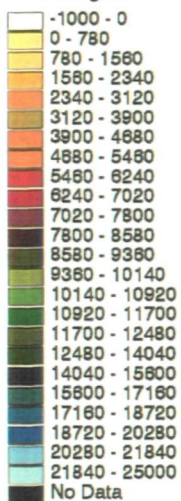
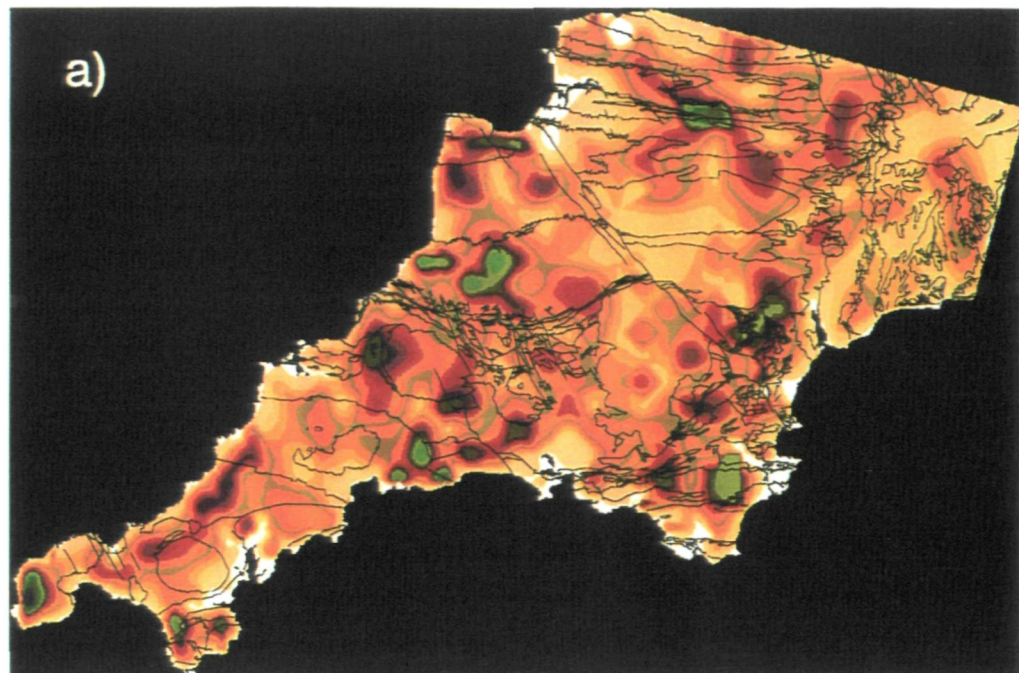
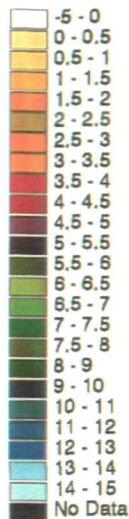


Fig. A2.5. Density maps of a) lineament frequency and b) lineament length of the linked directional families F and G, subsets of the SW England lineament population.

KEY
Outline of the
geology of SW
England

Lineament
frequency/
5km grid



KEY
Outline of the
geology of SW
England

Lineament
length (m)/
5km grid

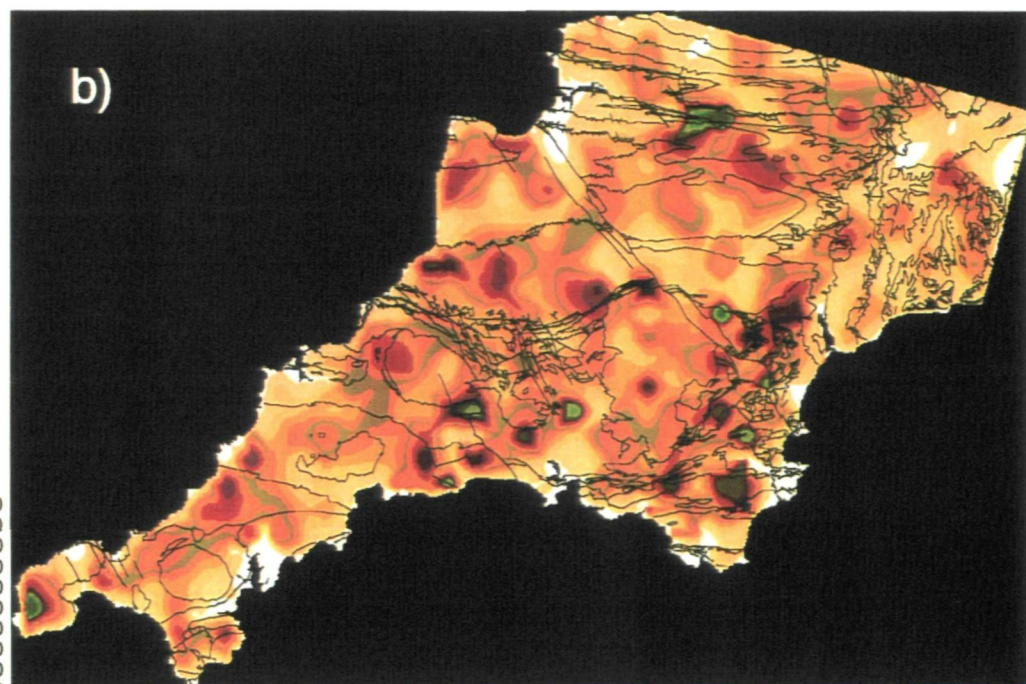
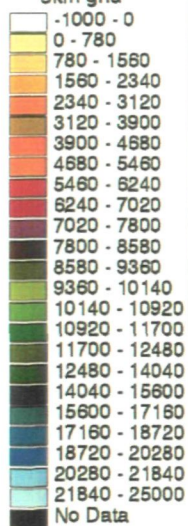
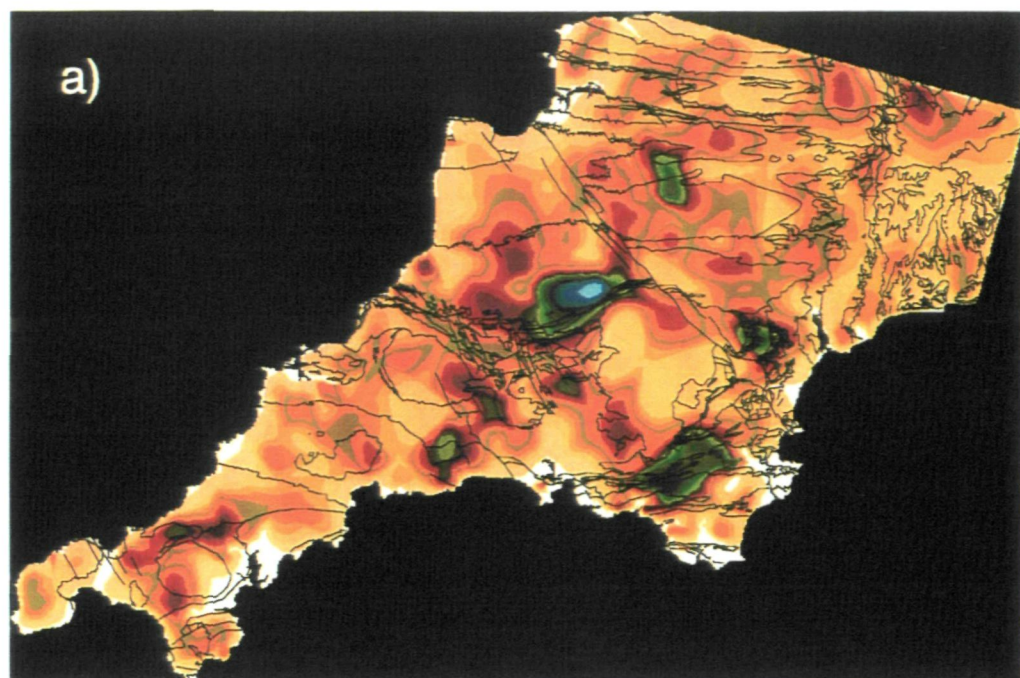
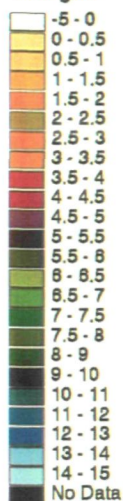


Fig. A2.6. Density maps of a) lineament frequency and b) length of the linked directional families H and I, identified from the regional lineament population.

KEY
Outline of the
geology of SW
England

Lineament
frequency/
5km grid



KEY
Outline of the
geology of SW
England

Lineament
length/
5km grid

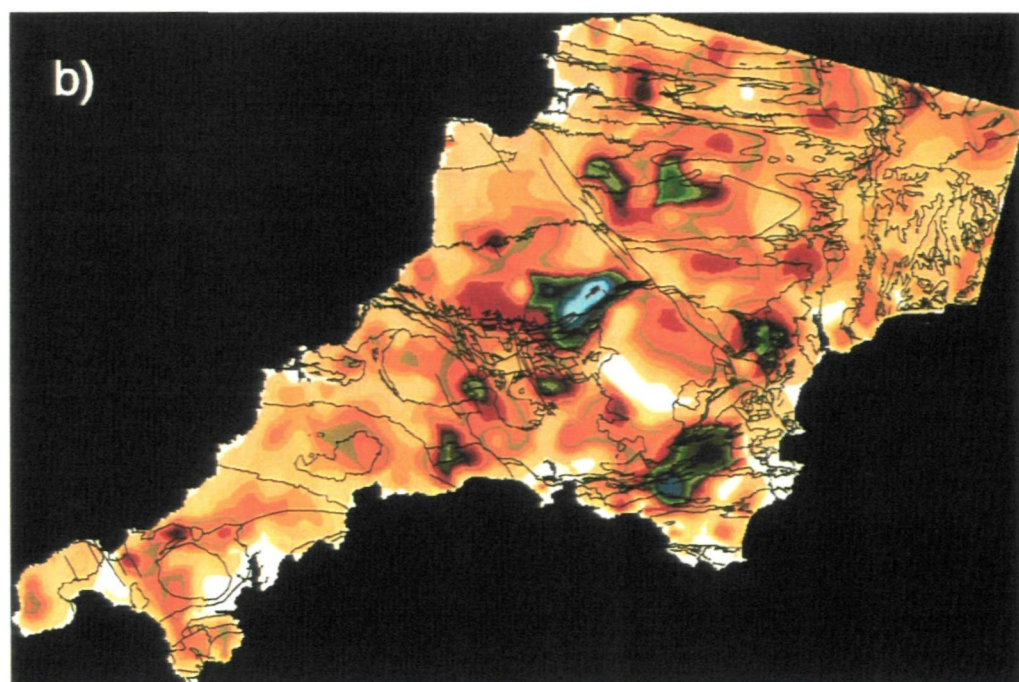
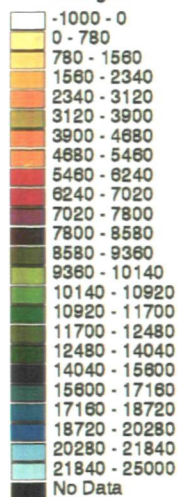
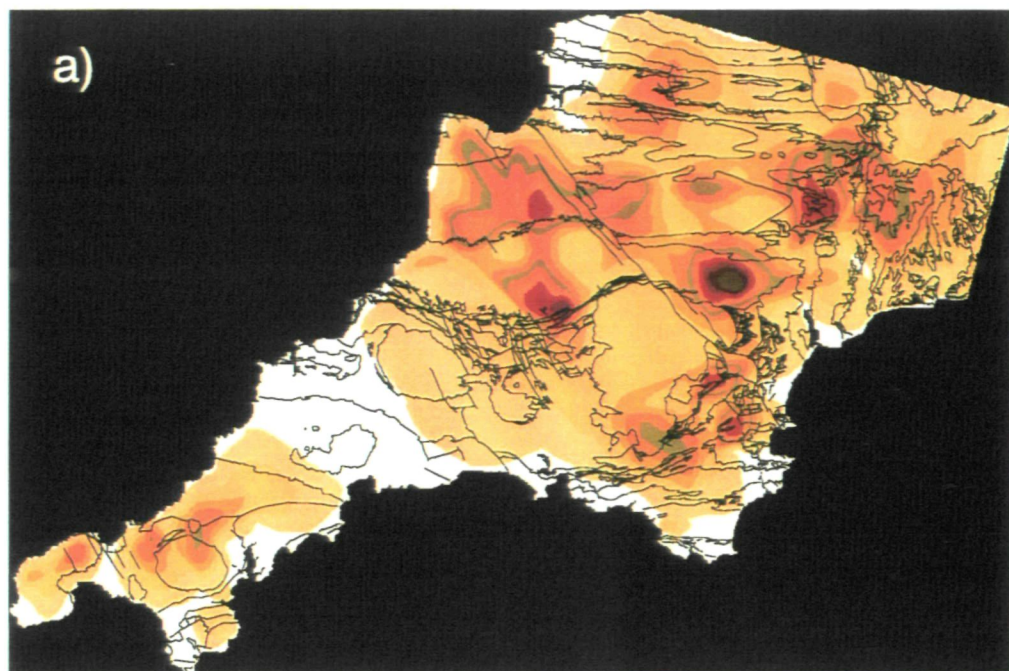
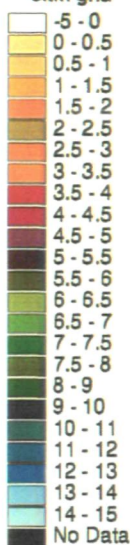


Fig. A2.7. Density maps of a) frequency and b) length of lineaments of the linked directional families J and K, subsets of the SW England lineament population.

KEY
Outline of the
geology of SW
England

Lineament
frequency/
5km grid



KEY
Outline of the
geology of SW
England

Lineament
length (m)/
5km grid

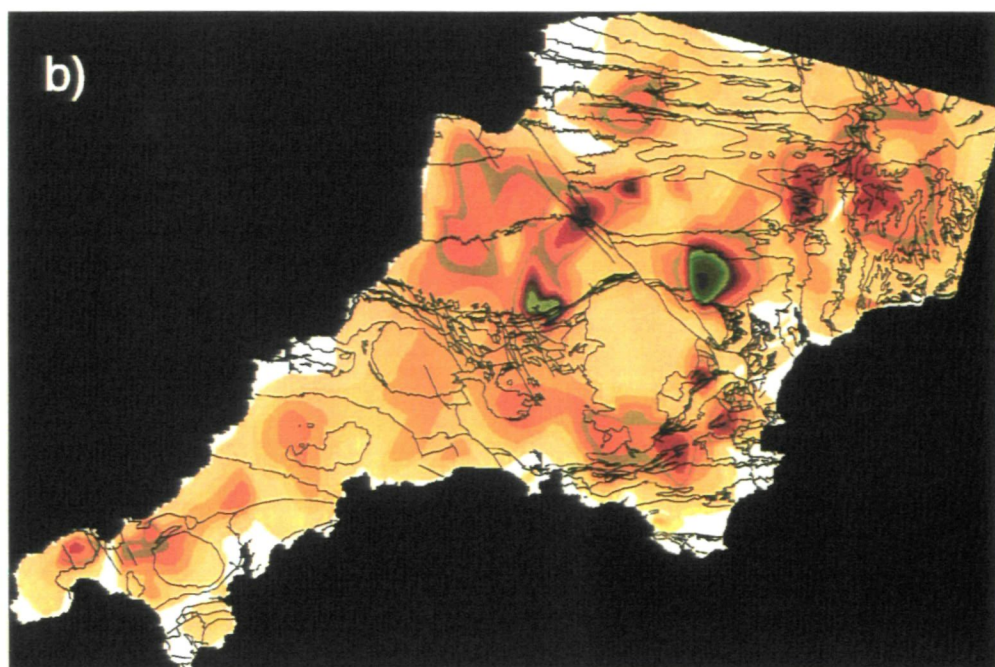
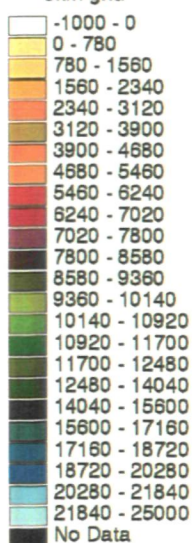
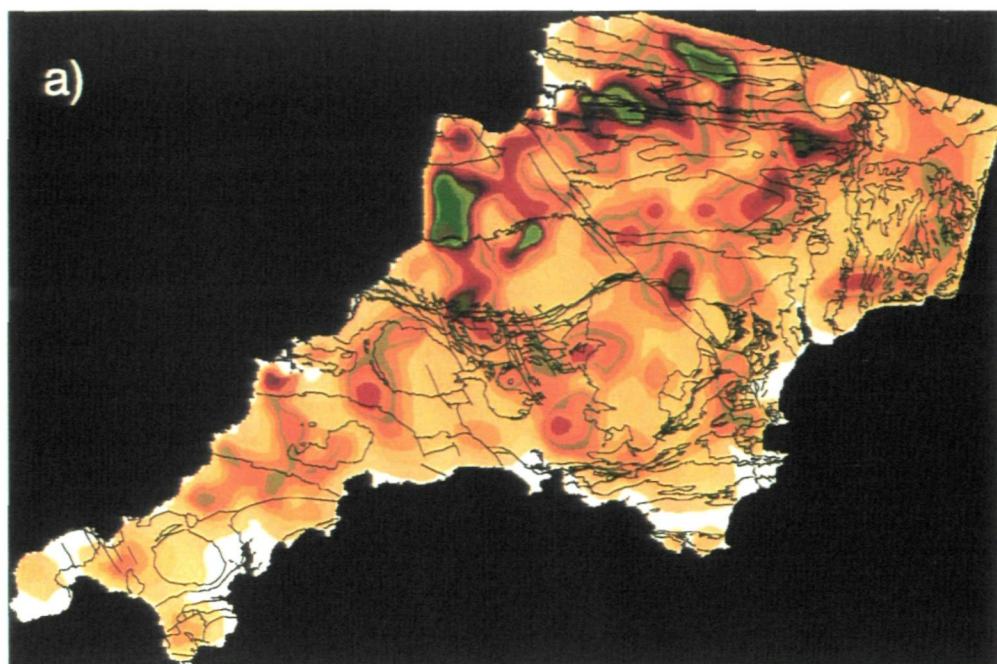
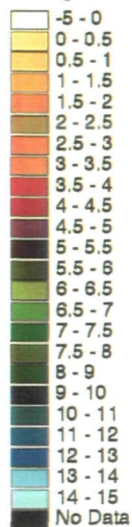


Fig. A2.8. Density maps of a) frequency and b) length of the directional family L identified from the SW England lineament population.

KEY
Outline of the
geology of SW
England

Lineament
frequency/
5km grid



KEY
Outline of the
geology of SW
England

Lineament
length (m)/
5km grid

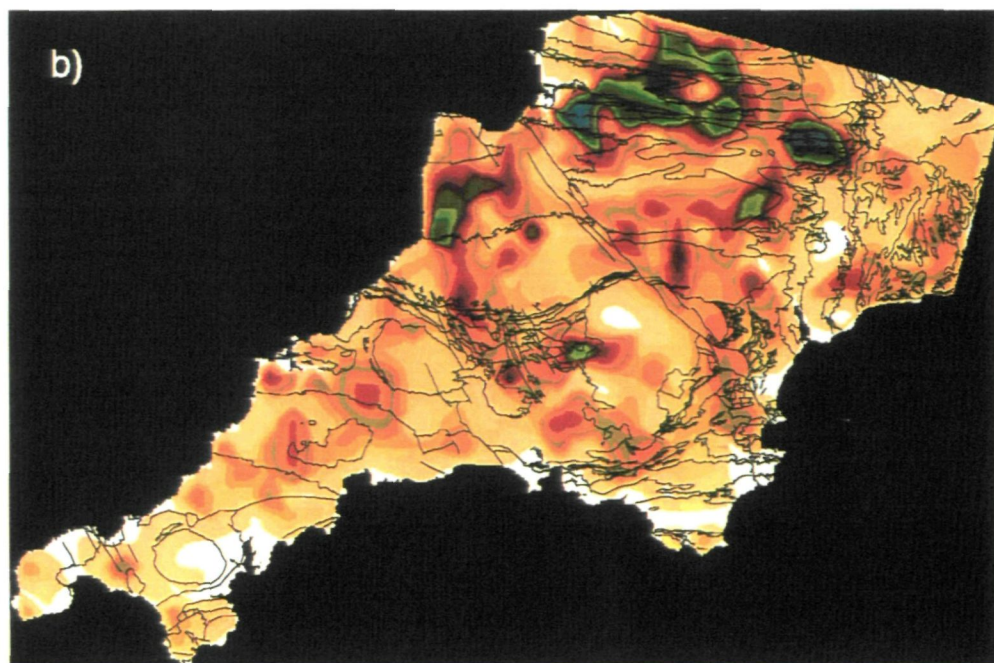
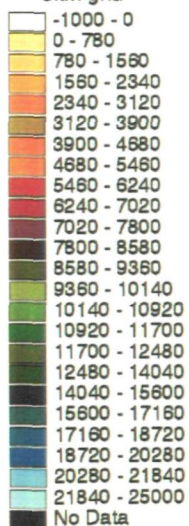
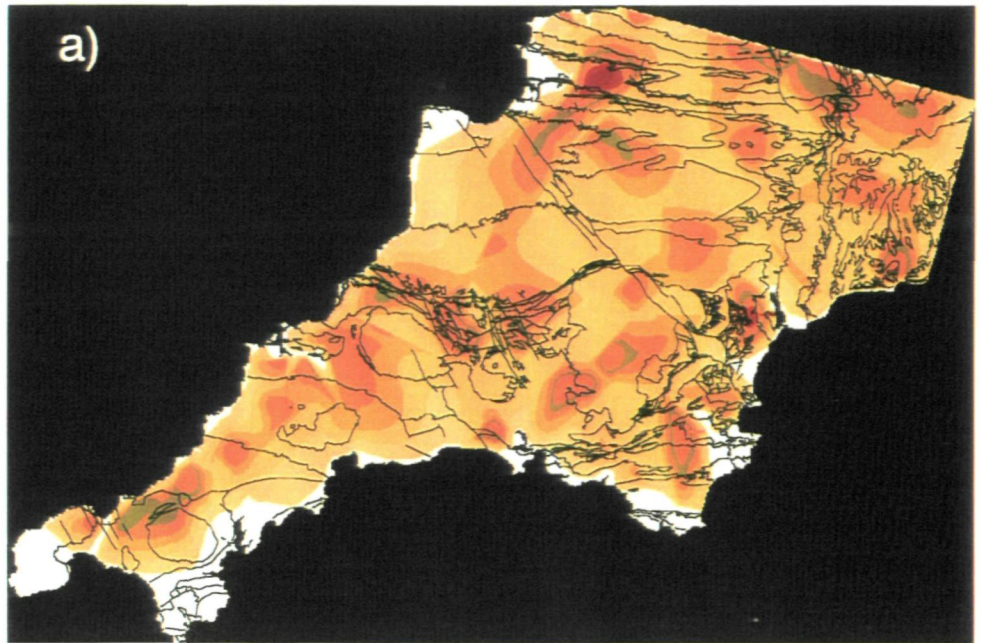
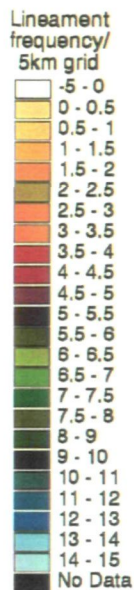


Fig. A2.9. Density maps of a) frequency and b) length of lineaments of the linked lineament directional families O and P, subsets of the SW England lineament population.

KEY
Outline of the
geology of SW
England



KEY
Outline of the
geology of SW
England

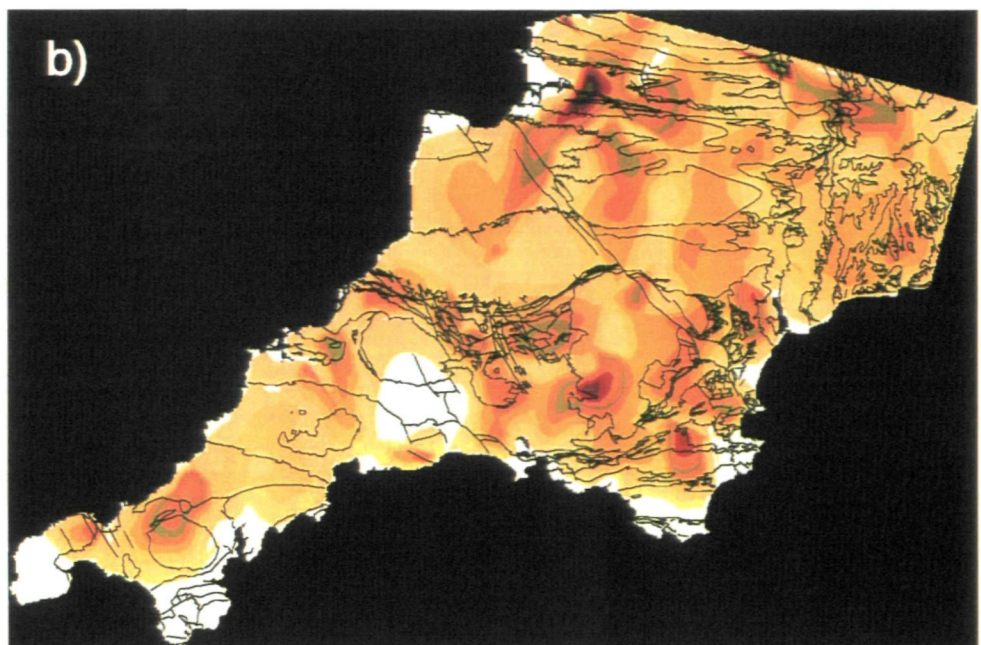
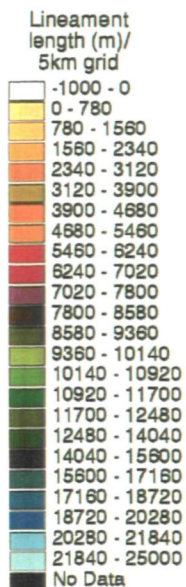
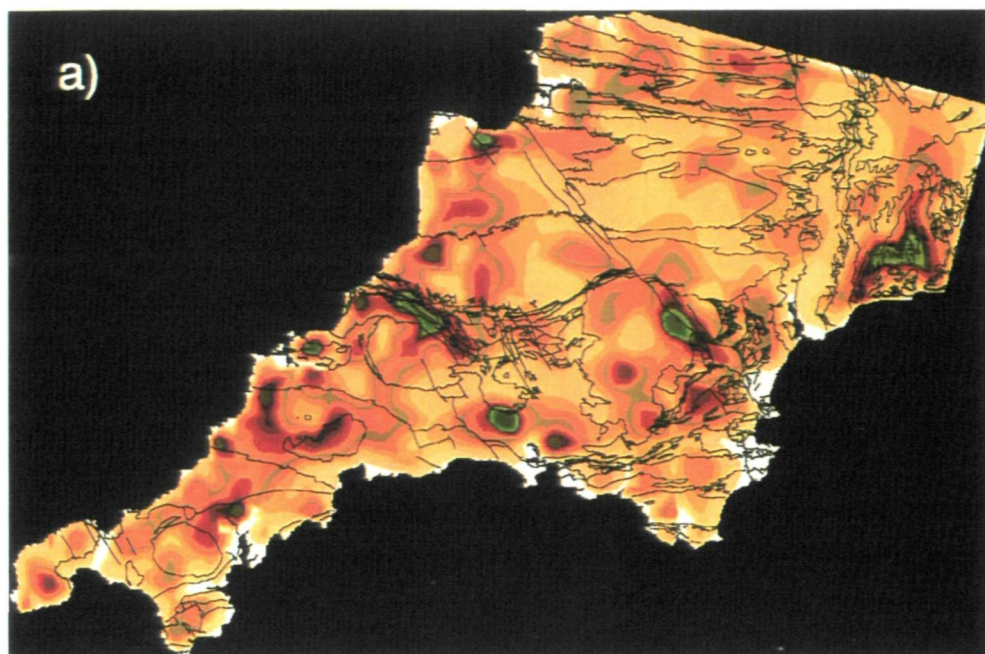
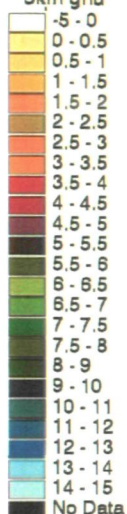


Fig. A2.10. Density maps of a) lineament frequency and b) lineament length of the directional family Q.

KEY

Outline of the
geology of SW
England

Lineament
frequency/
5km grid



KEY

Outline of the
geology of SW
England

Lineament
length (m)/
5km grid

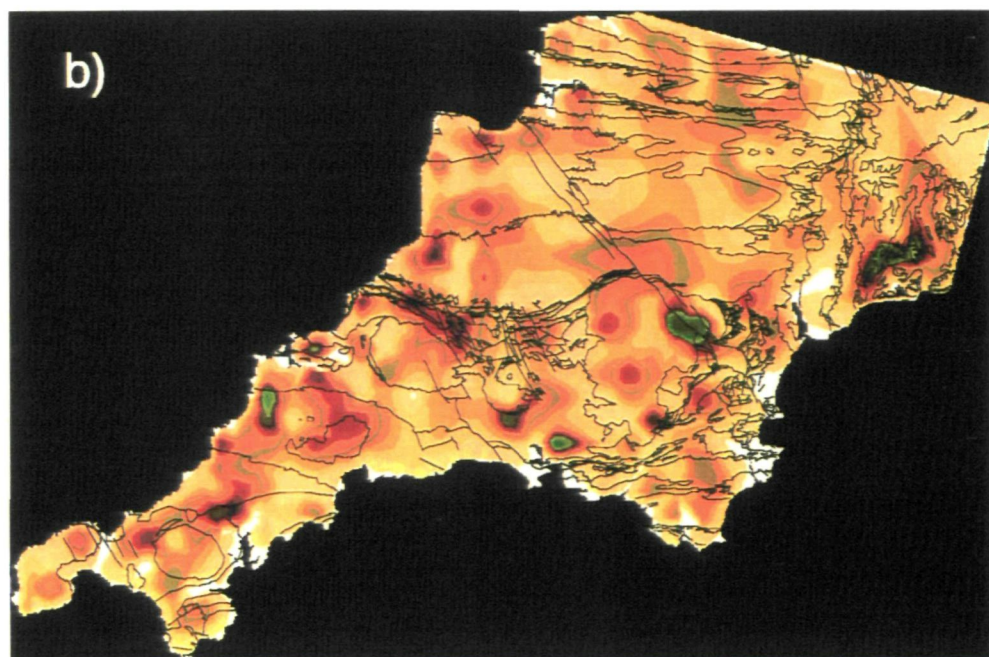
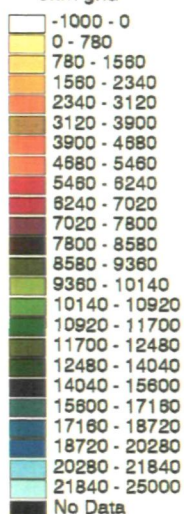
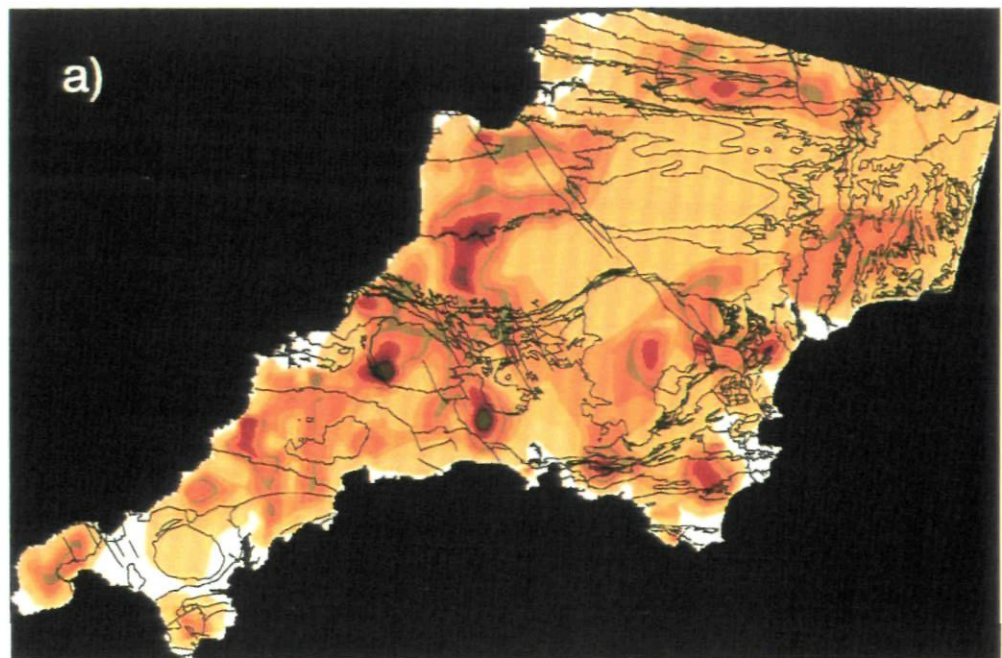
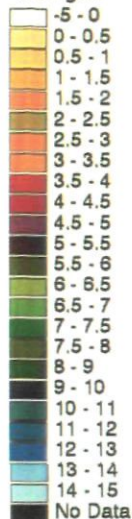


Fig. A2.11. Density maps of a) lineament frequency and b) lineament length of the linked density families R and S, subsets of the regional lineament population.

KEY
Outline of the
geology of SW
England

Lineament
frequency/
5km grid



KEY
Outline of the
geology of SW
England

Lineament
length (m)/
5km grid

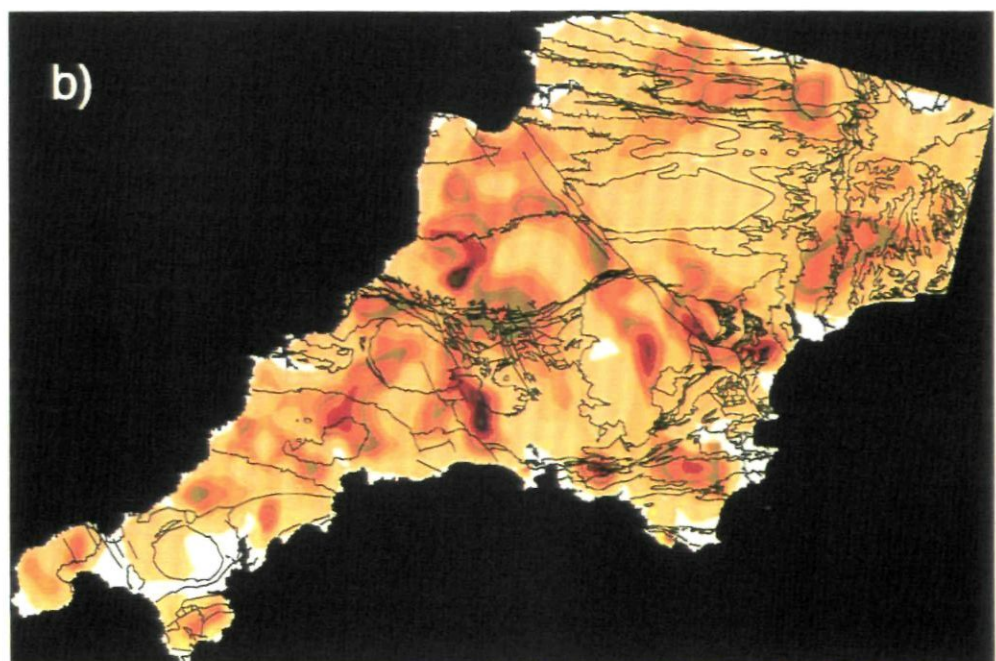
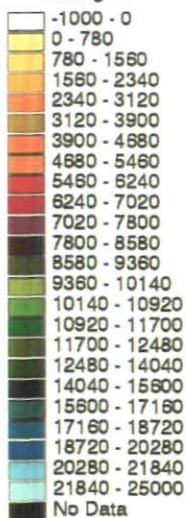
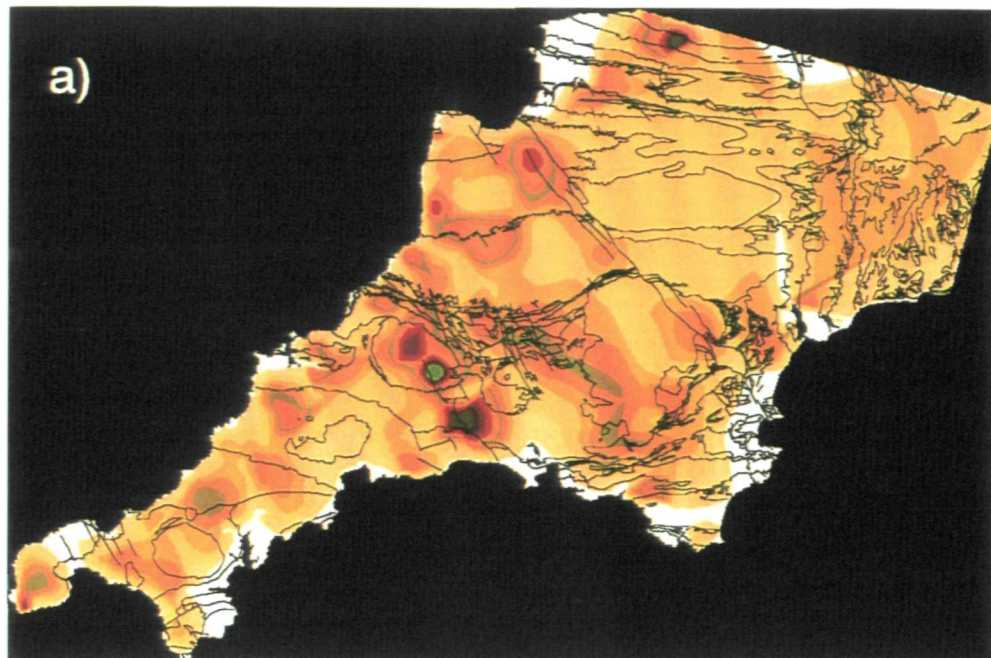
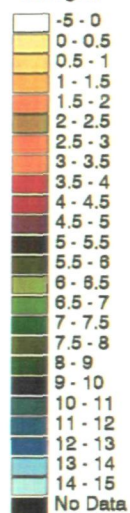


Fig. A2.12. Density maps of a) lineament frequency and b) lineament length of lineaments within the lineament directional family T, identified from the SW England lineament population.

KEY
Outline of the
geology of SW
England

Lineament
frequency/
5km grid



KEY
Outline of the
geology of SW
England

Lineament
length (m)/
5km

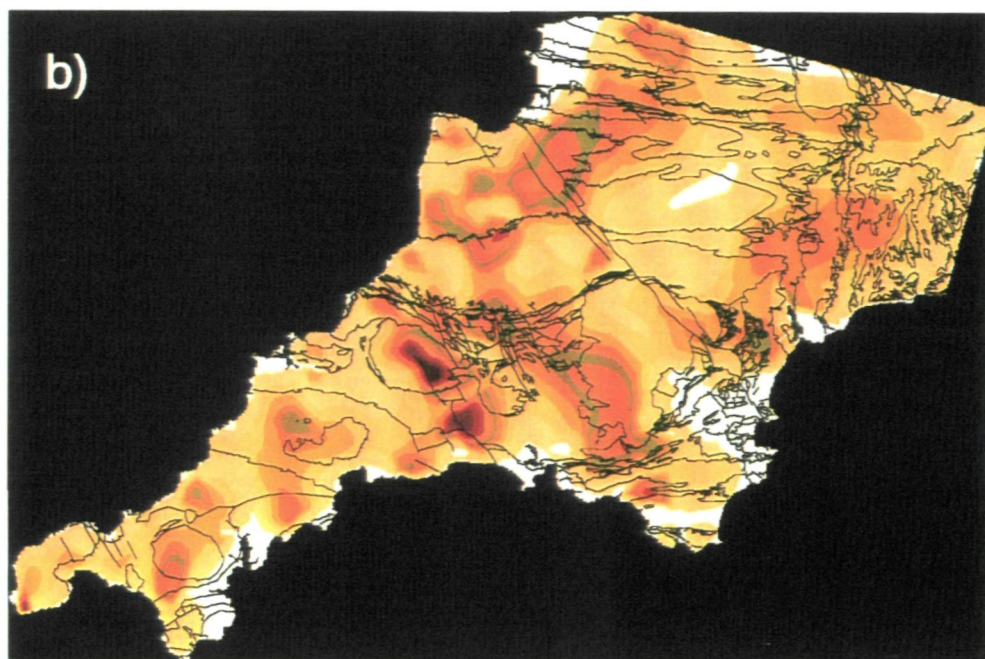
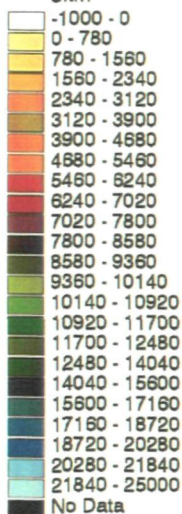


Fig. A2.13. Density maps of a) lineament frequency and b) lineament length of lineaments interpreted from TM images of SW England, and divided into the lineament directional families X and Y.

Publications

Rogers, J.D. 1994. Scaling relationships of lineament populations from Landsat TM imagery, South West England. (Extended abstract), *Tectonics Studies Group Special Meeting on Fault Populations*, 82-84.

The synoptic view provided by satellite imagery is ideal for the delineation of structural features at a high scale. To examine lineaments in SW England, Landsat Thematic Mapper imagery of bands 4, 5 and 7 with ground resolutions of 30m, 90m and 150m were processed by edge enhancing and directional filters. Lineaments were visually interpreted from these images and digitised using UNIX programmes; including the Geographical Information System, ARC/INFO. The scaling relationships between pixel resolution and the spatial variations of lineament length, frequency and trends were investigated from 15km² images of the north Cornwall coast, centred on the Rusey fault zone.

A *lineament* is defined by O'Leary *et al.* (1976) as a mappable, simple or composite feature of a surface, whose parts are aligned in a rectilinear or slightly curvilinear relationship and which differs distinctly from the patterns of adjacent features and presumably reflects a sub-surface phenomenon.

The landscape of SW England has been altered by man, particularly by modern agricultural methods. This causes several problems for lineament analysis, including a reduction in exposed rock, spurious noise produced by field boundaries and crops, linear man-made features, and the disturbance of the usually direct relationship between rock and soil. Seasonal changes in soil and vegetation water content result in varying spectral signatures, with solar illumination causing a bias towards a NE/SW trend (Drury 1986, Smithurst 1990). Drury (1986) has indicated that winter Landsat TM scenes are the most suitable

for structural analysis because the lower angle of solar illumination enhances topography and agricultural vegetation tonal differences are reduced. Results suggests there is a power-law relationship between lineament length and cumulative lineament frequency (Fig. 1). D-values increase with higher ground resolution with the values of 4.013 to 5.0732 being high compared with published data on fault populations (Childs *et al.* 1990, Walsh *et al.* 1991). Truncation is caused by the lower limit of the pixel resolution reducing the visual identification of the lineament population. Lineament length decreases with higher resolutions. Lineament frequency at the lower limit of resolution appears to have a linear relationship (Fig. 2), indicating the possibility of predicting lineament frequencies across a range of resolution and scales.

References.

- Childs, C., Walsh, J.J. & Watterson, J. (1990) A method for estimation of the density of fault displacements below the seismic resolution in reservoir formations. *In: Buller, A.T. (ed) North Sea Oil and Gas Reservoirs II. Graham & Trotman, London, 309-318.*
- Drury, S.A. (1986) Remote sensing of geological structure in temperate agricultural terrains. *Geological Magazine*, **123**, 113-121.
- O'Leary, D.W., Friedman, J.D. & Pohn, H.A. (1976) Lineament, linear, lineation: Some proposed new standards for old terms. *Geological Society of America*, **87**, 1463-1469.

Smithurst, L.J.M. (1990) Structural remote sensing of south-west England.

Proceedings of the Ussher Society, **7**, 236-241.

Walsh, J.J., Watterson, J. & Yielding, G. (1991) The importance of small scale faulting in regional extension. *Nature*, **351**, 391-393.

Figure 1. Lineament length against cumulative frequency for Landsat TM imagery from south west England.

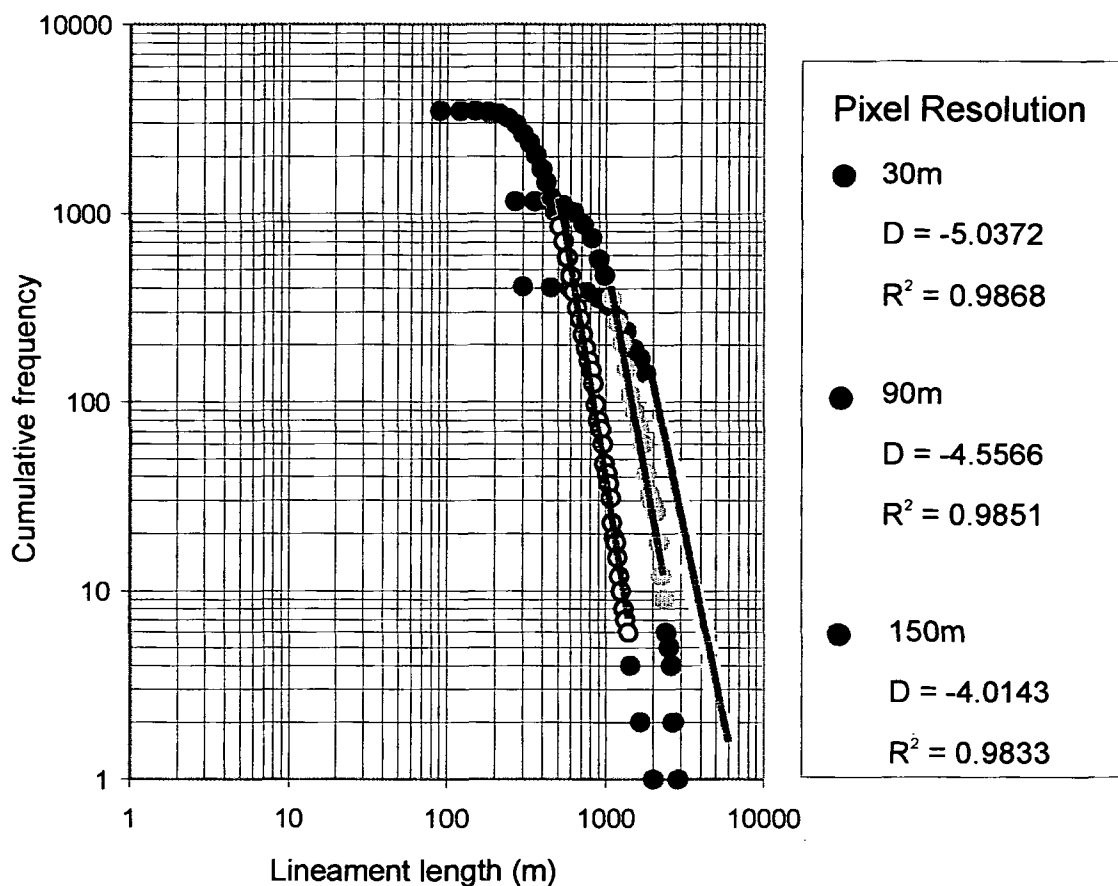
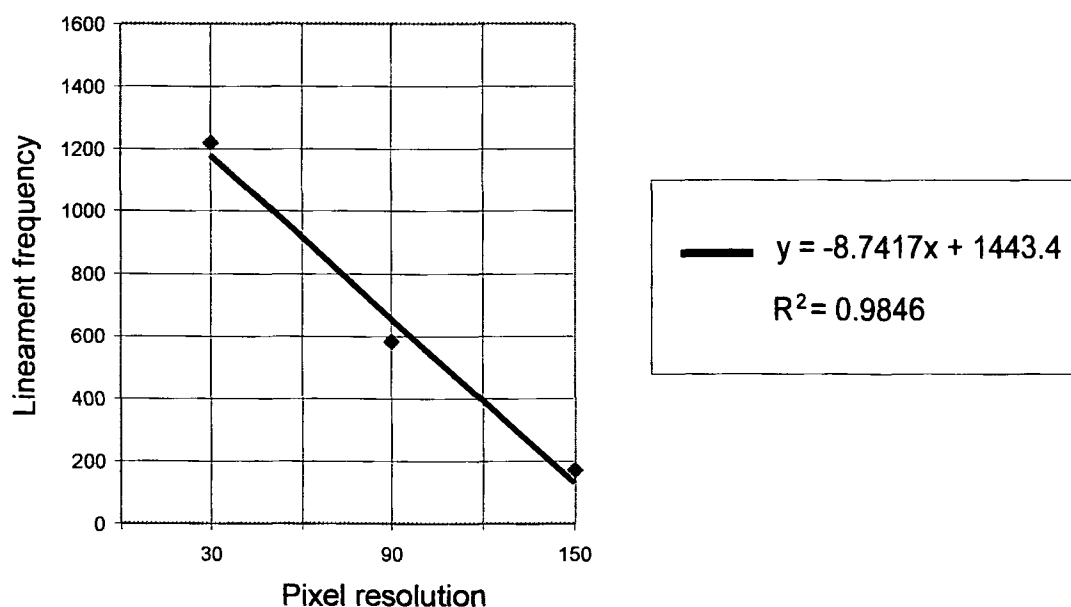


Figure 2. Graph indicating the relationship of the lower limit of resolution against lineament frequency.



Rogers, J.D. & Anderson, M.W. 1995. Interpretation of lineament populations from Landsat TM images. *Terra Nova*, 7,(1),27.

Lineament maps have been interpreted from Landsat TM imagery over a range of resolutions covering an area of North Cornwall, SW England. The area is a temperate agricultural terrain and related inherent linear features such as field boundaries and road networks cause spurious data over a pixel range of 30m to 150m. To increase lineament frequency, images of bands 4, 5 and 7 were enhanced with simple directional and high-pass filters. A geographic information system displaying elevation contours was used to distinguish between tonal and physiographic lineaments. Tonal linear features can then be corrected for field boundaries and man-made features. The frequency of spurious lineaments is found to increase with higher resolutions.

Lineament orientation, length and spacing over the resolution range have been analysed and linked to geological linear features identified from published geological maps. Lineament orientations increases in complexity with higher resolutions as smaller planar discontinuities with dissimilar trends fall within the observation threshold. Frequency-spacing distributions of a lineament population interpreted from images with a pixel size of 150m corresponding to stratigraphic bounded rock types have been found to be fractal. lineaments relating to faulting are found to be log-normal. This is consistent with published field-based data and suggests lineament maps showing such distributions are statistically valid.

Rogers, J.D. & Anderson, M.W. 1996. The Interpretation of Lineaments from Landsat TM Imagery of SW England and their Relationship to Regional Structural Trends. *Proceedings of the Ussher Society*, (9), 139.

Two scenes of Landsat TM imagery covering SW England have been interpreted for lineament trends and densities. Using a coarse pixel resolution of 150m, the local pixel variance reflecting small anthropogenic features is decreased, cleaning the interpreted map of spurious lineaments. Once cleaned, the scaling effects on directional lineament families have been investigated for a single sub-scene from North Cornwall.

The main lineament trend identified for SW England is E/W with subordinate trends to the N/S, NW/SE and NE/SW. The distribution of lineaments, along subordinate trends across the region, can be identified using computer generated contour maps of lineament length and frequency. Major E/W lineament trends are thought to reflect the trend of regional Variscan structures such as folds, lithostratigraphy and major thrust faults. Minor trends correspond with regional fracture patterns of uncertain origin. This apparently simple regional pattern implies little vertical axis rotation along major late/post Variscan structures. At increased resolutions, however, a higher directional complexity in the lineament populations is observed as smaller linear features fall within the image observation threshold. Consequently large scale lineaments may reflect linear zones of deformation of rotated linear features. The regional lineament trends may therefore oversimplify the actual nature of the deformation in SW England.